



EXPLORING THE INTERACTION OF DNA REPAIR PATHWAYS IN OVARIAN CANCER

Thesis submitted for partial fulfilment of the degree of Doctor of Philosophy

Aiste McCormick

CRUK Clinical Training Research Fellow

NICR

University of Newcastle upon Tyne

Supervisors

Richard J Edmondson

Professor of Gynaecological Oncology

Nicola J Curtin

Professor of Cancer therapeutics

2016

ABSTRACT

The dysregulation of DNA damage repair has a significant clinical impact in ovarian cancer. DNA double strand breaks (DSB) are repaired by the homologous recombination (HR) and the non homologous end joining (NHEJ) pathways. 50 % of ovarian cancers are HR defective (HRD), which makes these cancers sensitive to poly(ADP-ribose) polymerase inhibitors (PARPi). The role of PARP-1 in NHEJ, and the interaction between the two pathways in cancer chemo- and radio-sensitivity has been reported.

In this study, a primary ovarian cancer (PCO) culture model, derived from ascites, was optimised and the association of HRD with PARPi and cisplatin sensitivity confirmed. One PCO culture spontaneously immortalised, forming a novel cell line, NUOC-1, which was characterised demonstrating extensive genomic instability, clonal evolution and genomic aberrations consistent with an endometrioid / clear cell ovarian cancer.

NHEJ was found to be defective in 40 % of ovarian cancers, which was independent of HR and was associated with resistance to the PARPi, rucaparib. DNA-PKcs, Ku70 and Ku80 were found to be promising biomarkers for NHEJ function, however utility may be limited by intra-tumour heterogeneity. The role of PARP-1 in DNA DSB recognition and repair was assessed. Whilst PARP-1 expression and activity were independent of HR and NHEJ, PARP-1 was found to interact with DNA-PK and ATR in DSB recognition and repair.

HR recovery was found to lead to cisplatin and rucaparib cross resistance, and this appeared to be independent of BRCA and NHEJ function. Additionally, cisplatin resistant HRD cells were found to remain sensitive to rucaparib. Mutational and gene expression profiles were found to be cell and drug dependent with complex alterations in all resistant cell lines.

These results demonstrate the essential role of DSBs repair pathways in platinum and PARPi sensitivity. Stratification of tumours by HR and NHEJ function may therefore improve patient selection for treatment.

ACKNOWLEDGEMENTS

Despite having experience of laboratory environments and research projects, my PhD at times felt like a task too big to handle pushing me to complete limits academically and emotionally. Whilst my project has become significantly larger than initially planned and has created more questions than answers it has been an invaluable experience.

I thank my supervisors Richard and Nicola for their continuous support and guidance. Especially Richard, who throughout the past 7 years has not only supported my project, but has also been an invaluable source of advice for my future career (and family planning at times!).

I am grateful to all of my colleagues at the NICR in particular Nicola S, Sarah W, Rachel, Angelika, Peter, Michelle, James, Arman, Miranda, Amy, Alice, Kasturi and Sarah F for their help and support in the lab, the coffee room and the North Terrace. I am extremely grateful to Jim Allan for his invaluable help with the clever genomic work and support throughout. I also have to thank Vikki Rand for help with sequencing, John Lunec with p53 work and Huw and Helen for the mouse work.

Thanks also to my students – Laura, Anna, Charlie, Ellie, Katharine and Richard for doing amazing jobs on the projects and providing cakes and entertainment in their own individual ways.

I have to thank my parents for their constant support over the years, my family and friends for pretending to be interested in my science talk and especially Mark, who tirelessly supported me, encouraged me, acted as my chauffeur, proofread my thesis and forgave me for living in the lab. A special thank you also to Alex who made me take a break and get some life into my work life balance and Jonny, who gave me the much needed kick to finish the writing up.

And finally thank you to all those women who have battled ovarian cancer and donated samples to contribute to forwarding the understanding and future treatment of this devastating disease. And Cancer Research UK for generously funding this project and providing guidance throughout.

TABLE OF CONTENT

CHAPTER 1 INTRODUCTION.....	1
1.1 Background	1
1.2 Tumour Biology in Ovarian Cancer	2
1.2.1 Molecular Characteristics of Type I and Type II Tumours	3
1.2.2 Precursor Lesions for Ovarian Tumours	3
1.2.3 Treatment Considerations for Type I and Type II Tumours.....	5
1.2.4 Risk Factors	5
1.2.5 Hypotheses for Tumour Origin	6
1.3 Treatment of Ovarian Cancer	7
1.3.1 Surgery	7
1.3.2 Chemotherapy	8
1.3.3 Treatment of Recurrent Disease	13
1.3.4 Targeted Therapies.....	13
1.4 DNA Repair Pathways	15
1.4.1 Direct Repair by O6-methylguanine-DNA Methyltransferase	16
1.4.2 Mismatch Repair	16
1.4.3 Nucleotide Excision Repair	18
1.4.4 Base Excision Repair	19
1.4.5 DNA Double Strand Break Repair.....	20
1.4.6 Poly (ADP) Polymerase (PARP)	30
1.5 Rationale for This Project	33
1.6 Project Hypothesis	35
1.7 Project Aims	35
CHAPTER 2 MATERIALS AND METHODS.....	36
2.1 General Laboratory Practice	36
2.2 Cell Culture Methods	36
2.2.1 Routine Cell Culture	36
2.2.2 Primary Culture	36
2.2.3 Pancytokeratin Staining	38

2.2.4	Cell Passaging	39
2.2.5	Cell Counting	39
2.2.6	Cryopreservation of Cell Stocks.....	39
2.2.7	Resuscitation of Frozen Cell Stocks	40
2.3	Clinical Data and Survival Analysis	40
2.4	Measurement of DSB Induction and Repair	40
2.4.1	Induction of DNA Damage with Ionizing Radiation.....	41
2.4.2	Use of PARP Inhibitor, Rucaparib to Produce DSBs	41
2.4.3	Cell Fixation and Staining	41
2.4.4	Immunofluorescence Microscopy.....	42
2.4.5	Counting Foci.....	43
2.5	Cytotoxicity Assays	43
2.6	Non Homologous End Joining Assays	45
2.6.1	Cell Extract End Joining Assay	45
2.6.2	Luciferase Cellular End Joining Assay	50
2.7	Western Immunoblotting	51
2.7.1	Cytosol Preparation	52
2.7.2	SDS PAGE and Electrophoretic Transfer.....	52
2.7.3	Antibody Detection and Visualisation of Bound Proteins.....	53
2.7.4	Optimisation of Loading Control Protein.....	55
2.8	Immunohistochemistry	55
2.8.1	Formalin-Fixed Paraffin-Embedded Tissue.....	55
2.8.2	Antigen Retrieval.....	56
2.8.3	Antibody Detection.....	56
2.8.4	Imaging	57
2.8.5	Scoring.....	57
2.9	Cell Cycle Assessment using Flow Cytometry	58
2.9.1	Sample Preparation	58
2.9.2	Sample Analysis	58
2.9.3	Data Analysis	59
2.9.4	Optimising Flow Cytometry	59

2.10 Poly (ADP-ribose) Polymerase Assay	60
2.10.1 Data Analysis.....	61
2.11 Gene Expression Analysis by Quantitative Real-time PCR	61
2.11.1 RNA Extraction and Quantification	62
2.11.2 RNA Extraction from FFPE Tissue	62
2.11.3 Reverse Transcription of RNA into cDNA	63
2.11.4 Real-time PCR Setup	63
2.11.5 Data Analysis.....	65
2.12 RNA Genome Expression Arrays	65
2.12.1 Data Analysis.....	66
2.13 DNA Sequencing	67
2.13.1 DNA Extraction and Quantitation	67
2.13.2 PCR Amplification.....	67
2.13.3 Whole exome sequencing	68
2.14 SNP Array Analysis	69
2.14.1 Data Analysis.....	69
2.15 G-band Karyotyping	70
2.16 Fluorescence in Situ Hybridization for c-MYC	70
2.17 Mouse experiments	71
2.17.1 Subcutaneous Injection	71
2.17.2 Intraperitoneal Injection	71
2.18 Generation of Stable PTEN, DNA-PKcs and ATR Defective Cell Lines using Short Hairpin RNA-Mediated Gene Knockdown	73
2.18.1 shRNA Constructs	73
2.18.2 Assessment of Puromycin Sensitivity	74
2.18.3 Assessment of Transduction Efficiency	74
2.18.4 Lentiviral Transduction.....	75
2.18.5 Selection of Transduced Cells	76
2.18.6 Assessment of Knockdown Efficiency	76
2.19 Generation of Drug Resistant Cell Lines by Escalating Dosage	77

2.19.1	Concentration Finding Assay	77
2.19.2	Drug Dosing	77
2.19.3	Assessment or Resistance	78
2.20	Statistical Analysis	78
CHAPTER 3 FUNCTIONAL CHARACTERISATION OF OVARIAN CANCER MODELS....		79
3.1	Introduction	79
3.2	Aims for Chapter 3	80
3.3	Results	81
3.3.1	PCO Culture Characterisation.....	82
3.3.2	HR Function in PCO Cultures	86
3.3.3	Sensitivity of PCO Cultures to Rucaparib and Cisplatin	88
3.3.4	RNA Genome Expression Arrays to Assess HR Function	91
3.4	Characterisation of NUOC-1 Cell Line	95
3.4.1	Confirmation of Epithelial Origin.....	95
3.4.2	Assessment of Hormone and Tyrosine Kinase Receptor Expression	96
3.4.3	p53 Function Assessment.....	97
3.4.4	NUOC-1 DNA Repair Assessment.....	100
3.4.5	Drug Sensitivity Assessment.....	101
3.4.6	Assessment for ARID1A Mutations.....	102
3.4.7	PTEN Function.....	104
3.4.8	Assessment of the Tumourgenic Potential of NUOC-1 Cells	112
3.4.9	NUOC-1 Karyotype	116
3.4.10	Clonal Evolution in NUOC-1 Cells	117
3.4.11	Assessment of MYC Amplification	120
3.5	Chapter Summary	122
3.6	Discussion	123
3.6.1	Characterisation of PCO Cultures.....	123
3.6.2	HR Function in PCO Cultures	124
3.6.3	Prediction of HR Function by Genome Expression Arrays.....	125
3.6.4	Molecular Characterisation of NUOC-1 Cell Line.....	126

3.6.5	NUOC-1 Cell Line Represents Endometrioid / Clear Cell Ovarian Carcinoma.....	126
3.6.6	PTEN is a Potential Target for Ovarian Cancer Sensitisation to Cytotoxic Agents	127
3.6.7	NUOC-1 Cells are HRC, but BER Defective	128
3.6.8	Xenograft Development was not possible from NUOC-1 Cells	129
3.6.9	NUOC-1 Cells Reflect the Genomic Instability and Heterogeneity of Ovarian Cancer	129
3.7	Future Work	130
	CHAPTER 4 ASSESSMENT OF NHEJ FUNCTION IN OVARIAN CANCER.....	131
4.1	Introduction	131
4.2	Aims for Chapter 4	133
4.3	Results	133
4.3.1	Optimising NHEJ Assay	135
4.3.2	DNA End Joining in Established Epithelial Ovarian Cancer Cell Lines ...	138
4.3.3	DNA End Joining in PCO Cultures	139
4.3.4	Biomarker Development for NHEJ Function	144
4.3.5	Interaction of HR and NHEJ Pathways	150
4.3.6	Effect of NHEJ Function on Sensitivity to Rucaparib and Cisplatin.....	152
4.3.7	Correlation of NHEJ Status with Clinical Outcomes	156
4.3.8	Assessment of NHEJ Targets in FFPE Tissue.....	157
4.3.9	Assessment of NHEJ Heterogeneity	160
4.4	Chapter Summary	164
4.5	Discussion	164
4.5.1	NHEJ Function is Independent of HR and NHEJD is Associated with Rucaparib Resistance	164
4.5.2	Cisplatin Inhibits NHEJ Function.....	166
4.5.3	Protein Expression of Ku and DNA-PK are Potential Biomarkers for NHEJ Function	166
4.5.4	Tumour Heterogeneity of NHEJ Function	167
4.6	Future Work	169

CHAPTER 5 ASSESSMENT OF THE EFFECT OF ATR AND DNA-PK INHIBITION ON CELLULAR BIOLOGY AND PARPI SENSITIVITY	170
5.1 Introduction	170
5.1.1 ATR.....	170
5.1.2 DNA-PK	172
5.2 Aims for Chapter 5	174
5.3 Results	175
5.3.2 Assessment of the Effect of ATR and DNA-PK Inhibition on Cellular Biology 181	
5.3.3 Interaction of ATRi and DNA-PKi with PARPi	188
5.3.4 DNA Damage Recognition and Repair in Primary Cultures	196
5.4 Summary of Chapter	205
5.5 Discussion	206
5.5.1 Protein Inhibition and Knockdown may not be Directly Comparable	206
5.5.2 ATR and DNA-PK Inhibition Effects are Cell Line Specific.....	206
5.5.3 ATR and DNA-PK Inhibition are Cytostatic	207
5.5.4 DNA-PK is required for the Rapid Phase Whilst ATR in Slow Phase of DNA DSBs Repair.....	207
5.5.5 ATR Inhibition Sensitises to Rucaparib and Cisplatin whilst DNA-PK Inhibition to Irradiation.....	209
5.5.6 Interaction of ATR and DNA-PK with PARP-1	210
5.5.7 PARP-1 Affects DNA DSBs Recognition and Selection of Repair Pathway 210	
5.5.8 In PCO Cultures ATR and DNA-PK Expression Correlate but are Independent of PARP-1	211
5.5.9 DNA DSBS Recognition and Repair is Inhibited in NHEJ and HRD PCO Cultures.....	212
5.6 Future Work	213
CHAPTER 6 ASSESSMENT OF THE ROLE OF DNA REPAIR IN RESISTANCE TO RUCAPARIB AND CISPLATIN.....	214
6.1 Introduction	214
6.1.1 Mechanism of Platinum Chemotherapy	214

6.1.2	Mechanisms of Platinum Resistance	214
6.2	PARP Inhibitor Function	216
6.2.1	Mechanisms of PARP Inhibitor Resistance	217
6.3	Aims of Chapter 6	219
6.4	Results	220
6.4.1	Basal Cell Line Characteristics	220
6.4.2	Development of Resistant Cell Lines	225
6.4.3	Validation of Resistant Models	226
6.4.4	Assessment of Sensitivity to Rucaparib and Cisplatin	227
6.4.5	Mutation Analysis	233
6.4.6	Gene Expression Profiling and Analysis	245
6.5	Summary of Chapter	257
6.6	Discussion	257
6.6.1	Regaining of HRC is Associated with Rucaparib Resistance	257
6.6.2	NHEJ Pathway was not Altered During Resistance Development	259
6.6.3	Mutations Signatures are Dependent on Pre-existing Defects and Drug Treatment	260
6.6.4	Gene Expression Signatures are Dependent on Pre-existing Defects and Drug Treatment	260
6.7	Further Work	261
	CHAPTER 7 CONCLUDING DISCUSSION AND FUTURE DIRECTIONS	263
7.1	Summary of Results	264
7.2	Models for the Research of Ovarian Cancer	266
7.3	DNA DSBs Repair in Ovarian Cancer	267
7.4	Prediction of Response to PARPi	268
7.5	New Treatment Strategies for Ovarian Cancer	270
7.6	Strengths and Weaknesses of This Project	272
7.7	Future Work	273

APPENDICES	275
APPENDIX 1: NHEJ GENE DEFECTS IN HUMAN CANCERS	276
APPENDIX 2: SUMMARY OF CLINICAL TRIALS OF PARPI USE IN OVARIAN CANCER 279	
APPENDIX 3: NGOC CONSENT FORM.....	282
APPENDIX 4: MULTIPLE COMPARISONS FOR INHIBITION AND KNOCKDOWN OF ATR AND DNA-PK WITH PARPI	283
APPENDIX 5: PHD PUBLICATIONS	287
APPENDIX 6: PUBLISHED ABSTRACTS.....	289
APPENDIX 7: ORAL PRESENTATIONS	291
APPENDIX 8: POSTER PRESENTATIONS	292

LIST OF FIGURES

Figure 1-1 Schematic representation of the PI3K signalling pathway.....	9
Figure 1-2 Schematic representation of MAPK pathway.	10
Figure 1-3 Schematic representation of MMR pathway.....	17
Figure 1-4 Schematic representation of NER pathway.....	19
Figure 1-5 Schematic representation of BER pathway.....	20
Figure 1-6 Schematic representation of HR pathway.	22
Figure 1-7 Schematic representation of NHEJ.	26
Figure 1-8 Schematic representation of the pathway choice for the repair of a DSBs	29
Figure 2-1 Schematic representation of cellular extract NHEJ assay.....	46
Figure 2-2 Optimisation of BstXI digestion.	48
Figure 2-3 Optimisation of cell extract end joining assay.	49
Figure 2-4 Schematic representation of Luciferase cellular end joining assay.	50
Figure 2-5 Expression of α -tubulin and GAPDH across a panel of cell lines.	55
Figure 2-6 Graded scoring intensities for each antibody.	57
Figure 2-7 Gating for flow cytometry.	60
Figure 2-8 Cytocell MYC 'breakapart' probe set.	71
Figure 3-1 PCO characterisation panel.	83
Figure 3-2 Growth rate of PCO cultures.	84
Figure 3-3 Viral transduction of shRNA to DNA-PK and ATR into PCO 204.	85
Figure 3-4 Transfection of pGL2 luciferase expressing vector into PCO cultures.	86
Figure 3-5 HR function in PCO cultures. RAD51 foci fold rise above controls.	87
Figure 3-6 Kaplan-Meier survival curves for PFS/OS by HR status.	87
Figure 3-7 Correlation of rucaparib and cisplatin sensitivity of PCO cultures.	88
Figure 3-8 Rucaparib and cisplatin cytotoxicity in PCO cultures by HR function.	89
Figure 3-9 Kaplan-Meier survival curves for PFS/OS by sensitivity to rucaparib and cisplatin. Patients who had not progressed were censored at last follow up.	90
Figure 3-10 RNA Genome expression array.	92
Figure 3-11 Hierarchical clustering of HR pathway genes expression.	94
Figure 3-12 NUOC-1 characterisation panel.	95
Figure 3-13 Tyrosine kinase and endocrine receptor expression in the NUOC-1 cell line.....	97
Figure 3-14 Illustration of chromatogram of TP53 gene.	98
Figure 3-15 MDM2, p53, and p21 expression in response to Nutlin3.....	99
Figure 3-16 NUOC-1 cell line response to Nutlin3.....	99
Figure 3-17 Base excision repair of NUOC-1 assessed by competitive ELISA.	100
Figure 3-18 Illustration of chromatogram of ARID1A gene.....	103
Figure 3-19 A schematic of ARID1A protein product.....	103
Figure 3-20 Illustration of chromatogram of PTEN gene.	104
Figure 3-21 PTEN expression levels in NUOC-1 cells.	105
Figure 3-22 PTEN mRNA expression in OSEC-2 and NUOC-1 cells.....	106
Figure 3-23 The effect of PTEN knockdown on HR function.	107
Figure 3-24 Sensitivity of OSEC-2 and NUOC-1 to common therapeutics.	108

Figure 3-25 Illustration of sequence chromatograms of PTEN gene.	109
Figure 3-26 PTEN mRNA expression In PCO cultures.	110
Figure 3-27 PTEN mRNA expression divided by HR function status in PCO cultures.	111
Figure 3-28 Correlation of PTEN mRNA expression with sensitivity to cisplatin and rucaparib in PCO cultures.	111
Figure 3-29 PTEN association with survival benefits from TCGA database.	112
Figure 3-30 NUOC-1 tumourgenicity assessment bioluminescent images.	114
Figure 3-31 Quantification of bioluminescent imaging.	115
Figure 3-32 NUOC-1 karyotype.	116
Figure 3-33 Copy number variations in NUOC-1, NUOC-1-A1 and NUOC-1-A2 cells.	118
Figure 3-34 Copy number profiles of NUOC-1-A1 and NUOC-1-A2 cell lines.	119
Figure 3-35 Copy number profile of chromosome 8 in NUOC-1 cells.	120
Figure 3-36 FISH immunofluorescent images for MYC in NUOC-1.	121
Figure 4-1 NHEJ gene aberrations reported in the TCGA database.	134
Figure 4-2 Diagrammatic representation of BstXI digested products.	135
Figure 4-3 Rejoining of BstXI substrates.	136
Figure 4-4 Densitometry quantification of OSEC-2 rejoining of BstXI substrates. ...	136
Figure 4-5 PCR analysis of cell line rejoining of Co or 2I BstXI substrates.	137
Figure 4-6 Inhibition of end joining of BstXI digested Co substrates by NU7441.	137
Figure 4-7 End joining of compatible and 2I BstXI substrates by ovarian cell lines.	138
Figure 4-8 Intracellular end joining of linearised pGL2 vector by cell lines.	139
Figure 4-9 Correlation of luciferase cellular assay and cell extract assay.	139
Figure 4-10 End joining of compatible BstXI substrates by PCO cultures.	140
Figure 4-11 End joining of compatible BstXI substrates by PCO cultures. GelRed detection and quantification of end joining of BstXI compatible substrates.	142
Figure 4-12 Accuracy of rejoining of 2I BstXI substrates by PCO cultures.	143
Figure 4-13 NHEJ assessment by immunofluorescence.	144
Figure 4-14 DNA-PK autophosphorylation as a marker of NHEJ function.	145
Figure 4-15 Prediction of NHEJ function by mRNA and protein expression of pathway components.	146
Figure 4-16 PCO genome RNA expression microarray.	148
Figure 4-17 Rucaparib sensitivity and HR function in M059J and M059FUS-1 cells.	150
Figure 4-18 Growth of PCO cultures divided by HR and NHEJ status.	151
Figure 4-19 Rucaparib cytotoxicity in PCO cultures divided by NHEJ status.	153
Figure 4-20 Cisplatin cytotoxicity in PCO cultures divided by NHEJ status.	153
Figure 4-21 Rucaparib and cisplatin cytotoxicity plotted by NHEJ and HR status. ...	154
Figure 4-22 Cisplatin inhibition of end joining of Co and 2I BstXI substrates.	155
Figure 4-23 Kaplan-Meier survival curves for PFS/OS by NHEJ status.	157
Figure 4-24 DNA-PKcs, Ku70 and Ku80 protein expression grouped by NHEJ status.	159
Figure 4-25 DNA-PKcs, Ku70 and Ku80 mRNA expression grouped by NHEJ status.	159

Figure 4-26 Correlation of DNA-PKcs, Ku70 and Ku80 mRNA and protein expression.	160
Figure 4-27 Correlations of FFPE and ascites mRNA and protein expression.	161
Figure 4-28 Correlations of NHEJ protein expression in multiple biopsies.	162
Figure 4-29 DNA-PKcs, Ku70 and Ku80 protein expression grouped by tumour site.	162
Figure 4-30 DNA-PKcs, Ku70 and Ku80 protein expression in ovarian carcinoma and healthy control samples.	163
Figure 5-1 Assessment of HR in response to ATR and ATM inhibition.	176
Figure 5-2 Optimisation of inhibition of DNA-PK in OSEC-2 cell line.	176
Figure 5-3 Optimisation of inhibition of ATR in OSEC-2 cell line.	177
Figure 5-4 Silencing of ATR and DNA-PKcs in OSEC-2 and NUOC-1 cells.	178
Figure 5-5 ATR and DNA-PK double knockdown in OSEC-2 cells.	179
Figure 5-6 HR and NHEJ function in knockdown models.	180
Figure 5-7 The effect of ATR and DNA-PK inhibition on cell growth.	182
Figure 5-8 The effect of ATR and DNA-PK inhibition on cell survival.	183
Figure 5-9 The effect of ATR and DNA-PKcs on cell cycle.	184
Figure 5-10 DSBs formation and recovery after inhibition of ATR and DNA-PKcs.	185
Figure 5-11 Optimisation of inhibition of PARP.	189
Figure 5-12 The effect of PARPi combined with ATRi and DNA-PKi on cell growth.	190
Figure 5-13 The effect of PARPi combined with ATRi and DNA-PKi on cell survival.	192
Figure 5-14 DNA DSBs formation and recovery after inhibition of PARP-1.	193
Figure 5-15 DNA DSBs formation and recovery after inhibition of PARP-1 and ATR.	194
Figure 5-16 DNA DSBs formation and recovery after inhibition of PARP-1 and DNA-PK.	195
Figure 5-17 ATR and DNA-PKcs mRNA expression and correlation in PCO cultures.	197
Figure 5-18 PARP activity in PCO cultures correlated with ATR and DNA-PKcs mRNA expression.	198
Figure 5-19 PARP-1 activity in PCO cultures shown by NHEJ and HR status.	199
Figure 5-20 PARP-1 expression in PCO cultures shown by HR and NHEJ status.	199
Figure 5-21 Correlation between PAR activity and PARP-1 mRNA.	200
Figure 5-22 ATRi sensitisation of PCO cultures to rucaparib and cisplatin.	201
Figure 5-23 DNA DSBs formation and recovery in PCO cultures.	202
Figure 5-24 RAD51 foci fold rise and DNA-PK expression shown by HR or NHEJ status.	203
Figure 5-25 The association of γ H2AX foci formation and recovery with rucaparib and cisplatin sensitivity.	204
Figure 6-1 Schematic of the mechanisms contributing to platinum resistance.	215
Figure 6-2 Schematic of the mechanisms contributing to PARPi resistance.	217
Figure 6-3 HR status of model cell lines.	222
Figure 6-4 NHEJ status of model cell lines.	223
Figure 6-5 Chemo-sensitivity of cell lines assessed by Clonogenic assay.	224

Figure 6-6 Chemo-sensitivity of derived cell lines assessed by Clonogenic assay.	228
Figure 6-7 HR status of derivative cell lines.	230
Figure 6-8 End joining of Co BstXI substrates by resistant cell lines.	231
Figure 6-9 End joining of 2I BstXI substrates by resistant cell lines.	231
Figure 6-10 DNA-PKcs, Ku80 and Ku70 protein expression in resistant cell lines. .	232
Figure 6-11 BER function in resistant cell lines assessed by competitive ELISA. ...	233
Figure 6-12 Circos plots for rucaparib resistant cell line derivatives.	235
Figure 6-13 Circos plots for cisplatin resistant cell line derivatives.	236
Figure 6-14 Circos plots for irradiation cell line derivatives.	237
Figure 6-15 Differential expression analysis of resistant cell lines.	248
Figure 6-16 Differential expression analysis by drug treatment in resistant cell lines.	251
Figure 6-17 Expression of potential rucaparib resistance target genes in PCO cultures.	256
Figure 6-18 Expression of potential cisplatin resistance target genes in PCO cultures.	256

LIST OF TABLES

Table 1-1 Molecular classification of Ovarian Cancer.	4
Table 1-2 Risk Factors for Ovarian Cancer Development	6
Table 1-3 Second line systemic therapy for the treatment of ovarian cancer.	14
Table 1-4 Reported links to human cancers of HR gene alterations.	23
Table 1-5 Reported links to human cancers of NHEJ gene alterations.	27
Table 2-1 Cell lines used in the project.	37
Table 2-2 DNA damage induction and detection experiments.	41
Table 2-3 Antibody preparation for immunofluorescence experiments.....	42
Table 2-4 Leica DMR fluorescent microscope settings.	43
Table 2-5 Details of cytotoxic agents and small molecule inhibitors.....	44
Table 2-6 Antibodies used for protein detection by western blotting.	54
Table 2-7 Antibodies, concentrations and incubation times used for IHC.	56
Table 2-8 IHC scores for DNA-PKcs, Ku70 and Ku80.....	58
Table 2-9 Primers used for PCR.	64
Table 2-10 Viral titres and required volumes for each ShRNA construct.....	76
Table 2-11 Resistance development dosing.	77
Table 3-1 Patient characteristics for PCO culture samples.	82
Table 3-2 Summary of PCO antigen expression.	83
Table 3-3 Sensitivity of NUOC-1 and OSEC-2 cell lines to cytotoxic agents.....	102
Table 3-4 FISH for MYC results for NUOC-1.....	121
Table 4-1 PCO RNA differential expression after multiple test correlation.	149
Table 4-2 Rucaparib and cisplatin cytotoxicity and NHEJ status of cell lines.	152
Table 4-3 Patient characteristics for PCO samples divided by NHEJ status.	156
Table 4-4 DNA-PKcs, Ku70 and Ku80 mRNA and protein expression by NHEJ status.....	158
Table 5-1 Cell line models.	175
Table 5-2 Sensitisation of NUOC-1 and OSEC-2 cells to common therapeutics by ATR and DNA-PK inhibition and knockdown.....	187
Table 6-1 Cell line model characteristics.	221
Table 6-2 Sensitivity of UWB1-289 and PEO cell lines to rucaparib and cisplatin...225	
Table 6-3 Morphology and doubling time of UWB1.289 derived cell lines.....	226
Table 6-4 Morphology and doubling time of PEO1 derived cell lines.	227
Table 6-5 Cisplatin and Rucaparib sensitivity in derivative cell lines. LC ₅₀ assessed by clonogenics assay.	229
Table 6-6 Somatic mutations in DNA repair genes in derived cell lines not found in parent cell lines.	239
Table 6-7 Pathway enrichment of mutated genes in resistant cell lines.	241
Table 6-8 MAPK pathway genes mutated in resistant lines.	242
Table 6-9 Genes in PI3CA /AKT pathway mutated in resistant lines.....	243
Table 6-10 Calcium signalling pathway mutated genes.	244
Table 6-11 Top 10 genes differentially expressed in resistant cell lines.....	246
Table 6-12 Reported links to human cancer of genes with altered expression in resistant cell lines.	249

Table 6-13 Pathway enrichment analysis in resistant cell lines.....253

Table 6-14 Genes with mutations and altered expression in derived cell lines and
previously reported links to human cancers.254

Table 7-1 Project aims and outcomes264

LIST OF ABBREVIATIONS

3AB - 3-Aminobenzamide
53BP1 - p53 binding protein 1
8-OHdG - 8-oxo-7,8-dihydro-2'deoxyguanosine
8-oxoG - 8-oxoguanine
Ab - Antibody
ADP - Adenosine diphosphate ribose
A-EJ - Alternative end joining
AKT - Serine/threonine protein kinase
AKT2 - V-akt murine thymoma viral oncogene homolog 2
AML - Acute myeloid leukaemia
AT - Ataxia telangiectasia
ATCC - American Tissue Culture Collection
ATM - Ataxia telangiectasia mutated gene product
ATP - Adenosine 5'-triphosphate
ATR - Ataxia telangiectasia and Rad3 related
AUC - Area under curve
BER - Base excision repair
BioCOSHH - Biological Control of Substances Hazardous to Health Regulations
B-NHEJ - Backup NHEJ pathway
BRAF - V-raf murine sarcoma viral oncogene homolog B1
BRCA - Breast cancer susceptibility protein
BSA - Bovine serum albumin
CA125 - Cancer antigen 125
CDK2 - Cyclin-dependent kinase-2
CHK - Checkpoint kinase
CI - Confidence intervals
CK - Cytokeratin
CLL - Chronic lymphocytic lymphoma
CML - Chronic myeloid leukaemia
COSHH - Control of Substances Hazardous to Health Regulations
DAPI - 4',6-diamidino-2-phenylindole
DDR - DNA damage response
DMSO - Dimethyl sulphoxide
DNA - Deoxyribonucleic acid
DNA-PK - DNA-dependent protein kinase
DSB - Double strand break
DT - Doubling time
ECL - Enhanced chemiluminescence
EDTA - Ethylenediaminetetraacetic acid
EGFR - Epidermal growth factor
ELISA - Enzyme-linked immune absorbent assay
EOC - Epithelial ovarian cancer
EpCAM - Epithelial cell adhesion molecule
ERCC1 - Excision repair cross-complementing rodent repair deficiency

FACS - Fluorescence-activated cell sorting
 FANC - Fanconi anemia complementation group
 FCS - Foetal calf serum
 FFPE - Formalin-fixed paraffin-embedded
 FIGO - International Federation of Gynaecology and Obstetrics
 FISH - Fluorescent in situ hybridisation
 FITC - Fluorescein isothiocyanate
 GEM - Genetically engineered mice
 GI50 - Growth inhibition (50 %)
 GSH - Glutathione
 Gy - Gray (irradiation unit)
 H&E - Haematoxylin and eosin
 H2AX - H2A histone family, member X
 HCl - Hydrochloric acid
 HEPES - 4-(2-hydroxyethyl)-1-piperazineethanesulfonic acid
 HGSOC - High grade serous ovarian carcinomas
 HNPCC - Hereditary non-polyposis colorectal cancer
 HR - Homologous recombination repair
 HRC - Homologous recombination competent
 HRD - Homologous recombination deficient
 HRP - Horseradish peroxidase
 HU - Hydroxyurea
 ICC - Intra-class Correlation Coefficients
 IC50 - enzyme inhibition (50 %)
 IF - Immunofluorescence
 IHC - Immunohistochemistry
 IP - Intra-peritoneal
 IR - Ionising radiation
 KRAS - V-Ki-ras2 Kirsten rat sarcoma viral oncogene homolog
 KU70 - X-ray repair complementing defective repair in Chinese hamster cells 6
 KU80 - X-ray repair complementing defective repair in Chinese hamster cells 5
 LC50 - Lethal dose (50 %)
 LIG1 - DNA Ligase 1
 LIGIV - DNA Ligase IV
 LOH - Loss of heterozygosity
 MAPK - Mitogen activated protein kinase
 MGMT - O6-methylguanine-DNA methyltransferase
 MMEJ - Microhomology-mediated end joining
 MMR - Mismatch repair
 MOC31 - Antibody to an epithelial glycoprotein
 MRE11 - Meiotic recombination 11
 MRN - MRE11, RAD51, NBS1 complex
 MSI - Microsatellite instability
 NACT - Neoadjuvant chemotherapy
 NAD⁺ - Nicotinamide adenine dinucleotide
 NADH - Reduced form of NAD⁺

NBS1 - Nijmegen breakage syndrome 1
 NER - Nucleotide excision repair
 NGOC - Northern Gynaecological Oncology Centre
 NHEJ - Non homologous end joining
 NHEJC - Non homologous end joining competent
 NHEJD - Non homologous end joining deficient
 NSCLC - Non-small cell lung cancer
 Nt - Nucleotide
 OS - Overall survival
 OSE - Ovarian surface epithelium
 P16 - Cyclin-dependent kinase inhibitor 2A
 p53 - Tumour suppressor protein encoded by TP53 gene
 PALB2 - Partner and localiser of BRCA2
 PAR - Poly(ADP-ribose) polymer
 PARP - Poly(ADP-ribose) polymerase
 PARPi - Poly(ADP-ribose) polymerase inhibitor
 PBMCs - Peripheral blood mononuclear cells
 PBS - Phosphate buffered saline
 PCNA - Proliferating cell nuclear antigen
 PCO - primary ovarian cancer culture
 PCR - Polymerase chain reaction
 PDX - Patient derived xenograft
 PFS - Progression free survival
 P-Glyc - P-glycoprotein
 pH - Potential of hydrogen
 PI3K - Phosphatidylinositol 3-kinase
 PIK3CA- Phosphoinositide-3-kinase, catalytic, alpha polypeptide
 PolB - Polymerase (DNA directed), beta
 PR - Progesterone receptor
 PTEN - Phosphatase and tensin homologue deleted from chromosome 10
 RAD50 - RAD50 homolog (*S. cerevisiae*)
 RAD51 - Rad 51 homolog
 RCT - Randomised controlled trial
 RECIST - Response Evaluation Criteria in Solid Tumours
 RNA - Ribonucleic acid
 ROS - Reactive oxygen species
 RPA - Replication protein A
 RPM - Revolutions per minute
 RPMI - Roswell Park Memorial Institute developed medium
 SC - Subcutaneous
 SCID - Severe combined immune deficiency
 SD - Standard deviation
 SEM - Standard error of the mean
 SNP - Single nucleotide polymorphism
 SRB - Sulforhodamine B
 SSB - Single strand break

STIC - Serous tubal intraepithelial carcinoma
TBS - Tris-buffered saline
TCA - Trichloroacetic acid
TCGA - The Cancer Genome Atlas
TMA - Tissue micro array
TP53 - Gene encoding tumour suppressor protein (p53)
TTBS - Tris-buffered saline with 0.1 % Tween-20
UV - Ultraviolet
v/v - volume / volume
VEGF - Vascular Endothelial Growth Factor
w/v - weight / volume
XLF - XRCC4-like factor
XRCC - X-ray cross complementing

1.1 Background

Ovarian cancer poses challenges to clinicians due to advanced presentation, poorly understood aetiology, limited treatment modalities at relapse and a high mortality rate. Worldwide, ovarian cancer accounts for around 4 % of all cancers diagnosed in women. The risk of developing ovarian cancer by age 75 is between 0.5 % and 1.6 % (National Cancer Institute, 2014). Despite recent developments, overall mortality has changed little over the past 20 years, with the 5-year overall survival remaining low at 40 % (Jemal et al., 2009). The insidious onset of non-specific symptoms, coupled with a lack of a reliable detection method for early stage disease, results in a late stage at presentation at which time there are widespread metastases (Menon et al., 2009). The current standard treatment for epithelial ovarian cancer (EOC) is surgery accompanied by chemotherapy based on platinum compounds, with or without Taxanes (Ramirez et al., 2011). Although 70-80 % of women present with advanced stage disease, rates of response to primary chemotherapy are good, leading to improved median survival times. Aggressive surgical and medical treatment for primary and recurrent disease is thought to be responsible for the small improvement seen in survival (Kitchener, 2008). However, high rates of recurrence and the development of chemo-resistance limits further improvements (Kaye, 1996). Chemotherapy in platinum resistant disease is a challenge, and is associated with significant toxicity with the current chemotherapeutic agents (Markman, 2009). It is these reasons that also make ovarian cancer an important study target, as there is an urgent need for new therapeutic approaches and the means to identify patients who will benefit from them (Schilsky, 2010).

PARP inhibitors (PARPi) are an exciting new class of chemotherapeutic agents which act by exploiting defects in DNA repair pathways of cancer cells (Farmer et al., 2005, McCabe et al., 2006, Helleday et al., 2005, Ashworth, 2008b). The response of cancers known to have BRCA1/2 mutations, to PARPi, has been demonstrated in phase III clinical trials and they are now licensed for clinical use (Kim et al., 2015, Scott et al., 2015). With clinical trials continuing, a better understanding of the DNA repair pathway defects which results in cancer response to these drugs is now essential.

Attempts to stratify treatment have so far concentrated on identifying defects in the homologous recombination repair (HR) pathway (Mukhopadhyay et al., 2010). However, there is now increasing evidence for the role of PARP in the regulation of non homologous end joining (NHEJ) and alternative end joining (A-EJ) pathways; for interactive effects of PARPi and DNA-dependent protein kinase (DNA-PK) inhibitors; and for the role of the NHEJ pathway in PARPi resistance in HR deficient (HRD) cells (Boulton et al., 1999, Ruscetti et al., 1998, Veuger et al., 2003, Veuger et al., 2004, Mitchell et al., 2009a, Wang et al., 2006b, Audebert et al., 2006, Lu et al., 2006, Audebert et al., 2008, Hochegger et al., 2006, Saberi et al., 2007).

Established primary ovarian cancer culture (PCO) models provide us with an opportunity to improve the understanding of ovarian cancer response to PARPi and allow improved patient stratification by molecular pathology on an individual patient basis. Therefore, the primary aim of this project was to assess NHEJ function using the PCO model and provide further insight into the mechanisms of interaction of DNA double strand break (DSB) repair pathways in sensitivity and resistance to cisplatin and PARPi.

1.2 Tumour Biology in Ovarian Cancer

The term 'ovarian cancer' represents a complex group of tumours in terms of histology, molecular characterisation, prognoses and clinicopathological features. EOC is the most common subtype in the adult population (90 %) and the work in this project concentrates on EOCs. EOCs can be divided into low and high grade serous, mucinous, endometrioid, clear cell, transitional (Brenner type) and mixed tumour, according to their histological morphology. EOCs can be further subdivided into malignant and borderline tumours. However, following an understanding that ovarian cancer subtypes develop through the disruption of distinct genetic and biological pathways, new classification systems have emerged (Shih and Kurman, 2004, Kobel et al., 2008). The commonly referenced model classifies ovarian tumours into two groups based on the similarities of tumour presentation, evolution, and most importantly genetic mutations (Shih and Kurman, 2004). Type I cancers are the low grade serous, mucinous, endometrioid, or clear-cell histology. These cancers are often diagnosed at an early stage, grow slowly, and resist conventional chemotherapy. The more prevalent type II cancers are high grade serous, high grade

clear cell / endometrioid, or carcinosarcoma. These cancers present at a late stage, grow aggressively, and respond to conventional chemotherapy.

1.2.1 Molecular Characteristics of Type I and Type II Tumours

Clear differences in molecular alterations are also noted between the two groups (Table 1-1). Type I cancers tend to have a normal karyotype and wild-type *TP53* and *BRCA1/2*, but frequent mutations in the *B-RAF* and *KRAS* (Grisham et al., 2012). Clear-cell and endometrioid carcinomas share a similar gene expression pattern that is consistent with a common origin. These include *ANXA4* and *UGT1A1* genes, which are associated with chemo-resistance (Farley et al., 2008). Furthermore, inactivating mutations of *ARID1A* and *PTEN*, and activating mutations of *PIK3CA* that up-regulate phosphatidylinositol-3-kinase (PI3K) signaling, have been reported to be characteristic (Kuo et al., 2009, Wiegand et al., 2010, Jones et al., 2010).

Type II cancers are characterised by copy number abnormalities and marked genomic instability (Romero and Bast, 2012). The Cancer Genome Atlas Project, which analysed more than 300 high-grade serous cancers, detected amplification of more than 30 growth-stimulatory genes (Vockley et al., 2012). *BRCA1/2* germline and somatic mutations are common in type II ovarian cancers (Romero and Bast, 2012), whilst mutations of *TP53* are almost universal (Ahmed et al., 2010, Cancer Genome Atlas Research, 2011).

1.2.2 Precursor Lesions for Ovarian Tumours

Type I tumours appear to develop from well-established precursor lesions such as cystadenomas, atypical proliferative (borderline) tumours and endometriosis (Shih and Kurman, 2004). Molecular genetic alterations in *PTEN* and *ARID1A* and microsatellite instability, can be detected in the epithelial cells of endometriotic cysts and a clonal relationship between endometriosis and endometriosis related ovarian carcinomas has been demonstrated in several studies (Kim et al., 2014).

Recently, precursor lesions in the fallopian tube that pass through a stage of intraepithelial carcinoma, so-called “serous tubal intraepithelial carcinoma (STIC)” (Crum et al., 2007), have been suggested as precursors for type II tumours.

Table 1-1 Molecular classification of Ovarian Cancer.

EOC is classified into type I and type II tumours (Shih and Kurman, 2004).

Features	Type I tumours	Common Precursors	Most frequent mutations	Chromosomal instability
Slow growing	Low-Grade	Serous	KRAS	Low
Diagnosed at lower stages	Serous Carcinoma	cystadenoma / adenofibroma	BRAF	
Identifiable precursor lesions	Endometrioid Carcinoma	Endometriosis Adenofibroma Intraepithelial carcinoma	PTEN CTNNB1 KRAS MSI ARID1A PI3KCA MSI	Low
Resistant to platinum chemotherapy	Clear Cell Carcinoma	Endometriosis Adenofibroma Intraepithelial carcinoma	KRAS PI3KCA PTEN MSI HNF1- β up regulation ARID1A MMR pathway CTNNB1	Low
	Mucinous Carcinoma	Mucinous borderline tumour	KRAS	Low
Type II tumours				
Rapid growth	High-Grade	Not recognised	TP53	High
Early metastasis	Serous Carcinoma		BRCA1/2	
No clearly defined precursor lesions			Amplification of HER2 and AKT2	
Sensitive to platinum chemotherapy			Inactivation of p16 PIK3CA CCNE1	
	Carcinosarcoma	Not recognised	TP53	

1.2.3 Treatment Considerations for Type I and Type II Tumours

Regardless of subtype, EOC is uniformly treated with surgical de-bulking and a combination of carboplatin and paclitaxel. However, the treatment of type I and type II tumours must be individualised.

As type I tumours are slow growing, chemotherapeutic agents that are effective against the more rapidly proliferating type II tumours are not as effective. Many studies relate the poor prognosis of clear cell with resistance to platinum-based and taxane-based chemotherapy (Itamochi et al., 2008, Anglesio et al., 2011). In many type I carcinomas, there is constitutive activation of the MAPK signaling pathway because of mutations in *ERBB2*, *KRAS* or *BRAF*, the upstream regulators of MAPK. BRAF and other MAPK inhibitors could improve overall survival in patients with these types of tumours when combined with conventional chemotherapy (Shih and Kurman, 2004). Furthermore, hormone therapies such as progestogens, tamoxifen, luteinizing hormone releasing hormone agonists and more recently aromatase inhibitors, may have a role (Walker et al., 2007, Karagol et al., 2007).

Treatment for type II tumours should also be based on the detection of sensitive and specific biomarkers. Type II tumours have an 80 % response rate to platinum therapy (Anglesio et al., 2011). More recently it has been demonstrated that hereditary or acquired EOC with *BRCA* mutations and HRD are more sensitive to PARPi, as well as to platinum therapy (Mukhopadhyay et al., 2012).

1.2.4 Risk Factors

A hereditary predisposition to ovarian cancer occurs in 10 - 15 % of cases. This is caused by germline mutations in the tumour suppressor genes *BRCA1* and *BRCA2*, or in DNA mismatch repair (MMR) genes (Gayther and Pharoah, 2010). A genome wide association study identified a further EOC susceptibility locus at chromosome 9p22.2 (Song, 2009). The lifetime risk of developing EOC in women with a germline *BRCA1/2* mutation can be up to 66 % and 27 % respectively (Robles-Diaz, 2004). A greater understanding of the functional role of the various *BRCA1/2* mutations is urgently needed to predict which women will develop gynaecological cancers.

Although ovarian cancer aetiology remains unclear, a number of risk and protective factors have been identified for sporadic ovarian cancer detailed in Table 1-2

(Sueblinvong, 2009, Lahmann, 2010, Huncharek, 2003, Salehi, 2008). The most important risk factor is advancing age, with more than 85 % of patients being aged 50 years or older at diagnosis.

Table 1-2 Risk Factors for Ovarian Cancer Development

A list of risk and protective factors for the development of ovarian cancer (Sueblinvong, 2009, Lahmann, 2010, Huncharek, 2003, Salehi, 2008).

Risk Factors	Protective Factors
Increasing age	Parity
Family history	Breastfeeding
Early menarche/Late menopause	Combined Oral Contraceptive Pill
Hormone replacement therapy	Sterilisation
Polycystic ovarian syndrome	Hysterectomy
Obesity	
Smoking	
Nulliparity	
Fertility drugs	
White ethnicity	
Talcum powder	

1.2.5 Hypotheses for Tumour Origin

The initial proposed origin of ovarian cancer was from the less differentiated ovarian surface epithelial (OSE) cells. OSE are mesothelial-like cells that share embryological origin with the Mullerian tract epithelium, which eventually gives rise to the tubal, endometrial and endocervical epithelium (Ahmed et al., 2012).

Subsequently it was suggested that the invaginations which develop in the OSE may be incorporated into the ovarian stroma, forming inclusion cysts (Folkins, 2009). The formation of inclusion cysts lined by OSE cells was suggested as the origin of EOC, but this was later refuted (Dubeau, 1999).

A further hypothesis put forward for the development of EOCs included Mullerian trans-differentiation of trapped OSE cells after repeated ovulation (Roskelley and Bissell, 2002, Cheng et al., 2005); which goes some way to explain the risk reduction associated with pregnancy and oral contraception (Fathalla, 1971). Ovarian biopsies from women receiving ovulation stimulating fertility treatment have revealed a higher rate of dysplasia (Fathalla, 1971).

More recently, ovarian cancer development directly from mullerian derivatives has been suggested (Kindelberger, 2007, Lee et al., 2007b, Herrington, 2010). This is evident in some studies which showed dysplastic changes in fallopian tubes in women who underwent prophylactic removal of ovaries and fallopian tubes for BRCA gene mutation (Hartley et al., 2000, Carcangiu et al., 2006, McCluggage, 2011). Further studies systematically examined the tubes in patients with sporadic high grade serous ovarian carcinomas (HGSOC) and found similar lesions in up to 60 % of cases (Kindelberger, 2007, Przybycin, 2010).

The heterogeneous behaviour of ovarian cancers suggests that distinct morphological subtypes may indeed have different pathogenic processes (Shih and Kurman, 2004). HGSOC may originate from the fallopian tubes implanting into inclusion cysts or the peritoneal cavity. Endometrioid and clear cell ovarian cancers have been linked to retrograde menstruation (Kurman and Shih, 2011) and endometriosis (Worley, 2013), and therefore may originate from the endometrial cavity.

1.3 Treatment of Ovarian Cancer

The majority of women with ovarian cancer present with stage III / IV disease. The current gold standard for treatment of advanced ovarian cancer is cytoreductive surgery in combination with platinum-based chemotherapy.

1.3.1 Surgery

Surgery plays a pivotal role in the management of ovarian cancer. The significance of optimal resection (to no tumour or less than one centimetre nodules) is well-established and maximal cyto-reduction has been shown to be one of the most powerful determinants of survival among patients with EOC (Bristow et al., 2002, Elattar et al., 2011, Al Rawahi et al., 2013).

Surgery can be either primary debulking surgery, performed prior to administration of six cycles of adjuvant chemotherapy or interval debulking surgery, performed after three cycles of neoadjuvant chemotherapy, followed by three further cycles of chemotherapy post operatively. Recent major clinical trials have not shown any difference in survival after primary surgery compared to survival after neoadjuvant

chemotherapy with interval debulking surgery in advanced ovarian cancer (Vergote et al., 2010).

1.3.2 Chemotherapy

Primary surgery, even in early disease results in a significant proportion of cases relapsing and two large randomised controlled trials (RCTs): ICON 1 and ACTION, have shown that platinum-based adjuvant chemotherapy after complete cytoreduction improves OS as well as recurrence-free survival at 5 years (Colombo et al., 2003, Trimbos et al., 2003). Mixed results have been reported from trials assessing the addition of further agents. Several RCTs have shown the importance of the addition of paclitaxel to platinum therapy (Piccart et al., 2000, McGuire et al., 1996) with improvements in progression free survival (PFS) and overall survival (OS) (Piccart et al., 2000, McGuire et al., 1996, Bookman et al., 2003). ICON3 however, demonstrated that there was no survival benefit between first-line treatment with single-agent carboplatin or with the addition of paclitaxel, and the option of single or double agent chemotherapy is therefore currently tailored to the individual (Collaborators, 2002, Redman et al., 2011). Attempts to improve the standard two drug chemotherapy by adding a third agent failed to affect PFS or OS, but did result in increased adverse effects (Bookman et al., 2009, du Bois et al., 2006, Pfisterer et al., 2006, Hoskins et al., 2010). To date, standard treatment is offered to all patients irrespective of histological subtype, stage or surgical outcome.

1.3.2.1 Resistance to Chemotherapy

Both intrinsic and acquired resistance results from the numerous genetic and epigenetic changes occurring in cancer cells. The majority of resistance mechanisms described are common to several drugs. Specific changes have also been described for platinum and PARPi resistance development. These are discussed in more details in chapter 6. One of the most important determinants of drug sensitivity and resistance is the cancer cell ability to repair DNA damage. This is discussed in details in section 1.4.

1.3.2.1.1 Alterations in Proliferation Signalling Pathways

Dysregulation of proliferative signaling pathways is a characteristic of cancer cells (Rebucci and Michiels, 2013). Two important cell proliferation pathways are the

MAPK and the PI3K, both of which have been reported to be mutated in ovarian cancer (Geyer et al., 2009, Nakayama et al., 2006, Willner et al., 2007).

The PI3K pathway (Figure 1-1) transduces extra cellular signals, to promote cellular growth, proliferation and reduce apoptosis. PIK3CA proto-oncogene amplification or mutations increasing catalytic activity is associated with EOC (Meng, 2006, Yokomizo, 1998, De Luca et al., 2012). PIK3CA is increased in copy number in 40 % of ovarian cancer cell lines and patient tumour samples (Shayesteh, 1999). The PI3K inhibitor, LY294002, has been shown to inhibit ovarian cancer cell proliferation *in vitro* and to decrease ovarian cancer growth and ascites formation in mice (Hu, 2000). LY294002 has also been proven to increase the efficacy of paclitaxel in mice (Hu, 2000). More recently, a dual inhibitor of PI3K and PARP has been shown to significantly suppress tumour growth by downregulating BRCA1/2 in xenograph models (Ibrahim et al., 2012).

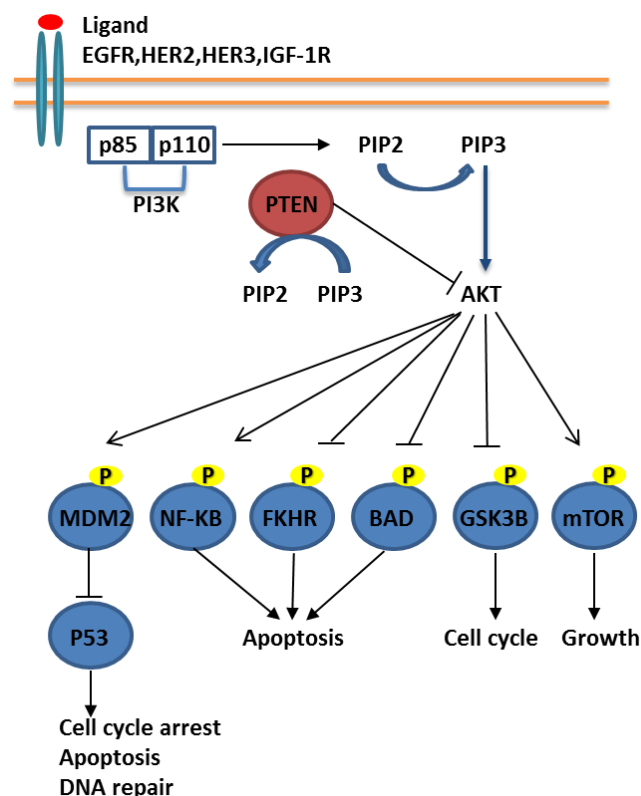


Figure 1-1 Schematic representation of the PI3K signalling pathway.

PI3K is coupled with a variety of growth factor-dependent tyrosine kinase receptors. Upon stimulation of its upstream receptors, PI3K is activated and generates Phosphatidylinositol (3,4,5)-triphosphate (PIP3) from Phosphatidylinositol 4,5-bisphosphate (PIP2)). PIP3 binds pleckstrin-homology domains to AKT and translocate to the plasma membrane where they are activated. All Akt isoforms (Akt1, Akt2, Akt3), once activated, promote cellular proliferation and inhibit apoptosis through phosphorylation of multiple substrates (Leary et al., 2013).

AKT1 and 2 are frequently amplified in ovarian cancer (Cheng et al., 1992, Sun, 2001). PI3K inhibitors and mTOR (downstream effectors related to growth and protein synthesis) inhibitors have been shown to increase the effectiveness of cisplatin and tamoxifen in ovarian cancer cells with activated Akt signaling (Treeck, 2006, Mabuchi, 2007).

A second signaling pathway that is often overexpressed in cancer cells is the Ras/Raf/MAPK pathway (Rebucci and Michiels, 2013). The pathway induces cell proliferation and differentiation; and several components have been found to be mutated in different cancers.

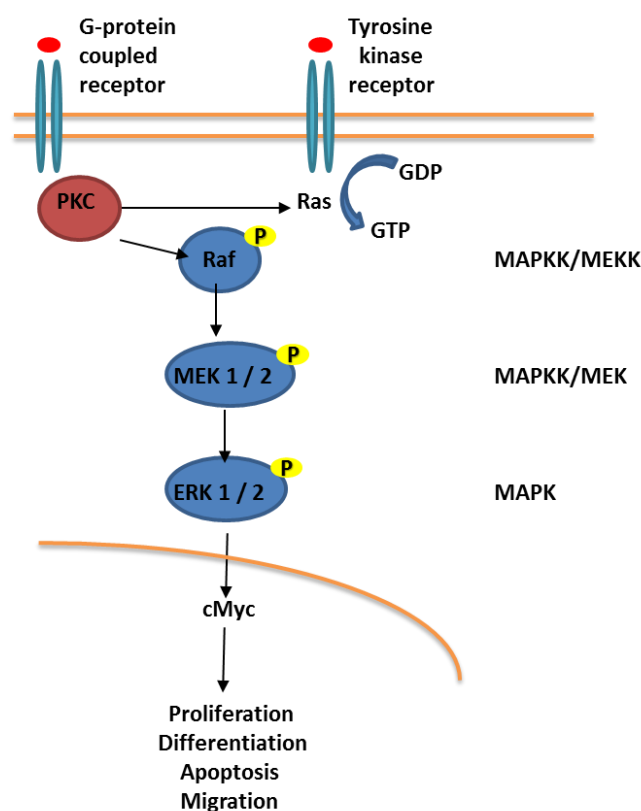


Figure 1-2 Schematic representation of MAPK pathway.

Binding of GTP, resulting in activation of the Ras-family GTPases, enables the transmission of external signals to the interior of the cell. The active GTP-Ras complex then interacts with Raf1 (Smalley, 2003) and a cascade of MEK phosphorylation activation steps follows, which in turn phosphorylate ERK. On activation, ERK enzymes phosphorylate cytoplasmic targets or migrate to the nucleus, where they phosphorylate and activate transcription factors (Treisman, 1994). They also target membrane bound proteins responsible for protecting cells against apoptosis (Lewis, 1998). The activation of the ERK MAPK pathway induces synthesis of cyclin D1 (Lavoie, 1996), promoting cell division.

Oncogenic mutations lead to activation of the pathway in the absence of a mitogenic signal, causing the cell to enter the S phase and continue to divide without any control. If cells divide before any DNA damage is repaired, the daughter cells inherit the mutations, and should these mutations confer a growth advantage leading to bypassing the apoptotic signals, growth of these cells will be selected for in that population.

In ovarian cancer mutations in *KRAS*, *BRAF* and *ERBB2* oncogenes, which result in constitutive activation of the MAPK pathway have been reported (Mayr, 2006, Gemignani, 2003). *KRAS* mutations are reported in 2/3rds of mucinous, 1/3rd of low grade / borderline serous and 1/5th of endometrioid cancers (Ho et al., 2004). The *KRAS* mutation is a functional variant located in the *KRAS* 3'UTR in a let-7 miRNA complementary site, which is a significant predictor of platinum resistance (Ratner, 2011). *BRAF* mutation is seen in 1/3rd of the low grade serous tumours (Nakayama et al., 2008). All known *BRAF* mutations occur within the kinase domain, with a single substitution of A for the T at nucleotide position 1796, accounting for at least 80 % of *BRAF* mutations (Davies et al., 2002, Rajagopalan, 2002). cMYC and *ERBB2* over expression is seen in 36 - 76 % and 10 - 20 % of advanced stage EOCs and is associated with poorer prognoses (Dimova, 2006).

1.3.2.1.2 Suppression of Tumour Suppressor Genes

In addition to induction of positive growth signals, tumour cells also down regulate tumour suppressor genes (Ertel et al., 2010). Phosphatase and tensin homologue deleted from chromosome 10 (*PTEN*) inhibits the PI3K/Akt pathway. Mutations leading to the loss of *PTEN* result in the activation of the PI3K/Akt pathway and increased cell survival (Nagata et al., 2004). Inactivating mutations of *PTEN* and activating mutations of *PIK3CA* that up-regulate phosphatidylinositol-3-kinase (PI3K) signaling have been reported to be characteristic of type I ovarian cancers (Romero and Bast, 2012, Munksgaard and Blaakaer, 2012).

The *TP53* tumour suppressor gene is involved in controlling cell cycle, apoptosis and maintaining the genome integrity. p53 levels rapidly increase following DNA damage; p53 activates genes involved in cell cycle arrest to prevent the cell from entering S phase until the damage is repaired. If the damage to the cell genome is too extensive to be repaired, p53 induces apoptosis. p53 has also been implicated in the regulation

of BRCA1 function (Bouwman et al., 2010) and in the transcriptional regulation of RAD51 (Arias-Lopez et al., 2006).

The majority of studies demonstrate that tumours harboring mutated *TP53* are associated with resistance (Lai et al., 2012) and treatment failure (Knappskog and Lonning, 2012) when compared to wild type. p53 over expression has been associated with shorter time to progression and overall survival as well as increased platinum resistance (Shahin et al., 2000, Reles et al., 2001, Folkins et al., 2008). In HGSOc, p53 mutations are reported to be ubiquitous (Ahmed et al., 2010, Cancer Genome Atlas Research, 2011). The therapeutic potential of restoration of wild-type p53 expression in tumour cells and use of oncolytic adenoviruses, which can only replicate in cells that have lost p53 have failed to show promising results in ovarian cancer patients (Buller et al., 2002, Vasey et al., 2002).

1.3.2.1.3 Insufficient Exposure of Cancer Cells to the Drugs

Pharmacokinetic approaches to overcome drug resistance are based on attempts to improve drug delivery to the cancer cells. Initial trials concentrating on increasing drug dose failed to overcome drug resistance (Gore et al., 1998). Intraperitoneal delivery of chemotherapy has been reported to improve PFS and OS. Other approaches that increase tumour-cell drug exposure include the development of Liposomes which increase tumour-cell-specific drug delivery. An example of this approach is liposomal doxorubicin, which is now approved for treatment (Strauss et al., 2008). Antibody-directed enzyme prodrug therapy and gene-directed enzyme prodrug therapy approaches also aim to increase tumour cell specific drug exposure to overcome drug resistance with minimal toxicity to normal tissues (Tong et al., 1998).

1.3.2.1.4 Changes to Drug Export

Decreased cellular drug accumulation by resistant cells is one of the major mechanisms of resistance. This may be due to either, an inhibition of drug uptake, an increase in drug efflux, or both. CTR1 regulates cellular influx of platinum (Holzer et al., 2006, Song et al., 2004). Two copper exporters, ATP7A and ATP7B, have also been proposed to be involved in cellular resistance to cisplatin (Samimi et al., 2004) and it has been shown that ovarian cancer patients with ATP7A expression have a lower survival rate than patients with undetectable levels (Samimi et al., 2003).

1.3.2.1.5 Tumour Microenvironment

Tumours are not only made up of cancer cells but also of stromal cells, macrophages and vasculature, which all play an important role in cancer biology and drug sensitivity (Rebucci and Michiels, 2013). Ovarian cancer cells can regulate the composition of their stroma by promoting the formation of ascitic fluid and by stimulating the differentiation of stromal cells. Stromal cells secrete cytokines which activate anti-apoptotic pathways and exchange drug efflux proteins enabling improved drug metabolism (Castells et al., 2012). Adipocytes secrete growth factors which activate TLR4 signalling in macrophages and thereby stimulate the production of pro-inflammatory mediators involved in chemo-resistance (Roodhart et al., 2011).

1.3.3 Treatment of Recurrent Disease

The treatment of recurrent ovarian cancer is mainly based on chemotherapy and is used with palliative, rather than curative intent (Hennessy et al., 2009, Herzog, 2004). Secondary cytoreductive surgery has a place in a well selected population (Lorusso et al., 2012, Harter et al., 2006). The main prognostic factor for successful treatment is the disease free interval from completion of chemotherapy until recurrence. The cancer is regarded as platinum-resistant if this time-interval is less than six months, and as platinum refractory if progression occurs during treatment (Markman et al., 1991). ICON 4 has shown increased survival in recurrent ovarian cancer with addition of paclitaxel to carboplatin treatment (Parmar et al., 2003). Numerous second line agents are now available for use in ovarian cancer (Table 1-3). Evidence for these therapies is limited and decisions are therefore made on individual patient basis.

1.3.4 Targeted Therapies

Besides increased toxicity with recurrent chemotherapies, development of resistance against the chemotherapy remains a problem. Novel biologically targeted agents target tumour cells and/or microenvironment by exploiting specific molecular abnormalities in the tumour. Multiple components of signaling cascades are aberrant in ovarian cancer, resulting in the activation of critical oncogenic pathways involved in processes such as cell proliferation, survival, migration and angiogenesis. In addition to PARPi, which will be discussed in detail in section 1.3.6, antiangiogenic agents are the most developed of the novel therapies.

Table 1-3 Second line systemic therapy for the treatment of ovarian cancer.

Agents	Target	Resulting effect	Licensed Indication	Side-effect Profile	Refs
Bevacizumab	A recombinant monoclonal antibody which binds to VEGF.	Prevention of angiogenesis and metastasis	Suboptimal cytoreduction and recurrent disease	Necrotising faciitis GI perforation / fistula Hypertension	(Monk et al., 2013)
Doxorubicin	Anthracycline antibiotic with antimitotic and cytotoxic activity.	Prevents DNA ligation by complexes with DNA by intercalation between base pairs and inhibiting topoisomerase II activity.	Platinum and paclitaxel refractory disease	Myelosuppression Mucositis/stomatitis Rash	(Strauss et al., 2008)
Gemcitabine	A nucleoside analogue activated intracellularly to dFdCTP by deoxycytidine kinase.	Inhibits DNA synthesis and induces apoptosis.	Pre-treated ovarian cancer	Myelosuppression Hepatic impairment	(Kodaz et al., 2015)
Topotecan	A synthetic camptothecin derivative that binds to the topoisomerase I-DNA complex	Interfers with the replication fork at SSB, leading to replication arrest and DNA DSB.	Platinum and paclitaxel refractory disease	Myelosuppression	(Markman et al., 2000)
Etoposide	A semisynthetic derivative of podophyllotoxin. Inhibits DNA topoisomerase II, thereby inhibiting DNA re-ligation	Causes critical errors in DNA synthesis and subsequent apoptosis.	Recurrent ovarian cancer	Myelosuppression Diarrhoea / vomiting	(Thavaramara et al., 2009)
Tamoxifen	Binds to oestrogen receptors altering the regulation of oestrogen dependent genes	Reduces DNA polymerase activity and impairs thymidine utilisation	ER positive cancers	Convulsions Respiratory distress	(Markman et al., 2004)

Angiogenesis, the formation of new blood vessels, is a critical component of cancer growth and metastasis. Bevacizumab is a monoclonal antibody against Vascular Endothelial Growth Factor (VEGF). Two randomised, phase III trials, GOG 0218 (Burger et al., 2011) and ICON7 (Perren et al., 2011) have demonstrated an improvement in PFS but not OS, when bevacizumab was added to the combination of carboplatin and paclitaxel followed by maintenance therapy, as the first line treatment for advanced EOC.

Furthermore, the addition of bevacizumab to chemotherapy in platinum sensitive (OCEANS) (Aghajanian et al., 2012) and platinum resistant (AURELIA) (Pujade-Lauraine et al., 2012) recurrent disease has been shown to improve PFS. A number of other angiogenesis inhibitors have also entered clinical trials (Karlan et al., 2012, Coleman et al., 2011).

The main challenges facing targeted therapies are toxicities (Burger et al., 2007, Cannistra et al., 2007) and identification of the appropriate target population. Circulating short VEGFA isoforms, expression of neuropilin-1 and VEGF receptor 1 and genetic variants in VEGFA are potential biomarkers for angiogenesis inhibitors (Lambrechts et al., 2013).

1.4 DNA Repair Pathways

The accumulation of DNA damage can initiate cancer and lead to genomic instability of the cell, which is then able to break and reform chromosomes, inactivate tumour suppressor genes, amplify drug resistance genes, and consequently become more malignant and drug resistant over time (Kennedy and D'Andrea, 2006, Lengauer et al., 1998). The cancer cell must first however be able to tolerate the DNA damage. This tolerance can be achieved firstly by the cancer cells losing DNA damage signaling and check point pathways such as those controlled by p53 (Macaluso et al., 2005, Bartkova et al., 2005). Secondly, the cancer cells may knock out one of the major DNA repair pathways (Kennedy and D'Andrea, 2006). Endogenous DNA damage occurs naturally in all cells with a high frequency of $>10^4$ spontaneous damage events per cell every day, as a result of replication errors, cellular metabolism-induced oxygen radicals, as well as environmental agents e.g. UV radiation (Ames and Gold, 1991, Hoeijmakers, 2001). Faulty DNA repair mechanisms not only predispose cells to becoming cancer cells, but also affect sensitivity to

treatment. Most cytotoxic chemotherapy agents induce DNA damage in order to kill cancer cells. Resistance to these agents can result from an ability to proliferate through loss of checkpoint function. This can also result in increased sensitivity as the cells go through the cell cycle unrepaired, which leads to cell death (Curtin, 2012).

There are six major mechanisms responsible for the repair of DNA lesions: direct repair, MMR, base excision repair (BER), nucleotide excision repair (NER), HR, NHEJ, and A-EJ (Hoeijmakers, 2001, Bernstein et al., 2002).

1.4.1 Direct Repair by O⁶-methylguanine-DNA Methyltransferase

Direct repair by O⁶-methylguanine-DNA methyltransferase (MGMT) removes the alkyl group of the O⁶ position of guanine, which causes a mismatch of the alkylated guanine with thymine, instead of cytosine during replication. Use of cancer agents such as temozolomide, dacarbazine and nitrosoureas causes alkylation of O⁶-methylguanine, which, if the MGMT pathway is deficient, results in persistent mismatching of bases during replication. The MMR pathway attempts to correct this mismatch, but as the alkylated base is permanently bound with the template DNA, is unsuccessful; thus triggering futile cycles of excision and repair, which ultimately results in apoptosis.

1.4.2 Mismatch Repair

MMR is responsible for the recognition and repair of DNA damage caused by deamination, oxidation and replication errors and also targets DNA dimers and alkylated bases (Duval and Hamelin, 2002). MMR is subdivided into 2 pathways according to the protein complexes that bind to the DNA lesion (Figure 1-3).

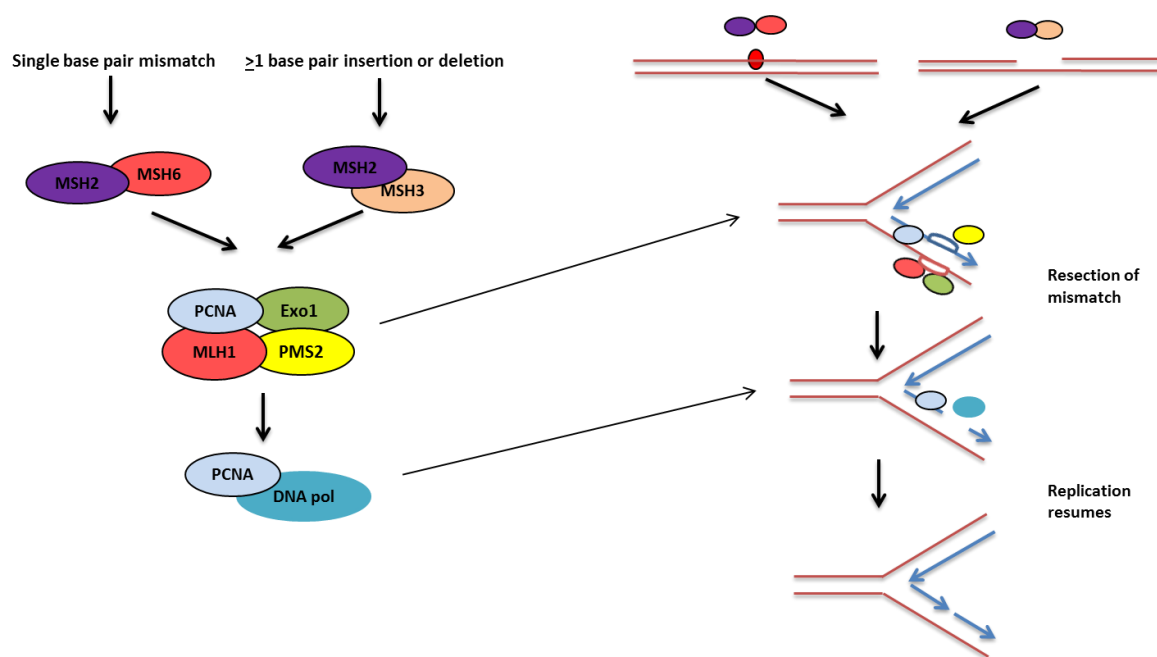


Figure 1-3 Schematic representation of MMR pathway.

The MutS α (consisting of MSH2: MSH6) complex binds in base-base and insertion/deletion mismatches, and the MutS β complex (MSH2: MSH3) binds only to insertion/deletion mismatches. These assemble at the DNA mismatch site and recruit hMutL α (MLH1:PMS2), along with other proteins to initiate the repair process.

The products of the genes participating in DNA MMR were originally identified for their involvement in the Hereditary Non Polyposis Colorectal Cancer (HNPCC) syndrome (Scartozzi et al., 2003). HNPCC is caused by germline mutations in one of the MMR genes (Bronner et al., 1994, Cyr et al., 2011). It results in an increased lifetime risk of colon (80 %) and ovarian (12 %) cancer (Watson and Lynch, 2001). Mutations in *MLH1*, *MSH2*, and *MSH6* account for the majority of reported MMR germline variants, but there are numerous other missense mutations which can also result in loss of MMR function (Peltomaki and Vasen, 2004).

Loss of MLH1 has been observed in 50 % of stage III/IV ovarian cancers (Scartozzi et al., 2003). Further to HNPCC syndrome, epigenetic silencing through promoter hypermethylation of hMLH1 has been reported in endometrial, gastric, colon and ovarian cancers (Geisler et al., 2003, Strathdee et al., 1999). Microsatellite instability (MSI) has been confirmed to be a marker of MMR deficiency and MMR deficiency has been reported in up to 39 % of ovarian tumours, mostly in endometrioid types (Helleman et al., 2006, Zhang et al., 2008).

Cisplatin and carboplatin function by binding to the DNA and forming DNA adducts, leading to intra-strand or inter-strand cross-links which disrupt the structure of the DNA molecule, resulting in steric changes in the helix (Sharma et al., 1995). When MMR is deficient, the cells bypass the intra-strand crosslinks and continue to proliferate in spite of the DNA damage, and are therefore resistant to platinum agents as well as DNA methylating agents and thiopurines (Helleman et al., 2006). Defects in the MMR pathway have been demonstrated to be significantly higher in tumours post chemotherapy, compared to untreated controls (Scartozzi et al., 2003, Cooke and Brenton, 2011, Watanabe et al., 2001). Therefore, research has focused on attempts to reactivate epigenetically silenced MLH1. After promising preclinical data that demonstrated chemo-sensitisation, clinical trials were stopped due to adverse reactions (Plumb et al., 2000).

1.4.3 Nucleotide Excision Repair

NER encompasses with the wide class of helix-distorting lesions that interfere with base pairing and generally obstruct transcription and normal replication (Hoeijmakers, 2001); for example, UV radiation induced thymidine dimers resulting in stalled replication forks. NER is the predominant pathway repairing platinum-DNA adducts (Figure 1-4). Different studies with ovarian cancer cell lines have demonstrated that high ERCC1 mRNA expression is correlated with increased capacity of cells to repair cisplatin-induced DNA damage, thus conferring resistance to the drug (Damia, 1998, Ferry, 2000, Li et al., 2000). *In vitro* studies have demonstrated sensitivity to platinum in NER defective human ovarian cell lines, in particular those with reduced levels of ERCC1 and XPF proteins. Knockdown of ERCC1 in cell lines and in mice, has shown increased sensitivity to platinum (Selvakumaran et al., 2003, Dabholkar et al., 1994, Kohn et al., 1994).

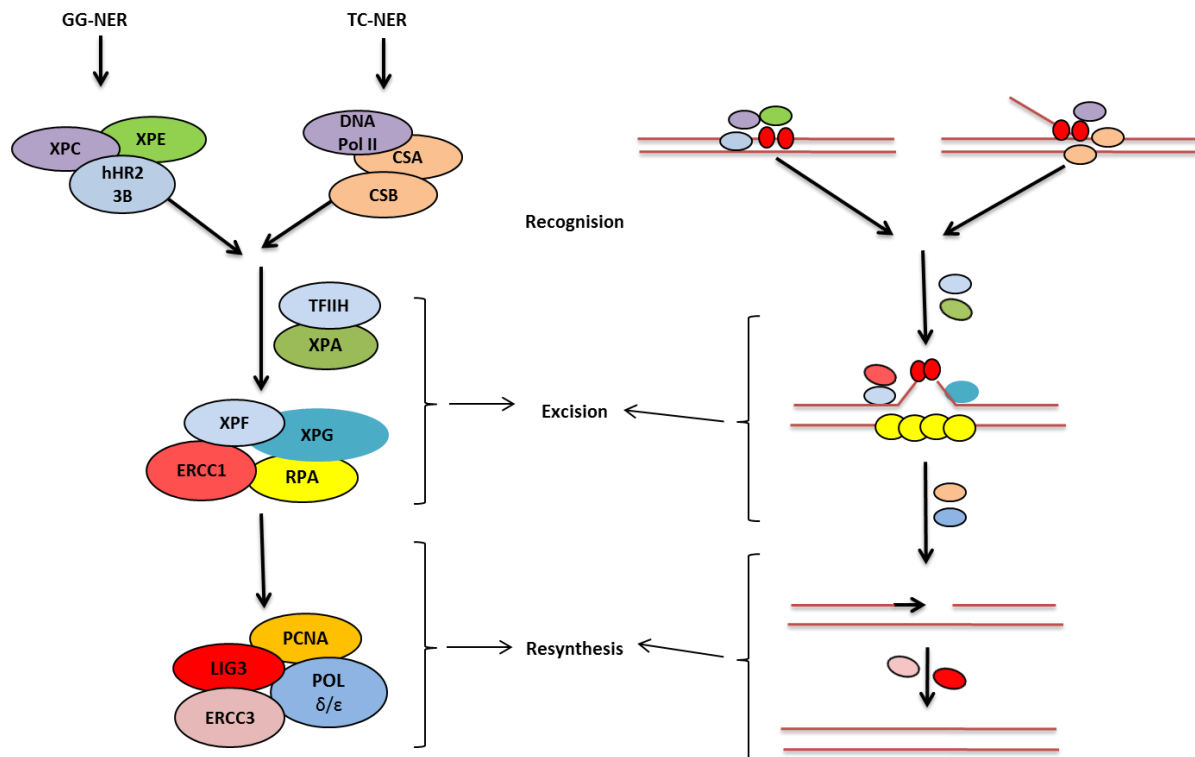


Figure 1-4 Schematic representation of NER pathway.

There are two NER sub-pathways to remove these lesions: global genome NER (GG-NER) which surveys the entire genome for distorting injury; and transcription-coupled repair (TCR) which focuses on damage that blocks elongating RNA polymerases (Christmann et al., 2003). Upon recognition of the DNA lesion, (either by binding of XPC-hHR23B or DNA polymerase II stalling) a cascade of proteins are recruited. These proteins are the same for both TC-NER and GG-NER. The XPF and XPA helicases and the multi-unit transcription factor TFIIH open the damaged region (Le Page et al., 2000). The single-stranded-binding protein replication protein A (RPA) binds to the corresponding undamaged strand and stabilises it. In the rate-limiting step, the endonucleases XPG and ERCC1-XRF complex then cleave the open DNA strands and excise the damaged 25 – 30 bases site. DNA polymerase δ/ϵ , ligase 3 and ERCC3 re-synthesise the removed region (Hoeijmakers, 2001).

1.4.4 Base Excision Repair

BER is the main guardian against damage due to cellular metabolism, including that resulting from reactive oxygen species, methylation, deamination and hydroxylation (Hoeijmakers, 2001). BER is involved in the removal of either a single damaged nucleotide (short patch repair) or a few (2-15) nucleotides (long patch repair) (Figure 1-5). Following DNA base damage, PARP-1 binds to the single strand breaks (SSB) (Benjamin and Gill, 1980). Activation of PARP-1 results in the production of PAR, which is attached to histones or PARP-1 itself. This leads to the relaxation of the chromatin fibre and facilitates the recruitment of proteins necessary for repair (Figure 1-5) (Althaus et al., 1993, Dantzer et al., 2000). Inhibition of PARP-1 activity inhibits

the formation of XRCC1 foci (El-Khamisy et al., 2003), and failure of BER results in DSB due to collision of the SSB with the progressing replication fork (Gottipati et al., 2010).

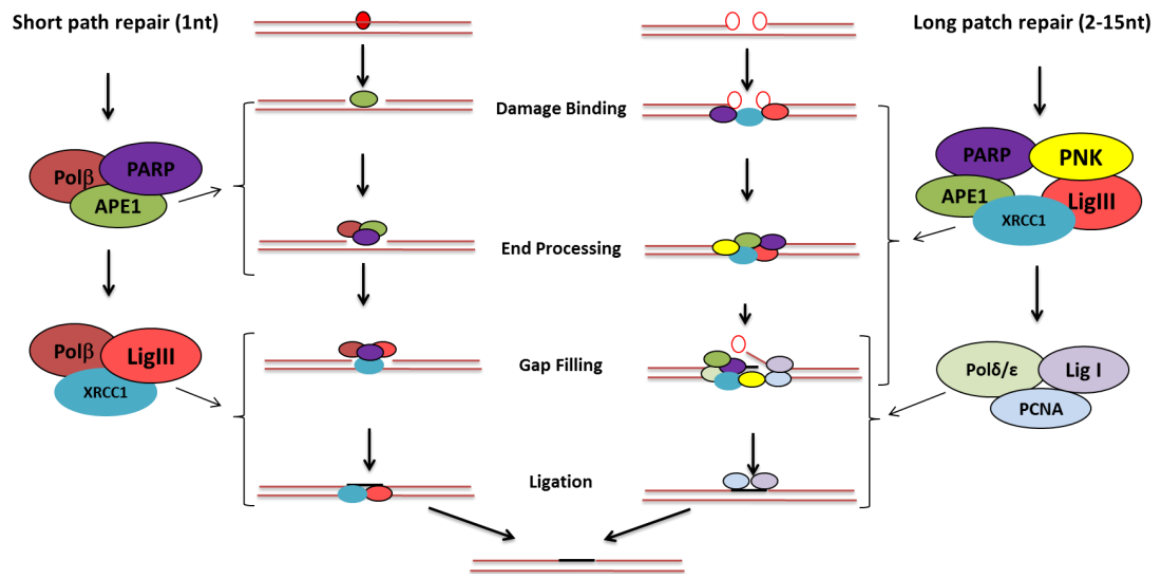


Figure 1-5 Schematic representation of BER pathway.

Short-patch repair takes place after the excision of a damaged base. It involves the PAR mediated recruitment of the scaffold protein XRCC1, followed by DNA polβ and DNA ligase III which conducts the ligation of the DNA. Long-patch repair occurs after direct DNA breaks (e.g. after IR damage); it involves recruitment of XRCC1 followed by polynucleotide kinase (PNK), which converts the damaged ends to 5'-phosphate and 3'-hydroxyl moieties. Proliferating cell nuclear antigen (PCNA) and DNA polymerase δ/ε extend and fill the gap by 2–15 nucleotides, and FEN1 cleaves the resulting flap. The nick is then ligated by DNA ligase I (Baute and Depicker, 2008).

APE1 has been shown to be overexpressed in 71.9 % of ovarian cancers and to correlate with tumour type, optimal debulking, and overall survival (Al-Attar et al., 2010). Additional studies have also demonstrated that altered APE1 expression or cytoplasmic localisation is associated with platinum resistance and overall prognosis (Sheng et al., 2012, Zhang et al., 2009). Furthermore, XRCC1 399 Arg/Arg genotype has been shown to be linked to a lower survival rate (Cheng, 2012).

1.4.5 DNA Double Strand Break Repair

DNA DSBs are repaired by one of three pathways: HR, NHEJ and A-EJ. HR involves alignment of a homologous chromatid to provide a template for error free repair and is therefore limited to the S or G2 phase of the cell cycle when a sister chromatid is present. NHEJ is the predominant method of repair in G0/G1 but functions in all

stages of the cell cycle. NHEJ does not require a complementary template as it repairs the defect by direct ligation and is therefore error prone (Helleday, 2010, Lieber, 2008). A-EJ has been shown to involve BER pathway genes; predominate in S and G2 phase of the cell cycle; and to compete with or compensate for the loss of HR. A-EJ uses short sequences of microhomology, which results in large excisions of DNA, and is therefore extremely error prone.

1.4.5.1 Homologous Recombination

HR is the principal repair pathway during the S-phase of the cell cycle and so appears to be a critical pathway for the maintenance of genomic stability. The HR pathway is activated by DNA DSBs (Kanaar et al., 1998, Shrivastav et al., 2008), and stalled and collapsed replication forks (McGlynn and Lloyd, 2002, Petermann et al., 2010). HR repair of DSBs uses the sister chromatid as a template, resulting in error-free repair (Figure 1-6). DSBs activate the ataxia telangiectasia-mutated (ATM) and ATM and Rad3 related (ATR) kinases, which triggers a cascade of phosphorylation events involving CHK2 and p53 to activate cell cycle checkpoints and promote DNA repair (Jacquemont and Taniguchi, 2007, Hartlerode and Scully, 2009). Mediated by BRCA1, the RAD50-MRE11-NSB1 (MRN) complex exposes the 3' ends on either side of the DSB (Paull and Lee, 2005, Zhong et al., 1999). The MRN complex binds to the damaged DNA and undergoes a series of conformational changes to activate and increase ATM affinity for its substrates, and retain active ATM at sites of DSBs (Paull and Lee, 2005). ATM phosphorylates H2AX, NBS1, BRCA1 and FANCD2 (Jacquemont and Taniguchi, 2007, Hartlerode and Scully, 2009). Single strand DNA is rapidly bound by the RPA, which unwinds the DNA's secondary structure (Sung and Klein, 2006). The RPA is replaced with RAD51, which is mediated by BRCA2 (Davies et al., 2001). The damaged 3' advancing strand then invades the complementary sequence of the homologous chromosome sets up a D-loop intermediate and primes DNA synthesis by using the duplex DNA as a template (Hartlerode and Scully, 2009, Sung and Klein, 2006). If the D-loop captures the second end of the break, Holliday junctions (HJs) are formed (Hartlerode and Scully, 2009, Sung and Klein, 2006).

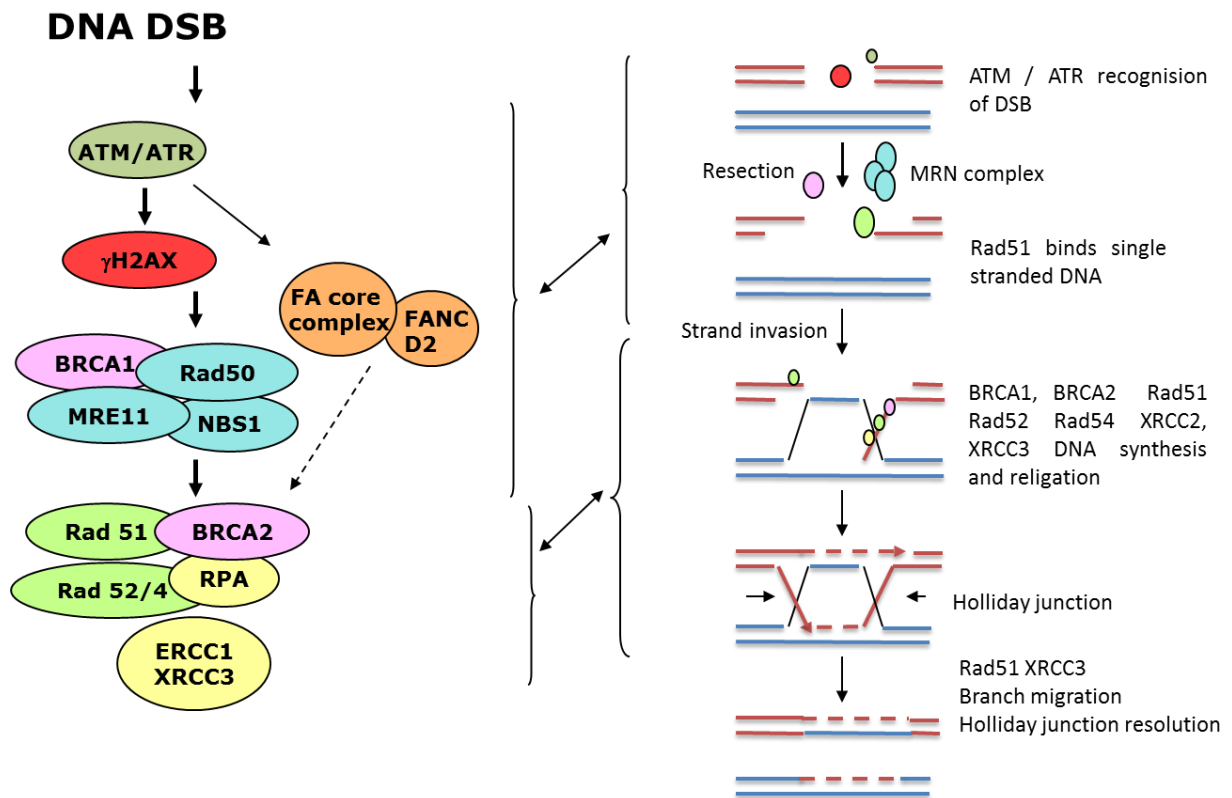


Figure 1-6 Schematic representation of HR pathway.

DSBs activate the ATM/ATR which in turn phosphorylates H2AX, NBS1, BRCA1 and FANCD2. Mediated by BRCA1 the MRN complex exposes the 3' ends on either side of the DSB. RPA binds to single strand DNA and unwinds the DNA's secondary structure. The RPA is replaced with RAD51, which is mediated by BRCA1, PALB2 and BRCA2. The 3' advancing strand from the damaged chromosome then invades the complementary sequence of the homologous chromosome. Following the synapsis, the invading strand sets up HJ and primes DNA synthesis by using the duplex DNA as a template. RAD54 promotes branch migration whilst BLM and GEN1 resolve the HJ (Cerbinskaite et al., 2012).

The resolution of a HJs can be executed by several enzyme complexes, such as BLM in complex with topoisomerase III α , which can dissolve double HJs to form non-crossover products (Wu and Hickson, 2003, Bohr, 2008), or GEN1, which promotes junction resolution by symmetrical cleavage (Ip et al., 2008). After replication has extended past the region of the DSB, the strand replication continues to the end of the chromosome (Hoeijmakers, 2001, Khanna and Jackson, 2001).

1.4.5.1.1 HR Defects in Cancer

A number of inherited syndromes show a defect in HR and a predisposition to cancer or premature aging i.e., Ataxia telangiectasia (Milne, 2009, Taylor et al., 1975), Ataxia-telangiectasia like disorder (Taylor et al., 2004), Nijmegen Breakage

syndrome (Chistiakov et al., 2008, Digweed and Sperling, 2004) and Fanconi anaemia (Alter, 1996, Kennedy and D'Andrea, 2005, Kutler et al., 2003). Cells deficient in this pathway are susceptible to several anti-cancer agents, however, recombination may also result in loss of heterozygosity (LOH), leading to inactivation of tumour suppressor genes, or cause gross gene rearrangements that can activate proto-oncogenes (Moynahan and Jasin, 1997). The function of the entire repair pathway can be affected if one or more genes involved in the pathway are defective.

Defects in the majority of genes involved in the HR pathway have been reported in human cancers, as summarised in table 1-4 and reviewed in (Cerbinskaite et al., 2012). For the purposes of this report, only HR gene defects reported in ovarian cancer will be discussed in detail.

Table 1-4 Reported links to human cancers of HR gene alterations.

Summary of HR genes which are reported to harbor mutations, function altering polymorphisms or epigenetic alterations leading to reduced function in human cancer (Cerbinskaite et al., 2012).

Cancer Site	HR Genes
Head and Neck	ATM, FANCF
Medullo-blastoma	FANCD1/BRCA2
Nasopharyngeal	ATM
Oral	ATM
Thyroid	XRCC3
Lung	NBS1, BRCA1, FANCF, XRCC2
Breast	ATM, RAD50, NBS1, BRCA1, BRCA2, RAD51, FANCI
Stomach	ATM, ATR, BRCA1, BRCA2
Pancreas	BRCA2, RAD51, FANCC
Colorectal	ATM, MRE11, BRCA1, BRCA2
Ovarian	MRE11, RAD50, BRCA1, BRCA2, FANCF
Endometrial	ATR
Cervical	BRCA1, FANCF
Prostate	ATM, NBS1, BRCA2
Multiple Myeloma	RAD51
Leukaemia	ATM, NBS1, RAD51, FANCA, FANCC, FANCF, FANCG
Melanoma	NBS1, XRCC3, BRCA2
Lymphoma	NBS1

1.4.5.1.2 Role of HR in Ovarian Cancer

The role of the HR pathway in ovarian cancer became an important research field due to the function of tumour suppressor genes *BRCA1* and *BRCA2*. These genes are best known as breast and ovarian cancer susceptibility genes (Gayther et al., 1999), however, they have also been linked to a number of different human cancers (Table 1-4). Inactivation of the *BRCA1* or *BRCA2* results in genetic instability and chromosomal rearrangements (Bishop and Schiestl, 2002, Ban et al., 2001). Knockout of the *BRCA1* is embryonically lethal in mice (Gowen et al., 1996) and down regulation of *BRCA1* halts the cell cycle at the G2 to M transition, which leads to cell cycle arrest or apoptotic cell death (Bouwman et al., 2010). *BRCA2* functions are largely limited to DNA repair and recombination (Chistiakov et al., 2008). The protein controls the availability, localisation, DNA binding and stabilisation of RAD51 (Ayoub et al., 2009, Shivji et al., 2009, Davies et al., 2001).

The lifetime risk of developing EOC in women with a germline *BRCA1/2* mutation can be up to 66 % and 27 % respectively (Robles-Diaz, 2004). Cancers containing *BRCA1* mutations are more common in younger women (<50 years at diagnosis), compared to cancers with *BRCA2* mutations in older women (>60 years) with hereditary ovarian cancers (Risch et al., 2001). Mutation rates vary between patients of different ancestry, being higher among Jewish (26 %), Italian (24 %), and Indo-Pakistani (14 %) and lower in British (3.5 % - 4.7 %) (Janezic et al., 1999, Stratton et al., 1997, Risch et al., 2001). They also vary with histological type, being higher in serous cancers (10.9 % *BRCA1* and 5.6 % *BRCA2* mutations) and lower in endometrioid cancers (2.1 % mutation rate for both *BRCA* genes) (Risch et al., 2001). Reports of *BRCA1/2* mutations in mucinous and borderline cancers are contradictory (Risch et al., 2001, Boyd et al., 2000, Stratton et al., 1997).

Epigenetic silencing of *BRCA* genes has also been noted. *BRCA1* alterations occurring by gene deletion, loss of gene expression (due to promoter methylation) or by loss of protein expression have been reported in about 5-31 % of sporadic ovarian cancers (Wang et al., 2004a, Jacinto and Esteller, 2007, Hilton et al., 2002).

BRCA1/2 deficiency, defined as mutations and loss of expression, was reported in 30 % of HGSOC (Hennessy et al., 2010). *BRCA1/2* associated tumours have distinct clinical features tending to be HGSOC, carboplatin sensitive and to be associated with an improved survival (Ramus and Gayther, 2009, Cass et al., 2003).

1.4.5.1.3 Concept of HRD and Therapy

Further to the loss of the BRCA genes HRD due to mutations in other genes involved in the HR pathway has also been described. These include mutations of *EMSY*, *MRE11*, *RAD50*, *XRCC2*, *XRCC3* and FANC pathway genes (Brown et al., 2006, Heikkinen et al., 2003, Heikkinen et al., 2006, Nagaraju et al., 2009, Kennedy and D'Andrea, 2006, Taniguchi et al., 2003). It is believed that in fact around 50 % of EOCs could be potentially HR deficient (Mukhopadhyay et al., 2010, Cancer Genome Atlas Research, 2011).

1.4.5.1.4 Inhibitors that Block HR Function

Novel inhibitors that block HR function have been developed. Mirin is an inhibitor of MRE11 endonuclease activity and thus of HR function (Dupre et al., 2008). However, MRE11 function is not limited to HR as it is also upstream of NHEJ, and so mirin also inhibits NHEJ (Rass et al., 2009). The BCR-ABL1 inhibitor imatinib blocks HR by inhibiting the activation of RAD51 and sensitized cells to DNA crosslinking agents and IR (Choudhury et al., 2009). Other RAD51 inhibitors have also been identified (Huang et al., 2011a). A further way to block HR is to inhibit CDK1, which activates BRCA1. Preclinical studies showed that the CDK1 inhibitor AG024322 is synthetically lethal with PARPi (Johnson et al., 2011). ATM and ATR have crucial roles by signalling DNA damage to cell cycle checkpoints and DNA repair pathways. ATM promotes HR by recruiting BRCA1 and NHEJ by recruiting p53 binding protein 1 (53BP1) to DSBs (Bouwman et al., 2010). ATM inhibitors have been reported to induce sensitisation to IR, etoposide and camptothecin *in vitro* (Hickson et al., 2004, Rainey et al., 2008). ATR is activated by the DNA single-strand–double-strand junction, and it activates MMR and HR pathways (Wang et al., 2004b). Preclinical studies have demonstrated ATR inhibitor induced *in vitro* chemo and radio-sensitisation (Reaper et al., 2011, Peasland et al., 2011). ATR role and inhibitors will be further discussed in chapter 5. The effects of HR inhibition on patient outcomes still needs to be evaluated.

1.4.5.2 Non Homologous End Joining

In the classical or DNA-PK dependent NHEJ pathway (Figure 1-7) the end-joining process starts with the binding of Ku70/Ku80 heterodimers to the DNA ends, followed by DNA-PKcs. The nuclease functions are performed by Artemis (Ma et al., 2002),

however, some resection is done by the MRN complex (Dinkelmann et al., 2009, Quennet et al., 2011). DNA polymerase μ and λ participate in the repair and DNA ligase IV, supported by two components called XRCC4 and XLF, catalyses the final end-joining reaction (Lieber et al., 2003, Ahnesorg et al., 2006, Buck et al., 2006). Recent studies have also shown a role for PARP in the NHEJ pathway (Spagnolo et al., 2012, Mitchell et al., 2009a), however, the mechanism of this is unclear.

NHEJ is an essential part of the DNA end-joining phase in V(D)J recombination, the mechanism that assembles coding regions for the variable domains of immunoglobulin and T cell receptors in developing lymphocytes (Grawunder et al., 1998, Tonegawa, 1983). Lymphoid-specific RAG proteins generate DNA double strand breaks which are re-joined by NHEJ (Tonegawa, 1983, Grawunder et al., 1998). Hypomorphic mutations in *XLF*, *Artemis* and *LIG4* lead to a number of rare hereditary disorders characterised by immunodeficiency (*Artemis*) and/or developmental abnormalities (*XLF*, *LIG4*), which underscore the general importance of the NHEJ pathway for genome integrity and development (Jeggo et al., 2004, Sekiguchi and Ferguson, 2006).

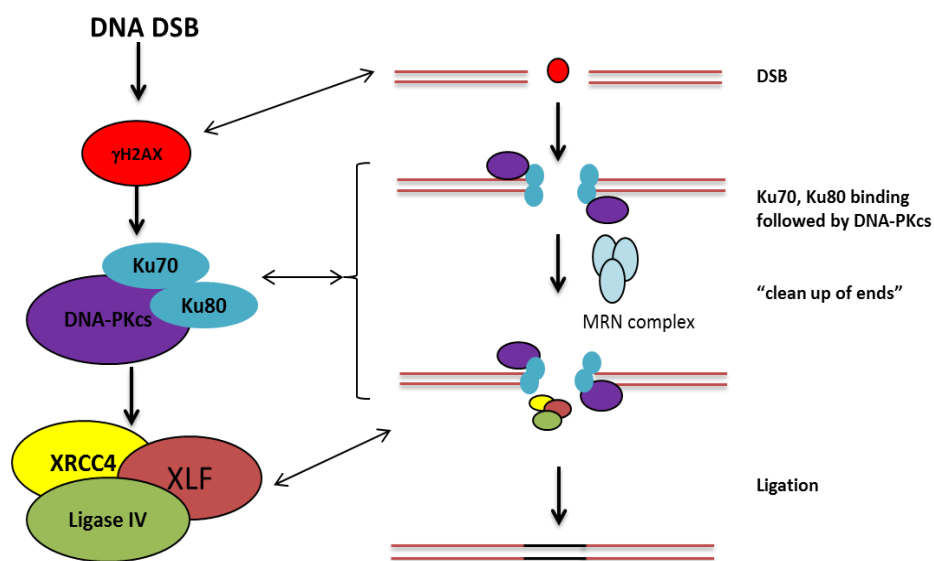


Figure 1-7 Schematic representation of NHEJ.

After phosphorylation of H2AX at DNA DSB sites, NHEJ is initiated by the binding of the Ku heterodimer (composed of Ku70 and Ku80). DNA-PKcs is then recruited and binds to the DNA end, activating its serine/threonine kinase activity. The Ku70/Ku80/DNA-PKcs complex, referred to as DNA-PK, holds the two DNA strands together in a synapse. Activation of DNA-PK by phosphorylation allows the alignment of the DNA strands, which are subsequently joined by the ligase IV/XRCC4 complex. This reaction is stimulated by XLF protein, which interacts with XRCC4 to catalyse the final end-joining reaction (Lieber et al., 2003, Ahnesorg et al., 2006, Buck et al., 2006).

1.4.5.2.1 Non Homologous End Joining Defects in Cancer

Further to the rare hereditary disorders, the NHEJ pathway activity has also been linked to a number of human cancers. NHEJ activity was reported to be reduced and increasingly error prone in bladder cancers (Bentley et al., 2009, Bentley et al., 2004, Windhofer et al., 2008). DNA end-joining capacities in peripheral blood mononuclear cells of breast cancer patients were reported to be consistently lower than those from healthy women (Bau et al., 2007) and dysregulated NHEJ has also been reported in leukaemia patients (Deriano et al., 2005, Gaymes et al., 2002).

A number of studies have investigated individual gene mutations and polymorphisms in the NHEJ pathway in human cancers. Table 1-5 summarises the NHEJ genes which are reported to harbor mutations, SNPs or epigenetic alterations leading to altered function in human cancers. Overexpression of NHEJ genes and pathway function has also been linked to drug resistance (Kim et al., 2000, Deriano et al., 2005).

Table 1-5 Reported links to human cancers of NHEJ gene alterations.

Summary of NHEJ genes which are reported to harbor mutations or epigenetic alterations leading to reduced function in human cancer. Adapted from manuscript in preparation. Full table in appendix 1.

Cancer Site	NHEJ Genes
Head and Neck	DNA-PK,
Laryngeal	PARP-1
Glioma	XRCC4, LIG IV
Nasopharyngeal	KU70
Lung	DNA-PK, XRCC4, LIG IV
Breast	DNA-PK, KU70, Ku80, XRCC4, Lig IV
Gastric/colorectal	DNA-PK, KU70, KU80
Pancreas	LIG IV
Cervical	DNA-PK, KU70, KU80
Bladder	DNA-PK, XRCC4, KU
Multiple Myeloma	Lig IV, Ku80
Leukaemia	DNA-PK, KU70, KU80, Lig IV, Artemis
Lymphoma	Lig IV
Neuroblastoma	DNA-PK
Fibrosarcoma	DNA-PK, Ku 80

1.4.5.2.2 BRCA1 Role in NHEJ Pathway

Although BRCA1 is thought to be primarily involved in the HR pathway (Turner et al., 2005), it has been implicated in the NHEJ pathway as well (Bau et al., 2004, Couplier et al., 2004, Bau et al., 2006). *In vitro* studies have demonstrated that cell extracts derived from BRCA1-deficient cells exhibit reduced end-joining activity (Bau et al., 2004, Zhong et al., 2002). Moreover, recent reports have indicated that BRCA1 functions to inhibit NHEJ (Bau et al., 2004, Wang et al., 2006a, Zhuang et al., 2006), this may be by protecting from excess trimming by exonucleases (Paull et al., 2001). This notion is also supported by the observation that, in BRCA1-deficient cells, there is an increased tendency towards the generation of large deletions (>2 kb) during NHEJ (Zhuang et al., 2006). It is therefore postulated that BRCA1 not only promotes HR but also reduces error-prone NHEJ processes. However, the role of BRCA1 in NHEJ, if any, is still poorly understood as conflicting results have been reported, including promotion, suppression, or no effect (Wei et al., 2008).

1.4.5.3 Alternative End Joining Pathway

An alternative end joining (A-EJ), also known as backup NHEJ pathway (B-NHEJ) or microhomology-mediated end joining (MMEJ), which lies somewhere between HR and NHEJ and is more error prone, has been suggested in eukaryotic cells (Wang et al., 2003, Iliakis et al., 2004, Yan et al., 2007, Corneo et al., 2007). Alternative end-joining is suggested to rely on microhomologies, which are short sequences of a few homologous base pairs. Unlike HR, A-EJ is inherently error-prone because the use of microhomology leads to deletions of sequences from the strand being repaired and chromosomal translocations. Evidence of this pathway comes from several *in vitro* assays (Cheong et al., 1999, Wang et al., 2003, Perrault et al., 2004) and *in vivo* studies (Liang and Jasin, 1996, Audebert et al., 2008). PARP-1 / DNA ligase III / XRCC1 / histone 1 module and Pol θ are suggested to be involved in A-EJ (Audebert et al., 2004, Wang et al., 2005, Wang et al., 2006b, Rosidi et al., 2008). Pol θ has been shown to be overexpressed in HGSOC (Ceccaldi et al., 2015a).

A-EJ is reported to be suppressed by the DNA-PK dependent NHEJ (Perrault et al., 2004), to show cell cycle dependence with a more pronounced function during the G2 phase (Wu et al., 2008), and may be compromised in non-cycling cells (Windhofer et al., 2007). Recent publications have shown that A-EJ and HR are competing pathways, as evidenced by the observation of increased HR in cells

lacking Pol θ . Furthermore, A-EJ has been demonstrated to compensate for the loss of HR, however, this results in chromosomal rearrangement and reduced ability of the cells to survive (Ceccaldi et al., 2015a, Mateos-Gomez et al., 2015).

1.4.5.4 Selection of DNA Double Strand Repair Pathway

The choice between which DSB pathway repairs a lesion is thought to be cell cycle dependent (Figure 1-8) (Symington and Gautier, 2011). In G1 phase, DSB 5' end resection is halted by the 53BP1/Rif1 proteins allowing Ku to bind and NHEJ predominance (Chapman et al., 2012a, Chapman et al., 2013). Synthesis of BRCA1 in S and G2 phases inhibits Rif1 and allows 5' end resection, subsequent inhibition of NHEJ and repair by HR (Chapman et al., 2012a, Chapman et al., 2013). As HR requires homologous sequences, it may only be active in cell cycle stages where these are available (S and G2 phases) (Lieber, 2010). A-EJ is also thought to act on 5' resected lesions (Wang et al., 2006b, Bentley et al., 2004). Like NHEJ, A-EJ rejoins lesions with minimal end processing, however, as the DNA ends have already been resected, large amounts of genetic material may be lost and this pathway is thought to be highly toxic (Bétermier et al., 2014). The choice between HR and A-EJ is thought to be decided by the length of resected segments, with HR principally dealing with long segments and A-EJ shorter (Bétermier et al., 2014). A-EJ requires PARP for its activity and is susceptible to PARP inhibition (Mansour et al., 2010).

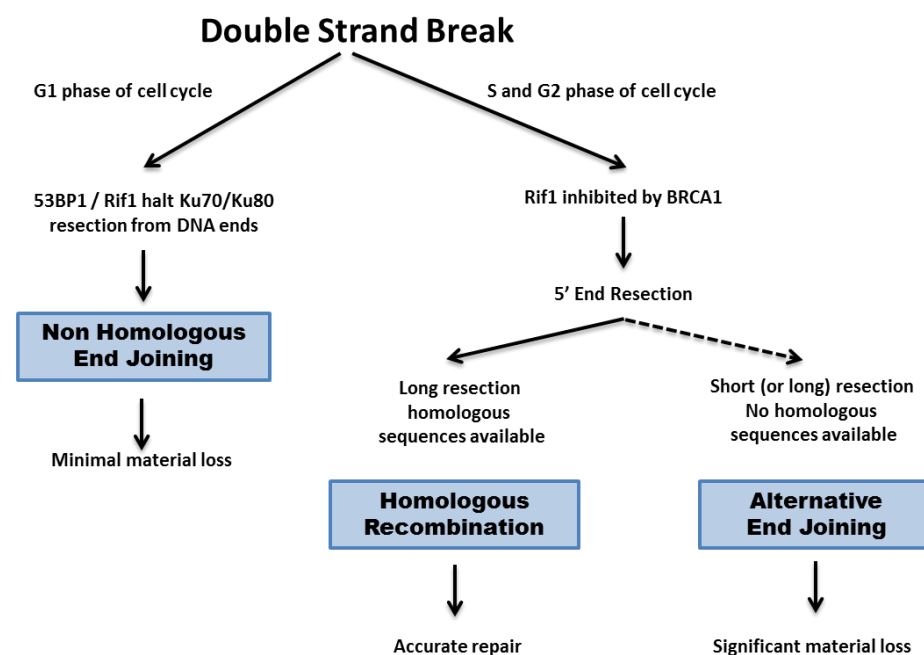


Figure 1-8 Schematic representation of the pathway choice for the repair of a DSBs (Bétermier et al., 2014, Chapman et al., 2013).

1.4.6 Poly (ADP) Polymerase (PARP)

PARP-1 has been the most studied and described enzyme in the family of 17 PARPs (Ame et al., 2004). The gene encoding PARP-1 protein is the *ADPRT-1* located on 1q41-q42 (Auer et al., 1989). PARP-1 is an abundant 113 kDa nuclear enzyme and plays a role in a number of cellular processes and therefore has a number of clinical applications (Sodhi et al., 2010, Pacher and Szabo, 2007, Lupachyk et al., 2011, Crawford et al., 2010, Giansanti et al., 2010), however, for the purposes of this report, only PARP-1 application in DNA repair and cancer will be discussed further.

1.4.6.1.1 PARP Role in SSB Repair

Following DNA base damage, PARP-1 binds to the SSB (Benjamin and Gill, 1980). Activation of PARP-1 results in the production of PAR, which is attached to histones or PARP-1 itself. This leads to the relaxation of the chromatin fibre and facilitates the recruitment of proteins necessary for repair (described in section 1.4.4) (Althaus et al., 1993, Dantzer et al., 2000). Inhibition of PARP-1 activity inhibits the formation of XRCC1 foci (El-Khamisy et al., 2003), and failure of BER results in DSBs due to collision of the SSB with the progressing replication fork (Gottipati et al., 2010).

1.4.6.1.2 PARP Role in DSB Repair

PARP-1 binds to and is activated by stalled replication forks (Bryant et al., 2009, Sugimura et al., 2008) and is necessary for the accumulation of MRE11 and NBS1 at the site of DSBs (Hegan et al., 2010, Benjamin and Gill, 1980, Haince et al., 2008). Inhibition of PARP has been shown to retard the rejoining of IR-induced DNA DSBs (Mitchell et al., 2009a, Boulton et al., 1999). Interaction of PARPi and DNA-PKi in radio-sensitisation has also been demonstrated (Ruscetti et al., 1998, Veuger et al., 2003, Veuger et al., 2004, Mitchell et al., 2009a). In irradiated cells, the higher affinity of Ku for DSBs has been suggested to limit PARP-1 contribution to DSB repair, however, when the classical NHEJ pathway is not functional PARP-1 may be recruited (Wang et al., 2006b). The function of PARP-1 in the A-EJ has been shown by both *in vitro* and *in vivo* studies (Wang et al., 2006b, Audebert et al., 2006, Lu et al., 2006, Audebert et al., 2008). In other studies, PARP-1 has been shown to have a protective role in HR by suppressing access of NHEJ to DNA DSBs (Hochegger et al., 2006, Saberi et al., 2007). With on-going studies into the clinical application of PARPi, further clarification of the role PARP in DNA DSB repair is needed.

1.4.6.1.3 PARP Activity in Cancer

V762A single nucleotide polymorphism (SNP) results in amino acid substitution in PARP-1 and can reduce PARP-1 catalytic activity by 30-40 % (Lockett et al., 2004). V762A SNP in PARP-1 has been reported to be associated with prostate cancer, colon cancer and multiple myeloma (Doll et al., 1996, Lyn et al., 1993, Lockett et al., 2004, Bernstein et al., 2002). Reduced PARP activity in response to DNA damage has also been reported in laryngeal cancer (Rajaei-Behbahani et al., 2002). Conversely, reports in breast cancer are contradictory; with studies reporting PARP-1 expression to be increased in more than 50 % of breast tumours (Bieche et al., 1996), while others report lower (Hu et al., 1997, Lockett et al., 2004, Wang et al., 2007, Smith et al., 2008) or no association of PARP-1 activity with risk of breast cancer (Zhai et al., 2006, Zhang et al., 2006).

PARP-1 and PARP-2 expression varies widely across all nucleated human cells excluding neutrophils (Schreiber et al., 2002, Csete et al., 2009). Pilot studies measuring PARP-1 activity in peripheral blood mononuclear cells from healthy volunteers and metastatic melanoma patients before and during temozolomide therapy and in tumour biopsies, revealed large inter-individual differences in PARP activity in both healthy volunteers (20-615 pmol/10⁶ cells) and cancer patients (15-430 pmol/10⁴ cells) (Plummer et al., 2005). This was also confirmed by a more recent study, comparing PARP activity in sarcoma patients with their monozygotic twins (Zaremba et al., 2011). This may explain the conflicting results seen in previous studies.

1.4.6.1.4 Synthetic Lethality and PARP Inhibitors

The concept of synthetic lethality describes a phenomenon where 2 non-lethal genetic mutations can lead to lethality in combination (Dobzhansky, 1946). This may involve genes in complementary pathways or acting along a single or related pathway, in which case, the loss of both genes, rather than just one, significantly affects pathway signaling and function. This concept has now been exploited in cancer therapy, whereby tumour cells harboring specific genetic lesions can be challenged by targeting the synthetically lethal partner genes or pathways leading to selective tumour cell death (Kaelin, 2005, Helleday et al., 2008, Brough et al., 2011). This allows a large therapeutic window whereby the non-cancerous cells in the body,

not harboring the gene defect, are not affected by the chemotherapeutic agent, allowing the chemotherapy to impact only on the cancerous cells.

Studies in cell lines have showed that HR defects result in sensitivity to PARPi; there was an observed 100-1000 fold increase in sensitivity to PARPi in cells homozygous for *BRCA1* or *BRCA2* mutation, compared to heterozygous or *BRCA* wild-type cell lines (Bryant et al., 2005, Farmer et al., 2005). Furthermore, siRNA-mediated depletion of *BRCA2* in *BRCA* wild type breast cancer cell lines also caused sensitivity to PARPi (Bryant et al., 2005). Cancers defective in HR pathway due to loss of function of other genes involved in this pathway are also hypersensitive to PARPi (Bryant and Helleday, 2006, McCabe et al., 2006, Drew et al., 2011). *BRCA1/2* mutation carriers are heterozygous for the defect in all other cells; therefore still have a functional HR pathway. PARPi are less cytotoxic to normal cells, therefore, their associated side-effects, including myelosuppression and nausea, are relatively mild (Plummer and Calvert, 2007, Mukhopadhyay et al., 2011).

Reversion mutations have been reported in *BRCA* gene in ovarian cancer *in vitro* (Taniguchi et al., 2003). Furthermore, it has been shown that in cell lines and tumour samples, secondary reverting mutations in *BRCA1/2* genes can lead to cisplatin resistance in *BRCA1/2* mutation carriers (Swisher et al., 2008, Sakai et al., 2008, Sakai et al., 2009, Edwards et al., 2008). This reversion has been suggested to be due to the function of the NHEJ pathway, which results in secondary reverting *BRCA* mutations resulting in restoration of HR function (Ashworth, 2008a, Sakai et al., 2009). Furthermore, pathway 'rewiring' may also alter responses to DNA damage in DNA repair deficient cells. An example of this is 53BP1 overexpression that results in the inhibition of NHEJ and upregulation of the HR pathway in *BRCA1* deficient tumours (Bouwman et al., 2010, Aly and Ganesan, 2011).

1.4.6.1.5 PARP Inhibitors in Cancer Clinical Trials

The first PARPi to enter a clinical trial was rucaparib in 2003. It was used to potentiate the effect of radio- and chemo-therapies, and showed a beneficial effect in several cancers (Plummer et al., 2005). In ovarian cancer the initial trials concentrated on hereditary EOCs with known *BRCA1/2* mutations (Fong et al., 2009, Audeh et al., 2010). The focus of research has subsequently been re-directed to evaluate the use of PARPi as a stand-alone therapy in patients with HRD beyond *BRCA1/2* mutations (Plummer and Calvert, 2007, Clinical_Trials.gov, 2012). The

application of PARPi in platinum resistant EOCs is also being explored (Fong et al., 2010, Audeh et al., 2010). Ongoing and completed clinical trials are summarised in Appendix 2. Further to on-going clinical trials into the application for PARPi, the identification of the HRD EOC population, through identification and validation of biomarkers is an active area of on-going research (Mukhopadhyay et al., 2010).

1.4.6.1.6 The Potential Role of NHEJ in PARPi Induced Cell Killing

It is thought the minimal end processing in NHEJ repair makes the pathway error prone and may lead to lethal genomic instability (Patel et al., 2011). Research published in 2011 suggested the erroneous repair mediated by the NHEJ pathway is critical in driving the lethality of PARPi in HRD cells (Patel et al., 2011). The group found that PARPi resulted in activation of DNA-PK and that genetic or pharmacological inhibition of NHEJ rescued PARP lethality in HRD cells. Although NHEJ may not be as toxic as A-EJ, it may still be crucial to PARPi mediated cell killing in HRD tumours (Bétermier et al., 2014).

1.5 Rationale for This Project

A number of questions still remain unanswered. Whilst there is a clear understanding of the importance of DNA repair in ovarian cancer, the study of DNA DSB repair has so far been limited to HR. The function of NHEJ and the more recently described A-EJ pathways have had little assessment in ovarian cancer to date. It is therefore, difficult to be certain of the exact proportion of human cancers which are NHEJ defective (NHEJD), as many of the mutations are rare and have been reported from studies with a limited number of samples; consequently it is not always clear what the impact of a polymorphism is on function of the protein transcribed. Individual risk increases due to each SNP reported are low, therefore, the impact to individuals carrying these variants may be limited. However, due to the frequency of occurrence of these SNPs the population based risk is likely to be significant. Large genome association studies to identify further SNPs and mutations in NHEJ genes, and therefore, estimate the true proportion of NHEJD cancers are essential. These are however, beyond the scope of this project.

Genome wide association studies will not provide all the answers, as the functional role of all mutations identified need to be assessed. The challenge is therefore to be able to identify the cancers which are functionally NHEJD or up-regulated, arising

from mutations or SNPs of any one or a combination of the genes described. Work is well underway to develop biomarker tests which will accurately identify those cancers which are HRD (Mukhopadhyay et al., 2010). Functional assays which are capable of assessing the NHEJ pathway are now needed to be applied in combination with those assessing HR. Such tests will be designed to spot defective functional pathways rather than just identifying one gene abnormality at a time and will hopefully allow treatment of patients based on tumour biology rather than by the organ of origin, thus potentially widening the therapeutic options available.

With increasing evidence supporting the application of PARPi, a clearer understanding is required into the role of this protein in the NHEJ pathway, and the biological significance of inhibition of PARP in the presence and absence of a functional NHEJ pathway. Furthermore, whilst the interaction of DSB repair pathways has been suggested, this relationship in ovarian cancer still remains to be determined.

The evidence to date has also demonstrated the role of DNA repair dysfunction in the development of chemo-resistance in ovarian cancer. Whilst a number of mechanisms for platinum resistance have been explored, these are still not fully understood and attempts to overcome this has not yet yielded clinically significant results. With the aim to introduce PARPi into clinical practice the mechanisms for resistance to PARPi also need to be understood. Furthermore, understanding the similarities and differences between PARPi and platinum resistance is essential for the clinical application of this new drug. Being able to understand, predict and prevent resistance development would put PARPi treatment at the forefront of ovarian cancer therapy in appropriately selected patients.

1.6 Project Hypothesis

The interactions of multiple DSB repair pathways have an important role in ovarian cancer biology and sensitivity to platinum and PARPi treatment.

1.7 Project Aims

The primary objective of this project was to investigate the interaction of DSB repair mechanisms in ovarian cancer biology and to assess their role in mediating therapeutic response to cisplatin and rucaparib. The strategies for achieving this were:

- To optimise models for the study of ovarian cancer by characterisation of the primary ovarian cancer (PCO) cultures and a novel ovarian cancer cell line.
- To assess NHEJ and HR function in a panel of PCO cultures and to correlate these with sensitivity to rucaparib and cisplatin.
- To assess the interactions of NHEJ and HR pathways in ovarian cancer biology, and the interaction of these two pathways with PARP-1, using drug inhibition and knockdown models.
- To develop rucaparib and cisplatin resistant cell line models and to assess the role of DNA repair pathways in resistance development. Furthermore, to perform genome-wide molecular analysis in order to investigate mechanisms of resistance development.

Further details of specific aims are described in each individual chapter.

2.1 General Laboratory Practice

All experiments were performed in accordance with the University standards for safe working with chemical substances in laboratories, which comply with the Control of Substances Hazardous to Health Regulations (COSHH) and BioCOSHH. Routinely used chemicals of analytical or molecular biology grade were purchased from Sigma-Aldrich Co. Ltd. (Dorset, UK), unless otherwise stated. Phosphate buffered saline (PBS) (137 mM NaCl, 83 mM KCl, 10 mM Na₂HPO₄) was prepared from PBS tablets (Invitrogen Life Technologies, Paisley, UK) and was autoclaved prior to use for sterility.

2.2 Cell Culture Methods

Tissue culture plastic ware was from Corning-Costar (supplied by VWR International Ltd., Leicestershire, UK). All cell culture was carried out in a class II microbiological safety cabinet (BIOMAT-2, Medical Air Technology Ltd., Oldham, UK) using an aseptic technique.

2.2.1 Routine Cell Culture

All cell lines were maintained as adherent cultures in media as detailed in Table 2-1 with 10 % (v/v) heat inactivated foetal calf serum (FCS), 20 mM L-glutamine and 50 µg/ml penicillin / streptomycin in 75 cm³ sterile cell culture flasks. All media were stored at 4 °C and warmed to 37 °C in a water bath prior to use. Cultures were incubated at 37 °C (OSEC-1 and OSEC-2 at 33 °C) in a humidified 5 % CO₂ incubator (Heraeus Equipment Ltd., Essex, UK). Testing for mycoplasma was performed by E.C. Matheson at 2 month intervals using a MycoAlert kit (Lonza Biologics, Slough, UK).

2.2.2 Primary Culture

Ascitic fluid was collected from patients undergoing primary surgery for ovarian cancer or primary peritoneal cancer debulking surgery at Queen Elizabeth Hospital, Gateshead. All patients gave informed consent. Consent form can be seen in appendix 3. Ethical approval was sought, and specimens were registered in

accordance with the Human Tissue Act 2004. All cultures were labelled PCO followed by a serial number which identifies the patient from whom the sample was collected. All collected primary cultures were entered in the NICR central tissue resource database. 20 mls of ascitic fluid was added to 20 mls of culture medium, which comprised of RPMI 1640 medium supplemented with 20 % FCS, 20 mM L-glutamine, and 1 % penicillin and streptomycin in 75 cm³ sterile tissue culture flasks and incubated at 37 °C / 5 % carbon dioxide. The medium was aspirated and 13 mls of warmed fresh medium replaced on day 4 to 5 of incubation. The medium was replaced every 4 to 5 days until cells reached >80 % confluence.

Table 2-1 Cell lines used in the project.

Cell line	Source	Medium	Characteristics
OSEC-1	Generated at Newcastle University (Davies et al., 2003)	RPMI 1640	BRCA2 heterozygote, HRC, telomerase and temperature sensitive SV40 large T antigen immortalised normal OSE cell line
OSEC-2	Generated at Newcastle University (Davies et al., 2003)	RPMI 1640	BRCA wild type, HRC, telomerase and temperature sensitive SV40 large T antigen immortalised normal OSE cell line
SKOV3	ATCC ® HTB-77	RPMI 1640	Ovarian adenocarcinoma cell line derived from ascites of a patient with moderately well differentiated ovarian adenocarcinoma (Debernardis et al., 1997)
OVCAR3	ATCC ® HTB-161	RPMI 1640	Derived from a patient with an ovarian epithelial adenocarcinoma
A2780	Provided by Prof. R. Brown (Beatson Laboratories, Glasgow, Scotland)	RPMI 1640	Human ovarian carcinoma p53 and MMR-proficient, (Anthony et al., 1996)
A2780-CP70	Provided by Prof. R. Brown (Beatson Laboratories, Glasgow, Scotland)	RPMI 1640	hMLH1 promoter hypermethylation (Strathdee et al., 1999) variant of A2780, 5-fold resistant to cisplatin relative to the parental A2780 cell line (Anthony et al., 1996)
IGROV-1	ATCC	RPMI 1640	Human ovarian adenocarcinoma (Benard et al., 1985)
MDAH	ATCC ® CRL-10303	RPMI 1640	Human ovarian adenocarcinoma

MO59J	ATCC ® CRL-2366	RPMI 1640	Malignant glioblastoma cells, DNA-PK mutated
MO59FUS-1		RPMI 1640	Paired cell line to MO59J. DNA-PK competent by virtue of transfer of portion of Chr8 (Virsik-Kopp et al., 2004)
V3	Provided by Dr. Penny Jeggo (University of Sussex, UK)	DMEM	DNA-PKcs deficient Chinese hamster ovary cells
V3-YAC	Provided by Dr. Penny Jeggo (University of Sussex, UK)	DMEM	Derived from V3 cells, transfected with a yeast artificial chromosome (YAC) carrying the human DNA-PKcs gene
UWB1-289	ATCC ® CRL-2945	50 % MEBM 50 % RPMI	BRCA1-null human ovarian cancer derived from papillary serous ovarian carcinoma (DelloRusso et al., 2007)
UWB1-289-BRCA1	ATCC ® CRL-2946	50 % MEBM 50 % RPMI	Ovarian carcinoma cell lines derived from UWB1.289, a BRCA1-null human ovarian cancer line, in which wild-type BRCA1 was restored (DelloRusso et al., 2007)
PEO1	PEA - 10032308	RPMI 1640	Derived from malignant effusion from the peritoneal ascites of a patient with a poorly differentiated serous adenocarcinoma contains BRCA2 mutation [5193C>G (Y1655X)]
PEO4	PEA - 10032309	RPMI 1640	Derived from the same patient as PEO1 after clinical resistance developed to chemotherapy. Contains a secondary BRCA2 mutation [5193C>T (Y1655Y)] that cancelled the inherited mutation

2.2.3 Pancytokeratin Staining

To confirm epithelial cell origin, pancytokeratin staining was used in PCO cultures. A sterilised 22 mm² cover slip was placed in 6-well plate prior to the seeding of cells at a density of 1 x 10⁶. The plates were incubated for 24 hours (hrs) to allow cells to adhere. Medium was removed and cells were fixed with ice-cold methanol for 10 minutes (min). Cells were washed with PBS and incubated in 250 µl (1:100 dilution)

of FITC conjugated Anti-Cytokeratin Pan mouse monoclonal antibody (Millipore) for 1 hr. Excess antibody was washed with PBS and coverslip mounted to glass slide with VECTASHIELD® Mounting Medium with DAPI (Vector Laboratories). Slides were examined using fluorescence microscope (Leica DMR, Leica Microsystems, UK). Cells incubated with no primary antibody were used as negative control. Cultures containing greater than 95 % epithelial cells were considered to be cytokeratin positive and were utilised in further assays.

2.2.4 Cell Passaging

Cell lines and established PCO cultures were passaged when cells were 80 % confluent in order to maintain cells in exponential growth phase. Medium was aspirated and the cells were rinsed with warm sterile PBS followed by incubation in 5 ml 0.25 % trypsin-EDTA (ethylene-diamine-tetra acetic acid, Sigma - Aldrich) for 5 min in the incubator (until all the cells had detached). Full medium was added to detached cells to neutralise the trypsin. Cell suspension was centrifuged at 230 x G for 5 min. The supernatant was discarded; the cell pellet was re-suspended in full medium and plated in new flasks / culture dishes as required. Cell lines were passaged a maximum of 30 times, after which fresh stocks were resuscitated from liquid nitrogen storage.

2.2.5 Cell Counting

Cells were trypsinised and resuspended in 10 ml of media. 10 µl of the solution was loaded onto a Neubauer Haemocytometer (VWR International Ltd.) and a minimum of 100 cells were recorded for each cell count.

2.2.6 Cryopreservation of Cell Stocks

Cells were trypsinised and centrifuged in sterile BD Falcon™ centrifuge tubes (BD Biosciences, Oxford, UK) at 230 x G for 5 min. The supernatant was discarded, after which cell pellets were resuspended in 1 ml freezing medium [usual growth medium supplemented with 10 % v/v FCS and 10 % (v/v) dimethyl sulphoxide (DMSO)] and transferred to sterile polypropylene cryovials (Invitrogen Life Technologies). Cells were frozen slowly (approximately 1 °C per minute) to -80°C and transferred to liquid nitrogen for long term storage.

2.2.7 Resuscitation of Frozen Cell Stocks

Cryopreserved cell aliquots were thawed rapidly and transferred to 5 ml pre-warmed RPMI medium. Suspensions were then centrifuged at 230 x G for 5 min, after which the supernatant was completely removed and discarded. Resulting cell pellets were re-suspended in 7 ml 10 % RPMI culture medium, transferred to 25 cm³ sterile cell culture flasks and incubated at 37 °C / 5 % CO₂. Cell cultures were checked daily for growth and used in experiments once normal exponential cell growth had resumed.

2.3 Clinical Data and Survival Analysis

Patient data including age, pretreatment tumor markers, operative details and histologic subtype, stage, and grade were recorded from the clinical database. Histologic diagnosis of primary ovarian/PPC was confirmed by independent gynecologic-specific pathologists. Surgical stage, histologic grade, and cell type were classified according to the World Health Organization (WHO) and Federation Internationale des Gynaecologistes et Obstetristes (FIGO) standards. All patients received platinum-based chemotherapy with or without paclitaxel as first-line treatment.

Survival data were calculated using the date of diagnosis, defined as the date of histologic or cytologic confirmation of EOCs. For progression free survival (PFS) patient who had documented progression were uncensored, whereas patients who had not progressed at last follow up were censored. For overall survival (OS), patients who died at follow-up (any cause) were considered uncensored, whereas patients alive at follow-up were censored. Statistical Package for Social Sciences Software (SPSS version 15.0; SPSS Inc.) was used for analyses. Univariate analyses for OS and PFS were generated by Kaplan–Meier survival curves and log-rank (Mantel–Cox) tests for statistical significance.

2.4 Measurement of DSB Induction and Repair

DSB recognition and repair was assessed by estimation of the foci formation of γH2AX (recognition) and RAD51 and DNA-PKcs (repair) using immunofluorescent staining. This technique involves permibilisation of cells after DNA damage and subsequent detection of target proteins of interest using immunofluorescence labelled antibodies. The antibody molecules which bind to each protein can be visualised as

foci and counted, therefore protein expression levels can be compared between cell lines. Cells were plated on cover slips in a sterile 6 well cell culture plate at a concentration of 5×10^5 / well and incubated for 24 hrs to allow cells to adhere followed by treatment with a DNA damaging agent.

2.4.1 Induction of DNA Damage with Ionizing Radiation

Ionising radiation (IR) was used to induce DNA damage in the experiments to assess DNA-PK phosphorylation, formation of double strand breaks and radio-sensitisation by inhibitors. Exposure to IR was performed using a D3300 X-ray system (Gulmay Medical Ltd., Surrey, UK) at a dose rate of 2.4 Gy / min, 310 kV, 10 mA.

2.4.2 Use of PARP Inhibitor, Rucaparib to Produce DSBs

Rucaparib (Clovis), a potent inhibitor of PARP-1 and PARP-2 ($K_i < 5$ nM/L) was used at a concentration of 10 μ M to prevent repair of endogeneous SSB leading to SSB accumulation and conversion to DSB in exponentially growing cell lines and primary cultures. Cells were incubated for 24 hrs following drug treatment.

Table 2-2 DNA damage induction and detection experiments.

Experiment	Protein detected	DNA-damage induction	Incubation prior to fixation
NHEJ pathway activation	pDNA-PKcs	2 / 4 Gy IR	1 hr
HR assay	RAD51 and γ H2AX	10 μ M rucaparib and 2 Gy IR	24 hrs
DNA DSB formation	γ H2AX	2 Gy IR	Time line: 0, 15min, 2, 6, 24 and 48 hrs

2.4.3 Cell Fixation and Staining

Following DNA damage, cells were incubated for an optimised length of time (Table 2-2). Cover slips in 6 well plates were then washed with cold PBS (4 °C), fixed with ice cold methanol for 10 min, re-hydrated with 2 changes of PBS for 20 min and transferred to 90 mm petri dishes covered with para film. Cells were then permeabilised with 150 μ l / cover slip blocking buffer [KCM buffer (120 mM KCl, 20 mM NaCl, 10 mM Tris-HCl, 1 mM EDTA, pH 8.0, 0.1 % v/v Triton X-100), 2 % (w/v)

bovine serum albumin, 10 % (w/v) milk powder, and 10 % (v/v) goat serum (DAKO, Denmark)] for 1 hr at room temperature (RT).

Table 2-3 Antibody preparation for immunofluorescence experiments.

Reagent	Dilution	Incubation time	Source/content
Primary Ab γH2AX	1:200	1 hr at RT	Anti-phospho-Histone H2AX (Ser139), clone JBW301 (IgG1 mouse monoclonal antibody) Upstate, Millipore Corp.
Primary Ab RAD51	1:200	1 hr RT and ON at 4 °C	Anti-RAD51 Rabbit pAb. (PC 130), Calbiochem, EMD Biosciences, Inc.
Primary Ab pDNA-PKcs	1:50	1 hr RT and ON at 4 °C	Anti-phospho-S2056 DNA-PK Abcam
Secondary Ab γH2AX	1:1000	1 hr at RT	Alexa Fluor R 546 Goat anti-mouse IgG (H + L). Invitrogen
Secondary Ab RAD51 / pDNA-PKcs	1:1000	1 hr at RT	Alexa Fluor 488 Goat anti- Rabbit IgG (H + L). Invitrogen

Primary antibody diluted in blocking buffer (Table 2-3) was added to the cover slips and incubated for the appropriate length of time. Cover-slips were then washed (3 x 15 min per wash). Secondary antibodies were added to the cover slips and incubated in the dark at RT for 1 hr each. KCM buffer (3 x 15 min per wash) was used after each change of antibodies. Cover slips were mounted on slides using Vectashield mounting medium containing DAPI (Vector Laboratories, Inc. Burlingame). Slides were air dried in the dark at RT before storing them at 4 °C. All experiments were done alongside untreated controls and treated slides with no primary antibodies.

2.4.4 Immunofluorescence Microscopy

A Leica DMR (Wetzlar, Germany) fluorescent microscope was used. All images were captured using RT SE6 Slider Camera Spot Advanced software version 3.408 (Diagnostic Instruments, Inc), and stored as tiff / bitmap images. The settings used to take pictures are detailed in Table 2-4.

Table 2-4 Leica DMR fluorescent microscope settings.

Stain	FilterColor	Gamma	Gain	Exposure time(ms)
DAPI	Blue	0.35	4/8	300
RAD51 / pDNA-PKcs	Green	0.35	16	3500
γ H2AX	Red	0.35	16	3500

2.4.5 Counting Foci

ImageJ software was used to count (Abramoff et al., 2004) the total number of cells across 3 fields. Overlapping cells, and cells with fragmented nuclear outline on DAPI staining were excluded to avoid over/under estimation of foci counts. The average number of foci / cell (mean, SD) was calculated for each field using ImageJ software and make mask and foci counting macros (Znojek PhD thesis). The final count was taken as the mean and SEM after 3 independent experiments.

2.5 Cytotoxicity Assays

Cytotoxicity assays were used throughout the project to assess drug or radiation response in cell lines and primary cultures. Cells were assessed in pairs with their parental cell lines, where available.

2.5.1.1 Reagents and Exposures

Stock solutions of chemotherapeutic agents for use in cytotoxicity assays were prepared according to Table 2-5 using appropriate solvents. All stock solutions were aliquoted and stored at -80 °C. Working solutions were stored at -20 °C.

2.5.1.2 Clonogenic Assay

Clonogenic assays were performed to study the effect of drug treatments on cell survival by assessing the ability of cells to form colonies. Cells were seeded in a 6 well plate for 24 hrs to allow attachment. Medium was gently aspirated and replaced with 2 ml of fresh full medium containing the required treatments. Cells were incubated for 24 hrs followed by aspiration of the medium, washed in PBS x 1, and 2 ml of fresh full medium was added. Cells were incubated at 33 °C / 5 % CO₂ for 14 days (OSEC-2) or 37 °C / 5 % CO₂ for 30 days (PEO1, PEO4, UWB1.289, UWB1.289+BRCA1 and NUOC-1) to check for colony formation. The medium was

aspirated, plates were washed in PBS once and then fixed using the Carnoy's fixative (acetic acid: methanol 1:3 v/v, stored at RT) followed by staining with 1 % crystal violet. Colony formation efficiency was calculated as number of colonies / number of cells seeded x 100. Survival was determined as a fold change over the untreated control.

Table 2-5 Details of cytotoxic agents and small molecule inhibitors.

Cytotoxic agent	Drug Class	Molecular weight g/mol	Solvent	Stock solution
Cisplatin	Bifunctional alkylating agent – inhibit DNA synthesis	300.01	SDW	4 mM
Paclitaxel	Plant Alkaloids - Mitotic spindle inhibitor: enhances tubulin polymerization	853.91	Methanol	10 mM
Camptothecin	Plant Alkaloids - Topoisomerase I inhibitor	348.35	DMSO	10 mM
Doxorubicin	Anthracycline antibiotic - Topoisomerase II inhibitors	543.52	SDW	10 mM
Rucaparib	PARP inhibitor	421.36	DMSO	10 mM
NU7441	Small molecule DNA-PK inhibitor	413.49	DMSO	4 mM
NU6027	A selective inhibitor ATR. Developed as an inhibitor of cyclin-dependent kinase-2 (CDK2)	251.28	DMSO	10 mM
KU55933	Small molecule ATM kinase inhibitor	395.5	DMSO	10 mM

2.5.1.3 SRB Assay

Primary cultures do not form colonies with a high frequency, so growth inhibition following various treatments was assessed using a 96 well SRB assay instead. The sulforhodamine B (SRB) assay is used for cell density determination, based on the measurement of cellular protein content (Skehan et al., 1990). SRB is a bright pink aminoxanthene dye, with two sulphonic groups that bind to basic amino-acid residues under mild acidic conditions, and dissociate under basic conditions. As the

binding of SRB is stoichiometric, the amount of dye extracted from the stained cells is directly proportional to the cell mass (Vichai and Kirtikara, 2006).

Cells were seeded at a concentration of 1000 cells per well in 96 well plates and left to attach overnight. After gently aspirating out the medium, 100 µl of fresh full medium containing drug treatments was added to each well, using 6 replicate wells per condition. The plates were incubated for 3 doubling times for the cell line or 10 days for PCO cultures, at which point the cells were fixed with 25 µl of 50 % trichloroacetic acid (TCA) per well, and stored at 4 °C for one hr. Plates were then washed and dried. 100 µl of 0.4 % SRB solution (4 g SRB in 1 litre 1 % acetic acid) was added to each well for 30 min at RT followed by five washes in 1 % acetic acid, to remove unbound SRB. 100 µl of 10 mM Tris (pH 10.5) was added to each well to solubilise bound SRB, and absorbance read at 570 nm using a Spectra Max 250 plate reader (Molecular Devices). The mean and SD of optical densities following each treatment were calculated.

2.6 Non Homologous End Joining Assays

In order to assess NHEJ function two previously published *in vitro* assays were selected.

2.6.1 Cell Extract End Joining Assay

A previously described protein extract end joining assay was selected to be used for this project (Diggle et al., 2003). End joining is assessed by the ability of cell extracts to rejoin linearised vector monomers into multimers (Figure 2-1). The vectors produce either compatible or incompatible ends when linearised using BstXI. Rejoining was visualised by agarose gel electrophoresis with gel red stain and quantified by densitometry. The results were expressed as: $100 \times (\text{density of multimers}) / (\text{density of multimers} + \text{monomers})$.

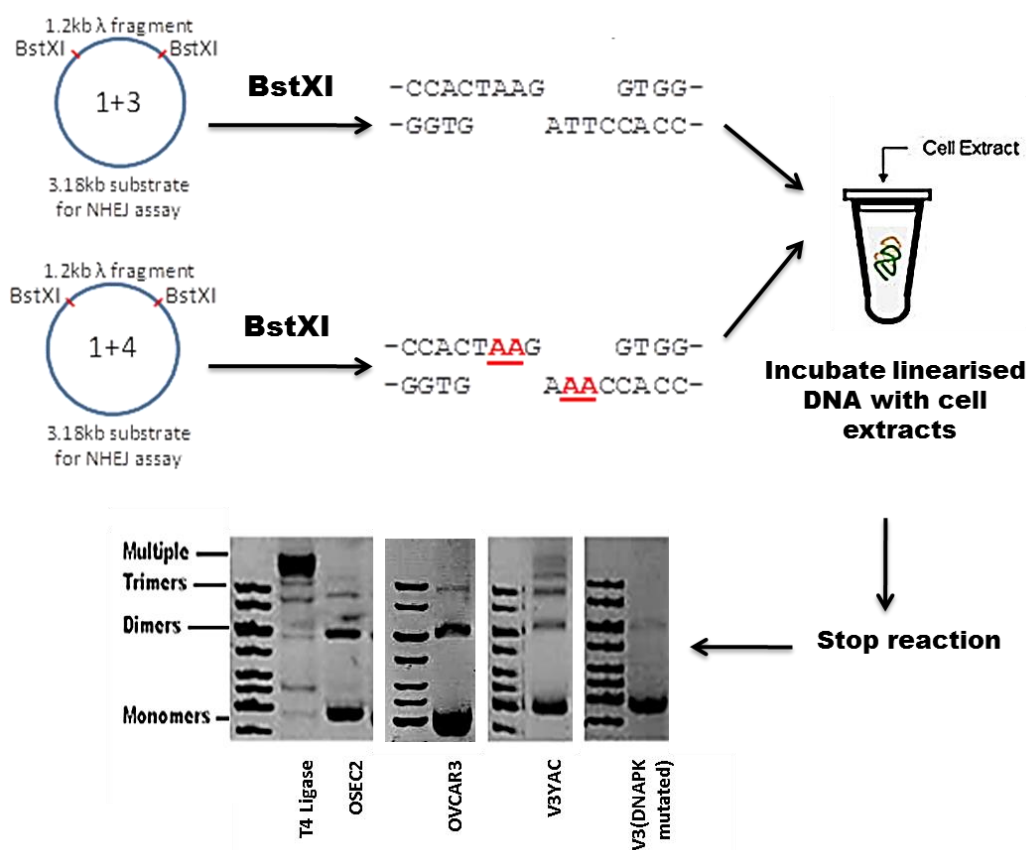


Figure 2-1 Schematic representation of cellular extract NHEJ assay.

2.6.1.1 Cell-free Extract Preparation

Cells were grown in 175 cm³ flasks until 70 % confluent. 3 flasks were used for each lysate sample. Cells were washed 3 times with cold PBS and once in hypotonic buffer (10 mM Tris–HCl pH 8.0, 1 mM EDTA, 1 mM DTT) by gently resuspending the cells by pipetting, followed by pelleting at 230 x G for 4 min. The cell pellets were resuspended in 400 μ l hypotonic buffer and left on ice for 20 min, with occasional gentle agitation, prior to homogenisation using a 20 g needle in the presence of protease inhibitors (0.17 mg / ml phenylmethylsulphonyl fluoride, 0.01 U / ml aprotinin, 1 μ g / ml pepstatin, 1 μ g / ml chymostatin, 1 μ g / ml leupeptin). The suspension was then left on ice for a further 20 min with occasional gentle agitation, then mixed with 0.5 volume of high salt buffer (50 mM Tris–HCl pH 7.5, 1 M KCl, 2 mM EDTA, 1 mM DTT). The samples were ultracentrifuged at 70000 rpm for 56 min in a Beckman TLA120 Optima table top ultracentrifuge using a TLA120 fixed angle rotor, then dialysed against dialysis buffer (20 mM Tris–HCl pH 8.0, 20 % v/v glycerol, 0.1 M KOAc, 0.5 mM EDTA, 1 mM DTT) for 2 hrs before storage at -80 °C.

Protein concentration was assessed using the Pierce Assay protein reagent kit according to the manufacturer's instructions (Pierce Biotechnology, Milwaukee, WI).

2.6.1.2 DNA Substrates

Vectors were digested using BstXI enzyme (New England Biolabs) as per manufacturer's instructions (Figure 2-2.A). Complete digestion was confirmed using gel electrophoresis and gelRed stain (Figure 2-2.B). A 1 % agarose gel was prepared by melting Ultrapure™ agarose (Invitrogen Life Technologies) in TBE buffer [89 mM Tris-HCl pH 8, 89 mM Boric acid, 2 mM EDTA]. Gels were stained with GelRED. GelRED is a DNA intercalating agent which, when exposed to UV light fluoresces brightly with a red colour when incorporated in nucleic acids. Its inclusion in the gel, therefore allows visualisation of the DNA following separation. The gel was allowed to set at RT.

The gel cassette was placed in a Sub-Cell® GT Agarose Gel Electrophoresis System (Bio-Rad Laboratories Ltd.) filled with TBE buffer. To allow estimation of the size of PCR products, 5 µl of quick-Load® 100 bp DNA Ladder (New England Biolabs (UK) Ltd., UK) was loaded in to the first well. Electrophoresis was performed at 100 V for 45 min. DNA was visualised using Gel Doc™ XR (Bio-Rad Laboratories Ltd.). The Gel Doc software (Quantity One® V4.5.0) was used to capture an image of the gel.

Digested bands were cut out and purified using a gel purification kit (Qiagen, UK), following the manufacturer's instructions. For each digestion reaction, PCR using NHEJ forward and reverse primers was performed to assess for any contamination with uncut vector. The presence of uncut vector was confirmed by a band at 551 bps (Figure 2-2.C). Any digested samples found to contain uncut vector were discarded. Digested vectors were resuspended to 5 ng / µl concentration in water and stored at -20 °C for up to 7 days before use.

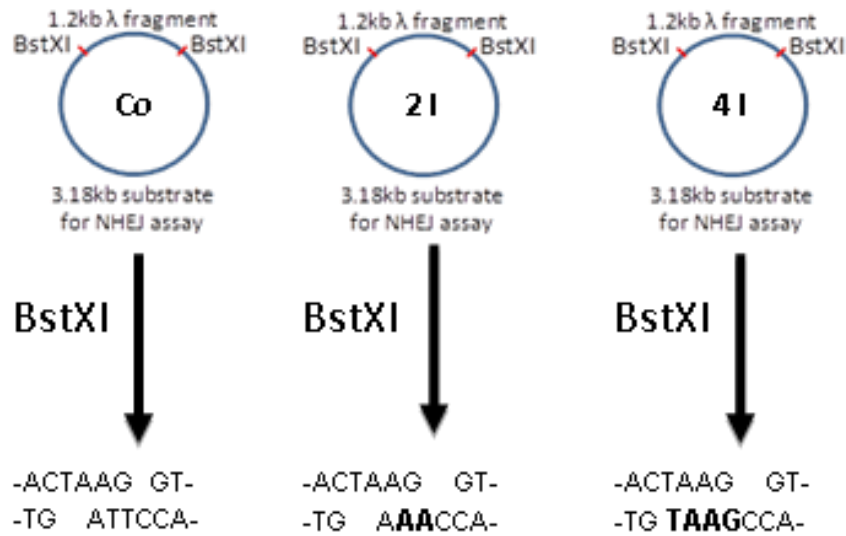
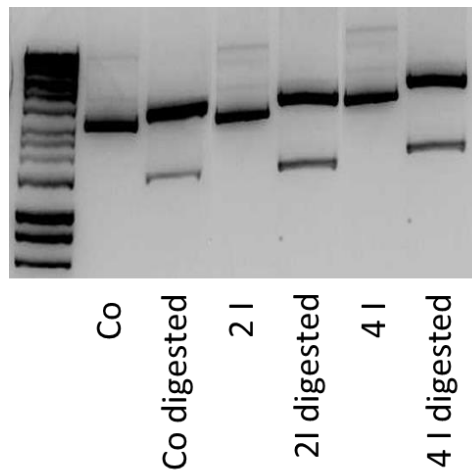
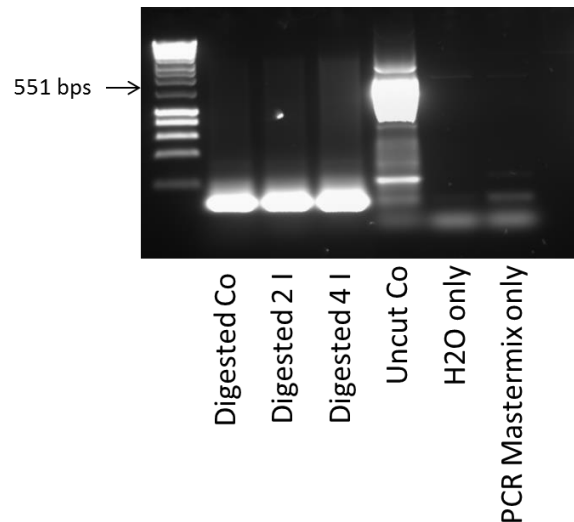
A**B****C**

Figure 2-2 Optimisation of BstXI digestion.

A. Diagrammatic representation of the three vectors and products. **B.** Confirmation of BstXI digestion using agarose gel electrophoresis and gelRed staining. Digestion produced a 3.2kb band by excising a 1.2kb λ fragment. **C.** Check for uncut vector contamination. PCR reaction was performed using forward and reverse primers for each digested sample (Co, 2I and 4I). Uncut vector was used as positive control for PCR reaction. H₂O and mastermix only reactions were used as controls for contamination.

2.6.1.3 DNA End Joining Assay

End-joining reactions (20 μ l) were carried out with 50 μ g protein extract and 100 ng DNA substrate in the presence of T4 ligase manufacturer's recommended buffer at 37 °C for 2 hrs. Extract from DNA-PK deficient cell lines (V3) and no protein loaded sample, was used as a negative control, DNA-PKcs competent (V3-YAK) and T4 ligase (New England Biolabs, Beverly, MA) were used as positive controls.

Monomers only are used in this assay, and therefore, repair by HR was not possible. Microhomology sequences in the DNA are a significant distance from the cut site. Repair by A-EJ therefore results in the large loss of DNA sequence and hence smaller product.

Samples were incubated with RNase A (80 µg / ml) for 10 min and then protein was removed by incubation with proteinase K (2 mg/ml) and 0.5 % (w/v) SDS for 10 min followed by incubation at 65 °C for 10 min. Analysis was performed by agarose (0.7 %) gel electrophoresis and GelRed staining. Gels were transferred to a dark box with CCD camera (Fuji LAS 3000 system, Raytek, Sheffield, UK). An image was acquired using Fuji LAS imaging software (version 1.1), which was then analysed using Aida Image Analyser software (version 3.28.001, Raytek).

2.6.1.4 Optimisation of Extract End Joining Assay

The quantity of vector DNA required, and the maximum concentration of DMSO which could be used in a reaction, was optimised using OSEC-2 cells. 100 ng vector DNA yielded bands that were, detectable and quantifiable (Figure 2-3.A). DMSO inhibited end joining (Figure 2-3.B) and therefore the concentration of DMSO was kept below 1 % when inhibitors were used in subsequent assays.

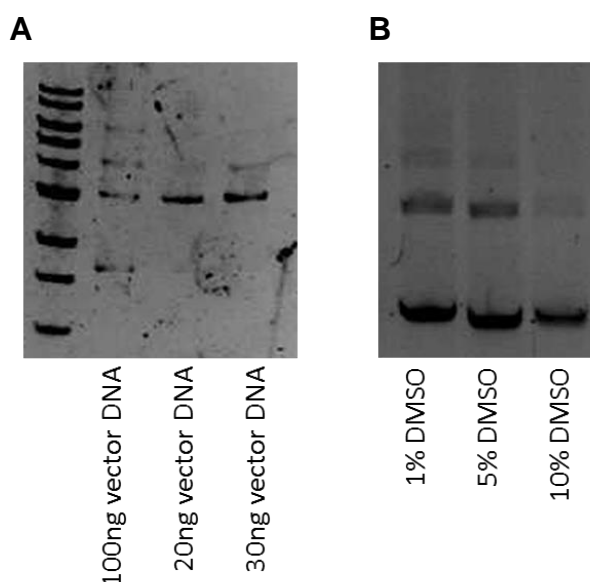


Figure 2-3 Optimisation of cell extract end joining assay.

A. Optimisation of amount of vector DNA loaded into the assay. **B.** Optimisation of amount of DMSO to be used in NHEJ assay.

2.6.2 Luciferase Cellular End Joining Assay

The cellular luciferase assay quantifies end joining of the linearised luciferase gene containing pGL2 plasmid using luciferase function. pGL2 plasmid was completely linearised using either HindIII or EcoRI and transfected into cells using Lipofectamine (Figure 2-4).

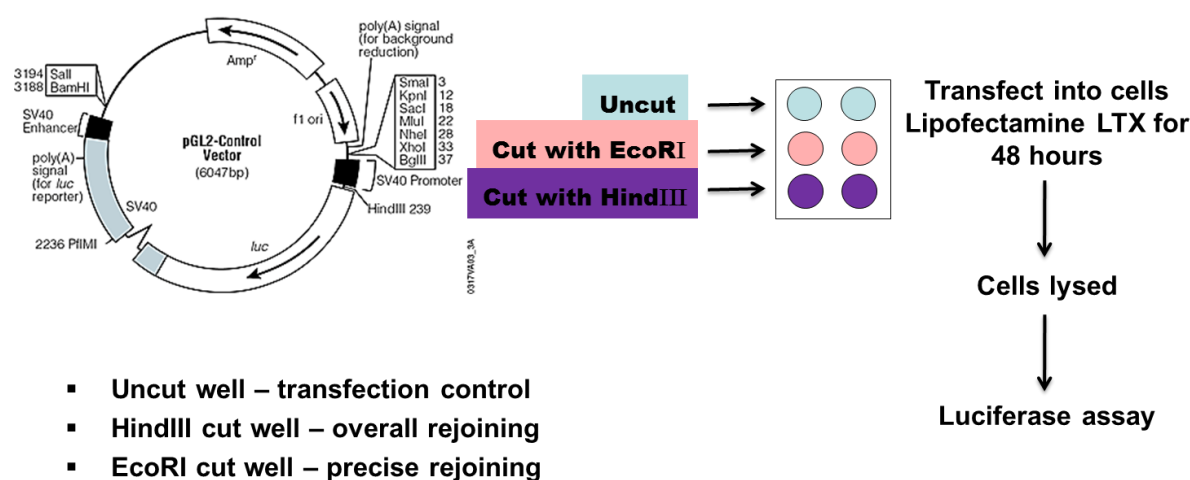


Figure 2-4 Schematic representation of Luciferase cellular end joining assay.

The transfectants were harvested 48 hrs after transfection and assayed for luciferase activity. Luciferase only functions when the vector is rejoined, thus demonstrating NHEJ. The vector linearisation produces blunt ends and does not contain any microhomology sequences preventing repair by HR and A-EJ.

The linearisation of the vector EcoRI cutting site is located within the luciferase gene, which therefore requires precise rejoining. The HindIII site is before the luciferase gene, therefore some loss of nucleotides would still result in functioning luciferase and thus assessed overall rejoining. Transfection of uncut vector acts as control for transfection efficiency for the cell line. Results were expressed as $100 * (\text{EcoRI cut} / \text{uncut}) / (\text{HindIII cut} / \text{uncut})$.

2.6.2.1 DNA Substrates

Plasmid pGL2 (Promega, Madison, WI) was completely linearised using either HindIII or EcoRI, as confirmed by agarose gel (1 %) electrophoresis and GelRed staining. DNA fragments were purified using spin columns (Qiagen, UK), dissolved in sterilised

water at 5 ng / μ l and stored at -20 °C (for up to 7 days), before use. Linearised plasmids were transfected into cells using Lipofectamine 2000 (Invitrogen).

2.6.2.2 Lipofectamine Transfection

The manufacturer's protocol for Lipofectamine TM 2000 (Invitrogen, USA, Cat No. 11668-027) was followed. Adherent cells were grown in 24 well plates for 24 hrs in 10 % FCS media (2 ml / well) to attain 80 % confluency. For each well, 500 μ l of DNA / Lipofectamine mix (1: 2.5 ratio) was prepared as follows: each of 500 ng of plasmid DNA in 8 μ l DSW and 0.5 μ l of PLUS reagent were added to 491.5 μ l of serum free media, shaken vigorously for 5 min then incubated at RT for 15 min. 3.0 μ l Lipofectamine LTX reagent was added, mixed well and incubated at RT for 30 - 60 min. Media was aspirated from the cells and replaced with the 500 μ l of DNA / lipofectamine mix. After 5 hrs of incubation, 1.5 ml of full media with 10 % FCS was added per well.

2.6.2.3 Transfection by Electroporation in Cell Lines and Primary Cultures

A cell suspension containing 1×10^6 cells / ml of media was prepared and 250 μ l placed in 4 mm electroporation Cuvettes (Eurogentec, Product code- CE0004-50). 1-5 μ g of pGL2 plasmid was added to the cell suspension. Electroporation was carried out using an EPI-2500 electroporator at 100 - 500 volts. The cell suspension was added to the media containing 10 % FCS in 6 well plates and incubated for 48 hrs before the transfectants were harvested and assayed for Luciferase activity.

2.7 Western Immunoblotting

To determine whether the levels of particular proteins differed in cell lines and PCO cultures, quantitation of protein expression was performed by western immunoblotting. This technique involves extraction of total cytosolic proteins, separation of proteins according to size, followed by immunoblotting onto a membrane, and subsequent detection of target proteins of interest using labelled antibodies. The number of antibody molecules which can bind to each protein (and hence the amount of label detected) is proportional to the amount of protein present, therefore, protein expression levels can be quantified and compared between samples.

2.7.1 Cytosol Preparation

Cells were plated in a 6 well plate at a concentration of 5×10^5 per well and incubated for 24 hrs to allow cells to adhere. The medium was then aspirated and 5 ml of fresh medium with required treatments was added. Cells were incubated for the appropriate time period.

Culture medium was removed and cells were washed with PBS, then harvested by adding 3 ml of chilled PBS and scrapping the plate to ensure all cells were removed. The cell suspension was transferred to chilled 15 ml falcon tubes and centrifuged at $500 \times G$ at $4^\circ C$ for 5 min after which the supernatant was removed. The pellet was lysed in 50 ml Merck phosphosafe buffer (Merck Chemicals Ltd.) by incubating at RT for 5 min, then centrifuged at $16000 \times G$ at $4^\circ C$ for 5 min. Protein concentration was estimated using Pierce® BCA Protein assay Kit (Fisher Scientific UK Ltd., Leicestershire, UK) as per the manufacturer's instructions.

2.7.2 SDS PAGE and Electrophoretic Transfer

Sodium dodecyl sulphate polyacrylamide gel electrophoresis (SDS-PAGE) was used to separate proteins in the cytosolic extracts according to size. To a 22.5 µl of sample 7.5 µl 4 x Bio-Rad XT Sample Buffer (Bio-Rad Laboratories Ltd.) was added and cell lysates were then denatured at $100^\circ C$ for 10 min prior to loading onto gels. 4 µl Seebule protein ladder was resolved alongside protein samples to assess protein size (4 kDa to 250 kDa). For analysis of ATR, the samples were loaded into Tris-glycine 4-15 % gel. For the analysis of all other proteins Criterion XT Tris-Acetate 3–8 % gels were used (both purchased from Bio-Rad Laboratories Ltd.).

Electrophoresis was performed in the reservoir buffer (77.9 % glycine, 16.6 % tris-base, 5.48 % SDS) using a constant voltage of 200 mV until the bromophenol blue dye front reached the bottom of the gel.

Following separation, proteins were transferred electrophoretically from the gels onto a nitrocellulose membrane (Hybond C-extra, Amersham, Biosciences). Gels were removed from their casing and placed in transfer cassettes with PVDF membrane (soaked in 100 % methanol immediately prior to use), sandwiched between 3 mm Whatman® chromatography papers (supplied by VWR International Ltd.) and transfer sponges, all of which had been pre-soaked in transfer buffer [10 mM CAPS-NaOH pH 11, 10 % (v/v) methanol]. Cassettes were placed in an Electrophoretic

Transfer Cell filled with transfer buffer (78.7 % glycine, 21.2 % tris-base) and electrophoresis was performed at a constant voltage of 100 mV for 1 hr using a magnetic stirrer to maintain ion distribution in the buffer.

2.7.3 Antibody Detection and Visualisation of Bound Proteins

PVDF membranes with bound proteins were removed from transfer cassettes and immersed in 5 % blocking solution [TBS-Tween, 5 % (w/v) BSA powder] with constant agitation for one hr at RT to block non-specific antibody binding sites. Following blocking, membranes were cut into appropriate sections (depending on which proteins were to be detected) and transferred to 50 ml BD Falcon™ centrifuge tubes containing 3 ml primary antibody solution (prepared according to dilution specified in Table 2-6). Incubation in most cases was over night at 4 °C with gentle agitation (using a roller mixer).

After incubation in primary antibody, membranes were washed in 5 ml TBS/Tween [0.01 M TrisHCl pH 7.5, 0.1 M NaCl, 0.05 % (v/v) Tween-20] at RT for 10 min (with gentle agitation). This wash step was repeated twice more to ensure removal of any unbound primary antibody. Membranes were then transferred to fresh 50 ml Falcon tubes containing 3 ml 1:1000 horseradish peroxidase (HRP) conjugated secondary antibody (goat anti-rabbit, rabbit anti-mouse or donkey anti-goat, Dako, Ely, UK) and incubated for 1 hr at RT (with gentle agitation). Following this, a total of 4 washes were performed, as above, to ensure any unbound antibody was completely removed.

Detection of bound antibodies was performed using ECL detection fluid (Amersham) according to the manufacturer's protocol. Visualisation of chemiluminescence was achieved via exposure of membranes to Kodak BioMax Light film (VWR International Ltd.) for the appropriate length of time (10 seconds to 10 min, depending on target protein). Films were developed using a Mediphot 937 X-Ray Film processor (ColentaLobortechnik, Austria).

Table 2-6 Antibodies used for protein detection by western blotting.

Primary Antibody	Size (kD)	Dilution	Supplier
Rabbit polyclonal anti Oestrogen receptor α	66	1:1000	Santa Cruz
Rabbit polyclonal anti Progesterone receptor	90	1:1000	Cell Signaling
Rabbit polyclonal anti Androgen receptor	110	1:1000	Santa Cruz
Mouse monoclonal anti EGFR	180	1: 10,000	Cell Signaling
Rabbit polyclonal anti Her-2	185	1:1000	Santa Cruz
Rabbit polyclonal anti Her-3	185	1:1000	Santa Cruz
Mouse monoclonal anti Alpha tubulin	50	1:4000	Sigma Aldrich
HRP linked anti GAPDH	37	1:30,00	Santa cruz
Rabbit polyclonal Anti pDNA-PKcs	471	1:500	Abcam
Rabbit polyclonal Anti DNA-PKcs	471	1:1000	Santa Cruz
Mouse monoclonal Anti Ku70	70	1:800	Abcam
Mouse monoclonal anti Ku80	80	1:800	Abcam
Mouse monoclonal Anti Lig IV	104	1:800	Abcam
Rabbit polyclonal anti XRCC4	38	1:1000	AbDSerotec
Goat polyclonal anti ATR	217	1:200	Santa Cruz
Rabbit polyclonal anti PTEN	47	1:200	Cell Signalling
Rabbit polyclonal anti ATM	350	1:1000	Calbiochem
Mouse monoclonal anti MDM2	90	1:300	Calbiochem
Rabbit monoclonal anti MDMX	80	1:1000	Bethyl
Mouse monoclonal anti P53	53	1:500	Vector
Mouse monoclonal anti P21	21	1:100	Calbiochem

2.7.4 Optimisation of Loading Control Protein

To ensure equitable protein loading, two commonly used loading controls, α -tubulin and GAPDH, were compared across different cell lines (Figure 2-5). Despite protein quantification using the Pearce protein assay, marked discrepancies were found between α -tubulin levels, whereas, GAPDH had uniform expression, and was therefore selected for subsequent experiments.

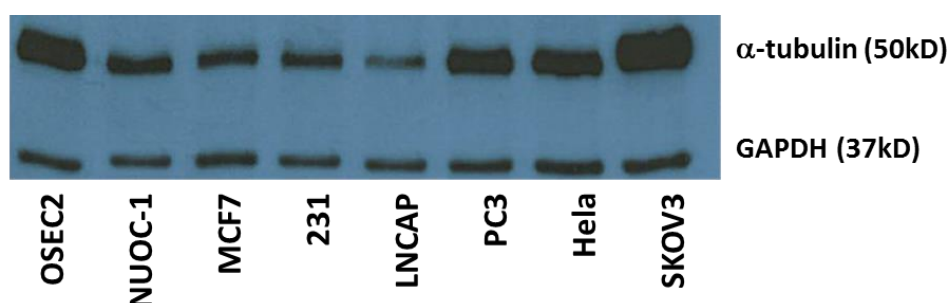


Figure 2-5 Expression of α -tubulin and GAPDH across a panel of cell lines. Blots are representative of three independent experiments.

2.8 Immunohistochemistry

Immunohistochemistry (IHC) involves the binding of a primary antibody specific to a protein of interest within histological tissue sections mounted on microscope slides. HRP is conjugated to the primary antibody (via a secondary antibody, where required) and the application of a chromogen (3,3'-Diaminobenzidine (DAB) to HRP) produces visible staining. Staining may be quantified by scoring based on colour intensity and the relative area occupied by graded intensities. Higher scores equate to a higher total protein expression.

2.8.1 Formalin-Fixed Paraffin-Embedded Tissue

Ovarian tissue from patients undergoing surgery at the Northern Gynaecological Oncology Centre (Gateshead, UK) was formed into formalin-fixed paraffin embedded (FFPE) blocks by the hospital histology department. FFPE tissue was used to analyse protein expression by IHC and mRNA expression by real time PCR (qPCR). Tissue micro arrays (TMA) were constructed by Dr Peter Donoghue. Two cores from each tumour, along with appropriate positive and negative control tissues, were included. The TMAs were sectioned at 4 μ m and mounted on adhesive slides (Leica, IL, USA) by Dr Peter Donoghue.

2.8.2 Antigen Retrieval

Slides were de-waxed in xylene for 5 min and hydrated through graded alcohols (99 %→95 %→70 %→50 %). Slides to be labelled with Ku70 and Ku80 primary antibodies underwent 10 min microwave-based antigen retrieval (2 x 5 min at 850 watts) in tris buffer (pH 9) (Sigma-Aldrich, Poole, UK). Slides to be labelled with DNA-PKcs primary antibody were subjected to antigen retrieval using an antigen decloaker for 30 seconds at 125 °C in citrate buffer (pH 6) (VWR, Leuven, Belgium). Following cooling and washing, sections were drawn around with a hydrophobic marker (Dako, Glostrup, Denmark) to prevent reagent loss. Endogenous peroxidase activity was blocked through application of 3 % hydrogen peroxide solution for 10 min (30 % hydrogen peroxide diluted in TBS buffer).

2.8.3 Antibody Detection

Primary antibodies were diluted in TBS buffer and applied as shown in Table 2-7. Negative controls were included in all runs (TBS buffer only). Antibody detection was carried out using the Menapath X-Cell detection kit (Menarini Diagnostics, Berkshire, UK). After antibody incubation, slides were subjected to 30 min application of universal secondary antibody probe. All slides underwent a 30 min application of HRP-polymer. DAB chromogen was diluted in the supplied buffer (1 drop of chromogen per 1 ml of buffer) and applied to the slides. Excess DAB solution was neutralised in sodium hypochlorite solution. Slides were counter-stained in Gills II haematoxylin (Leica) and blued in Scott's tap-water (Leica). Following rinsing, slides were dehydrated through graded alcohols (50 %→70 %→95 %→99 %) and cleared in xylene for 5 min before application of cover slips using DPX mounting agent (Sigma).

Table 2-7 Antibodies, concentrations and incubation times used for IHC.

Antibody	Dilution	Incubation Time	Manufacturer
Ku70	1:700	Overnight, at 4 °C	Abcam (Cambridge, UK)
Ku80	1:1250	Overnight, at 4 °C	Abcam (Cambridge, UK)
DNA-PKcs	1:750	1 Hr at 15-25 °C, at RT	Santa Cruz (TX, USA)

2.8.4 Imaging

Slides were scanned using the AperioScanScope slide scanner (Leica) and images viewed using Aperio Spectrum Webscope (Leica).

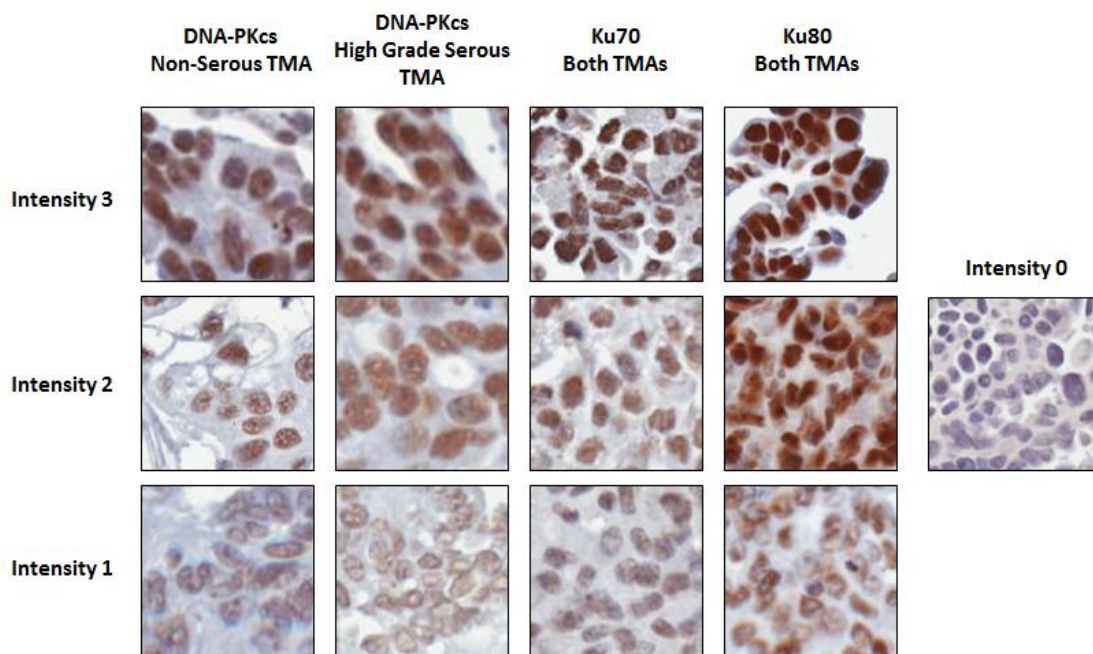


Figure 2-6 Graded scoring intensities for each antibody.

Tissue cores were graded from 1-3 depending on intensity of staining as shown above. For DNA-PKcs HGSOC and Non-Serous TMAs required different example intensities due to a slight discrepancy between the staining of the two slides.

2.8.5 Scoring

TMA cores were scored independently by Richard O'Sullivan (MRes 2014) and Dr Peter Donoghue using a modified H-score as previously described (McCarty et al., 1986).

Before scoring, the scorers discussed the range of intensities produced for each antibody and produced examples of each intensity from 1-3 (Figure 2-6). Intra-class Correlation Coefficients (ICC) were calculated to assess the correlation between the two scorers in the scoring of TMA cores (Hecht et al., 2008). Excellent reproducibility of scoring was found (Table 2-8).

Table 2-8 IHC scores for DNA-PKcs, Ku70 and Ku80.

ICC and 95 % confidence interval between the scorers for both raw scores and after discussion of heterogeneous results.

Primary Antibody	Intraclass Correlation Coefficient (95 % confident intervals)	
	Raw Scores	Post Discussion
DNA-PKcs	0.84 (0.76-0.90)	0.95 (0.92-0.97)
Ku70	0.91 (0.86-0.94)	0.95 (0.92-0.97)
Ku80	0.90 (0.85-0.93)	0.94 (0.91-0.96)

2.9 Cell Cycle Assessment using Flow Cytometry

Propidium Iodide (PI) staining was used to study cell cycle profiles. Stoichiometric binding of PI to DNA results in increased dye uptake as cells synthesise DNA and progress through cell cycles. PI fluorescence is detected in the FL2 channel of flow cytometers. This quantification of DNA content of the cells allows determination of cells in the sub G1 (apoptotic cells) G1, S and G2 phases of the cell cycle.

2.9.1 Sample Preparation

Cells were plated in a 6 well plate at a concentration of 5×10^4 per well and incubated for 24 hrs to allow cells to adhere, the medium was then aspirated and replaced with fresh full medium containing 1 μ M rucaparib, 1 μ M NU7441 and 10 μ M NU6027 individually and in combination. Cells incubated in full medium were used as positive control and stain free samples as negative controls. 48 hrs following treatment, cells were harvested and cell pellets were resuspended in 500 μ l of 2 % FCS in PBS, with the addition of 125 μ l of 0.25 % PI in 5 % Triton and 50 μ l RNaseA solutions. Samples were incubated at RT for 10 min prior to analysis with flow cytometry.

2.9.2 Sample Analysis

Samples were run through a Becton-Dickinson FACScan Flow Cytometer (BD Becton Dickinson UK Limited, Oxford, UK). Three detectors were used: one in line with the light beam (Forward Scatter), one perpendicular to it (Side Scatter) and fluorescent detector FL2 for PI fluorescence, measuring cell size, density, and fluorescence respectively.

The following settings were optimized for this assay:

Parameter	Detector	Voltage	Amp Gain	Mode
P1	FSC	E-1	3.94	Linear
P2	SSC	304	1.00	Linear
P3	FL1	535	N/A	Log
P4	FL2	443	N/A	Log

Events counted: 10000

2.9.3 Data Analysis

Data analysis was performed with the Window Multiple Document Interface software (WinMDI) version 2.8. For cell cycle analysis, forward scatter and side scatter dotplots were created with WinMDI software to define studied cell population and exclude debris and dead cells. The studied cell population were then plotted against cells with PI staining, with the relative DNA content which determined the proportion of cells in G1, G2 and S phase. Cells in G1, G2 and S phase were plotted on a frequency histogram and cell cycle areas designated with the use of marker settings with software calculated percentage of cells in each phase.

The data was transferred and interpreted using Microsoft Excel software. The mean and standard deviation of the percentage of cells in each phase of cell cycle were calculated. Final data represented the mean of three experimental repeats, each experiment containing 3 replicates, with SEM.

2.9.4 Optimising Flow Cytometry

Population gating was necessary to establish the cell cycle phases and discriminate doublets by relying upon cellular DNA content (Nunez, 2001). A third population was noted in the NUOC-1 cell line and hypothesised to be due to NUOC-1 tetraploidy (Figure 2-7). This work was carried out with Eleanor Earp (MRes 2013). Cell incubation in serum-starved conditions has been shown to arrest cells in G1 phase. To assess if the third population noted was the G2/M phase of multiploid cells, NUOC-1 cells were serum-starved for 3 doubling times prior to assessment of cell-cycle.

NUOC-1 cells grown in FCS-free media displayed unaltered cellular DNA populations, which did not aid in identifying the third population, but gave an insight into their possible resistance to starvation.

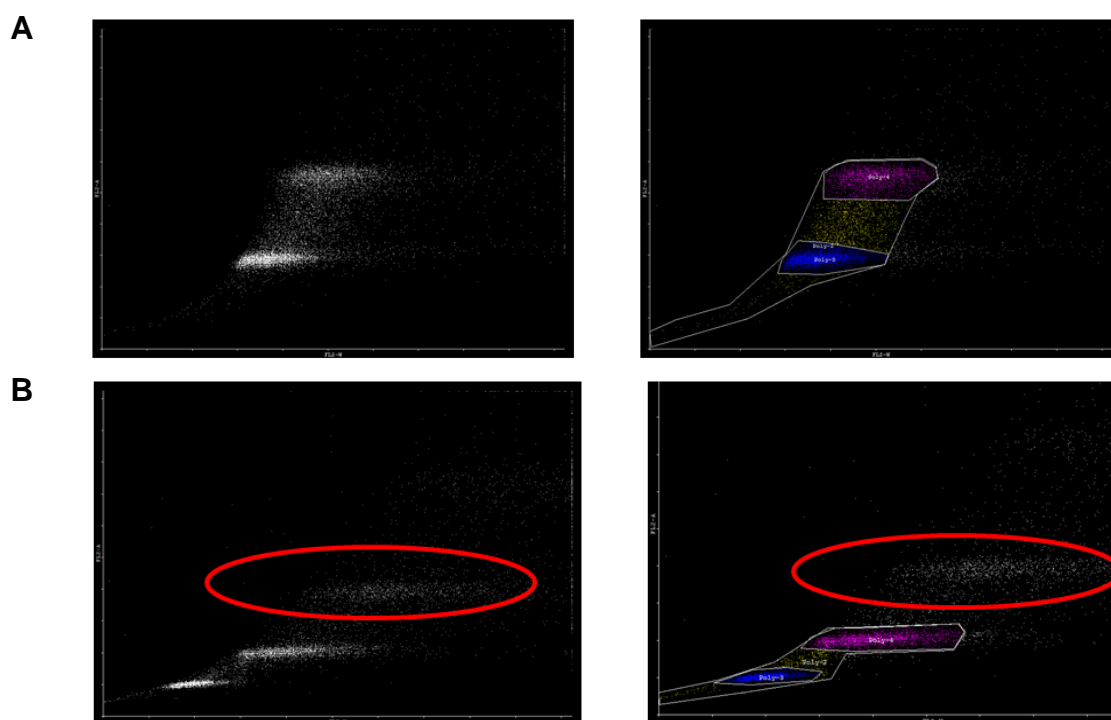


Figure 2-7 Gating for flow cytometry.

A. OSEC-2 and **B.** NUOC-1 cell line gating using cyflogic software. A third population (circled in red) appears in NUOC-1 cells that is absent from OSEC-2, hypothesised to be derived from tetraploidy.

2.10 Poly (ADP-ribose) Polymerase Assay

Poly(ADP-ribose) (PAR) is quantified following maximal stimulation of a defined quantity of permeabilised cells. Excess NAD⁺, a substrate for the PARP enzyme, alongside oligonucleotides that induce DSBs, thereby activating PARP, are added. Cells are blotted on to a membrane which is treated with anti PAR primary antibody followed by secondary antibody conjugated with HRP. A chemiluminescence agent is added, an image is captured and PARP activity is assessed as 'luminiscent arbitrary units'. This assay has been previously validated in our laboratory (Plummer et al., 2005) to GCLP standard and used as a pharmacodynamic endpoint for clinical trials (Plummer et al., 2008).

NICR standard operating procedure No.212 (revision 3) was followed. PCO cell pellets and one 10⁶ cell aliquot of L1210 (quality control) were defrosted, washed twice in ice cold PBS and permeabilised with digitonin (0.15 mg/ml) at RT for 5 min.

Nine volumes of ice-cold isotonic buffer (7 mM HEPES, 26 mM KCl₂, 0.1 mM Dextran, 0.4 mM EGTA, 0.5 mM MgCl₂, 45 mM sucrose dissolved in distilled water, pH 7.8) was added and the samples placed on ice. A 10 µl cell suspension was mixed 1:1 (v/v) with trypan blue and permeabilised cells counted. The cell suspension was diluted with isotonic buffer to a density of 6×10^5 cells / ml. Duplicate samples (1000 cells) were exposed to oligonucleotide at 200 µg / mL in the presence of excess NAD⁺ (7 mM) in reaction buffer (100 mM Tris–HCl, 120 mM MgCl₂, pH 7.8) for 6 min at 27°C, alongside unreacted cells. 500 µl of the PARP reaction mixture was loaded alongside PAR standards into a 48-well manifold containing a nitro cellulose Hybond-N membrane and drawn through using a vacuum pump. 400 µl 10 % trichloro acetic acid / 2 % sodium pyrophosphate followed by 800 µl 70 % ethanol were drawn through the membrane as a fixative. The membrane was PBS washed 3 times and blocked (5 % milk powder in 0.0005 % Tween-20 PBS) for 1 hr. Mouse monoclonal anti-PAR 10H antibody (1:1000) was added for 1 hr, followed by polyclonal goat anti-mouse IgG anti-PAR HRP antibody (1:1000). Secondary antibody was followed by Amersham ECL detection fluid and chemiluminescence recorded by Fujifilm LAS 3000 imager then analysed using Aida Image Analyser software (version 3.28.001).

2.10.1 Data Analysis

A standard curve was constructed by non-linear regression of the PAR standard values using Graph Pad Prism 6. The resulting equation relating PAR to chemiluminescence ($R^2 \geq 0.9$) was used to calculate the amount of PAR present in each well. Results were expressed as picomoles of ADP-ribose monomer incorporated per 10^6 permeabilised cells. Results were normalised to PAR in internal controls (L1210 cell line) to account for inter-assay variability.

2.11 Gene Expression Analysis by Quantitative Real-time PCR

In order to determine whether the expression of particular genes involved in DNA DSB repair was altered in PCO cultures relative to control cell lines and in knockdown and resistant derivatives relative to paired parental cell lines, gene expression analysis was performed by real time quantitative PCR using Syber green chemistry. This technique involves two stages; firstly, mRNA is reverse transcribed to cDNA; and secondly, PCR is performed using primers specific for the gene of

interest, during which accumulation of the PCR products is detected in real-time. This is achieved through the binding of syber green to double strand DNA and emitting a fluorescent signal when it is bound. As the target sequence is amplified the fluorescent signal amplifies. With progressive PCR cycles an exponential phase is reached where the quantity of product and associated magnitude of fluorescence of an intercalated reporter molecule doubles with each successive cycle. During this phase an absolute quantification of the amount of product can be calculated through comparison with a concurrently amplified standard curve of known concentrations. Multiple samples can be compared by normalising quantities to that of a 'housekeeping gene' assumed to be present at the same level in all samples. Relative quantification of expression of the target genes was performed and normalised to GAPDH for all cell line and PCO samples and HPRT1 for FFPE extracted RNA.

2.11.1 RNA Extraction and Quantification

For each cell line and primary culture, a frozen cell pellet obtained from a confluent 75 cm³ flask was thawed on ice. Total RNA was extracted from thawed cells using an RNAeasy® Mini kit (Qiagen, Crawley, UK) according to the manufacturer's protocol. Briefly, cells were lysed and homogenised, then RNA was bound to an RNAeasy® silica gel membrane in spin-column format, after which contaminants were removed by washing in the provided buffers. RNA was eluted in 30 µl nuclease-free distilled water (dH₂O) (Invitrogen Life Technologies). Quantification of RNA was performed using a NanoDrop® ND-1000 spectrophotometer (Thermo Scientific, DE, USA) which measures the absorbance of UV light at 260 nm passed through a 1 µl aliquot of extracted RNA, and performs the necessary calculations according to the Beer Lambert Law to provide the RNA concentration (in ng / µl).

2.11.2 RNA Extraction from FFPE Tissue

Samples were extracted from 10 µm sections cut from the donor FFPE tissue blocks. Extractions were performed using the All Prep DNA / RNA FFPE Kit (QIAGEN, Venlo, Netherlands) as per the manufacturer's instructions. Briefly, samples were deparaffinised twice in xylene and washed in 100 % ethanol. Tissues were lysed in the supplied Proteinase K and incubated at 80 °C to partially reverse formaldehyde crosslinking. The sample was added to the supplied spin column and centrifuged with

720 µL of 100 % ethanol to bind the RNA to the spin column membrane. Incubation with DNase1 was performed to remove contaminating DNA. Following subsequent wash and purification steps, RNA was eluted by centrifugation with 14 µL of RNase free water (Life Technologies, CA, USA).

2.11.3 Reverse Transcription of RNA into cDNA

2 µg of the total RNA was incubated at 65 °C for 5 min followed by 37 °C for 5 min prior to addition of Promega MMLV-reverse transcriptase master mix (4 µl 5 x Moloney Murine Leukaemia Virus RT buffer, 2 µl 4 mM dNTPs, 1 µl 50 µM Oligo dT15 and 0.3 µl MMLV reverse transcriptase) and incubation at 37 °C for 1 hr followed by 95 °C for 5 min. A blank reaction was also prepared using nuclease-free dH₂O in place of RNA, to ensure no contamination of reagents. Assuming a reverse transcription efficiency of 100 %, this yielded 20 µl of cDNA at the concentration of 100 ng / µl. This was subsequently adjusted to 20 ng / µl by addition of 80 µl nuclease-free dH₂O and stored at -20 °C until required.

2.11.4 Real-time PCR Setup

PTEN primer sequences were purchased from Sigma-Aldrich. All other primers were purchased from Sigma Genosys and all primers were diluted to 100 µM as per the manufacturer's instructions. Working stocks were diluted 1:40 by addition of 390 µl dH₂O to 10 µl of stock solution and aliquoted. Both stocks were stored at -20 °C. Sequences of primers are detailed in Table 2-9. 2 µl of cDNA was loaded on to a 386 well plate in triplicate with Invitrogen SYBR green Master Mix (dNTPs, optimised buffer, UDG, ROX reference dye, AmpliTaq DNA polymerase UP and SYBR green ER dye) and 2.5 mM of the appropriate forward and reverse primers. For each gene two controls were also prepared, using a blank reverse transcription reaction and a nuclease free dH₂O in place of cDNA, to ensure no contamination of reagents. Assays (and controls) were setup in triplicate for each gene in each cell line. Samples were run on an AbiPrism Applied Biosystems real time PCR machine for 10 min at 95 °C, 40 cycles (15 s at 95 °C, 60 s at 60 °C), 15 s at 95 °C, 15 s at 60 °C, 15 s at 95 °C.

Following completion of thermal cycling, detected fluorescence was converted to a Ct value for each reaction using the SDS2.3 software, using standard parameters. The

means of the triplicate Ct values generated for each gene (in each cell line) were used for quantification of gene expression, as described below.

Table 2-9 Primers used for PCR.

Primer Set	Sequence	Annealing temp
DNA-PKcs	5' – CTAACCTCGCCAGTTTATCAATC – 3' 5' – TTTTCCCAATCAAAGGAGGG – 3'	55
DNA-PKcs	5' – GATCTGAAGAGATATGCTGTG – 3' 5' – GTTTCAGAAAGGATTCCAGG – 3'	55
Ku70	5' – AAGAAGAGTTGGATGACCAG – 3' 5' – GTCACCTCTGTATGTGAAGC – 3'	55
Ku80	5' – TTCATTCACTGAGAGTCTGAG – 3' 5' – CGATTTATAGGCTGCAATCC – 3'	55
ATR	5' – CCTTCAGATTTCCCTTGAATAC – 3' 5' – GCAGTTCATGTTTTGATGAG – 3'	55
ATR	5' – GTAACAGAGTTCCCAAGATTC – 3' 5' – TCAAGTTCCTACAGAAGAGG – 3'	55
LIG IV	5'- TGAGTGGAAACAGATAGCCAGCCAA-3' 5' – ATTACACAGTACGTGTCTGGGCCT-3'	55
XRCC4	5'-CTGAAATGACTGCTGACCGAGATCCA-3' 5'- CTGAAGCCAACCCAGAGAGATCAGTT-3'	55
PTEN	5' – CAGAGCCATTTCCATCCTGC – 3' 5' – CATTACACCAGTTCGTCCCTTTC – 3'	55
PTEN	5' – CATGTTGCAGCAATTCAC – 3' 5' – GGTATGAAGAATGTATTTACCCA – 3'	55
PTEN	5' – CCACAAACAGAACAAGATGCTAA – 3' 5' – CATGGTGTTTTATCCCTCTTGAT – 3'	55
HPRT1	5' – TTGCTTTCCTTGGTCAGGCA – 3' 5' – AGCTTGCGACCTTGACCATCT – 3'	55
HPRT1	5' – TGAACGTCTTGCTCGAGATGTG – 3' 5' – CCAGCAGGTCAGCAAAGAATTT – 3'	55
HPRT1	5' – TTGTAGCCCTCTGTGTGCTCA – 3' 5' – TTTTATGTCCCCTGTTGACTGG – 3'	55
GAPDH	5' – CGACCACTTTGTCAAGCTCA – 3' 5' – GGGTCTTACTCCTTGAGGC – 3'	55
ARID1A	5' – TATGGAGGTCCTTATGACAG – 3' 5' – ATTGCCATAGGAATCATGTC – 3'	55
	5' – CCTTCTCTCCTCATACCTC – 3' 5' – CTTGATTGGTTCATGGAAGG – 3'	55
	5' – GGATTAATAGTATGGCTGGC – 3' 5' – TYGGATTTGGATTCTGTCTTG – 3'	55
P53	5' – CGAGCTGTCTCAGACACTGG – 3' 5' – CCTTGTCTTACCAGAACGTTG – 3'	58
	5' – CATGGGACTGACTTTCTGCTCTTG – 3'	55

5' – CGGGGACAGCATCAAATCATC – 3'	
5' – GTTCTGGTAAGGACAAGGGT – 3'	55
5' – ATACGGCCAGGCATTGAAGT – 3'	
5' – ATCTGTTCACTTGTGCCCTG – 3'	55
5' – CAACCAGCCCTGTCGTCTCTC – 3'	
5' – GCCTCTGATTCCTCACTGAT – 3'	55
5' – GGAGGGCCACTGACAACCA – 3'	
5' – AAGGCGCACTGGCCTCATCTT – 3'	60
5' – CAGGGGTCAGCGGCAAGCAGA – 3'	
5' – GAGCCTGGTTTTTTAAATGG – 3'	60
5' – TTTGGCTGGGGAGAGGAGCT – 3'	
5' – AGCGAGGTAAGCAAGCAGG – 3'	55
5' – GCCCCAATTGCAGGTAAACAG – 3'	
5' – CTTCTCCCCCTCCTCTGTTGC – 3'	60
5' – GAAGGCAGGATGAGAATGGA – 3'	
5' – TGGTCAGGGAAAAGGGGCAC – 3'	58
5' – GAGAGATGGGGGAGGGAGGC – 3'	

2.11.5 Data Analysis

Relative quantification using the $2^{-\Delta\Delta Ct}$ method (Livak and Schmittgen, 2001) was performed to determine the expression level of each gene of interest. Briefly, analysis by this method first involved normalisation of the expression of each gene of interest to the expression of house-keeping gene in all cell lines. The normalised expression levels of genes of interest were then compared to control cell lines, generating values representing fold change in expression for each gene. All calculations were performed using Microsoft Excel. The entire investigation was repeated a total of three times, using new frozen cell pellets each time.

2.12 RNA Genome Expression Arrays

RNA was extracted as described in section 2.7.1, quality checked, then processed by the Oxford Genomics Centre (Oxford, UK) using Illumina Genome Studio and HumanHT 12v4.0 R1 15002873 array, as per manufacturer's instructions.

RNA concentration and purity was checked by Agilent RNA bioanalyser and RNA 6000 Nano Lab chip kit (Agilent Technologies, USA) as per manufacturer's instructions. Briefly, 2 μ l samples of concentrated RNA extract are treated for 2 min at 70 °C before adding 1 μ l aliquots to the Agilent RNA chip. A 6-peak RNA nano ladder is included in the chip for control. Data analysis was done using the 2100 Expert software. Good quality RNA was verified by the presence of a sharp

distinction at the small side of both the 18 S and 28 S ribosomal RNA bands and peaks. Any smearing or shouldering to the rRNA bands or peaks was indicative of RNA degradation. An RNA integrity number (RIN) of >8.0 was considered satisfactory.

The HumanHT-12 v4 Expression BeadChip consist of oligonucleotides immobilised to beads held in microwells on the surface of an array substrate and provides genome-wide transcriptional coverage of well-characterized genes, gene candidates, and splice variants, with high-throughput processing of 12 samples per BeadChip. Each array on the HumanHT-12 v4 Expression BeadChip targets more than 47,000 probes derived from the National Centre for Biotechnology Information Reference Sequence (NCBI) RefSeq Release 38 (2009). Labelled cRNA are detected by hybridisation to 50-mer probes on the Beadchip. After washing and staining steps using the Direct Hybridization Assay, beadchips are scanned on the HiScan or iScan systems.

2.12.1 Data Analysis

Arrays processing, background correction, normalisation and quality control checks were performed using the R package 'Lumi'. Probes intensity values were converted to VSD (variance stabilized data) using variance stabilising transformation. The robust spline normalisation (RSN) was used as an array normalization method. Irrelevant samples, poor quality probes (detection threshold < 0.01), and probes that are not detected at all in the remaining arrays were removed prior downstream analysis. The remaining probe normalised intensity was used in the differential expression analysis. Differential expression analysis was performed using the R package 'Limma', and p values were adjusted to control the false discovery rate (FDR) using the Benjamini–Hochberg method.

Illumina Genome Studio Gene expression software is used to extract relative gene expression across samples, clustering them into differential groups. The comparative Ct ($\Delta\Delta\text{Ct}$) method was used to assess the expression level of components of each pathway relative to endogenous controls normalised to the reference panel. The fold change differences in expression of each gene between sample categories (HRC and HRD; NHEJC and NHEJD) was calculated.

2.13 DNA Sequencing

Sequencing of *TP53* and *ARID1A* was performed by PCR amplification and Sanger sequencing.

2.13.1 DNA Extraction and Quantitation

Frozen cell pellets consisting of $\sim 5 \times 10^6$ cells were thawed and resuspended in 100 μ l PBS. Genomic DNA was extracted using a QIAmp DNA Mini Kit (Qiagen) according to the supplied manufacturer's protocol. Briefly, DNA extraction was achieved through binding of DNA to a QIAmpR silica gel membrane (in spin column format) after which contaminants were removed by washing using the provided buffers. DNA was eluted in 200 μ l Buffer AE [10 mM Tris-CHL, 0.5 mM EDTA, pH 9.0], quantification of DNA was performed using a NanoDropR ND-1000 spectrophotometer which measures the absorbance of UV light at 260 nm passes through a 1 μ l aliquot of extracted DNA, and performs the necessary calculations according to the Beer Lambert Law to provide DNA concentration (in ng / μ l).

For each sample, a 20 μ l aliquot of DNA at a concentration of 100 ng / μ l was prepared using buffer AE and stored at 4 °C for use in PCR reactions. Remaining DNA was stored at -20 °C.

2.13.2 PCR Amplification

PCR primer sequences are shown in Table 2-9. PCR reaction conditions were the same for each gene/exon and consisted of 1 x ReddyMix PCR buffer (Thermo Scientific), 10 pmol primers, 0.2 mM (each) dNTPs (Invitrogen Life Technologies), 1.5 mM MgCl₂, 0.5 units ThermoPrimeTaq DNA polymerase (Thermo Scientific) and 100 ng cDNA in a total volume of 10 μ l. For setup of reactions, the appropriate volume of PCR mastermix was initially prepared and 19 μ l was dispensed into the appropriate number of wells on a 96 well PCR plate on ice. To this, 1 μ l of 100 ng / μ l DNA was added. Controls were also prepared using nuclease free dH₂O in place of DNA, to ensure no contamination of reagents. Thermal cycles were performed as follows: 1 min at 94 °C, 40 cycles (30 s at 94 °C, 30 s at 55 °C, 30 s at 72 °C), 5 min at 72 °C.

In order to confirm successful PCR amplification of exons, a 5 μ l aliquot of each reaction was assessed using GelRED stained agarose gel electrophoresis as described in section 2.4.4. and 15 μ l of PCR reactions were diluted by addition of 85

µl of dH₂O and sent for Sanger sequencing (Beckman Coulter Genomics). The samples were analysed with mutation surveyor (Softgenetics) and mutations were searched for in the literature using Cancer Gene Census of the Catalogue of Somatic Mutations in Cancer (COSMIC) database (Wellcome Trust Sanger Institute, 2013). Both forward and reverse sequences were analysed to ensure accurate coverage of entire exons.

2.13.3 Whole exome sequencing

DNA was extracted from parent and resistant cell lines as previously described. Whole exome sequencing was performed off site by Oxford gene technology (OGT) (Oxfordshire, UK). Briefly, Agilent SureSelect All Exon Plus v4+UTR was used for exome capture and Illumina HiSeq 2000 minimum (San Diego, CA) for 100 bp paired end sequencing. Multiple sample vcf files were created by OGT using individual raw bam files. Raw bam files were generated from the sequencer and contained the whole sequenced data aligned to the reference genome of the parental cell line. Genome Analysis Toolkit (GATK; Broad Institute) was used for data quality assurance as well as variant discovery. Variant characterization, including filtering, annotation, classification, prioritization and inheritance pattern analysis was performed using SNP & Variation Suite (SVS) v8.1.5 (Golden Helix, Inc., Bozeman, MT, www.goldenhelix.com). Briefly, quality-control metrics (QC) were set to only retain variants in the positions with Read Depth ≥20 and Genotype Quality ≥20. Variants were classified, annotated, and functionally profiled in SVS v8.1.5 using multiple publicly available databases. The impact of the mutations on protein function was evaluated by database of non-synonymous functional predictions (dbNSFP). Functional predictions were performed using track of SVS for SNPs, and Indel SIFT webtool for Indel mutations (http://sift.bii.atar.edu.sg/www/SIFT_indels2.html). These analyses were carried out by OGT.

To identify those mutations that were of potential importance to the chemo-resistant phenotype from the data received, a selection criteria was applied. Firstly known SNPs were excluded during the analysis. Secondly the frequency of mutation reported in both parent and resistant lines; mutations which were present in >5 % of read in the parent line were excluded. Additionally, only mutations that were present in more than 25 % of reads (and therefore 50 % of cells, assuming heterozygosity) in

the resistant lines, and were either not observed in parental cells or had more than a 3 fold increase in frequency, were taken forward for further analysis.

2.14 SNP Array Analysis

SNP arrays were performed on NUOC-1 cell line subpopulations and matched genomic DNA. SNP arrays assess the expression of both SNPs and non-polymorphic sites distributed throughout the entire genome using probes hybridised to a chip. This data can be used to demonstrate copy number aberrations (CNAs) in individual samples, indicated by the deletion or amplification of particular probes. It can also reveal regions of copy-neutral loss of heterozygosity (cn-LOH) by comparing of SNP genotype to those of matched germline DNA. SNP arrays were performed offsite by Almac Diagnostics Ltd. (Craigavon, UK) using the Affymetrix SNP 6.0 platform. The SNP 6.0 array includes more than 906,600 SNPs and 946,000 non-polymorphic probes.

For SNP array analysis DNA was extracted using QIAmp DNA Kit as per the manufacturer's instructions. A minimum of 10 µl of DNA at a concentration of 50 ng / µl was analysed.

2.14.1 Data Analysis

Raw array-generated data in the form of .CEL files were received from Almac Diagnostics Ltd. Processing of raw data to identify CNAs and regions of cn-LOH in each samples was kindly performed by Prof J.M. Allan using Genotyping Console v4.0 (Affymetrix, Ca, USA).

The work flow for data processing briefly involved initial generation of SNP genotype calls using the birdseed v2 algorithm. This was followed by quantile normalisation of data and copy number and LOH analyses (via Hidden Markov Model) using default software settings (with regional GC correction applied). Matched germline DNA was used as reference model for LOH analysis. Segment analysis of CN data was performed to identify regions of CAN (with detection thresholds set to exclude regions smaller than 100 kb and involving fewer than 5 markers).

CNAs and regions of LOH were compared between sub-populations and parent line of NUOC-1 cell line, using affymetrix Genotyping Console Browser (version 1.0.12).

This also allowed identification of genes within affected regions (of CAN or LOH) based on annotations taken from the NCBI RefSeq database.

Quality control assessment of data was performed by determining the call rate at control SNPs, and by measurement of concordance between sub populations and parent line.

2.15 G-band Karyotyping

Karyotyping was performed offsite by the Cancer Cytogenetics department at Newcastle University, according to established protocols. Briefly, tetraphase chromosome spreads were prepared by incubating proliferating cells with 100 ng/ml colcemid for 4 h followed by resuspension in 75 mM KCl for 7 min. Cells were fixed by resuspension in 3:1 methanol:acetic acid before karyotyping. Slide-fixed cells were incubated overnight at 60 °C and G-banded by soaking in the trypsin solution (1.9 mg/ml trypsin, 74 mM NaCl, 0.469 mg/ml NaH₂PO₄ and 0.937 mg / ml Na₂HPO₄) for 10 s and in the staining solution [(8 ml Giemsa stain, 0.5 ml Leishman stain and 40 ml Gurr buffer (0.469 mg / ml NaH₂PO₄ and 0.937 mg / ml Na₂HPO₄)] for 3 min. Four metaphase chromosome spreads were analysed for each population and the karyotypes recorded.

2.16 Fluorescence in Situ Hybridization for c-MYC

Fluorescence in situ hybridization (FISH) is a cytogenetic technique that uses fluorescent probes that bind to only those parts of the chromosome with a high degree of sequence complementarity. It is used to detect and localise the presence or absence of specific DNA sequences on chromosomes. Fluorescence microscopy can be used to find out where the fluorescent probe is bound to the chromosomes. FISH analysis was performed offsite by the Cancer Cytogenetics department at Newcastle University, according to established protocols. Briefly, the Cytocell MYC 'breakapart' Probe set (Figure 2-8) was hybridised to nuclei as recommended by the suppliers. Slides were heated to 72 °C for 5 min and then incubated for 24 hr at 37 °C in a humidified hybridisation chamber (HYBrite; Abbott Molecular). After hybridisation, slides were counterstained with 4',6-diamidino-2-phenylindole (Vector Laboratories, Peterborough, UK). FISH was scored with an Olympus BX-61 fluorescence microscope (Olympus, Southend-on-Sea, UK) with a x 100 oil objective. Images were analysed using the CytoVision 7.2 SPOT counting system (Leica Microsystems,

Gateshead, UK). A minimum of 100 nuclei were scored per test by two independent analysts.

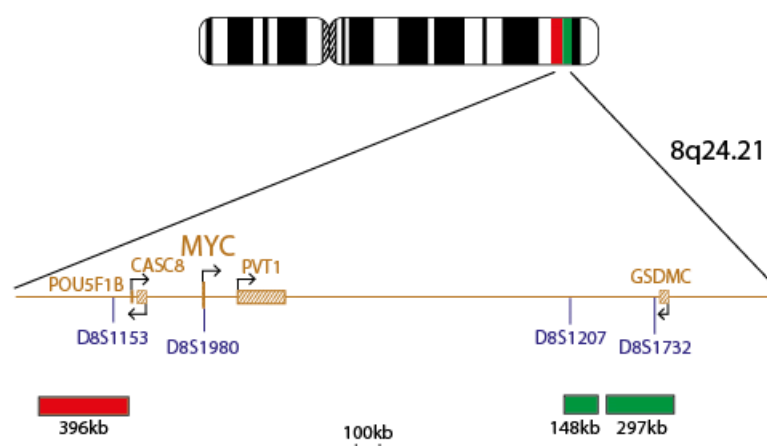


Figure 2-8 Cytocell MYC 'breakapart' probe set.

2.17 Mouse experiments

To assess the ability of NUOC-1 cells to generate tumours, their ability to form explants in mice was assessed. The mouse injections and monitoring was kindly performed by Huw Thomas. All animal studies were performed in compliance with the UK Home Office Animals (Scientific Procedures) Act 1986 for the use of animals in scientific procedures, and have undergone local ethical review; project license number PPL 60/42222.

2.17.1 Subcutaneous Injection

Exponentially growing NUOC-1 cells were trypsinised and resuspended at a concentration of 2×10^8 / ml in 500 μ l 10 % FCS RPMI 1640, mixed with 50 % (v/v) matrigel (Becton Dickinson) making a total volume of 300 μ l. Cells were transferred on ice to the animal house and injected subcutaneously into the right flank of 5, 8-10 week old mice under sterile conditions. Mice were then monitored for tumour growth and wellbeing for a maximum of 100 days.

2.17.2 Intraperitoneal Injection

Intraperitoneal (IP) injection of cells better represents ovarian cancer in humans, and therefore, NUOC-1 cells were injected IP into 5 further mice.

2.17.2.1 *Cell Labelling*

To allow monitoring of IP injected NUOC-1 cells, they were first labelled with luciferase by transfection of a vector containing luciferase. The vector was kindly gifted by Dr Alex Elder. An 800 µg / ml stock solution of hexadimetrine bromide was prepared by dissolving 800 µg hexadimetrinebromide in 1 ml sterile dH₂O. The stock solution was filter sterilised using a 0.2 µM filter (VWR International Ltd.), stored at 4 °C and used neat, as required.

Cells were seeded at 5×10^5 / 6 well plate, and after 24 hrs incubation (to allow adherence) 100 µl of viral vector, and 10 µl 8 µg/ml of hexadimetrine bromide was added to the well. A control well had hexadimetrine bromide added only. The plate was then wrapped in paraffin and centrifuged at 900 x G for 50 min at 34 °C; following which the cells were incubated at 37 °C / 5 % CO₂ until confluent. Control cells were treated in the same way. Cells were incubated and passaged as required to reach the required cell numbers.

2.17.2.2 *Confirming Cell Transfection*

Once cell populations had resumed normal exponential growth, transduction efficiency was determined by assessment of the expression of GFP by flow cytometry (the principles of flow cytometry are described in section 2.8). A suspension containing 2×10^5 cells was dispensed into a BD Falcon™ capped polystyrene tube. Cells were centrifuged at 450 x G for 4 min, supernatant discarded, and cells resuspended in 500 µl PBS. Flow cytometry was performed using a FACSCalibur flow cytometer with BD CellQuest Pro software (BD Biosciences) using pre-optimised instrument settings for detection of GFP fluorescence. A total of 10,000 cells were assessed from each transduced cell population. For assessment of GFP-expressing cells, cell debris and dead cells were first excluded from the analysis based on forward and side scatter signals. Percentage of GFP-expressing cells in the remaining cell population was then determined based on detection of GFP fluorescence.

2.17.2.3 *Injections into Mice*

Cells were trypsinised, washed in PBS, then 5×10^6 cells were resuspended in 300 µl PBS. This was transferred to the animal house and injected into the peritoneum of

five mice by Huw Thomas. The animals were housed under sterile conditions in a laminar flow environment with ad-lib access to food and water.

2.17.2.4 *Imaging Mice*

Tumour formation was assessed by non-invasive whole-body imaging at 0, 10 and 55 and 85 days after implantation using the IVIS Spectrum Imaging system (Caliper Life Sciences, Hopkington, MA, USA). Animal handling was kindly performed by Dr Helen Blair. Mice were injected IP with 3 mg / mouse D-luciferin (Promega) solution 10 min before being anaesthetized for the imaging procedure. Photon emission was captured and expressed in p/s/cm²/sr using Living Image software (version 4.3.1., CaliperLifeSciences). Mice were labelled using ear notching to ensure fluorescence in each mouse could be followed over time. The mice were then returned to an incubator to recover.

2.18 Generation of Stable PTEN, DNA-PKcs and ATR Defective Cell Lines using Short Hairpin RNA-Mediated Gene Knockdown

Stable knockdown subclones of cell lines OSEC-2 and NUOC-1 were generated using Short Hairpin RNA (shRNA)-mediated gene knockdown. In this process, lentiviral particles are used to deliver shRNA constructs into cells which become incorporated into the host genome. Transcription by RNA polymerase III (due to the H1 promoter sequence included in the construct) results in continual production of shRNA molecules. These molecules are cleaved to produce small interfering RNA (siRNA) molecules. The siRNA molecules become bound to the RNA-induced silencing complex molecules, which subsequently binds to and cleaves mRNA molecules which match the siRNA, hence permanently blocking expression of the target gene.

2.18.1 *shRNA Constructs*

Pre-packaged lentiviral transduction particles containing verified MISSION®shRNA constructs, targeting the coding domain sequence of DNA-PKcs and ATR and PTEN (in pLKO.1-puro plasmid vectors) were purchased from Sigma-Aldrich, UK. The sequences of the shRNA constructs were not disclosed by the supplier. In addition, Lentiviral transduction particles containing a random shRNA construct confirmed not to target any known human or mouse genes (MISSION® Non-Target shRNA Control

Transduction Particles), were also purchased to use as controls for transduction. All purchased lentiviral particles were received as frozen stock and stored at -80 °C. Upon first use, particles were aliquoted appropriately and stored at -80 °C until required.

2.18.2 Assessment of Puromycin Sensitivity

The pLKO.1-puro plasmid used as a vector for the shRNA constructs contains a puromycin resistance gene, meaning the antibiotic can be used to select cells which have been successfully transduced. However many cell lines are inherently sensitive to the effect of puromycin, hence preliminary investigations were necessary to establish the minimum puromycin concentration required to kill all non-transduced cells. The following investigation was performed for OSEC-2 and NUOC-1 cells.

A cell suspension at a density of 7.5×10^3 cells / ml was established in RPMI medium (20 ml). 2 ml of solution was added to each well of a sterile 6 well culture plate and allowed to adhere overnight. An appropriate volume of working puromycin solution was then added to each well. Puromycin concentrations of 0 (control), 2, 4, 6, 8 or 10 µg / ml were tested, as recommended by the manufacturer (Sigma-Aldrich). Plates were incubated at 37 °C / 5 % CO₂ (33 °C for OSEC-2) and assessed microscopically each day for cell death.

In the case of both cell lines 72 hrs in culture following puromycin administration, all cells in all treated cultures were found to be dead upon microscopic inspection. Therefore, for both cell lines, selection of transduced cells was performed using media supplemented with puromycin at a concentration of 2 µg / ml.

2.18.3 Assessment of Transduction Efficiency

Prior to performing transduction with lentiviral particles containing shRNA constructs, it was necessary to determine the optimum multiplicity of the infection (MOI) required for transduction of each cell line using MISSION®TurboGFP™ Control Transduction Particles. This also served as a control to determine whether the transduction process itself had any effect on cell growth, so that these could be separated from the effects of shRNA-mediated gene knockdown. Lentiviral transduction of OSEC-2 and NUOC-1 cells was performed using MISSION®TurboGFP™ Control

Transduction Particles according to Section 2.17.4. MOIs of 0 (Control), 1, 2 and 5 were prepared as recommended by manufacturer (Sigma-Aldrich).

Once cell populations transduced with MISSION®TurboGFP™ Control Transduction Particles had resumed normal exponential growth following puromycin selection, transduction efficiency was determined by assessment of the expression of GFP by flow cytometry (as described in section 2.16.2). Expression of GFP was similar for all MOIs tested, in both cell lines. Based on the time taken to recover exponential cell growth MOI of 2 was selected for subsequent lentiviral transductions.

It was also noted at this point that the growth kinetics of transduced cells was not significantly different from non-transduced cells, demonstrating that the transduction process itself has no apparent effect on the growth of OSEC-2 cells. The transduction process did, however, slow the growth of NUOC-1 cells. Therefore, all comparisons were made between non target control samples and knockdown samples, to take into account the slowed cell growth due to the transduction process.

2.18.4 Lentiviral Transduction

Cells were seeded at a density of 1×10^5 per well in a sterile 6 well plate. After 24 hrs an appropriate volume of thawed lentiviral particle suspension was added directly to the cell suspension (Table 2-10). A normal control was prepared for each cell line / shRNA combination according to the same procedures, but without the addition of lentiviral particles. After 24 hrs incubation, the media was aspirated, washed with 2 ml of warm PBS and replaced by warmed 10 % RPMI media.

Table 2-10 Viral titres and required volumes for each ShRNA construct.

Construct	Viral Titre (TU/ml)	Volume to give MOI 2 (µl)
DNA-PK 6255	8.0 x 10 ⁶	25.0
DNA-PK 6256	1.3 x 10 ⁷	15.4
DNA-PK 6257	1.5 x 10 ⁷	13.3
DNA-PK 6258	4.5 x 10 ⁶	44.4
DNA-PK 6259	1.5 x 10 ⁷	13.3
ATR 10300	7.8 x 10 ⁶	25.6
ATR 10301	6.7 x 10 ⁶	29.9
ATR 10302	6.4 x 10 ⁶	31.3
ATR 39613	9.2 x 10 ⁶	21.7
ATR 39614	9 x 10 ⁶	22.2
PTEN 2745	1.7 x 10 ⁷	11.8
PTEN 2746	1.3 x 10 ⁷	15.4
PTEN 2747	1.4 x 10 ⁷	14.3
PTEN 2748	1.7 x 10 ⁷	11.8
PTEN 2749	1.6 x 10 ⁷	12.5

2.18.5 Selection of Transduced Cells

After 72 hrs incubation, the media was aspirated and replaced with 2 ml of 10 % RPMI media supplemented with 2 µg / ml puromycin. Cultures were incubated at 37 °C / 5 % CO₂ and selection media was replaced every 72 hrs until normal exponential cell growth had resumed. At this point, cell populations were deemed to consist entirely of transduced cells, given that only cells which had taken up a plasmid could survive in selection media due to acquired puromycin resistance.

Control non-transduced parental cell populations were treated in the same way as above, except normal 10 % RPMI culture media was used in place of selection media.

2.18.6 Assessment of Knockdown Efficiency

The efficiency of shRNA-mediated knockdown of target genes, relative to control non-transduced cells, was assessed by real time q-PCR and western immunoblotting according to the protocols described in sections 2.6 and 2.10. The cellular amounts of DNA-PKcs and ATR mRNA and proteins were also assessed in cells transduced with the non-target shRNA control to exclude any effects of transduction and shRNA processing on target gene expression.

2.19 Generation of Drug Resistant Cell Lines by Escalating Dosage

In order to model the development of chemo-resistance *in vitro*, HRD cell lines were cultured in the presence of escalating doses of either rucaparib or cisplatin, in an attempt to generate drug-resistant subclones for analysis of HR status and NHEJ status. PEO1 and UBW1-289 cell lines were used.

2.19.1 Concentration Finding Assay

In order to identify a suitable concentration for each drug in each cell line, concentration finding assays were performed by treating the cell lines with a range of concentrations of each drug, and LC₅₀ was selected as a starting concentration. Concentration finding assays were performed using SRB and clonogenics assays in all cases as described in section 2.3. The selected treatment doses are detailed in Table 2-11.

Table 2-11 Resistance development dosing.

Cell line	Treatment	Initial Dose	Dose Increment	Final Dose
PEO1	Rucaparib	1 µM	1 µM	20 µM
PEO1	Cisplatin	10 nM	0.2 µM	2 µM
PEO1	IR	5 Gy	5 Gy	Total IR of 60 Gy
UWB1.289	Rucaparib	1 µM	1 µM	20 µM
UWB1.289	Cisplatin	10 nM	0.2 µM	3 µM
UWB1.289	IR	5 Gy	5 Gy	Total IR of 60 Gy

2.19.2 Drug Dosing

For each cell line and drug combination, 1 x 10⁶ cells were resuspended in 5 ml of appropriate medium supplemented with the appropriate volume of drug, and transferred to a sterile 25 cm³ cell culture flask. At the same time, a similar culture was set up using medium supplemented with DMSO but no drug. Cultures were incubated at 37 °C / 5 % CO₂ and assessed at regular intervals for resumption of normal exponential growth (by microscopic appearance). Once normal growth had resumed in the dosed culture, the next drug dose was applied using the same procedure (Table 2-11).

2.19.3 Assessment of Resistance

Following recovery of exponential cell growth after the final drug dose, acquired resistance to the drug with which cells were treated and cross resistance was assessed relative to respective parental cultures using SRB and clonogenics assays.

2.20 Statistical Analysis

Statistical analysis was performed using GraphPad Prism version 6.00 (GraphPad Software, La Jolla California USA). Unpaired student *t* tests or Mann–Whitney tests were used depending on a D'Agostino & Pearson omnibus normality test. Multiple comparisons were performed using 1-way or 2-way Anova with appropriate multiple comparisons correction. All statistical tests were considered statistically significant if the *p* value was less than 0.05. Statistical tests were two-sided.

CHAPTER 3 FUNCTIONAL CHARACTERISATION OF OVARIAN CANCER MODELS

3.1 Introduction

The term 'ovarian cancer' represents a heterogeneous group of tumours in terms of histology, molecular characterisation, prognoses and clinical and pathological features (Vaughan et al., 2011, Kurman and Shih, 2010). The differences between type I and type II ovarian cancer biology and treatment are discussed in chapter 1. To investigate novel treatments in ovarian cancer, representative models are needed for the different groups. A number of experimental models for the study of ovarian cancer are available to the research community, however all have limitations.

Cell lines that are derived from tumours are the most frequently utilised models in cancer research. Existing human ovarian cancer cell lines possess the advantages of high proliferative capacity, clonogenicity and extended life span in culture. However, most have acquired significant genetic alterations from their cells of origin, loss of heterogeneity and are rarely derived from chemotherapy-naïve patients (Daniel et al., 2009, Domcke et al., 2013). Additionally, there is evidence to suggest that many cell lines contain significant misidentification, duplication, and loss of integrity (Korch et al., 2012, Ertel et al., 2006, Stein et al., 2004, Gillet et al., 2011, Sandberg and Ernberg, 2005).

Primary cells isolated from patients are often considerably different from established cell lines of similar origin. The ability to culture and characterise freshly isolated cancer cells from patients provides an important experimental system that has the potential to resemble the patient situation more accurately (Dunfield et al., 2002, Mukhopadhyay et al., 2010). However, primary cultures have slow growth rates and short life spans, which limit their use.

Mouse models have been extensively used in research. Genetically engineered mice (GEM) develop cancer either spontaneously (Hardisty, 1985) or following various 'environmental' exposures such as radiation (Vankranen et al., 1995). The most sophisticated animal models, have either knockout of tumour suppressor genes or overexpression of oncogenes (Jonkers and Berns, 2002, Frese and Tuveson, 2007). The drawback of GEM models is that they do not encompass a human origin and

different mutations in the same gene may elicit different phenotypes (Frese and Tuveson, 2007). Additionally, human cancers are thought to develop from a single mutated cell, whereas in GEM the oncogenic event is initiated simultaneously throughout the organ (Frese and Tuveson, 2007). The development of patient derived xenograft (PDX) models enabled *in vivo* assessment of tumour tissue and cell lines in immunocompromised mice (Kendall et al., 2006, Rubio-Viqueira and Hidalgo, 2009). The drawback of PDX models is the long graft latency, the specialised skill set which significantly increases the cost of research and varied engraftment success, which has been reported to be higher in more clinically aggressive tumours (DeRose et al., 2011, Loukopoulos et al., 2004). Furthermore, genetic alterations are more prevalent in engrafted tumours compared with their parental cancers (Ding et al., 2010), with less differentiated tumours being more prone to changes (DeRose et al., 2011).

The Helene Harris Memorial Trust meeting in 2004 (Balkwill et al., 2004), outlined a number of actions required to improve ovarian cancer outcomes. Development of more appropriate and better characterised experimental models was one of the actions and is the focus of this chapter.

3.2 Aims for Chapter 3

For this study two models for ovarian cancer were optimised. The first model was a primary ovarian cancer culture (PCO) model. PCO cultures are derived from ascitic fluid collected at the time of surgery for ovarian cancer. This model was previously established in the group (Mukhopadhyay et al., 2010, O'Donnell et al., 2014).

The specific aims of characterisation were:

- To optimise antigen expression characterisation and storage of PCO cultures.
- To assess the growth of PCO cultures.
- To assess HR function of PCO cultures.
- To assess PCO cultures sensitivity to rucaparib and cisplatin and correlate with HR function.

During this project one of the ascitic cultures (PCO 142) immortalised spontaneously. This novel cell line was named NUOC-1 and is the basis for the second model to be used. The specific aims were to perform the following:

- Molecular characterisation, including expression of surface antigens and receptors
- P53 function analysis
- PTEN functional analysis
- DNA repair assessment
- Drug sensitivity assessment
- Mutational analysis
- Assessment of tumourgenicity
- Copy number alterations analysis
- Clonal evolution assessment

3.3 Results

Between 2011 and 2013, ascites samples were collected from 78 patients. Samples were collected by me, Rachel O'Donnell and Angelika Kaufman. Patients enrolled in this study were treated at the NGOC at Queen Elizabeth Hospital, Gateshead. The histological diagnosis of ovarian cancer was confirmed by independent pathologists and surgical stage, grade and cell type were classified according to WHO and FIGO standards (Prat 2013). Demographic, surgical and pathological data was collected from the hospital and pathology databases (Table 3-1).

Ascites samples were collected at the time of surgery (65 patients, 83 %) or at the time of drainage of symptomatic ascites (13 patients, 16 %). Of the samples collected intra-operatively, 53 (82 %) were collected during primary surgery and 12 (18 %) during interval surgery following chemotherapy. Erythrocytes and cellular debris from ascites did not adhere to the culture flask and were removed following media change. Successful growth was achieved in 69 cases (88 %). Three cultures were discarded due to infection, three due to failed epithelial characterisation, and 5 cultures were excluded based on the pathology reporting non-ovarian cancer. 58 (74 %) cultures were used in further experiments.

Table 3-1 Patient characteristics for PCO culture samples.

Age at diagnosis	Median (range)	63 (43-85)
Histology	HGSOC	41
	Endometrioid / clear cell	6
	Mixed	2
	Mucinous	2
	Carcinosarcoma	2
	Low grade serous	1
	Non ovarian pathology	4
Stage	1	2
	2	2
	3 A	1
	3 B	1
	3 C	42
	4	6
	NA	4
Pre-op Ca125	Median	790
Type of surgery	Primary surgery	39
	IDS following NACT	17
	No surgery	2
Outcome of surgery	Complete	11
	Optimal	38
	Suboptimal	7
	No surgery	2

3.3.1 PCO Culture Characterisation

In general, the appearance of each culture was that of a cobblestone monolayer pattern (Figure 3-1.A), as previously described (Dunfield et al., 2002). As they approached senescence, cells developed a more mesenchymal phenotype, becoming elongated and exhibiting a markedly reduced growth rate.

3.3.1.1 Antigen expression in PCO Cultures

Ascitic fluid is composed of multiple cellular components, and in order to confirm exclusive growth of cancer cells, characterisation of cultured cells is required.

Immunofluorescent characterisation of the cultures was carried out using a panel of antibodies to detect expression of pancytokeratin, CA125, EpCAM, MOC-31, D2-40 and Vimentin (Figure 3-1.B-G). Cultures were rejected if they failed to demonstrate greater than 95 % cytokeratin positivity. This work was conducted by me, Rachel

O'Donnell, Michelle Dixon and Angelika Kaufmann. Further to expression of cytokeratin, the majority of PCO cultures expressed an epithelial marker (EpCAM or MOC31) or the ovarian marker (CA125) (Figure 3-1 and Table 3-2).

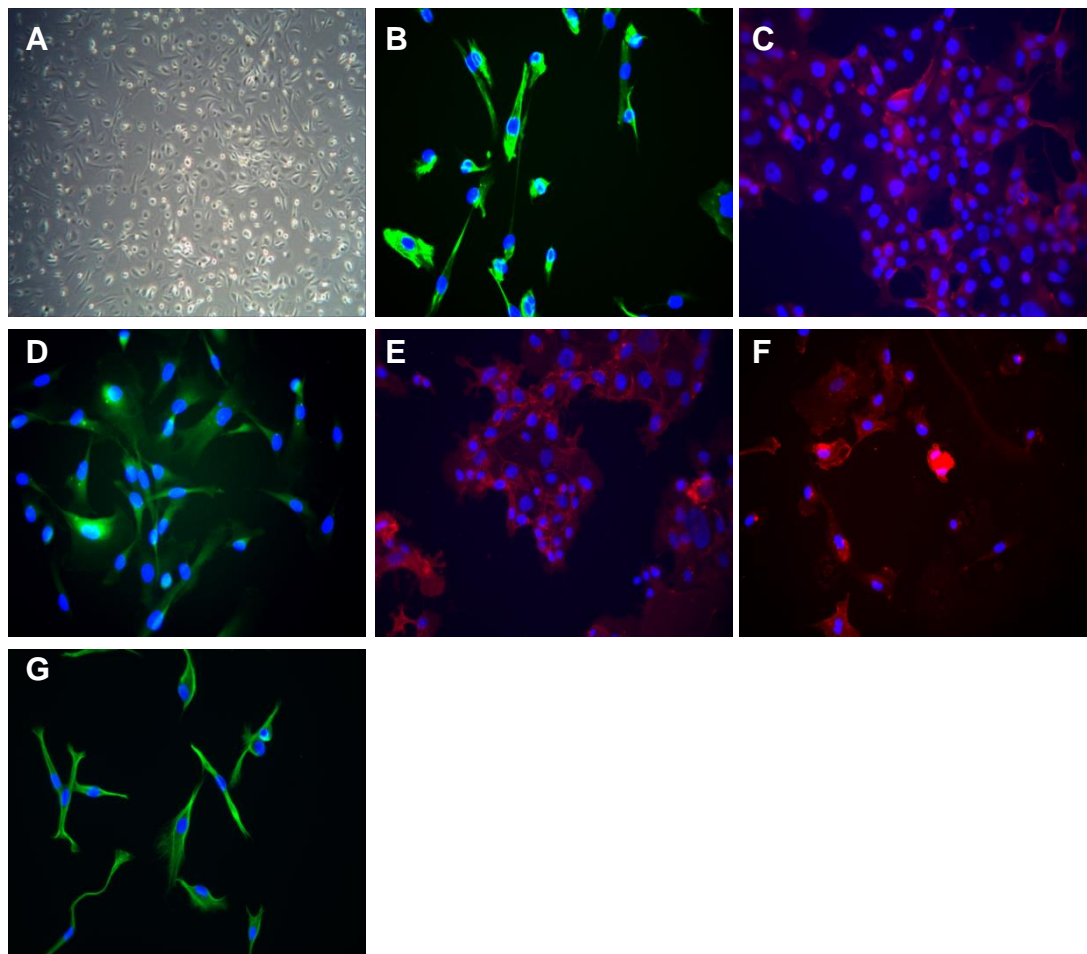


Figure 3-1 PCO characterisation panel.

A. Brightfield demonstrating cobblestone monolayer; immunofluorescent images with antibodies targeted against; **B.** FITC-anti-CK; **C.** Alexafluor 596 anti-CA125; **D.** Alexafluor 488 anti-EpCAM; **E.** Alexafluor 596 anti-MOC 31; **F.** Alexafluor 488 anti-Vimentin; **G.** Alexafluor 596 anti-D240 (PCO 160 – dysgerminoma).

Table 3-2 Summary of PCO antigen expression.

Tissue marker	Antigen	Number tested	Expression N (%)
Epithelial	CK	n=50	46 (100 %)
	EpCAM	n=38	13 (44.8 %)
	MOC31	n=29	11 (45.8 %)
Ovarian	CA125	n=24	11 (45.8 %)
Germ cell	D240	n=21	0 (0 %)
Mesenchymal	Vimentin	n=25	23 (95.8 %)

3.3.1.2 PCO Cultures Growth

The growth rate of PCO cultures was assessed using SRB assay over a period of 10 days. The median PCO growth rate was markedly slower than many of the commercially available cell lines and highly variable. The median doubling time was 135 hrs (95 % CI = 104.2 to 284.6 hrs, Figure 3.2). Senescence occurred between the 2nd and 8th passages, most commonly between 4th and 5th. Cultures were considered unsuccessful when no growth was seen after 28 days (ODonnell et al., 2014).

No correlation was demonstrated between growth rate, histological subtype or stage of disease at presentation. The relatively slow growth rate may be a consequence of the artificial culture environment and lack of factors from the tumour micro-environment.

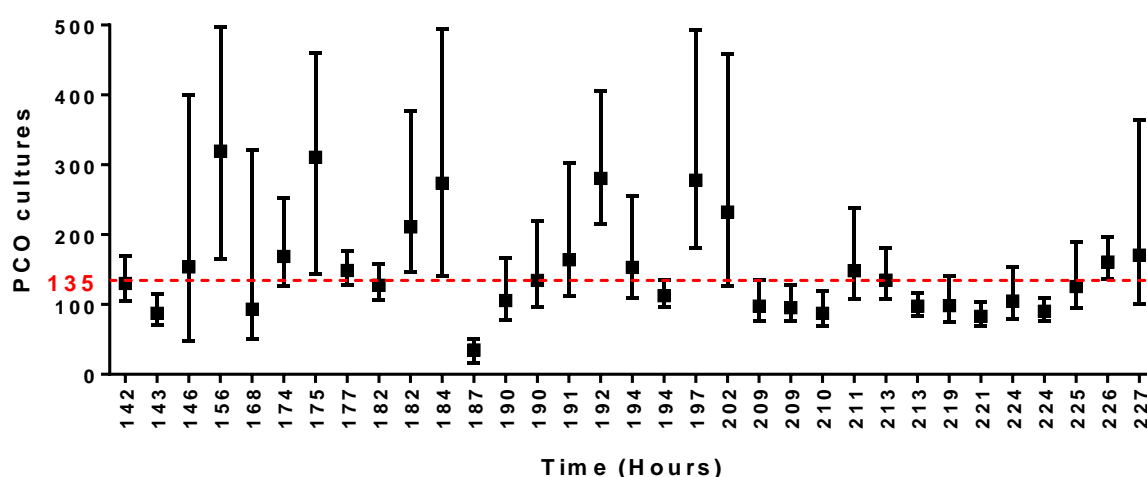


Figure 3-2 Growth rate of PCO cultures.

Results are doubling time with 95 % CI. Results are average of 6 experimental repeats grown for 10 days. Median doubling time was 135 hrs.

3.3.1.3 PCO Cultures Storage

Paired sets of 50 ml aliquots of ascitic fluid were centrifuged at 400 x G for 5 min (N = 6). The resultant cell pellets were resuspended in cryopreservative media, stored at -80°C or in liquid nitrogen and thawed at 6 weeks and 6 months. Cultures were successfully grown from both storage conditions after 6 weeks, with no difference observed in morphology, growth rate or functional assessment (ODonnell et al.,

2014). However, following 6 months, a significant difference in success of subsequent culture from the two conditions was observed. Ascitic pellets stored in liquid nitrogen were successfully cultured in 83 % cases, whereas, no cultures stored at -80°C could be successfully grown.

3.3.1.4 Transfection into PCO cultures

A number of functional assays require transfection of vectors into cells (Bau et al., 2007, Ohashi et al., 2005). Two methods of transfection were optimised in PCO cultures. Firstly, viral transduction using MISSION™ shRNA lentiviral transduction particles was attempted. Cells continued to grow in puromycin media following the transduction thus suggesting successful transfection (Figure 3-3). Long term transduction could not be assessed due to the short term life-span of the PCO cultures.

Viral transduction is not applicable to all assays and therefore transfection of pGL2 luciferase expressing vector using Lipofectamine LTX and electroporation was attempted. Transfection efficiency was assessed by luciferase expression and compared to control cell lines. Despite optimisation, both lipofectamine and electroporation transfection methods failed to yield a high enough transfection efficiency in PCO cultures for functional assays (Figure 3-4).

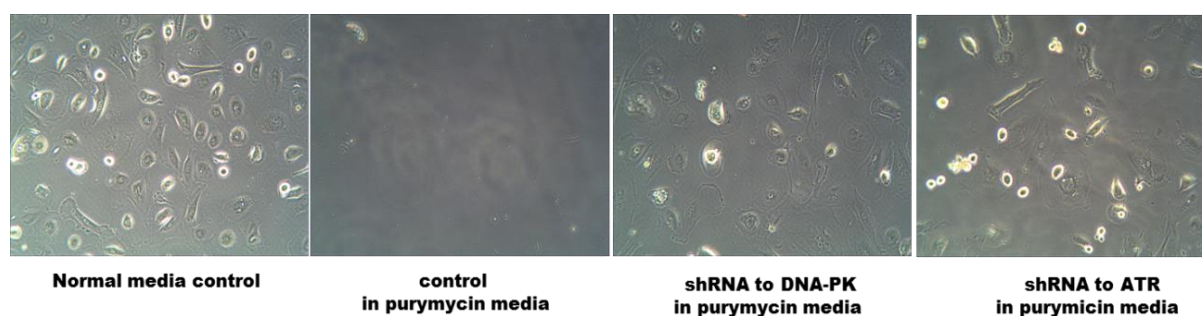


Figure 3-3 Viral transduction of shRNA to DNA-PK and ATR into PCO 204.

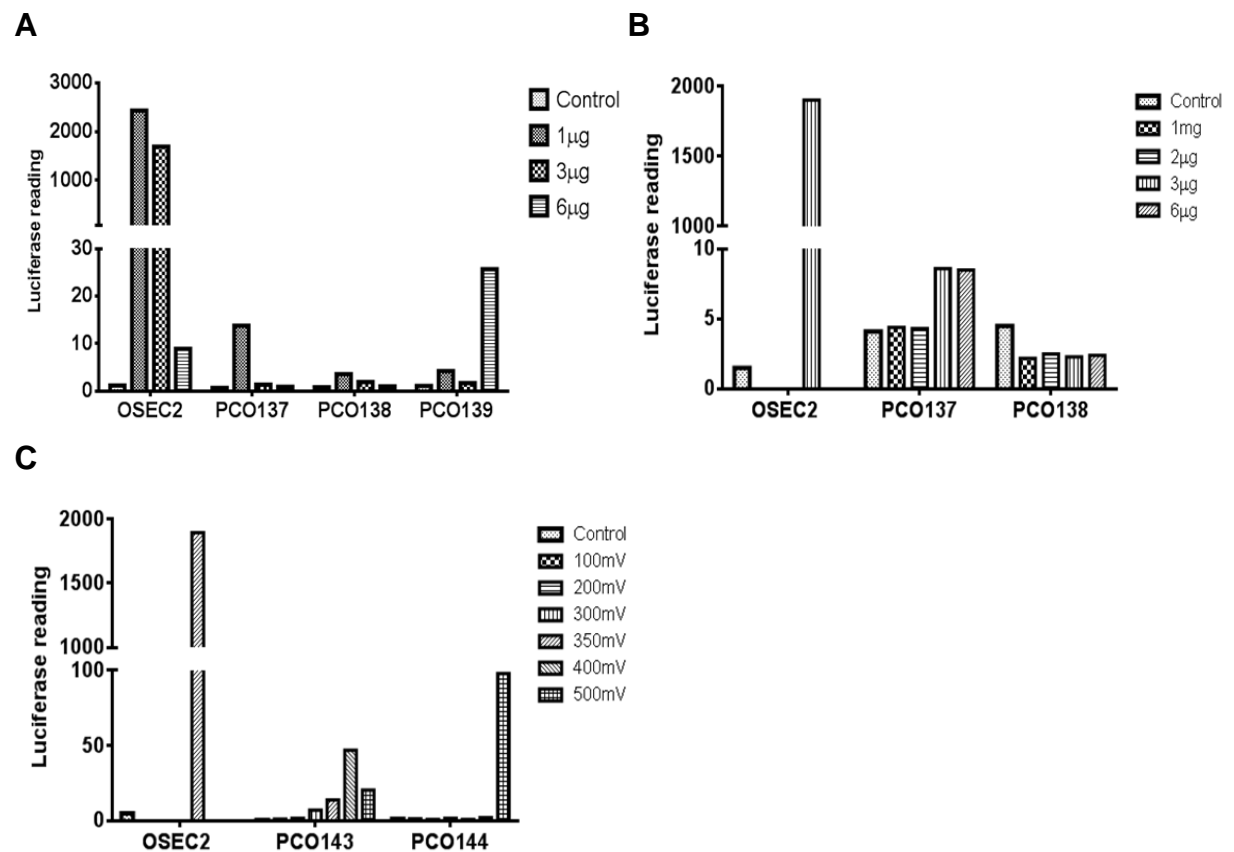


Figure 3-4 Transfection of pGL2 luciferase expressing vector into PCO cultures.

A. Transfection using Lipofectamine LTX (positive control - OSEC-2 cell line); **B.** Transfection using electroporation at 350mV; **C** Transfection of 3mg vector using increasing voltage. Results are expressed as luciferase readings.

3.3.2 HR Function in PCO Cultures

HR function assessment was performed in 41 PCO cultures. HR assays were performed by me, Michelle Dixon and Rachel O'Donnell.

Hypothesis: HR function is defective in 50 % of ovarian cancer cultures

A two fold increase in γ H2AX and RAD51 is used as a cut off to define HRC. > 2 fold increase in γ H2AX and RAD51 cells are deemed HRC, whilst > 2 fold increase in γ H2AX but < 2 fold increase in RAD51 cells are deemed HRD (Mukhopadhyay et al., 2010, Drew et al., 2011). 19 out of 41 (46 %) PCO cultures were deemed HRD and 22 out of 40 (54 %) of PCO cultures were HRC. However, as can be seen in Figure 3-5, the foci fold increase from control was highly variable.

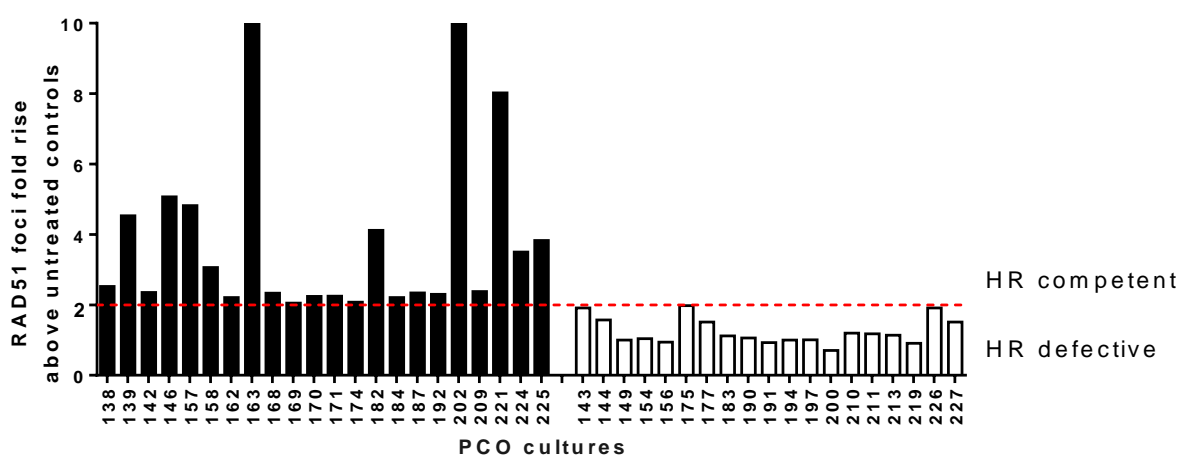


Figure 3-5 HR function in PCO cultures. RAD51 foci fold rise above controls.

3.3.2.1 Correlation of HR with Progression Free and Overall Survival

Previously published data demonstrated an association of HRD with improved survival (Mukhopadhyay et al., 2012). In this study no significant difference in PFS or OS was seen between HRC and HRD groups (Figure 3-6).

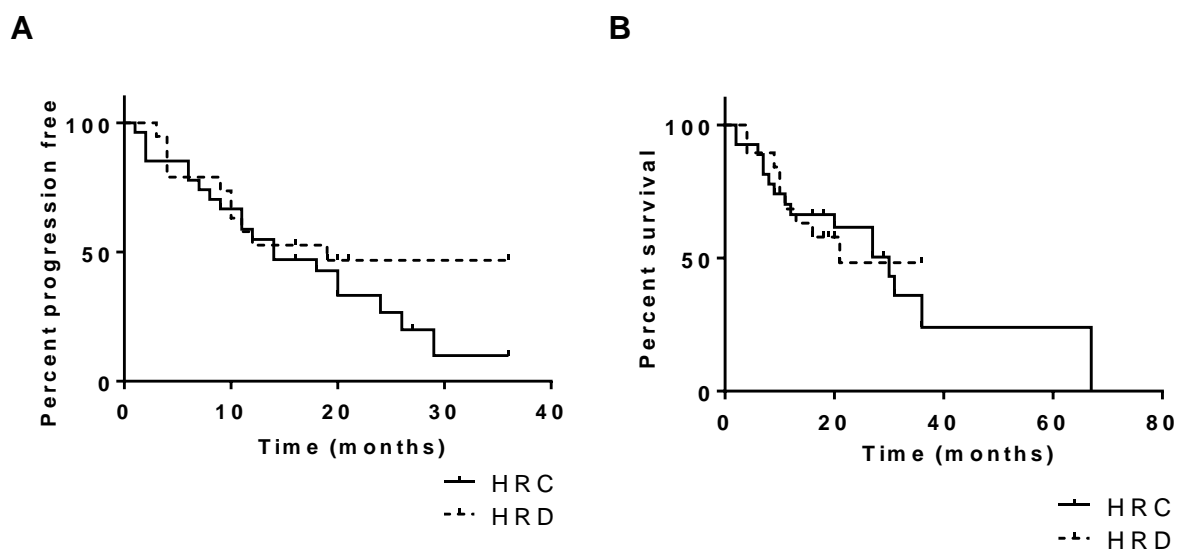


Figure 3-6 Kaplan-Meier survival curves for PFS/OS by HR status.

A. Median progression free survival was 14 months for HRC compared to 19 months for HRD group, log rank Chi square 1.0 $p = 0.31$. Patients who had not progressed were censored at last follow up. **B.** Median overall survival was 30 months for HRC group and 21 months for HRD group. Log rank Chi square 0.004 $p = 0.94$. Patients were censored at last follow up.

3.3.3 Sensitivity of PCO Cultures to Rucaparib and Cisplatin

For immortalised cell lines, cytotoxicity is assessed over 3 doubling times using SRB assay. For PCO cultures it was not feasible to determine the doubling time of each culture prior to cytotoxicity assay due to their limited life span. The median doubling time for PCO was 134.6 hrs and therefore, a standard incubation time of 10 days was adopted.

The sensitivity of PCO cultures to both rucaparib and cisplatin was assessed using SRB assay. The sensitivity for both drugs varied greatly; the median survival of cells after 10 days of treatment with 10 μ M rucaparib was 63.34 %, and the median survival after 10 days of treatment with 10 μ M cisplatin was 43.49 %. There was good correlation between sensitivity to both agents (Pearson R^2 was 0.245 and $p = 0.001$).

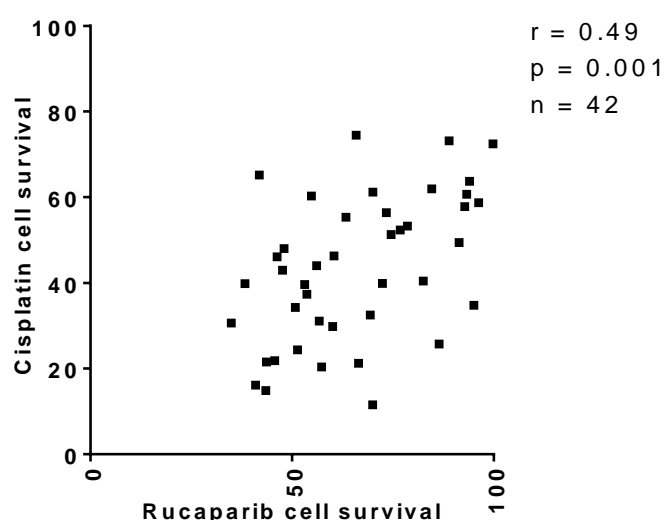


Figure 3-7 Correlation of rucaparib and cisplatin sensitivity of PCO cultures.

Results are the percentage cell survival after 10 μ M rucaparib and the percentage cell survival after 10 μ M cisplatin treatment. $N = 42$.

3.3.3.1 Correlation of Rucaparib and Cisplatin Sensitivity with HR Function

HRD cultures were more sensitive to rucaparib ($p = 0.011$, Figure 3-8) and more sensitive to cisplatin ($p = 0.041$, Figure 3-8) compared to HRC cultures.

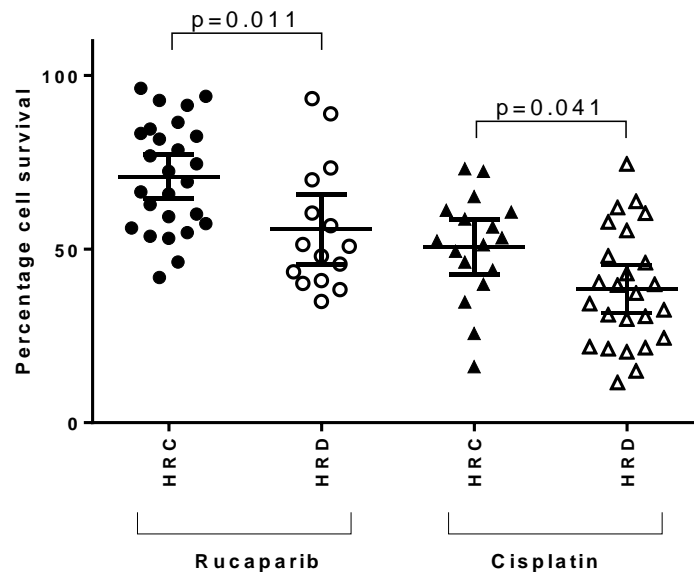


Figure 3-8 Rucaparib and cisplatin cytotoxicity in PCO cultures by HR function.

Cell survival calculated as cell growth after 10 days treatment with 10 μ M rucaparib or 10 μ M cisplatin as a fraction of DMSO. Control growth for PCO cultures was assessed by SRB assay, and results were divided by HR status. Error bars are SEM.

3.3.3.2 Correlation of Sensitivity to Rucaparib and Cisplatin with Progression Free and Overall Survival

The correlation of *in vitro* sensitivity to rucaparib and cisplatin with patient survival was assessed. Cultures with < 60 % survival after 10 day treatment with 10 μ M rucaparib and < 40 % growth after 10 day treatment with 10 μ M cisplatin were deemed sensitive. Longer PFS and OS were found for cultures deemed to be sensitive to rucaparib and cisplatin (Figure 3-9), however the differences were not found to be statistically significant.

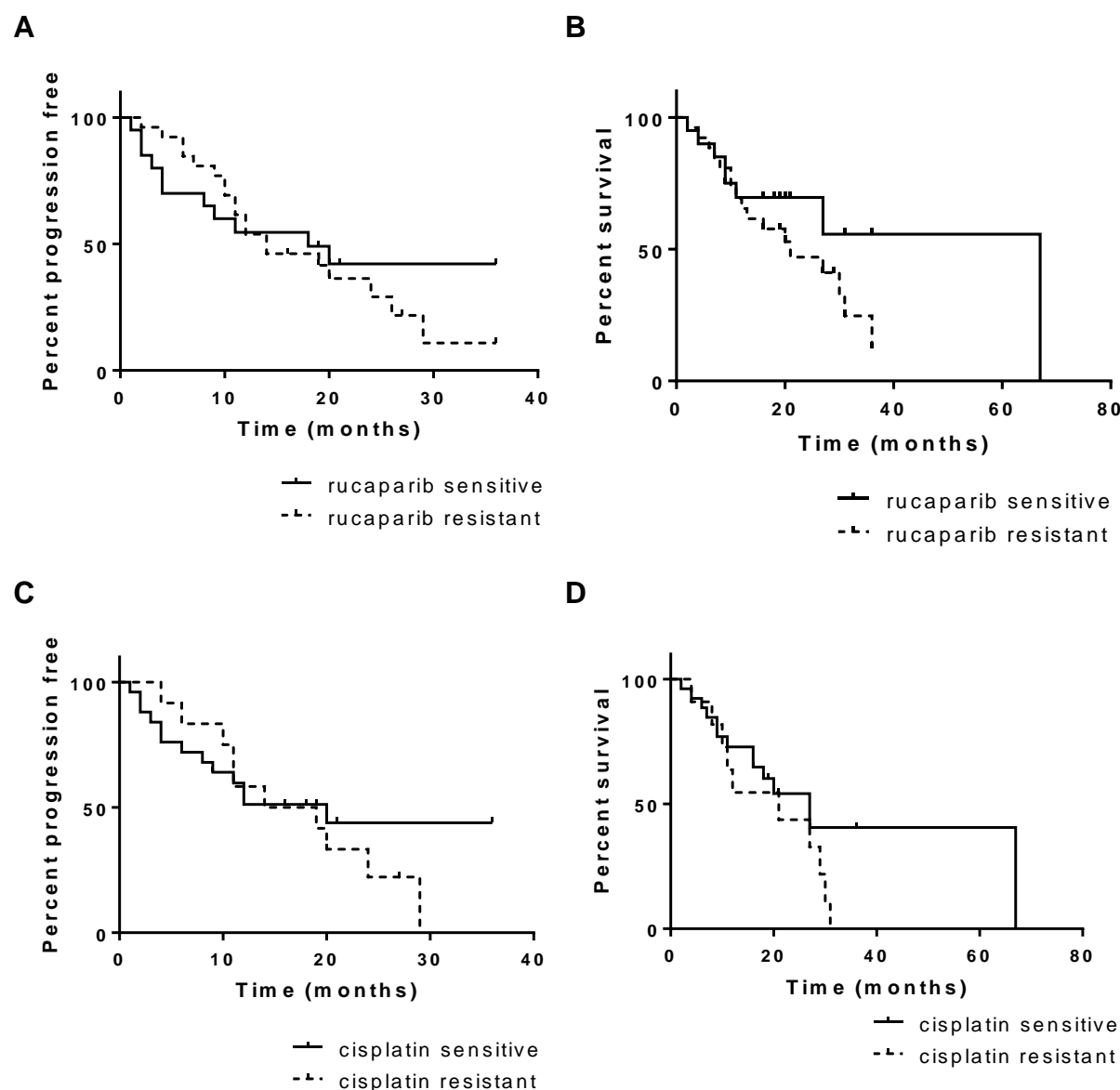


Figure 3-9 Kaplan-Meier survival curves for PFS/OS by sensitivity to rucaparib and cisplatin. Patients who had not progressed were censored at last follow up.

A. Median PFS was 18 months for rucaparib sensitive compared to 14 months for resistant cultures, log rank Chi square 0.15 $p = 0.7$. $N = 20$ sensitive and $N = 26$ resistant cultures. Patients who had not progressed were censored at last follow up. **B.** Median OS was 67 months for rucaparib sensitive compared to 21 months for resistant cultures. Log rank Chi square 2.1 $p = 0.14$. Patients were censored at last follow up. **C.** Median PFS was 20 months for cisplatin sensitive compared to 16.5 months for resistant cultures, log rank Chi square 0.2 $p = 0.6$. $N = 25$ sensitive and $N = 12$ resistant cultures. Patients who had not progressed were censored at last follow up. **D.** Median OS was 27 months for cisplatin sensitive compared to 21 months for resistant cultures. Log rank Chi square 1.2 $p = 0.27$. Patients were censored at last follow up.

3.3.4 RNA Genome Expression Arrays to Assess HR Function

DNA micro-arrays have become an established tool to study gene expression patterns in ovarian cancers for both diagnostic and prognostic markers (Hibbs, 2004, Spentzos, 2004). This approach has the advantages of high throughput analysis, as well as using RNA, which can be extracted easily from clinical material including FFPE tissues. Gene expression profiling using FFPE samples showed a BRCA-like profile in many of the sporadic EOC (Jazaeri, 2002, Konstantinopoulos et al., 2010). The 'BRCAness profile', now understood to be HRD has been shown to correlate with responsiveness to platinum and PARPi.

Hypothesis: Gene expression profiles for HRD and HRC cultures differ and can be used as an assay to predict HR status

Using RNA extracted from the PCO ascitic cultures characterised for HR function, genome wide expression was determined by the Oxford genomics centre (Oxford, UK) using Illumina Genome Studio and HumanHT 12v4.0 R1 15002873 array, as per manufacturer's instructions, and as described in section 2.12. All RNA samples were extracted from the same ascitic fluid primary culture as used in the functional HR assay and cytotoxicity assays.

3.3.4.1.1 Unsupervised Hierarchical Clustering

In order to identify a potential HRD signature, RNA expression was analysed using unsupervised hierarchical clustering (Figure 3-10). PCOs 157 and 142 were clear outliers in terms of expression clustering. PCO 142 was later renamed as the NUOC-1 cell line, as it spontaneously immortalised. The difference in mRNA expression for this cell line may therefore be linked to its spontaneous immortalisation. PCO 157 however, did not immortalise and the reason for its obvious difference in mRNA expression is unclear.

Despite removal of the two outlier samples no clustering by HR function was observed of the PCO cultures (Figure 3-10.C-D).

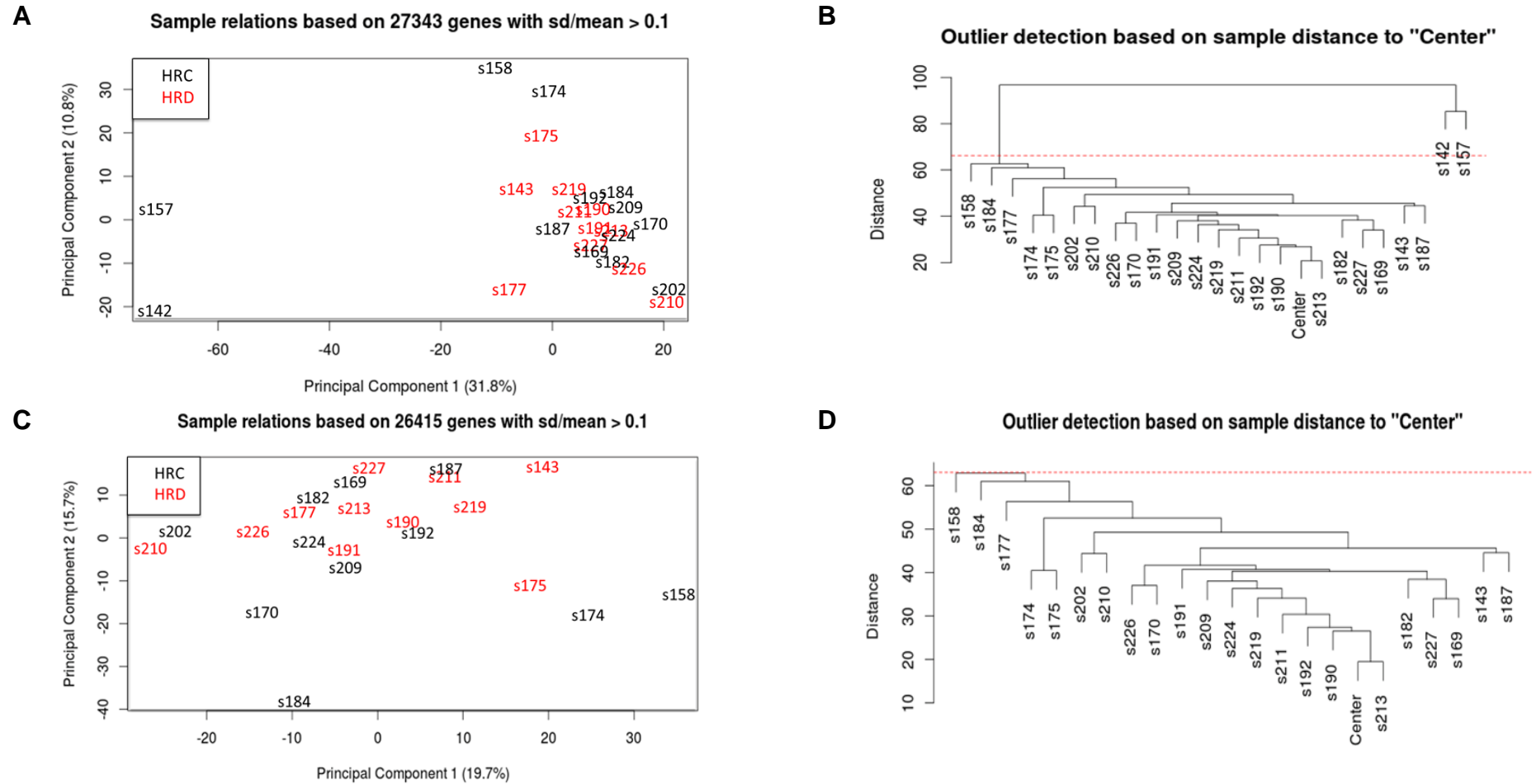


Figure 3-10 RNA Genome expression array.

A. PCA plot of all PCO samples. Sample relation based on 27343 genes with $sd/mean > 0.1$ HRD cultures are in red and HRC in black. **B.** Dendrogram after normalization. PCO142 and PCO 157 were deemed outliers. **C.** PCA plot after outlier cultures were removed. Sample relation based on 26415 genes with $sd/mean > 0.1$. **D.** Dendrogram after normalization after outlier cultures were removed from analysis.

3.3.4.1.2 Hierarchical Clustering of RNA Expression

In view of the lack of association in unsupervised clustering, the relative expression of 15 key components of the HR pathway were assessed and compared between HRD and HRC cultures (Figure 3-11).

Illumina Genome Studio Gene expression software was used to extract relative gene expression across samples, clustering them into functional groups. The comparative Ct ($\Delta\Delta\text{Ct}$) method was used to assess the expression level of the components of each pathway, relative to endogenous controls normalised to the reference panel. The expression of two genes were significantly different between the two groups; RAD51 ($p = 0.008$) and XRCC2 ($p < 0.0001$) were both downregulated in the HRC group. Further evaluation of these components for use as a biomarker for HR status is required.

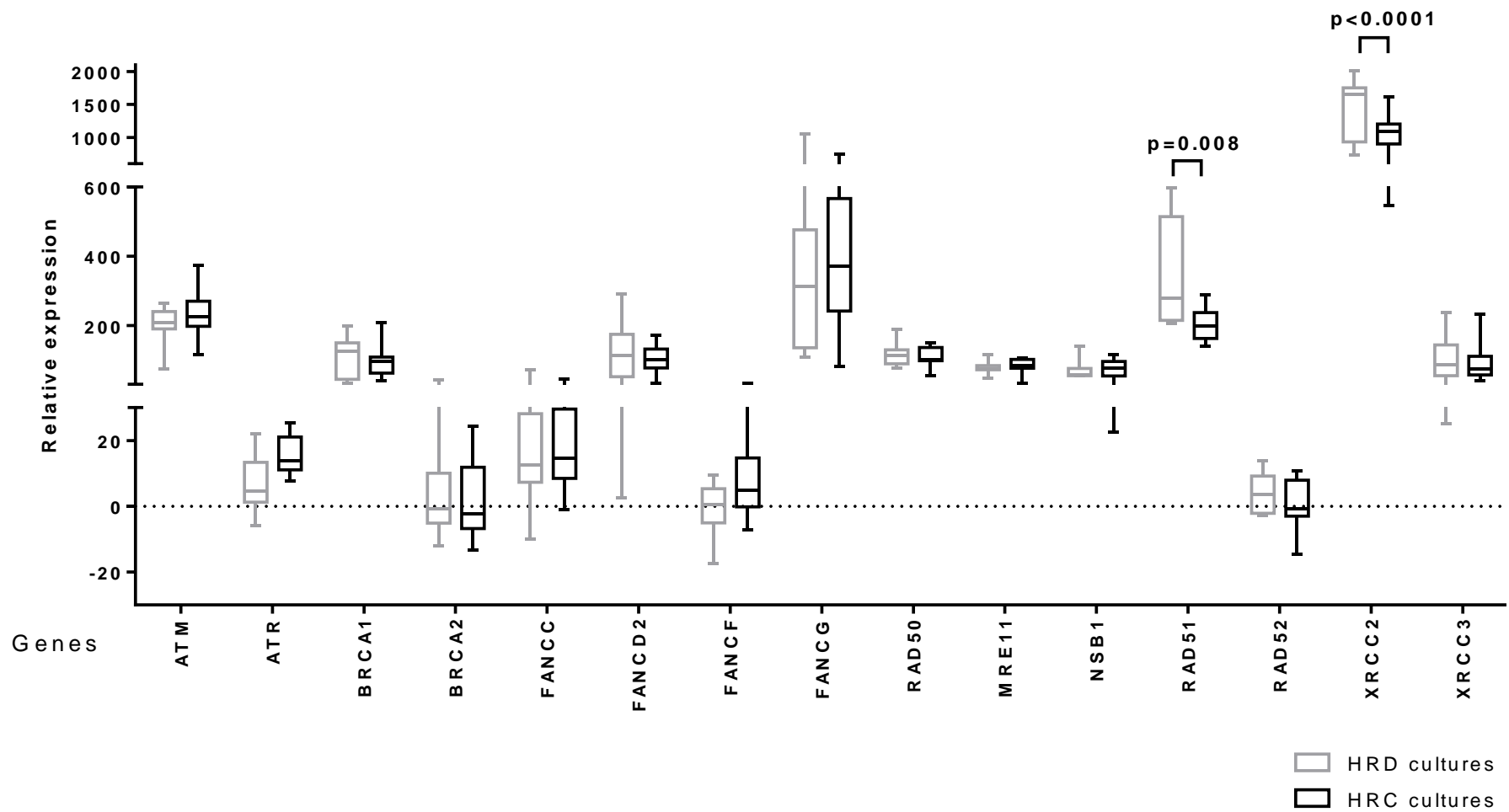


Figure 3-11 Hierarchical clustering of HR pathway genes expression.

3.4 Characterisation of NUOC-1 Cell Line

The NUOC-1 cell line was derived from the ascites of a chemotherapy naive patient with a mixed histology tumour. The patient was of Caucasian background and was 62 years old at the time of diagnosis. She presented with stage IIIC high grade mixed ovarian carcinoma and underwent primary surgery. Ascites was collected at the time of surgery. The patient was considered optimally debulked, however, due to frailty did not receive any chemotherapy and only survived 52 days following surgery. She did not have any known relevant familial history. Pathology of the tumour consisted of 80 % endometrioid, 15 % clear cell and 5 % serous carcinoma.

The ascites was prepared and processed as described in section 2.2.2. The growth of NUOC-1 cells was initially slow, with a 128 hr doubling time at passage 2; but with continued culture this decreased to 58 hrs at passage 14.

3.4.1 Confirmation of Epithelial Origin

Hypothesis: NUOC-1 cells are epithelial cells

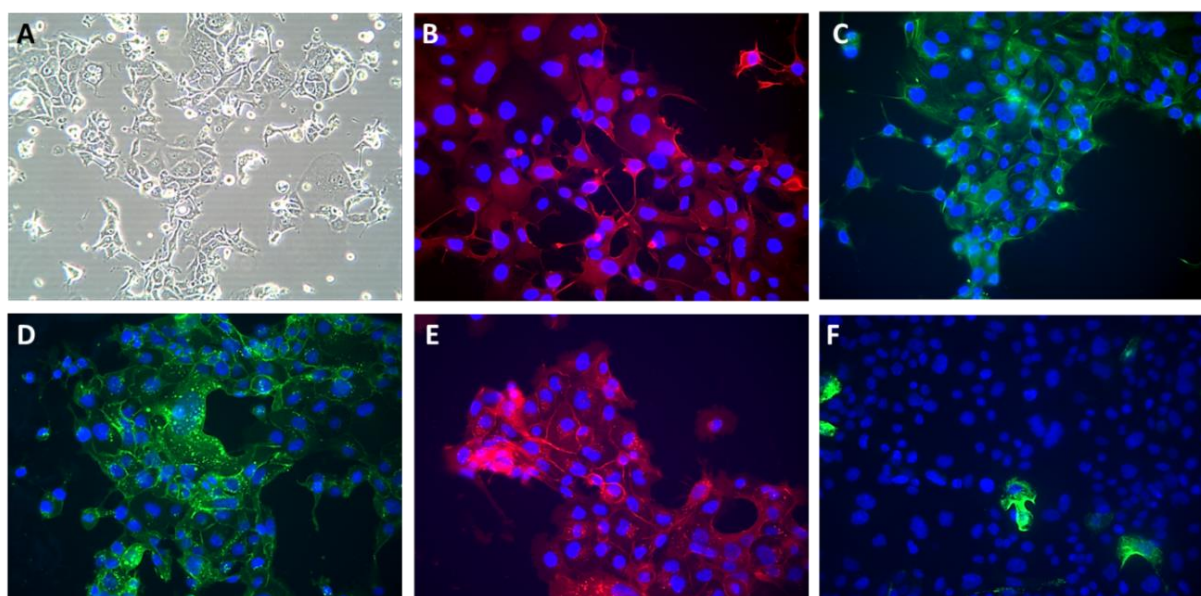


Figure 3-12 NUOC-1 characterisation panel.

A. Brightfield demonstrating cobblestone monolayer; immunoflourescent images with antibodies targeted against: **B.** Alexafluor 596 anti-CA125; **C.** FITC-anti-pancytokeratin; **D.** Alexfluor 488 anti-EpCAM; **E.** Alexafluor 596 anti-MOC 31; **F.** Alexafluor 596 anti-Vimentin.

Upon bright field microscopy examination, a cobblestone morphology, characteristic of epithelial cells, was noted; this was maintained during repeated passage. NUOC-1 cells stained positive for proteins characteristic of epithelial ovarian carcinoma (pancytokeritin, EpCAM, MOC31 and CA125), and stained negative for Vimentin (Figure 3-12). The epithelial cell phenotype of the NUOC-1 cells and the expression of antigens commonly expressed in ovarian cancer were consistently expressed at passage 2 and 14.

3.4.2 Assessment of Hormone and Tyrosine Kinase Receptor Expression

Hypothesis: NUOC-1 cells express hormone and tyrosine receptors

The effect of steroid hormones in carcinogenesis has been studied in breast and endometrial cancer, with well-known and promising results for therapy. However, for ovarian cancer, the results have been conflicting (de Toledo et al., 2014). In NUOC-1, hormone receptor expression was characterised using western blotting. This work was carried out with Eleanor Earp (MRes, 2013).

For the expression of hormone and tyrosine receptors, appropriate controls were selected. The MCF7 cell line was used as a positive control for ER, PR and HER3 expression; the LnCap cell line was used as a positive control for AR, HER2 and HER3 expression. The MDA-MB-231 triple negative breast cancer cell line and AR negative PC3 cell lines were used as negative controls. NUOC-1 cells stained negative for oestrogen, progesterone and androgen receptors (Figure 3-13). The NUOC-1 cells were found to express the HER-3 receptor and the HER-2 receptor at a higher level than LnCap and SKOV3 cell lines (Figure 3-13).

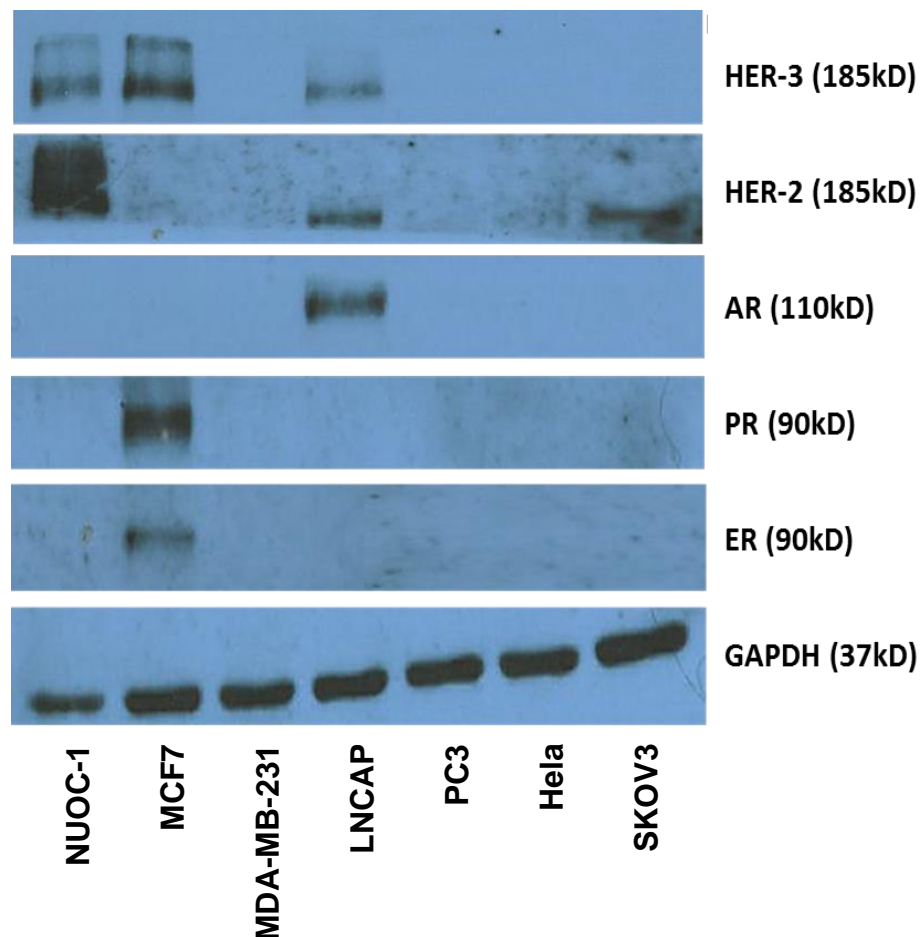


Figure 3-13 Tyrosine kinase and endocrine receptor expression in the NUOC-1 cell line.

NUOC-1 cells express the HER-3 receptor (positive control MCF7) and over-express the HER-2 receptor (positive control LNCAP and SKOV3). NUOC-1 cells do not express the oestrogen receptor (positive control MCF7), the progesterone receptor (positive control MCF7) or the androgen receptor (positive control LNCAP). Blots are representative of three independent experiments.

3.4.3 p53 Function Assessment

HGSOC of the ovary is genomically characterised by ubiquitous *TP53* mutations (Ahmed et al., 2010, Cancer Genome Atlas Research, 2011). *TP53* mutational and p53 functional status was determined. This work was undertaken with Katharine Elliot (MRes, 2013).

Hypothesis: NUOC-1 cells are wildtype for p53 consistent with endometrioid / clear cell origin

3.4.3.1 Assessment for P53 Mutations

TP53 mutation status was assessed by PCR amplification and off-site Sanger dideoxy sequencing. No mutations were detected in exons 3-9, but a codon 72 C→G (Arg/Pro) polymorphism in exon 4 was detected (Figure 3-14).

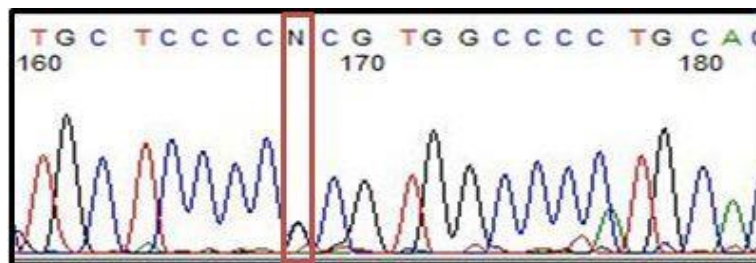


Figure 3-14 Illustration of chromatogram of *TP53* gene.

Exon 4 sense sequence codon 72 C→G polymorphism highlighted.

3.4.3.2 Functional P53 assessment

p53 transcriptionally activates MDM2, which then acts to inhibit further p53 mediated transactivation by binding to the transactivation domain located in the N-terminal (Kussie et al., 1996). MDM2 exerts further regulatory action by inducing the nuclear export and degradation of p53 (Gorringe et al., 2007). The MDM2 antagonist Nutlin-3 inhibits the MDM2-p53 interaction by binding MDM2 in the hydrophobic cleft, where p53 would normally bind. MDM2 antagonism leads to the stabilisation of p53, with increases in transcriptional activity, leading to elevated p21 and MDM2 expression (Vassilev et al., 2004).

Treatment with Nutlin-3 resulted in an accumulation of MDM2 in NUOC-1 cell lines, corresponding to a concentration-dependent increase in p53 (Figure 3-15). The p53 downstream growth inhibitory target, p21, also increased in a concentration-dependent manner. This was consistent with the results in the *TP53* wildtype A2780 cell line. Analysis of the same Nutlin-3 treatment in *TP53* mutant CP70 cells showed significantly higher p53 levels with no induction of p53 upon treatment.

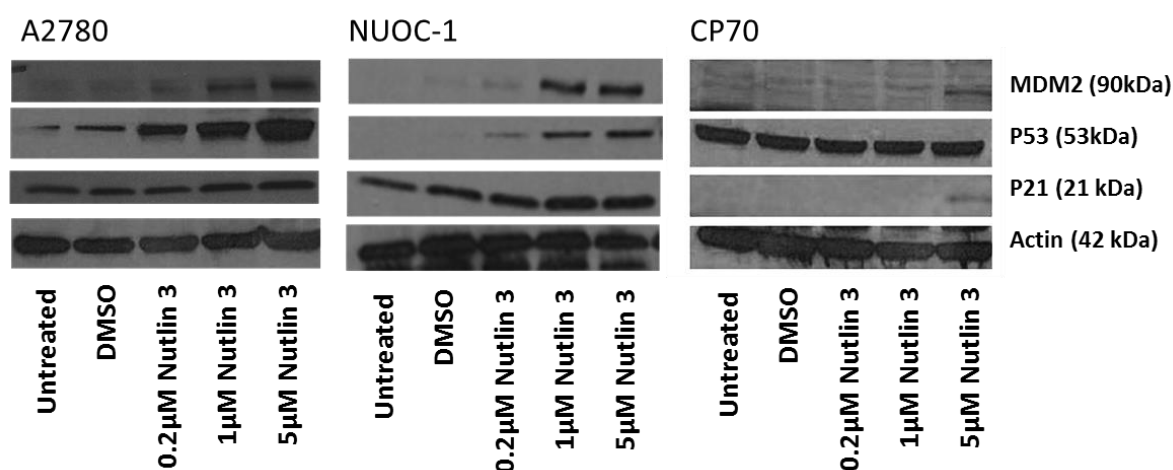


Figure 3-15 MDM2, p53, and p21 expression in response to Nutlin3.

Blots are representative of three independent experiments.

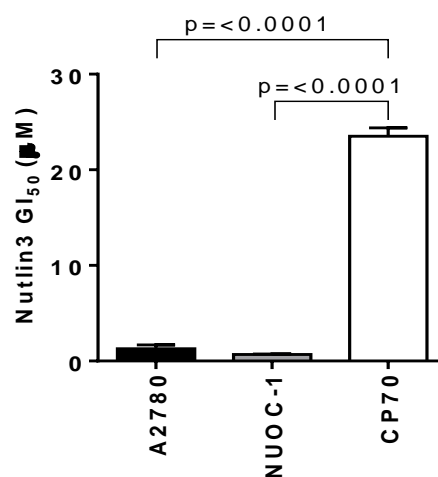


Figure 3-16 NUOC-1 cell line response to Nutlin3.

Results are mean GI₅₀ values between the CP70, TP53 mutant cell line and each TP53 wild-type cell line: A2780, NUOC-1. Results are mean of three independent experiments. Error bars are SEM.

Nutlin-3 had a higher growth inhibitory effect in TP53 wild-type NUOC-1 cells (GI₅₀ 0.7 μM +/- 0.03 μM) compared to mutant CP70 cells (23.5 μM +/- 0.9 μM; $p < 0.00001$), but comparable to TP53 wildtype A2780 (1.3 μM +/- 0.4 μM) (Figure 3-16).

3.4.4 NUOC-1 DNA Repair Assessment

Functional assessment of NUOC-1 HR was undertaken as part of PCO culture characterization, as discussed in section 3.3.2. NUOC-1 cells were deemed HRC with a 2.84 fold rise in RAD51 foci, compared to untreated controls.

3.4.4.1 BER Function in NUOC-1 Cells

Previous studies have reported APE1 overexpression in ovarian cancer as described in section 1.4.4 and XRCC1 SNPs. Defects in BER pathway in ovarian cancer have not been reported.

Hypothesis: NUOC-1 cells are BER competent

Excess production of 8-OHdG inferred the non-functioning of BER and was quantified by competitive ELISA in NUOC-1 cells (Figure 3-17). AA8 (BER competent) with its derivative EM9 cell lines (BER deficient due to XRCC1 mutation) were used as positive and negative controls. The HT 8-oxo-dG ELISA kit II (Trevigen, USA, 4380-096-K), is a competition ELISA of immobilised 8-OHdG on pre-coated wells with 8-OHdG in the sample for monoclonal antibody binding, which is then quantified by spectrophotometry. High 8-OHdG corresponds to low BER.

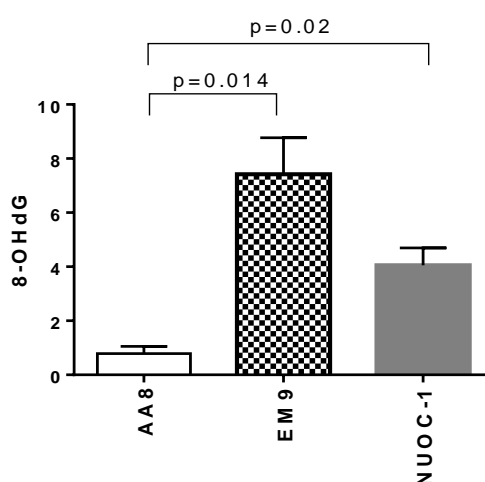


Figure 3-17 Base excision repair of NUOC-1 assessed by competitive ELISA.

Results are the measurement of 8-OHdG levels. AA8 (BER proficient) cell line was used as positive control, EM9 (BER deficient) cell line was used as a negative control.

The mean 8-OHdG in EM9 cells with XRCC1 mutation conferring BER dysfunction was 7.42 nM +/- 2.7 nM, compared to parental BER function in the AA8 cell line of 0.79 nM +/- 0.54 nM, $p = 0.014$. NUOC-1 cell 8-OHdG level was 4.0 nM +/- 0.64 nM, indicating that NUOC-1 cells were BER defective. Mechanisms of BER deficiency were not assessed in this project but may have an important role in NUOC-1 cell chemo-sensitivity.

3.4.5 Drug Sensitivity Assessment

Ovarian clear cell carcinoma is associated with chemo-resistance and poor prognosis (Itamochi et al., 2008). The literature reports an initial response rate (RR) to first-line treatment of 22 - 56 % in clear cell carcinoma, which is significantly lower than the initial RR of other subtypes of EOC of 80 % (Anglesio et al., 2011).

Hypothesis: NUOC-1 cells exhibit a chemoresistant phenotype consistent with clear cell carcinoma

The sensitivity to common cytotoxics was assessed using a SRB assay, comparing the NUOC-1 cells to the OSEC-2 cells (Table 3-3). This work was done with Eleanor Earp (MRes, 2013).

Compared to the OSEC-2 cells, NUOC-1 cells were found to be more sensitive to camptothecin (mean GI_{50} 6.35 nM +/- 2.6 nM for NUOC-1 compared to 172.4 nM +/- 71.55 nM for OSEC-2, $p < 0.0001$). NUOC-1 cells were more resistant to paclitaxel (mean GI_{50} 251.7 nM +/- 36.5 nM for NUOC-1 compared to 100.9 nM +/- 29.4 nM for OSEC-2, $p = 0.003$).

Table 3-3 Sensitivity of NUOC-1 and OSEC-2 cell lines to cytotoxic agents.

Results are mean GI₅₀ and 95 % CI assessed by SRB assay. Results are the average of 3 independent experiments.

Cytotoxic agent	Mean GI ₅₀ and 95 % confidence interval		Paired t-test
	OSEC-2	NUOC-1	P =
Cisplatin (μM)	2.73 0.83 to 8.95	1.46 0.59 to 3.6	0.97
Paclitaxel (nM)	100.9 71.63 to 142.2	251.7 116.2 to 545.4	0.003
Camptothecin (nM)	172.4 86.41 to 343.9	6.35 2.98 to 13.53	<0.0001
Doxorubicin (nM)	35.52 21.80 to 57.86	31.30 7.41 to 132.3	0.96
Rucaparib (μM)	5.53 2.62 to 11.68	5.48 1.67 to 1.80	0.99
Irradiation (Gy)	5.1 3.92 to 6.64	3.15 2.23 to 4.45	0.98

3.4.6 Assessment for ARID1A Mutations

Located on chromosome 1, the ARID1A gene encodes for the adenine-thymine (AT)-rich interactive domain-containing protein 1A. This protein forms an integral part of a complex essential in chromatin remodeling, known as the adenosine triphosphate-dependent chromatin modeling complex switch/sucrose-nonfermentable (SWI/SNF). Functioning through epigenetic regulation of gene expression and chromatin, the SWI/SNF complex has roles in cell-cycle control, DNA repair and apoptosis (Guan et al., 2011, Wu and Roberts, 2013). Mutations in the ARID1A gene are reported in 46 % of ovarian clear cell carcinomas (Wiegand et al., 2010, Jones et al., 2010).

Hypothesis: NUOC-1 cells contain ARID1A mutation commonly found in clear cell carcinomas

Assessment of the ARID1A mutation status in NUOC-1 cells and germline DNA was undertaken using PCR amplification and off-site Sanger dideoxy sequencing. This work was carried out with Eleanor Earp (MRes, 2013). A single T nucleotide insertion within exon 9 of the ARID1A gene was found (Figure 3-18). Using the TRANSLATE tool within ExPASy (Bioinformatics resource portal) it was predicted that this insertion frame shift mutation causes a premature stop codon and shortened protein.

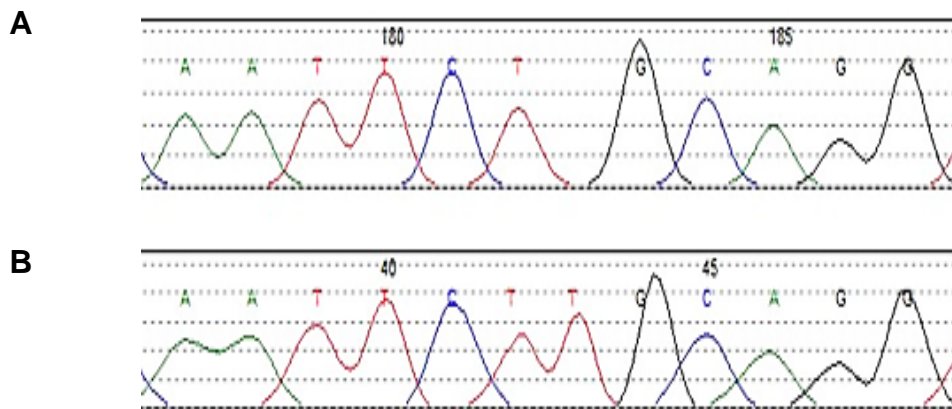


Figure 3-18 Illustration of chromatogram of ARID1A gene.

A. Reference sequence and **B.** Somatic insertion of T in exon 9 of ARID1A gene in NUOC-1.

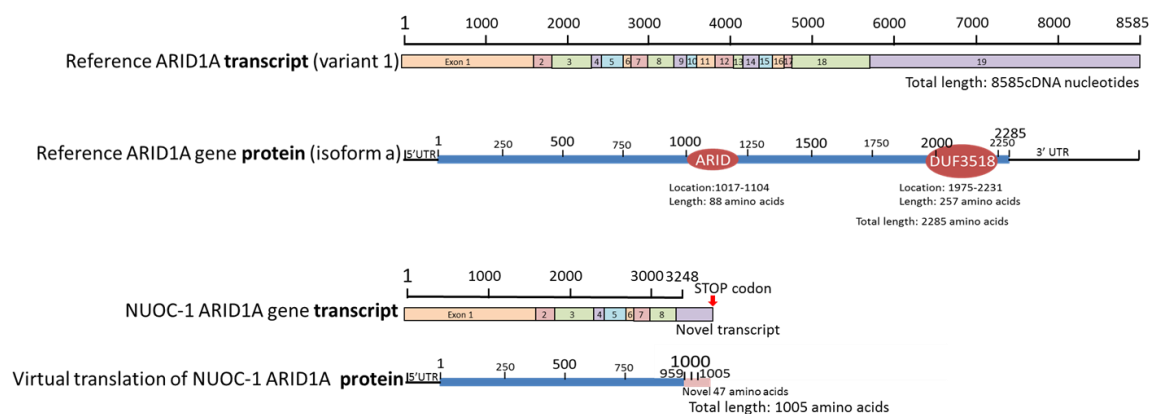


Figure 3-19 A schematic of ARID1A protein product.

Top panel - reference ARID1A transcript and protein. The protein product shows 2 conserved domains: ARID (located at amino acid position 1017-1104) and DUF3518 (located amino acid position 1975-2231). Bottom panel - NUOC-1 ARID1A transcript and protein. The truncated protein product is 1280 amino acids shorter than the wild-type and is missing the 2 conserved domains.

As this missense mutation occurs upstream of the two known ARID1A gene conserved domains- ARID/BRIGHT DNA binding domain and Domain of unknown function (DUF3518), it would almost certainly affect protein function, and it is likely to result in a loss of function mutation (Figure 3-19). However, it should be noted that, these are virtual translations, and may never be translated due to nonsense mediated decay. A review of the COSMIC database did not identify previous reports of this exact mutation. Due to the time constraints of this project, protein expression of ARID1A was not analysed.

3.4.7 PTEN Function

Located on chromosome 10, PTEN is the primary negative regulator of the PI3K pathway. Activation of PI3K signaling is associated with poor prognosis in multiple tumour types, including ovarian clear cell carcinoma (Huang et al., 2011b, Kuo et al., 2009). PTEN's role in drug sensitivity is still unclear due to conflicting evidence. PTEN function in the NUOC-1 cell line and role in drug sensitivity was assessed in this study.

Hypothesis: NUOC-1 cells contain PTEN mutations commonly found in endometrioid / clear cell carcinomas

PTEN mutations in exons 2-5, 6-7 and 9-10 were assessed using PCR amplification and off-site Sanger dideoxy sequencing in the NUOC-1 cell line and matched genomic DNA. A point mutation was detected (1508G>GA, 159R>R, Figure 3-20), however, no somatic mutations were observed in any of the PTEN coding sequences.

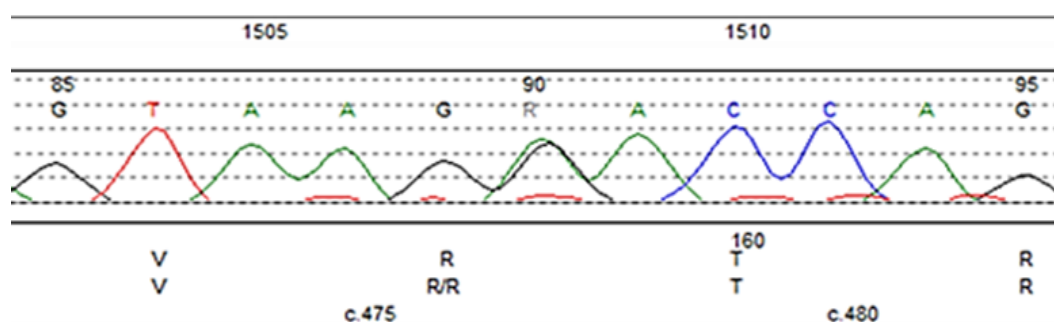


Figure 3-20 Illustration of chromatogram of PTEN gene.

Point mutation of PTEN gene in NUOC-1.

PTEN expression at mRNA and protein level was assessed in NUOC-1 cells using RT-qPCR and western blotting (Figure 3-21). OSEC-2 cells were used as positive control; LnCap cells, which carry a single deletion of PTEN and a mutated remaining allele (McMenamin et al., 1999), and PC3 cells, which have a homozygous deletion, were used as negative controls. This work was done with Charlotte Leeson (Undergrad, 2013).

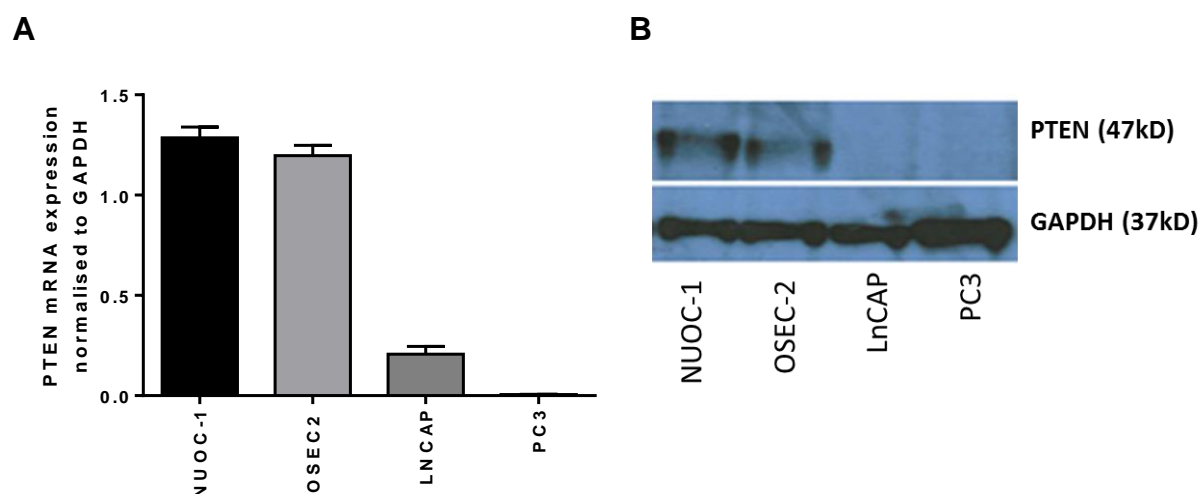


Figure 3-21 PTEN expression levels in NUOC-1 cells.

A. mRNA expression assessed by real time RT-PCR and **B.** protein expression assessed by western blot analysis. LNCap and PC3 cells serve as negative controls whilst OSEC-2 is a positive control.

PTEN mRNA expression in NUOC-1 was comparable to OSEC-2 cells and was significantly higher than negative controls: LNCap ($p = 0.0001$) and PC3 ($p = 0.0017$) (Figure 3-21.A). When the protein levels were assessed, NUOC-1 expression of PTEN was again comparable to OSEC-2 cells, and no protein bands were visualised in LNCap and PC3 cells (Figure 3-21.B).

3.4.7.1 PTEN Knockdown in OSEC-2 and NUOC-1 Cells

OSEC-2 and NUOC-1 cells were virally transduced with MISSION®shRNA lentiviral transduction particles containing PTEN shRNA, as described in section 2.18. Five constructs were used to achieve optimal silencing. Controls were transduced with a non-target control construct. In OSEC-2 cells, knockdown was assessed for all 5 constructs. In NUOC-1 cells, only constructs 2746 and 2747 grew successfully. Knockdown levels were confirmed at mRNA level by RT-PCR (Figure 3-22). This work was done with Charlotte Leeson (Undergrad, 2013).

Significant knockdown was achieved in OSEC-2 cells with constructs 2745 (53 %, $p = 0.005$) and 2746 (68 %, $p = 0.0005$), and in NUOC-1 cells with constructs 2746 (87 %, $p < 0.0001$) and 2747 (82 %, $p < 0.0001$). For consistency, knockdown with construct 2746 was selected to be used in further experiments for both cell lines.

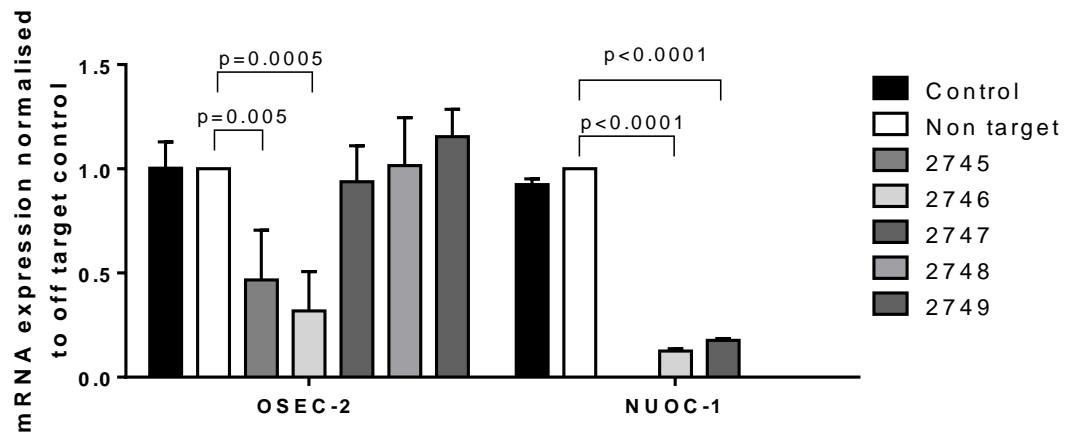


Figure 3-22 *PTEN* mRNA expression in OSEC-2 and NUOC-1 cells. mRNA expression was normalised to expression of GAPDH. Results are then normalised to non target shRNA = 1. Results are average of three independent experiments. Error bars are SEM.

3.4.7.2 *PTEN* Knockdown Effect on HR

A link between *PTEN* loss and HR deficiency is debated, with some groups reporting that *PTEN* attenuates *RAD51* gene expression and recruitment to DSBs and stabilises replication forks (McEllin et al., 2010, He et al., 2015), whilst others refute this (Fraser et al., 2012, Hunt et al., 2012).

Hypothesis: Loss of PTEN results in HRD

PTEN knockdown did not significantly affect HR function in either OSEC-2 or NUOC-1 cells (Figure 3-23).

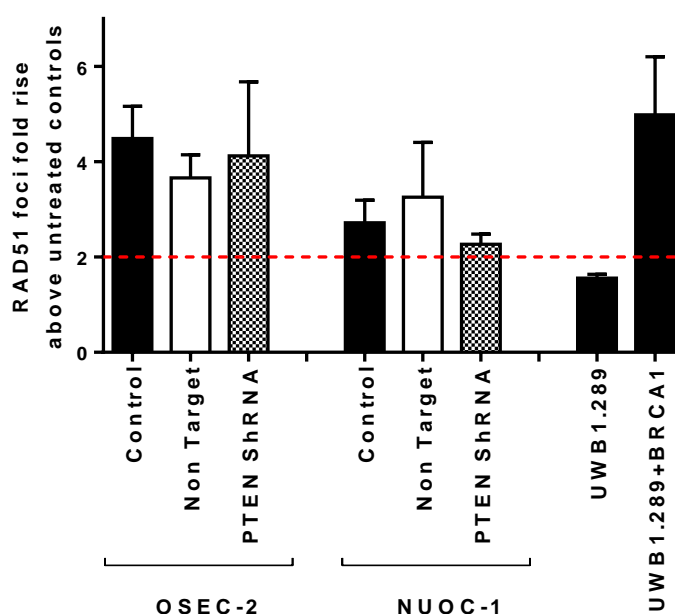


Figure 3-23 The effect of PTEN knockdown on HR function.

Assessed by γ H2AX/RAD51 foci formation assay after 24 hr treatment with 10 μ M rucaparib and 2 Gy IR and compared to DMSO treated un-irradiated control. BRCA1 mutated UWB1.289 cells were used as a HRD control and BRCA1 reconstituted UWB1.289+BRCA1 cells were used as a HRC control. Results are mean of 3 independent experiments. Error bars are SEM.

3.4.7.3 PTEN Knockdown Effect on Sensitisation to Common Cytotoxics

PTEN's role in drug sensitivity is still unclear due to conflicting evidence. The effect of PTEN knockdown on drug sensitivity was therefore assessed by measuring growth inhibition using a SRB assay. This work was carried out with Eleanor Earp (MRes, 2013).

Hypothesis: PTEN in an important determinant of ovarian cancer sensitivity to common therapeutic agents

In OSEC-2 cells, PTEN knock-down had no significant effect on any of the cytotoxic agents, sensitivity; whilst in NUOC-1 cells, PTEN knockdown enhanced sensitivity to all the cytotoxics assessed, with the exception of camptothecin to which NUOC-1 was exquisitely sensitive (Figure 3-24).

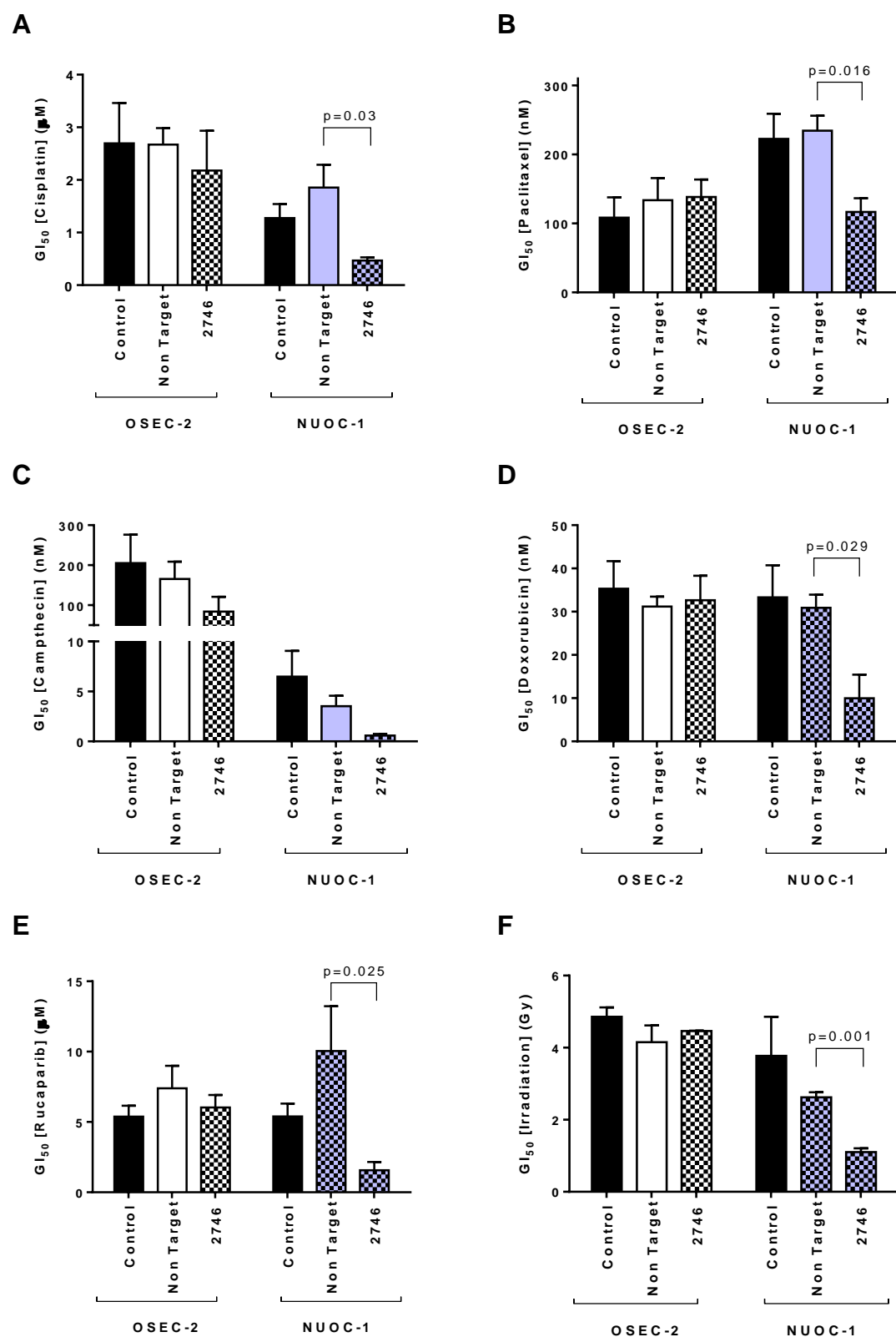


Figure 3-24 Sensitivity of OSEC-2 and NUOC-1 to common therapeutics.

A. Cisplatin, **B.** Paclitaxel, **C.** Campthecin, **D.** Doxorubicin, **E.** Rucaparib, **F.** Irradiation. Results are average of three independent experiments. Error bars are SEM.

The results from this study suggest that PTEN inhibition increases the sensitivity of NUOC-1 cells, but not normal epithelium cells, to cytotoxic agents. Potentially, PTEN could be a tumour specific target for chemo and radiotherapy sensitisation if these results can be replicated in other models of tumour vs normal tissue.

3.4.7.4 PTEN Mutations and Expression in PCO Cultures

Hypothesis: PTEN mutations in ovarian cancer are independent of HR function, but are associated with chemo-sensitivity and improved survival

To further explore the role of PTEN in ovarian cancer, PTEN expression was assessed in 28 unselected PCO cultures. DNA from PCO cultures and matched genomic DNA were screened for PTEN mutations in exons 2-5, 6-7 and 9-10 using PCR amplification and off-site Sanger dideoxy sequencing.

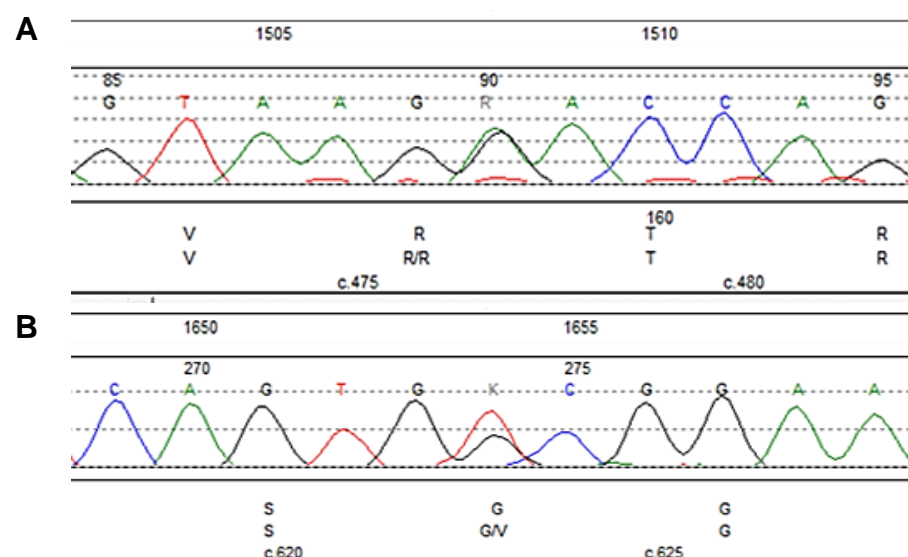


Figure 3-25 Illustration of sequence chromatograms of PTEN gene.

Two point mutations were noted in PTEN gene in PCO cultures. **A.** 1508G>GA, 159R>R in 4 cultures and **B.** 1654G>GT, 208G>G/V in 6 cultures.

The cultures included 20 high grade serous, 7 endometrioid / clear cell and 1 mucinous carcinoma. Mutations that were observed in genomic DNA as well as PCO cultures, were excluded. Two somatic point mutations were detected in PCO cultures (1654G>GT, 208G>G/V in 6 cultures and 1508G>GA, 159R>R in 4 cultures) (Figure 3-25). Neither mutation resulted in amino acid change in the PTEN coding sequences. The mutations that were found also did not correlate with histological

type. Mutations were noted in 2 endometrioid / clear cell carcinomas and 8 high grade serous carcinomas.

Expression of PTEN mRNA was assessed in 34 PCO cultures (Figure 3-26). LnCap and PC3 cells were used as negative controls for PTEN expression. The median PTEN expression mRNA expression normalised to GAPDH for PCO cultures was 0.79 this was significantly higher than LnCap (0.212 +/- 0.014, $p < 0.0001$) and PC3 (0.006 +/- 0.0007, $p < 0.0001$). Point mutations which were detected in the panel analysed, did not correlate with the mRNA expression in this panel (Figure 3-26). This result suggests that the two point mutations have no functional significance.

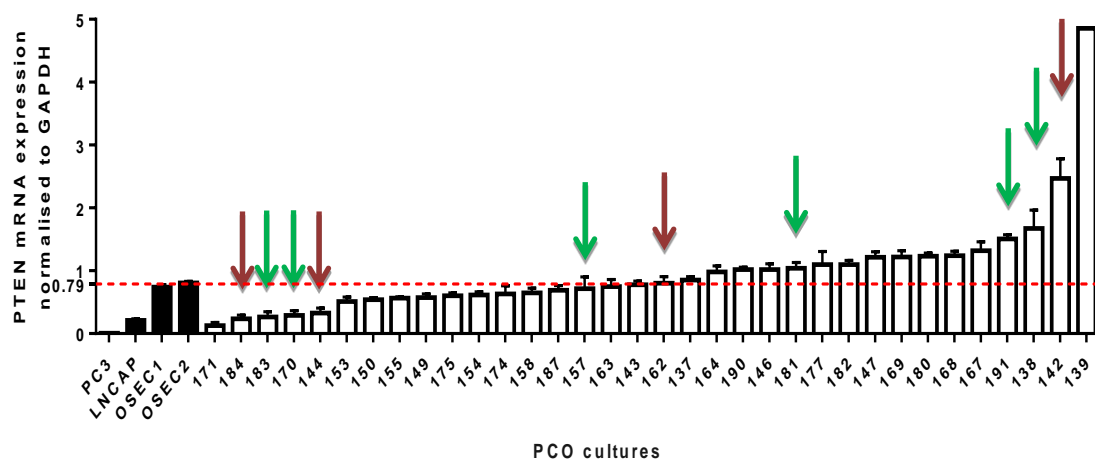


Figure 3-26 PTEN mRNA expression In PCO cultures.

Black bars – cell line controls (negative – PC3 and LNCAP, positive – OSEC-1 and OSEC-2). Expression is normalised to GAPDH expression. Cultures with point mutations are marked with red (1508G>GA) and green (1654G>GT) arrows.

Supporting the findings of knockdown experiments, PTEN mRNA expression was not found to correlate with HR function (Figure 3-27). There was also no correlation of PTEN expression with the sensitivity to rucaparib or cisplatin. Pearsons correlation was $R^2 = 0.018$, $p = 0.57$ for rucaparib and $R^2 = 0.045$, $p = 0.47$ for cisplatin (Figure 3-28).

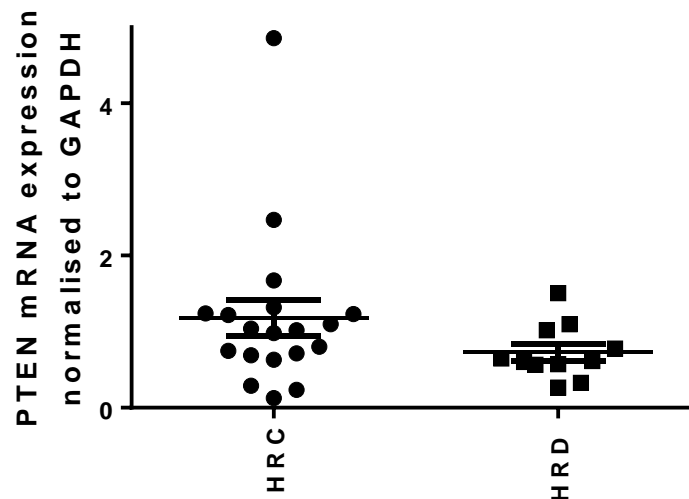


Figure 3-27 PTEN mRNA expression divided by HR function status in PCO cultures. mRNA results are normalised to GAPDH housekeeper gene.

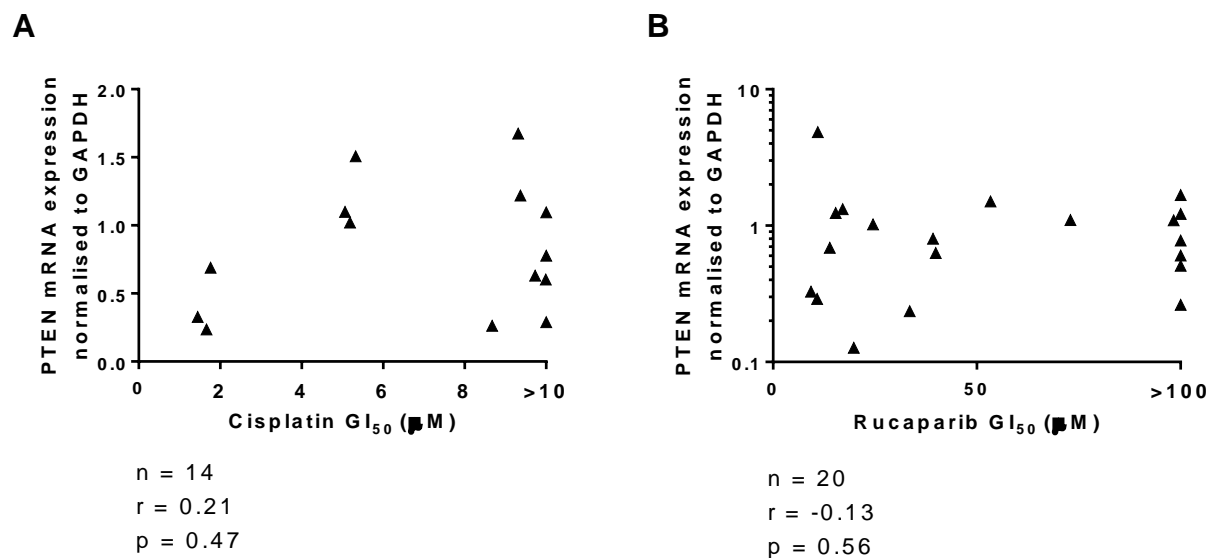


Figure 3-28 Correlation of PTEN mRNA expression with sensitivity to cisplatin and rucaparib in PCO cultures.

mRNA results are normalised to GAPDH housekeeper gene. Sensitivity is expressed as GI₅₀ in μM.

3.4.7.5 PTEN Influence on Survival of Ovarian Cancer Patients

The TCGA 2011 ovarian cystadenocarcinoma database was used to validate findings in our patient cohort. The alteration rate of PTEN in the TCGA dataset was 25/316 (8 %) with 2 mutations (1 missense and 1 truncating), and 23 putative copy number

changes (2 amplification and 21 deep deletion). A trend approaching significance was found for PFS in PTEN mutation cases (Figure 3-29). Median disease free survival was 21.22 months in PTEN mutated cases, compared to 15.64 months in control cases (logrank test $p = 0.06$). A similar trend was observed for overall survival (median overall survival 55.88 months in PTEN mutated cases, compared to 43.5 months in control cases (Logrank test $p = 0.13$), (Figure 3-29).

Differential PTEN expression was found in 39/316 (12 %) of tumours (upregulation in 6 and downregulation in 33 cases). There was no association between PTEN mRNA expression and PFS ($p = 0.22$) and OS ($p = 0.21$).

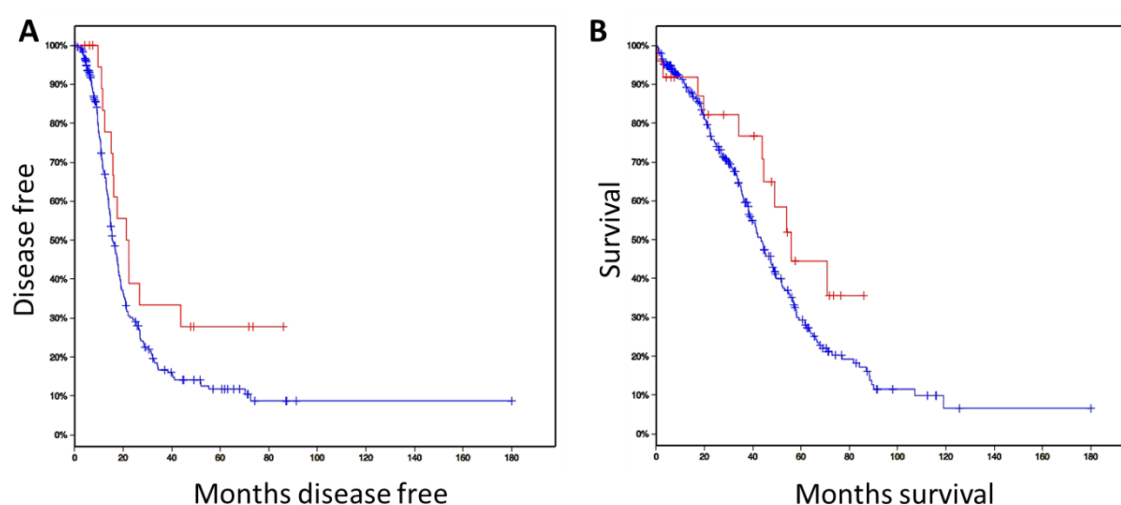


Figure 3-29 PTEN association with survival benefits from TCGA database.

Survival curves for PTEN mutated cases $N=25$ (red line) and control cases $N = 291$ (blue line). **A.** Disease free survival. PTEN alterations $N = 21$, cases relapsed $N = 13$, median months disease free 21.22. Cases without PTEN alteration $N = 239$, cases relapsed $N = 176$, median months disease free 15.64. Logrank test $P = 0.06$ **B.** Overall survival Kaplan-meier estimate. PTEN alterations $N = 25$, cases deceased $N = 11$, median months survival 55.88. Cases without PTEN alteration $N = 290$, cases deceased $N = 170$, median months survival 43.5. Logrank test $p = 0.13$.

3.4.8 Assessment of the Tumourigenic Potential of NUOC-1 Cells

Hypothesis: NUOC-1 cells are capable of forming xenografts in SCID mice

The tumourigenic potential of the cell line was assessed based on its ability to form tumours in 8-10 week old female SCID mice at subcutaneous right gluteal sites. Five mice were transplanted with 5×10^6 cells suspended in 50 % medium / 50 % v/v matrigel subcut. The animals were housed under sterile conditions in a laminar flow

environment with *ad-lib* access to food and water. Tumour formation was assessed by observation for 100 days, after which no tumour formation was detected. This work was kindly performed by Huw Thomas.

As subcutaneous site is not the site for ovarian cancer growth, the tumorigenic potential of this cell line was then assessed based on its ability to form intraperitoneal (IP) tumours in 8-10 week old female SCID mice.

Firstly, the NUOC-1 cells were transduced with SLIEW lentiviral vector. This vector was kind gift from Dr Alex Elder. Transfection was confirmed by an increase in GFP expression on FACS flow cytometry, as described in section 2.17.2. Five mice were transplanted with 5×10^6 cells suspended in PBS. The animals were housed under sterile conditions in a laminar flow environment with *ad-lib* access to food and water.

Tumour formation was assessed by non-invasive whole-body imaging at 0, 10, 55 and 85 days after implantation (Figure 3-30) using the IVIS Spectrum Imaging system (Caliper Life Sciences, Hopkington, USA). Animal handling was performed by Dr Helen Blair. No formation of ascites was noted in the animals. Luciferase signal was present at day 10 and in one mouse at day 55, however the signal reduced over time (Figure 3-31) and no signal could be found in any of the mice at day 85.

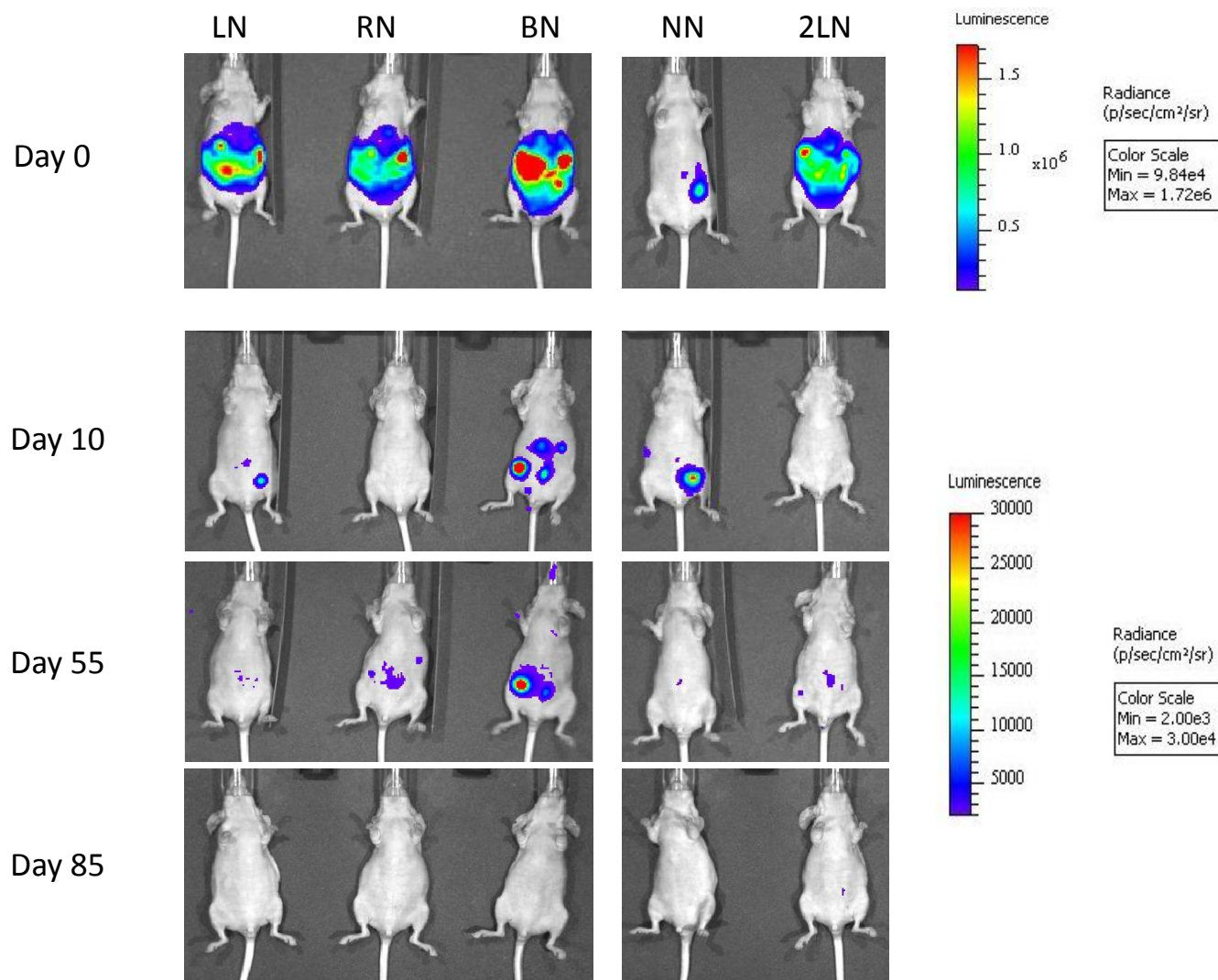


Figure 3-30 NUOC-1 tumourgenicity assessment bioluminescent images.

Mice were transplanted with luciferase-expressing NUOC-1 cells IP. Bioluminescent imaging was performed on day 0, 10, 55 and 85. Mice were marked with ear notches to allow recognition (left notch (LN), Right notch (RN), bilateral notches (BN), no notches (NN) and 2 left notches (2LN). Day 0 images are shown on a different radiance scale to avoid image saturation.

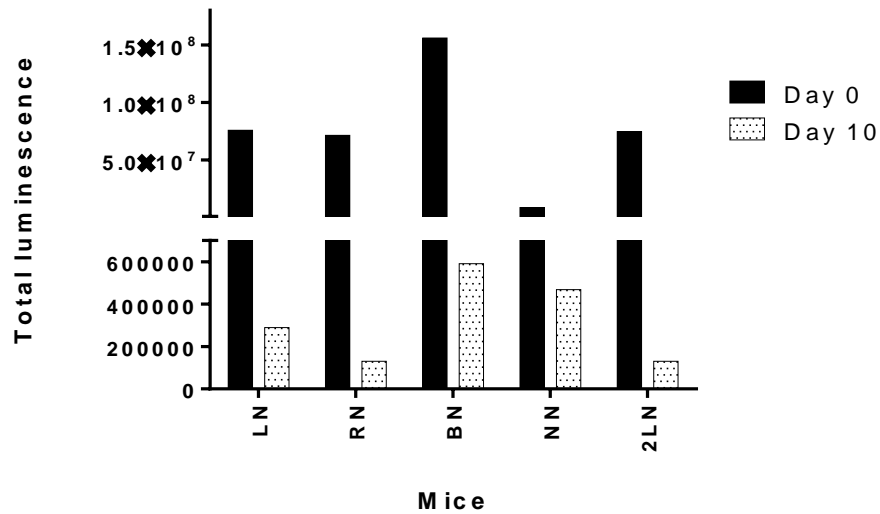


Figure 3-31 Quantification of bioluminescent imaging.

Mice were transplanted with luciferase-expressing NUOC-1 cells IP. Bioluminescent imaging was performed on day 0 and day 10. Mice were marked with ear notches to allow recognition (left notch (LN), Right notch (RN), bilateral notches (BN), no notches (NN) and 2 left notches (2LN). Graph shows the total luminescence for each mouse at the two time points.

3.4.9 NUOC-1 Karyotype

The NUOC-1 karyotype was assessed off-site by the Cytogenetics Laboratory at the Newcastle Institute of Genetic Medicine. The result was a composite of four metaphases (Figure 3-32). NUOC-1 cells revealed a complex, near-tetraploid karyotype, with loss of chromosomes 3,6,11,16 and 19, and structural abnormalities including rearrangements of 5q, 9q, 17p and 18q.



Figure 3-32 NUOC-1 karyotype.

Picture is a representative G-banded metaphase. The result is a composite of 4 metaphases. Arrows indicate the chromosomal abnormalities present in all metaphases assessed.

3.4.10 Clonal Evolution in NUOC-1 Cells

Hypothesis: NUOC-1 cell line is a mixed population of cells which contain gene alterations commonly described in Type I ovarian cancers

To assess clonal evolution, two NUOC-1 subpopulations were derived. NUOC-1 cells were split at passage 4 and either grown continuously to passage 14 (NUOC-1-A1) or frozen and stored in liquid nitrogen for 12 months before being thawed and the also grown to passage 14 (NUOC-1-A2).

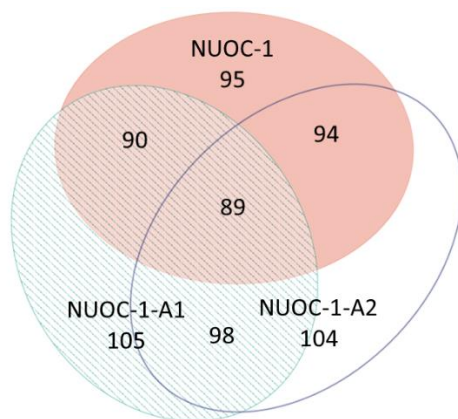
Intra-chromosomal copy number alterations deviating from the baseline copy number state (tetraploid) were identified in NUOC-1-A1, NUOC-1-A2 and parent NUOC-1 cells using OmniExpress Exome BeadChip genotyping data. Both sub population cell lines carried numerous common copy number alterations, indicating a shared recent ancestry (Figure 3-33). However, each cell line also carried a small number of unique copy number alterations not seen in the other cell line, indicating ongoing genomic evolution. Specifically, NUOC-1-A1 and NUOC-1-A2 carried a total of 121 and 116 copy number/CN LOH alterations, respectively; of which 107 were common to both cell lines. The vast majority (>95 %) of copy number alterations were gains, indicating a pro-amplification genotype in both cell lines, with an average amplicon size of 2.6 Mb and 1.2 Mb in NUOC-1-A1 and NUOC-1-A2, respectively. Furthermore, there was clear evidence that both NUOC-1-A1 and NUOC-1-A2 were heterogeneous with respect to copy number alterations, with some alterations being present in virtually all of the cells whereas, other alterations were clearly carried in sub-clones. There was also clear evidence of multiple independent alterations affecting the same genomic regions.

The vast majority of copy number alterations shared by NUOC-1-A1 and NUOC-1-A2 were also visible in parental NUOC-1 cells. Furthermore, the vast majority of copy number alterations seen in NUOC-1-A2 but not NUOC-1-A1 were visible in the parental line, but not those copy number changes which were seen in NUOC-1-A1 but not NUOC-1-A2. The low quality of data derived from parental NUOC-1 cells prohibits the visualisation of some small and/or low magnitude copy number alterations. The majority of copy number alterations unique to NUOC-1-A1 were not discernible in the data derived from parental NUOC-1 cells, thus suggesting that the cell population from which NUOC-1-A1 derived was present as a very minor sub-

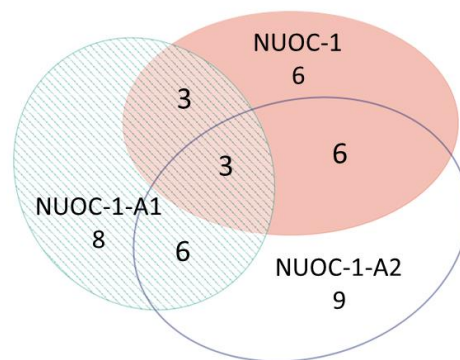
clone in the parental NUOC-1 cells. In contrast, the evidence suggests that the cells from which NUOC-1-A2 ultimately derived constituted the major population of NUOC-1 cells.

With regard to the unique copy number alterations, genes implicated in type II ovarian cancer pathogenesis are also affected by copy number alterations in NUOC-1-A1 and/or NUOC-1-A2 (Figure 3-34). For example, the HINF1B and ERBB2 genes are captured by amplicons of 405Kb and 115Kb, respectively, on chromosome 17 in both NUOC-1-A1 and NUOC-1-A2 cells. Likewise, the AKT1 gene is captured by a 155Kb amplicon on chromosome 14. The ARID1A gene is captured by a large region of copy neutral loss of heterozygosity on chromosome 1, which could unmask a recessive gene mutation.

Gains



Losses



Copy neutral LOH

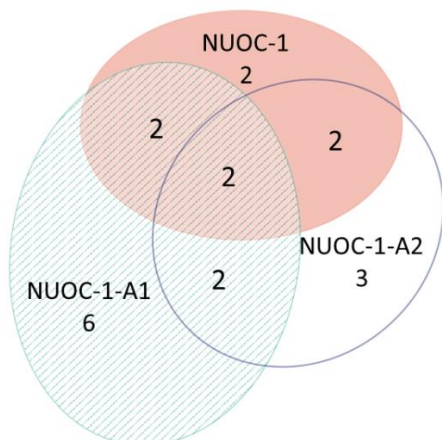


Figure 3-33 Copy number variations in NUOC-1, NUOC-1-A1 and NUOC-1-A2 cells.

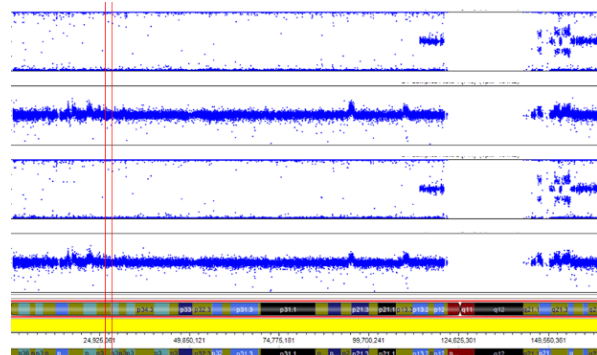
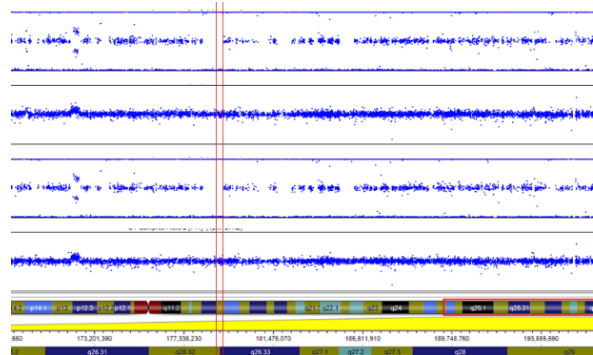
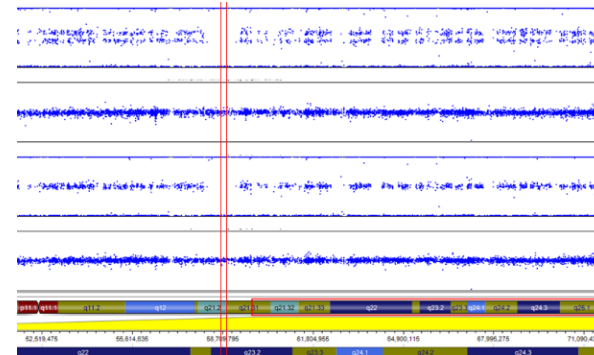
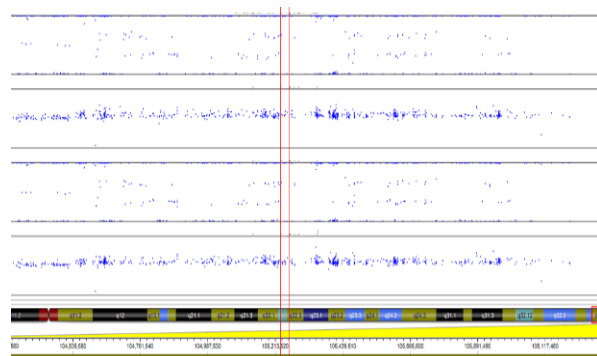
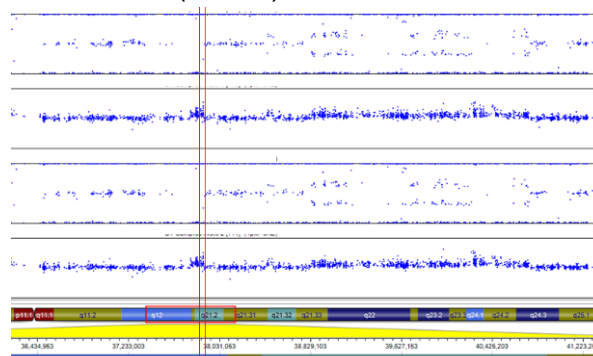
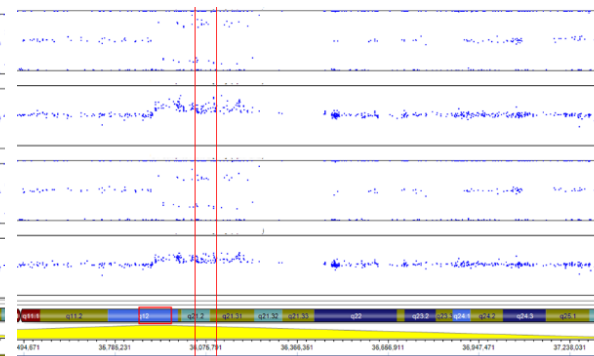
A- ARID1A, chr 1**B - PIK3CA, chr 3****C - PPM1D, chr 17****D - AKT1, chr 14****E - ERBB2 (HER2), chr 17****F - HINF1B, chr 17**

Figure 3-34 Copy number profiles of NUOC-1-A1 and NUOC-1-A2 cell lines.

Each SNP marker is represented and aligned to its position on the chromosomes as well as its designated copy number state. An ideogram of the chromosome is positioned below the SNP marker plots. **A.** ARID1A captured by a large region of copy neutral LOH on chr 1. **B.** PIK3CA located in a region of apparent copy neutral LOH. **C.** PPM1D located in a region of apparent copy neutral LOH. **D.** AKT1, captured by a 155Kb amplicon on chr 14. **E.** ERBB2 (HER2), captured by amplicon of 405Kb on chr 17. **F.** HINF1B, captured by amplicon of 115Kb on chr 17.

NUOC-1-A1 cells had a low level copy number gain affecting the long arm and some of the short arm of chromosome 8 that was not seen in NUOC-1-A2. However, NUOC-1-A2 has a complex high level amplification on chromosome 8 that captures the c-MYC locus (Figure 3-35), and which was present in the dominant clone. It is not possible to discern from the genotyping data the exact copy number in either cell line, although it is clear that NUOC-1-A1 and NUOC-1-A2 will differ significantly in c-MYC gene copy number.

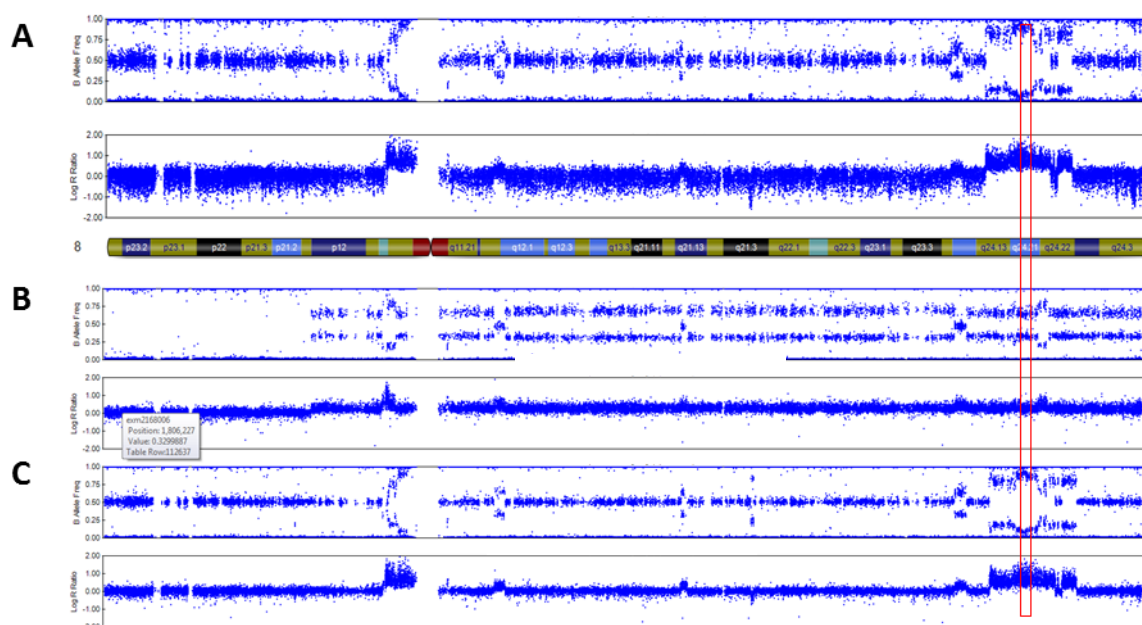


Figure 3-35 Copy number profile of chromosome 8 in NUOC-1 cells.

A. NUOC-1, **B.** NUOC-1-A1 and **C.** NUOC-1-A2 cell lines. Each SNP marker is represented and aligned to its position on the chromosomes as well as its designated copy number state. An ideogram of chromosome 8 is positioned below the SNP marker plots. MYC gene location is marked.

3.4.11 Assessment of MYC Amplification

To further analyse the amplification of MYC and the differences observed between NUOC-1-A1 and NUOC-1-A2, FISH for MYC analysis was carried out off-site by the Cytogenetics Laboratory at the Newcastle Institute of Genetic Medicine. MYC was assessed in samples at four stages of cell line development. These included FFPE tissue of the tumour (collected at the time of surgery), ascites sample from which NUOC-1 was derived (frozen on the day of collection) and the two subpopulations of NUOC-1 – NUOC-1-A1 and NUOC-1-A2, using a break apart MYC probe as described in section 2.15. The results are shown in Table 3-4 and Figure 3-36.

Table 3-4 FISH for MYC results for NUOC-1.

MYC was assessed in paraffin embedded tumour sample from the patient NUOC-1 cell line was derived, ascites sample, NUOC-1-A1 and NUOC-1-A2 cells. The percentage of normal, increased chromosome and MYC amplified cells is stated. HSR - homogeneously staining regions.

Sample	Normal MYC (%)	Modal signal pattern MYC x3~6 (%)	MYC amplification (%)
Paraffin section	20	69	11
NUOC-1 Ascites	14	4	82, HSR
NUOC-1-A1	0	98 MYC x3 (55 %) and MYC x6 (28 %)	2
NUOC-1-A2	0	0	100

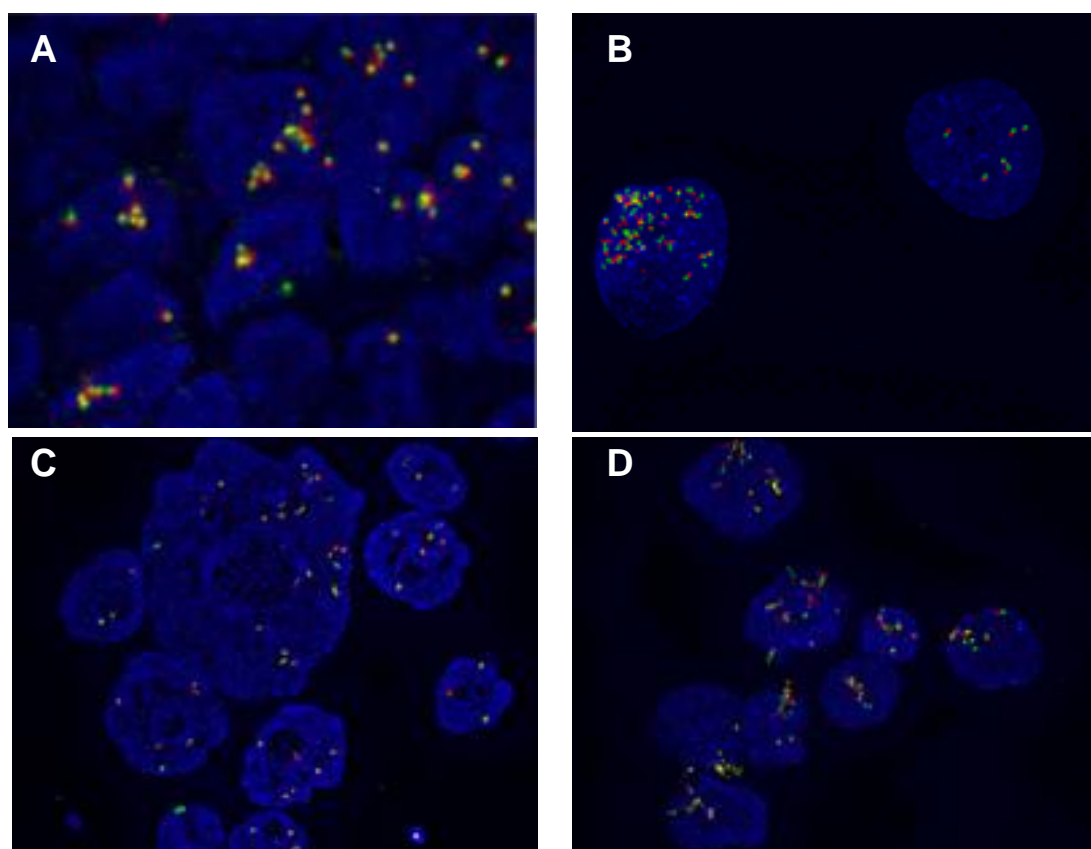


Figure 3-36 FISH immunofluorescent images for MYC in NUOC-1.

Results are **A.** FFPE embedded tumour sample, **B.** NUOC-1 ascites sample, **C.** NUOC-1-A1, **D.** NUOC-1-A2.

FFPE section of tumour was found to contain a modal MYC signal pattern x 3~6 in 69 %, MYC amplification in 11 % and normal MYC signal in 20 % of cells analysed. Ascites sample contained 14 % normal MYC expressing cells. These cells are likely

to be normal mesenchymal cells present in ascites. The majority of cells contain MYC amplification (82 %) with a small number of modal signal pattern (4 %) also. This finding demonstrates heterogeneity between ascites and solid tumour.

The differences of MYC between NUOC-1-A1 and NUOC-1-A2 are very clear and closely relate to the findings from the SNP array. Mostly modal signal pattern was detected in NUOC-1-A1 (98 %), which would be seen as normal copy number in the SNP array, in comparison to 100 % MYC amplification observed in NUOC-1-A2. Also consistently the results support the hypothesis that NUOC-1-A2 forms the major and NUOC-1-A1, the minor clones in the original cell line. Importantly NUOC-1-A1 is likely to represent a major clone in the solid tumour based on MYC expression. However, this hypothesis needs to be assessed using other targets.

No separation of MYC probes was seen in cells with increased chromosome numbers, suggesting that MYC translocation was not present. In cells with HRS amplification, greater numbers of first compared to second probe were observed. This suggests the presence of varied size amplicons.

3.5 Chapter Summary

In this study two models of ovarian cancer were characterised. PCO cultures were generated with an 88 % success rate. The main findings included:

- Slow growing and to senesce at passage 4-5.
- Variable expression of antigens including epithelial markers and CA125.
- Viral particle transduction into PCO cultures was optimised, but transfection using Lipofectamine and electroporation was not possible.
- 46 % of PCO cultures were found to be HRD. HRD correlated with increased sensitivity to rucaparib and cisplatin *in vitro*, but not clinical survival outcomes.

During the project one PCO culture immortalised and was therefore characterised as a novel ovarian cancer cell line. NUOC-1 was derived from the ascites of a chemo naive, caucasian patient at the time of primary surgery. Evidence of intra-tumour heterogeneity between solid and ascites samples was found during the analysis of MYC expression. The main findings included:

- Expression of Pancytokeritin, EpCAM, MOC31 and CA125, but not Vimentin.

- No expression of oestrogen, progesterone and androgen receptors, but positive expression of HER-3 and overexpression of HER-2 receptor.
- NUOC-1 cells were wildtype for p53 and PTEN.
- ARID1A mutation.
- Knockdown of PTEN resulted in, growth inhibition and sensitisation to cytotoxic agents.
- Near tetraploid karyotype, with chromosomal abnormalities of all chromosomes and mixed population of cells.
- Failure to form tumours in SCID mice.
- Unstable and pro-amplification tendency.
- Two subpopulations were derived which were isogenic for MYC amplification. NUOC-1-A1 formed minority population in NUOC-1 parent line whilst NUOC-1-A2 formed the majority subpopulation.

3.6 Discussion

In order to establish new cellular models of ovarian cancer, all the samples of ovarian tissue collected by our group were processed to derive PCO cultures (ODonnell et al., 2014). Two distinct models for the study of ovarian cancer were characterised in this chapter.

3.6.1 Characterisation of PCO Cultures

The ability to generate and utilise primary cultures of ovarian cancer has several advantages over other models, including established cell lines and animal models. It is now recognised that many cell lines in long term culture will undergo further genetic aberrations rendering them dissimilar from their tissue of origin. Furthermore, even a large panel of cell lines cannot accurately represent the heterogeneity that is seen in EOC. The 88 % success rate of viable cultures of epithelial cells is sufficiently high to justify the feasible use of these techniques in clinical practice if diagnostic tests were developed. Furthermore, the ability to store cultures in liquid nitrogen long term allows the possibility of collaboration for research or *post hoc* diagnostic analysis. One of the strengths of developing models of viable cancer cells is that it allows for the use of functional assays which would not be possible using FFPE tissue or even fresh frozen tissue. This is likely to become increasingly important in

the development of biomarkers for treatments which depend upon the dysregulation of a complete pathway, as opposed to aberration of a single gene.

It is not clear why culture from ascites is unsuccessful in a proportion of cases, why senescence occurs at variable passages or why only one culture has immortalised. It is likely, that this is a consequence of a lack of the essential factors required for growth, which are provided *in vivo* by the complex interactions within the tumour microenvironment, but are absent in the artificial culture setting. A recent study described a novel method for establishing cell lines from primary tumour cells using a novel medium with a much higher success rate of immortalisation (Ince et al., 2015). A further explanation could be that cells in the ascites are not always the most viable of tumour cells and stem cells need to be considered.

3.6.2 HR Function in PCO Cultures

As previously demonstrated (Mukhopadhyay et al., 2010), 46 % of PCO cultures were found to be HRD; and HRD cultures were found to be more sensitive to rucaparib and cisplatin, compared to HRC cultures. Replication of these findings provides further support for the constancy of HRD in ovarian cancer, and the importance of HRD in platinum and rucaparib sensitivity. The literature suggests a correlation between chemo sensitivity to platinum and PARPi. In clinical studies, response to the oral PARPi olaparib correlated with platinum free interval (Fong et al., 2010). The result from PCO cultures supports this finding with a positive correlation between *ex vivo* sensitivity to rucaparib and cisplatin.

Lack of association between HR function and survival was contradictory to previous evidence (Mukhopadhyay et al., 2012). Furthermore, *ex vivo* sensitivity to rucaparib and cisplatin was also not associated with a statistically significant difference in survival. The lack of association observed may be due to a number of factors. Firstly, the survival data is not complete, due to time limitations of the project. Assessment of this data in a few years with complete set of clinical data may provide different findings. Secondly, the standardised SRB protocol used, which did not take into account the doubling time of individual cultures, may have overestimated sensitivity in rapidly growing cultures and underestimated sensitivity in slow growing cultures. Thirdly, the assessment of *ex vivo* cultures only translates into clinical survival if the cultures are representative of the tumour. The adherent monolayer of cells cultured

may only represent one subpopulation of ascitic cells collected. Assessment of how representative PCO cultures are of the residual microscopic tumour following surgery are still required. Evidence from NUOC-1 MYC assessment demonstrate discordance between the ascites and solid tumour sample as well as a mixed population which over time developed into two separate cell lines. To capture the heterogeneity of PCO cultures the characterisation of PCO cultures should therefore ideally be performed at time 0, prior to passage. Finally, this analysis has not taken into account histological subtype, the residual volume of tumour at the end of surgery, and chemotherapy treatments actually given, which have all previously been identified as being important in the prediction of clinical outcome (Von Heideman, 2014).

3.6.3 Prediction of HR Function by Genome Expression Arrays

There is a pressing need to identify biomarkers of HRD which would predict the benefit from PARPi in ovarian cancer and potentially multiple other cancer types, regardless of the underlying molecular mechanism (Turner, 2011). Several approaches to the identification of HRD tumours using mutational screening, gene expression profiling, loss of heterozygosity (LOH) assays, telomeric allelic imbalances and large scale transition scores have been developed (Watkins et al., 2014). These gene signatures, however, have not yet achieved widespread use. Several unsupervised multi-strategy approaches and statistical methods have been developed from a high throughput genomic data to identify differentially expressed genes (Liu, 2010, Li, 2008, Kang, 2012) and may represent a superior method of analysis in future studies. The ongoing ARIEL 2 (NCT01891344), a phase 2 trial of rucaparib therapy for women with relapsed HGSOE or endometrioid ovarian cancer, aims to identify a molecular signature of HRD. This will be evaluated further in ARIEL 3 (NCT01968213) which aims to assess rucaparib as a maintenance therapy.

The unsupervised hierarchical clustering in this small dataset found no difference in RNA expression signatures between HRD and HRC cultures. The upregulation of RAD51 and XRCC2 in HRD cultures is promising, but should not be over interpreted. It is unlikely that one marker in isolation is capable of predicting function of the entire pathway. The significantly higher RAD51 expression in HRD cultures in comparison to HRC cultures was unexpected. Based upon the HR pathway, higher RAD51 expression was hypothesised in HRC cultures. The HR assay is not based upon

absolute levels of RAD51 to determine functional status, but a change in level in response to DNA damage. This higher baseline level in the HRD cultured may therefore represent dysfunctional Rad51 present in the nucleus of HRD cells. This finding needs to be explored further.

3.6.4 Molecular Characterisation of NUOC-1 Cell Line

In this study the establishment and characterisation of a novel ovarian cancer cell line, derived from a chemotherapy naïve patient has been described. PCO cultures provide a model that better represents the tremendous heterogeneity of ovarian cancer. This however, has a major limitation, in that the very short life span and slow growth limits the characterisation that is possible in these cultures, as well as their use in repeat experiments. Of the 156 primary cultures established in our laboratory so far, NUOC-1 is the only culture to spontaneously immortalise. NUOC-1 cells continue to maintain their morphology and epithelial marker expression over repeated passages.

A recent meta-analysis found that progesterone receptor (PR) expression predicted favourable survival, while HER2 expression had a negative effect on survival. NUOC-1 was found to be hormone receptor negative and tyrosine receptor positive. This is consistent with the very poor survival observed in this patient. This phenotype of NUOC-1 cells would make this cell line a useful model in study of receptor function.

3.6.5 NUOC-1 Cell Line Represents Endometrioid / Clear Cell Ovarian Carcinoma

NUOC-1 cells were found to contain a polymorphism in exon 4, however functional assessment determined that NUOC-1 cells were wildtype for p53. NUOC-1 cell line was derived from ascites of a mixed histology tumour. *TP53* mutations are reported in the majority of serous ovarian cancer (Ahmed et al., 2010, Cancer Genome Atlas Research, 2011), therefore the p53 wildtype phenotype of NUOC-1 is inconsistent with HGSOC histology and suggests that the small proportion of HGSOC cells were not represented in the sample or failed to immortalise in culture. A recent study has also demonstrated that HGSOC establish cell lines less frequently (Domcke et al., 2013).

Therefore, the NUOC-1 cell line probably represents endometrioid / clear cell ovarian carcinoma. The endometrioid and clear cell carcinomas are both linked to endometriosis and contain similar driver mutations. Endometrioid / clear cell histology for NUOC-1 is also supported by the findings of alterations in genes that are commonly altered in these tumours. These included an insertion mutation in the ARID1A gene. As well as the ARID1A gene being captured by a large region of copy neutral LOH on chromosome 1 found on SNP array. ARID1A is reported to be lost or mutated in 50 % of clear cell carcinoma (Anglesio et al., 2011, Tan et al., 2013). Other genes located in regions of copy neutral LOH included PIK3CA and PPM1D. PIK3CA has been reported to be mutated in 40 %, and PPM1D in 10 %, of clear cell carcinomas (Anglesio et al., 2011, Tan et al., 2013). SNP array also found AKT1, ERBB2 and HINF1B to be captured by amplicons. HINF1B is reported to be upregulated in almost 100 % of clear cell carcinoma (Anglesio et al., 2011, Tan et al., 2013). AKT and ERBB2 amplifications are reported in 14 % of clear cell carcinoma (Anglesio et al., 2011, Tan et al., 2013). Resistance to paclitaxel, as exhibited by NUOC-1 cells, is also commonly seen in clear cell carcinoma (Itamochi et al., 2008).

3.6.6 PTEN is a Potential Target for Ovarian Cancer Sensitisation to Cytotoxic Agents

PTEN mutations are reported in 50 % of clear cell / endometrioid carcinomas. NUOC-1 cells were found to be wildtype for PTEN. As a negative regulator of growth it was hypothesised that PTEN inhibition would increase chemo-resistance. Chemo-resistance, particularly to cisplatin has been reported in PTEN-mutated cancers (Keniry and Parsons, 2008, Stewart, 2007). However, in this study, PTEN knockdown caused chemo- and radio-sensitisation in NUOC-1 cells, but had no effect in OSEC-2 cells.

In the PCO model, no association between PTEN expression and sensitivity to rucaparib or cisplatin was observed. This was supported by a lack of association of PTEN expression with survival in the TCGA cohort. This difference may be due to histological differences between NUOC-1 and PCO cohorts, as the majority of PCO cultures were HGSOc, and only 8 endometrioid / clear cell. A further explanation for the difference may be that knockdown models represent *in vitro* alteration of PTEN expression, which may not be representative of baseline activity in PCO cultures (Hunt et al., 2012). Previous groups have similarly found that experimentally removed

PTEN in cell line models do not behave like cancer cells developed in a PTEN-null genotype context, possibly due to accumulated genetic aberrations that occur in a PTEN-independent manner (Hunt et al., 2012). An important further reason for the lack of association is that only mRNA expression was assessed. Post translational modification including phosphorylation, acetylation, methylation, oxidation have been reported (Minami et al., 2014).

Additionally PTEN loss has been demonstrated to induce sensitivity to PARPi in cell line models, however recent findings from TOPARP trial (NCT01682772) indicate that PTEN loss does not confer sensitivity to PARPi (Mateo et al., 2015). However, association of PTEN mutations with a trend towards improved survival suggests that PTEN loss may be a useful biomarker for treatment sensitivity and survival outcomes. These results need to be validated in further large cohorts of ovarian cancer.

A link between PTEN loss and HR deficiency is debated with some groups reporting that PTEN attenuates RAD51 gene expression and recruitment to double strand DNA breaks (McEllin et al., 2010), whilst others refute this (Fraser et al., 2012, Hunt et al., 2012). In this study no association of PTEN with HR function was found, either in knockdown models or our primary culture cohort. These results provide further evidence to suggest that PTEN has little or no role in HR pathway function.

3.6.7 NUOC-1 Cells are HRC, but BER Defective

Functional assessment found NUOC-1 cells to be HRC. This finding is supported by the sensitivity of NUOC-1 to rucaparib, cisplatin and irradiation, being equivalent to the OSEC-2 cell line, which was derived from normal ovarian epithelium.

NUOC-1 cells were found to be BER defective. NUOC-1 cells were also exquisitely sensitive to the Topo I poison camptothecin. Sensitivity to Topo I poisons due to BER defects has been previously demonstrated comparing isogenic cell lines EM9 and AA8 (Plo et al., 2003). Further confirmation of BER defects could be confirmed by assessing sensitivity to H₂O₂ and temozolomide and topotecan. BER defective cells have been shown to be sensitive to all these therapies (Illuzzi and Wilson, 2012). Stratification of ovarian cancer by BER status would be useful in selection for second line therapy with topotecan versus liposomal doxorubicin. The NUOC-1 cell line is

therefore a useful model for the assessment of further novel therapeutics in BER defective ovarian cancer.

3.6.8 Xenograft Development was not possible from NUOC-1 Cells

NUOC-1 cells were not able to form xenografts in SCID mice. It has been previously suggested that cell lines derived from patients with indolent disease exhibit low tumourgenicity (Laks et al., 2009). This is not the case for the NUOC-1 cell line, as the patient from which the cell line originated had extremely aggressive disease and lived only 52 days post optimal debulking surgery. Whilst the inability of NUOC-1 cells to form xenografts limits its use by some researchers, this should not detract from the phenotype of this cell line. Furthermore, NUOC-1 tumourgenicity in mice with complete absence of immune function was not assessed due to the time and resource limitations of this study.

3.6.9 NUOC-1 Cells Reflect the Genomic Instability and Heterogeneity of Ovarian Cancer

The results obtained with the G-banding karyotype reflect previously published karyotype studies on epithelial ovarian cancer, where high genomic instability is observed (Deger et al., 1997). Low grade cancers generally have a normal karyotype and therefore the NUOC-1 karyotype would suggest it to be a high grade clear cell / endometrioid tumour.

The heterogeneity of cells observed in NUOC-1 better reflects the heterogeneity of ovarian cancer not seen in cell lines derived from a single clonal population. SNP array results provide further insight into the extensive genomic alterations present in this cell line. Further investigation of the lesions in this cell line in the NUOC-1-A1 and NUOC-1-A2 subpopulations may provide insights into the molecular events that contribute to ovarian cancer initiation and progression.

High levels of c-MYC have been linked to poor PFS and OS in ovarian cancer and siRNA-mediated c-MYC silencing has been explored as a potential target in platinum resistant ovarian cancer with positive results (Reyes-Gonzalez et al., 2015). SNP and FISH analyses of MYC provide evidence for heterogeneity of solid tumour and ascites samples and for NUOC-1-A2 subpopulation being derived from a majority

and NUOC-1-A1 from a minority population of the ascites. The two subpopulations of NUOC-1 provide a good isogenic model for the exploration of c-MYC.

3.7 Future Work

Validation of targets identified by SNP array are planned to be carried out. Validation of ERB2 expression by IHC in FFPE tissue of the tumour is also planned. ERB2 validation will be carried out in collaboration with the Pathology Lab at the Royal Victoria Infirmary. Completion of ARID1A protein and function assessment in NUOC-1 culture would add to the characterisation of the cell line. Furthermore, assessment of PTEN mutational and functional status in a larger cohort of PCO cultures would add to the body of knowledge of the role of PTEN in ovarian cancer.

Further to the submission of the NUOC-1 cell line manuscript for publication, the immediate plan for the cell line is to make it commercially available. The unique phenotype of the cell line which has been extensively characterised here, would make NUOC-1 an invaluable model for the study of type I ovarian cancer.

CHAPTER 4 ASSESSMENT OF NHEJ FUNCTION IN OVARIAN CANCER

4.1 Introduction

The NHEJ pathway plays an important role in genome maintenance after DNA damage. NHEJ has been demonstrated to repair up to 90 % of DNA DSBs in human cells and to function throughout the cell cycle (Valerie and Povirk, 2003). As discussed in section 1.4.5.2, the classical NHEJ pathway is initiated by the binding of the Ku heterodimer (Ku70 and Ku80) to a DNA DSB and subsequent association, and autophosphorylation of the DNA-dependent protein kinase catalytic subunit (DNA-PK_{cs}) (Walker et al., 2001). This trimeric DNA-PK complex facilitates ligation by recruitment of the XRCC4/LIG4 complex. Mutations in classical NHEJ pathway components have been linked to immunodeficiency and developmental abnormalities (O'Driscoll et al., 2004, Sekiguchi and Ferguson, 2006). Furthermore, underactivity of the NHEJ pathway has also been linked to bladder cancer (Bentley et al., 2004, Bentley et al., 2009, Windhofer et al., 2008) and leukaemia (Gaymes et al., 2002, Deriano et al., 2005). These findings underscore the importance of the NHEJ pathway for maintaining genome integrity.

The DNA damage response (DDR) is becoming increasingly recognised as an important determinant of response to cancer therapeutics. This interest was initially provoked by the paradigm shifting discovery that inhibition of BER with PARPi was synthetically lethal in HRD tumours (Bryant et al 2005, Farmer et al 2005). PARPi were therefore selectively targeting the defect arising in the tumour, but not in normal tissues (Ashworth, 2008b, Bryant et al., 2005, McCabe et al., 2006). Given the finding that ≥ 50 % of ovarian cancer were HRD (Mukhopadhyay et al., 2010, Cancer Genome Atlas Research, 2011), as well as building evidence for efficacy of PARPi in ovarian cancer, means that PARPi are likely to play an important role in the future treatment of ovarian cancer. A number of studies also indicate a connection between NHEJ and PARP-1. In particular, PARP-1 interacts with the Ku proteins *in vitro* and *in vivo* (Wang et al., 2006b, Galande and Kohwi-Shigematsu, 1999, Couto et al., 2011), and Ku70, Ku80 and DNA-PKcs have been shown to be capable of binding to ADP ribose polymers (Pleschke et al., 2000, Li et al., 2004a, Gagne et al., 2008). The genetic ablation of KU70 and LIG4 has been shown to restore the survival of PARP1-deficient cells exposed to agents inducing DSBs (Wang et al., 2006b, Hochegger et

al., 2006). Also, DNA-PK inhibition and depletion has been shown to result in HR function recovery and PARPi resistance *in vitro* (Patel et al., 2011).

Many *in vitro* studies have demonstrated that complementary DNA ends are joined in an efficient and accurate manner by NHEJ (Baumann and West, 1998, Labhart, 1999). However, *in vivo*, DSBs are often chemically modified, staggered, and/or are comprised partially or completely of incompatible DNA ends that require modification before joining can take place (Valerie and Povirk, 2003). The recruitment of proteins involved in the processing of DNA ends depends on the type of modification required (Bentley et al., 2004). Such end processing may result in the loss of a small number of terminal nucleotides at the resultant junctions, such that NHEJ is an error prone repair pathway and is potentially a mutagenic process (Lieber et al., 2003).

In the absence of the classical NHEJ pathway, there is evidence that an alternative Ku-independent mechanism for the end-joining (A-EJ) of DSBs can be utilised (Pannunzio et al., 2014, Rai et al., 2010, Iliakis et al., 2004, Wang et al., 2003, Yan et al., 2007, Corneo et al., 2007). This mechanism uses small regions of microhomology at internal sites on the DNA substrate, but unlike HR, A-EJ is inherently error-prone. This is because the use of microhomology leads to deletion of sequences from the strand being repaired, and also to chromosomal translocations (Ceccaldi et al., 2015a, Mateos-Gomez et al., 2015). A-EJ has recently been reported to be overexpressed in HGSOC (Ceccaldi et al., 2015a), however, to date NHEJ function in ovarian cancer is unknown. The selection of repair mechanisms has been discussed in section 1.4.5.4.

A number of methods for assessing the function of a pathway are described in the literature. Mutations of the genes in question can be used to assess the function of a pathway. The benefit of this method is the applicability of a high throughput approach in analysing large numbers of samples. Furthermore, many publically available databases have already analysed mutations in genes in the NHEJ pathway. However, not all mutations result in functional alterations and therefore may not have any impact on the function of the gene or the overall pathway. In the NHEJ pathway, the majority of mutations reported are SNPs, with many of them having contradicting reports of functionality and association with cancer, as summarised in appendix 1.

mRNA and protein expression may be a better assessment of pathway function. However, the minimal expression required for the pathway to function is unclear for

many proteins. Functional assessment of the pathway would evaluate its function independently of alterations of specific genes. For this study, NHEJ function was examined using functional assays. Furthermore, possible biomarkers for clinical application and heterogeneity of the NHEJ function were assessed.

4.2 Aims for Chapter 4

Despite the mounting evidence for NHEJ role in PARPi sensitivity, NHEJ function has not been investigated in ovarian cancer *in vivo* to date. The aim for these investigations was therefore to assess NHEJ function in ovarian cancer cultures, and to relate the function to HR competence and to rucaparib and cisplatin sensitivity. Specifically the experimental aims were as follows:

- Optimise functional NHEJ assays.
- Assess NHEJ function in a panel of ovarian cancer cell lines and a panel of primary ovarian cancer cultures.
- Correlate rucaparib and cisplatin sensitivity with NHEJ function.
- Assess the expression of NHEJ mRNA and protein, and correlate the expression with end joining competence. Assess the feasibility for the use of mRNA and protein expression as possible biomarkers.
- Assess DNA-PK autophosphorylation, as a potential biomarker for NHEJ function.
- Validate NHEJ biomarkers in FFPE tissue from tumour samples matched to ascites samples.
- Examine heterogeneity of NHEJ function in ovarian cancer.

4.3 Results

The TCGA bioportal was used to assess the frequency of NHEJ gene aberrations in a primary ovarian cancer cohort (Figure 4-1). Assessment of the TCGA data found aberrations in NHEJ genes in 60 % of cases. The majority of alterations (41 %) were found in XRCC6 (Ku70). The alterations included amplifications, deletions and mutations. At mRNA level both up and downregulation were reported. It is unclear as to which of the alterations results in functional loss of NHEJ.

Altered in 190 (60%) of 316 cases/patients

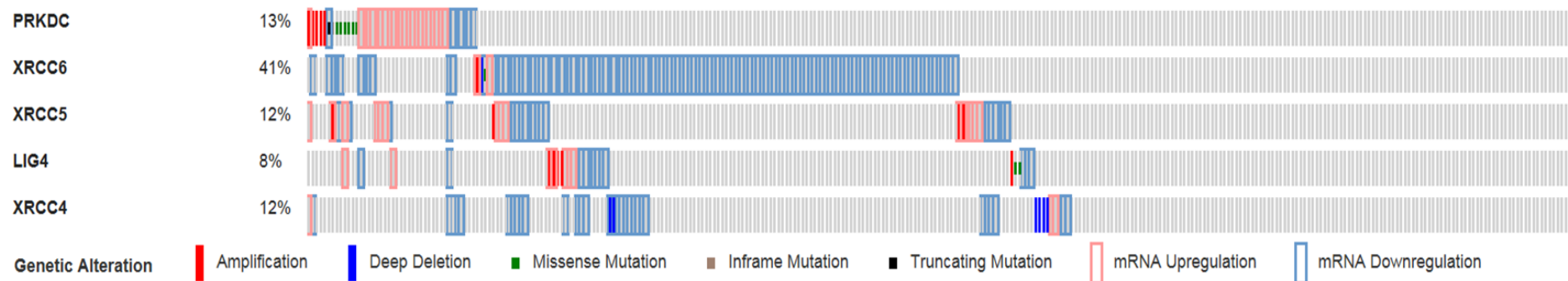


Figure 4-1 NHEJ gene aberrations reported in the TCGA database.

NHEJ genes were found to be altered in 190 (60 %) of 316 cases / patients.

4.3.1 Optimising NHEJ Assay

A number of assays are described in the literature for assessing end joining. Two assays were selected from a literature review, and optimised for this study. The selected end joining assays were initially optimised in a cell line derived from normal ovarian epithelium (OSEC-2) and cell lines with known NHEJ function, by using DNA-PKcs competent and defective isogenic cell lines.

4.3.1.1 End Joining Accuracy Depends on DSBs Compatibility

Three vectors were used for this assay, all were a kind gift from Dr A. Kiltie, Oxford. Digestion with BstXI resulted in the formation of either compatible DSB (Co), 2 base mismatch (2I) or 4 base mismatch (4I) (Figure 4-2). The digestion optimisation is described in section 2.6.1.2.

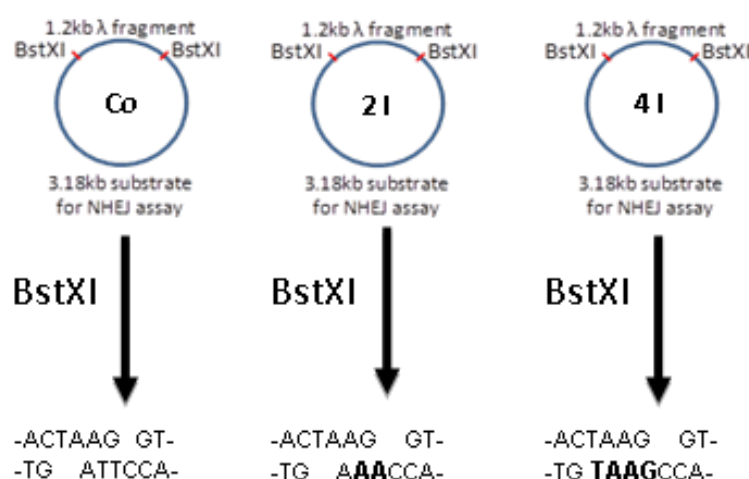


Figure 4-2 Diagrammatic representation of BstXI digested products.

T4 ligase ligated Co substrates, but incompatible substrates could not be joined without the addition of the appropriate λDNA (Figure 4-3). OSEC-2 cells were able to rejoin 34.8 % of Co, 15.9 % of 2I and 13.7 % of 4I substrates (Figure 4-3 and Figure 4-4). The addition of the λDNA fragment increased the rejoining rate of incompatible substrates (50.8 %, $p < 0.001$ of 2I and 43.3 %, $p = 0.0004$ of 4I), but had no effect on the rejoining of compatible substrates. As both 2I and 4I had similar rejoining rates, assessment of cell line and PCO panels was performed using Co and 2I substrates only.

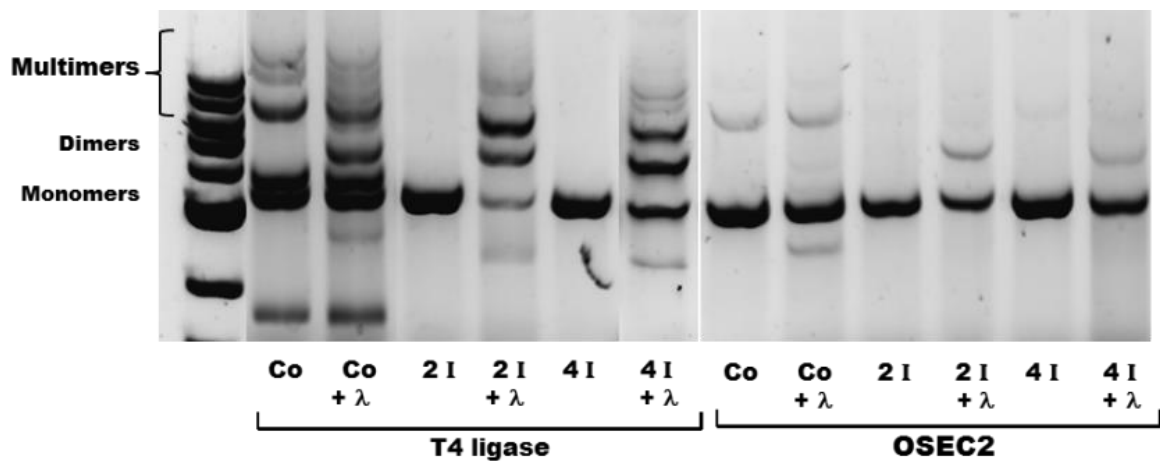


Figure 4-3 Rejoining of *Bst*XI substrates.

Results are for compatible (Co), 2 base mismatch (2I) and 4 base mismatch (4I) substrates with or without addition of λ substrate by T4ligase and OSEC-2 cells. Successful rejoining is demonstrated by the presence of multimer bands. Gels are representative of 3 independent experiments.

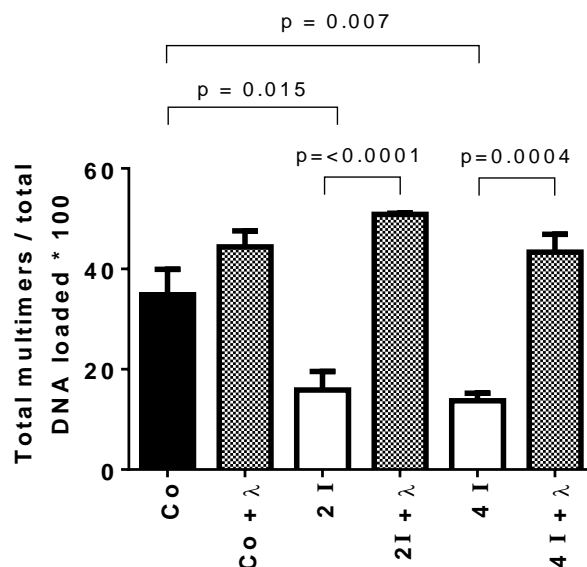


Figure 4-4 Densitometry quantification of OSEC-2 rejoining of *Bst*XI substrates.

Results are for compatible (Co), 2 base mismatch (2I) and 4 base mismatch (4I) substrates, with or without addition of λ substrate. Rejoining of results are expressed as total rejoined products / total DNA loaded. Error bars are SEM.

Comparison of the rejoining undertaken in paired DNA-PK deficient and proficient cell lines, demonstrated that whilst compatible ends are largely rejoined correctly by all cell lines, DNA-PK deficient V3 and M059J cells were unable to rejoin 2I substrates (Figure 4-5).

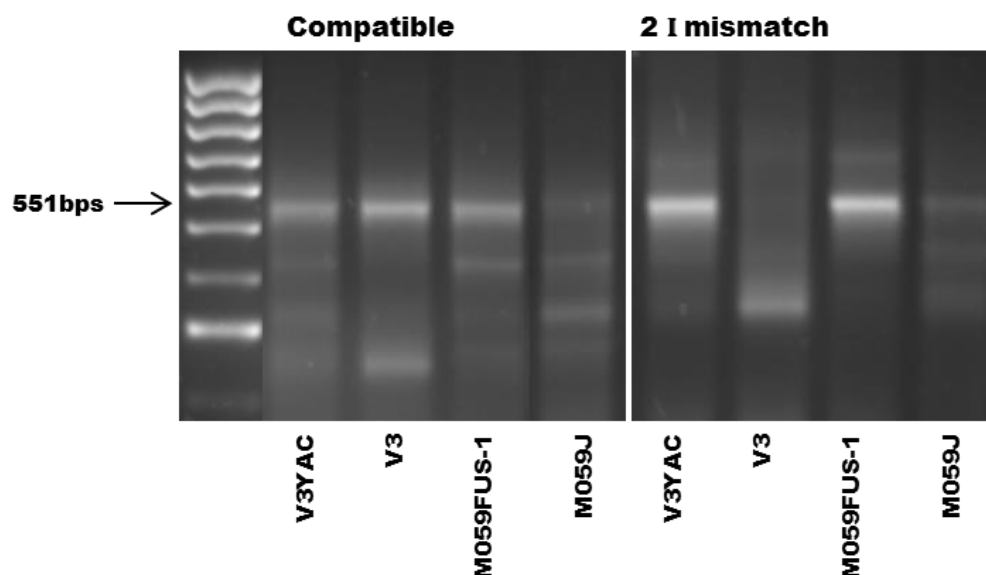


Figure 4-5 PCR analysis of cell line rejoining of Co or 2I BstXI substrates.

Cell lines used were: V3YAC (DNA-PKcs corrected) and V3 (DNA-PKcs deficient), M059FUS-1 (DNA-PKcs corrected), M059J (DNA-PKcs deficient). The rejoin products were amplified using pFOR and pREV primers. Correct rejoining produces products of 551bps. Inaccurate rejoining with loss of bases results in smaller or no product formation. Gels are representative of 3 independent experiments.

4.3.1.2 Confirmation of NHEJ Inhibition by NU7441

The DNA-PK inhibitor NU7441 was found to inhibit end joining in a concentration-dependent manner in DNA-PKcs complemented V3YAC cells, but had no effect in DNA-PKcs deficient V3 cells (Figure 4-6).

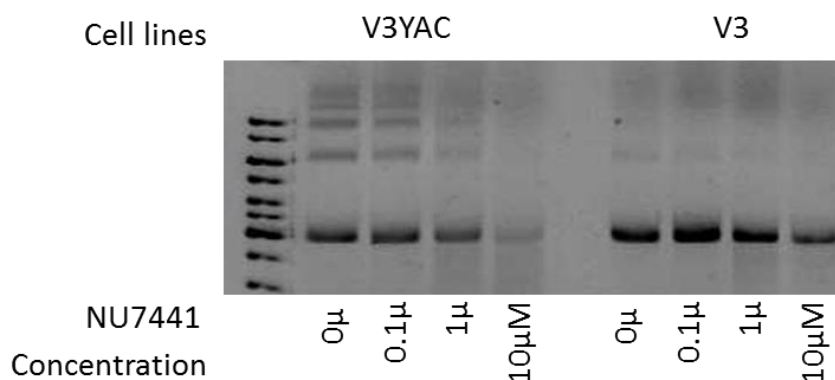


Figure 4-6 Inhibition of end joining of BstXI digested Co substrates by NU7441.

Results are for V3YAC (DNA-PKcs proficient) and V3 (DNA-PKcs deficient) cell lines. End joining is analysed by agarose gel electrophoresis and GelRed staining. Gels are representative of three independent experiments.

4.3.2 DNA End Joining in Established Epithelial Ovarian Cancer Cell Lines

To ensure the cell free extract assay represented the cellular end joining accurately, NHEJ function was assessed in a panel of immortalised cell lines using both the cell extract assay and a cellular luciferase assay.

Whilst immortalised non-cancerous ovarian surface epithelium OSEC cells were able to rejoin 2I ends accurately, four of the six EOC cell lines were unable to rejoin 2I substrate, thus indicating NHEJ deficiency (Figure 4-7). This correlated with a mean accurate rejoining rate of 24.6 % (95 % confidence interval (CI) = 11.5 to 37.6 %) by cell lines capable of rejoining 2I substrates, compared to 11.5 % (95 % CI = 6.8 to 16.3 %, $p = 0.03$) by cell lines unable to rejoin 2I substrates, when assessed using the luciferase cellular assay (Figure 4-8), (pearson correlation $r = 0.79$ $p=0.007$, Figure 4-9).

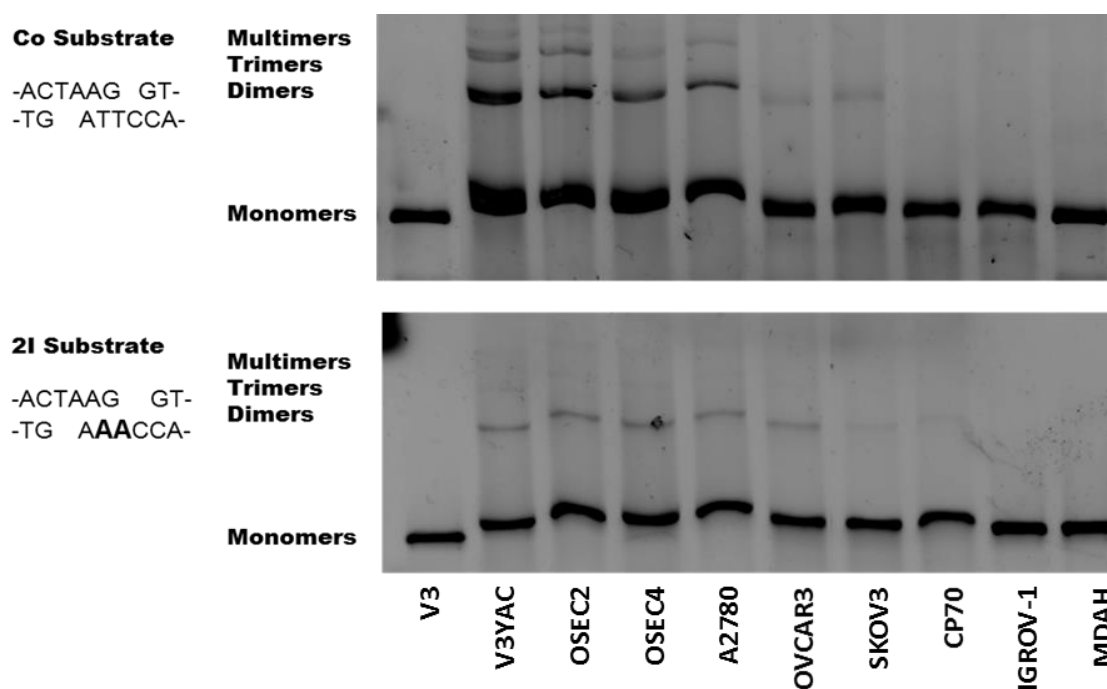


Figure 4-7 End joining of compatible and 2I BstXI substrates by ovarian cell lines. Gels are representative of 3 independent experiments.

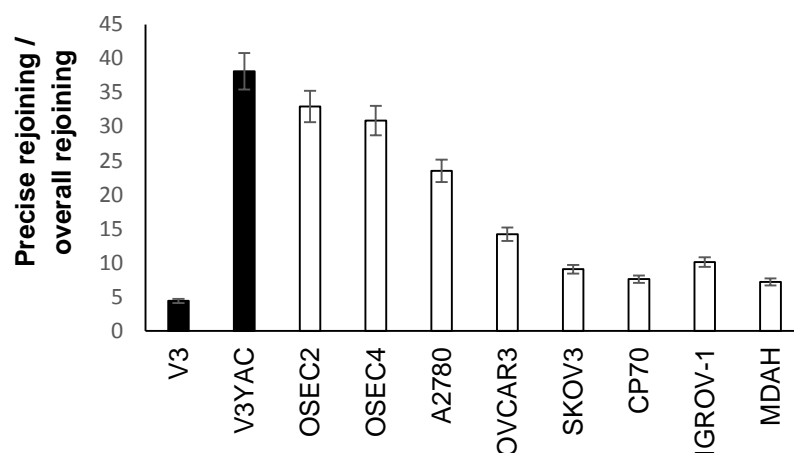
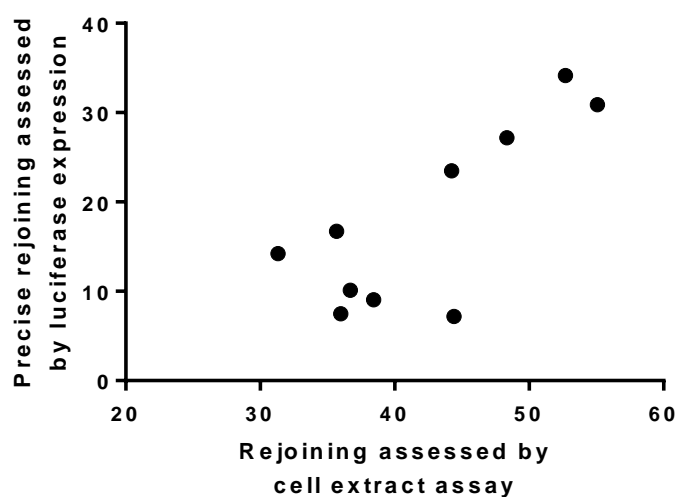


Figure 4-8 Intracellular end joining of linearised pGL2 vector by cell lines.

Measured as precise rejoining / overall end joining x 100. Data are average of three independent experiments. Error bars are SEM.



n = 10
r = 0.79
p = 0.007

Figure 4-9 Correlation of luciferase cellular assay and cell extract assay.

4.3.3 DNA End Joining in PCO Cultures

To understand if the frequency of NHEJ defects in immortalised cell lines represents the frequency in ovarian cancer *in vivo*, NHEJ function was assessed in a collection of PCO cultures.

4.3.3.1 Cell Extract NHEJ Assay Optimisation in PCO Cultures

Hypothesis: Functional assessment of NHEJ can be undertaken in primary ovarian cancer cultures

Rejoining by PCO extracts was optimised using PCO 138, 139 and 142 (Figure 4-10). For each PCO culture two extracts were prepared from passages 1 and 2. Consistent rejoining was noted between passages. For the remainder of the study, end joining was quantified using 3 separate lysates for each PCO culture from passage 1-3.

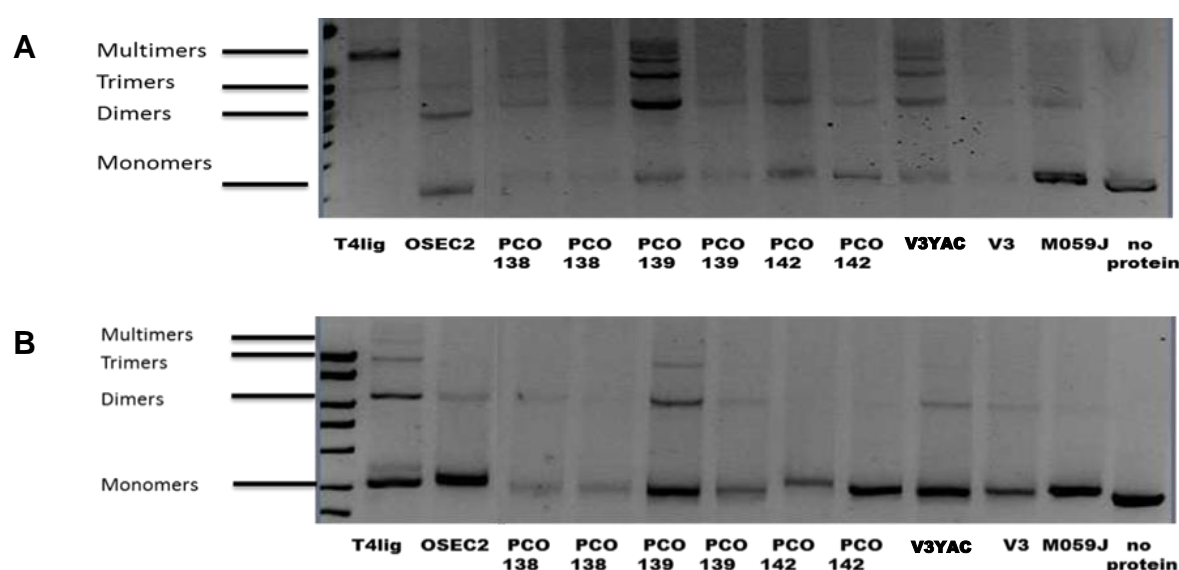


Figure 4-10 End joining of compatible BstXI substrates by PCO cultures.

GelRed detection and quantification of end joining of BstXI **A.** compatible and **B.** 2I incompatible substrates. Gels are representative of 3 independent experiments. T4Ligase, OSEC-2 and V3YAC (DNA-PKcs corrected) were used as positive controls. V3 and M059J (both DNA-PKcs deficient) cell lines were used as a negative controls. Water was used as a contamination control.

As described in section 3.3.1.4, transfection of vectors into PCO cultures was not possible. Therefore, the decision was made to assess end joining function using the cell extract assay only.

4.3.3.2 NHEJ Function in PCO Cultures

Hypothesis: NHEJ pathway is defective in a significant proportion of ovarian cancer cultures

NHEJ was assessed in 40 PCO cultures. There was significant inter-sample variability (rejoining range 5 % to 39 % of loaded DNA). The majority of extracts end joined DNA substrates to form dimers whilst 5 cultures (12.5 %) also formed trimers and further multimers. (Figure 4-11). PCR analysis of the junctions formed demonstrated that the rejoining of the Co substrate was accurate (Figure 4-12).

18 of the 40 PCO cultures were found to be NHEJD, as demonstrated by incubation with 2I substrates producing either no products, or forming products of significantly smaller size (Figure 4-12). Furthermore, some cultures formed multiple bands of different sizes indicating loss of differing numbers of nucleotides. Extensive resection has been demonstrated to be due to use of microhomologies in this vector in the absence of the functional NHEJ pathway (Bentley et al., 2004).

Repair of 2I substrates was independent of the repair of competent substrates (median 23.59 % (95 % CI = 13.72 to 28.31 %) by NHEJC cultures, compared to 17.05 % (95 % CI = 12.9 to 27.65 %) by NHEJD cultures, unpaired t test $p = 0.59$).

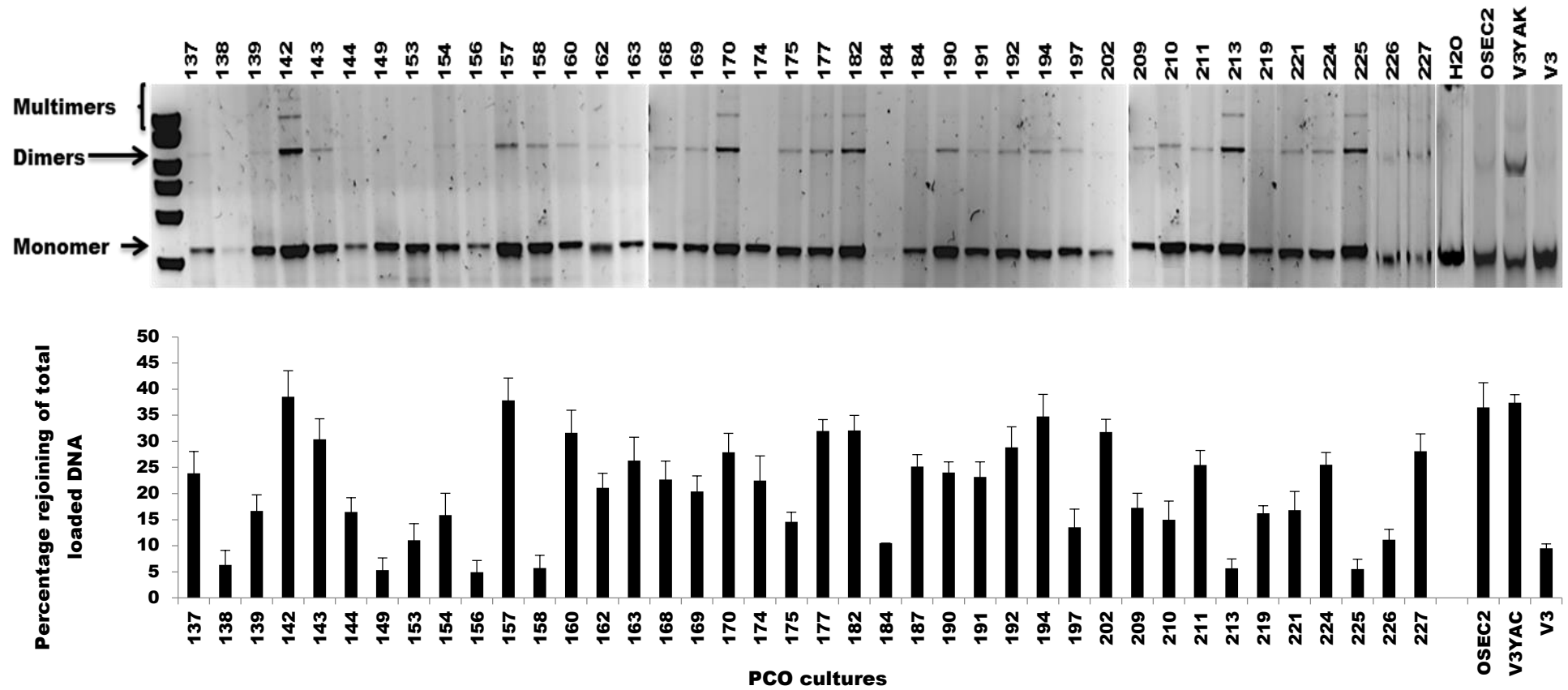


Figure 4-11 End joining of compatible *Bst*XI substrates by PCO cultures. GelRed detection and quantification of end joining of *Bst*XI compatible substrates.

Gels are representative of 3 independent experiments. OSEC-2 and V3YAK (DNA-PKcs corrected) were used as positive controls. V3 (DNA-PKcs deficient) cell line was used as a negative control. Water was used as a contamination control. Error bars are SEM. N = 40.

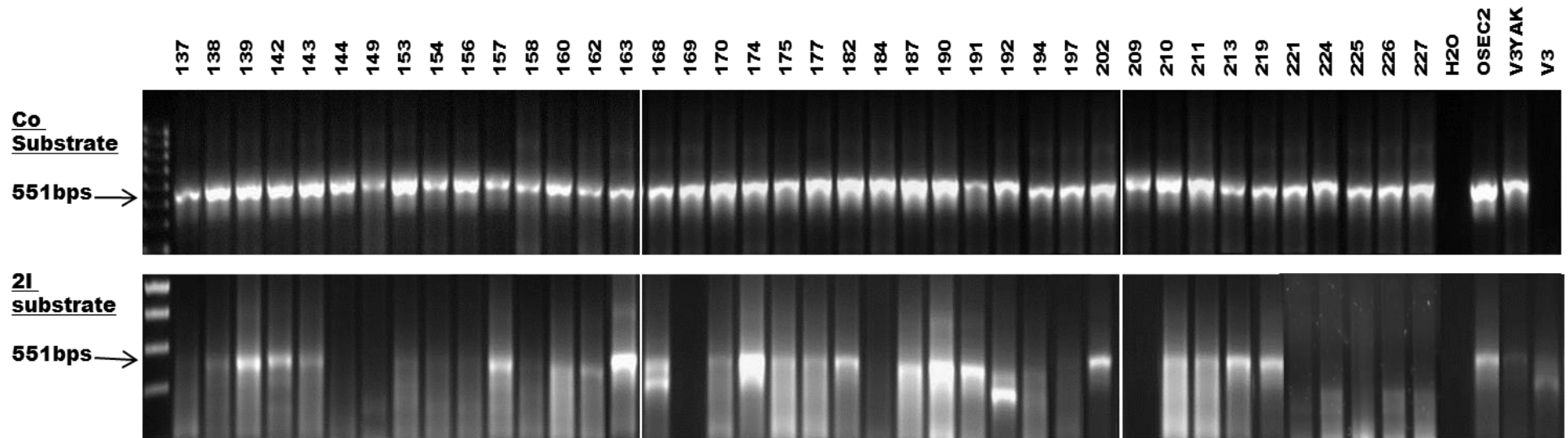


Figure 4-12 Accuracy of rejoining of 2I BstXI substrates by PCO cultures.

PCR analysis of rejoined DNA of Co and 2I substrates amplified using pFOR and pREV primers. Correct rejoining produces products of 551bps. Inaccurate rejoining with loss of bases results in smaller or no product formation. Gels are representative of three independent experiments. N = 40.

4.3.4 Biomarker Development for NHEJ Function

In order to identify potential biomarkers of the NHEJ pathway which would be suitable for clinical use, a panel of RNA and protein species was examined and correlated with NHEJ function.

Hypothesis: DNA-PK autophosphorylation is a potential biomarker for NHEJ function

4.3.4.1 pDNA-PK Foci Formation Correlation with NHEJ Function

The first potential biomarker which was assessed was the use of phospho-DNA-PK foci formation after irradiation. Consistent with the cell extract and cellular assays, a statistically significant increase in phospho-DNA-PKcs foci formation was demonstrated in NHEJC cell lines. Meanwhile, NHEJD cell lines did not show a significant increase in the formation of phospho-DNA-PKcs foci after DNA damage (Figure 4-13).

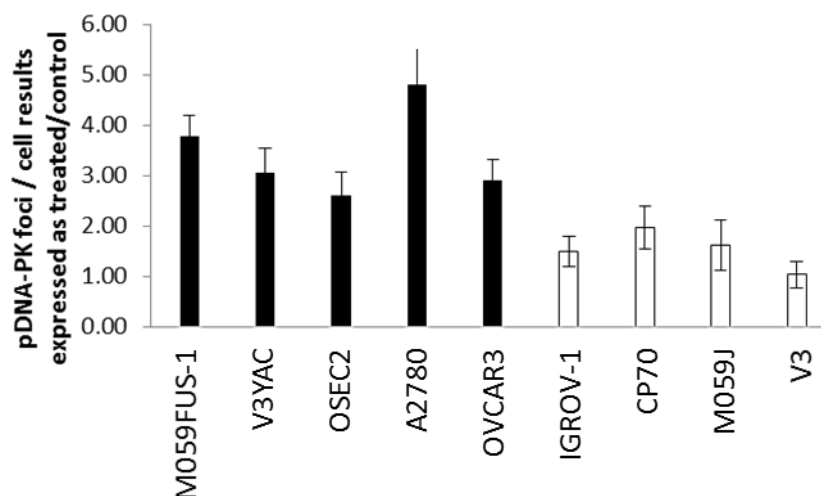


Figure 4-13 NHEJ assessment by immunofluorescence.

Phospho-DNA-PK foci count per cell in cell lines. Results are foci numbers 1 hr after irradiation normalised to un-irradiated controls. Results are the average of 3 independent experiments. Error bars are SEM. Cell lines found to be functionally NHEJC are shown in black and NHEJD in white bars.

However, DNA-PK autophosphorylation did not correlate with NHEJ function in PCO cultures (Figure 4-14). Phospho-DNA-PKcs formation in PCO cultures also did not

correlate with γ H2AX foci formation, therefore the amount of DNA damage induced is not responsible for the lack of association observed.

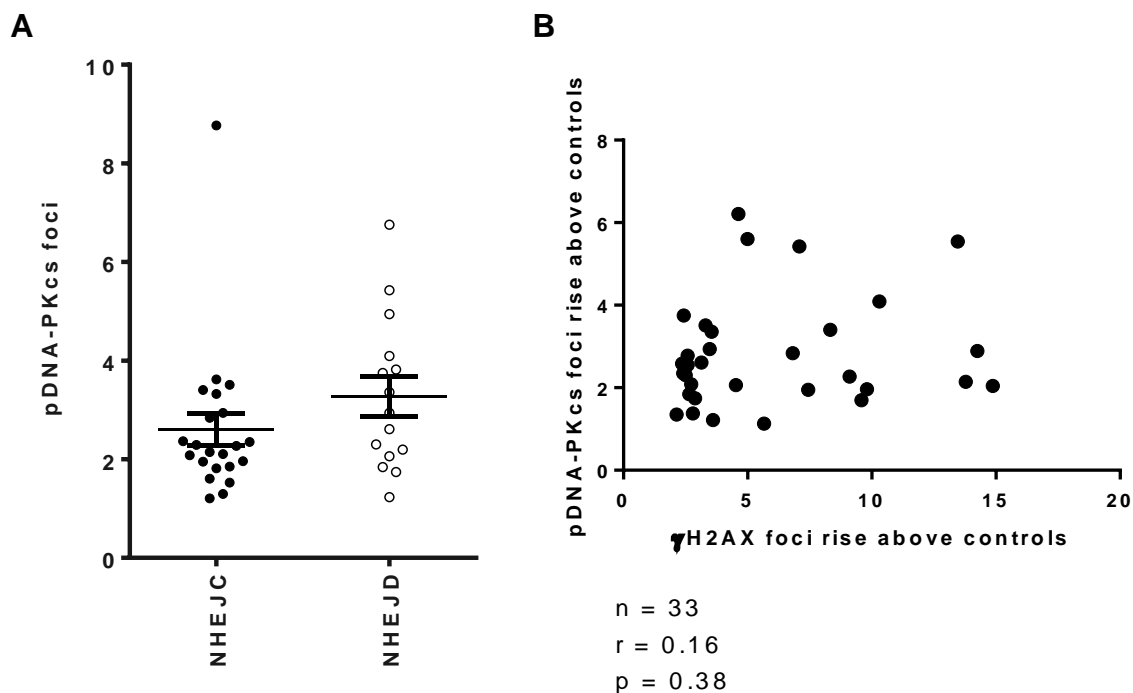


Figure 4-14 DNA-PK autophosphorylation as a marker of NHEJ function.

A. DNA-PK foci fold rise above controls 1 hr after 2Gy IR in primary ovarian cancer cultures. Divided by NHEJ status. Results are average of 3 independent experiments. **B.** Correlation of pDNA-PK and γ H2AX foci fold rise above controls after 2Gy IR in primary ovarian cancer cultures. Results are average of 3 independent experiments.

4.3.4.2 Correlation of Protein and mRNA Expression with NHEJ Status

The proteins involved in the NHEJ pathway are required for pathway function. Therefore, the expression of Ku, DNA-PKcs, LIG4 and XRCC4 was assessed at both mRNA and protein level.

Hypothesis: NHEJ function correlates with mRNA and protein expression levels of essential NHEJ protein

The analysis of the NHEJ pathway components showed protein, but not mRNA expression of Ku70, Ku80 and DNA-PKcs, were all significantly lower in NHEJD cultures (Figure 4-15.A-B).

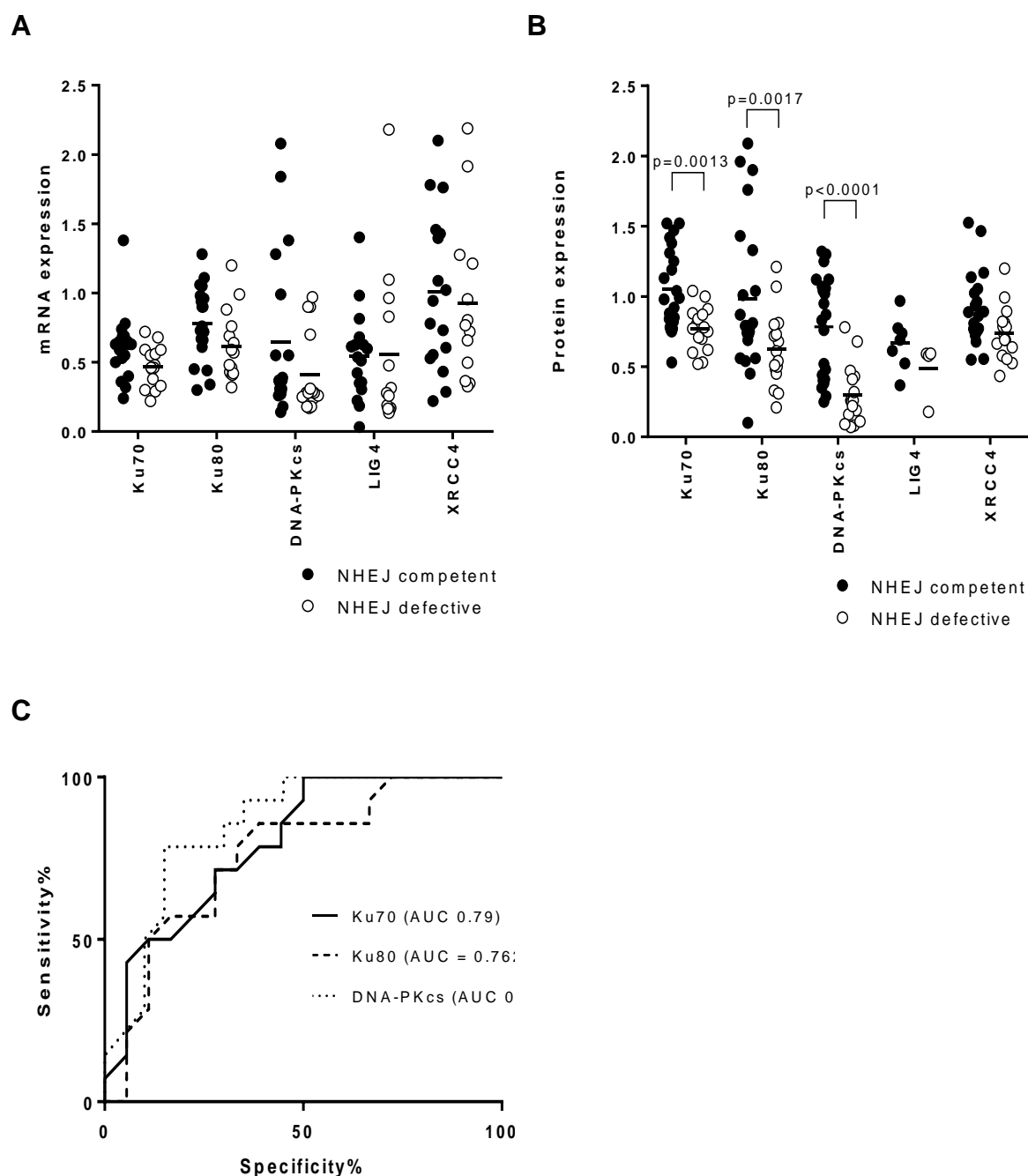


Figure 4-15 Prediction of NHEJ function by mRNA and protein expression of pathway components.

A. mRNA expression of NHEJ components PCO cultures assessed by RT-qPCR. Full circles are NHEJC, open circles are NHEJD. **B.** Protein expression of NHEJ components in PCO cultures assessed by western blotting. Western bands were quantified using Fuji LAS-300 Image Analyser System. Full circles – NHEJC, open circles – NHEJD. Protein and mRNA levels were normalised to GAPDH expression. Results are average of 3 independent experiments. Error bars are SEM. **C.** ROC curves for Ku70, Ku80 and DNA-PKcs protein expression as predictors of NHEJ function. ROC curves were generated and AUC calculated using PRISM software. NHEJC N = 22; NHEJD N = 18.

Ku70, Ku80 and DNA-PKcs protein expression levels were found to be good predictors (AUC 0.798, 0.762 and 0.852 respectively) for NHEJ function (Figure 4-15.C). Discordance between protein and mRNA expression was noted.

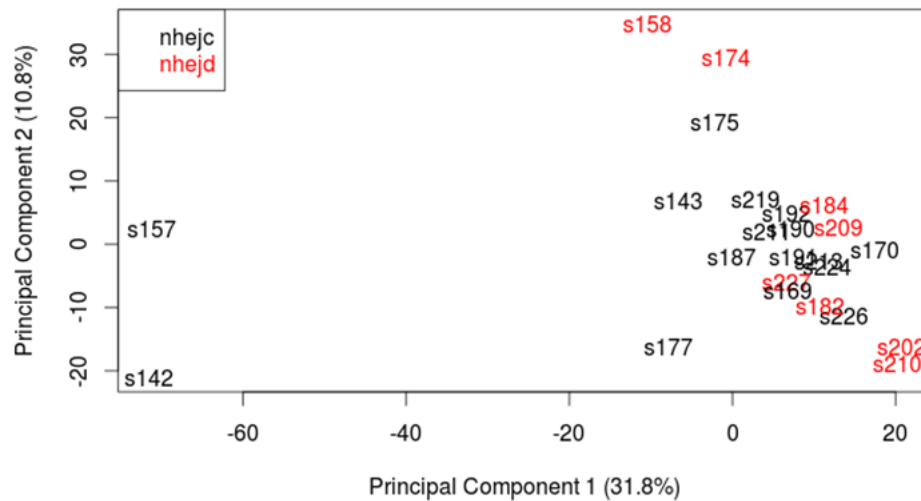
4.3.4.3 Prediction of NHEJ Function by Genome RNA Expression Arrays

Using RNA extracted from the PCO ascitic cultures characterised for NHEJ function, the relative expression of genes was determined by the Oxford genomics centre (Oxford, UK) using Illumina Genome Studio and the HumanHT 12v4.0 R1 15002873 array, as per the manufacturer's instructions, as described in section 2.12. All RNA samples were extracted from the same ascitic fluid primary culture used in the functional NHEJ assay and cytotoxicity assays. RNA expression was analysed using unsupervised hierarchical clustering (Figure 4-16). No clustering by NHEJ function was observed in the PCO cultures.

Differential expression analysis confirmed that after multiple test correlations, no genes were significantly differentially expressed between NHEJD and NHEJC cohorts (Table 4-1). The top 20 genes, when ranked by p value without multiple test correlation, did not include any DNA repair genes. This is consistent with the RNA expression analysis of NHEJ genes assessed by PCR in section 4.3.4.2.

A

Sample relations based on 27343 genes with $sd/mean > 0.1$

**B**

Sample relations based on 26415 genes with $sd/mean > 0.1$

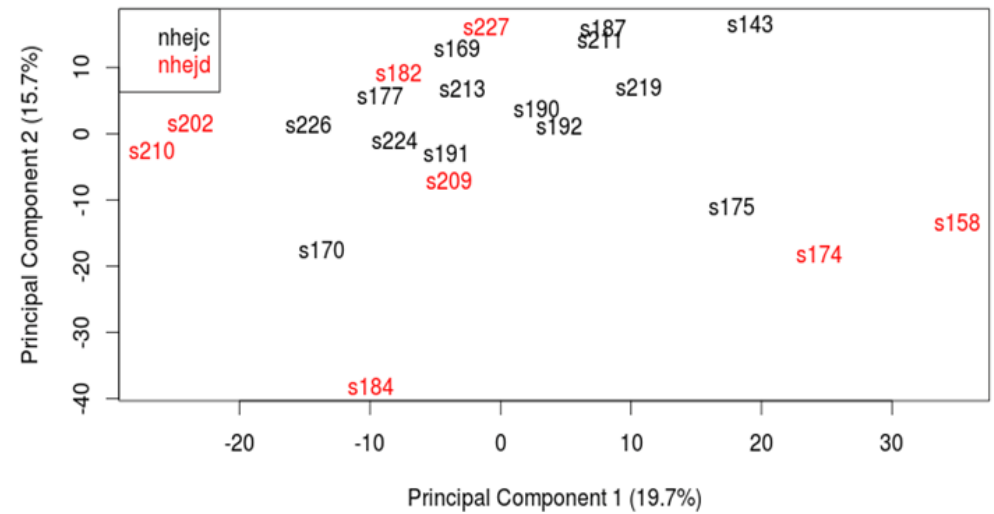


Figure 4-16 PCO genome RNA expression microarray.

A. PCA plot of all PCO samples. Sample relation based on 27343 genes with $sd / mean > 0.1$ NHEJD cultures are in red and NHEJC in black. **B.** PCA plot after outlier cultures were removed. Sample relation based on 26415 genes with $sd / mean > 0.1$.

Table 4-1 PCO RNA differential expression after multiple test correlation.

No genes were found to have a significant difference in expression ($\text{adj } p < 0.05$). Table demonstrates the top 20 results ranked by p value. $N = 24$.

Gene symbol	Gene name	Av. Expr	t	p =	adj. p =
UQCC1	ubiquinol-cytochrome c reductase complex assembly factor 1	9.55	4.24	0.0003	0.93
IRX5	iroquois homeobox 5	7.67	4.15	0.0004	0.93
KYNU	kynureninase	8.56	4.03	0.0006	0.93
GALNT6	polypeptide N-acetylgalactosaminyltransferase 6	8.37	3.89	0.0008	0.93
TXLNA	taxilin alpha	11.00	-3.81	0.0010	0.93
FBLN1	fibulin 1	9.21	-3.73	0.0012	0.93
TNIP3	TNFAIP3 interacting protein 3	8.00	3.71	0.0012	0.93
BHLHE41	basic helix-loop-helix family, member e41	8.43	3.65	0.0014	0.93
IFNAR2	interferon (alpha, beta and omega) receptor 2	8.80	3.51	0.0020	0.93
DMKN	dermokine	8.78	-3.48	0.0021	0.93
TNFSF14	tumor necrosis factor (ligand) superfamily, member 14	7.80	3.39	0.0026	0.93
KYNU	kynureninase	8.13	3.39	0.0026	0.93
CBLL1	Cbl proto-oncogene-like 1, E3 ubiquitin protein ligase	9.28	-3.36	0.0029	0.93
FNIP2	folliculin interacting protein 2	8.39	3.35	0.0029	0.93
SCARA3	scavenger receptor class A, member 3	8.26	-3.32	0.0031	0.93
TRIM24	tripartite motif containing 24	7.68	3.31	0.0032	0.93
RBPM5	RNA binding protein with multiple splicing 2	9.71	-3.31	0.0032	0.93
HTRA4	HtrA serine peptidase 4	8.16	3.28	0.0034	0.93
PRPF38A	pre-mRNA processing factor 38A	7.84	-3.27	0.0035	0.93
ADD3	adducin 3 (gamma)	9.66	3.27	0.0036	0.93

4.3.5 Interaction of HR and NHEJ Pathways

In vitro studies have demonstrated an interaction between HR and NHEJ pathways (Edwards et al., 2008, Tavecchio et al., 2012). Furthermore NHEJ pathway has been suggested to be critical in driving the lethality of PARPi in HRD cells (Patel et al., 2011).

Hypothesis: NHEJ function correlates with rucaparib sensitivity

4.3.5.1 Effect of DNA-PKcs on Rucaparib Sensitivity and HR

To assess the hypothesis that NHEJ function has a role in rucaparib sensitivity, DNA-PKcs defective M059J and the paired competent M059FUS-1 cell line were used. DNA-PKcs competent M059FUS-1 cells were significantly more sensitive to rucaparib compared to DNA-PKcs defective M059J cells (mean GI₅₀ 2.75 μ M 95 % CI = 0.90 to 2.93 μ M vs 17.45 μ M, 95 % CI = 13.0 to 22.25 μ M, $p < 0.0001$, Figure 4-17.A).

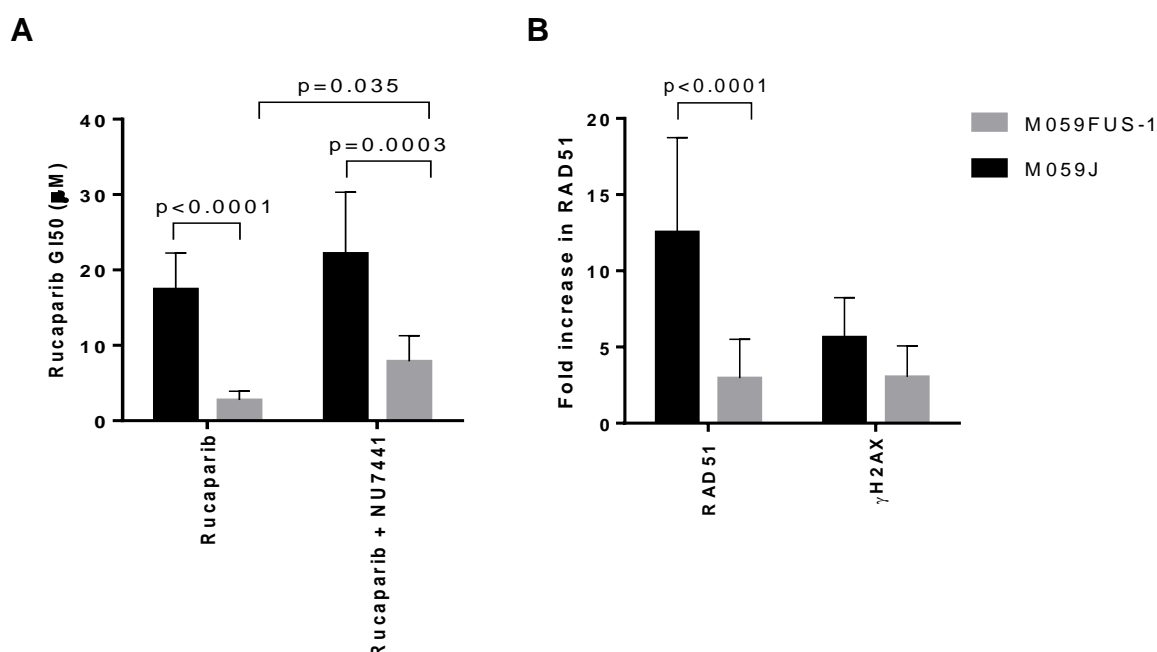


Figure 4-17 Rucaparib sensitivity and HR function in M059J and M059FUS-1 cells.

A. sensitivity to rucaparib was assessed using SRB assay. DNA-PKcs was inhibited by addition of 1 μ M NU7441 at the time of treatment. Results are mean of 3 independent experiments and error bars are SEM. **B.** RAD51 and γ H2AX focus formation was assessed 24 hrs after 2 Gy irradiation compared to untreated controls. Foci were counted across > 100 nuclei and results are expressed as fold rise above controls.

The role of DNA-PK kinase activity in this sensitivity was further confirmed by a significant induction of resistance in M059FUS-1 cells by the addition of the DNA-PK inhibitor NU7441 (mean GI_{50} 7.89 μ M, 95 % CI = 5 to 11.29 μ M, p = 0.035). NU7441 had no significant effect in DNA-PKcs defective M059J cells. To assess if HR function was different between the two cell lines, the γ H2AX/RAD51 formation assay was used. Both cell lines were deemed HRC with a >2 fold rise in RAD51 foci formation after induction of DNA damage compared to controls. However, the mean fold rise in RAD51 foci in M059J cells was significantly higher compared to M059FUS-1 cells (mean 12.54 \pm 6.2 fold compared to 2.96 \pm 2.5 fold, p < 0.0001, Figure 4-17.B). This finding suggests that in the absence of NHEJ function, HR is increased.

4.3.5.2 Interaction of NHEJ and HR in PCO Cultures

In the cohort of PCO cultures, NHEJ function was independent of HR competence. 12 cultures were functional for both pathways, 6 cultures were defective for both pathways, while 10 and 12 cultures showed defects in either NHEJ or HR but not both, respectively.

HR and NHEJ function were found to be independent of PCO culture growth rate (Figure 4-18).

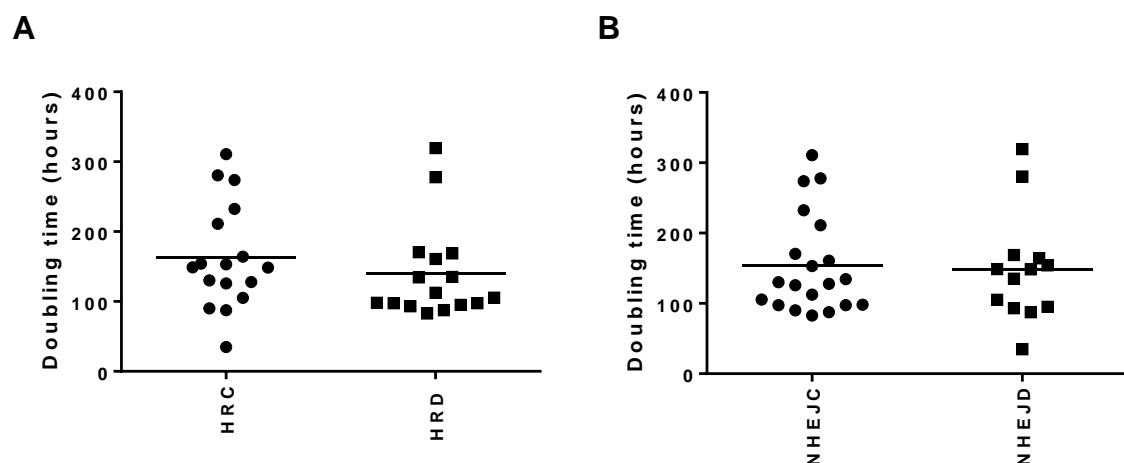


Figure 4-18 Growth of PCO cultures divided by HR and NHEJ status. Growth was assessed by SRB assay over 10 days.

4.3.6 Effect of NHEJ Function on Sensitivity to Rucaparib and Cisplatin

Increased sensitivity of HRD PCO cultures to rucaparib and cisplatin has been previously demonstrated (Mukhopadhyay et al., 2010), and has been confirmed in chapter 3. Sensitivity of immortalised cell lines and each PCO culture to rucaparib and cisplatin was determined using SRB proliferation assays. Sensitivity was assessed over 3 doubling times for immortalised cell lines and 10 days for PCO cultures.

When cell lines were grouped by NHEJ status, NHEJC cell lines were found to be more sensitive to rucaparib (mean GI₅₀ 2.6 µM 95 % CI = 0 to 11.6 µM vs 14.15 µM, 95 % CI = 1 to 27.3 µM, $p = 0.036$, Table 4-2). The difference in cisplatin sensitivity was not statistically significant.

Table 4-2 Rucaparib and cisplatin cytotoxicity and NHEJ status of cell lines. GI₅₀ was determined by SRB assay.

Cell line	NHEJ status	GI ₅₀ for Rucaparib (µM)	GI ₅₀ for Cisplatin (µM)
OVCAR3	NHEJC	0.93	0.26
A2780	NHEJC	0.14	2.49
CP70	NHEJD	8.10	2.22
SKOV3	NHEJD	17.87	4.13
IGROV-1	NHEJD	16.46	1.79
MDAH	NHEJD	Not determined	Not determined

4.3.6.1 Correlation of Rucaparib and Cisplatin Sensitivity with DNA DSBs Repair

There was no association between end joining rates of Co BstXI substrates and drug sensitivity. Co substrates assessed overall end joining which includes end joining by A-EJ pathway. Therefore, the lack of association is not surprising. Defects in the NHEJ pathway, as defined by the inability to rejoin 2I BstXI substrates, were associated with resistance to rucaparib in PCO cultures ($p = 0.002$, Figure 4-19). NHEJ function had no significant effect on cisplatin sensitivity (Figure 4-20). Inhibition of DNA-PK resulted in rucaparib resistance in sensitive cultures ($p = 0.002$, Figure 4-19). DNA-PK inhibition had no effect on rucaparib resistant cultures and no effect on cisplatin sensitivity (Figure 4-20).

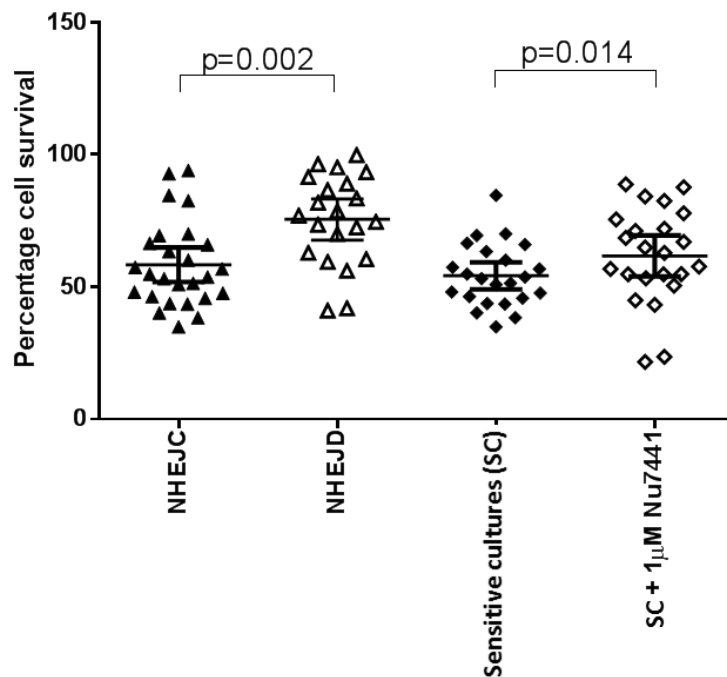


Figure 4-19 Rucaparib cytotoxicity in PCO cultures divided by NHEJ status.

Cell survival calculated as mean cell growth after 10 days treatment with 10 μ M rucaparib, as a fraction of DMSO control growth for PCO cultures, as assessed by SRB assay. Results were divided by NHEJ status (NHEJC/ NHEJD) or comparison of sensitive cultures +/- 1 μ M Nu7441. Error bars are SEM.

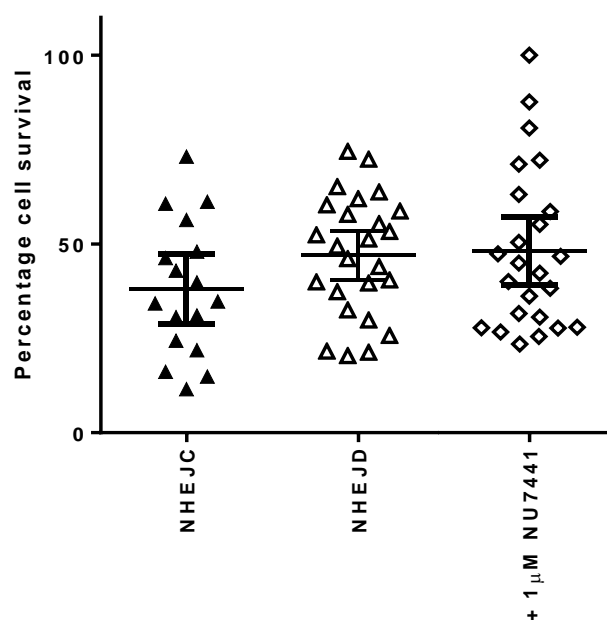


Figure 4-20 Cisplatin cytotoxicity in PCO cultures divided by NHEJ status.

Cell survival calculated as mean cell growth after 10 days treatment with 10 μ M cisplatin as a fraction of SDW control growth for PCO cultures, as assessed by SRB assay. Results were divided by NHEJ status (NHEJC / NHEJD) or cell growth after addition of 1 μ M NU7441 to cisplatin. Error bars are SEM.

When HR and NHEJ functions were taken into account, only NHEJC/HRD cultures were sensitive to rucaparib (Figure 4-21). As predicted from HR function association with rucaparib sensitivity, both groups with HRC cultures were resistant to rucaparib (NHEJC/HRC and NHEJD/HRC). The surprising and interesting group, however, was the NHEJD/HRD group. From HR function alone, this group would be expected to be sensitive to rucaparib, however the percentage of cells surviving at 10 μ M rucaparib was similar to that of the two HRC groups. Importantly this also correlated positively with the RAD51 foci rise after DNA DSBs induction (Pearson $r^2 = 0.9486$, $p = 0.03$).

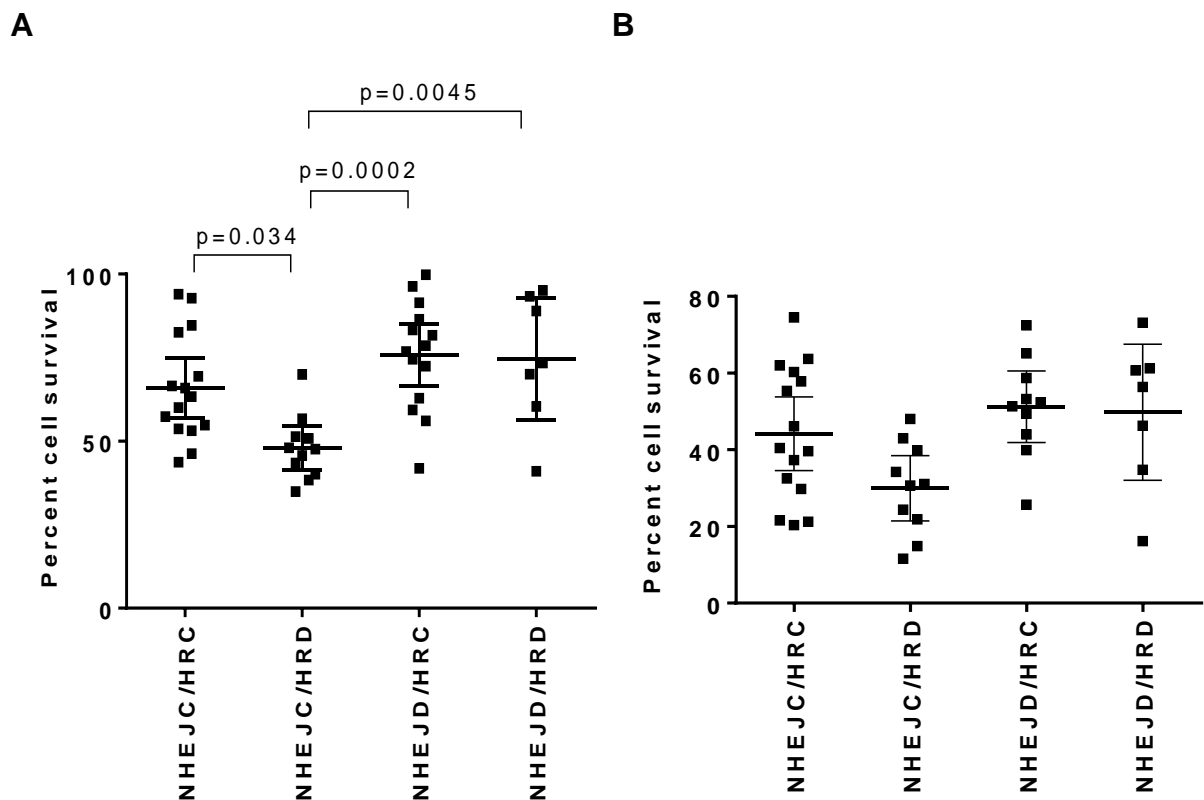


Figure 4-21 Rucaparib and cisplatin cytotoxicity plotted by NHEJ and HR status.

Results are percent mean cell survival after 10 days treatment with **A.** 10 μ M rucaparib compared to DMSO control and **B.** 10 μ M cisplatin compared to SDW control for PCO cultures shown by HR and NHEJ status. Error bars are SEM.

4.3.6.2 The Effect of Cisplatin on NHEJ Function

Cisplatin has previously been reported to inhibit NHEJ (Diggle et al., 2005). In view of the lack of association of NHEJ function with cisplatin sensitivity in both cell lines and PCO cultures, the effect of cisplatin on NHEJ function was assessed in OSEC-2 cells. Cisplatin was found to inhibit rejoining of Co and 2I ends significantly at a concentration of 4 nM, when compared to the control (Figure 4-22). Therefore the lack of association observed at 10 μ M of cisplatin treatment is likely to be due to cisplatin inhibition of NHEJ.

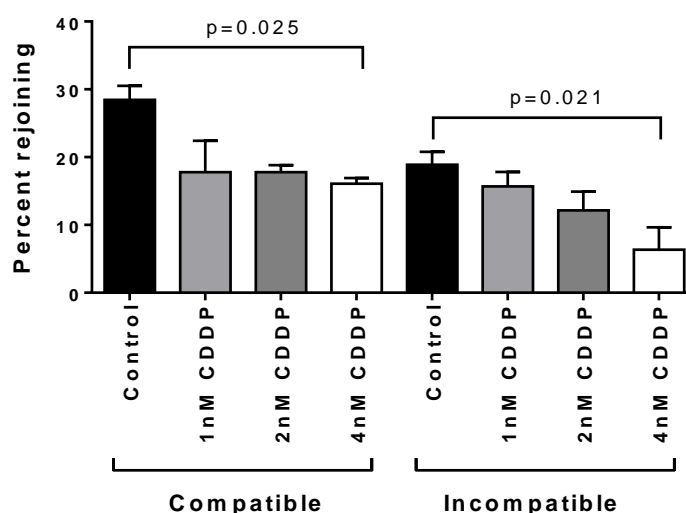


Figure 4-22 Cisplatin inhibition of end joining of Co and 2I BstXI substrates.

End joining was assessed in OSEC-2 cell line. Results are average of three independent experiments. Error bars are SEM.

4.3.7 Correlation of NHEJ Status with Clinical Outcomes

No significant differences were observed between the clinical outcomes and histological characteristics of the NHEJC and NHEJD PCO culture groups (Table 4-3).

Table 4-3 Patient characteristics for PCO samples divided by NHEJ status.

		Total (N=40)	NHEJ C (N=22)	NHEJ D (N=18)	P =
Age at diagnosis	Median	66	68	64	0.42
	Range	45-85	46-85	45-78	-
Histology	HGSOC	28	16	12	0.88
	Endometrioid / clear cell	5	3	2	>0.99
	Mixed	3	1	2	0.85
	Mucinous	2	1	1	> 0.99
	Carcinosarcoma	1	0	1	0.92
	Low grade serous	1	1	0	0.97
Stage	1	1	0	1	0.99
	2	1	0	1	0.99
	3 A	1	0	1	0.99
	3 B	1	1	0	0.99
	3 C	32	19	13	0.58
	4	4	2	2	> 0.99
Pre-op Ca125	Median	1087	1354	699	0.30
Type of surgery	Primary diagnosis	29	16	13	0.85
	Following NACT	11	6	5	0.85
Outcome of surgery	Complete	5	2	3	0.83
	Optimal	28	15	13	0.98
	Suboptimal	6	4	2	0.86
	No surgery	1	1	0	0.96

4.3.7.1 Correlation of NHEJ with Progression Free and Overall Survival

As the patients from whom the PCO cultures were collected were treated with standard therapy, and NHEJ function did not correlate with cisplatin sensitivity, it was hypothesised that no correlation with clinical outcomes would be seen.

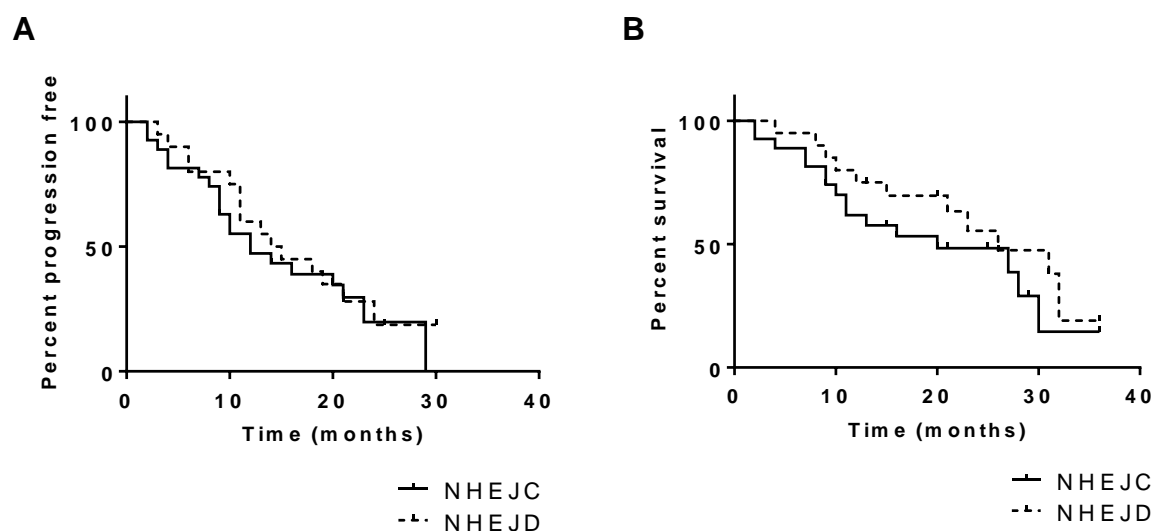


Figure 4-23 Kaplan-Meier survival curves for PFS/OS by NHEJ status.

A. Median PFS was 14.5 months for NHEJD compared to 12 months for NHEJC group, log rank Chi square 0.16, $p = 0.68$. **B.** Median overall survival was 27 months for NHEJC group, and 26 months for NHEJD group. Log rank Chi square 1.0, $p = 0.32$.

There was no significant difference between the PFS or the OS between NHEJC and NHEJD groups (Figure 4-23). When PFS was sub divided into NHEJ and HR competence there was no significant difference between PFS (NHEJC/HRC - 11.5 months, NHEJC/HRD - 9.3 months, NHEJD/HRC - 18 months, NHEJD/HRD group failed to reach median follow up).

4.3.8 Assessment of NHEJ Targets in FFPE Tissue

Tumours collected during surgery in clinical practice were formalin fixed and paraffin embedded. The DNA-PK complex protein (DNA-PKcs, Ku70 and Ku80) were individually assessed as biomarkers of the NHEJ pathway. This work was performed with Richard O'Sullivan (MRes, 2014) and Dr Peter Donoghue.

Hypothesis: NHEJ function can be assessed in FFPE tissue by using differentially expressed protein targets

Table 4-4 DNA-PKcs, Ku70 and Ku80 mRNA and protein expression by NHEJ status.

PCO	Functional NHEJ Assay	IHC Protein Expression			qPCR mRNA expression Normalised to HPRT		
		DNA-PKcs	Ku70	Ku80	DNA-PKcs	Ku70	Ku80
139	Competent				0.27		0.60
142	Competent	6.71	12.40	8.45	0.78	18.57	1.14
143	Competent	14.38	2.04	7.79	0.15	2.25	0.18
144	Competent	4.57	1.55	4.22	0.03	0.29	0.08
156	Competent				0.34	2.97	0.34
160	Competent	5.16	2.73	4.97	1.18	0.44	1.10
168	Competent	12.05	3.07	4.27	1.05	1.68	1.46
187	Competent	16.15	13.25	14.97	0.29	0.05	0.36
197	Competent				0.14	2.55	0.16
202	Competent	11.81		11.36	0.51	0.10	0.47
211	Competent	9.48	9.18	11.65	0.36	3.18	0.28
149	Defective	11.30	11.86	12.44	0.12	0.20	0.25
153	Defective	12.07	9.96	12.19	0.29	0.90	0.28
154	Defective	6.25			0.77	6.07	0.49
157	Defective	13.32	1.90	5.70	0.19	0.05	0.19
158	Defective	12.85	6.10	13.47	0.55	3.70	0.46
162	Defective	10.77	8.16	6.47	0.70	10.75	0.70
163	Defective	15.65	12.73	16.56	0.37	0.05	0.32
174	Defective	9.64	1.53	6.46	0.38	2.95	0.38
175	Defective	5.27	11.37	8.94	0.19	0.51	0.22
184	Defective	14.86	9.94	12.94	0.75	2.60	0.46
209	Defective				0.56	1.34	0.49
210	Defective	12.03	9.44	13.44	0.22	0.81	0.31
221	Defective	7.71		11.93	0.82	0.15	0.61

4.3.8.1 Protein Expression of DNA-PKcs, Ku80, Ku70

Ovarian cancer TMA sections were stained for DNA-PKcs, Ku70 and Ku80 as described in section 2.8. No significant differences in biomarker expression were noted between tumours matched to NHEJC and NHEJD PCO cultures (Figure 4-24).

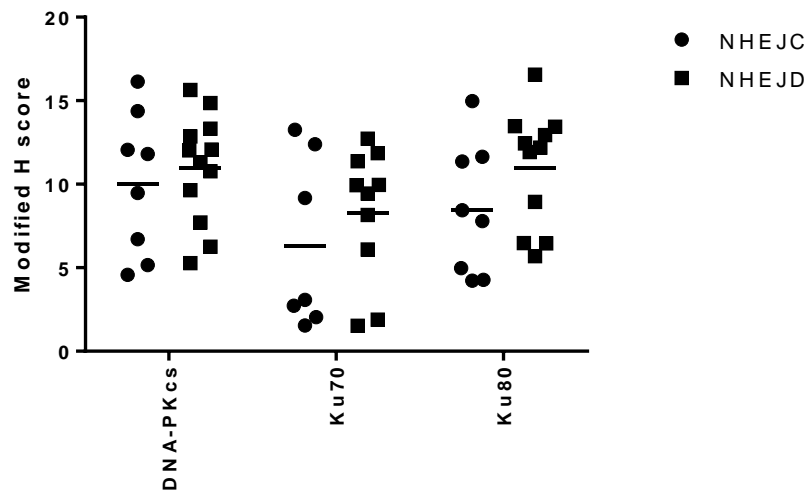


Figure 4-24 DNA-PKcs, Ku70 and Ku80 protein expression grouped by NHEJ status. Protein expression was assessed by modified H Score. Scoring was performed by 2 scorers.

4.3.8.2 mRNA Expression of DNA-PKcs, Ku80, Ku70

24 study samples were amplified by QPCR. No significant differences in biomarker expression were noted between NHEJC and NHEJD tumours (Figure 4-25).

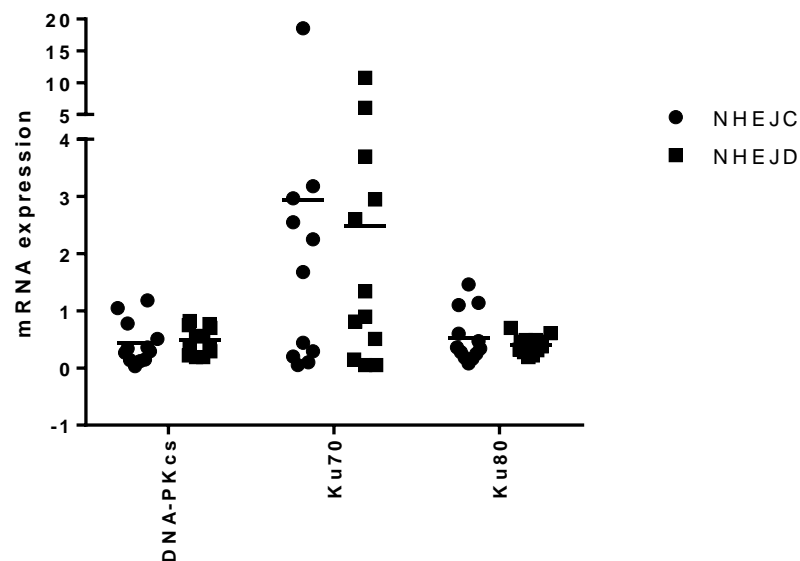


Figure 4-25 DNA-PKcs, Ku70 and Ku80 mRNA expression grouped by NHEJ status. mRNA expression is normalised to HPRT1 expression.

Discordance was found between the protein and mRNA expression of all targets assessed (Figure 4-26).

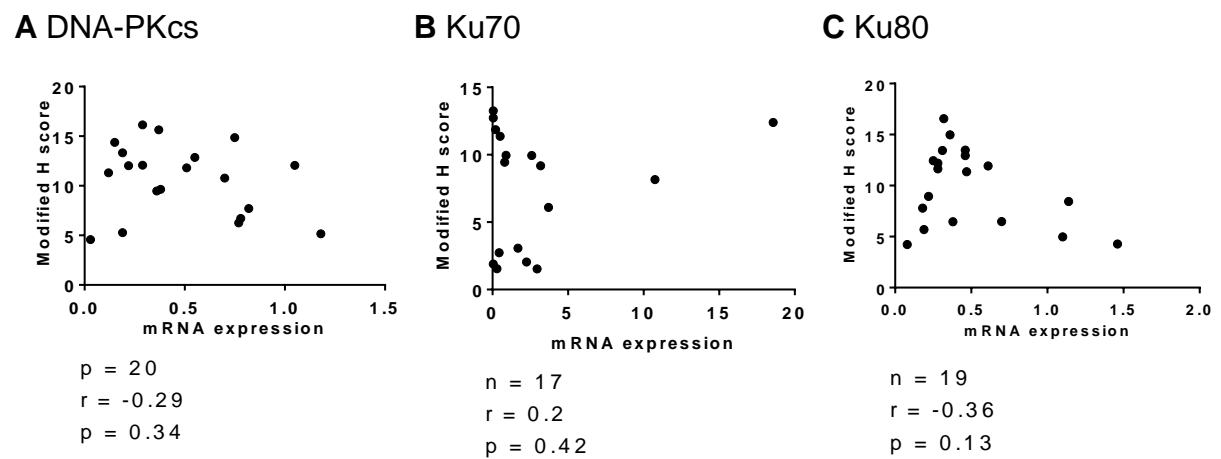


Figure 4-26 Correlation of DNA-PKcs, Ku70 and Ku80 mRNA and protein expression.

4.3.9 Assessment of NHEJ Heterogeneity

Hypothesis: Subpopulations of ovarian cancer cells exist exhibiting heterogeneity in NHEJ function

Inter and intra tumour heterogeneity of HR function has been demonstrated in ovarian cancer (O'Donnell et al., 2015). For NHEJ function biomarkers to be used to select patients for treatment, an assessment of heterogeneity is required. From the data so far, inter tumour heterogeneity of NHEJ is clear, with important effects on rucaparib sensitivity. Gene expression studies have indicated different biological profiles in the cancer cells derived from ascites and solid ovarian cancer tumours from the same patient, in terms of metastasis, invasion and angiogenesis (Le Page et al., 2006).

4.3.9.1 Protein and mRNA Expression in FFPE Tissue and Matched Ascites

In view of lack of correlation between DNA-PK complex protein expression in FFPE tissue and NHEJ function of matched ascites samples, the expression of the mRNA and protein from FFPE and ascites samples were correlated. Spearman's rank correlation was performed to assess correlation between FFPE and ascites mRNA and protein expression (Figure 4-27). No positive correlation was noted between protein or mRNA expression in FFPE and in ascitic samples from matched patients.

Expression discordance could be due to the different techniques used to assess protein expression, and different house keeper genes used for mRNA quantification.

Different housekeeper genes were used for FFPE tissue mRNA due to excessive degradation of GAPDH in FFPE extracted mRNA (Richard O'Sullivan MRes thesis, 2014). However, more importantly, discordance may also be due to intra tumour heterogeneity between the solid cancer cells captured in FFPE and that of cancer cells in ascites samples.

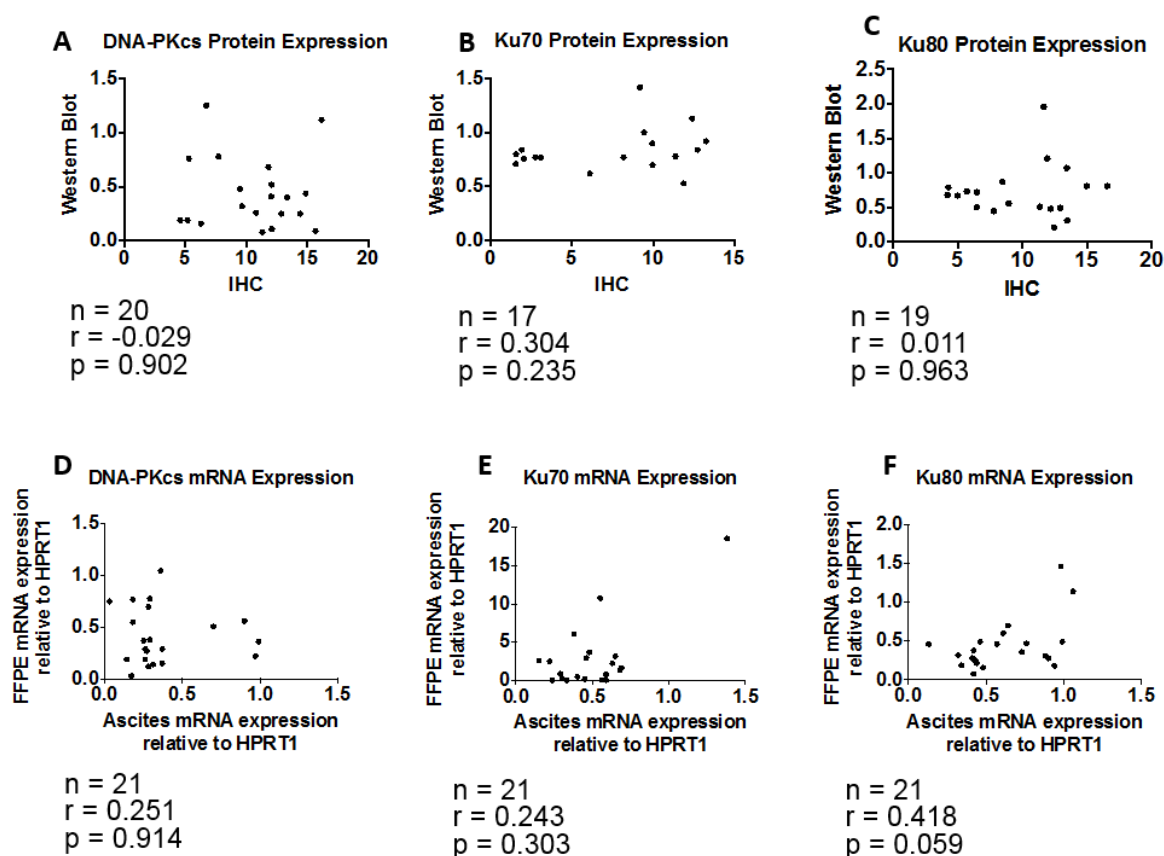


Figure 4-27 Correlations of FFPE and ascites mRNA and protein expression.

4.3.9.2 Intra-tumour Heterogeneity of NHEJ Protein Expression

To explore tumour heterogeneity further, multiple solid samples were collected from six patients undergoing primary surgery for ovarian carcinoma. There was no correlation noted between DNA-PK, Ku70 or Ku80 protein expression in multiple biopsies (Figure 4-28). The expression for both samples was analysed using the same method of extraction and western blotting technique. The discordance noted is therefore, likely to be due to intra-tumour heterogeneity.

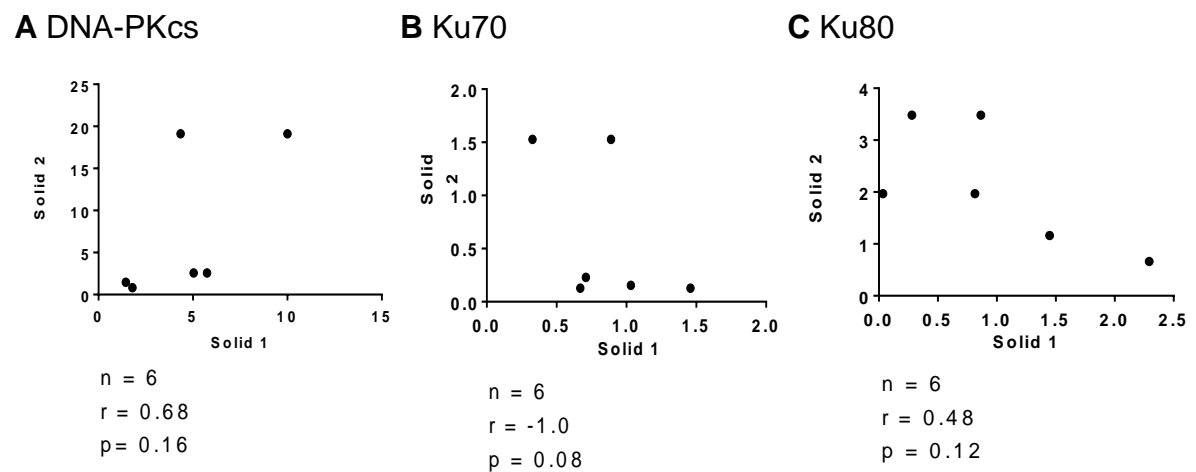


Figure 4-28 Correlations of NHEJ protein expression in multiple biopsies.

A. DNA-PKcs, **B.** Ku80, **C.** Ku70 protein expression normalised to expression of GAPDH. Two solid samples were collected at the time of surgery. The site of solid sample varied between cases.

In order to assess if the tissue of origin affected the expression of DNA-PK complex protein, multiple solid samples collected from patients were assessed. Ovarian, fallopian tube and omental cancer deposits were sampled. There was no significant difference noted between the expression of DNA-PKcs, or Ku protein between the three sampling sites (Figure 4-29).

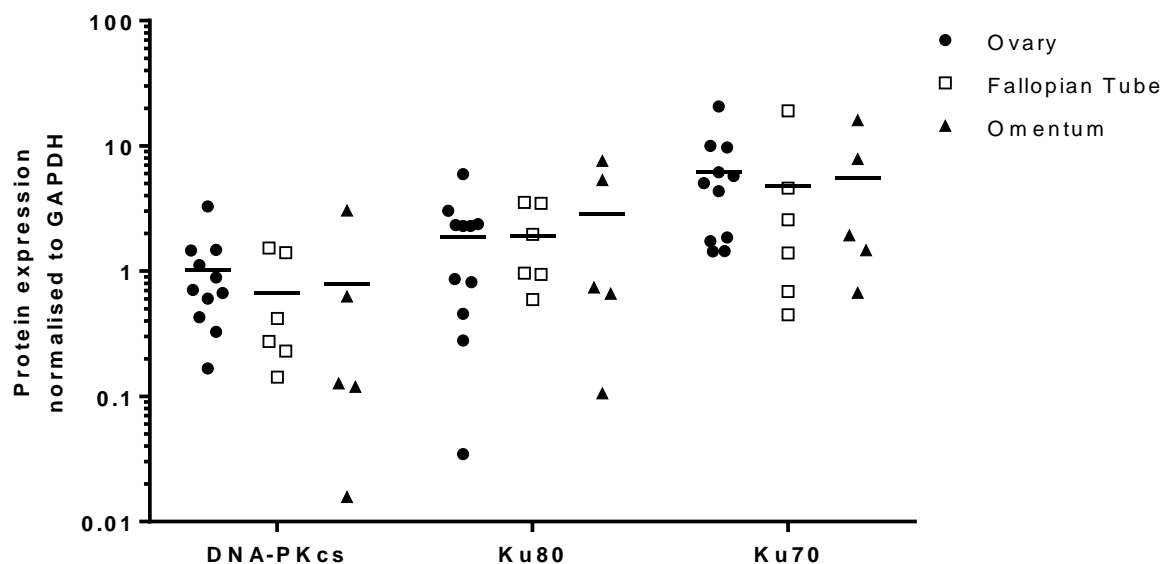


Figure 4-29 DNA-PKcs, Ku70 and Ku80 protein expression grouped by tumour site. Protein expression was normalised to the expression of GAPDH.

4.3.9.3 Expression of NHEJ Proteins in Tumour and Ascites Samples Compared to Normal Ovarian / Fallopian Epithelium from Healthy Volunteers

Solid samples from ovarian and fallopian tube tissue were collected from patients undergoing hysterectomy for menorrhagia. Samples from these patients were used as normal controls to cancer samples. The expression of DNA-PKcs, Ku80 and Ku70 protein was assessed using western blotting and correlated with solid samples collected from patients undergoing surgery for ovarian carcinoma and PCO ascites cultures (Figure 4-30).

Expression of all three proteins was significantly lower in PCO ascites samples compared to normal controls. When comparing normal control samples to solid cancer samples, there was significantly higher expression of DNA-PKcs in normal samples compared to cancer samples (normalised to GAPDH mean expression 3.62 \pm 1.4 fold vs 0.67 \pm 0.17 fold, $p = 0.005$). The differences for Ku protein were not statistically significant. The expression of Ku70 was significantly higher in cancer samples compared to ascites cultures (normalised to GAPDH mean expression 4.4 \pm 1.2 fold in solid cancer samples vs 0.93 \pm 0.05 fold in ascites, $p < 0.0001$).

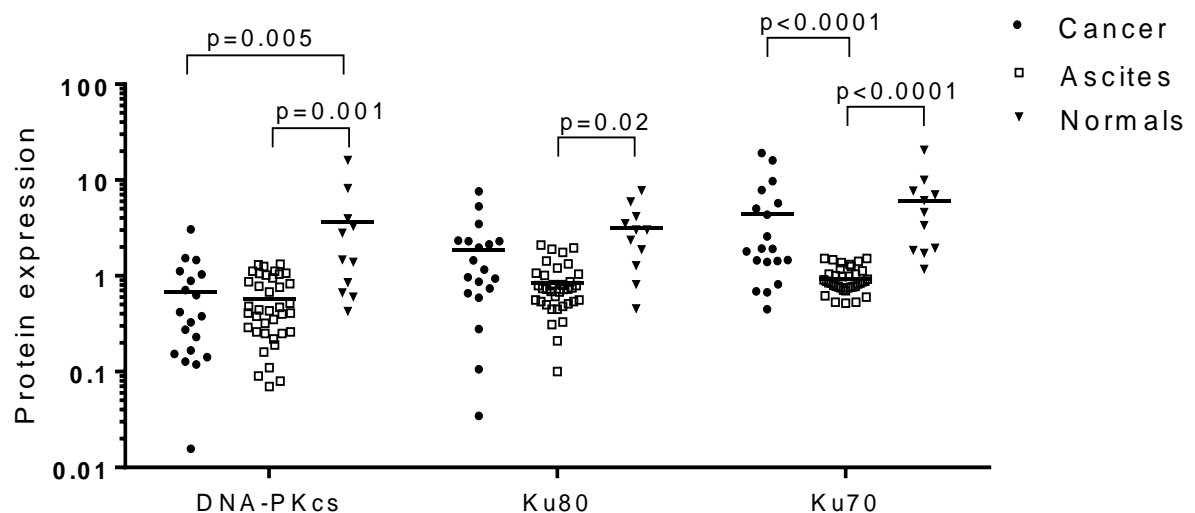


Figure 4-30 DNA-PKcs, Ku70 and Ku80 protein expression in ovarian carcinoma and healthy control samples.

Protein expression was assessed by western blotting and normalised to GAPDH expression. Results are mean of 3 independent experiments. N = 19 cancer solid samples, 11 normal control samples and 38 ascites culture samples.

4.4 Chapter Summary

- NHEJ function can be measured in extracts from ovarian cancer cell lines and primary cultures and 40 % of PCO cultures are NHEJD.
- NHEJD is associated with resistance to rucaparib.
- Cisplatin was found to inhibit NHEJ function and cisplatin sensitivity was independent of NHEJ.
- NHEJ function was found to be independent of HR competence.
- There was no significant correlation of NHEJ function with clinical outcomes in this cohort.
- NHEJ function can be predicted by the protein expression of DNA-PKcs, Ku70 and Ku80, in primary cultures. However, further biomarker development is required, as these correlations could not be demonstrated in FFPE or fresh solid tissue.
- Heterogeneity of NHEJ function was noted in primary ovarian cancer.

4.5 Discussion

In this chapter NHEJ function was measured in extracts from ovarian cancer cell lines and PCO cultures. NHEJ function assessment was optimised by two different functional assays. 60 % of ovarian cancer cell lines and 40 % of PCO cultures were found to be NHEJD. This is the first study to assess NHEJ function in a primary ovarian cancer cohort and to quantify the frequency of defects. The differences in the frequency of NHEJ defects between cell lines and PCOs may be due to a small number of cell lines assessed. The cell lines assessed are also known to harbor other defects. Such as p53 status and MMR status, namely the CP70 cell line was derived from the A2780 and is MMR deficient and mutant for p53, which are also known to affect sensitivity to cisplatin.

4.5.1 NHEJ Function is Independent of HR and NHEJD is Associated with Rucaparib Resistance

Contrary to HRD association with rucaparib sensitivity, NHEJD was found to be associated with resistance to rucaparib. Previous studies in cell lines have shown that deletion of DNA-PK can restore HR function and PARPi resistance in BRCA mutated cells (Patel et al., 2011). This is the first study to demonstrate this correlation

in primary cultures. The sensitivity of HRD cancers to PARPi has been attributed to the concept of synthetic lethality, however, the exquisite sensitivity of HRD cells seen *in vitro* has not been reproduced in clinical trials. The concept of synthetic lethality has been based on the theory that HRD cells are unable to repair DNA DSBs. However, as HR repairs unpaired DSBs (such as collapsed replication forks) and is not functional in the G0/G1 phases of the cell cycle, the majority of DSBs are repaired by the NHEJ pathway (Bentley et al., 2004). The role of NHEJ function in error free repair has been shown in this study by the mainly error free rejoining by DNA-PKcs proficient V3YAC and M059-FUS1 cell lines compared to the mainly error prone repair in DNA-PK deficient V3 and M059J counterparts. The role of NHEJ function in PARPi sensitivity is supported by the observation that NU7441 caused rucaparib resistance in all sensitive cultures, independent of HR function. Therefore, NHEJ is an important determinant of DSB repair and as shown in this study, sensitivity to PARPi.

HR and NHEJ function were found to be independent of one another; with some PCO cultures were found to be competent in both, some defective in just one, whilst a small cohort were defective in both pathways. Independence of the two pathways is documented in the literature (Bee et al., 2013). The two pathways function in different stages of the cell cycle and repair different forms of DSBs (Bee et al., 2013). As PARPi causes collapsed replication forks in cycling cells, which can only be repaired by HR, it is also unsurprising that HRC cultures were resistant to rucaparib (Bryant et al., 2009, Sugimura et al., 2008). However, the role of PARP1 in DSBs, beyond causation of collapsed replication forks due to unrepaired SSBs, is also documented in the literature (Hegan et al., 2010, Benjamin and Gill, 1980, Haince et al., 2008); as well as the interaction between PARP1 and the NHEJ pathway (Ruscetti et al., 1998, Veuger et al., 2003, Veuger et al., 2004, Mitchell et al., 2009a). The independent role of NHEJ function in PARPi sensitivity is demonstrated in this study. The hypothesis put forward for the role of NHEJ in PARPi resistance is based on the error proneness of NHEJ. The errors in repair are suggested to cause lethal defects in DNA, which, in the absence of HR, results in apoptosis. Therefore, NHEJC/HRD cells are sensitive to PARPi. Cells with competent NHEJ and HR pathways are able to repair DNA damage and are, therefore, resistant to PARPi. In the absence of NHEJ, the slower error free HR takes over repair. This notion is supported by findings of greater HR function, demonstrated by greater RAD51 foci formation in the DNA-PK deficient cell

line in this study as well as literature (Middleton et al., 2015). Therefore, in the absence of NHEJ function, the lack of error prone repair results in resistance to PARPi (Patel et al., 2011). In cells which are NHEJD/HRD repair is undertaken A-EJ, which is a mutagenic process due to excessive resection. The interaction of A-EJ is still not fully understood and its assessment was beyond the scope of this project. The precise interaction between HR, NHEJ and PARP-1 is further explored in chapter 5.

4.5.2 Cisplatin Inhibits NHEJ Function

An important observation is the finding of a lack of association of NHEJ function with cisplatin sensitivity in the primary cultures. Whilst HRD has been shown to sensitise cancers to cisplatin and PARPi (Mukhopadhyay et al., 2012), NHEJ appears to be important for PARPi sensitivity only. Inhibition of NHEJ function by cisplatin has been previously reported (Diggle et al., 2005), and has been reproduced in this study, which is likely to be the reason for the lack of association observed. Whether cisplatin inhibition of NHEJ has important consequences to ovarian cancer genomic instability remains to be explored.

There was also no association noted between NHEJ status and the clinical outcomes of patients the PCO cultures were collected from. As all patients in this cohort were treated with standard platinum based therapy, the lack of correlation is therefore not surprising. To assess the role of NHEJ in patient outcomes, NHEJ function needs to be determined in a cohort of patients treated with PARPi.

4.5.3 Protein Expression of Ku and DNA-PK are Potential Biomarkers for NHEJ Function

For an assay to be clinically applicable, simple and reliable biomarker tests are required. This study suggests that expression of the NHEJ related proteins Ku70, Ku80 and DNA-PKcs may be useful as biomarkers to determine NHEJ status in cancer samples. Failure to see a positive correlation between mRNA expression and pathway function in PCR and genome expression arrays may be due to a number of reasons. Firstly, this may be due to assay limitations as only single mRNA samples were collected, and therefore, repeat expression assessment was not possible. As mRNA extraction was performed in batches and stored at -80 °C prior to use, different handling of the samples may affect the results. Furthermore, samples for

this cohort were collected over a period of two years, and so different biological or experimental mRNA and protein degradation rates might affect the mRNA and protein correlations. Secondly, differences between mRNA and protein expression may also be due to biological processes, i.e. transcriptional splicing, post-transcriptional splicing, translational modifications and regulation, and protein complex formation; these might all affect the relative quantities of mRNA and protein, to various degrees (Guo et al., 2008, Chen et al., 2002). Discordance between mRNA and protein has been reported previously in the literature in other cancer tissues (Guo et al., 2008, Chen et al., 2002).

4.5.4 Tumour Heterogeneity of NHEJ Function

The assessment of Ku70, Ku80 and DNA-PKcs in FFPE and fresh solid samples did not correlate with the same proteins assessed by WB, or with NHEJ function in the PCOs. A number of explanations may account for these findings. Firstly, both FFPE and fresh solid samples studies were limited by the small sample size available. Secondly, it was clear from the scatter plots presented that within both competent and defective tumours there was a wide range of protein and mRNA expression. This could point to both tumour and sample heterogeneity. IHC scoring only assessed an extremely small area of tumour and it was noted that varying intensities of expression were observed between cores from the same tumour, and also within individual cores. Some areas of a tumour may be NHEJC, whilst others are NHEJD, and so a more widespread assessment of a tumour, with possibly more cores, is required. Differences between populations of cells in ascites and within solid tumour may also account for the differences seen. Gene expression studies have indicated different biological profiles in the cancer cells derived from these two sources from the same patient in terms of metastasis, invasion and angiogenesis (Le Page et al., 2006). A further explanation for the differences however, could also be the difference in the sample nature and handling; namely ascites samples were cultured in the laboratory whilst solid samples were lysed directly. Significant genetic alterations in cell line during culture have been reported (Korch et al., 2012). This notion is supported by the finding of significantly lower expression of DNA-PKcs and Ku protein in ascites compared to both normal and cancer solid samples. Assessment of ascites directly after collection may provide lower heterogeneity in the samples.

Tumour heterogeneity of NHEJ function is an important finding of this study to consider. Whilst the areas of tumour which are NHEJC, and so are sensitive to PARPi treatment, are likely to respond to treatment and regress, areas of NHEJD tumour would remain refractory to treatment and continue to grow. Therefore, only partial response to treatment would be seen, with refractory disease developing over time. Treatment with PARPi in clinical practice has been found to prolong life, rather than cure, and NHEJD areas of tumour may be one of the explanations for the refractory disease development. For this theory to be assessed, repeat biopsies for NHEJ function assessment over the length of treatment are required.

The expression of DNA-PKcs protein in cancer samples was overall, lower than in solid samples collected from healthy patients. Ku70 and Ku80 were also reduced in the ascites cultures, suggesting an overall reduction in NHEJ capacity. Lower NHEJ function has been reported in other cancers; namely, in the peripheral blood mononuclear cells of breast cancer patients (Bau et al., 2007). Furthermore, a dose-response relationship is reported between end joining capacity and the risk of breast cancer (Bau et al., 2007). NHEJ activity has been reported to be reduced and increasingly error prone in invasive, as compared to non-invasive, bladder cancers (Bentley et al., 2009, Bentley et al., 2004, Windhofer et al., 2008). The evidence for the role of the NHEJ pathway in tumourigenesis is further provided by reports of increased DNA binding by Ku in low grade, low stage bladder tumours (grade 1–2, pTa–T1), but a 1.5 to 3 fold decrease in Ku binding in high grade invasive tumours (Stronati et al., 2001). Therefore, defects in the NHEJ pathway may cause sufficient genomic instability for cancer to develop due to failure to repair DSBs. The frequency of NHEJ defects noted in ovarian cancer may have important implications beyond PARPi sensitivity. HGSOC have been reported to almost universally carry inactivating mutations in p53 and a large number of genomic deletions/amplifications, as well as a copy number alterations (Ahmed et al., 2010, Cancer Genome Atlas Research, 2011). NHEJD combined with p53 mutation, resulting in the highly mutagenic joining of DSBs via sequence microhomologies, may contribute to the increased genomic instability observed.

The ability to select the correct patient for the correct treatment at the right time is required for personalised medicine. Whilst attempts are currently being made to develop predictive biomarkers of HR function, this study suggests that in ovarian cancer, NHEJ function is also an independent predictor of sensitivity to PARPi.

4.6 Future Work

Assessment of NHEJ function in a larger cohort of homogenised fresh / frozen tumour tissue, along with biomarker expression, is required to gather further evidence for the role of NHEJ function in ovarian cancer. It is also not clear if NHEJ has a role in ovarian cancer development. This needs to be assessed by analysing NHEJ in multiple biopsies from different stages of EOCs.

NHEJ function will only have an important role in cancer biology, if it is associated with clinical outcomes. As the patients in this cohort were treated with platinum chemotherapy and platinum has been found to inhibit NHEJ, the lack of association was not surprising. However, the effect of NHEJ function on survival outcomes in patients undergoing PARPi therapy is an important future study to undertake.

CHAPTER 5 ASSESSMENT OF THE EFFECT OF ATR AND DNA-PK INHIBITION ON CELLULAR BIOLOGY AND PARPI SENSITIVITY

5.1 Introduction

As cells face an ongoing assault from environmental and endogenous sources of DNA damage, the DNA damage response (DDR) is essential to maintain genomic stability (Hoeijmakers, 2009). The DDR signals cell cycle checkpoints that arrest the cell cycle to allow sufficient time for repair or apoptosis to be completed. The response to DSBs and collapsed replication forks is crucial, as these are difficult to repair. The independent functions of the NHEJ and HR pathways that were found in chapter 3 in PCO cultures require further investigation. The aim of this chapter is, therefore, to assess the biological interaction of the two pathways in ovarian cancer and normal ovarian epithelium, and to assess the interaction of HR and NHEJ with PARP-1.

Three PI3-Kinase-related kinases (PIKKs), ATM, ATR and DNA-PKcs are intimately connected with DDR (Thompson, 2012). This study concentrates on two – ATR and DNA-PKcs.

5.1.1 ATR

The ATR gene is located at chromosome position 3q23 and comprises 2644 amino acids (approximately 301kDa) (Bentley et al., 1996). ATR^{-/-} mice die on embryonic day 7 due to increased apoptosis and chromosomal fragmentation (Brown and Baltimore, 2000). No human germ-line homozygous ATR deletions have been identified, however, autosomal-recessive disease Seckel syndrome sufferers have a hypomorphic mutation in ATR resulting from an A2101G substitution, causing changes in splicing and resulting in low levels of the protein. Sufferers exhibit growth restriction, short stature, microcephaly and are hypersensitive to UV (O'Driscoll et al., 2003).

5.1.1.1 Role of ATR in DNA Damage Repair

ATR is possibly the most versatile of the three PIKKs in that it is activated by single-stranded DNA adjoining double-stranded DNA that occurs during NER, following resection of DSBs and collapsed replication forks (Cortez, 2003, Dunkern et al.,

2001, Minca and Kowalski, 2011, Cortez, 2005). ATR is activated by these lesions to phosphorylate a number of targets involved in HR and the re-start of replication forks, but its major target is CHK1 (Chen et al., 2012). By phosphorylation of CHK1, ATR initiates the S and G2 checkpoint cascade (Zhao and Piwnicka-Worms, 2001). ATR has also been shown to be activated by the MMR protein (Yoshioka et al., 2006), to phosphorylate DNA-PKcs (Yajima et al., 2006), and to indirectly influence the BER pathway (Stauffer et al., 2007).

5.1.1.2 ATR Activity in Cancer

Many studies have investigated ATR mutations in relation to breast and ovarian cancer risk; however, no germline mutations have been reported to be involved (Durocher et al., 2006, Heikkinen et al., 2005, Kontorovich et al., 2008). A high frequency frameshift mutation of the A(10) repeat from the codon 774 of the ATR gene, resulting in a truncated form of ATR, was noted in 21 % of stomach cancers (Menoyo et al., 2001). The A(10) repeat has also been found to be altered in a third of MSI positive endometrial cell lines (Mironov et al., 1999, Lewis et al., 2005, Vassileva et al., 2002). Microsatellites are unstable in MMR defective cancers. MMR deficiency has been reported in up to 39 % of ovarian tumours, and therefore the A(10) repeat in ATR may have an important role in some ovarian cancers (Buller et al., 2001, Helleman et al., 2006).

Many of the anticancer agents that are in routine clinical use act by causing DNA damage. Platinum agents cause bulky adducts or ICLs, IR and topoisomerase II poisons induce DSBs, and gemcitabine is incorporated into DNA causing chain termination and therefore, stalled replication forks (Hoeijmakers, 2001). All these lesions trigger ATR, thus inhibition of ATR should promote cell killing. Cancer cells undergo continuous proliferation and often have dysregulated G1 control, making them reliant on their remaining S and G2 checkpoints (Massague, 2004). This means that cancerous cells are much more likely than normal cells to enter S-phase with damaged DNA. Therefore, they have a high level of replicative stress, stalled replication forks and DSBs. In addition, there are higher levels of ROS in tumours due to increased metabolic activity, mitochondrial dysfunction and various oxidases (Storz, 2005). These give rise to approximately 100-fold higher levels of oxidative DNA lesions in tumours than in normal tissues (Wiseman and Halliwell, 1996).

Therefore, inhibition of ATR is thought to have a significant effect on the tumour, but not normal cells, thus limiting toxicity to the patient.

5.1.1.3 ATR as a Therapeutic Target

Recent studies identified that numerous cellular defects confer sensitivity to single agent ATR inhibitors (ATRi). These include defects in ATM, XRCC1 and BRCA1 and overexpression of DNA-PKcs (Peasland et al., 2011, Sultana et al., 2013, Middleton et al., 2015, Mohni et al., 2014). Inactivation of ATR is also synthetically lethal in oncogene-activated cancer cells (Gilad et al., 2010), and cells with induced overexpression of cyclin E (Toledo et al., 2011). Two ATRi, VX-970 and AZD-6738, are currently undergoing clinical evaluation. VX-970 is being evaluated both as a single agent and in combination with both platinum-based chemotherapy (clinicaltrials.gov identifier: NCT02157792) and AZD-6738 in haematological malignancies with 11q deletions (ATM defective) (clinicaltrials.gov identifier: NCT01955668). In this study, the Newcastle-developed ATR inhibitor, NU6027, which has K_i of 100nM and IC_{50} of 6.7 μ M, was used. NU6027 was developed as a CDK2 inhibitor, and although its potency for CDK2 is limited, it has to be noted that, some of the effects seen, may be through CDK2 inhibition rather than ATR.

5.1.2 DNA-PK

DNA-PKcs is a key player in the NHEJ pathway of DSB repair and has additional functions in the mammalian cell including telomere maintenance and induction of apoptosis (Burma and Chen, 2004, Kim et al., 1999). The *DNA-PKcs* is located at chromosome position 8q11 and comprises 4128 amino acids (approximately 469kDa). Mouse knockout models remain viable but demonstrate growth restriction, whilst mouse DNA-PKcs mutant models demonstrate immunodeficiency (Thacker and Zdzienicka, 2003, Burma et al., 2006).

5.1.2.1 Role of DNA-PKcs in DNA Damage Repair

The recruitment of DNA-PKcs to DSBs by Ku results in activation of its kinase function such that it can now phosphorylate other proteins as well as itself. DNA-PKcs tethers the broken ends to facilitate rejoining (Cary et al., 1997), and also recruits and activates proteins involved in DNA end-processing and ligation. The dissociation of DNA-PKcs from DNA breaks is dependent on phosphorylation of

several S/TQ residues, most notably on T2609 and S2056 (Burma and Chen, 2004, Chen et al., 2005). DNA-PKcs interacts with artemis and the artemis:DNA-PKcs cuts various forms of damaged DNA ends (Ma et al., 2005). Pol μ and pol λ can bind to the Ku:DNA complex, and are capable of template-dependent, and in the case of pol μ , template independent synthesis. DNA-PKcs also stimulates the ligase activity of the XLF:XRCC4:LIGIV complex which can ligate across gaps and ligate incompatible DNA ends with high efficiency (Gu et al., 2007b, Gu et al., 2007a). DNA-PKcs is also phosphorylated by ATM and ATR (Yajima et al., 2006, Chen et al., 2007).

5.1.2.2 *DNA-PKcs Activity in Cancer*

DNA-PKcs down regulation, in many instances through SNPs of the *DNA-PKcs* gene, has been reported in several human cancers (McKean-Cowdin et al., 2009, Moll et al., 1999, Sakata et al., 2001, Danoy et al., 2008, Lee et al., 2007a, Kurimasa et al., 1999, Someya et al., 2006, Robinson-Bennett et al., 2008). A further mechanism for loss of DNA-PKcs function is by mutation in one of the two microsatellite mononucleotide repeats [poly(A8) and poly(A10) tracts]; this has been reported in gastric, colorectal and urothelial carcinomas (Lee et al., 2007a, Li et al., 2004b, Mongiat-Artus et al., 2006). Loss of DNA-PKcs function has also been reported to be associated with a higher risk of metastasis to lymph nodes, tumour progression and poor survival in malignant spindle cell tumours of the extremities, lung and gastric cancers (Cho et al., 2002, Xing et al., 2008, Lee et al., 2007a, Lee et al., 2005).

On the other hand, DNA-PKcs over expression was reported in oral cancer (Shintani et al., 2003, Um et al., 2004) and neuroblastoma (Deutsch et al., 2001). In breast and lung cancers, *DNA-PKcs* has been suggested to be a potential susceptibility gene (Someya et al., 2006), with significantly lower DNA-PK activity in peripheral blood lymphocytes in cancer patients compared to healthy controls (Moll et al., 1999, Fu et al., 2003, Auckley et al., 2001). Contrary to the prognostic effects of loss of DNA-PKcs function, increased DNA-PKcs expression has been reported to be associated with drug resistance in B-CLL (Shen et al., 1998, Kim et al., 2000, Deriano et al., 2005). The increased DNA-PKcs expression in cancer tissues is likely to be due to increased genomic stress, and its association with poor survival may not only provide a useful prognostic marker but also a treatment target. It would appear, therefore, that in addition to SNPs which predispose to various cancers, perturbations in the

DNA-PKcs gene are common. In general, loss of expression is associated with poor survival, but interestingly, increased expression may be associated with chemotherapy resistance.

5.1.2.3 DNA-PK as a Therapeutic Agent

Cells defective in NHEJ are not only sensitive to IR, but also topoisomerase II poisons that cause DSBs (Jeggo et al., 1989). Inhibition of DNA-PK is, therefore, an attractive target for modulating resistance to therapeutically induced DSBs. DNA-PKi have been suggested as radio- and chemo- potentiators by *in vitro* and *in vivo* studies (Rosenzweig et al., 1997, Boulton et al., 2000, Kashishian et al., 2003, Shinohara et al., 2005, Tavecchio et al., 2012, Zhao et al., 2006). A proof-of-principle study of dual DNA-PK and PI3K inhibitor (KU-0060648) has demonstrated chemo-sensitisation *in vitro* and *in vivo* with limited toxicity, thus suggesting that further evaluation of DNA-PKi is required (Munck et al., 2012). PARP-1 and DNA-PK interaction in radio-sensitisation has also been demonstrated, which suggests that the combined use of these inhibitors may also be effective; although, whether this would be by mutual stimulation or competition is still unclear (Ruscetti et al., 1998, Veuger et al., 2003, Veuger et al., 2004, Mitchell et al., 2009a, Boulton et al., 1999). In this study the Newcastle-developed potent DNA-PKi, NU7441 was used. NU7441 has an IC₅₀ of only 13 nM and at least 100-fold selectivity for this enzyme compared with other PI3KK family kinases (Leahy et al., 2004).

5.2 Aims for Chapter 5

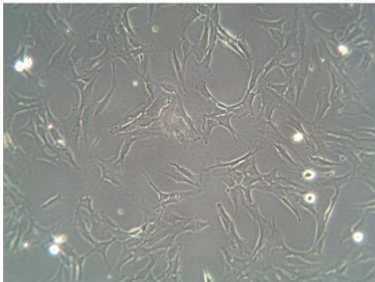
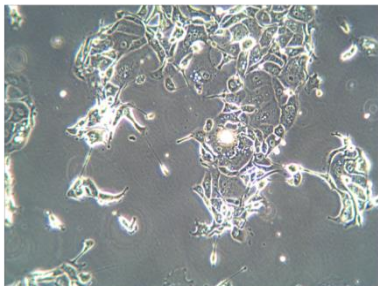
The aim of this study was to assess the role and the interaction of ATR and DNA-PK in DNA damage recognition in ovarian cancer. Furthermore, this study aimed to assess the interaction of DNA-PK and ATR with PARP inhibitors. Specific aims were:

- to assess the effect of ATR and DNA-PK inhibition on cell growth, cell survival, cell cycle, and DSBs recognition and repair, in normal ovarian epithelium and in ovarian cancer.
- to assess the interaction between ATR and DNA-PK with PARP-1 inhibition in terms of cell growth, cell survival and DSBs recognition and repair.
- to assess DSB recognition and repair in PCO cultures.

5.3 Results

Two cell line models were selected – a normal ovarian epithelial cell line (OSEC-2) and an ovarian carcinoma cell line (NUOC-1) (Table 5-1). OSEC-2 cell line was developed at Newcastle University (Davies et al., 2003). NUOC-1 cell line is a spontaneously immortalised PCO culture that was characterised in chapter 3.

Table 5-1 Cell line models.

Cell line	Morphology	Derived from	Doubling time (hrs)
OSEC-2		Derived from normal ovarian surface epithelium. Immortalised with SV40 large T antigen, hTERT	27
NUOC-1		Spontaneously immortalised primary culture derived from ascites collected from a patient with clear cell / endometrioid ovarian carcinoma.	58

5.3.1.1 Selection of ATR vs ATM for Inhibition of HR Function

Both ATR and ATM are signaling proteins that are reported to initiate HR. The HR assay was carried out using ATR and ATM inhibitors to assess which of the two proteins has a more important role in HR. A two fold increase in γ H2AX and RAD51 is used as a cut off to define HRC. > 2 fold increase in γ H2AX and RAD51 cells are deemed HRC, whilst > 2 fold increase in γ H2AX but < 2 fold increase in RAD51 cells are deemed HRD.

Relative to un-irradiated controls, neither ATR nor ATM inhibitors had a significant effect on γ H2AX foci number 24 hrs after treatment with 10 μ M rucaparib and 2Gy IR (Figure 5-1). ATR inhibition caused HRD, as there was only a 1.4-fold increase in RAD51 foci after IR+rucaparib. ATM inhibition did not impair HR, as there was a 2.2-fold increase in RAD51 foci after IR+rucaparib in ATM inhibited cells. Therefore, ATR was selected for this study. Inhibition of NHEJ by the DNA-PK inhibitor NU7441 was confirmed in chapter 4.

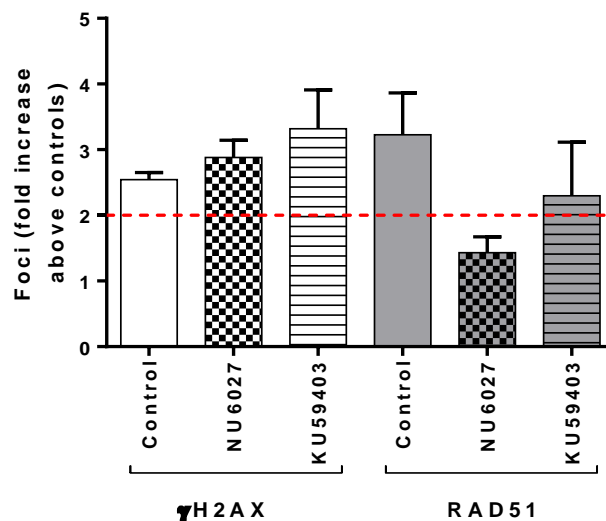


Figure 5-1 Assessment of HR in response to ATR and ATM inhibition.

DNA damage by γ H2AX foci and HR function assessed by the formation of RAD51 foci 24 hrs after 2Gy IR in OSEC-2 cells. ATR (NU6027) and ATM (KU59403) inhibitors were added 1 hrs prior to IR treatment.

5.3.1.2 Optimisation of Inhibition of ATR and DNA-PK

To avoid the complication of off-target cytotoxicity of the inhibitors the minimum concentration needed to inhibit enzymatic activity in cells by 80 % was determined by assessing phosphoDNA-PK expression after 2 Gy IR by western blotting. Although significant inhibition of DNA-PK phosphorylation was found at all concentrations, 1 μ M NU7441 was selected, as it produced a mean 78 % reduction in activity, and this concentration had been used in previous studies with this compound (Figure 5-2).

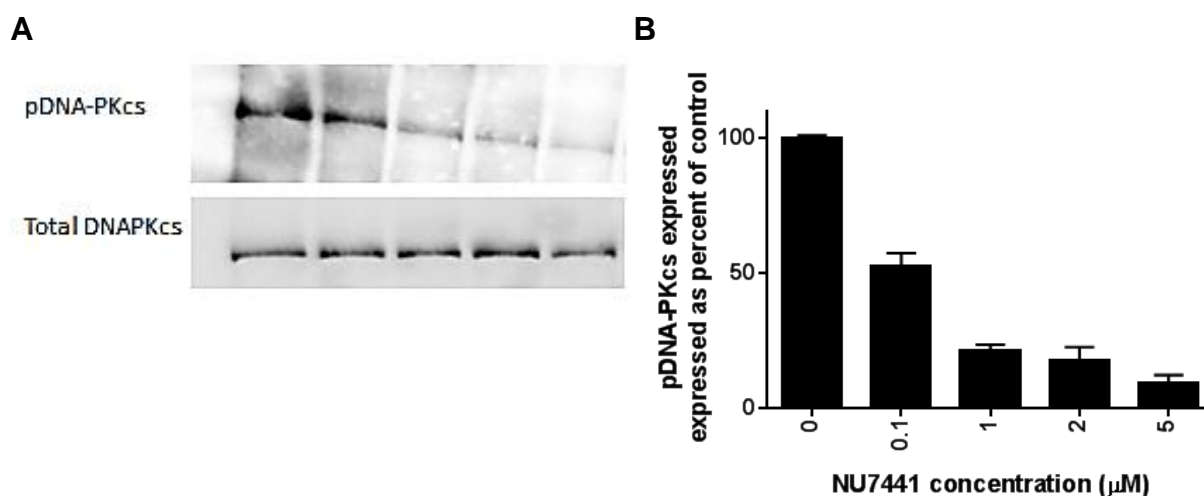


Figure 5-2 Optimisation of inhibition of DNA-PK in OSEC-2 cell line.

A. Representative western blot and B. band density results for pDNA-PK inhibition by NU7441 1 hr after 2 Gy IR.

ATR function was assessed by the assessment of phosphorylation of CHK1 after treatment with HU. All those concentrations tested except 1 μM NU6027, significantly reduced pCHK1 (Figure 5-3). 10 μM NU6027 was selected, as it produced a mean 80 % reduction in activity and this concentration had been used in previous studies with this compound.

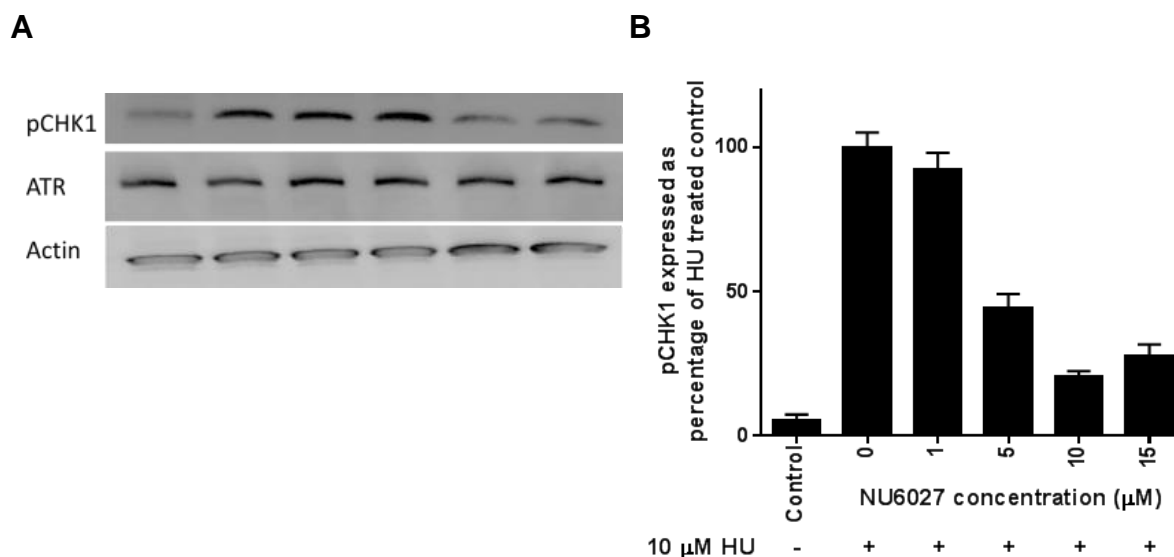


Figure 5-3 Optimisation of inhibition of ATR in OSEC-2 cell line.

Western blot and band density results of pCHK1 inhibition after 24 hr incubation with NU6027. 10 μM Hydroxyurea (HU) was used to induce DNA damage.

5.3.1.3 Development of Knockdown Models for ATR and DNA-PK

Knockdown models of ATR and DNA-PKcs were generated to assess the effect of an absent protein, as compared to an inhibited protein. OSEC-2 and NUOC-1 cells were virally transduced with MISSION®shRNA lentiviral transduction particles. Five constructs for each protein were assessed. A non target control construct was used for control of transduction. In OSEC-2 cells knockdown was assessed for all 5 constructs for ATR and DNA-PKcs. In NUOC-1 cells 4 DNA-PKcs and 3 ATR knockdowns grew successfully for analysis.

5.3.1.3.1 Assessment of Knockdown by mRNA and Protein Expression

Knockdown levels were confirmed at mRNA level by RT-qPCR and at protein level by western blotting. This work was done with Charlotte Leeson (Undergrad, 2013).

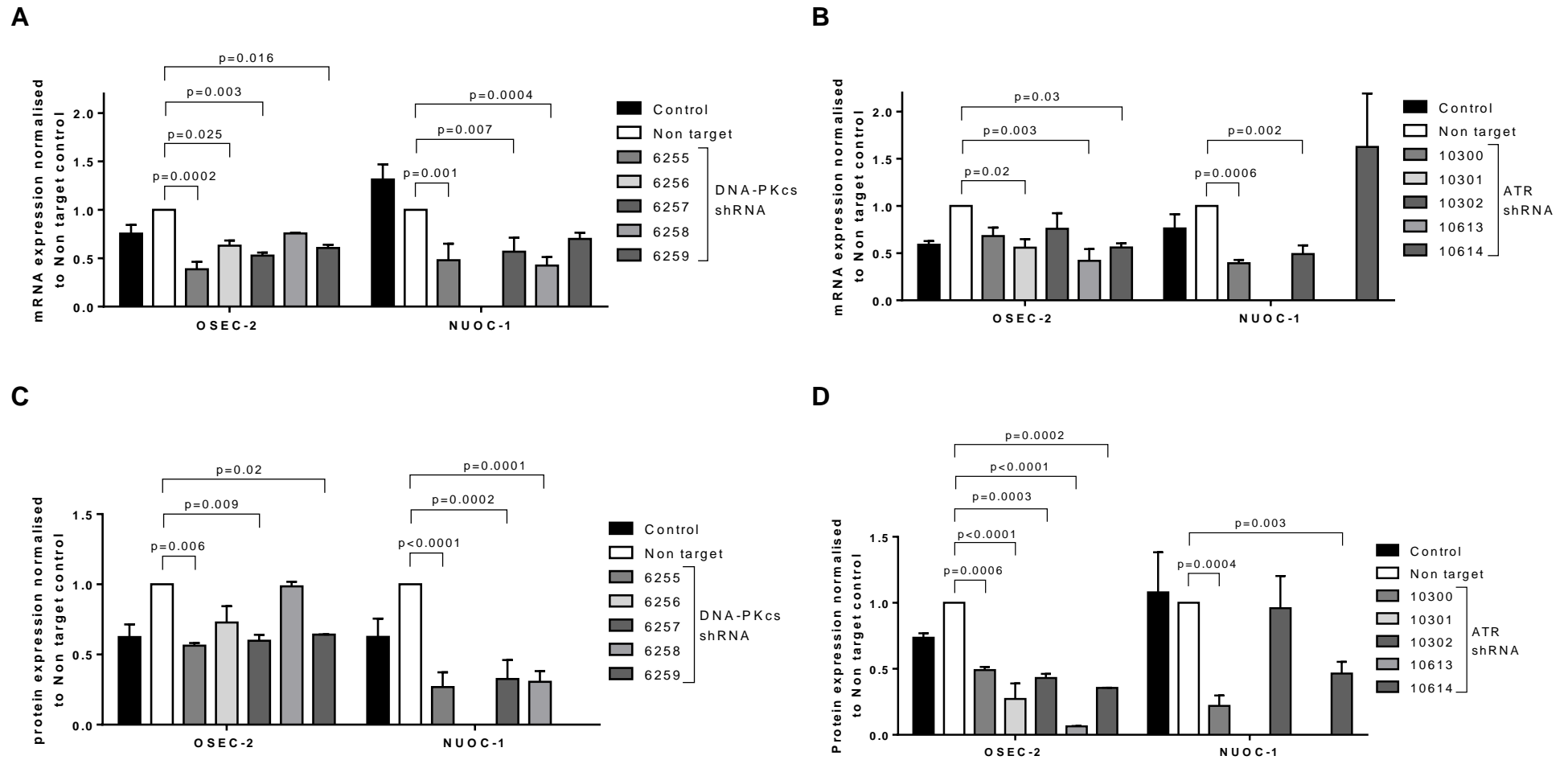


Figure 5-4 Silencing of ATR and DNA-PKcs in OSEC-2 and NUOC-1 cells.

A. DNA-PKcs mRNA expression analysed by real time RT-qPCR. Expression was normalised to GAPDH housekeeper gene. Results were then normalised to non target control. **B.** ATR mRNA expression. **C.** DNA-PKcs protein expression analysed by western blotting. Densitometry was normalised to α -tubulin loading control. Results were then normalised to non target control. **D.** ATR protein expression. All results are average of three independent experiments. Error bars are SEM.

For DNA-PKcs knockdowns the 6255 construct achieved the best knockdown, as measured by both mRNA (61 % knockdown in OSEC-2, $p = 0.0002$, and 52 % knockdown in NUOC-1 cells, $p = 0.001$) and protein (46 % knockdown in OSEC-2, $p = 0.006$ and 73 % knockdown in NUOC-1 cells, $p < 0.0001$) levels in both OSEC-2 and NUOC-1 cells, and therefore, this construct was selected for use in further experiments (Figure 5-4).

For ATR knockdown no single construct was comparable in both cell lines, and therefore, construct 10613 was selected for OSEC-2 (68 % knockdown at mRNA, $p = 0.003$, and 94 % knockdown at protein level, $p < 0.0001$) cells and 10300 for NUOC-1 cells (61 % knockdown at mRNA, $p = 0.0006$, and 78 % knockdown at protein level, $p = 0.0004$) for use in further experiments.

5.3.1.3.2 Development of Double Knockdown Models

To analyse the interactions of ATR and DNA-PK, double knockdown models were created. The models were firstly developed in OSEC-2 cells.

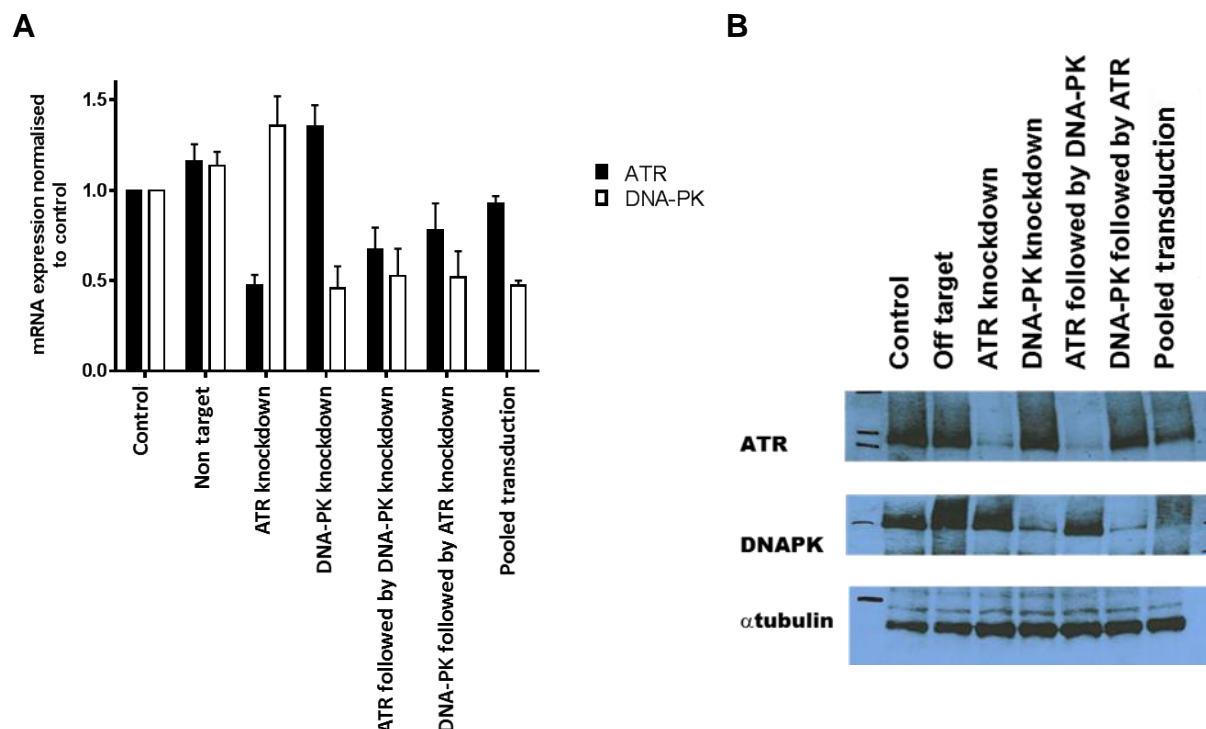


Figure 5-5 ATR and DNA-PK double knockdown in OSEC-2 cells.

A. DNA-PKcs and ATR mRNA expression was analysed by real time RT-qPCR. **B.** DNA-PKcs and ATR protein expression was analysed by western blotting. Expression was normalised to GAPDH housekeeper gene. Results were then normalised to controls. All results are average of three independent experiments. Error bars are SEM.

Greater than 50 % DNA-PK knockdown was successful in all combinations of knockdown (Figure 5-5). However, the only combination where ATR knockdown was successful was when ATR knockdown was performed first, followed by DNA-PK knockdown, thus producing a 30 % ATR and 50 % DNA-PK knockdown. The level of knockdown was below that achieved with individual knockdowns. Furthermore, when protein levels were assessed double knockdown was found not to be possible. Therefore, the decision was made to combine knockdown with drug treatments.

5.3.1.3.3 Assessment of HR and NHEJ Function in Knockdown Models

Functional assessment of knockdown models for HR and NHEJ was undertaken using validated assays. Knockdown of ATR blocked the increase in RAD51 foci after DNA damage (mean 1.0 \pm 0.1 fold rise in OSEC-2 10613 knockdown, compared to 2.6 \pm 0.1 fold in OSEC-2 controls, $p = 0.003$, and mean 1.3 \pm 0.3 fold in NUOC-1 10300 knockdown, compared to 2.5 \pm 0.2 fold in NUOC-1 controls, $p = 0.007$) (Figure 5-6.A). ATR knockdown cells were therefore deemed HRD.

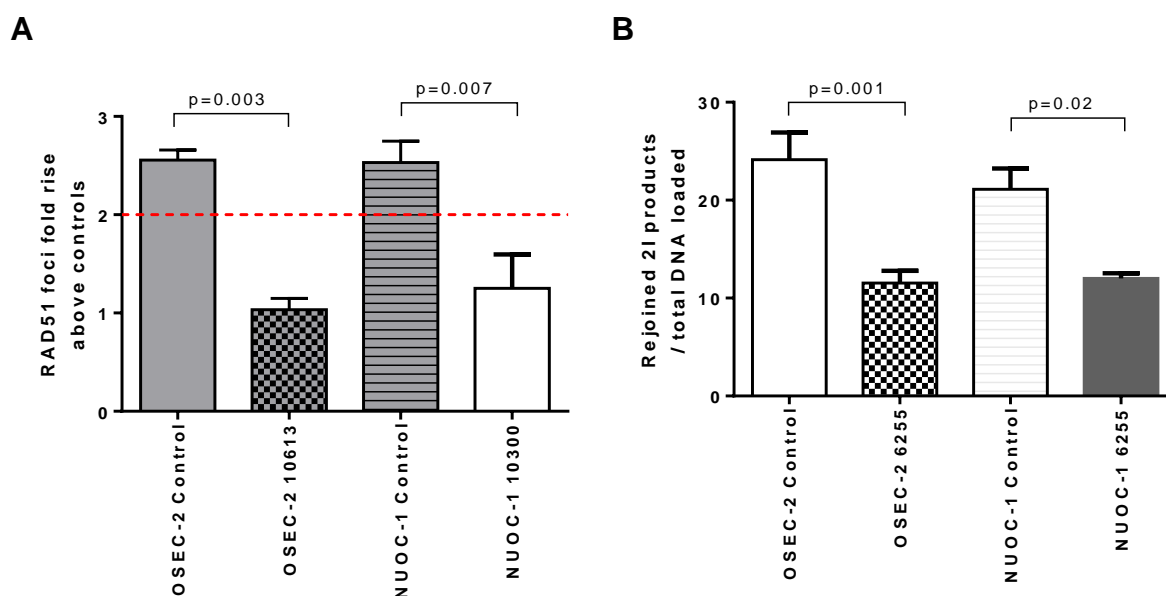


Figure 5-6 HR and NHEJ function in knockdown models.

A. HR function assessed by fold rise in RAD51 foci after 2Gy IR and 24 hr treatment with 10 μ M rucaparib in OSEC-2 and NUOC-1 non target shRNA controls and ATR knockdowns (10613 and 10300). RAD51 foci were assessed by immunofluorescence and quantified using ImageJ. **B.** NHEJ function assessed by rejoining of 2I BstXI cut vector DNA by OSEC-2 and NUOC-1 non target shRNA and DNA-PKcs knockdown (6255). Rejoining was assessed by GelRed stained agarose gel and quantified by densitometry. All results are mean of three independent experiments. Error bars are SEM.

To determine NHEJ function, the rate of rejoining of 2I BstXI substrates was assessed. Knockdown of DNA-PKcs approximately halved the rejoining of 2I BstXI cut vectors (mean 11.5 +/- 1.3 % in OSEC-2 6255 knockdown compared to 24.1 +/- 2.8 fold in OSEC-2 controls, $p = 0.001$, and mean 12.0 +/- 0.5 % in NUOC-1 6255 knockdown compared to 21.1 +/- 2.1 fold in NUOC-1 controls, $p = 0.02$), and so were deemed NHEJD (Figure 5-6.B).

5.3.2 Assessment of the Effect of ATR and DNA-PK Inhibition on Cellular Biology

Both ATR and DNA-PKcs have cellular effects outside the DDR. Therefore, the effect on cellular biology was assessed for the inhibitors and knockdown models individually and combined.

Hypothesis: Inhibition of ATR and DNA-PK results in reduction in cell growth and cell survival with synergistic effect due to inhibition of DNA repair

5.3.2.1 The Effect of ATR and DNA-PK on Cell Growth

Inhibition of ATR resulted in significant growth inhibition in OSEC-2 and NUOC-1 cells (Figure 5-7). The results were consistent between inhibitor (47 % reduction, $p = 0.007$ for OSEC-2, and 78 %, $p < 0.0001$ for NUOC-1) and shRNA knockdown (29 % reduction, $p = 0.03$ for OSEC-2, and 41 % reduction, $p = 0.02$ for NUOC-1). This finding is likely to be due to the impairment of DNA damage repair.

DNA-PK inhibition was found to have inconsistent results between knockdown and inhibition in NUOC-1 cells (30 % reduction when treated with inhibitor and 40 % increase in growth seen in shRNA knockdown) and had no effect in OSEC-2 cell growth.

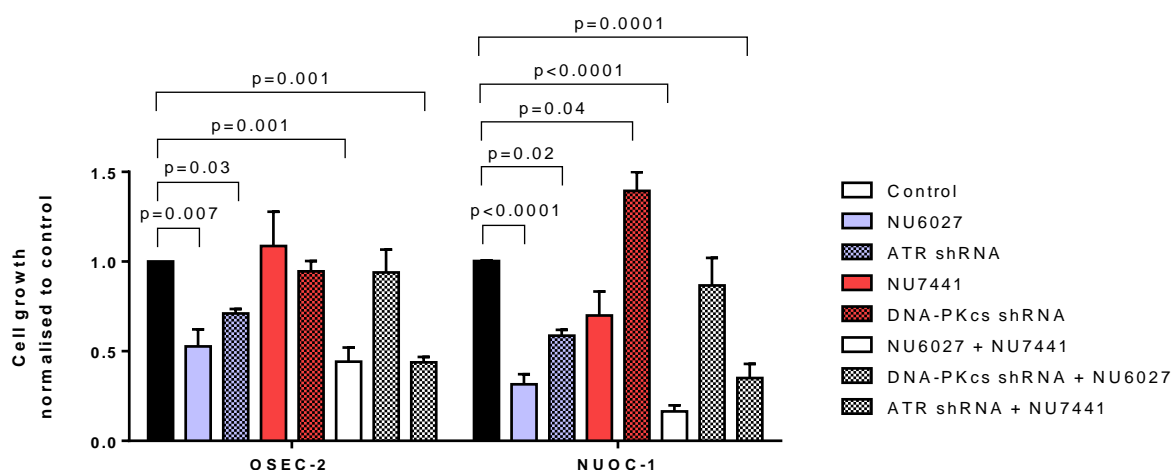


Figure 5-7 The effect of ATR and DNA-PK inhibition on cell growth.

All results are normalised to DMSO controls for drug treatments and non target shRNA for knockdown models. All treatments were grown for three doubling times. Results are average of three independent experiments with 6 experimental repeats. Error bars are SEM. Statistical significance was assessed by two way Anova with Bonferroni correction for multiple analysis.

Combined pharmacological inhibition of ATR and DNA-PKcs resulted in significant inhibition of cell growth in both cell lines (56 % reduction, $p = 0.001$ for OSEC-2, and 82 % reduction, $p < 0.0001$ for NUOC-1), which was similar to the result of ATR knockdown combined with NU7441 (56 % reduction, $p = 0.001$ for OSEC-2, and 65 % reduction, $p = 0.0001$ for NUOC-1). However, the addition of NU6027 to DNA-PK knockdown was found to have no effect on cell growth in either cell line compared to controls. In the NUOC-1 cell line, addition of NU6027 to DNA-PK shRNA did significantly reduce cell growth compared to DNA-PK shRNA alone (39 % reduction, $p < 0.0001$).

5.3.2.2 The Effect of ATR and DNA-PK on Cell Survival

To assess if, further to inhibition of cell growth, overall cell survival is inhibited by loss of ATR and DNA-PKcs, clonogenics assays were used (Figure 5-8). Despite significant growth inhibition by ATRi in OSEC-2 cells, the only treatment found to have a significant reduction in cell survival was the combination of ATR shRNA with NU7441 (65 % reduction in cell survival, $p = 0.045$).

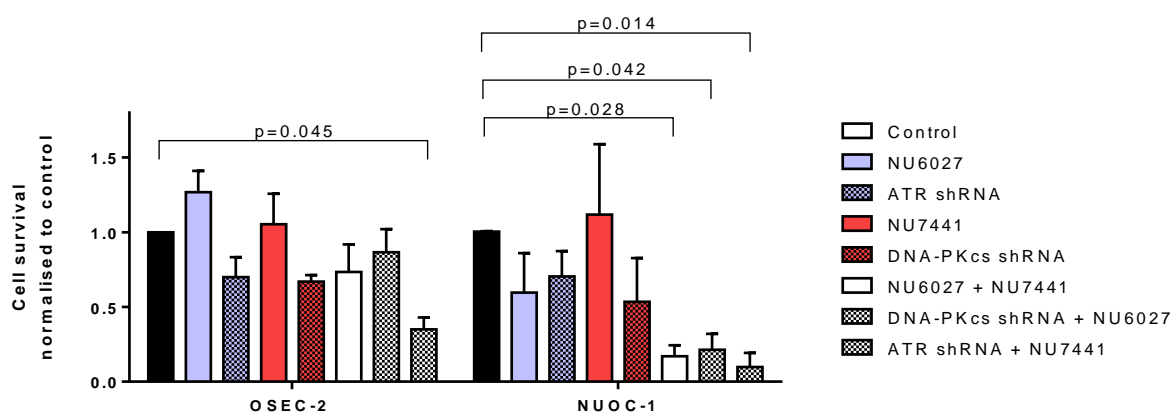


Figure 5-8 The effect of ATR and DNA-PK inhibition on cell survival.

All results are normalised to DMSO controls for drug treatments and non target shRNA for knockdown models. OSEC-2 treatments were grown for 14 days and NUOC-1 for 30 days. All treatments were grown for three doubling times. Results are average of three independent experiments with 3 experimental repeats. Error bars are SEM. Statistical significance was assessed by two way Anova with Bonferroni correction for multiple analysis.

In NUOC-1 cells, neither inhibition, nor knockdown of ATR or DNA-PK individually reduced cell survival significantly. Combination of ATR and DNA-PK inhibitors together (83 % reduction in cell survival, $p = 0.028$) and shRNA knockdown with ATRi (79 % reduction in cell survival, $p = 0.042$) and DNA-PKi (90 % reduction in cell survival, $p = 0.014$) resulted in reduced cell survival.

5.3.2.3 The Effect of ATR and DNA-PK on Cell Cycle

Hypothesis: Inhibition of ATR and DNA-PK results in cell cycle arrest

Due to the observed discrepancy between growth inhibition and cell survival assays, cell cycle analysis was performed. The effects of ATR and DNA-PKcs inhibition and knockdown on phases of the cell cycle were analysed using PI staining and FACS analysis (Figure 5-9).

In OSEC-2 cells, ATR inhibition resulted in significant G1 arrest (15 %, $p < 0.0001$), whilst knockdown of DNA-PKcs resulted in a significant G2/M arrest (9 %, $p = 0.0007$). The results between knockdown and drug inhibition were not consistent. Also non target shRNA produced a significant G1 arrest (14 %, $p < 0.0001$), which suggests off target cell cycle effects. This effect of non target shRNA may also be masking any effects from the ATR and DNA-PK knockdown. Due to NUOC-1

tetraploid and mixed population phenotype, cell cycle analysis could not be performed in NUOC-1 cells (determined in section 2.9.4).

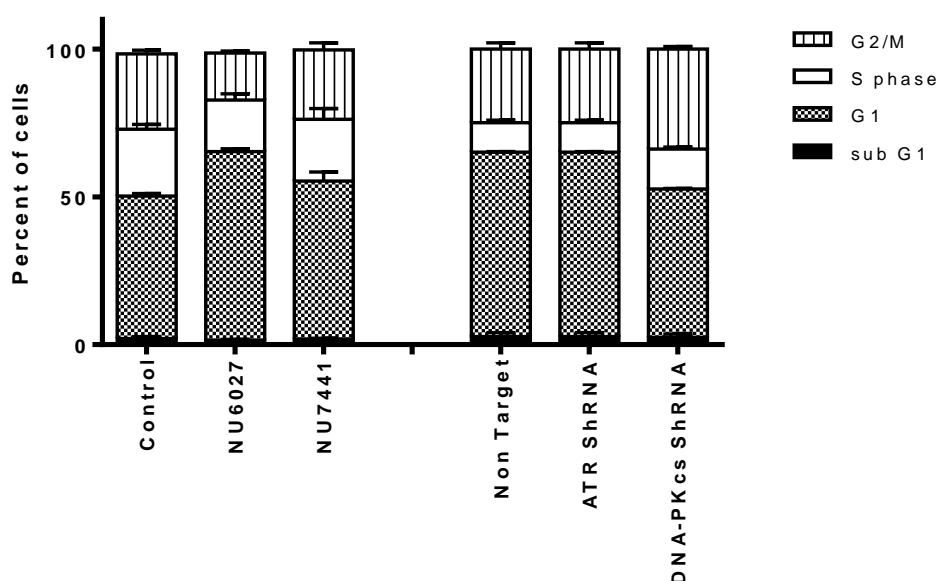


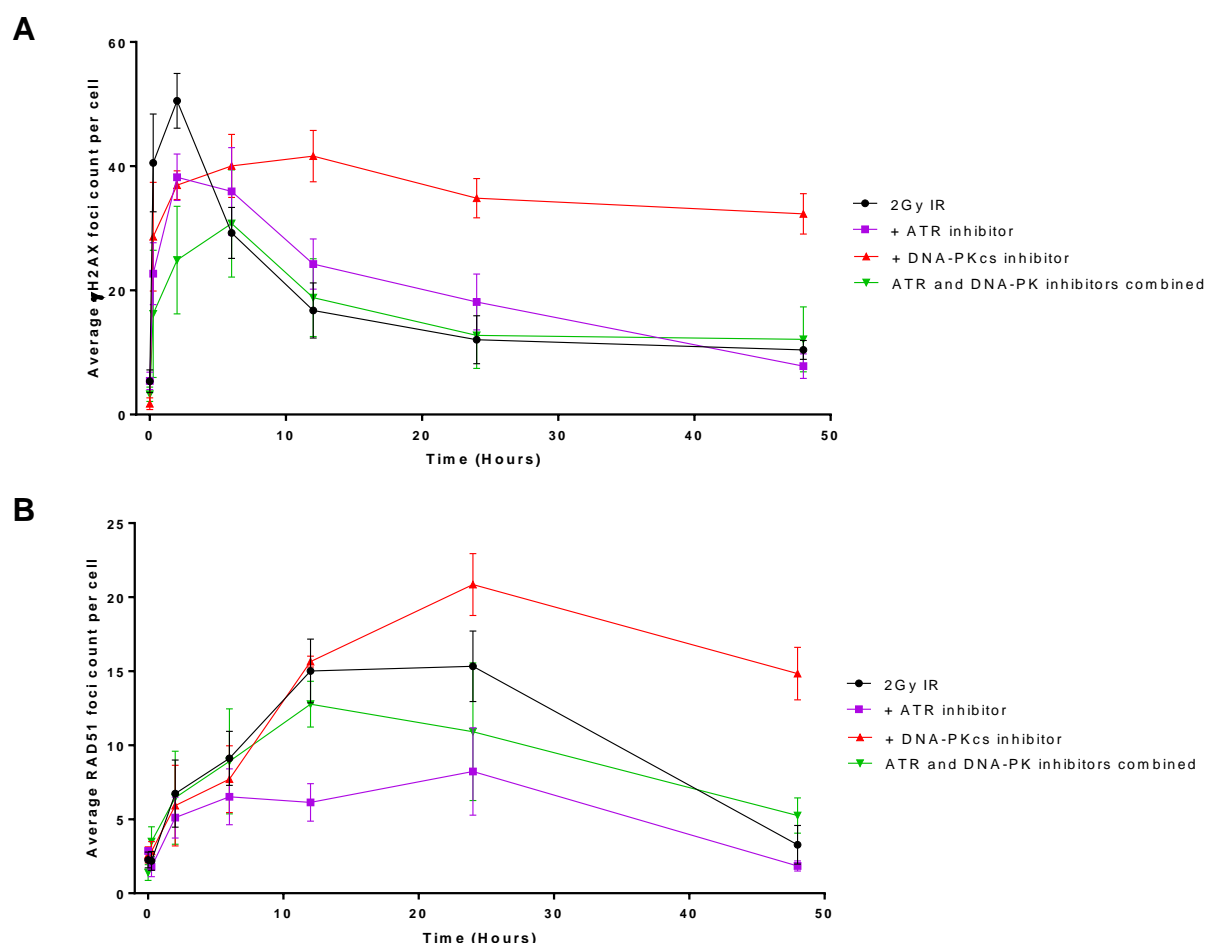
Figure 5-9 The effect of ATR and DNA-PKcs on cell cycle.

DNA-PKcs was inhibited with NU7441 or knockdown with shRNA, and ATR was inhibited with NU6027 or shRNA knockdown in exponentially growing cells. 10,000 cells were counted. Pharmacologically inhibited cells are compared to DMSO control, and shRNA-knockdown cells are compared to non target shRNA control. Results are mean of 3 independent experiments.

5.3.2.4 The Effect of ATR and DNA-PK on DNA Repair

ATR and DNA-PK are essential for DSB repair. DSBs repair was assessed by inducing DSBs using 2 Gy IR, and measuring the mean numbers of γ H2AX foci, a marker for DSBs, and the mean numbers of RAD51, a marker for HR. OSEC-2 cells were used for these experiments.

Hypothesis: Inhibition of ATR and DNA-PK results in reduction of DNA damage recognition. DNA-PK is involved in fast phase of repair via NHEJ, whilst ATR activates slow phase of repair via HR



*Figure 5-10 DSBs formation and recovery after inhibition of ATR and DNA-PKcs. Inhibitors were added to OSEC-2 cells 1 hr prior to irradiation. Foci formation was assessed using immunofluorescence after 2Gy IR. Foci numbers were quantified using ImageJ. Average number of foci per nucleus are expressed. **A.** γ H2AX foci, **B.** RAD51 foci. The results are average of three independent experiments. Error bars are SEM.*

An initial rapid peak in γ H2AX foci was seen after 2 Gy IR, peaking at 2 hrs in this cell line model (Figure 5-10). After the initial peak, the γ H2AX foci disappeared in a biphasic manner with an initial rapid disappearance, followed by a more gradual decline. RAD51 foci increased steadily peaking at 12 hrs after irradiation; the counts were then maintained until 24 hrs, after which, the number of foci had returned to the baseline count by 48 hrs.

Inhibition of ATR with NU6027 resulted in the inhibition of γ H2AX foci formation, consistent with γ H2AX phosphorylation by ATR, with 25 % lower foci counts at 2 hrs ($p = 0.033$, Figure 5-10.A); and also in the reduction of RAD51 foci formation, with 55 % lower RAD51 foci counts at 12 hrs ($p = 0.004$), and 43 % lower at 24 hrs ($p = 0.03$) (Figure 5-10.B).

Inhibition of DNA-PK with NU7441 resulted in a lower peak γ H2AX foci count at 2 hrs (28 % lower, $p = 0.03$), consistent with γ H2AX phosphorylation by DNA-PK; and a delay in γ H2AX foci recovery, consistent with the impairment of DSB repair by NHEJ, with 69 % higher γ H2AX foci counts at 6 hrs ($p = 0.008$), 200 % higher at 12 hrs ($p = 0.004$), 250 % higher at 24 hrs ($p = 0.005$) and 230 % higher at 48 hrs ($p = 0.007$) (Figure 5-10.A.). Furthermore, significantly higher RAD51 foci counts were found at 24 hrs (21 % higher, $p = 0.047$) and 48 hrs (297 % higher, $p < 0.0001$) (Figure 5-10.B).

Combination of ATR and DNA-PKcs inhibitors resulted in a lower γ H2AX peak, with 60 % lower mean counts at 15 min ($p = 0.005$), and 50 % lower at 2 hrs ($p = 0.003$). The γ H2AX foci peak was also delayed to 6 hrs after IR, compared to 2 hrs in the controls. This result demonstrates the synergistic actions of ATR and DNA-PKcs in DSBs recognition. RAD51 foci numbers were found to be lower than in IR control cells, but higher than in cells treated with ATR inhibitor alone; these differences were not statistically significant. ATR and DNA-PK, therefore, have opposing effects on the numbers of RAD51 foci forming in these cells after irradiation.

5.3.2.5 The Effect of ATR and DNA-PK Inhibition on Chemo-sensitivity Ovarian Cells

Further to the baseline assessment of the sensitivities of NUOC-1 and OSEC-2 cell lines to common therapeutics, as discussed in chapter 3, the role of ATR and DNA-PKcs inhibition in chemo-sensitivity was assessed.

Hypothesis: Inhibition of ATR results in sensitisation to common therapeutics due to inhibition of HR, whilst inhibition of DNA-PK results in radio-sensitisation, but resistance to PARPi due to inhibition of NHEJ

Growth inhibition assays were performed to evaluate the effect of ATR and DNA-PKcs inhibition in OSEC-2 and NUOC-1 cell line sensitivity to irradiation, rucaparib, cisplatin and paclitaxel. Inhibition and shRNA knockdown models for ATR and DNA-PKcs were used. Inhibition was compared to DMSO treated controls, and shRNA knockdown to non target shRNA controls.

Table 5-2 Sensitisation of NUOC-1 and OSEC-2 cells to common therapeutics by ATR and DNA-PK inhibition and knockdown.

Treatments assessed were radiation, rucaparib, cisplatin and paclitaxel with ATR or DNA-PKcs inhibition using drug and shRNA knockdowns. Multiple T tests compared to controls were carried out, with bonferroni adjustment for multiple comparisons. Significant results are marked in bold.

	Drug	Irradiation GI ₅₀	p=	Rucaparib GI ₅₀	p=	Cisplatin GI ₅₀	p=	Paclitaxel GI ₅₀	p=
NUOC-1	Control	4.14	-	8.3	-	1.18	-	0.41	-
	ATR inhibited	4.46	0.82	4.67	0.003	0.51	0.014	0.35	0.06
	DNA-PK inhibited	2.01	0.009	6.55	0.41	0.97	0.18	0.32	0.53
	Non target	2.95	-	7.01	-	1.07	-	0.32	-
	ATR shRNA	2.53	0.50	2.53	0.014	0.38	0.044	0.18	0.53
	DNA-PK shRNA	0.75	<0.0001	5.19	0.09	0.80	0.61	0.25	0.90
OSEC-2	Control	5.84	-	17.47	-	2.83	-	0.44	-
	ATR inhibited	3.77	0.17	12.82	0.39	1.43	0.11	0.39	0.89
	DNA-PK inhibited	1.36	0.025	34.76	0.12	2.33	0.51	0.45	0.19
	Non target	2.99	-	7.21	-	4.33	-	0.24	-
	ATR shRNA	3.63	0.95	4.82	0.009	2.96	0.49	0.24	0.74
	DNA-PK shRNA	3.35	0.88	8.38	0.26	4.35	0.99	0.15	0.14

DNA-PK inactivation was found to have significant radio-sensitisation in the NUOC-1 cell line as seen in the inhibition (51 % reduction in GI_{50} , $p = 0.009$) and shRNA knockdown (75 % reduction in GI_{50} , $p < 0.0001$) cells (Table 5-2). In OSEC-2 cells, the radio-sensitisation was statistically significant for NU7441 treatment (76 % reduction in GI_{50} , $p = 0.025$), but not shRNA knockdown.

ATR inhibition resulted in significant sensitisation of NUOC-1 cells to rucaparib (44 % reduction in GI_{50} , $p = 0.003$ for ATR inhibition, and 64 % reduction in GI_{50} , $p = 0.014$ for shRNA knockdown), and cisplatin (57 % reduction in GI_{50} , $p = 0.014$ for ATR inhibition, and 65 % reduction in GI_{50} , $p = 0.044$ for shRNA knockdown). The only statistically significant sensitisation of OSEC-2 cells was to rucaparib in ATR shRNA knockdown ($p = 0.009$).

Neither ATR nor DNA-PKcs inhibition had any significant effect on sensitivity of either cell line to Paclitaxel. This result was anticipated as paclitaxel is a mitotic spindle inhibitor; and thus DNA is not its primary target.

5.3.3 Interaction of ATRi and DNA-PKi with PARPi

Interaction of PARPi and DNA-PKi in radio-sensitisation has also been demonstrated (Ruscetti et al., 1998, Veuger et al., 2003, Veuger et al., 2004, Mitchell et al., 2009a). In other studies, PARP-1 has been shown to have a protective role in HR by suppressing the access of NHEJ to DSBs (Hocheegger et al., 2006, Saberi et al., 2007). The interaction of PARPi with DNA-PKi and ATRi in cell biology was assessed in this study.

5.3.3.1 Optimisation of PARP Inhibition

To reduce the complication of off-target cytotoxicity, the minimum concentration of rucaparib necessary to inhibit PARP activity by > 80 % was determined. 1 μ M rucaparib dose was selected for further experiments (Figure 5-11).

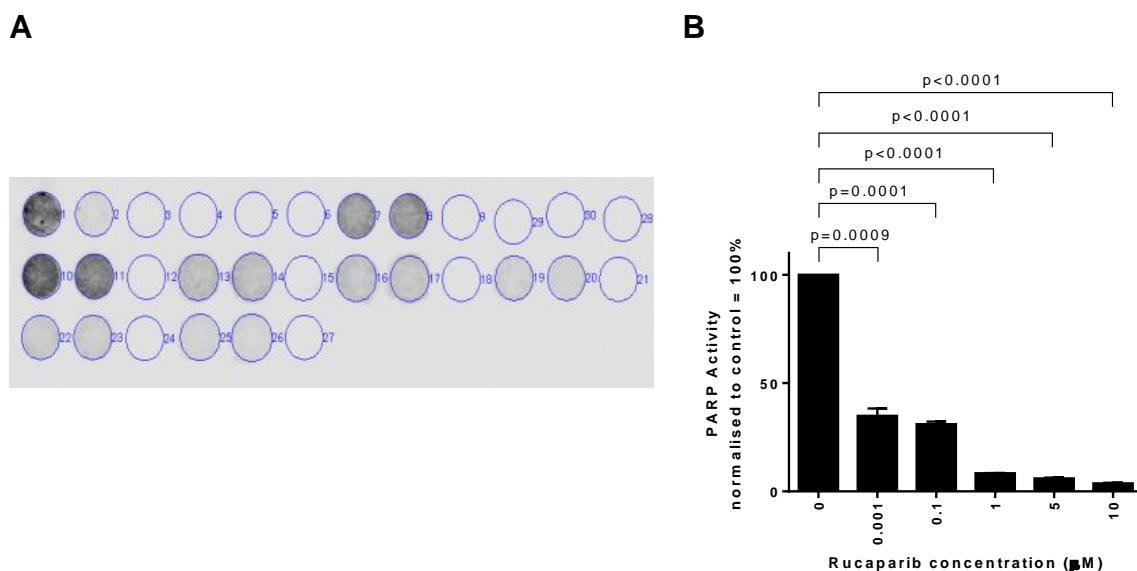


Figure 5-11 Optimisation of inhibition of PARP.

PAR assay A. representative blot and B. band density results for PARP activity inhibition by rucaparib.

5.3.3.2 The Interaction of PARP Inhibition with ATR and DNA-PK Inhibition on Cell Growth

Hypothesis: Addition of rucaparib results in synergistic inhibition of cell growth and survival with ATRi, but opposing effects with DNA-PKi

The growth of OSEC-2 and NUOC-1 cells was not inhibited by 1 μM of rucaparib alone. The interaction of PARPi with ATRi and DNA-PKi on cell growth was assessed by treatment with 1 μM of rucaparib with 1 μM NU7441 or 10 μM NU6027 or shRNA knockdown of either protein.

In OSEC-2 cells, there was no additional growth inhibitory effect of rucaparib above ATRi or ATR shRNA (Figure 5-12 and Appendix 4). Furthermore, no significant alteration of cell growth, compared to controls, was seen when rucaparib was combined with DNA-PKi or DNA-PKcs shRNA.

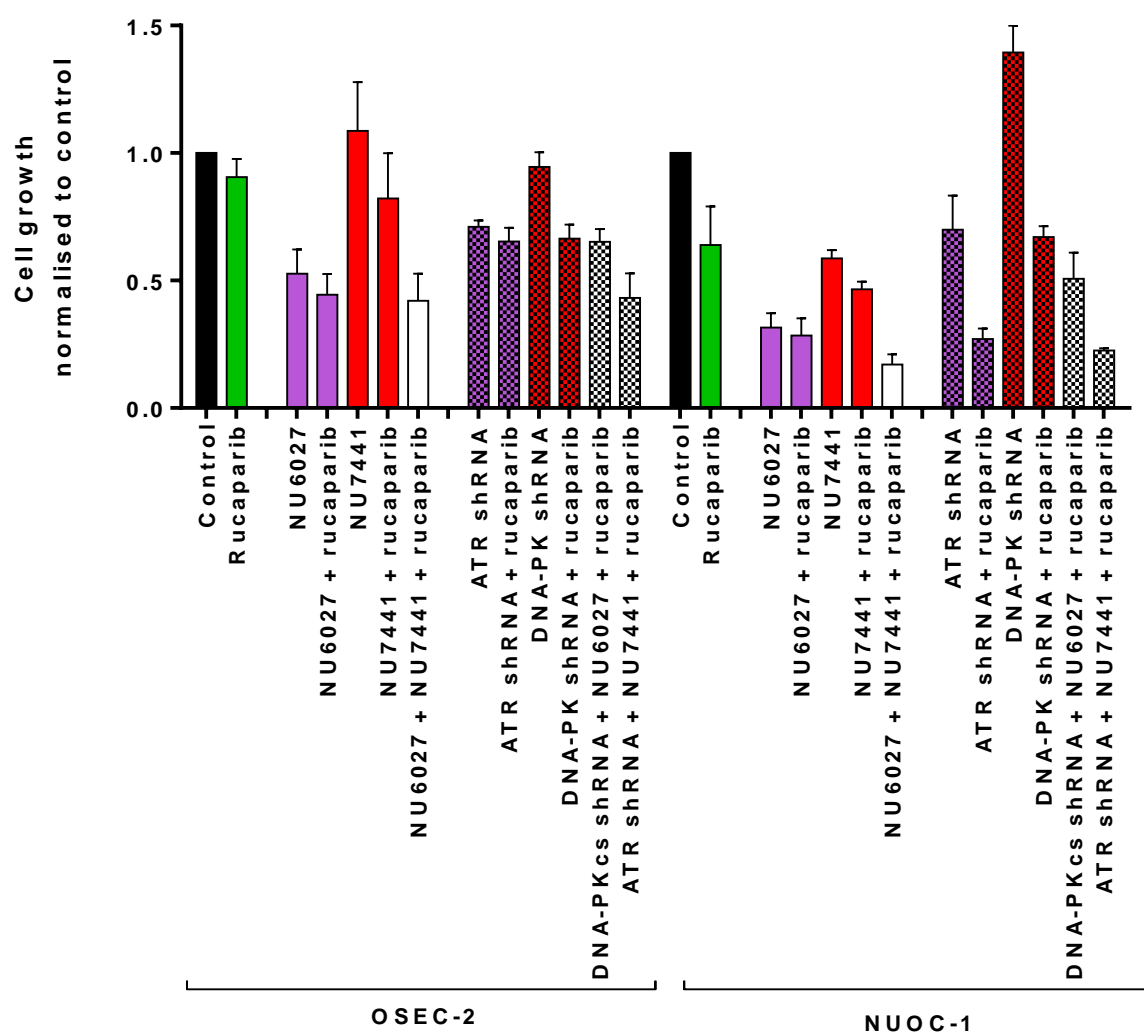


Figure 5-12 The effect of PARPi combined with ATRi and DNA-PKi on cell growth.

All results are normalised to appropriate control. All treatments were grown for three doubling times. Results are average of three independent experiments with 6 experimental repeats. Error bars are SEM. Statistical comparisons are in appendix 4.

In NUOC-1 cells, inhibition with rucaparib resulted in a significant reduction in cell growth when added in combination with ATR shRNA (61 % growth reduction, $p < 0.0001$), and DNA-PKcs shRNA (52 % growth reduction, $p < 0.0001$) knockdowns (Figure 5-12 and Appendix 4). This growth inhibition was not reproduced when inhibitor combinations were used. However, the combination of all three inhibitors resulted in a significant reduction of cell growth compared to rucaparib alone (52 % reduction, $p = 0.02$, in OSEC-2, and 66 % growth reduction, $p = 0.03$, in NUOC-1 cell lines), but not compared to ATRi or DNA-PKi alone.

5.3.3.3 *The Interaction of PARP Inhibition with ATR and DNA-PK Inhibition on Cell Survival*

To assess if the combination of rucaparib with ATRi and DNA-PKi were cytotoxic, as well cytostatic, clonogenic assays were performed (Figure 5-13 and Appendix 4).

In the OSEC-2 cell line, rucaparib resulted in a 27 % reduction in cell survival, compared to DMSO control. The combination of rucaparib with NU6027 resulted in a 51 % reduction in cell survival, compared to NU6027 alone, but this change was not significant compared to rucaparib alone. After correction for multiple comparisons, these results were also not found to be statistically significant. The addition of rucaparib to ATR shRNA resulted in a 63 % reduction in cell survival, compared to rucaparib alone, and a 61 % reduction in cell survival, compared to ATR shRNA. Consistent reduction in cell survival was also seen when rucaparib was added to NU7441 (52 %) and DNA-PK shRNA (52 %).

The combination of the three inhibitors only produced a 27 % reduction in cell survival, however, triple inhibition when either DNA-PK shRNA or ATR shRNA were used produced a 50 % and a 77.5 % ($p = 0.04$) reduction in cell survival, respectively, compared to untreated controls.

In NUOC-1 cells rucaparib alone, and also in combination with ATRi and DNA-PKi did not produce a significant reduction in cell survival. However, the addition of rucaparib to ATR shRNA resulted in a 67 % reduction in cell survival, compared to ATR shRNA, and 99 % reduction, when compared to rucaparib alone ($p = 0.01$). The addition of rucaparib to DNA-PK shRNA also resulted in a reduction of cell survival (38.5 % compared to DNA-PK shRNA and 86 % compared to rucaparib).

In NUOC-1 cells, using triple inhibitors produced a 47 % reduction in cell survival, however, triple inhibition when shRNA was used resulted in only 1.5 % cell survival for DNA-PK shRNA + NU6027 + rucaparib ($p = 0.013$), and no cell survival at all when ATR shRNA was combined with NU7441 and rucaparib ($p = 0.011$).

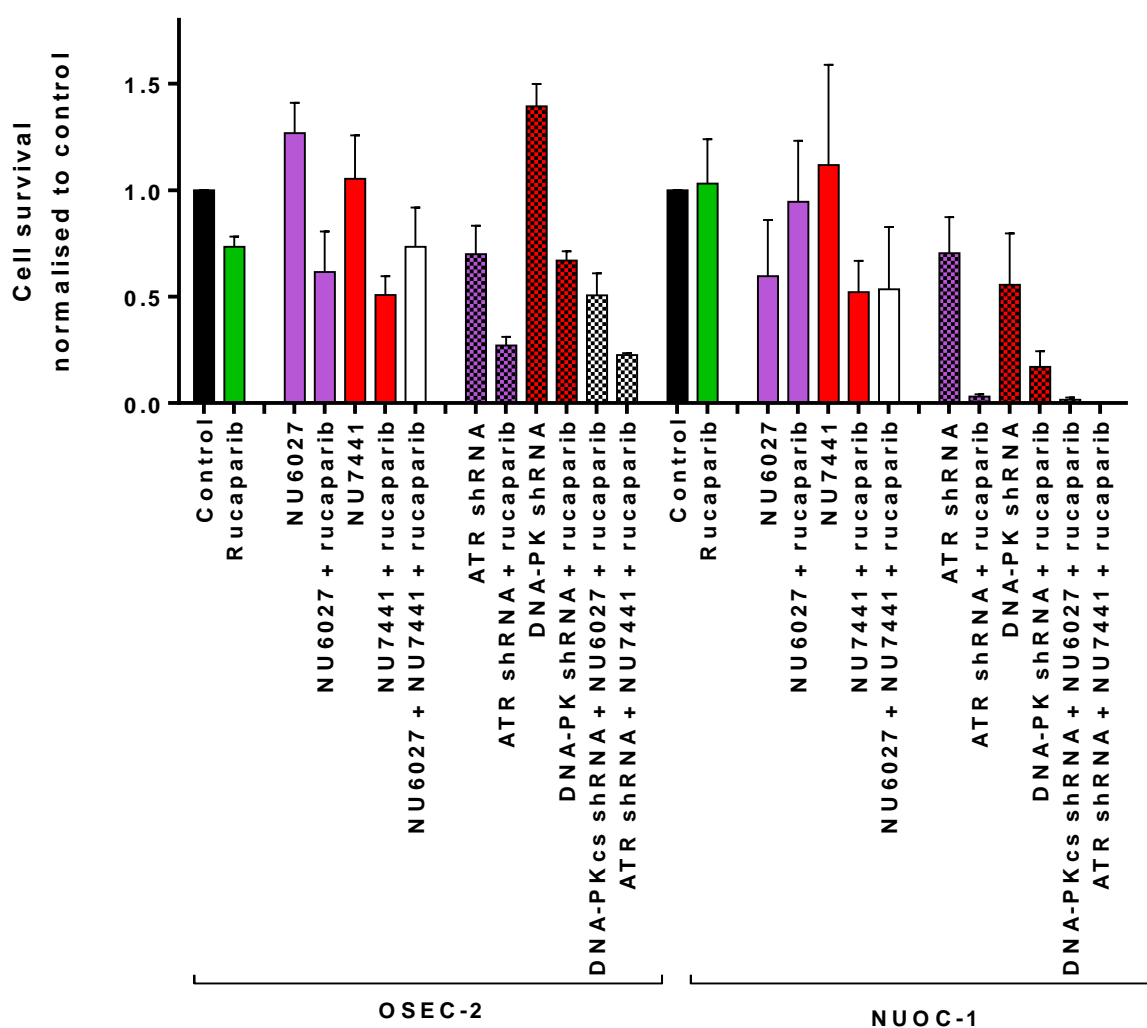


Figure 5-13 The effect of PARPi combined with ATRi and DNA-PKi on cell survival. All results are normalised to appropriate control. OSEC-2 treatments were grown for 14 days and NUOC-1 for 30 days. All treatments were grown for three doubling times. Results are average of three independent experiments with 3 experimental repeats. Error bars are SEM. Statistical comparisons are in appendix 4.

5.3.3.4 The Interaction of PARP Inhibition with ATR and DNA-PK Inhibition on DNA Repair

PARP-1 binds to and is activated by stalled replication forks (Bryant et al., 2009, Sugimura et al., 2008) and is necessary for the accumulation of MRE11 and NBS1 at the site of DSBs (Hegan et al., 2010, Benjamin and Gill, 1980, Haince et al., 2008). The role of PARP-1 in DSBs recognition and repair was assessed by time-course of γ H2AX / RAD51 foci formation and recovery.

Hypothesis: Inhibition of PARP inhibits DNA DSBs recognition and repair via HR

PARP-1 inhibition resulted in a 35 % reduction in γ H2AX foci numbers at 2 hrs (mean 32.6 \pm 7.6 foci / cell in rucaparib treated, compared to 50.5 \pm 4.4 foci / cell in untreated controls, $p = 0.025$) (Figure 5-14). The number of RAD51 foci was lower in PARPi treated cells, but this was not statistically significant.

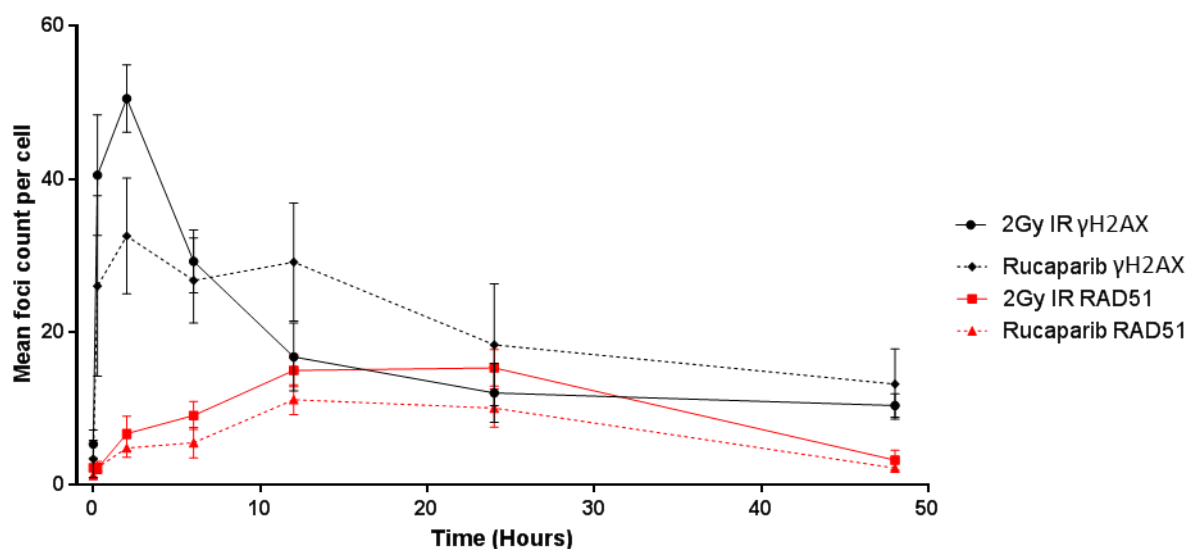


Figure 5-14 DNA DSBs formation and recovery after inhibition of PARP-1.

Assessed by γ H2AX and RAD51 foci formation in OSEC-2 cells. Inhibitors were added 1 hr prior to irradiation. Foci formation was assessed using immunofluorescence after 2Gy IR. Foci numbers were quantified using ImageJ macro. Average number of foci per nucleus are expressed. Black lines – γ H2AX foci, red lines – RAD51 foci. The results are average of three independent experiments. Error bars are SEM.

To test the interaction of PARP-1 with DNA-PK and ATR in DSBs repair, cells were treated with a combination of PARPi, ATRi, and DNA-PKi and γ H2AX and RAD51 foci formation was then assessed (Figure 5-15).

The combination of ATRi and PARPi resulted in a rise in γ H2AX foci, compared to control level at 2 hrs, and whilst a delay in foci recovery was seen, this was not statistically significant. RAD51 foci formation again returned baseline IR levels when both inhibitors were combined.

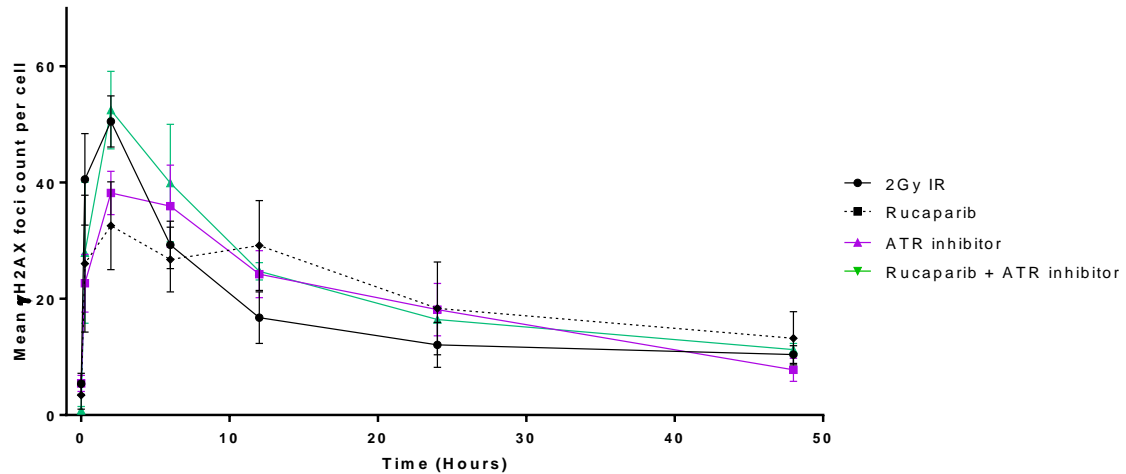
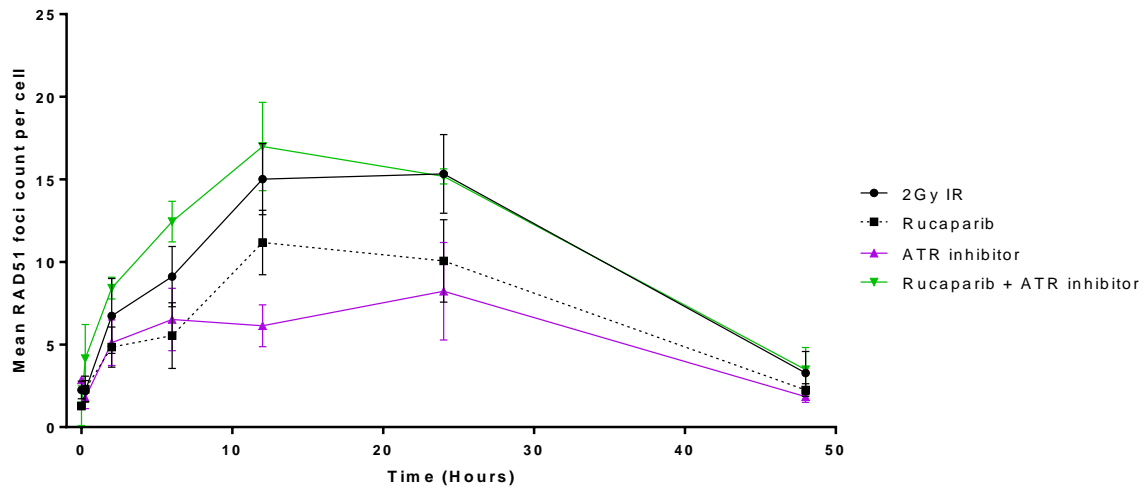
A**B**

Figure 5-15 DNA DSBs formation and recovery after inhibition of PARP-1 and ATR.

*Assessed by γ H2AX and RAD51 foci formation in OSEC-2 cells. Inhibitors were added 1 hr prior to irradiation. Foci formation was assessed using immunofluorescence after 2Gy IR. Foci numbers were quantified using ImageJ macro. Average number of foci per nucleus are expressed. **A.** γ H2AX foci, **B.** RAD51 foci. The results are average of three independent experiments. Error bars are SEM.*

A statistically significant delay in γ H2AX foci recovery was seen after the combination of PARPi and DNA-PKi (Figure 5-16). 59 % more foci, compared to IR controls were found at 8 hrs, 157 % more foci at 12 hrs (Tukeys multiple comparison $p = 0.015$), 222 % at 24 hrs ($p = 0.014$) and 188 % at 48 hrs ($p = 0.044$). The difference between DNA-PKi and the combination of inhibitors was not significant. This finding demonstrates the predominant role of NHEJ in DSBs repair.

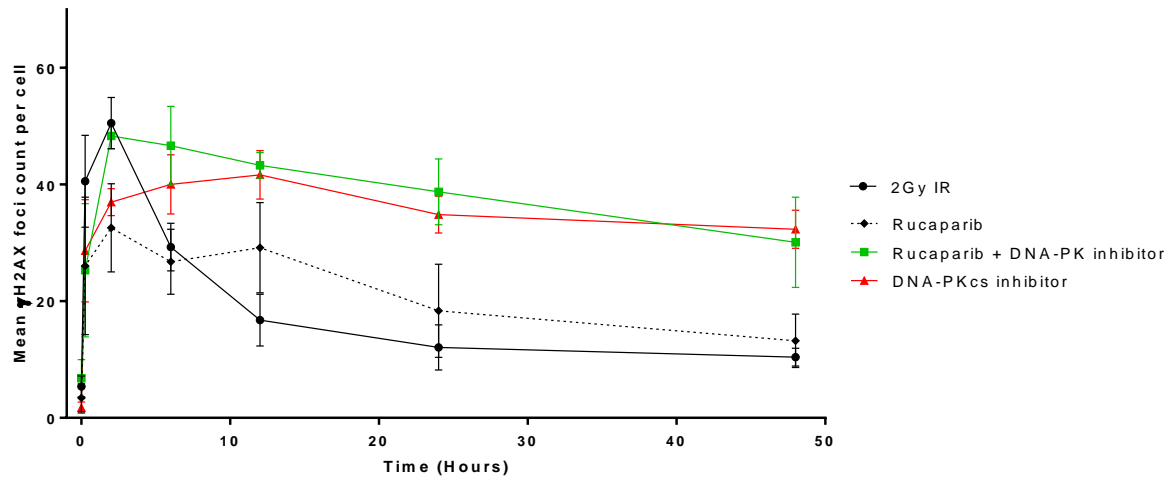
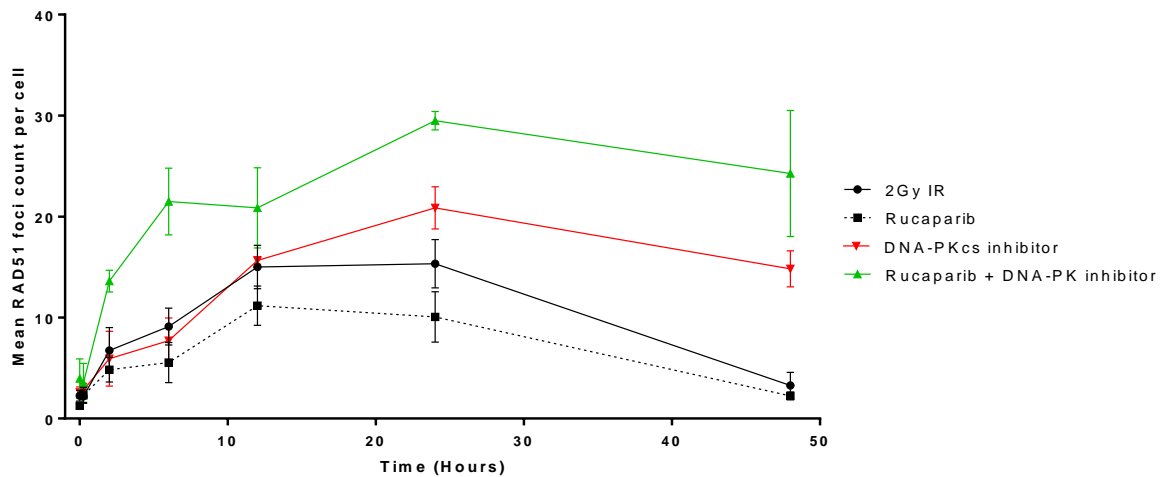
A**B**

Figure 5-16 DNA DSBs formation and recovery after inhibition of PARP-1 and DNA-PK.

*Assessed by γ H2AX and RAD51 foci formation in OSEC-2 cells. Inhibitors were added 1 hr prior to irradiation. Foci formation was assessed using immunofluorescence after 2Gy IR. Foci numbers were quantified using ImageJ macro. Average number of foci per nucleus are expressed. **A.** γ H2AX foci, **B.** RAD51 foci. The results are average of three independent experiments. Error bars are SEM.*

Whilst PARPi resulted in a non-statistically significant reduction in RAD51 foci formation, RAD51 foci formation was significantly increased when the inhibitors were combined above the level for DNA-PKi alone at 6 hrs (133 % higher, $p = 0.0006$, compared to IR; 290 % higher, $p < 0.0001$, compared to rucaparib; and 179 % higher, $p = 0.0001$ compared to DNA-PKi), at 24 hrs (92 % higher, $p < 0.0001$, compared to IR; 180 % higher, $p < 0.0001$, compared to rucaparib; and 41 % higher, $p = 0.026$, compared to DNA-PKi.) and at 48 hrs (643 % higher, $p < 0.0001$, compared to IR; 977 % higher, $p < 0.0001$, compared to rucaparib; and 64 % higher,

$p = 0.013$, compared to DNA-PKi) (Figure 5-16.B). This finding suggests that PARP-1 inhibits HR. This is in contradiction to reports of the PARP-1 protective role of HR (Hochegger et al., 2006). However, it is in agreement with reports that in the absence of PARP-1, HR is increased (Helleday et al., 2005). PARP-1 has been reported to function in the A-EJ pathway, and A-EJ has been reported to compete with HR (Ceccaldi et al., 2015a, Mateos-Gomez et al., 2015). In the absence of NHEJ and A-EJ, HR appears to be increased.

5.3.4 DNA Damage Recognition and Repair in Primary Cultures

To see if the findings from cell line experiments could be extended to primary human tissue the PCO culture collection was used.

Hypothesis: Expression of ATR and DNA-PK and PARP function are variable and independent of each other in PCO cultures

5.3.4.1 Expression of ATR and DNA-PKcs at mRNA Level

The expression of ATR and DNA-PKcs mRNA was assessed by RT-qPCR. A range of expression of both ATR and DNA-PKcs mRNA was found in all the PCO cultures assessed. All PCO cultures expressed a lower level of ATR and DNA-PK mRNA, compared to the OSEC-2 cell line. The mRNA level in OSEC-1 closer resembled the expression in PCO cultures. Therefore, differences are unlikely to be due to higher expression in normal cells as both OSEC-1 and OSEC-2 were derived from normal epithelium. There was a positive correlation between expression of ATR and DNA-PKcs mRNA in PCO cultures (Pearson $r = 0.44$, $p = 0.007$) (Figure 5-17).

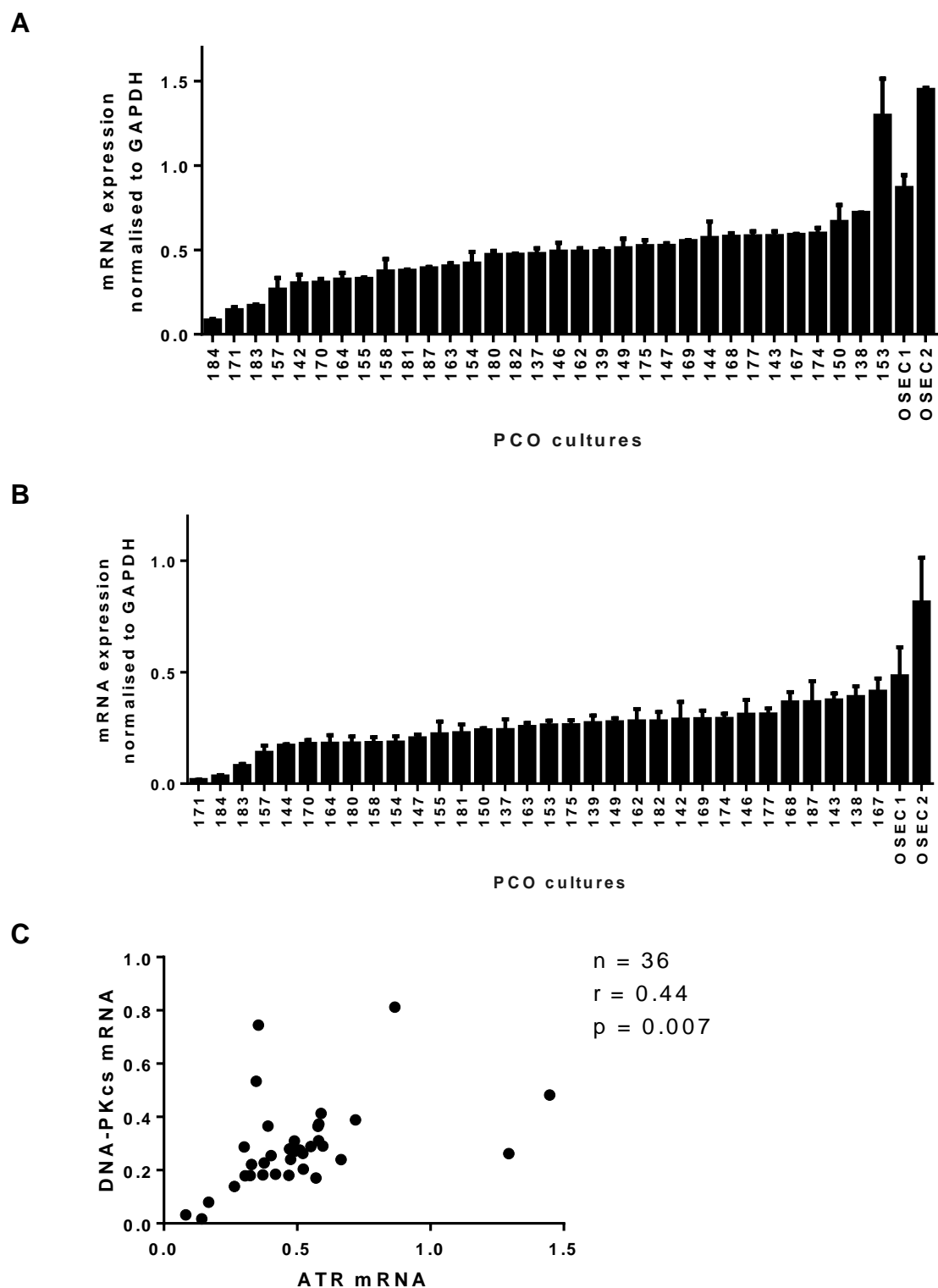


Figure 5-17 ATR and DNA-PKcs mRNA expression and correlation in PCO cultures. Expression was assessed by RT-qPCR and normalised to expression of housekeeper gene GAPDH. **A.** ATR mRNA expression. **B.** DNA-PKcs mRNA expression. **C.** Correlation between ATR and DNA-PKcs mRNA expression.

PARP activity was analysed in a selection of PCO cultures. The experiments were kindly performed by James Murray. A range of PARP activity was found in PCO cultures. There was no correlation with the expression of ATR or DNA-PKcs mRNA levels and PARP-1 activity (Figure 5-18.B-C).

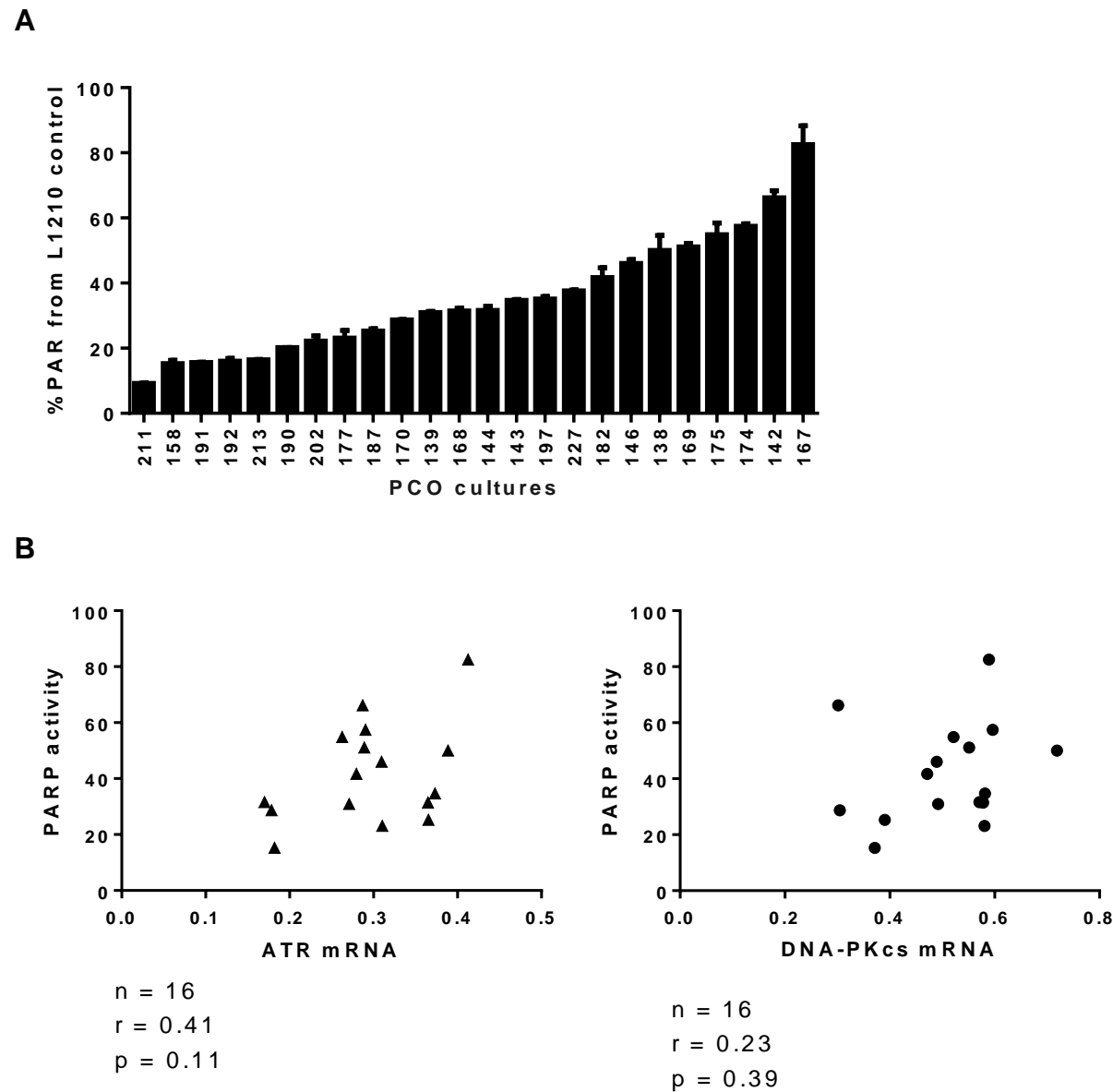


Figure 5-18 PARP activity in PCO cultures correlated with ATR and DNA-PKcs mRNA expression.

A. PAR assay band density results for activated PAR. Activity in each PCO was normalised to activity in control cell line L1210. **B.** correlation between PAR activity and ATR mRNA. **C.** Correlation between PAR activity and DNA-PKcs mRNA.

As previously discussed, the interaction of PARP-1 with HR and NHEJ is still not clear. Therefore the correlation of PARP activity with HR and NHEJ function in PCO

cultures was assessed. No positive correlation between PARP function and either HR or NHEJ was noted (Figure 5-19).

The expression of PARP-1 mRNA was assessed in a RNA Genome expression array (Figure 5-20). Consistent with PARP activity, the expression of PARP-1 mRNA was independent of HR and NHEJ function in PCO cultures. Furthermore, no correlation between PARP-1 mRNA and PAR activity was detected (Figure 5-21).

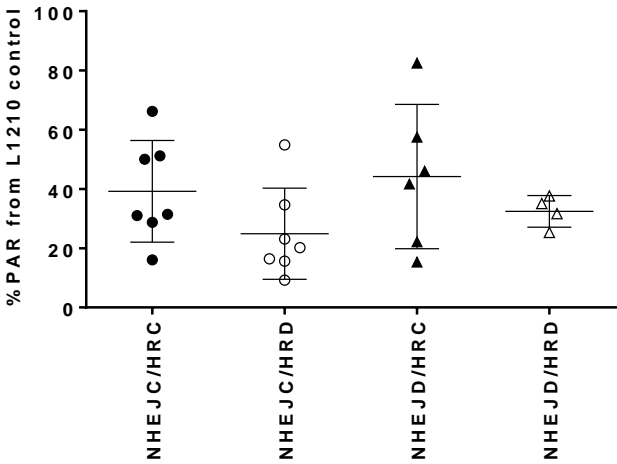


Figure 5-19 PARP-1 activity in PCO cultures shown by NHEJ and HR status.

Stimulated PAR activity expressed as mean PAR pmol/ 10^6 cells was assessed in duplicate and normalised to L1210 control. Error bars are SD.

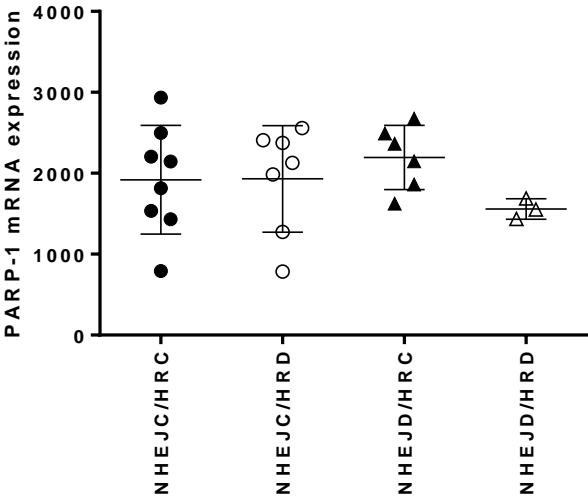


Figure 5-20 PARP-1 expression in PCO cultures shown by HR and NHEJ status. Error bars are SD. Expression was assessed using RNA genome microarray.

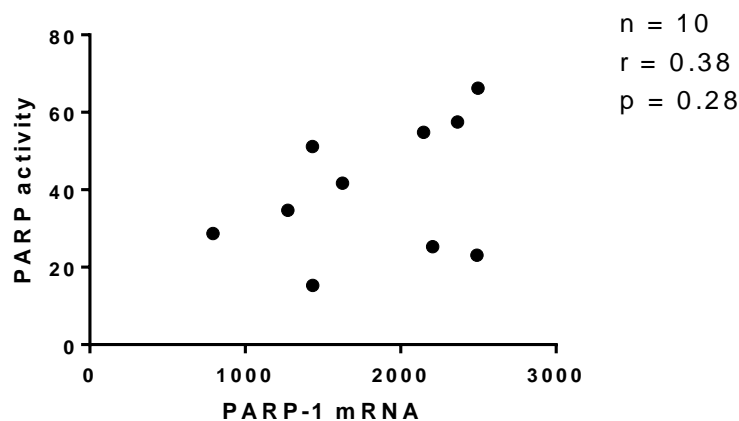


Figure 5-21 Correlation between PAR activity and PARP-1 mRNA.

PAR assay band density results for activated PAR. Activity in each PCO was normalised to activity in control cell line L1210. Expression was assessed using RNA genome microarray.

5.3.4.2 ATR Induced Sensitisation to Rucaparib and Cisplatin

The results from section 5.3.2.5 demonstrating ATRi sensitisation to rucaparib and cisplatin were encouraging. Therefore, in a cohort of PCO cultures the effect of ATRi on sensitivity to rucaparib and cisplatin was assessed (Figure 5-22). The addition of ATRi reduced the mean survival after 10 days treatment with 10 μ M rucaparib from 56 % to 42 % ($p = 0.0065$), and the mean survival after 10 days treatment with 10 μ M cisplatin from 34 % to 22 % ($p = 0.0028$).

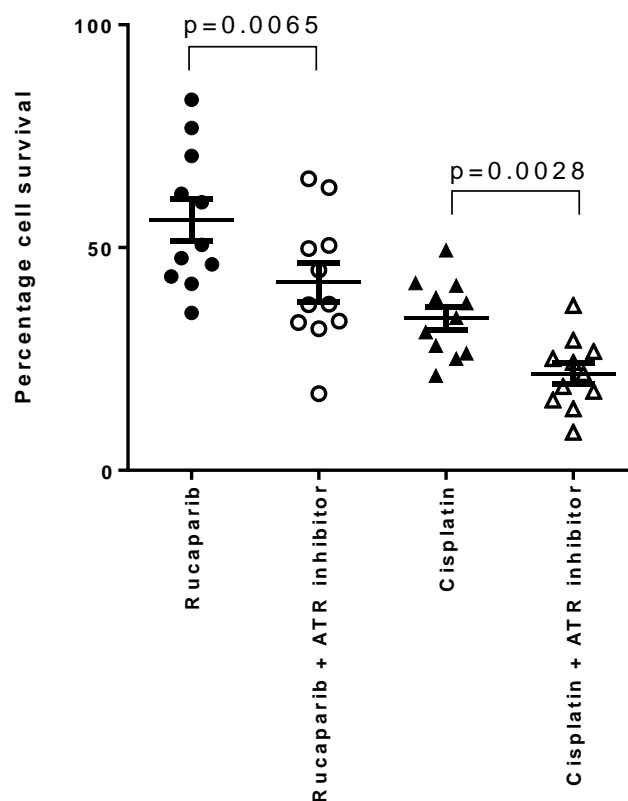


Figure 5-22 ATRi sensitisation of PCO cultures to rucaparib and cisplatin.

Results are percent cell survival after 10 days treatment with 10 μ M rucaparib and 10 μ M cisplatin, +/- 10 μ M NU6027, compared to DMSO control. Error bars are SEM.

5.3.4.3 DSB Activation and Repair in Primary Ovarian Cultures

In the cell line experiments in section 5.3.2.4, inhibition of ATR resulted in a reduced peak of γ H2AX foci formation. Meanwhile, inhibition of DNA-PK reduced the peak of γ H2AX foci formation and delayed recovery. To confirm the results from cell line inhibition experiments, the rate of γ H2AX formation and recovery was assessed in PCO cultures.

Hypothesis: γ H2AX foci formation in HRD cells is lower than in HRC cells. γ H2AX foci formation is lower and recovery delayed in NHEJD, compared to NHEJC cultures

Each culture was irradiated at 2Gy and cover slips were fixed at the following time points: pre-IR, 10 min, 1 hr, 2 hrs, 4 hrs, 12 hrs, 24 hrs and 48 hrs.

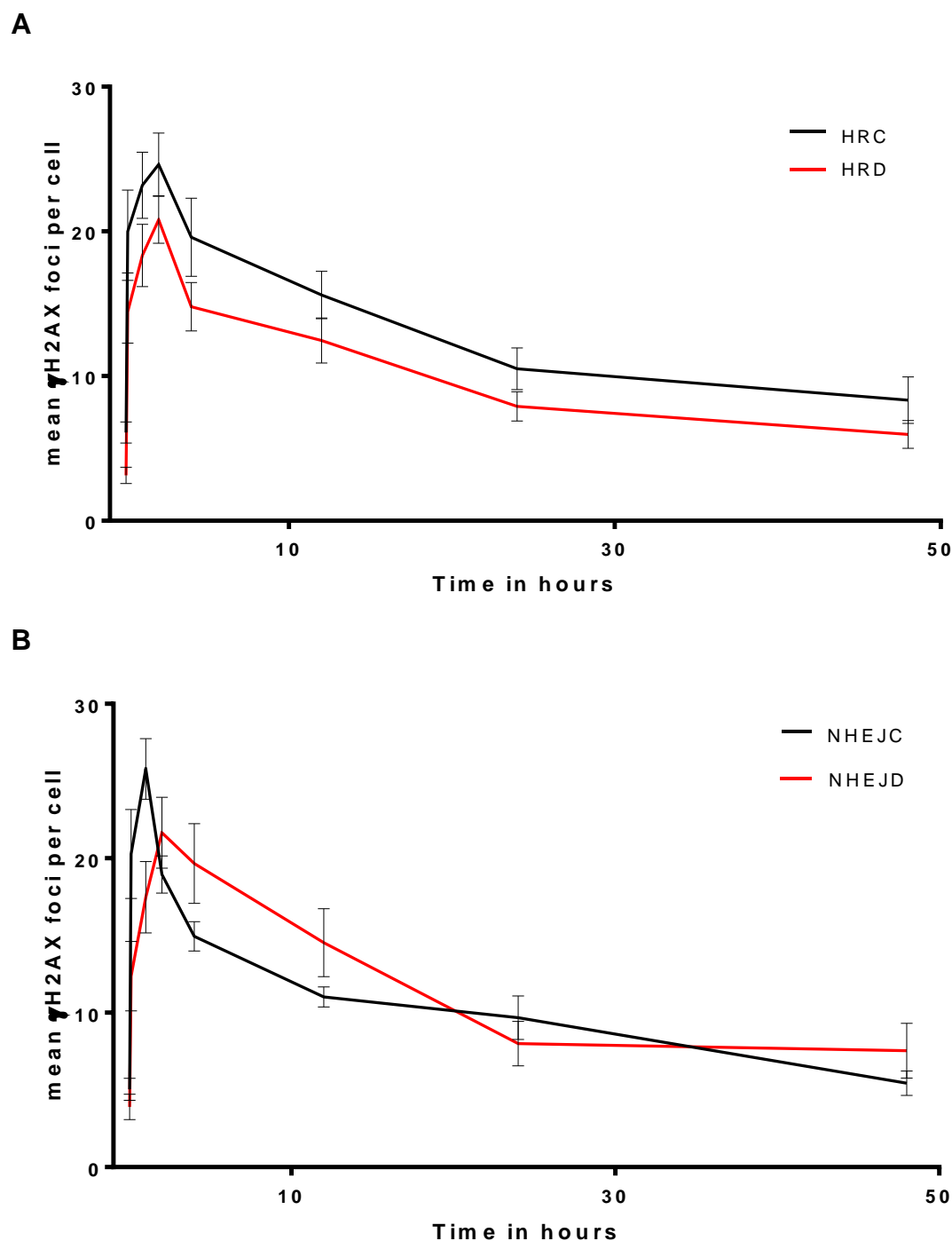


Figure 5-23 DNA DSBs formation and recovery in PCO cultures.

*Assessed by γ H2AX foci formation after 2Gy IR using IF in **A**. HRC compared to HRD cultures, and **B**. NHEJC compared to NHEJD cultures. Foci numbers were quantified using ImageJ macro. Average number of foci per nucleus are expressed. The results are average of three independent experiments. Error bars are SEM.*

Confirming the results of the cell line experiments, the HRD cultures had a lower peak of γ H2AX foci. However, the difference was not statistically significant (Figure 5-23.A). NHEJD cultures had a delayed peak of γ H2AX foci (Figure 5-23.B).

Significantly lower number of foci formed immediately after irradiation (mean 20.3 +/- 2.9 foci in NHEJC, compared to mean 12.4 +/- 2.2 foci in NHEJD, $p = 0.029$) and at 1 hr (mean 25.8 +/- 1.9 foci in NHEJC, compared to mean 17.5 +/- 2.3 foci in NHEJD, $p = 0.01$). A slower recovery of γ H2AX foci was also observed in NHEJD PCO cultures (Figure 5-23.B).

In PCO cultures RAD51 foci formation was assessed at 24 hrs only. The mean increase in RAD51 foci above controls was significantly higher at 5.45 fold in HRC compared to 1.28 fold HRD cultures ($p < 0.0001$) (Figure 5-24.A). The increase in RAD51 foci was also higher in NHEJD cultures compared to NHEJC cultures ($p = 0.03$). The increase in HR in the absence of DNA-PK is consistent with the inhibition results in section 5.3.2.4, and previous studies (Cornell et al., 2015) suggesting that when NHEJ is impaired there is a shift to HR.

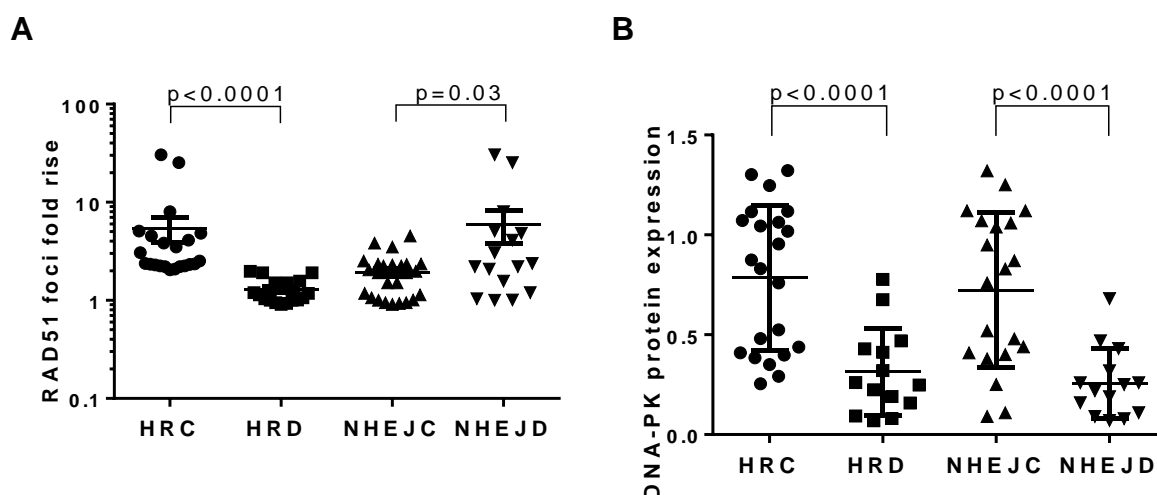


Figure 5-24 RAD51 foci fold rise and DNA-PK expression shown by HR or NHEJ status.

A. RAD51 foci fold rise above controls in primary ovarian cancer cultures divided by HR or NHEJ status. RAD51 foci were assessed as mean foci count per cell in samples after 24 hrs of 10 μ M rucaparib and 2 Gy IR treatment, compared to untreated controls. Foci were counted across 3 fields of view for each sample counting >50 cells in each sample. $N = 40$. Error bars are SEM. **B.** DNA-PKcs protein expression in primary ovarian cancer cultures shown by HR or NHEJ status. DNA-PK protein expression was assessed by western blotting and normalised to GAPDH house keeper gene. $N = 36$. Error bars are SEM.

DNA-PKcs expression was 64 % higher in NHEJC (0.72 of GAPDH expression, 95 % CI = 0.5 - 0.9), compared to NHEJD cultures (0.26, 95 % CI = 0.2 - 0.4, $p < 0.0001$) (Figure 5-24.B). Interestingly, DNA-PKcs expression was also 59 % higher in HRC

cells (0.78 of GAPDH expression, 95 % CI = 0.6-0.9), compared to HRD cells (0.32, 95 % CI = 0.2-0.4, $p < 0.0001$) (Figure 5-24.B).

5.3.4.4 Correlation between γ H2AX foci recovery and sensitivity to rucaparib and cisplatin

To validate the observation that γ H2AX foci formation and recovery differs depending on HR and NHEJ function, the association of γ H2AX foci formation and recovery with rucaparib and cisplatin sensitivity was assessed (Figure 5-25).

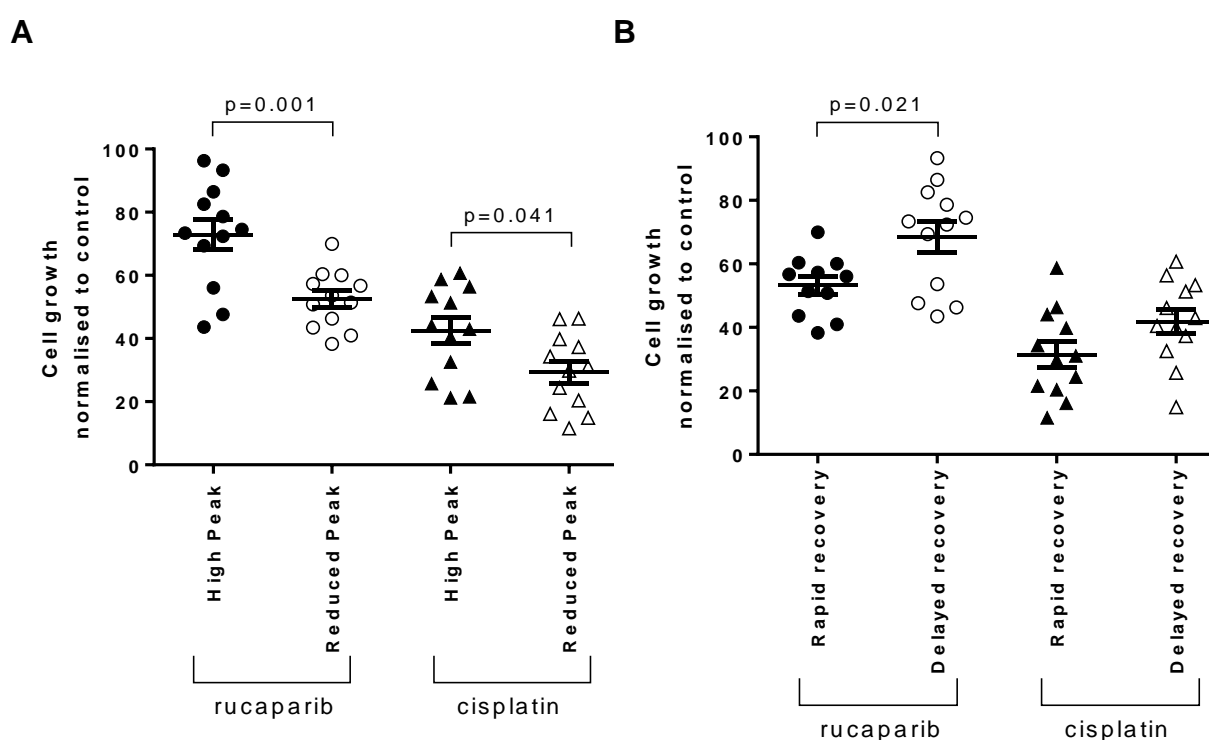


Figure 5-25 The association of γ H2AX foci formation and recovery with rucaparib and cisplatin sensitivity.

A. PCO cultures were divided into two groups based on median foci numbers at 2 hrs. Sensitivity was assessed by SRB assay after 10 days growth in 10 μ M rucaparib and 10 μ M cisplatin treatment, compared to DMSO treated controls. **B.** PCO cultures were divided into two groups based on median foci numbers at 4 hrs. Sensitivity was assessed by SRB assay after 10 days growth in 10 μ M rucaparib and 10 μ M cisplatin treatment, compared to DMSO treated controls. One way Anova with Sidak multiple analysis correction was performed. Error bars are SEM.

Cultures with a reduced peak in γ H2AX foci at 2 hrs were found to be more sensitive to rucaparib ($p = 0.001$) and cisplatin ($p = 0.04$). Cultures which had a delay in γ H2AX foci recovery, with above median γ H2AX foci numbers at 4 hrs were found to be less sensitive to rucaparib ($p = 0.021$) but not cisplatin. These cultures were predicted to be NHEJD. Therefore the results are consistent with sensitivity

association found in chapter 4. The results suggest that sensitivity to rucaparib and cisplatin could be predicted by a single test assessing overall DSBs repair in PCO cultures.

5.4 Summary of Chapter

In this study HR and NHEJ pathway interaction was assessed using pharmacological inhibition and shRNA knockdown models of ATR and DNA-PK in OSEC-2 (cell line derived from normal epithelium) and NUOC-1 (cell line derived from endometrioid / clear cell carcinoma).

Both ATR and DNA-PK inhibition was found to be cytostatic and causing G1 and G2 arrest, respectively. Inhibition of DNA-PK resulted in reduced recognition of DNA DSBs and delay in repair. It was also found to increase HR. Inhibition of ATR resulted in reduced DSBs recognition and reduction in HR, but not in the overall rate of DSBs repair. Combination of the two inhibitors resulted in continued HR, suggesting an alternative activation. Previously reported radio-sensitisation induced by DNA-PKi, and sensitisation to rucaparib and cisplatin by ATRi were confirmed. The sensitisation was specific to the NUOC-1 cell line, and was not reproducible in OSEC-2 cells, thus suggesting a cancer cell specificity. ATRi sensitisation to rucaparib and cisplatin was confirmed in PCO cultures.

ATR and DNA-PK interaction with PARP-1 was assessed by the addition of a nontoxic dose of rucaparib to ATR inhibited and DNA-PKcs inhibited models. The previously reported role for PARP-1 in DSB recognition was confirmed. Combination of PARPi and DNA-PKi resulted in a delay in DSBs repair and a synergistic increase in HR. The combined inhibition of ATR and PARP also caused a reduction in DSB recognition, but an increase in HR, overcoming the inhibition of HR by ATRi.

The observations were validated by assessing the interaction of ATR and DNA-PKc in PCO cultures. In PCO cultures a positive correlation was found between ATR and DNA-PK mRNA expression. PARP function was independent of HR and NHEJ. Reduced DSBs recognition in HRD, and reduced recognition and delayed repair in NHEJD cells was observed. Rucaparib and cisplatin sensitivity correlated positively with a high γ H2AX foci peak at 2 hrs, and rucaparib sensitivity correlated with a rapid recovery of γ H2AX foci. These results suggest that rucaparib and cisplatin sensitivity could be predicted by a single test.

5.5 Discussion

In this study interaction of NHEJ, HR and PARP-1 was assessed by using cell line and PCO culture models.

5.5.1 Protein Inhibition and Knockdown may not be Directly Comparable

The level of inhibition achieved using inhibitors was higher than that achieved using knockdown. Whilst both HR and NHEJ function were reduced in both knockdown and inhibited cells, some function of both pathways remained. It was not ascertained if a critical level of either protein exists in the cells. Thus, some of the differences observed may be due to different levels of inhibition of each protein. Furthermore, the presence of inactive protein rather than absence of the protein achieved in knockdown models may have a dominant negative effect. A further important point to consider is that NU6027 is also a CDK2 inhibitor. Therefore some of the observed effects may be CDK2 driven. Confirmation of these findings in a larger cohort of cell lines, and by using different inhibitors for ATR and DNA-PK is required.

5.5.2 ATR and DNA-PK Inhibition Effects are Cell Line Specific

The most important observation noted was that throughout the study the loss of ATR or DNA-PKcs had a significantly more pronounced effect in NUOC-1 than in OSEC-2 cells, suggesting that NUOC-1 cells are more reliant on the DDR mechanism than OSEC-2 cells. Cancer cells often contain dysregulation of their cell cycle control (Massague, 2004), have high levels of replicative stress, stalled replication forks and DSBs, therefore, inhibition of DDR is thought to have a significant effect in tumour, but not normal cells (Wiseman and Halliwell, 1996), thereby limiting toxicity to the patient.

However, these observations may also be due to differences seen in the level of inhibition of both ATR and DNA-PK between the two cell lines and baseline levels of these proteins. Knockdown achieved by shRNA was different between the two cell lines, DNA-PK was only 44 % knockdown in OSEC-2, compared to 73 % in the NUOC-1 cell line. This is likely to explain the lack of radio-sensitivity observed in the OSEC-2 cell line after DNA-PK shRNA knockdown, despite the documented role of DNA-PK in radio-sensitivity in the literature, and the observation with NU7441 inhibitor. The converse was seen in ATR knockdown where >90 % knockdown was

achieved in OSEC-2, but only 78 % knockdown in NUOC-1 cells. In this case, despite a higher level of knockdown OSEC-2 cells were not sensitised to rucaparib or cisplatin by the absence of ATR. This was consistent with the NU6027 inhibitor, and is therefore, likely to represent a true difference between reliance of NUOC-1 and OSEC-2 cells on ATR.

5.5.3 ATR and DNA-PK Inhibition are Cytostatic

Both ATR and DNA-PK inhibition was found to be cytostatic, but not cytotoxic, as assessed by SRB and Clonogenics assays. Cytostatic effects are likely to be due to cell cycle arrest induced by the lack of both proteins. This is in agreement with multiple studies, that inactivation of ATR causes a G2/M checkpoint failure and subsequent G1 arrest (Brown and Baltimore, 2003, Peasland et al., 2011). Conversely, G2 arrest follows DNA-PK inhibition, as DNA-PK is thought to phosphorylate p53, which mediates G1 arrest (Kachnic et al., 1999). The cytotoxic effects of ATRi have, however, been described in the presence of BER defects (Peasland et al., 2011, Sultana et al., 2013, Mohni et al., 2014) in cells with oncogene-activation (Gilad et al., 2010) and cyclin E over-expression (Toledo et al., 2011). NUOC-1 cells were found to be BER defective, as described in chapter 3, therefore, would be expected to be sensitive to ATR inhibition. These results are contradictory and demand further investigation.

The inhibition of both ATR and DNA-PK was found to be cytotoxic in NUOC-1 but not OSEC-2 cells, and underlies the importance of DDR mechanisms in cancer cell survival. This finding has also been observed with the combination of NU7441 and VE-821 ATRi (Middleton et al., 2015).

5.5.4 DNA-PK is required for the Rapid Phase Whilst ATR in Slow Phase of DNA DSBs Repair

The role of ATR and DNA-PKs in DSB repair is well described. In this study the interaction between the two proteins in DSB repair was assessed. Inhibition of either ATR or DNA-PK resulted in lower mean γ H2AX foci numbers. The combination further impaired focus formation, reflecting the phosphorylation of H2AX by both DNA-PK and ATR. The recovery of γ H2AX foci was significantly delayed in DNA-PK inhibited cells, but the speed of recovery was not significantly affected by ATRi.

When repairing DSBs, HR is more accurate than NHEJ, because it uses an undamaged sister chromatid as a template for repair, but it is therefore, restricted to the S-G2 phases of the cell cycle (San Filippo et al., 2008). HR is a more complex form of repair and takes more than 7 hrs to complete, whereas, NHEJ can be completed in 30 min (Mao et al., 2008). Therefore, the effect of inhibition of DNA-PK, and thus NHEJ, has a pronounced effect on the rapid phase of γ H2AX foci decline; whilst ATR, and thus HR inhibition, does not affect this phase of γ H2AX foci decline.

The combination of ATRi and DNA-PKi resulted in a further reduction in mean γ H2AX foci and delay in the timing of the peak foci numbers. Curiously, inhibition of both ATR and DNA-PK did not appear to affect the rate of disappearance of γ H2AX foci, suggesting other mechanisms of repair may be activated under these circumstances. To confirm this, physiological measures of DNA breakage and repair, e.g. Comet assay, would be needed.

As the rapid phase of repair was completed, the emergence of RAD51 foci was observed, which accumulated during the slow phase of γ H2AX foci resolution. This demonstrates the shift from the faster NHEJ to the slower HR repair. The later accumulation of RAD51 foci could also reflect IR induced single-stranded lesions encountering the replication fork. Experiments in synchronised cells would need to be performed to assess this finding.

Assessment of RAD51 foci noted opposing effects of ATR and DNA-PK. As expected, the absence of DNA-PK resulted in an increase in RAD51 foci, and thus, HR, despite DNA-PK having no direct role in HR. This data suggests that when NHEJ is inhibited there is a shunting of DSB repair to HR, which has been observed previously (Allen et al., 2003). This is consistent with NHEJ and HR competing for DSB repair (Allen et al., 2003, Chapman et al., 2012b). Potential crosstalk between HR and NHEJ, mediated by DNA-PK, has been investigated, and certain specific phosphorylation sites on DNA-PKcs which promote HR whilst inhibiting NHEJ have been identified (Convery et al., 2005, Neal et al., 2011).

As previously demonstrated, inhibition of ATR, essential in HR, resulted in a reduction of RAD51 foci (Peasland et al., 2011). Inhibition of RAD51 by the ATRi was lower when combined with the DNA-PKi. This observation has been previously described in isogenic cell lines (Middleton et al., 2015). This finding suggests that that DNA-PKcs suppresses HR and in the absence of both ATR and DNA-PK, HR

continues and must be reliant on another mechanism of activation. The primary activation of HR in this setting is likely to be ATM. ATM signals in response to chromosomal DNA damage by phosphorylating BRCA1, NBS1 and RAD51 (Cortez et al., 1999, Gatei et al., 2000). To validate these findings the effect of ATM inhibition alone, and in combination with ATR and DNA-PK inhibition needs to be determined. Further investigations could be to use comet assays to assess overall DSBs repair, and to repeat these experiments in other cell lines.

5.5.5 ATR Inhibition Sensitises to Rucaparib and Cisplatin whilst DNA-PK Inhibition to Irradiation

Inhibition of DNA-PK has been consistently shown to cause radio-sensitisation in a number of different studies (Price and Youmell, 1996, Rosenzweig et al., 1997, Boulton et al., 2000, Kashishian et al., 2003, Shinohara et al., 2005, Tavecchio et al., 2012, Zhao et al., 2006). This has been confirmed in this study.

The HRD phenotype has been demonstrated to result in cisplatin and rucaparib sensitivity (Mukhopadhyay et al., 2012, Mukhopadhyay et al., 2010, Li et al., 2016). This has been confirmed by the inhibition of ATR in the NUOC-1 cell line, and in PCO cultures. In clinical terms, the effect of ATRi and DNA-PKi combination suggests that the inhibition of ATR on the background of functional NHEJ, would result in a HRD phenotype. Therefore, ATRi may be an important chemo sensitiser in ovarian cancer. An ongoing trial investigating ATRi as a single agent, and in combination with platinum-based chemotherapy (clinicaltrials.gov identifier: NCT02157792), is likely to provide important knowledge in this field. However, the mechanisms of HR activation, independent of ATR, need to be assessed.

Importantly, sensitisation was achieved in NUOC-1 cells, but not OSEC-2 cells. These findings are important on 2 counts. Firstly, this provides evidence for the use of ATRi to sensitise HRC cancers to platinum based chemotherapy and PARPi. Secondly, this data suggests that the intrinsic molecular defects in cancer cells combined with DDR inhibition causes chemo- and radio-sensitisation, supporting the concept of cancer-cell specific synthetic lethality. It has to be noted that the OSEC-2 cell line has been altered, and is functionally p53 mutant, therefore, its function cannot be directly extrapolated to represent normal ovarian epithelium. However, it is the closest model of normal ovarian epithelium available in laboratory settings and

sets a useful basis for hypothesis generating. This observation does need to be validated by *in vivo* studies.

The failure of paclitaxel sensitisation with the DSB repair pathway inhibition is unsurprising, given its chemotherapeutic effects do not come through elicitation of DNA damage. However, this finding is contradictory to reported paclitaxel sensitisation by DNA-PK inhibition in multidrug resistant ovarian cancer cell lines (Mould et al., 2014), and needs to be evaluated in other cell line models.

5.5.6 Interaction of ATR and DNA-PK with PARP-1

The overall aim of this project was to improve the understanding of the interaction between NHEJ, HR and PARP-1. In the second part of this study the interaction between ATR and PARP-1, and DNA-PK and PARP-1 was analysed. In terms of growth, the combination of 1 μ M rucaparib with either 1 μ M NU7441 or 10 μ M NU6027, did not produce additional growth inhibition in either cell line. The addition of 1 μ M of rucaparib to ATR and DNA-PK knockdown in NUOC-1 cells, however, resulted in significant growth inhibition compared to each knockdown alone. The result is cell line specific as this effect was not observed in OSEC-2 cells. The result is also in contradiction to resistance induced by NU7441 inhibition in PCO cultures, as described in chapter 4. PARP-1 inhibition has been reported to lead to the activation of DNA-PK in BRCA2-deficient cells, but not in cells with wild-type BRCA2 (Patel et al., 2011). The interaction between DNA-PK and PARP-1 may therefore be cell specific, and dependent on other cell defects. An alternative explanation may be that the effect of experimental knockdown of DNA-PK is different to that of the defective NHEJ pathway. These findings need to be further evaluated in other cell line models.

5.5.7 PARP-1 Affects DNA DSBs Recognition and Selection of Repair Pathway

The role for PARP-1 in DNA DSBs repair has been previously described. PARP-1 binds to and is activated by stalled replication forks (Bryant et al., 2009, Sugimura et al., 2008) and is necessary for the accumulation of MRE11 and NBS1 at the site of DSBs (Hegan et al., 2010, Benjamin and Gill, 1980, Haince et al., 2008). Inhibition of PARP-1 has been shown to retard the rejoining of IR-induced DNA DSBs (Mitchell et al., 2009b, Boulton et al., 1999). In this study 1 μ M rucaparib significantly reduced the peak number of γ H2AX foci and delayed the recovery of γ H2AX. This supports the

essential role for PARP-1 in DDR. The effect on RAD51 foci was not significant, suggesting that PARP inhibition does not affect HR directly. This is in contrast to studies reporting PARP-1 to have a protective role in HR by suppressing access of NHEJ to DSBs (Hochegger et al., 2006, Saberi et al., 2007).

When combined with ATR inhibition, both the mean number of γ H2AX and RAD51 foci at each time point resembled that of the IR control, and not each inhibitor alone. This supports previous reports that the role of PARP-1 in DSB repair is in the A-EJ pathway. The function of PARP-1 in the A-EJ has been shown by both *in vitro* and *in vivo* studies (Audebert et al., 2006, Lu et al., 2006, Audebert et al., 2008). A-EJ has been described to compete with HR, as well as act in the absence of HR (Nik-Zainal et al., 2012, Ceccaldi et al., 2015a, Mateos-Gomez et al., 2015). Therefore, PARP inhibition may re-establish HR by inhibiting the A-EJ pathway. This may be the possible explanation for the observed resistance of NHEJD/HRD PCO cultures to rucaparib in chapter 4.

The combination of rucaparib with DNA-PK inhibition resulted in a lower peak of γ H2AX foci and slow recovery, which is similar to DNA-PKi alone. This finding agrees with previous reports, which suggest that PARP-1 and DNA-PK are epistatic (Mitchell et al., 2009a). The combination of DNA-PKi and PARPi resulted in a further increase in RAD51 foci formation, again suggesting that PARPi increases HR. This finding is consistent with that of ATR and PARPi combination, however, it is in contradiction to the finding of sensitisation of ATR inhibitor to rucaparib treatment. These findings therefore, need to be further explored.

5.5.8 In PCO Cultures ATR and DNA-PK Expression Correlate but are Independent of PARP-1

To determine the clinical relevance of the cell line findings, the interaction of ATR and DNA-PK in PCO cultures was assessed. Whilst the expression of each protein varied in the unselected cohort of PCO cultures, a positive correlation between ATR and DNA-PK mRNA levels was found. This finding suggests that the expression of ATR and DNA-PKs may be concomitantly regulated in certain tumours. This has been previously noted in glioblastoma (Middleton et al., 2015). The correlation was suggested to be due to DNA-PKs and ATR being held in a complex with cMYC and CHK1. Discordance between mRNA and protein levels were seen in chapter 4. A

comparison of the expression of ATR and DNA-PK protein is required for this finding to be validated.

There was no correlation observed between PARP activity and either ATR or DNA-PK mRNA levels. Furthermore, the assessment PARP activity by HR and NHEJ function confirms the independence of PARP activity from the HR and NHEJ functions. This result is supported by the finding of no correlation of PARP-1 mRNA expression with either the HR or NHEJ status of PCO cultures. These findings are in contrast to previous studies describing the interaction of PARP-1 with HR, and need to be explored further.

5.5.9 DNA DSBs Recognition and Repair is Inhibited in NHEJ and HRD PCO Cultures

Confirming the findings of inhibition experiments, a lower peak of γ H2AX in both the NHEJD and HRD PCO cultures. Lower peak of γ H2AX foci was associated with increased sensitivity to both rucaparib and cisplatin. Also, as seen in the inhibition experiments, NHEJD cultures were found to have a delay in γ H2AX foci recovery, whilst the recovery rate was not significantly different between HRD and HRC cells. Confirming association of NHEJD with rucaparib resistance, PCO cultures with delayed recovery of γ H2AX foci were less sensitive to rucaparib. These findings suggest that HR and NHEJ function can be predicted by the assessment of γ H2AX foci formation and recovery. Whilst further development is required, a single assay for DNA DSBs formation and repair may be a potential tool for patient selection for treatment.

RAD51 foci time line experiments were not performed in PCO cultures, however, the RAD51 foci fold increase at 24 hrs was assessed as part of the HR assay. Similarly to the inhibition experiments NHEJD PCO cultures also had a mean RAD51 foci which was higher than NHEJC cultures. Therefore, NHEJD may result in an increase in HR, however, this may be dependent on the type of defect resulting in HRD. The effect of DNA-PK inhibition in HRD cells due to different mutations is assessed in the next chapter.

5.6 Future Work

In this study, inhibitors and shRNA knockdown were used to assess the roles of ATR and DNA-PK. Inhibitors are known to have off target effects, and therefore, validation with knockdown supports the findings. To further strengthen these findings, validation using isogenic cell lines is important undertake in the future.

The assessment of DNA repair by different methods is also required. To further develop on the possibility to assess HR and NHEJ by a single method, assays such as, single point comet assays, need to be explored. The benefit of this assay over a functional NHEJ / HR assay is that it does not require growing cells. Therefore, frozen cells could be used. Use of frozen cells is a more likely to translated into clinical practice compared to cell culture.

Although growth inhibition data demonstrated that ATRi significantly sensitised cells to cisplatin, and that rucaparib and DNA-PK inhibition potentiated radiation sensitivity, this needs to be confirmed in an *in vivo* setting. An *in vivo* study design could involve xenograft studies to confirm the enhanced efficacy of the combinations, and to confirm that they are specific to cancer cells by assessing the toxicity of the combinations. Furthermore, the toxicity of the combinations of inhibitors with chemotherapy agents could be evaluated. If this study yielded positive findings, a human explant xenograft study would then be undertaken to further evaluate the role of ATR and DNA-PK inhibitors.

CHAPTER 6 ASSESSMENT OF THE ROLE OF DNA REPAIR IN RESISTANCE TO RUCAPARIB AND CISPLATIN

6.1 Introduction

The current standard treatment of ovarian cancer, in both early and advanced stages, consists of cytoreductive surgery followed by chemotherapy, based on carboplatin with or without paclitaxel (Bristow et al., 2002, Elattar et al., 2011, Al Rawahi et al., 2013). The initial response rate is high (70 - 80 %), but the majority of patients with advanced disease relapse within two years. Recurrent ovarian cancer is not curable, due to the development of chemo-resistance (du Bois et al., 2005). Platinum-resistant disease is also characterised by resistance to other cytotoxic agents (Ledermann and Kristeleit, 2010). Studies have confirmed a correlation between platinum sensitivity and PARPi response, with higher response rates in platinum sensitive compared with platinum-resistant and refractory patients (Fong et al., 2010). However, responses in the platinum resistant and refractory cases provide evidence for different mechanisms of resistance and suggest incomplete crossover of sensitivity. The mechanisms for cisplatin and rucaparib resistance were investigated in this study.

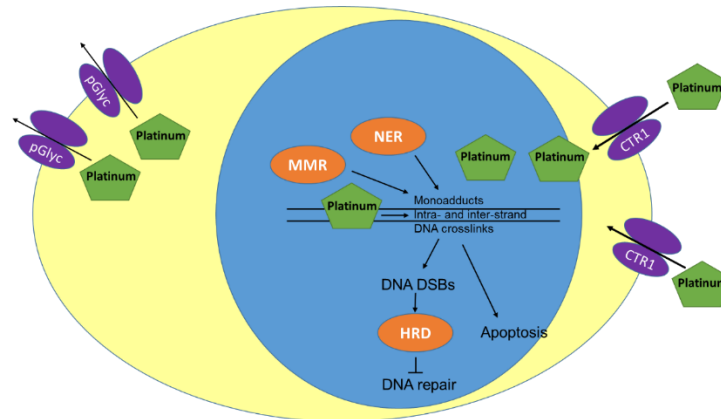
6.1.1 *Mechanism of Platinum Chemotherapy*

Platinum agents are transported into the cell by passive diffusion or mediated by a copper transporter (CTR1). Once inside the cell, cisplatin / carboplatin are activated and bind DNA (Jamieson and Lippard, 1999), forming monoadducts. Intra- and inter-strand DNA crosslinks are subsequently formed causing conformational DNA changes, impairing replication and DNA synthesis (Siddik, 2003). Platinum-induced DNA lesions attract DNA binding proteins which either signal for apoptosis or initiate DNA repair (Tapia, 2012).

6.1.2 *Mechanisms of Platinum Resistance*

Whilst platinum resistance is still not completely understood, three main mechanisms have been documented. These include reduced intracellular accumulation of platinum, intracellular inactivation of platinum, and increased DNA repair. Each mechanism will be discussed in turn and summarised in Figure 6-1.

Platinum sensitive cell



Platinum resistant cell

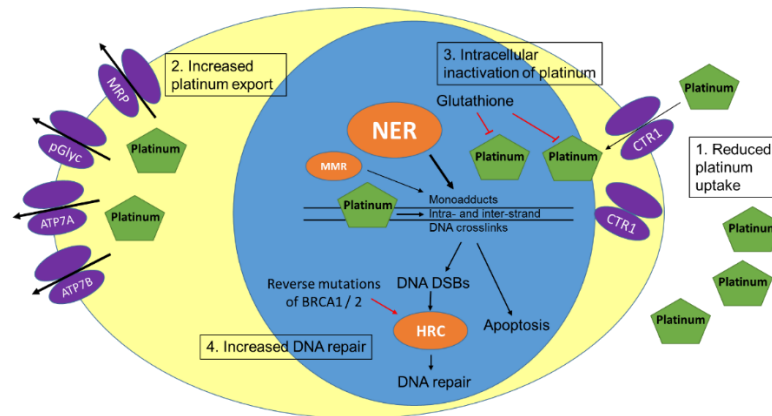


Figure 6-1 Schematic of the mechanisms contributing to platinum resistance.

6.1.2.1 Reduced Intracellular Drug Accumulation

Decreased cellular uptake of cisplatin by resistant cells is one of the major mechanisms of resistance described *in vitro*. This is either by reduced influx mediated by internalisation of the CTR1 copper transporter (Holzer et al., 2004), or by increased efflux, with exporters ATP7A, ATP7B, MRP-related transport proteins and P-glycoprotein (P-Glyc) (Samimi et al., 2004, Korita et al., 2010, Hoffmann et al., 2010).

6.1.2.2 Intracellular Cisplatin Inactivation

Glutathione (GSH) contributes to the detoxification and inactivation of many cellular toxins, including cisplatin and its analogues. GSH has been associated with cisplatin resistance in ovarian, cervical and lung cancer cell lines (Li et al., 2009b).

6.1.2.3 Increased DNA Repair

The NER pathway is predominantly responsible for repairing intra-strand platinum-DNA adducts in cellular DNA, and increased NER has been correlated with cisplatin resistance (Dabholkar et al., 1994). Loss of DNA MMR has also been linked to platinum resistance (Helleman et al., 2006).

During DNA replication inter-strand DNA cross-linking causes DNA DSBs. These DSBs are repaired by HR. HRD has been linked to increased platinum sensitivity and concomitant survival benefits (Mukhopadhyay et al., 2012). However, *BRCA1/2* mutated cancers also develop platinum resistance, which has been suggested to be mediated by secondary intragenic mutations in *BRCA1/2*. Secondary mutations can reverse stop codons, usually resulting in an open reading frame, thereby restoring HR function (Sakai et al., 2008, Swisher et al., 2008, Edwards et al., 2008). *BRCA1/2* restoration does not, however, explain all cases of cisplatin resistance, therefore further investigations are still required.

6.2 PARP Inhibitor Function

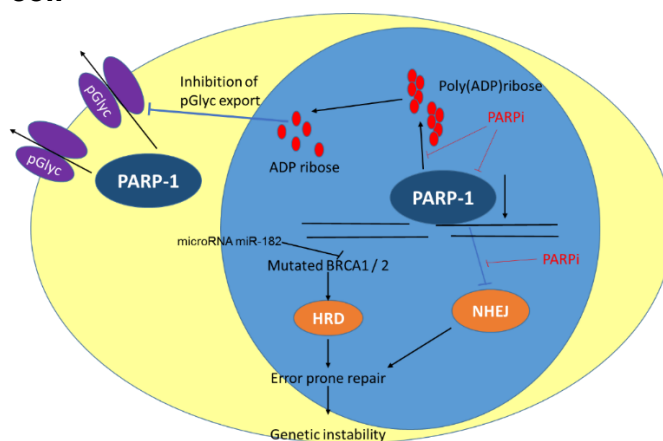
PARP-1 reaches DNA damage sites rapidly and activates different cellular responses to DNA damage (Javle and Curtin, 2011). The activated PARP-1 splits the substrate nicotinamide adenine dinucleotide (NAD^+) to release ADP-ribose, nicotinamide, and protons (Shah et al., 2011). PARP-1 then forms polymers of ADP-ribose (PAR) that post-translationally modify nuclear proteins, largely PARP-1 itself and histones. PARP-1 controls a wide array of cellular processes, such as cell death, transcription, cell division, and DNA repair (Krishnakumar and Kraus, 2010). Among the DNA repair pathways, PARP-1 is widely recognised for its impact on BER, but it also influences HR, NHEJ, MMR and NER (Pines et al., 2012, De Vos et al., 2012, Liu et al., 2011). Competitive PARPi are analogs of nicotinamide that compete with the substrate NAD^+ to bind to the enzyme (Montoni et al., 2013). PARPi have been shown to be lethal as a monotherapy to HRD cells (Aly and Ganesan, 2011, Mukhopadhyay et al., 2010, Patel et al., 2011). Furthermore, it has been suggested that since PARP-1 plays a role in reactivating stalled replication forks, this may be a further mechanism of PARPi function (Helleday, 2011). PARPi sensitivity has also been reported via inhibition of NF- κ B, which mediates transcription of prosurvival genes in breast cancer cells (Nowsheen et al., 2012). Further to use as

monotherapy, PARPi also potentiates lethality of chemotherapeutic agents or IR (Javle and Curtin, 2011).

6.2.1 Mechanisms of PARP Inhibitor Resistance

PARP inhibitor resistance has been described via four main mechanisms. These are, decreased levels or activity of PARP-1, decreased intracellular availability of PARPi, increased HR capacity and altered NHEJ capacity (Montoni et al., 2013). The mechanisms of PARPi resistance are summarised in Figure 6-2.

PARPi sensitive cell



PARPi resistant cell

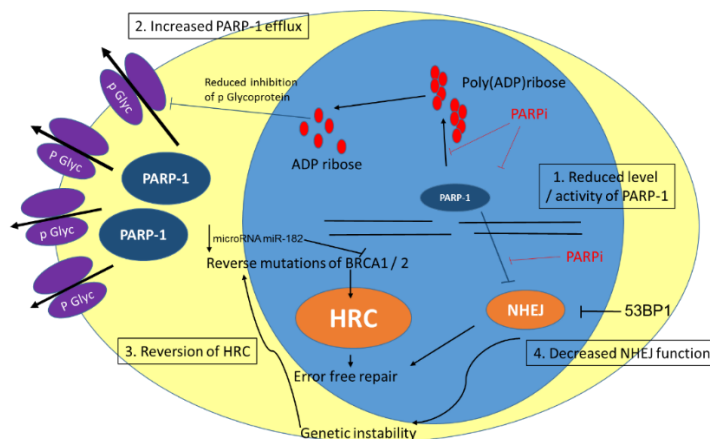


Figure 6-2 Schematic of the mechanisms contributing to PARPi resistance.

6.2.1.1 Decreased Levels or Activity of PARP-1

PARPi prevent activation of the PARP-1 that is bound to DNA strand breaks to form PAR, or facilitate DNA repair events. Therefore, reduced levels of PARP-1 could result in resistance to PARPi, as has been demonstrated in colorectal carcinoma (Liu et al., 2009). The effectiveness of PARPi is also linked to the catalytic activity of

PARP-1. Thus, decreased activity of PARP-1 independent of normal expression could influence the efficacy of PARPi (Oplustilova et al., 2012, Gottipati et al., 2010). Furthermore, variant forms of PARP-1 with decreased catalytic activity, such as those created by the single nucleotide polymorphism (SNP)V⁷⁶²/A (Lockett et al., 2004), could make cancer cells resistant to PARPi.

6.2.1.2 Decreased Intracellular Availability of PARPi

Further to the role of P-glycoprotein in cisplatin resistance described earlier, P-Glyc is also involved in the efflux of the PARPi Olaparib (Oplustilova et al., 2012). Inhibition of P-Glyc has been reported to re-sensitise PARPi-resistant BRCA1 deficient cells to PARPi (Rottenberg et al., 2008, Jaspers et al., 2013).

6.2.1.3 Increased HR Capacity

Resistance to PARPi in BRCA deficient tumours can occur via reverse mutations in *BRCA1/2* and restoration of HR function (Sakai et al., 2008, Swisher et al., 2008, Edwards et al., 2008, Barber et al., 2013, Norquist et al., 2011). The genomic instability associated with BRCA loss could be a cause for reverse mutations of *BRCA* genes (Aly and Ganesan, 2011). Selection of cells with restored BRCA function could confer resistance to PARPi. A further alteration to BRCA function is by regulation of BRCA expression. BRCA1 expression is negatively regulated by the microRNA miR-182, and overexpression sensitises BRCA1-proficient breast cancer cells to PARPi, whereas, downregulation results in resistance (Moskwa et al., 2011).

53BP1 is a nuclear protein that plays a key role in DNA repair responses and checkpoint control (Bunting et al., 2010). Together, BRCA1 and 53BP1 determine the balance between NHEJ and HR. Loss of 53BP1 suppresses NHEJ and promotes HR. While cells with a defect in BRCA1 alone are susceptible to PARPi, an additional loss of 53BP1 was shown to increase HR repair and induce PARPi resistance (Bunting et al., 2010, Brandsma and Gent, 2012, Oplustilova et al., 2012).

6.2.1.4 Altered NHEJ Capacity

It has been suggested that one of the causes of synthetic lethality of PARPi in HRD cells is an upregulation of the error-prone NHEJ pathway that is normally suppressed by PARP-1 (Patel et al., 2011). However, data from chapters 4 and 5 do not support this model. Decreased NHEJ capacity in HRD cells has been suggested to lead to

resistance to PARPi. This has been demonstrated *in vitro* in BRCA2-deficient cell lines, where inhibition or downregulation of Ku80, Artemis, or DNA-PK resulted in resistance to PARPi (Patel et al., 2011), and which has been confirmed in chapters 4 and 5.

A further mechanism implicating NHEJ in PARPi resistance, is the suggestion that normal NHEJ function leads to genomic instability. This could be responsible for the reversion of mutated *BRCA1/2*, restoration of partial HR capacities and development of resistance to PARPi in HRD tumours (Chiarugi, 2012). Depletion of NHEJ components DNA-PK and Ku80 also results in PARPi sensitivity in HRC cells (Bryant and Helleday, 2006). Thus, both increased and decreased NHEJ capacity has been hypothesised to result in PARPi resistance. The results in chapter 4 suggest that in ovarian primary culture NHEJ is defective in 40 % of cultures, which is associated with PARPi resistance.

Research into resistance mechanisms (“insights into treatment failure”) was outlined as one of the key lines of research in the “Focus on Cancer” March 2011 issue of Nature Medicine. Resistance to cisplatin has been intensively researched and a number of mechanisms have been described, however, it still remains poorly understood. Furthermore, PARPi are a new treatment still in clinical trial settings, therefore, further insight into the mechanisms of function will emerge as the trials mature. Understanding of the overlapping and separate mechanisms of resistance not only provides the ability to better select the correct treatment for patients based on the cancer genetics, but also possibly provide targets for overcoming the resistance of both platinum and PARPi.

6.3 Aims of Chapter 6

The purpose of these investigations was to determine the roles of DNA repair pathways in chemo-resistance in ovarian cancer. Furthermore, to investigate whether common or different mechanisms are involved in the resistance to cisplatin and rucaparib. Specifically the experimental aims were as follows:

- Treat cell lines with escalating doses of cisplatin or rucaparib over an extended period of time to determine if stable drug resistant cultures could be established.
- Determine the HR, NHEJ and BER status of the resistant cultures.

- Assess the mechanisms of resistance by performing exome mutational analysis and whole genome expression array.
- Identify any potential targets of resistance to cisplatin and rucaparib.

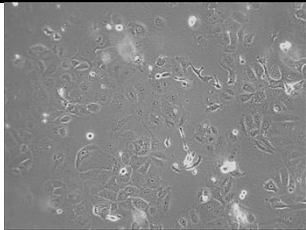
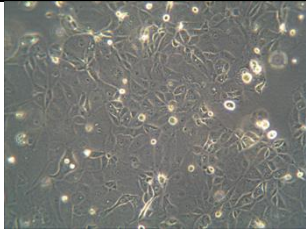
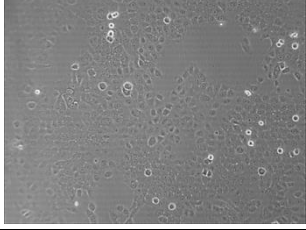
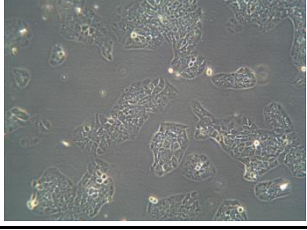
6.4 Results

Two HRD cell lines were selected for use in these experiments, UWB1.289 and PEO1 cells. These cell lines were selected as they harbor *BRCA1* and *BRCA2* gene mutations respectively. They also have paired HRC isogenic cell lines for controls. The PEO1 cell line was also selected as it has been previously used in the development of cisplatin resistance.

6.4.1 Basal Cell Line Characteristics

Cell line pairs were characterised prior to resistance induction. The cell line morphology was assessed using light microscopy. Both cell line pairs had cobblestone appearance and were morphologically similar to their BRCA complemented pairs. Cell doubling time was determined using the SRB assay as described in chapter 2, and consistently the *BRCA*-mutant cells showed a slower growth rate compared to BRCA competent controls.

Table 6-1 Cell line model characteristics.

Cell line	BRCA status	Histology of tumour from which cell line was derived	Patient characteristics	Source	Morphology	Doubling time (hrs)
UWB1.289	Germline BRCA1 mutation within exon 11 and a deletion of the wild-type allele p53 mutant	Derived from papillary serous histology carcinoma	The patient developed breast cancer at age 42, ovarian cancer at age 54, and died at age 56	ATCC		136
UWB1.289 +BRCA1	Wild-type BRCA1 was restored	Derived from UWB1.289 cell line by transfection of human <i>BRCA1</i>	Derived from UWB1.289 cell line	ATCC		96
PEO1	BRCA2 mutation [5193C>G (Y1655X)]	Derived from peritoneal ascites of a patient with a poorly differentiated serous adenocarcinoma	The patient previously received cisplatin, 5-fluorouracil and chlorambucil treatment	PEA		100
PEO4	Secondary BRCA2 mutation [5193C>T (Y1655Y)] which restored full length BRCA2	Derived from the same patient as PEO1 after clinical resistance developed to chemotherapy	The patient previously received cisplatin, 5-fluorouracil and chlorambucil treatment	PEA		91

6.4.1.1 HR Status of Cell Line Models

The HR status of the four cell lines was determined using the previously described γ H2AX/RAD51 foci assay. > 2 fold rise in γ H2AX was used as an indication of induction of DNA DSBs. >2 fold rise in RAD51 was used as a definition of HRC. As expected, in BRCA1 and BRCA2 deficient cell lines there was no significant increase in RAD51 foci after IR+rucaparib (Figure 6-3). HR function was not significantly affected by DNA-PK inhibition in UWB1.289+BRCA1 and PEO4 cells, as expected. However, treatment with NU7441 of BRCA1-mutant UWB1.289 cells recovered HR function, and there was a nearly 3-fold increase in RAD51 foci following exposure to IR+rucaparib. NU7441 treatment did not, however, recover HRC in the BRCA2 mutant PEO1. Thus, HR function recovery in BRCA1 but not BRCA2 mutant cells, suggests that the effect of DNA-PK inhibition may be lesion specific.

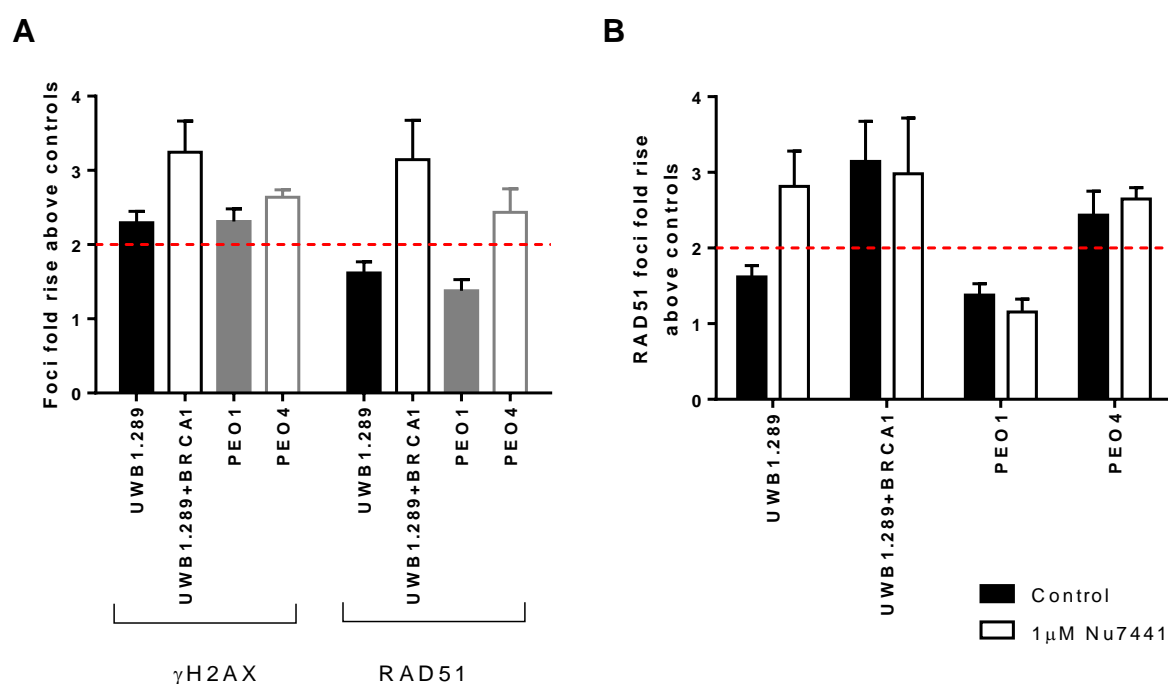


Figure 6-3 HR status of model cell lines.

HR status was assessed using γ H2AX/RAD51 assay. **A.** Cells were treated with 2 Gy IR and 10 μ M rucaparib for 24 hrs before number of γ H2AX and RAD51 foci in each cell was determined. Two fold RAD51 foci increase above controls in deemed HR competent. **B.** RAD51 foci counts of HR assay performed +/- 1 μ M NU7441. Results are average of 3 independent experiments. Error bars are SEM.

6.4.1.2 NHEJ Status of Cell Line Models

The NHEJ status of the four cell lines was assessed using the previously described cellular luciferase vector rejoining assay. The DNA-PKcs deficient V3 cell line was used as a negative control, and its DNA-PK corrected cell line, V3YAC, provided a positive control for rejoining. All four human ovarian cancer cell lines were deemed NHEJ competent (Figure 6-4).

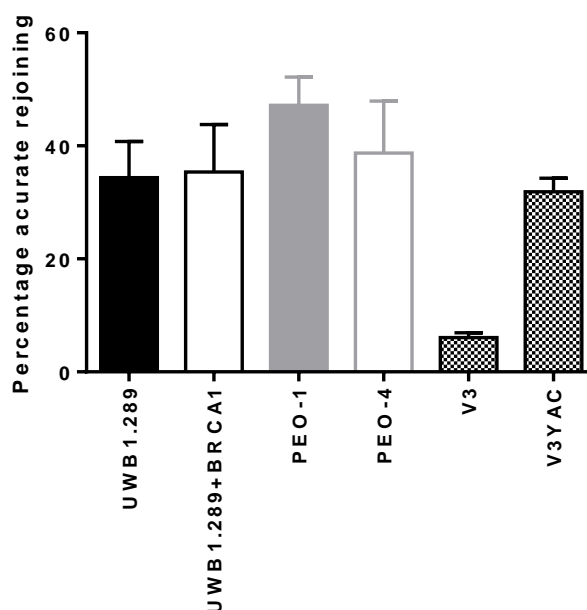


Figure 6-4 NHEJ status of model cell lines.

NHEJ status was assessed by using luciferase vector rejoining assay. Intracellular end joining of linearised pGL2 vector by cell lines was measured by luciferase activity. Measured as precise rejoining / overall end joining x 100. Data are average of three independent experiments. Error bars are SEM.

6.4.1.3 Sensitivity to Rucaparib and Cisplatin

As expected *BRCA* mutant cells were found to be significantly more sensitive to both rucaparib and cisplatin (Figure 6-5). Mean GI₅₀ and LC₅₀ are listed in Table 6-2.

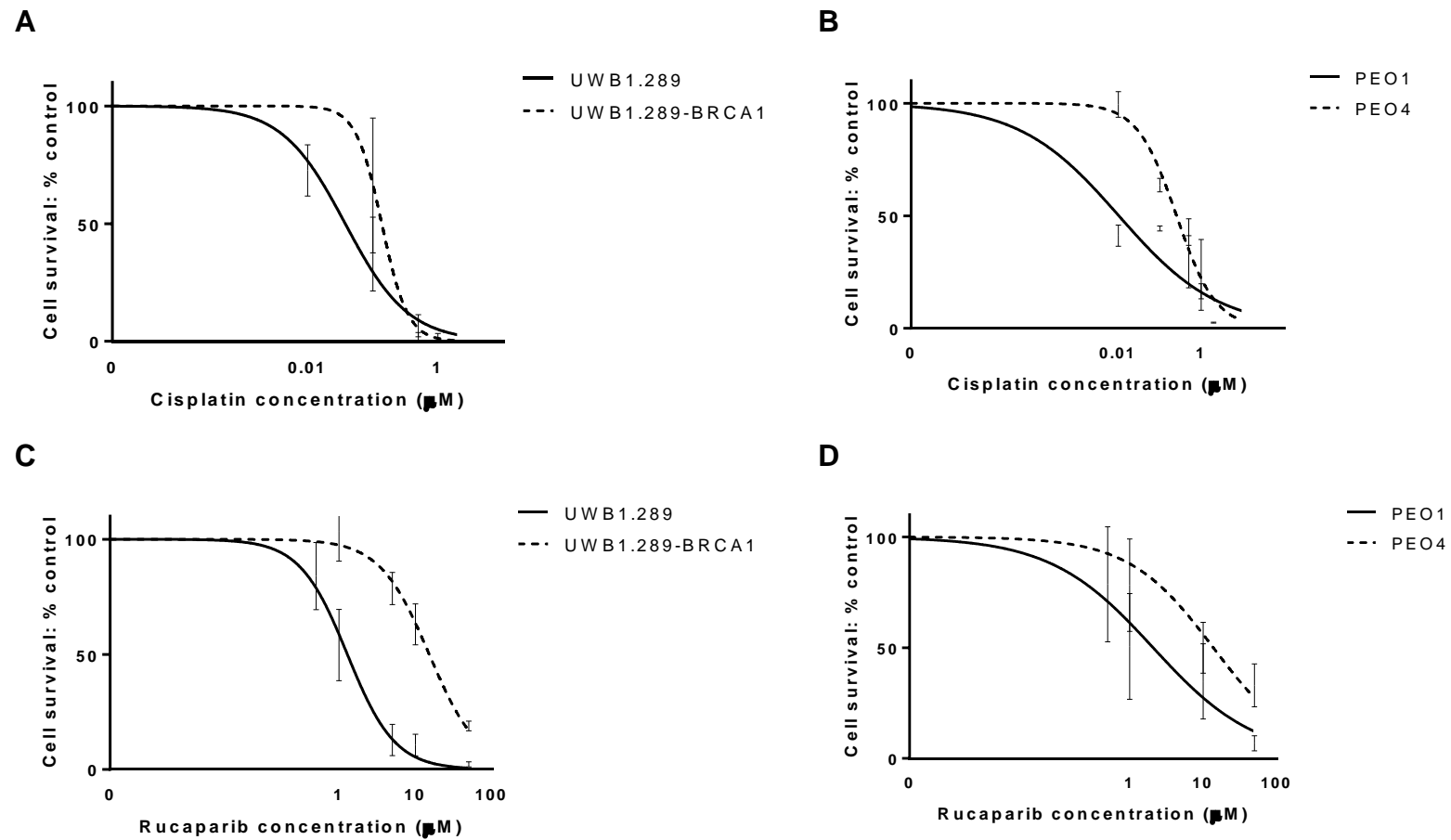


Figure 6-5 Chemo-sensitivity of cell lines assessed by Clonogenic assay.

A. UWB1.289 cell sensitivity to Cisplatin. **B.** PEO cells sensitivity to cisplatin. **C.** UWB1.289 cells sensitivity to rucaparib. **D.** PEO cells sensitivity to rucaparib. Results are average of 3 independent experiments with 3 experimental repeats. Error bars are SEM.

Table 6-2 Sensitivity of UWB1-289 and PEO cell lines to rucaparib and cisplatin.

Rucaparib and cisplatin GI_{50} (assessed by SRB assay) and LC_{50} (assessed by clonogenics) in paired UWB1-289 and PEO cell lines.

Cells	GI_{50} rucaparib	LC_{50} rucaparib	GI_{50} cisplatin	LC_{50} cisplatin
UWB1-289	1.6 μ M	1.3 μ M	280nM	75nM
UWB1-289-BRCA1	14.3 μ M	13.92 μ M	1420nM	183nM
Fold increase (t-test p =)	8.9 (0.035)	10.7 (< 0.0001)	5.0 (0.041)	2.4 (0.008)
PEO1	7.8 μ M	0.78 μ M	552nM	9.3nM
PEO4	16.59 μ M	9.6 μ M	1238nM	1440nM
Fold increase (t-test p =)	2.1 (0.005)	12.3 (0.034)	2.24 (0.0007)	155 (< 0.0001)

6.4.2 Development of Resistant Cell Lines

Hypothesis: Stable drug resistant cell lines can be derived from HRD cell lines by treatment with escalating doses of drug and incremental irradiation.

UWB1.289 and PEO1 cells were grown in T75 flasks in recommended media at 37 °C, and supplemented with increasing concentration of cisplatin or rucaparib over a period of 18 months. The starting drug concentrations were the LC_{50} for each drug for each cell line. The media was changed twice a week, and cells were passaged as required. The concentration of drug was increased when exponential growth was achieved at each concentration. Parallel flasks at the lower concentration were maintained alongside higher concentration, in case the higher concentration proved lethal. In those cases a smaller incremental increase in drug concentration was used. The final drug concentrations achieved were 20 μ M rucaparib for PEO1 (2.5 x GI_{50} and 25 x LC_{50}) and UW1.289 (12.5 x GI_{50} and 15 x LC_{50}) 2 μ M cisplatin for PEO1 (3.6 x GI_{50} and > 200 x LC_{50}) and 3 μ M cisplatin for UWB1.289 (10.7 x GI_{50} and 40 x LC_{50}). The final concentrations exceeded the LC_{50} and GI_{50} of BRCA corrected paired cell lines PEO4 and UWB1.289+BRCA1.

A further method for the assessment of resistance development is the induction of nonspecific DNA mutations prior to selection for resistance. Irradiation was used to induce DNA mutations in PEO1 and UWB1.289 cells. The flasks were exposed to fractional irradiation of 5 Gy, followed by cell recovery, and the next irradiation was performed after a single passage and exponential growth was regained. Total

irradiation for each derived cell line was 60 Gy. The 5 Gy fractioning was used as it has been previously described in other studies (Wade et al., 2015).

6.4.3 Validation of Resistant Models

Resistant lines were passaged without additional drug 3 times before being used for further experiments. Initially the cells were characterised by assessing morphology, growth and sensitivity to cisplatin and rucaparib. No changes in the morphology of the UWB1.289 resistant lines were noted (Table 6-3). Rucaparib resistant PEO1 lines were morphologically similar to PEO1. However, PEO1-CDDPR cells were morphologically more similar to the PEO4 cell line (Table 6-4).

Table 6-3 Morphology and doubling time of UWB1.289 derived cell lines.

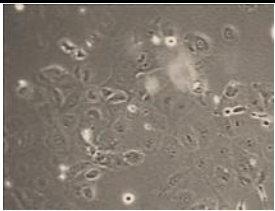
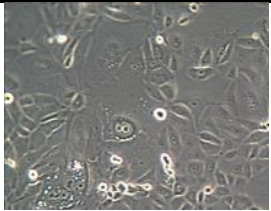
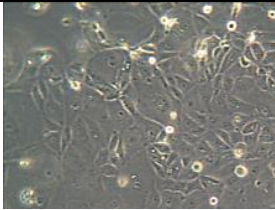
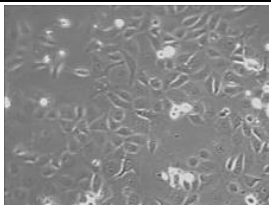
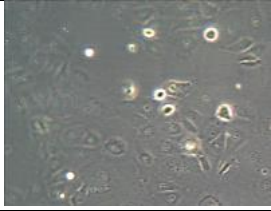
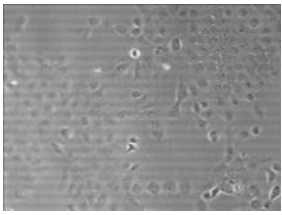
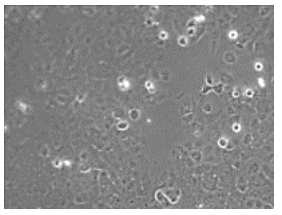

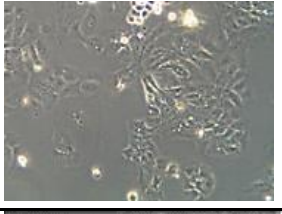
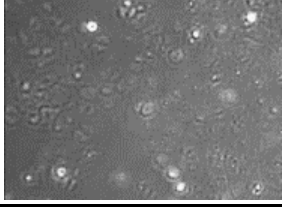
Parent cell lines	Morphological appearance	Doubling time (hrs)	Derived cell lines	Morphological appearance	Doubling time (hrs)
UWB1.289		136	UWB1.289-699R		128
UWB1.289 +BRCA1		96	UWB1.289-CDDPR		82
			UWB1.289-IR		113

Table 6-4 Morphology and doubling time of PEO1 derived cell lines.

Parent cell lines	Morphological appearance	Doubling time (hrs)	Derived cell lines	Morphological appearance	Doubling time (hrs)
PEO1		100	PEO1-699R		89
PEO4		91	PEO1-CDDPR		105
			PEO1-IR		84

BRCA competent UWB1.289+BRCA1 and PEO4 were found to have faster growth rates compared to their BRCA deficient pairs. The growth of resistant cell lines was also found to be consistently higher than the parent lines.

6.4.4 Assessment of Sensitivity to Rucaparib and Cisplatin

Cytotoxicity assays following passage in drug free media demonstrated that all UWB1.289 derivatives were resistant to cisplatin, compared to UWB1.289 cells. This indicates that the mechanisms of resistance were stable and that cells did not require continuous exposure to the drugs they were derived in. The sensitivity was not significantly different from that of the UWB1.289+BRCA1 cell line. The only exception was UWB1.289-CDDPR cells, which were significantly more resistant to cisplatin than all the other derivatives, including the UWB1.289+BRCA1 cell line (Figure 6-6.A and Table 6-5). This suggests that there are multiple methods of resistance beyond HR function.

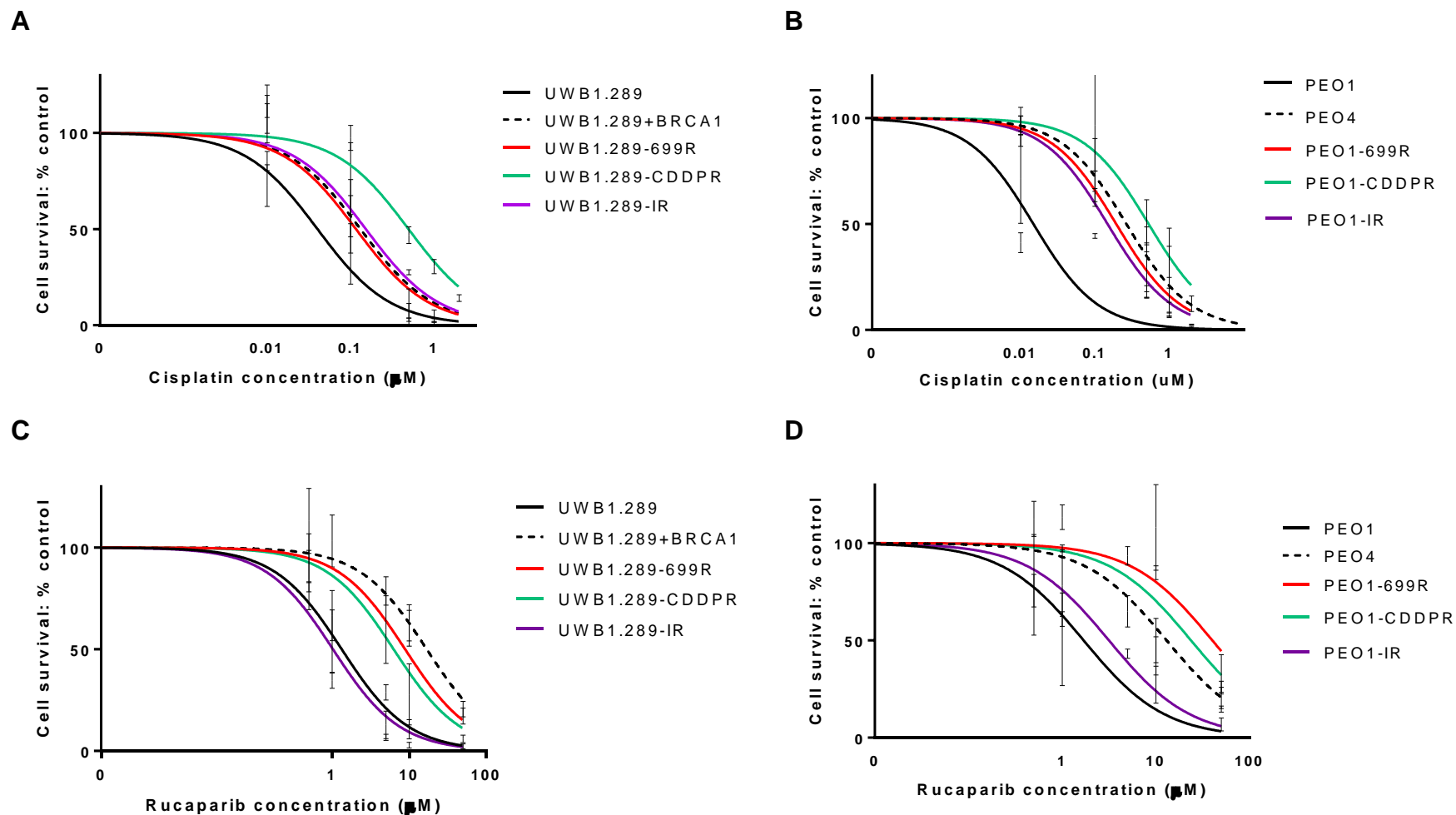


Figure 6-6 Chemo-sensitivity of derived cell lines assessed by Clonogenic assay.

A. UWB1.289 derivative cells sensitivity to Cisplatin. **B.** PEO derivative cells sensitivity to cisplatin. **C.** UWB1.289 derivative cells sensitivity to rucaparib. **D.** PEO derivative cells sensitivity to rucaparib. Results are average of 3 independent experiments with 3 experimental repeats. Error bars are SEM.

Table 6-5 Cisplatin and Rucaparib sensitivity in derivative cell lines. LC_{50} assessed by clonogenics assay.

Cell line	Cisplatin $LC_{50}(\mu M)$	95 % CI (μM)	Comparison to parent line Fold increase (F test p =)	Comparison to BRCA competent line Fold increase (F test p =)	Rucaparib $LC_{50}(\mu M)$	95 % CI(μM)	Comparison to parent line Fold increase (F test p =)	Comparison to BRCA competent line Fold increase (F test p =)
UWB1.289	0.04	0.02 to 0.07	-	0.3 (0.015)	1.33	0.82 to 2.17	-	0.08 (<0.0001)
UWB1.289-699R	0.12	0.07 to 0.2	3.0 (0.0079)	0.9 (0.77)	8.86	4.81 to 16.34	6.7 (<0.0001)	0.5 (0.12)
UWB1.289-CDDPR	0.49	0.4 to 0.7	12.25 (<0.0001)	3.8 (0.0005)	6.29	1.45 to 27.23	4.7 (0.022)	0.4 (0.15)
UWB1.289-IR	0.15	0.1 to 0.2	3.75 (0.0001)	1.2 (0.69)	1.03	0.60 to 1.75	0.8 (0.41)	0.06 (<0.0001)
UWB1.289+BRCA1	0.13	0.06 to 0.3	3.25 (0.015)	-	16.92	9.68 to 29.55	12.7 (<0.0001)	-
PEO1	0.015	0.006 to 0.04	-	0.06 (0.0004)	1.69	0.57 to 5.0	-	0.1 (0.018)
PEO1-699R	0.19	0.2 to 0.4	12.7 (0.002)	0.7 (0.2)	40.07	12.54 to 128.0	23.7 (0.0007)	3.0 (0.11)
PEO1-CDDPR	0.53	0.21 to 1.35	35.3 (0.0013)	2.0 (0.15)	23.72	8.04 to 70.00	14.0 (0.0045)	1.8 (0.4)
PEO1-IR	0.15	0.11 to 0.2	10.0 (0.0059)	0.6 (0.14)	3.16	2.22 to 4.49	1.9 (0.3)	0.2 (0.004)
PEO4	0.27	0.17 to 0.4	18.0 (0.0004)	-	13.03	5.44 to 31.22	7.7 (0.018)	-

UWB1.289-699R and UWB1.289-CDDPR derivatives were resistant to rucaparib (Figure 6-6.C and Table 6-5). Again, resistance was not significantly different from the UWB1.289+BRCA1 cell line. UWB1.289-IR cells were sensitive to rucaparib at a similar level to the UWB1.289 parent line, which was significantly lower than UWB1.289+BRCA1 cells (Figure 6-6.C and Table 6-5).

All PEO1 derivatives showed similar levels of resistance, compared to the BRCA2 competent PEO4 cells (Figure 6-6.B and Table 6-5). Again, all derivatives with the exception of PEO1-IR were resistant to rucaparib (Figure 6-6.D and Table 6-5).

6.4.4.1 Assessment of HR Status in Resistant Cell Lines

Hypothesis: Resistant cell lines regain HR competence

HR function was assessed using the γ H2AX/RAD51 assay for all derivatives. All derivatives grown in rucaparib and cisplatin were found to be HRC (Figure 6-7). Both PEO1 and UWB1.289 IR derivatives remained HRD, consistent with the HR status of the parent lines.

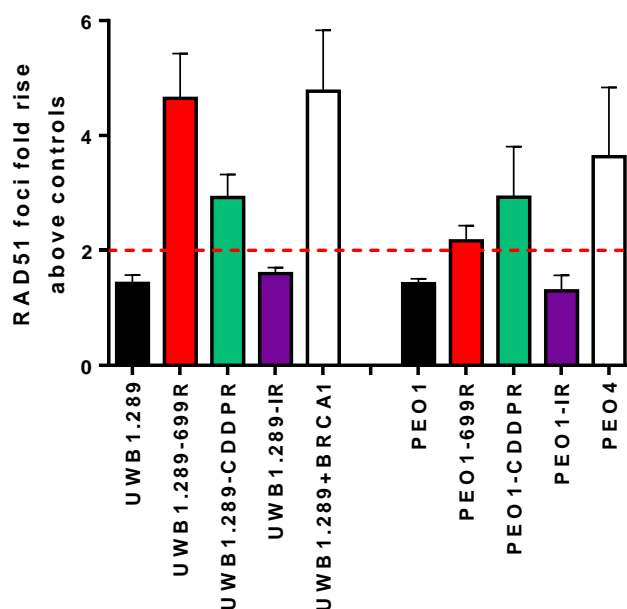


Figure 6-7 HR status of derivative cell lines.

HR status was assessed using the γ H2AX/RAD51 assay. Cells were treated with 2 Gy IR and 10 μ M rucaparib for 24 hrs before the number of γ H2AX and RAD51 foci in each cell was determined. Two fold RAD51 foci increase above controls is deemed HR competent. Results are average of 3 independent experiments expressed as fold increase above controls. Error bars are SEM.

6.4.4.2 Assessment of NHEJ status in Resistant Cell Lines

Hypothesis: Resistant cell lines will develop NHEJ deficiency during the process of resistance development.

All derivatives were able to rejoin compatible (Co) and incompatible (2 base mismatch - 2I) BstXI vectors (Figure 6-8 and Figure 6-9).

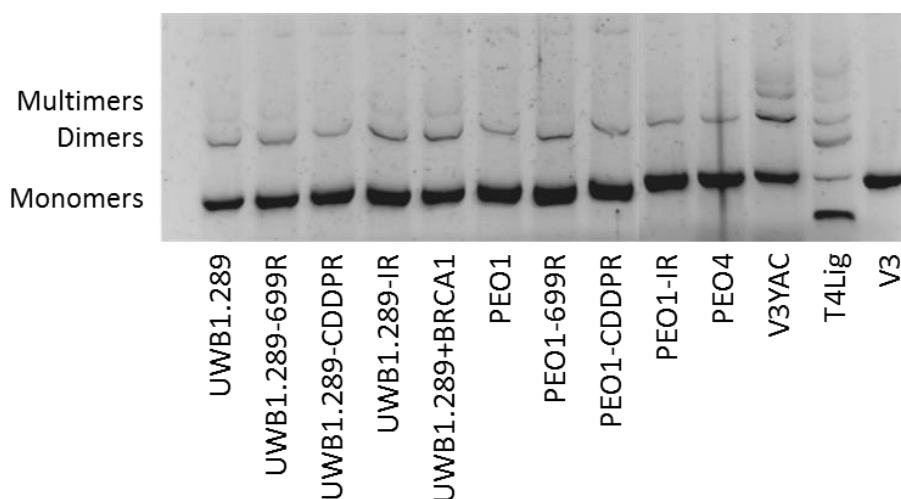


Figure 6-8 End joining of Co BstXI substrates by resistant cell lines.

V3YAC and T4Lig were used as positive controls, V3 was used as a negative control. Gels are representative of three independent experiments.

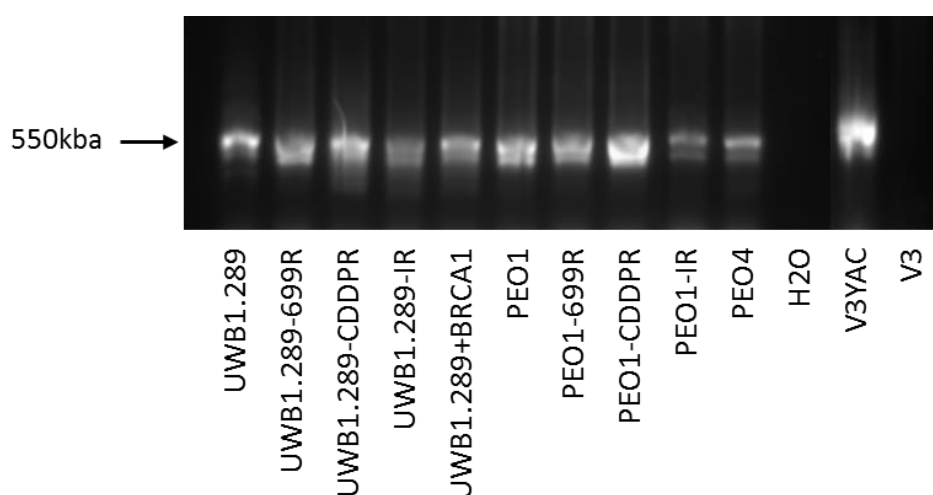


Figure 6-9 End joining of 2I BstXI substrates by resistant cell lines.

V3YAC was used as a positive control and V3 as negative control. H₂O was used as a control for PCR contamination. Gels are representative of three independent experiments.

The ability to rejoin both indicated NHEJ competence. A second band was seen in all derived cell lines, suggesting some error prone rejoining, however, competent rejoining was also evident (Figure 6-9). No change of end joining from the parent lines was seen. When protein expression was assessed, again no change in expression of DNA-PKcs, Ku70 or Ku80 was seen in the derived cell lines, compared to the parent lines (Figure 6-10).

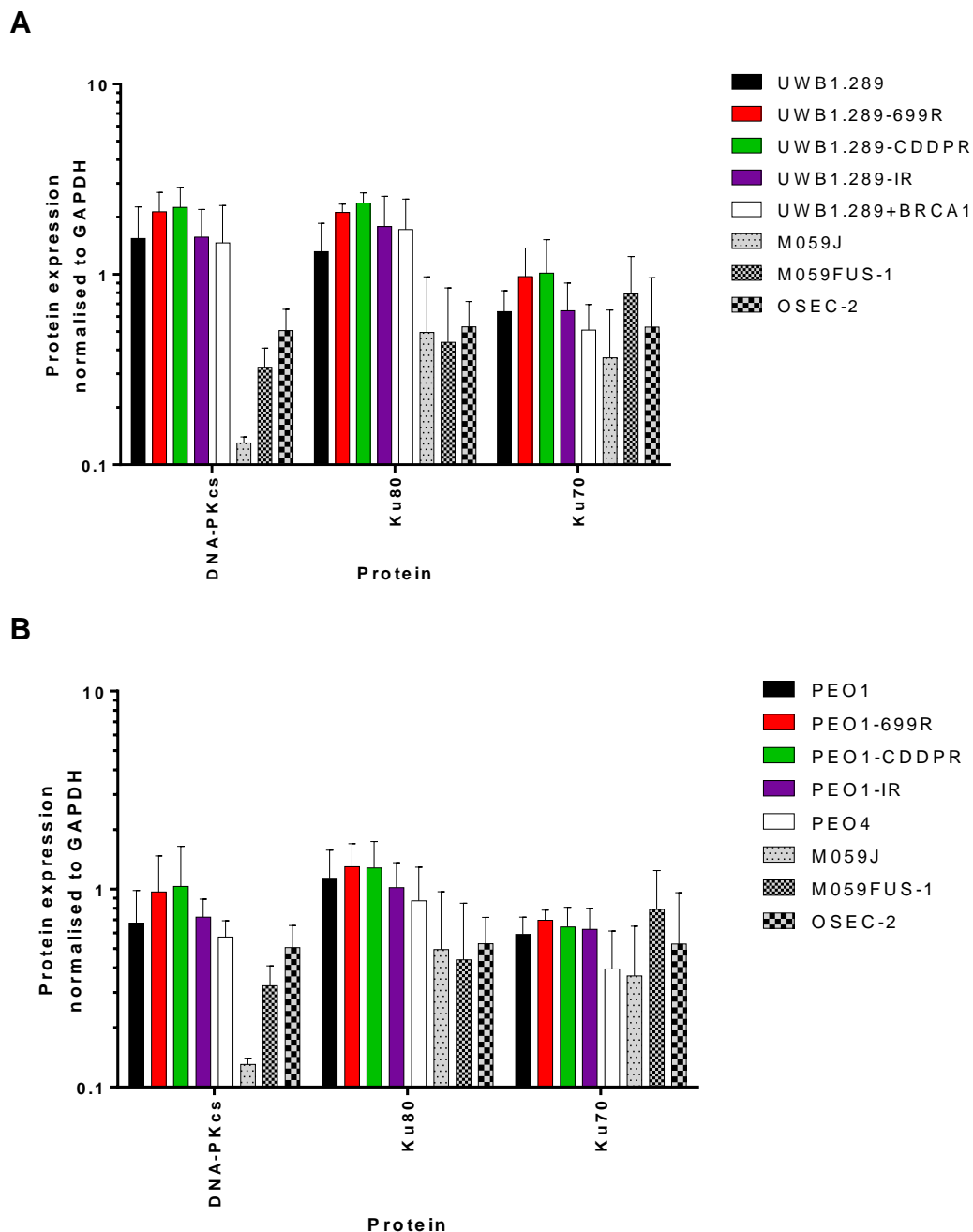


Figure 6-10 DNA-PKcs, Ku80 and Ku70 protein expression in resistant cell lines.

M059J was used as a negative control, M059FUS-1 and OSEC-2 as positive controls. **A.** UWB1.289 derivative cell lines, **B.** PEO1 derivative cell lines. The results are mean of three independent experiments. Error bars are SEM.

6.4.4.3 Assessment of BER Function in Resistant Cell Lines

Hypothesis: Resistant cell lines will develop BER deficiency during the process of resistance development.

The BER status of all cell lines was assessed using the previously described competitive ELISA assay. AA8 (BER competent) with its derivative EM9 cell lines (BER deficient mutant with XRCC1 mutation) were used as positive and negative controls. Mean 8-OHdG for cell line models ranged from 3.11 to 5.26 (Figure 6-11). No significant change of 8-OHdG levels from the parent lines were observed for any of the resistance cell lines.

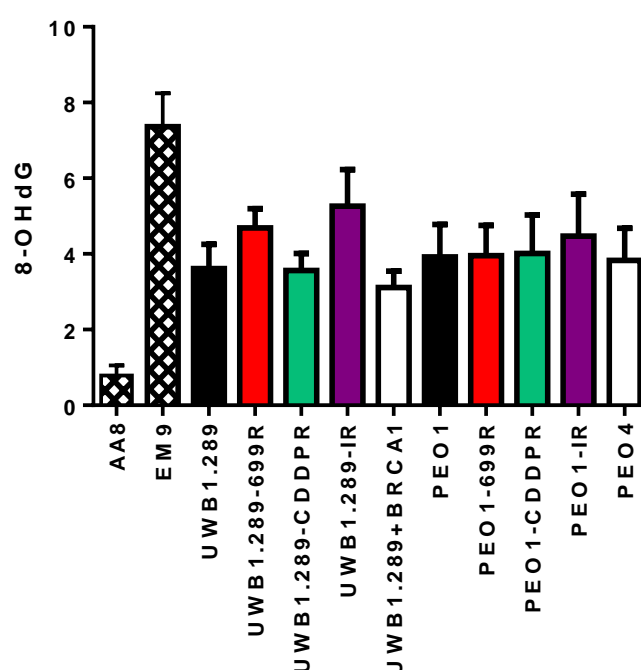


Figure 6-11 BER function in resistant cell lines assessed by competitive ELISA.

Results are the measurement of 8-OHdG levels. AA8 (BER proficient) cell line was used as positive control, EM9 (BER deficient) cell line was used as a negative control.

6.4.5 Mutation Analysis

Exome sequencing analysis was performed off site by Oxford Gene Technology (OGT). A number of novel somatic mutations were noted in the resistant, compared to parent cell lines. The majority of the mutations were heterozygous. Numerous

mutations were present in the parent line at low allelic frequency, but were noted at a higher frequency in the derived lines. These mutations are likely to have been selected for in the resistance development process.

To identify those mutations that were of potential importance to the chemo-resistant phenotype, selection criteria was applied to the raw data. Firstly known SNPs were excluded during the analysis. Secondly, the frequency of mutation reported in both parent and resistant lines was determined; mutations which were present in > 5 % of read in the parent line were excluded. Mutations that were present in less than 25 % of reads (and therefore < 50 % of cells, assuming heterozygosity) in the resistant lines were excluded. And lastly, mutations which were found to be less than three times higher in resistant compared to parent cell line were excluded. The mutations which met the selection criteria were plotted on circos plots using <http://circos.ca/> (Krzywinski et al., 2009) by Dr Sirintra Nakjang (Figures 6-12 to 6-14). Mutations are located throughout all the chromosomes. OGT software applied predictions for the likely mutations which had deleterious protein consequences.

Hypothesis: Mutational analysis will show different targets for rucaparib compared to cisplatin resistant cell lines.

Novel gene mutations in UWB1.289-699R and PEO1-699R are shown in Figure 6-12. Significantly more new mutations were noted in the UWB1.289-699 model, compared to the parental PEO1-699R model, although this did not include mutations in *BRCA1/2*. This suggests that HR function recovery in both cell lines was by mechanisms other than BRCA gene reversion. Numerous post translational modifications of the HR protein have been described (Heyer et al., 2010) and would need to be assessed in these cell lines. Common to both rucaparib resistant cell lines was a novel mutation in the *GMPT2* gene, which is involved in metabolism, and has been reported to promote monocytic differentiation of leukemia cells (Zhang et al., 2003).

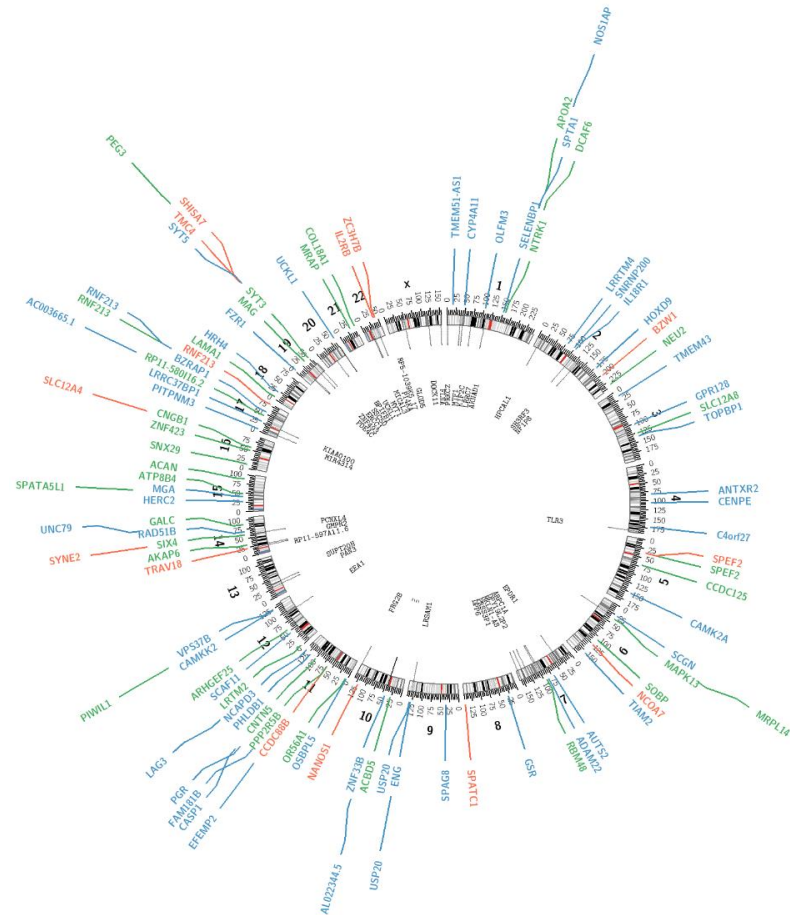
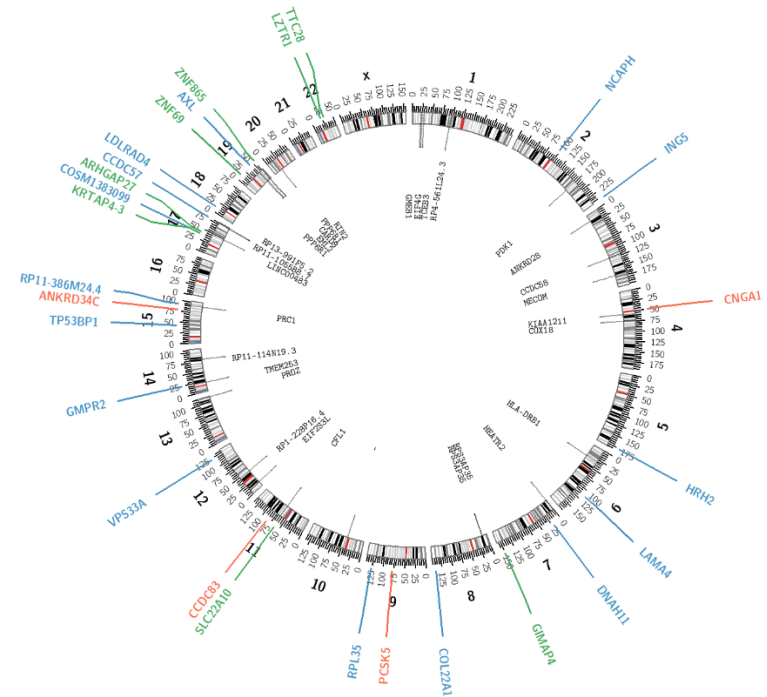
A**B**

Figure 6-12 Circos plots for rucaparib resistant cell line derivatives.

A. New mutations in UWB1.289-699R compared to UWB1.289. **B.** New mutations in PEO1-699R compared to PEO1. Genes with mutations present in parent line but selected for in resistant lines are noted in black, novel mutations are shown in blue, mutations which are predicted to be deleterious are shown in red, and those which are novel and predicted to be deleterious are shown in green.

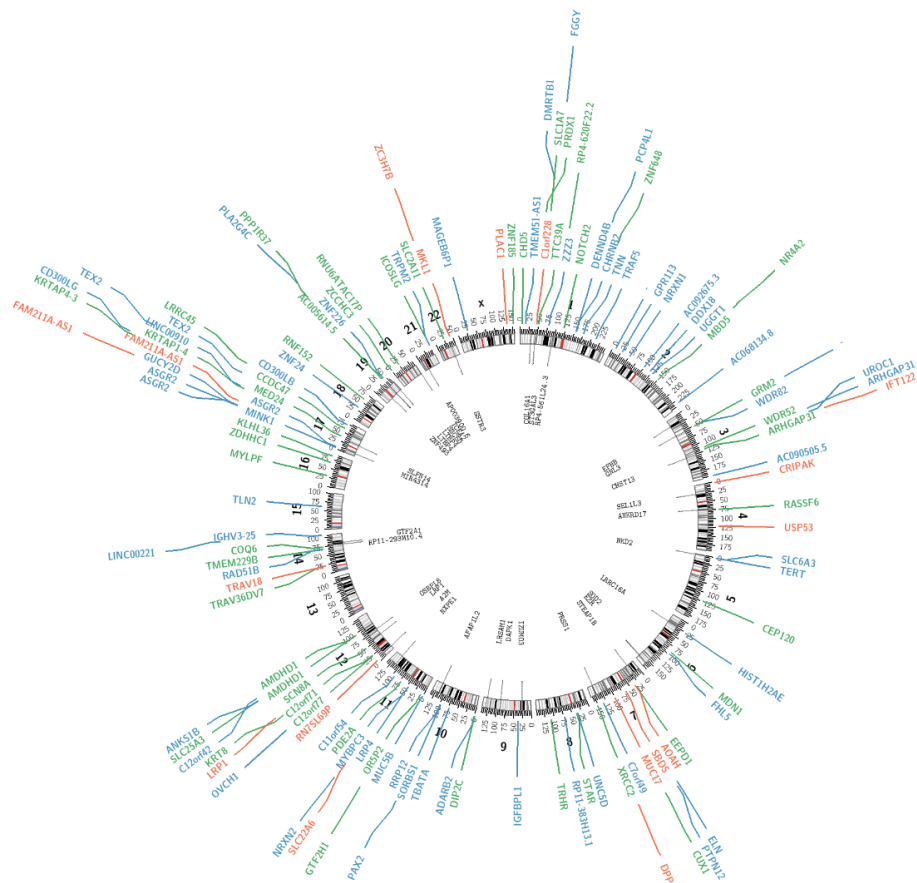
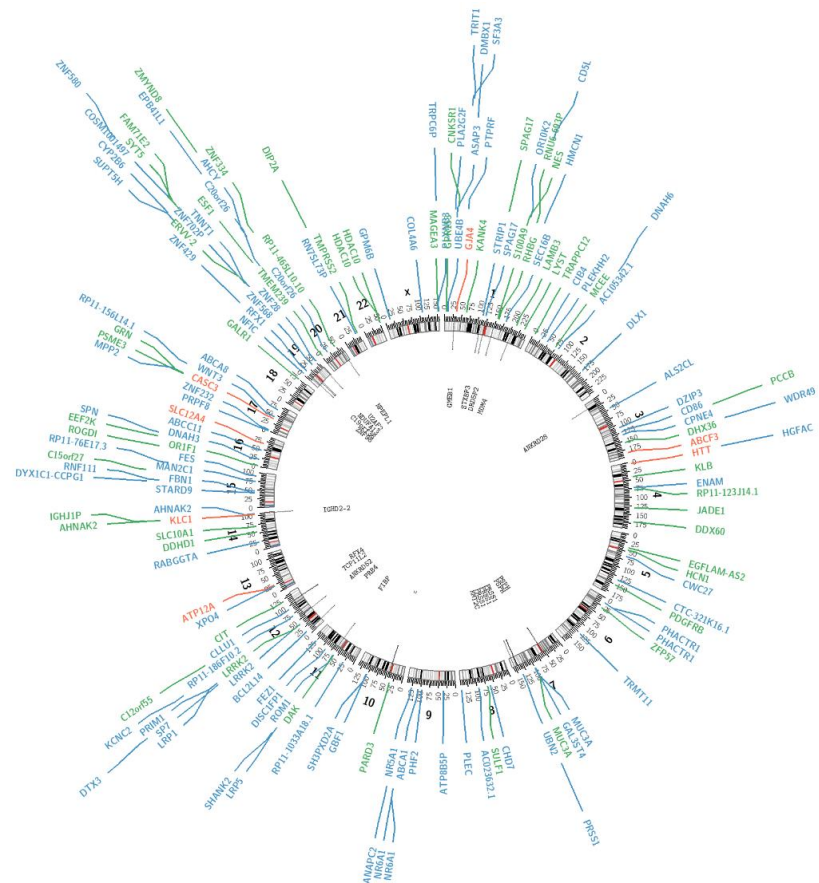
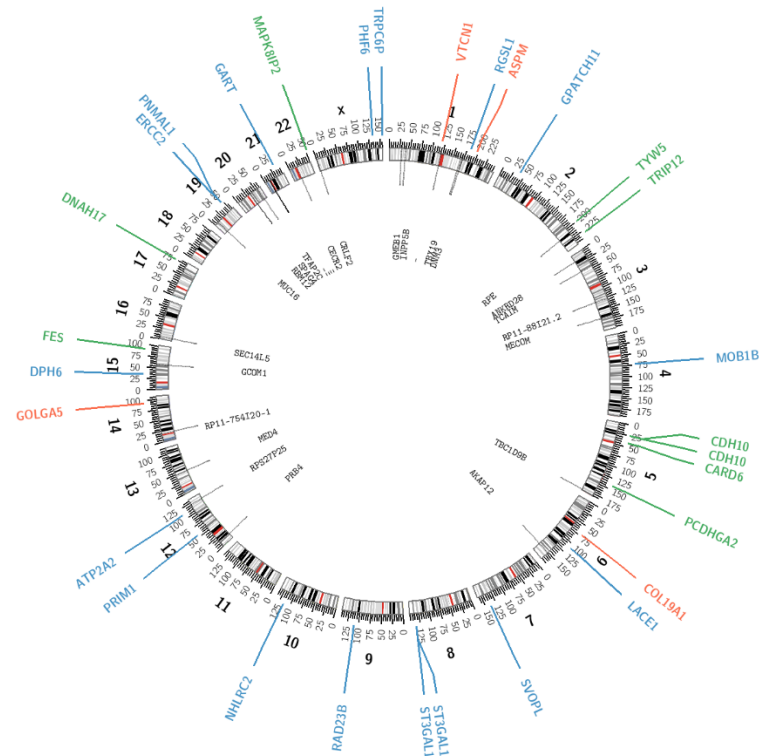
A**B**

Figure 6-13 Circos plots for cisplatin resistant cell line derivatives.

A. New mutations in UWB1.289-CDDPR compared to UWB1.289. **B.** New mutations in PEO1-CDDPR compared to PEO1. Genes with mutations present in parent line, but selected for in resistant lines are noted in black, novel mutations are shown in blue, mutations which are predicted to be deleterious are shown in red, and those which are novel and predicted to be deleterious are shown in green.



A. New mutations in UWB1.289-IR compared to UWB1.289. **B.** New mutations in PEO1-IR compared to PEO1. Genes with mutations present in parent lines but selected for in resistant lines are noted in black, novel mutations are shown in blue, mutations which are predicted to be deleterious are shown in red, and those which are novel and predicted to be deleterious are shown in green.

Figure 6-13 demonstrates the novel mutations in UWB1.289-CDDPR and PEO1-CDDPR cells, which carry mutations across all chromosomes. Again, whilst HR function was regained in both cell lines, no novel *BRCA* mutations were noted. Two common genes were found to contain mutations - *PRSS1* and *LRP1*. *LRP1* codes for an endocytic receptor involved in several cellular processes, including intracellular signaling, lipid homeostasis, and clearance of apoptotic cells. *PRSS1* encodes for a trypsinogen, which is a member of the trypsin family of serine proteases, and mutations in this gene are associated with hereditary pancreatitis (Pfuetzner et al., 2001).

As noted in rucaparib resistant cell line derivatives, UWB1.289-IR was found to contain significantly more novel mutations, compared to PEO1-IR (Figure 6-14). Two commonly mutated genes were found. *RGSL1* (Regulator Of G-Protein Signaling Like 1) has been reported to be mutated in breast cancer (Wiechec et al., 2011). *COL19A1* codes for the alpha chain of type XIX collagen, although there are no reports of this gene being involved in ovarian cancer or radio-sensitivity.

6.4.5.1 Mutations in DNA Repair Genes in Resistant Cell Lines

The first aim was to identify mutated genes involved in DNA repair pathways. No novel *BRCA1* or *BRCA2* mutations were noted in any of the derived cell lines when compared to the parent cell lines. A number of other DNA repair genes were somatically mutated (Table 6-6). In all three UWB1.289 resistant derivative lines, an identical A to T base change substitution was noted on Chromosome 14, at position 68331668, mapping to the *RAD51B*. This mutation was not observed in the parental cells. Mutation in other HR gene *EME1* was noted in UWB1.289-IR cell line.

No novel mutations in the BER genes were noted. This is consistent with the functional assessment of BER of the derivative and the parent cell lines.

Table 6-6 Somatic mutations in DNA repair genes in derived cell lines not found in parent cell lines.

Derived cell lines	Gene Name	Position	Ref.	Variant	Ref. read in parent cell line	Variant read in parent cell line	Ref. read in resistant cell line	Variant read in resistant cell line	% read variant in resistant cell line	Amino acid change	Pathway
UWB1.289-699R	RAD51B	68331668	A	T	22	0	21	13	38	W	HR
	ERCC1	45918893	C	+AA	24	2	18	8	31	*/+AA	NER
UWB1.289-CDDPR	XRCC2	152346278	G	C	152	0	95	51	35	S	HR
	GTF2H1	18380070	A	T	33	0	34	13	28	W	NER
	RAD51B	68331668	A	T	22	0	18	8	31	W	HR
UWB1.289-IR	RAD51B	68331668	A	T	22	0	25	9	26	W	HR
	EME1	48456440	T	A	28	0	19	15	44	W	HR
PEO1-699R	TP53BP1	43739686	G	-A	22	0	14	7	33	*/-A	NHEJ
PEO1-CDDPR											
PEO1-IR	RAD23B	110086162	G	A	26	0	6	20	77	A	NER
	ERCC2	45859053	C	A	69	0	41	24	37	M	NER

No novel mutations were noted in the NHEJ pathway genes. This finding is consistent with no change in the NHEJ function in the derived cell lines. A novel mutation in *TP53BP1* was noted in PEO1-699R. Overexpression of 53BP1 results in inhibition of NHEJ and upregulation of HR. The effect of this mutation on protein expression is not known, but no significant effect on NHEJ function was noted in the PEO1-699R cell line.

A number of NER pathway genes were found to be mutated in the UWB1.289-699R, UWB1.289-CDDP and PEO1 derived cell lines. As functional assessment of NER was not undertaken, the significance of these mutations is unknown.

6.4.5.1.1 Pathway Analysis of Novel Mutations in Resistant Cell Lines

To understand the mechanism of resistance development, pathway analysis was performed on the mutated genes list. Analysis was performed with Dr. Sirintra Nakjang. Ingenuity (<http://www.ingenuity.com>) and KEGG pathway analysis programs were used, and the results are detailed in Table 6-7. The two different analysis programs yielded different pathways for the mutated genes. Differences between the two software programs are likely to be due to the differences in the annotation used by each software package, and have been reported previously (Li et al., 2009b). This, therefore, warrants further investigation.

Cell proliferation MAPK and the PI3K pathways have both been reported to be mutated in ovarian cancer (Geyer et al., 2009, Nakayama et al., 2006, Willner et al., 2007). Pathway analysis found that at least one gene in the MAPK pathway was mutated in all the resistant cells (table 6-8).

Furthermore, although not yet functionally validated, mutations in the PI3CA/AKT pathway were noted in all except the PEO1-IR derivative (Table 6-9). The frequent mutation of this pathway suggests an important role in cisplatin resistance. Importantly, *in vivo* studies have demonstrated that inhibition of PI3K downregulates *BRCA1/2* and sensitises to PARPi. Phase one trial combining PI3Ki and olaparib in HGSOC is underway (NCT01623349).

Table 6-7 Pathway enrichment of mutated genes in resistant cell lines.

Resistant cell line	Ingenuity (top canonical pathways)	KEGG (top pathways)
UWB1.289-699R	CDK5 Signaling (p=1.12E-03) IL-15 Signaling (p=8.23E-03) STAT3 Pathway (p=9.99E-03) BMP signaling pathway (p=1.08E-02)	Endocytosis PI3K-AKT signaling pathway MAPK signaling pathway cAMP signaling pathway
UWB1.289-CDDPR	Glutamate Receptor Signaling (p=1.04E-02) Histidine Degradation (p=2.15E-02) Estrogen Receptor Signaling (p=4.64E-02)	Neuroactive ligand-receptor interaction Ribosome biogenesis in eukaryotes Focal adhesion Glutamatergic synapse
UWB1.289-IR	Glutathione Redox Reactions II (p=8.25E-03) CNTF Signaling (p=9.06E-03) Growth Hormone Signaling (p=1.56E-02) Selenocysteine Biosynthesis II (p=1.64E-02)	TNF signaling pathway cAMP signaling pathway PI3K-Akt signaling pathway Focal adhesion
PEO1-699R	Phototransduction Pathway (p=2.83E-02) Regulation of Cellular Mechanics by Calpain Protease (p=3.04E-02) Gs Signaling (p=5.75E-02) eNOS Signaling (p=7.43E-02)	Purine metabolism Ribosome
PEO1-CDDPR	Methylmalonyl Pathway (p=3.84E-05) 2-oxobutanoate Degradation I (p=6.39E-05) Methionine Degradation (p=3.03E-03)	ABC transporters Spliceosome Neuroactive ligand-receptor interaction Endocytosis Cell adhesion molecules
PEO1-IR	Cell Cycle: G2/M DNA Damage Checkpoint Regulation (p=2.86E-02) Cytokine Signaling (p=3.66E-02)	Purine metabolism Nucleotide excision repair MAPK signaling pathway Thyroid hormone signaling pathway

Table 6-8 MAPK pathway genes mutated in resistant lines.

Resistant cell line	Genes affected	Position	Ref.	Variant	Ref. read in parent cell line	Variant read in parent cell line	Ref. read in resistant cell line	Variant read in resistant cell line	% read variant in resistant cell line	Amino acid change
UWB1.289-699R	NTRK1	156843742	C	A	80	0	56	21	27	C → M
	MAPK13	36098412	C	T	64	0	32	19	37	C → Y
	FLNA	153581219	C	A	37	0	19	17	47	C → M
UWB1.289-CDDPR	PLA2G4C	48591828	T	G	37	0	17	13	43	T → K
UWB1.289-IR	RPS6KA4	64128672	C	T	39	2	45	15	25	C → Y
	AKT1	105242929	A	C	50	0	9	11	55	A → M
PEO1-699R	MECOM	168862931	A	- ACACAC	32	1	20	7	26	A → */- ACACAC
PEO1-CDDPR	PDGFRB	149500563	C	G	35	0	16	20	56	C → S
PEO1-IR	MAPK8IP2	51042447	G	A	62	0	43	28	39	G → R
	MECOM	168862931	A	- ACACAC	32	1	20	7	26	A → */- ACACAC

Table 6-9 Genes in PI3CA /AKT pathway mutated in resistant lines.

[illegible]

Table 6-10 Calcium signalling pathway mutated genes.

Resistant cell line	Genes affected	Position	Ref.	Variant	Ref. read in parent cell line	Variant read in parent cell line	Ref. read in resistant cell line	Variant read in resistant cell line	% read variant in resistant cell line	Amino acid change
UWB1.289-699R	CAMK2A	149631531	T	A	40	0	35	12	25.53	T → W
UWB1.289-CDDPR	TRHR	110100496	G	C	25	0	15	8	34.78	G → S
UWB1.289-IR	RYR2	237617933	G	T	45	0	17	8	32	G → K
	BDKRB2	96707166	G	A	43	0	22	12	35.29	G → R
PEO1-699R	HRH2	175112511	C	T	126	0	89	31	25.83	C → Y
PEO1-CDDPR	PDGFRB	149500563	C	G	35	0	16	20	55.56	C → S
PEO1-IR	ATP2A2	110788113	G	T	77	0	29	15	34.09	G → K

Calcium is a prominent regulator of cell migration, exerting multiple effects on the contractility of the actin cytoskeleton (Leung et al., 2014, Furukawa et al., 2003). Furthermore, dysregulation of calcium signaling has been linked to platinum resistance and ovarian cancer metastasis *in vitro* (Al-Bahlani et al., 2011, Leung et al., 2014). Mutations in the genes involved in the calcium signaling pathway were noted in all derived cell lines (Table 6-10). This data supports previous reports suggesting a role for calcium signaling in cisplatin resistance.

6.4.6 Gene Expression Profiling and Analysis

Further to the assessment of gene mutations, gene expression profiling was undertaken. Gene expression profiling studies have reported putative signatures for resistance to a number of chemotherapies (Devapatla et al., 2014, Sherman-Baust et al., 2011). Gene expression profiling offers functional assessment of the cell alteration in resistance development, which is not possible to see from gene mutation analysis alone.

Hypothesis: mRNA expression analysis will show different gene alterations for rucaparib compared to cisplatin resistant cell lines.

The top 10 upregulated and top 10 downregulated genes for each derived cell line compared to parent control expression are listed in Table 6-11. LogFC is also listed for each gene. A number of genes were noted in more than one cell line list, and these are highlighted.

S100A4 was upregulated in both UWB1.289-IR and PEO1-IR. Considerable evidence suggests that activation of the WNT signaling pathway plays an important role in human tumorigenesis and radio-sensitivity (Chang et al., 2008b). A further inhibitor of WNT signaling is DKK1, which inhibits cell motility and blocks invasion (Anastas and Moon, 2013), was downregulated in both UWB1.289-BRCA1 and PEO4. Furthermore, DKK1 negatively regulates cellular resistance to cisplatin in head and neck cancers (Shen et al., 2012).

Table 6-11 Top 10 genes differentially expressed in resistant cell lines.

Top 10 upregulated and top 10 downregulated genes in each cell lines compared to parent line controls were selected. Genes which are common to two or more cell lines are marked in red.

UWB1.289-699R	log FC	UWB1.289-CDDPR	log FC	UWB1.289-IR	log FC	UWB1.289-BRCA1	log FC	PEO1-699R	log FC	PEO1-CDDPR	log FC	PEO1-IR	log FC	PEO4	log FC
Top 10 upregulated genes															
CA2	3.1	PAEP	2.9	BGN	3.4	IGFBP5	3.7	CLDN23	1.7	TXNIP	2.3	CRABP2	2.7	CRABP2	5.0
TPK1	2.6	TNC	2.7	TUBB2B	2.4	TMEM178A	2.4	TRIB1	1.4	MMP7	2.2	FOXC1	2.3	MX1	4.6
S100A9	2.6	OBP2B	2.2	FBLN1	2.1	NPR3	2.3	ARHGEF35	1.3	MID1	2.2	FST	2.1	AKR1D1	4.2
IGFBP7	2.3	PAEP	2.2	APOE	1.9	KCNIP1	2.3	MARCKSL1	1.2	MMP7	2.1	CDH2	1.3	IFIT1	4.2
DUSP1	2.2	COMMD1	2.0	THY1	1.7	TPK1	2.2	PKD1L1	1.1	FOXC1	1.8	LTB	1.2	IFITM1	3.9
SNAR-A1	2.2	TNC	1.9	FBLN1	1.7	ACKR2	2.2	ARPC1B	1.1	TM4SF1	1.8	CUTA	1.2	EMX2	3.8
SPOCK1	1.9	FAM107A	1.9	S100A4	1.6	ABCA4	2.2	LY6E	1.0	MECOM	1.8	KRT13	1.1	ISG15	3.8
CCNA1	1.9	GAMT	1.9	GAMT	1.6	PASD1	2.1	CARD9	1.0	SLC16A3	1.7	S100A4	1.1	IFI44	3.6
CRYAB	1.8	DKK3	1.9	TFPI2	1.5	TMEM178A	1.9	BAIAP2L1	1.0	EFEMP1	1.7	SGK1	1.1	IFIT2	3.5
CXXC5	1.8	GLRX	1.8	HKDC1	1.5	LMCD1	1.9	BTBD2	0.9	CBR3	1.6	GPNUMB	1.1	IFITM2	3.5
Top 10 downregulated genes															
ETFB	-2.4	KRT6A	-2.9	KRT6A	-2.1	TM4SF1	-3.2	RASIP1	-2.7	IL1R2	-3.9	DIRAS3	-2.5	IL1R2	-4.4
UCHL1	-2.1	LAD1	-2.3	PI3	-2.1	MUC1	-3.1	IER3	-2.1	IER3	-3.5	LRRFIP2	-1.8	PROM1	-4.2
BCAT1	-2.1	ANGPTL4	-2.2	LCN2	-1.9	REC8	-2.8	SLIT2	-1.6	MKX	-3.2	ACAA1	-1.5	MKX	-3.6
COCH	-2.0	CDH6	-2.1	ANXA2	-1.4	DKK1	-2.7	MKX	-1.6	FLG	-2.2	RPL14	-1.4	BEX1	-3.2
KLHL35	-2.0	MGST1	-1.9	SOD2	-1.3	MUC1	-2.3	IL1R2	-1.5	CBLN1	-2.1	GJB2	-1.4	RBP7	-3.2
ETFB	-2.0	IL1RL1	-1.9	SLPI	-1.2	VIM	-2.2	CBLN1	-1.3	C1QTNF1	-1.9	CTSH	-1.4	SCG5	-3.0
MARCKSL1	-1.8	THBS1	-1.9	RNASET2	-1.1	CLDN11	-2.1	P3H2	-1.3	PNOC	-1.9	SDHAF3	-1.4	HOXB8	-3.0
MGST1	-1.8	STEAP1	-1.9	RHPN2	-1.0	VIM	-2.0	CSRP1	-1.1	SLC4A11	-1.9	MYD88	-1.3	DKK1	-2.9
CLDN11	-1.8	IFI27	-1.8	AADAC	-1.0	CAMK2N1	-2.0	HDGFRP3	-1.1	CPA4	-1.9	OXSR1	-1.3	DIRAS3	-2.9
MCOLN2	-1.8	TXNRD1	-1.8	SNHG7	-1.0	FOXQ1	-1.9	GLIPR1	-1.0	GABBR2	-1.8	GSTP1	-1.3	IER3	-2.8

TPK1 and *CLDN1* were commonly altered in UWB1.289-699R and UWB1.289-BRCA1. *TPK1* is reported to potentiate the growth inhibitory effects of cisplatin in ovarian cancer cell lines (Arora et al., 2010). *CLDN11* encodes the extracellular matrix protein that functions as cell-cell adhesion molecules, and when disrupted, may contribute to the invasion and metastasis of cancer (DelloRusso et al., 2007).

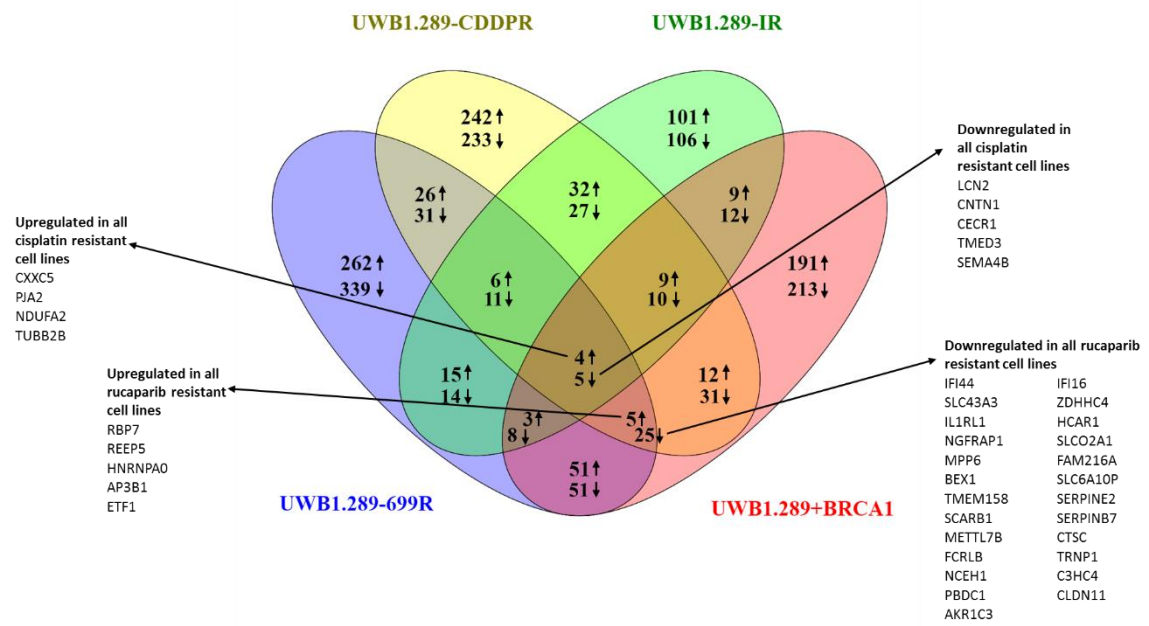
Contrary to previous studies reporting that *MGST1* is elevated in cisplatin resistant ovarian cell lines (Li et al., 2007), in this study *MGST1* was downregulated in both UWB1.289-699R and UWB1.289-CDDPR derivatives. *FOXC1* was upregulated in both PEO1-CDDP and PEO1-IR cell lines. This gene has been previously associated with cisplatin resistance in lung cancer (Guo et al., 2010), and may also have an important role in cisplatin resistance in these cell lines.

In the top 10 altered genes, *MARCKSL1* was upregulated in PEO1-699R, but downregulated in UWB1.289-699R. This finding suggests no consistent role in resistance development.

6.4.6.1 Common Gene Expression Alterations in Resistant Cell Lines

Gene expression profiling from the two parent cell lines identified very different expression signatures, which were initially analysed separately. The majority of the over- and under-expressed genes were specific for each derived cell line, but some were common to both cell lines. All UWB1.289 cell line derivatives were found to overexpress four, and under-express five common genes (Figure 6-15.A). Common genes found to be upregulated in platinum resistant UWB1.289 cells, including *CXXC5*, *PJA2*, *NDUFA2* and *TUBB2B*, have not been previously reported in the cancer literature. However, some of the downregulated genes have been reported to be linked to a number of human cancers, including *LCN2*, *TMED3*, and *SEMA4B*, as summarised in Table 6-12. All three are reported to have roles in the inhibition of progression, growth and metastasis. Therefore, the downregulation seen in the platinum resistant cell lines may be important in resistance development.

A



B

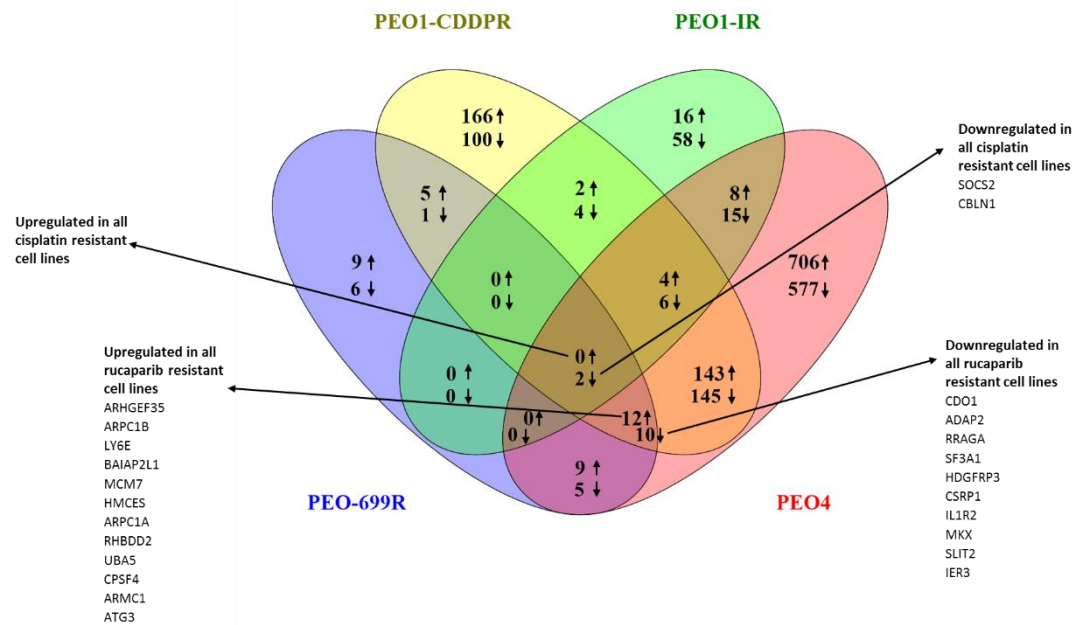


Figure 6-15 Differential expression analysis of resistant cell lines.

Venn diagrams of differentially expressed gene counts in each cell lines compared to parent line controls (<http://bioinfogp.cnb.csic.es/tools/venny>). Genes included in analysis were found to have > 1.5 fold alteration in expression and adjusted $p < 0.05$.

Table 6-12 Reported links to human cancer of genes with altered expression in resistant cell lines.

Gene	Potential role	Cancer	Reference
LCN2	Early detection Progression	Pancreatic cancer Breast cancer	(Cheng et al., 2014, Slater et al., 2013)
TMED3	Drug target Metastatic suppressor	Prostate cancer Colon cancer	(Duquet et al., 2014, Vainio et al., 2012)
SEMA4B	Inhibits growth	Lung cancer	(Jian et al., 2015)
SOCS2	Tumourgenesis Promote growth Oxaloparib resistance	GI cancers Prostate and breast cancers Ovarian cell lines	(Zhou et al., 2015, Hoefer et al., 2014, Haffner et al., 2007) (Varma et al., 2005)
IFI16	Growth suppressor	Prostate cancer	(Bui et al., 2009)
SLCO2A1	Mediate invasion Modulate susceptibility	Lung cancer Colorectal cancer	(Zhu et al., 2015) (Pereira et al., 2014)
BEX1	Biomarker for resistance to neoadjuvant chemotherapy	HER-2-negative breast cancer	(de Ronde et al., 2013)
TMEM158	Biomarker for cisplatin sensitivity	Lung cancer	(Mohammed et al., 2012)
SERPINE2	Promotor for lymph node metastasis	Testicular cancer	(Nagahara et al., 2010)
AKR1C3	Regulator of proliferation and doxorubicin resistance Pathogenesis	Breast cancer Prostate cancer	(Murugan et al., 2012) (Zhong et al., 2015) (Liu et al., 2015, Yepuru et al., 2013)
BAIAP2L1	Promotion of cell proliferation and inhibiting apoptosis	Ovarian cancer	(Chao et al., 2015)
MCM7	Progression	Prostate cancer	(Ren et al., 2006)
RHBDD2	Over expressed	Breast cancer and advanced colorectal cancer	(Lacunza et al., 2012, Abba et al., 2009)
SF3A1	Polymorphisms increase the risk	Pancreatic and colorectal cancer	(Tian et al., 2015, Chen et al., 2015)
SLIT2	Hypermethylation Poor prognosis and metastases	Ovarian cancer Breast cancer, esophageal and pancreatic cancers	(Dong et al., 2012) (Gonin et al., 2010, Qin et al., 2015) (Gohrig et al., 2014, Tseng et al., 2015)
IER3	Mediate of apoptosis	Cervical cancer	(Jin et al., 2015)

When PEO1 derivatives were analysed, no common overexpressed genes were noted, however two under expressed genes were common to all the cell line derivatives these were *SOCS2* and *CBLN1* (Figure 6-15.B). The *SOCS2* reported role in promoting growth and oxaloparib resistance (Table 6-12) suggests that it may be an important target for resistance to both platinum and rucaparib.

When only rucaparib resistant cell lines were analysed, five common genes were found to be upregulated and twenty five downregulated (Figure 6-15.A). Of those that were downregulated, a number may be potential targets for drug resistance; with previously reported roles in growth, metastasis and chemo resistance, these include *IFI16*, *SLCO2A1*, *BEX1*, *TMEM158*, *SERPINE2* and *AKR1C3* (Table 6-12) (Bui et al., 2009, Zhu et al., 2015, de Ronde et al., 2013, Mohammed et al., 2012, Nagahara et al., 2010, Murugan et al., 2012, Zhong et al., 2015).

In PEO1 derivatives resistant to rucaparib, twelve upregulated and ten downregulated genes were found to be common (Figure 6-15.B). Of these genes, two may be important targets; these are *BAIAP2L1*, which promotes cell proliferation and inhibits apoptosis (Chao et al., 2015), and *MCM7* which promotes progression (Ren et al., 2006). Of the genes which were found to be under expressed, a number have also been reported in the literature to be linked to human cancers, and therefore, could be potential therapeutic targets; these include *SLIT2*, which is associated with metastases (Gonin et al., 2010, Qin et al., 2015, Gohrig et al., 2014, Tseng et al., 2015), and *IER3*, a mediator of apoptosis (Jin et al., 2015). The altered function of all of these genes may represent potential mechanisms for rucaparib resistance, which are independent of platinum sensitivity. However, no common targets were found between the two cell lines.

Next, gene expression profiles in cell lines derived by exposure to the same treatment were compared (Figure 6-16). Rucaparib derived cell lines share only 2 commonly upregulated genes (*ARHGEF35* and *BAIAP2L1*) and no down regulated genes (Figure 6-16.A). Irradiated cell lines were found to have three upregulated and four downregulated genes in common (Figure 6-16.B). Cisplatin derived cell lines had 24 upregulated and 26 downregulated genes in common (Figure 6-16.C). Of the genes discussed already, *SLIT2* and *SOD2* were found to be upregulated in both PEO1-CDDPR and UWB1.289-CDDPR cells, and are therefore, likely to be important targets which need to be explored further.

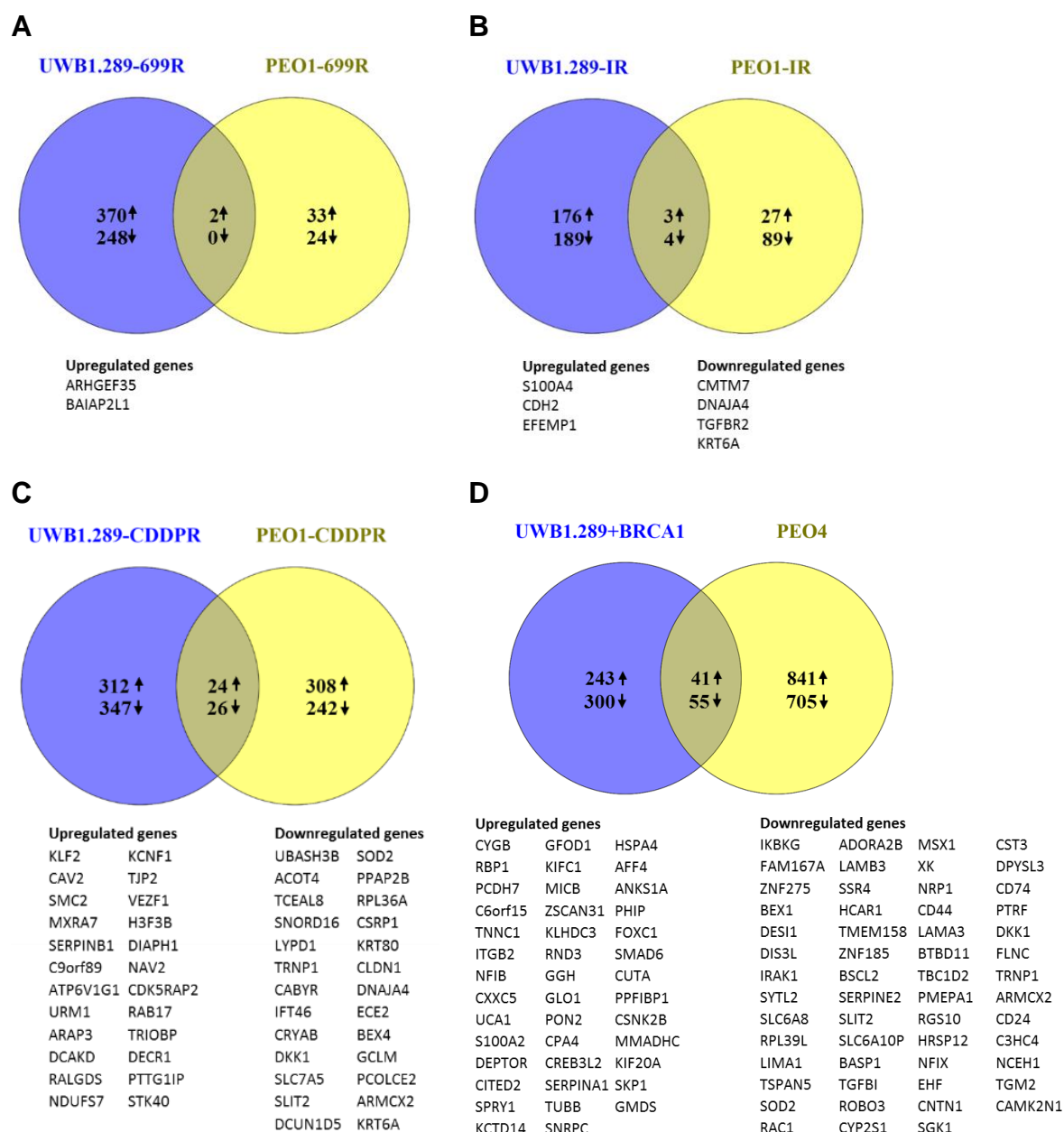


Figure 6-16 Differential expression analysis by drug treatment in resistant cell lines.

Venn diagrams of differentially expressed gene counts in each cell line compared to parent line controls. **A.** Rucaparib derived cell lines, **B.** Irradiated derivative cell lines, **C.** Cisplatin treatment derived cell lines, **D.** BRCA competent paired cell lines. Genes included in analysis were found to have >1.5 fold alteration in expression and adjusted $p < 0.05$.

Interestingly, the largest similarities were found between the two BRCA competent cell line controls, UWB1.289+BRCA1 and PEO4 (Figure 6-16.D), with 41 upregulated and 55 downregulated commonly shared genes. These two cell lines were generated in very different ways; UWB1.289+BRCA1 was derived from UWB1.289 by transfection of BRCA1, whilst PEO4 was derived from the same patient as PEO1

after clinical resistance development. This finding is therefore surprising and needs further exploration.

6.4.6.2 Pathway Enrichment of Genes with Altered Expression in Resistant Cell Lines

In order to gain some insight into the possible mechanisms that are important in the development of resistance to these drugs, pathway analysis was performed using genes that were found to show significant differences in expression, in each resistance phenotype. KEGG, GO, and IPA databases were used for enrichment of any potential pathways/terms in the drug resistant cell lines (Table 6-13). While many pathways were found to be enriched in each resistant phenotype, some pathways emerged as consistently identified in at least two databases.

In UWB1.289-699, the predominant pathway noted was involved in cell cycle control (Table 6-13), which has been linked to anoikis and taxol resistance in ovarian cancer *in vitro* (Carduner et al., 2014, Wang et al., 2013a). In contrast, in PEO1-699R, actin regulation was the predominant pathway with altered expression (Table 6-13). A recent study reported actin remodelling as a potential mechanism in cisplatin resistance (Sharma et al., 2012). The ribosome biogenesis was the pathway consistently altered in UWB1.289-CDDPR cells. Altered ribosomal biogenesis has been linked to PFS in serous ovarian cancer (Flavin et al., 2008).

Table 6-13 Pathway enrichment analysis in resistant cell lines.

Pathways/Terms found enriched in the indicated databases for each of the resistance derivatives.

Cell line	Ingenuity (top canonical pathways)	KEGG (adjP<0.05)	GO (p<0.02)
UWB1.289-699R	Cyclins and Cell Cycle Regulation (p=3.25E-05) Isoleucine Degradation I (p=7.78E-05)	Cell cycle (adjP=0.0005) Metabolic pathway (adjP=0.042)	Apoptosis (adjP=0.001) Amino acid metabolism (adjP=0.001) Protein binding (adjP=4.99e-08)
UWB1.289-CDDPR	Mitochondrial Dysfunction (p=1.32E-03) Protein Ubiquitination (p=1.63E-03) Putrescine Degradation III (p=3.30E-03)	Metabolic pathways (adjP=0.004) Glycosphingolipid biosynthesis (adjP=0.04) Ribosome biogenesis (adjP=0.04)	Apoptosis (adjP=0.009) Ribosome biogenesis (adjP=0.009) Cellular component biogenesis (adjP=0.0004) Response to chemical stimulus (adjP=0.001) rRNA metabolic process (adjP=0.009) Response to oxidative stress (adjP=0.009)
UWB1.289-IR	Histamine Degradation (p=8.96E-04) Fatty Acid oxidation (p=1.79E-03)	-	Protein binding (adjP=0.002)
PEO1-699R	Cleavage and Polyadenylation of Pre-mRNA (p=1.09E-03) Actin Nucleation (p=1.62E-03) Regulation of Actin-based Motility (p=5.64E-03) Endocytosis Signalling (p=7.16E-03)	Fc gamma R-mediated phagocytosis (adjP=0.0009) Regulation of actin cytoskeleton (adjP=0.005)	Actin polymerization (adjP=0.01) Negative regulation of chemotaxis (adjP=0.01)
PEO1-CDDPR	Endocytosis Signaling (p=2.13E-03) Phagosome maturation (p=6.03E-03) Phosphatidylcholine Biosynthesis (p=6.60E-03) Superoxide Radicals Degradation (p=6.60E-03)	-	Cellular component organization (adjP=0.005) Cell morphogenesis and migration (adjP=0.01) Cell-substrate junction assembly (adjP=0.01) Cell growth (adjP=0.014) Signal transduction (adjP=0.014) Protein binding (adjP=1.60e-05)
PEO1-IR	Mismatch Repair (p=6.17E-03) Cell junction signalling (p=6.26E-03) ERK5 Signalling (p=1.11E-02)	-	Tumour necrosis factor receptor binding (adjP=0.007)

Table 6-14 Genes with mutations and altered expression in derived cell lines and previously reported links to human cancers.

Derived cell line	Gene	logFC	AveEx pr	t	adj.P. Val	Reported in	Ref
UWB1.289-699R	EFEMP2	-1.33	8.48	-8.62	0.00	Biomarker for early detection of colorectal cancer	(Yao et al., 2012)
	PCNXL4	-0.65	9.09	-4.74	0.01		
	TIAM2	0.59	8.01	4.23	0.01		
UWB1.289-CDDPR	SOD2	-1.11	9.92	-10.70	0.00	Increased risk of ovarian cancer and pro-survival in ovarian cancer cells <i>in vitro</i> . Implicated in lung, colon and prostate.	(Dier et al., 2013, Miar et al., 2015)
	LRSAM1	0.75	8.89	10.07	0.00		
	PDE2A	0.82	7.14	7.06	0.00		
	LTBP4	0.84	7.40	4.91	0.01		
	GNL3	-0.62	10.67	-4.73	0.01	Biomarker predicting treatment response in breast cancer Metastasis susceptibility gene in prostate cancer	(Tamura et al., 2010, Lee et al., 2015)
UWB1.289-IR	ETFA	-0.61	10.51	-6.08	0.00		
	PHLDB1	0.81	8.24	4.80	0.01		
	LAMA1	0.63	7.05	3.95	0.04		
PEO1-699R	LZTR1	-0.66	8.56	-5.95	0.02		
PEO1-CDDPR	DLX1	-0.98	8.42	-5.50	0.00		
	SF3A3	0.61	10.22	4.99	0.01		
	ABCA1	0.92	7.03	4.06	0.02	Poor prognosis in serous ovarian carcinoma	(Hedditch et al., 2015, Chou et al., 2015)
	PCCB	0.70	10.39	4.03	0.02		
	LAMB3	-0.89	9.32	-3.72	0.04	Susceptibility gene in cervical cancer Pro-metastasis gene in lung cancer	(Wang et al., 2013b, Zhou et al., 2010)

6.4.6.3 *Genes with Mutations and Altered mRNA Expression*

A subset of genes was noted in which gene mutations were accompanied with an altered expression (Table 6-14), with either up or down regulation at the mRNA level. Assessment of the protein level alteration is needed before the functional effects can be ascertained, however these genes may potentially be important resistance targets. Of the genes in Table 6-14, two, *ABCA1* and *SODS2* have previously been reported in association with ovarian cancer. *LAMB3*, *EFEMP2* and *GNL3* have been reported in association with other human cancers, and may be potential targets for chemo-resistance.

6.4.6.4 *The Expression of Potential Target Genes in PCO Cultures*

The effect of gene alteration on survival would provide the greatest information of the role of these targets in resistance development. However, publically available databases that contain gene alteration and survival outcomes are for patients treated with standard therapy and not PARPi. Therefore, targets for PARPi resistance may not have a measurable effect on survival outcomes. In order to address this question, a selected sample of PCO cultures were assessed for gene expression, and for rucaparib and cisplatin resistance *in vitro*. Differences for the expression of potentially important genes were assessed.

Of those genes assessed, *SERPINE2* and *IER3* were significantly differentially expressed between the rucaparib resistant and sensitive PCO cultures (Figure 6-17). In PCO cultures, expression was higher in resistant cohorts, but expression from this gene was downregulated in the resistant cell line derivatives. *IER3* gene expression was found to be significantly lower in resistant cell lines and PCO cultures, and may therefore be an important target to explore in further studies. Of the potential targets selected for platinum resistance, no significant differential gene expression was noted in PCO cultures (Figure 6-18).

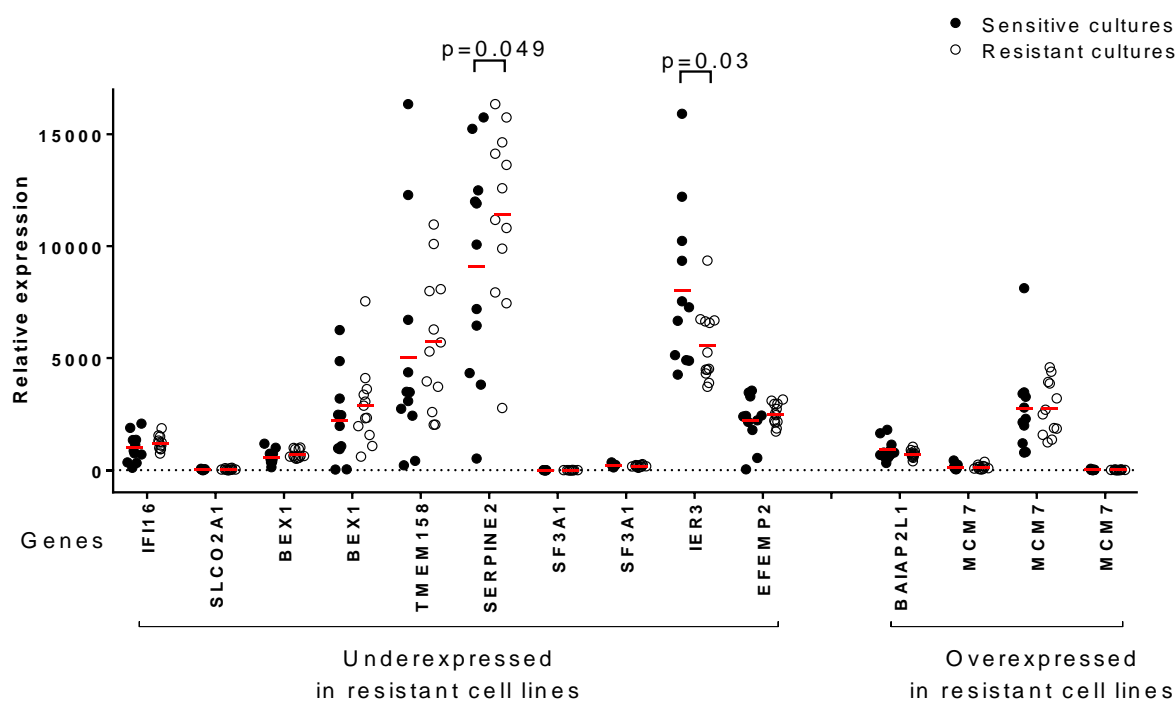


Figure 6-17 Expression of potential rucaparib resistance target genes in PCO cultures.

Expression was assessed by full genome array. Expression of individual genes was plotted by level of PCO sensitivity to rucaparib, assessed by SRB assay.

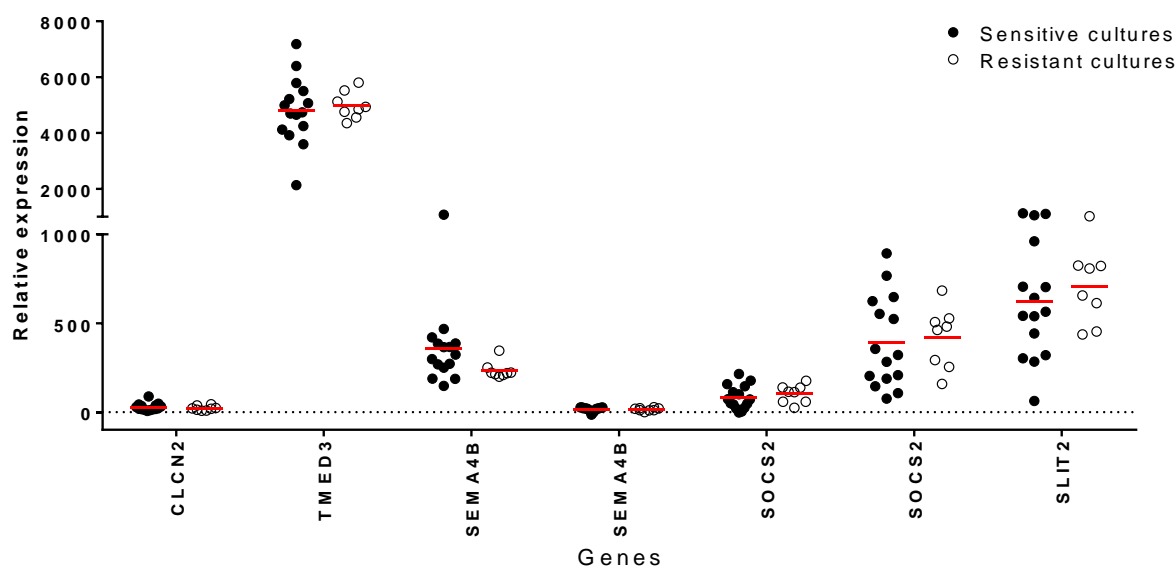


Figure 6-18 Expression of potential cisplatin resistance target genes in PCO cultures.

Expression was assessed by full genome array. Expression of individual genes was plotted by level of PCO sensitivity to cisplatin, assessed by SRB assay.

6.5 Summary of Chapter

In this study resistant cell lines were derived from *BRCA* mutant ovarian cancer cell lines by continued exposure to cisplatin, rucaparib or fractionated irradiation.

Characterisation of these cell lines found that:

- Cell lines derived by exposure to cisplatin and rucaparib were cross resistant to both drugs, whereas, cell lines derived by fractionated irradiation were only resistant to cisplatin.
- Cell lines derived by increasing the concentration of cisplatin and rucaparib were HRC.
- No significant alteration in NHEJ or BER pathways was seen in resistant derivatives.
- Multiple mutations were noted in all derived cell lines, compared to parent lines. The majority were somatic single nucleotide alterations.
- Genome expression arrays found a number of gene expression levels to be altered. Gene expression levels of each parent cell line derived lines were very different from each other.
- A few potential targets for resistance mechanisms were identified, which had altered expression in common across all rucaparib or all cisplatin resistant lines.

6.6 Discussion

In this study six resistant cell lines were derived from two parent HRD cell lines. In both models cells grown in either rucaparib or cisplatin were resistant to both agents. Therefore, significant overlap between the two resistance mechanisms is evident. In both models, cells which were irradiated were resistant to cisplatin, but not rucaparib, thus suggesting that some mechanisms which result in cisplatin resistance do not produce resistance to rucaparib. This is evident from studies demonstrating the response of cisplatin resistant tumours to PARPi in clinical trials (Fong et al., 2010).

6.6.1 *Regaining of HRC is Associated with Rucaparib Resistance*

In these models rucaparib and cisplatin derived resistant cells regained HR function. Irradiation derived cell lines did not regain HR function. Results from this study confirm the importance of the HR function in rucaparib resistance reported in the

literature (Sakai et al., 2008, Swisher et al., 2008, Edwards et al., 2008, Barber et al., 2013, Norquist et al., 2011). However, in contrast to published reports, reverse mutations in *BRCA* were not found in any of the resistant cell lines. Also, no significant change in expression level of *BRCA* were found in any of the resistant cell lines. Epigenetic alterations and protein expression of *BRCA* genes was not assessed in this study. Furthermore, the genome expression arrays carried out did not include microRNA, and so the expression of microRNA miR-182 which negatively influences *BRCA1* expression (Moskwa et al., 2011) could not be assessed. Therefore alteration in *BRCA* function may still be a potential mechanism for HRC recovery however, not by mutation or *BRCA* genes.

A somatic point mutation in 53BP1 in PEO1-699R was noted in 33 % of reads. This translates to 66 % of cells harboring a 53BP1 mutation. The evidence from the literature supports an interaction of 53BP1 with *BRCA1* (Bunting et al., 2010, Brandsma and Gent, 2012, Oplustilova et al., 2012). The PEO1 cell line harbors a *BRCA2* and not a *BRCA1* mutation. Therefore, mutations in 53BP1 may also have a role in regaining HR competence beyond interaction with *BRCA1*. An increase of HR function by 53BP1 mutation could be the explanation for gaining HR function in this cell line, and may be linked to rucaparib resistance. However, further assessment of this interaction is required before conclusions could be drawn. Also 53BP1 mutations were not found in any of the other derived cell lines, therefore, it alone is unlikely to explain HR function recovery.

RAD51B mutations were noted in all three UWB1.289 derivatives. The most likely explanation for finding the same point mutation in all three cell lines is that this mutation is found in a subclone of the parent line. UWB1.289-IR also harbors the *RAD51B* mutation, however this cell line derivative did not regain HR function. It is therefore unlikely that this mutation has an important role in HR function or rucaparib resistance. *RAD51B* mutations have been reported as a predisposition risk for breast cancer (Golmard et al., 2013, Orr et al., 2012). The patient from whom the UWB1.289 cell line was derived developed breast cancer at age 42, followed by ovarian cancer at age 54. Therefore, as well as the *BRCA1* mutation, the *RAD51B* mutation may be a germline mutation that this patient carried. As germline DNA for this patient is not available this hypothesis cannot be confirmed.

Mutations in a number of NER pathway genes were also noted in derived cell lines. These include *ERCC1*, *GTF2H1*, *RAD23B* and *ERCC2*. Platinum-based chemotherapy forms DNA adducts, which subsequently inhibit DNA replication. Removing platinum intra-strand DNA adducts requires the NER pathway. Links between NER defects and platinum sensitivity are well described. However, a recent study, using the TCGA ovarian dataset, has described a subgroup of HGSOC with NER alterations associated with a phenotype of platinum sensitivity similar to that of *BRCA1/2* mutated tumors, with improved OS and PFS (Gayarre et al., 2016, Ceccaldi et al., 2015b). Importantly however, NER alterations were also linked to PARPi resistance. The reported alterations were polymorphisms of genes *ERCC4* and *ERCC6*, which were not noted to be mutated in resistance lines from this cohort (Ceccaldi et al., 2015b). However, an *ERCC1* mutation was noted in the UWB1.289-699R cell line in this project. Therefore, NER defects may have a potential role in rucaparib resistance in this cell line. Validation of NER pathway function in all the cell lines is required before any conclusions could be drawn.

6.6.2 NHEJ Pathway was not Altered During Resistance Development

Contrary to the evidence of NHEJ function in the resistance to rucaparib in the literature and in chapter 4, no change in NHEJ function was found in any resistant cell lines. The explanation for this may be that NHEJ function is an inherent determinant of sensitivity, and is not an acquired resistance mechanism. Further evidence for this is the fact that the BRCA competent counterparts of these cell lines had the same NHEJ function as the BRCA defective cell lines at the start of the study. Cisplatin has been shown to inhibit NHEJ function in this study and by other groups (Diggle et al., 2005). The fact that NHEJ function remained unchanged after cisplatin treatment was removed would suggest that NHEJ inhibition by cisplatin is only a temporary effect whilst the drug is applied to the cells. This finding needs to be further assessed as it may have important implications for clinical practice.

Combination therapy is commonly used in the treatment of ovarian cancer, a number of trials are underway combining platinum and PARP inhibitors. These include phase one trials to assess the maximum tolerated dose of olaparib in combination with carboplatin (NCT02418624), as well as in combination with carboplatin and/or paclitaxel (NCT00516724) and a phase 1b trial of olaparib plus weekly carboplatin and paclitaxel in relapsed ovarian cancer (NCT01650376). Therefore, as NHEJ inhibition results in PARPi resistance, the combination of PARPi and platinum based

therapy could be predicted to have no significant benefits. Results of ongoing combination trials will be important for observation of this effect.

6.6.3 Mutations Signatures are Dependent on Pre-existing Defects and Drug Treatment

The mutation signatures obtained were very different for each derived cell line. This echoes a number of studies in the literature which all report different signatures for resistance. Furthermore, the signatures for resistance to different drugs, whilst very different, resulted in cross resistance in -699R and -CDDPR derivatives. This finding suggests that mutations in the cells are dependent on existing defects, as well as the drug treatment used. The important differences observed were between the number of mutations noted in UWB1.289 derivatives, compared to PEO1 derivatives treated with rucaparib and irradiation. The relatively few mutations in PEO1 cell lines suggest that the resistance in this line is more likely to be clone selection, rather than mutation based. This cannot be concluded without validating each mutation that was found.

No point mutations in PARP-1 were noted in these resistance cell lines, and PARP-1 expression at mRNA level was not significantly altered. Due to the time limit of this study, PARP activity was not assessed, which may provide important answers into the resistance mechanisms of these cell lines.

Mutations in PI3CA/AKT and MAPK pathways were found in all resistant cell lines, and therefore are likely to have an important role in platinum resistance. Again, as mutations in these pathways are found in all derivative cell lines, these are likely to be a generic resistance mechanism, as described in the literature.

6.6.4 Gene Expression Signatures are Dependent on Pre-existing Defects and Drug Treatment

Expression array analysis demonstrated that the derivatives of the two cell lines were very different from each other. This adds further evidence to the complexity of resistance development, as both cell lines were exposed to the same drug and irradiation treatments at the same time. The evidence for the significant difference between RNA profiles of cells resistant to different drugs has previously been published (Sherman-Baust et al., 2011, Koussounadis et al., 2014). The results from

this study provide support to the notion that resistance development is both drug and tissue specific. A possible explanation for this clear difference may be that the majority of the resistance mechanisms are found in subclones in the parent lines and the drug treatments select for these subclones. This is supported by the finding of a number of mutations which were selected for from parent to resistant line. Therefore, assessing the common expression profiles of all the derived cell lines resistant to rucaparib, from PEO1 and UWB1.289 derivatives, produced a short list of potential targets for rucaparib resistance. An assessment of literature has noted that a number of these targets have been reported to be associated with either cancer susceptibility, metastasis, drug resistance or poor outcome. However, most of the evidence is from small studies in different cancers. Assessment of publically available databases, such as the TCGA database, provides some insight into the role of targets in ovarian cancer chemo-sensitivity; however, as the patients in the database were treated with standard platinum therapy and not PARPi, it does not provide all the answers. An assessment of these targets in a rucaparib treated population is required for full validation.

6.7 Further Work

To validate the findings of this study, identified targets will need to be validated. This is planned to be done firstly by RT-qPCR of the selected top candidates of the genes. Furthermore, as protein expression can be altered post transcription, western blotting validation is required for the top candidates. Validation of these targets by experimental inhibition / upregulation is then required to assess their function. The assessment of BRCA1 and BRCA2 protein expression is especially important, as the literature reports BRCA mutations as the mechanism for HR recovery. Protein expression and function of other proteins involved in HR would give a greater insight, demonstrating any post translational modification which resulted in HR recovery.

An assessment of the other DNA repair pathways documented to result in platinum resistance needs to be undertaken in the resistant cell lines. This includes NER and MMR function of all derived cell lines. These assays were not performed in the laboratory at the time of this project, but the NER assay has now been optimised (Woodhouse et al., 2014) and assessment of these cell lines is planned. Assessment of PARP activity in resistant cell lines would also provide further insight into PARP resistance.

Important further work planned, is to develop xenografts from the parent and derived cell lines, and assess their biology *in vivo*. This would give insight into tumour development and the spread of HR defective and HR recovered resistant cell lines.

Increased understanding of the underlying genetics and aetiology of ovarian cancer provides further insights into its complexity, and subsequently, the hope that a single cure will be developed begins to dissipate. A major limitation for the treatment of ovarian cancer is the late stage of presentation. The search for effective screening tools has so far failed to translate into improved outcomes (Menon et al., 2009). Earlier diagnosis would rely on a better understanding of the development and progression of ovarian cancer. It is therefore more realistic, whilst further understanding is being gathered, to concentrate on life prolonging treatment and patient selection for treatment, rather than a cure. The immediate aim should therefore be to turn ovarian cancer into a chronic disease, rather than the 'silent killer' which it is currently regarded as.

Surgery plays an essential role in the management of ovarian cancer, and this should be undertaken at a time when complete cytoreduction is thought to be achievable. A good response at presentation is observed from the combination of platinum and taxane agents, and more recently by addition of bevacizumab. At relapse the development of resistance limits the available choice of agents. The polypharmacy of secondary chemotherapy agents has not been shown to be effective. Furthermore, the toxic profile of most of the available agents, coupled with the typically advanced age and multiple comorbidities of patients, limit the use of polypharmacy (Markman, 2009). A better treatment strategy would be to select patients for the appropriate treatment at the appropriate stage of the disease, based on the biomarkers for response. This strategy is restricted by our limited ability to accurately predict the response to treatment. Further understanding of the response and resistance mechanisms, for not only standard chemotherapy, but also novel agents and biomarkers to predict response is essential. This understanding would not only allow prediction and monitoring for resistance development and clinical relapse, but also selection of the most appropriate novel agents for each phase of treatment, which may add overall survival benefit, whilst limiting toxicity.

DNA damaging chemotherapy has been at the forefront for cancer therapy since the discovery of nitrogen mustard (Gilman, 1963). Genomic instability is an enabling characteristic of cancer (Hanahan and Weinberg, 2011), with dysregulation of DNA repair contributing to the instability, and ovarian cancer is no exception.

Chemotherapy drugs have become increasingly more targeted, however, they still rely on the underlying derangement of DNA repair mechanisms in the cancerous cells. DSBs are the most toxic form of DNA damage, and if unrepaired result in cell death. The application of PARPi in clinical practice is currently limited to *BRCA* mutant tumours. This is based on the association of HRD with sensitivity to PARPi. However, DSBs are repaired by the three pathways described so far, and in ovarian cancer only HR has been evaluated. Also, understanding of the interaction of the three pathways is still incomplete. This project addressed the function and interaction of the two main DNA DSBs repair pathways NHEJ and HR, and their role in determining chemo-sensitivity.

7.1 Summary of Results

A summary of the main objectives, and the additional objectives added during the evolution of the project are shown in Table 7-1.

Table 7-1 Project aims and outcomes

Aim	Comment	Publication / presentation
To characterise PCO cultures	PCO cultures were successfully derived with an 88 % success rate. Varied growth and expression of epithelial antigens and CA125 was noted. 46 % of PCO cultures were found to be HRD and associated with increased sensitivity to rucaparib and cisplatin <i>in vitro</i> , but not survival outcomes.	(ODonnell et al., 2014)
To characterise a novel ovarian cancer cell line	NUOC-1 cells were found to be of epithelial origin, and to be hormone receptor negative, but tyrosine kinase receptor positive. NUOC-1 cells were found to be wildtype for <i>P53</i> and <i>PTEN</i> , but to carry mutations in <i>ARID1</i> . NUOC-1 cells were HRC and NHEJC, but BER deficient. Two subpopulations of NUOC-1 were derived which contain a number of differences including copy number changes and MYC amplification. New genomic alterations occurred during the growth of each cell line.	Manuscript submitted for publication
To assess the role of PTEN in ovarian cancer	PTEN mutations in ovarian cancer are rare, but may be associated with a survival benefit. Inhibition of PTEN is a potential chemo-sensitiser.	(McCormick et al., 2016)

To assess NHEJ function in PCO cultures and correlate with sensitivity to rucaparib and cisplatin	Assays to assess NHEJ function were optimised, and 40 % of PCO cultures were found to be NHEJD. HR and NHEJ function in PCO cultures were independent of each other. Intra-tumour heterogeneity of NHEJ function was noted. NHEJD was associated with resistance to rucaparib. When combined together, only HRD/NHEJC cultures were sensitive to rucaparib. Cisplatin inhibited NHEJ function.	Oral and poster presentations. Manuscript provisionally accepted by Clinical Cancer Research
To assess the interactions of NHEJ and HR pathways in ovarian cancer biology	ATR and DNA-PK inhibition was found to be cytostatic. DNA-PKi resulted in reduced recognition and delay in DSBs repair and increase in HR. Inhibition of ATR resulted in reduced DSBs recognition and reduction in HR. Combination of the two inhibitors resulted in continued HR, suggesting an alternative activation. DNA-PKi induced radio-sensitisation, whilst ATRi induced sensitisation to cisplatin and rucaparib in NUOC-1 but not OSEC2 cells.	Poster presentation
To assess the interactions of NHEJ and HR with PARP-1	PARPi inhibited DSBs recognition and repair. Combination of PARPi and DNA-PKi resulted in a delay in DSBs repair, and synergistic increase in HR. The combined inhibition of ATR and PARP caused a reduction in DSBs recognition, but an increase in HR, overcoming the inhibition of HR by ATRi.	
To develop rucaparib and cisplatin resistant cell lines, and to assess the role of DNA repair in resistance	Resistant cell lines were derived from two HRD cell lines. Cross resistance between rucaparib and cisplatin was linked to HR recovery. Cisplatin resistance in the HRD cell line model was also noted. NHEJ and BER pathways were not altered in resistant cell lines.	Poster presentation
To perform genome-wide molecular analysis to investigate the mechanisms of resistance	A number of mutations and gene expression alterations were discovered in resistant cell lines. BRCA1 deficient cell line derivatives were found to contain more mutations, compared to BRCA2 deficient cell line derivatives. No <i>BRCA</i> revertant mutations were noted in any of the resistant lines. No single target for resistance was identified.	Will form the basis for subsequent grant applications

7.2 Models for the Research of Ovarian Cancer

Two models for the study of ovarian cancer biology were characterised: primary cultures and a novel ovarian cancer cell line. The use of primary ascitic cultures, described in this project, has provided a valuable resource for the study of ovarian cancer biology. Use of this model has many advantages over commercially available cell lines, but also has several limitations. The heterogeneity of PCO cultures in terms of antigen expression, growth rate, morphology, and DNA DSB repair is now clear. Whilst the multiple biopsy cohort in this study was small, intra-tumour heterogeneity of NHEJ function was also evident. Without assessing the intra-tumoural heterogeneity, it is unrealistic to expect a single assay to accurately predict the response to a particular cytotoxic agent, and there is a danger that clinical trials that do not take this into account may underestimate the actual clinical benefit.

Cell lines are the most commonly used models to study ovarian cancer with a number of advantages; including high proliferative capacity, clonogenicity and extended life span in culture. However, a number of disadvantages have also been reported with acquired genetic alterations from their cells of origin and loss of heterogeneity (Daniel et al., 2009, Domcke et al., 2013). Furthermore, the majority of the most commonly used cell lines have been shown not to represent HGSOC (Domcke et al., 2013). These disadvantages question the application of many cell lines as models for the heterogeneous nature of ovarian cancer. However with increasing understanding of the genomics of ovarian cancer, appropriate cell lines models can be selected. The novel ovarian cancer cell line (NUOC-1), has provided further insight into the complexity of ovarian cancer, as well as clonal evolution during the growth of the cell line. The mixed population of NUOC-1 cells represents a better model for the study of the heterogeneous nature of ovarian cancer compared to cell lines derived from single clone cells. Further models of this nature are required for the academic community.

An important aspect to consider for the academic community is the difference between protein absence and protein inhibition. In this study opposing results were found between absence and inhibition of PTEN and of DNA-PKcs. Previous groups have also reported that experimentally knockdown protein in cell line models do not behave like cancer cells developed in absence of that protein (Hunt et al., 2012, Middleton et al., 2015). The differences may be due to the accumulated genetic

aberrations in absence of PTEN or DNA-PKcs. However, inhibited protein may also produce effects which are not seen in its absence; namely DNA-PKcs auto-phosphorylation is thought to be necessary for its dissociation from DNA for the NHEJ pathway to complete DSB repair. DNA-PKcs binding to DNA DSB may also obstruct the recruitment of HR protein. Therefore, inhibition of the kinase activity may hinder DNA-PKcs dissociation and hence further impair DNA repair, leading to cell death. These differences between inhibition and knockdown have also been observed for PARPi (Horton and Wilson, 2013), ATMi (Yamamoto et al., 2012) and for the combination of NU7441 and VE-821 ATRi (Middleton et al., 2015). The differences between the role of the protein and the pathway also need to be considered. Many protein involved in DNA repair have other described functions, therefore, inhibition may exert effects through the alternative roles. An example of this is increased sensitivity of Ku80 but not in DNA-PKcs defective cell lines to ATRi VE-821 (Middleton et al., 2015).

7.3 DNA DSBs Repair in Ovarian Cancer

This study provides growing evidence of the degree of dysfunction within the DNA repair pathways in ovarian cancer. This is the first study to assess NHEJ function in primary ovarian cancer and to quantify the frequency of the deficiencies. Importantly, this study has shown that whilst inhibition of NHEJ results in an increase in HR, the competencies of the two pathways in PCO cultures are independent. Therefore, assessment of both pathways is needed for best selection of patients for treatment with PARPi. The lack of assessment of NHEJ function may be one of the factors responsible for the variable response to PARPi seen in clinical trials (summarised in appendix 2).

The evolution of HR and NHEJ loss within the pathogenesis of ovarian cancer remains however unknown. Whilst evidence exists for the loss of HR being a driving mechanism for ovarian cancer, understanding of NHEJ is lacking. The evidence from this project suggests that NHEJ is an inherent mechanism of resistance, and not acquired during treatment. Evidence in the literature shows a reduced NHEJ function in the healthy cells of cancer patients (Bau et al., 2007) – does this mean that NHEJ is a driver for carcinogenesis? The assessment of NHEJ function in healthy cells of ovarian cancer patients is still required.

The third mechanism of DSBs repair, A-EJ, was not formally assessed during this project, however, evidence is building for the role of A-EJ in ovarian cancer, (Ceccaldi et al., 2015a, Mateos-Gomez et al., 2015). In this project evidence of A-EJ was also seen in primary cultures which were NHEJD. Formal assessment of A-EJ and its interaction with HR and NHEJ still remains to be investigated.

Further to the three DNA DSBs pathways, three DNA SSBs repair pathways have been described. All of these have also been shown to have variable functions, with clinical implications in ovarian cancer. However, DNA repair is only a small fraction of the biological function in the cell, with a number of other pathways altered in ovarian cancer. As the ability to profile tumours continues to grow, and the effects of molecular aberrations on overall function of the cells and subsequent response to therapy increases, then more questions arise. If multiple pathways are dysfunctional, then how will the pathways interact? Are there dominant pathways or mutations that are most important, and if present, do they dictate management? Understanding the interplay of all the important pathways in ovarian cancer, alongside the highly variable and influential clinical factors, is a sizable challenge for the academic community. This challenge is perhaps unachievable using current technologies and with groups working in isolation on single aspects. The introduction of novel technologies, such as biological programming with artificial intelligence systems (Enshaei, 2015), will allow greater profiling and selection of patients for the best available therapy.

7.4 Prediction of Response to PARPi

Olaparib has been licensed for clinical use for BRCA mutated patients. It has been recently demonstrated that 15-20 % of ovarian cancers are BRCA mutated, and therefore mainstream clinical testing for germline BRCA mutations is being rolled out at present. However, this approach will limit the number of patients who are likely to benefit from PARPi, due to much higher rates of HRD in the ovarian cancer population. Conversely, not all patients who harbor a *BRCA1/2* mutation are HRD, and are therefore there will be non responders to PARPi in this group. NHEJ function will not be assessed in these patients. Results from this and previous studies have demonstrated NHEJD results in resistance to PARPi. Furthermore, the loss of the 53BP1 protein has been shown to restore PARPi resistance in previously sensitive *BRCA1* mutant models. As demonstrated in chapter 6, *BRCA* mutated cancers can

develop HRC during the process of resistance development through cell and drug specific complex mechanisms, which are yet to be fully understood. Therefore, these patients will be wrongly selected for a treatment from which they will not benefit.

Identification of HRD cells by a functional RAD51 assay, and NHEJD cells by a functional end joining assay, have been described in this study. The function of both of these pathways has been shown to affect *in vitro* sensitivity to PARPi. Application of these assays in clinical practice would allow the selection of patients for the correct treatment, however, this approach is still a long way off. A number of weaknesses in using such assays have previously been put forward, although many of which have been addressed. Firstly, obtaining viable replicating cancer cells from patient sources, such as ascites or pleural fluid. The growth and storage of ascitic fluid cultures was optimised in chapter 3, with an 88 % success rate. Expanding the use of the assay to solid culture biopsies (ODonnell et al., 2014) and effusion from other cancers (Patterson et al., 2014) widens the applicability of the assay.

There is a risk that in developing primary cultures one might exhibit a selection pressure on the cell tumour burden. Significant differences have been described between cultured cells and primary tumour samples. Heterogeneity between the ascites that the NUOC-1 cell line was derived from, and the solid tumour from the same patient, as well as observed clonal evolution, further demonstrates these differences. Therefore, functional assays need to be optimised to use fresh tissue, without the development of primary cultures. An example of this, NHEJ function using the monomer end joining assay can be assessed directly using fresh solid samples, as described in chapter 4 and also previously described in bladder cancer (Diggle et al., 2003). Efforts were also made to adapt the HR assay to be used on fresh tissue (ODonnell et al., 2014), however, this has so far been unsuccessful and needs further study.

Another challenge for the development of biomarkers is that the DNA repair function may be dependent on the tumour environment. For example, Chan and colleagues demonstrated that chronic hypoxia results in the reduced synthesis of essential HR proteins, with a three-fold reduction in HR capacity and increased sensitivity to DNA damaging agents and PARPi (Chan and Bristow, 2010, Chan et al., 2008). This is supported by recent findings that antiangiogenic treatments increase the sensitivity of

cancers to PARPi (Benafif and Hall, 2015). Hypoxia is a common feature of solid tumours, however may not be replicated in laboratory environment.

A number of genome wide sequencing approaches are being explored to predict HR function. These include sequencing of all HR genes (Turner et al., 2004, Pennington et al., 2014), gene expression profiling (<http://www.almacgroup.com/news/almac-validates-novel-test-for-ovarian-cancer-patients>), assessing methylation (Ibragimova and Cairns, 2011), and patterns of genomic profiling (Abkevich et al., 2012, Stefansson et al., 2009). However, as shown in chapter 6, it is not always possible to predict HR function from gene mutations or expression studies. More recently combination scores encompassing a number of tests, such as genome wide SNP profiles, BRCA1/2 mutation screening, and BRCA1 promoter methylation data combined HRD score have been explored (Timms et al., 2014). These assays utilise high through put technology, do not rely on live cells and have demonstrated an association with HRD and cisplatin sensitivity (Telli et al., 2016). Patterns of genomic profiling may be acquired during cancer development in HRD tumours, however, tumours whose genome has undergone one or more events that restore HR function are likely to be misclassified as HRD as a result of prior repair deficiency and its genomic scarring (Watkins et al., 2014). Proposals have been made to integrate a genomic scar-based biomarker with a marker of resistance in an attempt to improve the performance of any companion diagnostic for PARPi, but as yet this has not been tested in clinical samples (Watkins et al., 2014). Furthermore, as demonstrated in chapter 6, clear biomarkers for resistance to PARPi are still required. In the current climate, the cost of genomic studies also need to be taken into account, as it is currently not practical for every cancer patient to undergo genomic profiling of the tumour.

7.5 New Treatment Strategies for Ovarian Cancer

Unlike other cancers, development and approval of new chemotherapy agents in ovarian cancers has been limited in the last decade. Bevacizumab and Olaparib are the first two drugs to have been approved since 2006. This is likely to be due to the improved understanding of ovarian cancer biology and the move away from managing ovarian cancer as one disease. These new therapies move us a step closer to targeted therapy, and make ovarian cancer an exciting field of development, both academically and clinically. A combination of debulking surgery paired with the

proven most effective cytotoxic agent, platinum, should remain central to the primary management. However, the addition of targeted agents should be based on biomarker selection. Importantly, in view of tumour heterogeneity, it is the residual tumour that cannot be excised at the time of surgery that should be sampled for biomarker selection, as it is this residual tumour that will expand and cause relapse/recurrence, and therefore, it is the biology of this tumour that is important for targeted therapy.

In view of the altered function of HR in a resistance setting, as shown in chapter 6, at the time of relapse, the tumour should be re-biopsied and re-characterised with regards to a biomarker panel. This will enable the selection of the subsequent targeted cytotoxic agent, and thus enable the provision of an effective therapy, whilst minimising side effects and, hopefully, improve the survival for the patient.

However, this treatment strategy is not currently possible. Despite the excitement from the introduction of the new drugs, the current choice of cytotoxic agents available for the treatment of ovarian cancer is relatively limited. Furthermore, no current treatments have been paired with a reliable biomarker. This project adds to the understanding of sensitivity of ovarian cancer to PARPi and platinum agents. Further mechanisms of sensitivity and resistance still need to be explored to ensure the correct selection of therapy with minimal toxicity. Further novel agents also still need to be developed, which will work predictably in cancers identified by a clinically useful assay to be sensitive to that agent.

A major finding of this study is the complex mechanism of resistance development to cisplatin and rucaparib. This study adds to the knowledge of tissue and drug specific mechanisms of resistance. Furthermore, the results demonstrate that in addition to the published mechanisms of HRC recovery, there are likely to be further mechanisms that will need to be explored.

As well as novel therapies and patient selection, patient monitoring also needs to be updated. RECIST (Response Evaluation Criteria In Solid Tumours) is a set of published rules that define responsive, stable or progressive disease during treatment (Eisenhauer, 2009). RECIST helps to categorise tumours based upon their radiological appearance, giving an overall summary of the changes seen. With the knowledge of the presence of intra-tumour heterogeneity and the appreciation that

distinct areas of tumour are likely to behave differently, modification of RECIST may be needed to enable the description of individual tumour areas.

7.6 Strengths and Weaknesses of This Project

There are numerous models for the study of cancer that can be applied by the research community, and a broad selection of these were used throughout this study. The demonstration of the differences between experimental alteration of a target, compared to the biological absence in clinical samples is an important strength of this project. Whilst this does mean that conflicting results were found in some cases, it demonstrates the importance of good models, and use of primary tissue to elucidate true roles of targets in ovarian cancer.

A significant limitation of this project is the lack of complete assessments of the mechanisms of resistance in chapter 6. This was mostly due to time limitations, as the resistance development took significantly longer than initially expected, thus limiting the remaining time for characterisation. Importantly, however the results obtained provide evidence of extreme complexity of resistance development. This provides an explanation for why, despite extensive research and a number of suggested targets, chemo-resistance remains a huge burden to the treatment of ovarian cancer. This work will also form the basis of a planned grant application.

The heterogeneous group of primary cultures, in terms of histological subtypes, timing and outcome of surgery, initially appears to be a limitation of this project; especially in regard to the current move of clinical trials to separate different histological subtypes. However, this is also a great strength of this project, as it demonstrates that functional characterisation of tumours is a superior method of categorisation, compared to histology, in predicting outcome or response to treatment.

The fact that the patients were treated with standard therapy and not PARPi was another important limitation of this study, as the effect on clinical survival could not be assessed. However, one strength of our study, in terms of clinical, pathological and survival data, is that it was a prospective study collecting sequential samples. The clinicians involved in managing the patients were not aware of the *in vitro* results from any of the samples.

The limited number of solid samples is an important limitation of this study. However, even this number was able to provide evidence of tumour heterogeneity, in terms of NHEJ function, and provides sufficient pilot data to justify a larger trial. Clearly, standardisation of the number and location of biopsies and a larger number of participants will be required for a meaningful analysis of the effect of heterogeneity upon patient outcome.

7.7 Future Work

The work in this study adds to the growing evidence regarding the importance of the DNA DSBs recognition and repair pathways within ovarian cancer. However, it has also generated a number of further questions. In order to answer these questions, a number of potential future projects are being considered. The immediate plan for the NUOC-1 cell line is to make the cell line commercially available, and to undertake a MYC project in collaboration with Prof JM. Allan, utilising the isogenic nature of the two NUOC-1 subcultures in terms of MYC amplification. Validation of the targets that have been identified by SNP array in NUOC-1 cell line, is also planned.

The assessment of NHEJ function in a larger cohort of fresh / frozen tumour tissue, along with biomarker expression in PARPi treated patients is required to gather further evidence for the role of NHEJ function in ovarian cancer. As recognition and repair of DSBs in NHEJD cells is lower than NHEJC cells, it may be possible to predict NHEJD cultures by experiments, such as single point comet assay. This needs to be explored alongside assessment of NHEJ function.

In vivo xenograft studies to confirm ATRi and DNA-PKi interactions are required. *In vivo* experiments would also allow toxicity of the combinations of inhibitors with chemotherapy agents to be evaluated.

To validate the findings of the resistance mechanism study, a number of further experiments are planned, and the identified targets will need to be validated. In the first instance, this is planned to be done by RT-qPCR of the selected top candidates of genes. As the protein expression can be altered post transcription, western blotting validation is required for these candidates as well. The next step of validation planned is to perform resistance target identification, by experimental knockdown or upregulation of selected targets, and to assess if sensitivity is restored in the

resistant cell lines. Assessment of PARP activity in resistant cell lines would also provide further insight into PARP resistance.

To gain further understanding into the mechanism for HR recovery, it is important to assess the protein expression and function of individual HR genes. This would provide a greater insight into any post translational modification which resulted in HR recovery. An assessment of the other DNA repair pathway documented to result in platinum resistance, would need to be undertaken in the resistant cell lines too. This includes NER and MMR function of all the derived cell lines. These assays were not performed in the laboratory at the time of this project, but the NER assay has now been optimised (Woodhouse et al., 2014), and assessment of these cell lines is planned.

And lastly, the development of xenografts from the parent and derived cell lines, and assessment of their biology *in vivo*, would give insight into tumour development and spread of the HR defective and HR recovered resistant cell lines, as well as, the ability to assess therapies in a resistant setting.

APPENDICES

Appendix 1: NHEJ Gene Defects in Human Cancers

Gene	dbSNP ID	Intron/ Exon	Original Study ID	Chrom position	Nucleot ide change	Amino Acid change	MAF	Increased Cancer Risk	Reference	Decreased Cancer Risk	Reference
KU70	rs2267437	5'UTR	C-61G	42016699	C>G		0.278	Breast	(Willems et al., 2008, Fu et al., 2003)		
	rs5751129	5'UTR	T-991C	42015765	C>T		0.288	Renal cell, Gastric	(Chang et al., 2012, Wang et al., 2012, Yang et al., 2011)		
	rs132770	5'UTR	A-31G	42017264	A>G		0.157	Renal cell	(Chang et al., 2012, Wang et al., 2012)		
	rs132793	3'UTR	A46922G	42063681	A>G		0.157	Breast	(Sobczuk et al., 2010)		
KU80	rs2440	3'UTR	G841A	217070766	C>T		0.466	Breast	(Willems et al., 2008)		
	rs1051677	3'UTR	G-238A	217070248	T>C		0.125	Thyroid	(Gomes et al., 2010)		
	rs1051685	3'UTR	A466G	217070376	A>G		0.143	Thyroid	(Gomes et al., 2010)		
DNA-PKcs	rs7003908	Intron 48	6721G	48770702	C>A		0.291	Glioblastoma	(McKean-Cowdin et al., 2009)		
	rs6869366	5'UTR	T-1394G	82371746	T>G		0.095	Gastric, lung, breast, prostate, colorectal, bladder	(Fu et al., 2003, Chiu et al., 2008b, Bau et al., 2010),(Hsu et al., 2009,	Prostate, lung, bladder	(Mandal et al., 2011),(Yu et al., 2011),(Chang et al., 2009)

								Zhou et al., 2012, Chang et al., 2008a), (Bau et al., 2010),(Mittal et al., 2012)		
rs28360071	Intron 3	intron3 DIP	82438112	->Ins*		N/A	Prostate, oral	(Mandal et al., 2011),(Chiu et al., 2008a)		
rs28360317	Intron 7	intron7 DIP	82619560	->CCT		N/A	Bladder, prostate	(Mandal et al., 2011, Mittal et al., 2012)		
rs3734091	Exon 6	G739T	82500734	G>T	Ala247Ser	0.037	Oral	(Tseng et al., 2008)		
rs2075685	5'UTR	G-652T	82372665	G>T		0.386			Breast	(Zhou et al., 2012)
rs10057194	3'UTR	A9509G	82658571	A>G		0.184			Breast	(Zhou et al., 2012)
rs10080123	Intron 7	A-30323C	82461266	A>C		0.284			Breast	(Monsees et al., 2011)
rs2075686	5'UTR	C-571T	82372746	C>T		0.092	Breast	(Zhou et al., 2012)		
rs1193693	Intron 6	G-17030A	82537319	G>A		0.304			Breast	(Monsees et al., 2011)
rs1017794	Intron 1		82382055	C>A		0.404			Breast	(Monsees et al., 2011)
rs10040363	Intron 3		82473645	A>G		0.404			Breast	(Monsees et al., 2011)
rs1011981	Intron 1		82393688	A>G		0.314			Breast	(Monsees et al., 2011)
rs10042854	intron 3		82439695	C>T		0.399			Breast	(Monsees et al., 2011)

	rs4591730	Intron 3		82447802	G>A		0.4			Breast	(Monsees et al., 2011)
	rs11949301	Intron 6		82505153	C>A		0.224			Breast	(Monsees et al., 2011)
LIG IV	rs1805388	Exon 4	C54T	108863591	C>T	Thr9Ile	0.153	Pancreatic, NSCLC,	(Li et al., 2009a, Lieber et al., 2003, Tseng et al., 2009, Hill et al., 2006)	Childhood ALL, NHL, MM, CML, follicular lymphoma, B-cell lymphoma	(Andreae et al., 2007, Roddam et al., 2002, Sallmyr et al., 2008),(Hill et al., 2006)
	rs3093739	Intron 1	T5482C	107665402	T>C		0.131	Glioma	(Liu et al., 2008)		
	rs2232641	Exon 4	A2245G	108861645	A>G	Ile658Val	0.008	Adenocarcinoma and squamous carcinoma of the lung	(Sakiyama et al., 2005)		
	rs1805386	Exon 4	T1977C	108861913	T>C	Asp568Asp	0.093	Breast	(Goode et al., 2002),(Han et al., 2004)	Breast	(Kuschel et al., 2002)
	rs104894421	Exon 4	G833A	108862784	G>A	Agr278His	ND	Leukaemia	(Riballo et al., 1999)		
	rs1805389	Exon 4	C26T	107661610	C>T	Ala3Val	0.057			MM, ALL	(Roddam et al., 2002),(Andreae et al., 2007)

Appendix 2: Summary of Clinical Trials of PARPi use in Ovarian Cancer

Cancer Study Population	Regimen	Phase	Outcome	Refs
BRCA1/2 breast/ovarian, Triple negative breast, Sporadic ovarian	Olaparib 100 mg bd to 600 mg bd	I	RECIST criteria partial / complete response reported in 23 %. GCIG criteria of the CA-125 level, six patients with a BRCA mutation had a decline of more than 50 %. Most toxicities were grade 1-2, consisting of nausea (32 %), fatigue (30 %), vomiting (20 %), taste alteration (13 %), anorexia (12 %), anaemia (5 %), and 3 % developed grade 4 thrombocytopenia.	(Fong et al., 2009)
Advanced stage pre-treated ovarian with BRCA1/2 mutations	Olaparib 40mg od to 600mg bd.	I	Overall clinical benefit in 46 % (95 % CI, 32 % to 61 %) of BRCA patients. Median response duration was 28 weeks. RECIST criteria stable disease / partial / complete response or CA125 response was reported in 69 %, 45 % and 23 % respectively in platinum sensitive, platinum resistant and platinum refractory subgroups.	(Fong et al., 2010)
BRCA1/2 ovarian Recurrent sporadic ovarian	Olaparib 400mg bd or 100mg bd	II	Objective tumour response in 33 % for 400mg dose. The median progression free survival was 5.8 months and clinical benefit rate (complete response / partial response / stable disease for ≥ 8 weeks) was 52 % in the 400 mg bd cohort. Grade 1-2 toxicity: nausea (42 %), fatigue (30 %) and anaemia (15 %). Grade 3-4 toxicity: nausea (6 %), fatigue (3 %) and anaemia (3 %).	(Audeh et al., 2010)

Sporadic triple negative breast Sporadic ovarian	Olaparib 400mg bd	II	25/63 ovarian cancer patients had clinical response (28 of which were BRCA1/2 mutant).	(Gelmon, 2011)
Platinum sensitive relapsed ovarian pre-treated with 2+ platinum agents	Olaparib 400mg bd vs. placebo	RCT	PFS: median, 8.4 months for Olaparib vs. 4.8 months for placebo. Hazard ratio for progression or death - 0.35. No significant difference was seen for OS. Grade 1-2 toxicity - nausea (68 % vs. 35 %), fatigue (49 % vs. 38 %), vomiting (32 % vs. 14 %), and anaemia (17 % vs. 5 %).	(Ledermann et al., 2012)
BRCA1/2 relapsed ovarian after platinum therapy	Olaparib 400mg bd vs. doxorubicin 50mg/m2 iv every 4 weeks	II		(NCT00628251)
BRCA1/2 breast and ovarian	Rucaparib	II	Dose escalation followed by open-label multicentre study.	(NCT00664781)
Platinum-sensitive and platinum-resistant ovarian	Olaparib 400 mg BID PO d1-7 q21d with escalating dosages of carboplatin	II	Grade 3/4 neutropenia (23 %) and thrombocytopenia (20 %).	(Chiou et al., 2015)
Recurrent ovarian, breast, pancreatic, and prostate with BRCA1/2 mutations	Olaparib 400 mg BID PO daily	II	Tumor response rate 31.1 % (ovarian); 12.9 % (breast); 21.7 % (pancreatic); 50.0 % (prostate).	(Kaufman et al., 2015)
BRCA1/2 positive ovarian with recurrence <12	Olaparib 200 mg BID PO daily vs. olaparib 400 mg BID PO daily vs.	II	PFS and RECIST assessed odds ratio not significant for combined olaparib doses vs. PLD.	(Kaye et al., 2012)

months post platinum therapy	PLD 50 mg/m ² i.v. q28 days			
Platinum sensitive, HGS ovarian, platinum pretreated, progression free at least 6 months	Paclitaxel 175 mg/m ² i.v. day 1 + / - olaparib 200 mg BID PO d1–10 followed by monotherapy 400 mg BID daily Carboplatin	II	PFS for olaparib 12.2 months vs. 9.6 months ChemoRx arm. Hazard ration 0.51 (0.21 for BRCA mutation carriers). Grade 3 toxicity: neutropenia and anemia.	(Oza et al., 2013)
Platinum sensitive, recurrent, HGS / endometrioid ovarian, tubal / peritoneal with BRCA1/2 mutations	Olaparib 400 mg BID PO or olaparib 200 mg BID PO plus cediranib 30 mg PO daily	II	median PFS 17.7 vs.9.0 months (hazard ration 0.42). Grade 3-4 toxicity: fatigue, diarrhea, hypertension.	(Liu et al., 2014)
HGS / endometrioid with BRCA1/2 mutations platinum sensitive	Olaparib	III		(NCT01844986)
HGS / endometrioid	Valiparib	III		GOG3005
Relapsed HGS / endometrioid with BRCA1/2 mutation. Platinum sensitive	Olaparib	III		NCT01874363
Relapsed HGS / endometrioid, platinum sensitive	Rucaparib	III		NCT01968213
Relapsed HGS with BRCA1/2 mutations	Niraparib	III		NCT01847274

Appendix 3: NGOC Consent Form



Cancer Research Involving Tumour Samples Blood and Patient Information

CONSENT FORM

Please
initial
box

1. I have read the attached information sheet on the above project and have been given a copy to keep. I have had the opportunity to ask questions and understand why tumour samples, blood and patient information is being collected. ☐
2. I agree to donate a sample of tumour tissue and blood for research. I understand how the sample will be collected, that giving the sample for this research is voluntary and that I am free to withdraw my approval at any time without giving a reason and without my medical treatment or legal rights being affected. ☐
3. I give permission for certain anonymised medical details, as have been explained to me, to be looked at and information taken from them to be analysed in strict confidence by staff at the Northern Gynaecological Oncology Centre or from organisations supervising the research. ☐
4. I understand that future research using the sample I have given may include genetic research aimed at understanding the genetic influences relating to cancer, but that the results of these investigations are unlikely to have any implications for me personally. ☐
5. I agree that the samples I have given and the information gathered about me can be looked after and stored in the Northern Gynaecological Oncology Centre for use in future projects, as described in the attached information sheet. I understand that some of these projects may be carried out by researchers other than from the NGOC. ☐
6. I understand that all studies will be anonymised, coded and unlinked. This means that no results will be given to me directly of any research carried out on tissue, blood or data that I donate. ☐
7. I understand some research may take part in conjunction with commercial organisations. I will not benefit financially if this research leads to the development of a new treatment or medical test. ☐
8. I know how to contact the research team if I need to. ☐

Name of patient: Signature: Date:

Name of doctor: Signature: Date:

Thank you for agreeing to participate

White Copy – Patient Copy

Appendix 4: Multiple Comparisons for Inhibition and Knockdown of ATR and DNA-PK with PARPi

Table 8-1 Tukey's adjusted for multiple comparisons two way Anova comparisons of treatments in OSEC-2 and NUOC-1 cells.

Significant results are marked in bold.

Comparisons	OSEC-2 Percent reduction in cell growth	Tukey's adjusted P =	NUOC-1 Percent reduction in cell growth	Tukey's adjusted P =
Control vs. Rucaparib	9.4	0.9999	36	0.1854
Control vs. NU6027	47	0.0189	68	< 0.0001
Control vs. NU6027 + rucaparib	56	0.0024	72	< 0.0001
Control vs. NU7441	-8.7	> 0.9999	41	0.0698
Control vs. NU7441 + rucaparib	18	0.9619	53	0.0042
Control vs. NU6027 + NU7441 + rucaparib	58	0.0013	83	< 0.0001
Control vs. ATR shRNA	29	0.4982	30	0.4381
Control vs. ATR shRNA + rucaparib	35	0.2302	73	< 0.0001
Control vs. DNA-PK shRNA	5.4	> 0.9999	-39	0.0992
Control vs. DNA-PK shRNA + rucaparib	34	0.2722	33	0.2985
Control vs. DNA-PKcs shRNA + NU6027 + rucaparib	35	0.2238	49	0.0116
Control vs. ATR shRNA + NU7441 + rucaparib	57	0.0018	77	< 0.0001
Rucaparib vs. NU6027 + rucaparib	50.6	0.0244	36.3	0.2008
Rucaparib vs. NU7441 + rucaparib	9.23	> 0.9999	26.56	0.9679
Rucaparib vs. NU6027 + NU7441 + rucaparib	52.8	0.0142	73.4	0.0203
Rucaparib vs. ATR shRNA + rucaparib	27.5	0.6987	37.8	0.1596
Rucaparib vs. DNA-PK shRNA + rucaparib	26.4	0.7538	-4.7	> 0.9999
Rucaparib vs. DNA-PKcs shRNA + NU6027 + rucaparib	27.5	0.6893	20.3	0.9965
Rucaparib vs. ATR shRNA + NU7441 + rucaparib	51.7	0.0183	64	0.0670
NU6027 vs. NU6027 + rucaparib	15.7	> 0.9999	9.4	> 0.9999

NU6027 vs. NU6027 + NU7441 + rucaparib	20.75	0.9996	43.8	0.9928
NU6027 vs. DNA-PKcs shRNA + NU6027 + rucaparib	-22.6	0.9982	-19.4	0.9372
NU6027 + rucaparib vs. NU6027 + NU7441 + rucaparib	5.23	> 0.9999	39.3	0.9992
NU6027 + rucaparib vs. DNA-PKcs shRNA + NU6027 + rucaparib	-21.7	0.8952	-22	0.8430
NU7441 vs. NU7441 + rucaparib	24.6	0.6314	20.3	0.9985
NU7441 vs. NU6027 + NU7441 + rucaparib	60.9	0.0001	71.2	0.0638
NU7441 vs. ATR shRNA + NU7441 + rucaparib	60	0.0002	13.7	0.1791
NU7441 + rucaparib vs. NU6027 + NU7441 + rucaparib	40.8	0.0886	30.8	0.4661
NU7441 + rucaparib vs. ATR shRNA + NU7441 + rucaparib	43.0	0.1091	24	0.7609
ATR shRNA vs. ATR shRNA + rucaparib	8	> 0.9999	61.4	0.0506
ATR shRNA vs. ATR shRNA + NU7441 + rucaparib	39.4	0.5579	67.1	0.0183
ATR shRNA + rucaparib vs. ATR shRNA + NU7441 + rucaparib	33.9	0.8452	17	> 0.9999
DNA-PK shRNA vs. DNA-PK shRNA + rucaparib	29.5	0.5407	51.4	< 0.0001
DNA-PK shRNA vs. DNA-PKcs shRNA + NU6027 + rucaparib	30.5	0.4716	63.6	< 0.0001
DNA-PK shRNA + rucaparib vs. DNA-PKcs shRNA + NU6027 rucaparib	2	> 0.9999	23.9	0.9800

Table 8-2 Tukey's multiple comparisons adjusted two way Anova comparisons of treatments with PARPi in OSEC-2 and NUOC-1 cells. Significant results are marked in bold.

Comparisons	OSEC-2	Tukey's adjusted P =	NUOC-1	Tukey's adjusted P =
	Percent reduction in cell growth		Percent reduction in cell growth	
Control vs. Rucaparib	26.6	0.9968	-3	> 0.9999
Control vs. NU6027	-26.8	0.9966	40.4	0.9137
Control vs. NU6027 + rucaparib	38.5	0.9372	5.4	> 0.9999
Control vs. NU7441	5.3	> 0.9999	11.8	> 0.9999
Control vs. NU7441 + rucaparib	49.2	0.7388	48	0.7700
Control vs. NU6027 + NU7441 + rucaparib	26.6	0.9969	46.6	0.8007
Control vs. ATR shRNA	30.1	0.9905	29.6	0.9917
Control vs. ATR shRNA + rucaparib	72.9	0.1774	97	0.0151
Control vs. DNA-PK shRNA	-39.4	0.9258	44.4	0.8460
Control vs. DNA-PK shRNA + rucaparib	33	0.9797	83	0.0250
Control vs. DNA-PKcs shRNA + NU6027 + rucaparib	49.4	0.7354	98.5	0.0127
Control vs. ATR shRNA + NU7441 + rucaparib	77.5	0.0352	100	0.0105
Rucaparib vs. NU6027 + rucaparib	11.8	> 0.9999	8.4	> 0.9999
Rucaparib vs. NU7441 + rucaparib	22.6	0.9993	51	0.6947
Rucaparib vs. NU6027 + NU7441 + rucaparib	0.9	> 0.9999	49.6	0.7291
Rucaparib vs. ATR shRNA + rucaparib	46.3	0.8083	100	0.0106
Rucaparib vs. DNA-PK shRNA + rucaparib	6.4	> 0.9999	86	0.0512
Rucaparib vs. DNA-PKcs shRNA + NU6027 + rucaparib	22.7	0.9993	100	0.0088
Rucaparib vs. ATR shRNA + NU7441 + rucaparib	50.9	0.6977	100	0.0073
NU6027 vs. NU6027 + rucaparib	65.2	0.3216	-35	0.9684
NU6027 vs. NU6027 + NU7441 + rucaparib	53.3	0.6320	6.2	> 0.9999
NU6027 vs. DNA-PKcs shRNA + NU6027 + rucaparib	76.1	> 0.9999	58.1	0.5010

NU6027 + rucaparib vs. NU6027 + NU7441 + rucaparib	-11.9	> 0.9999	41.2	0.9016
NU6027 + rucaparib vs. DNA-PKcs shRNA + NU6027 + rucaparib	10.9	0.9307	93.0	0.0237
NU7441 vs. NU7441 + rucaparib	54.6	0.5974	59.8	0.4564
NU7441 vs. NU6027 + NU7441 + rucaparib	31.9	0.9846	58.4	0.4923
NU7441 vs. ATR shRNA + NU7441 + rucaparib	82.8	0.0707	112	0.0024
NU7441 + rucaparib vs. NU6027 + NU7441 + rucaparib	-22.7	0.9993	1.3	> 0.9999
NU7441 + rucaparib vs. ATR shRNA + NU7441 + rucaparib	28.3	0.9945	52.1	0.6655
ATR shRNA vs. ATR shRNA + rucaparib	42.8	0.8758	67.4	0.2761
ATR shRNA vs. ATR shRNA + NU7441 + rucaparib	47.4	0.7830	70.4	0.2179
ATR shRNA + rucaparib vs. ATR shRNA + NU7441 + rucaparib	4.5	> 0.9999	3.1	> 0.9999
DNA-PK shRNA vs. DNA-PK shRNA + rucaparib	72.4	0.1848	38.5	0.9366
DNA-PK shRNA vs. DNA-PKcs shRNA + NU6027 + rucaparib	88.8	0.0379	54	0.6130
DNA-PK shRNA + rucaparib vs. DNA-PKcs shRNA + NU6027 rucaparib	16.4	> 0.9999	15.5	> 0.9999

Appendix 5: PhD Publications

- **A McCormick**, P Donoghue, R O’Sullivan, M Dixon, RL O’Donnell, A Kaufman, NJ Curtin, RJ Edmondson. Ovarian Cancers Harbor Defects in Non-Homologous End Joining Resulting in Error Prone Repair and Resistance to Rucaparib. **Provisionally accepted by Clinical Cancer Research**
- **A McCormick**, E Earp, C Leeson, M Dixon, RL O’Donnell, A Kaufman, RJ Edmondson. PTEN is a potential target for ovarian cancer sensitisation to cytotoxic agents. Int J Gynecol Cancer 2016
- RL O’Donnell, A Kaufmann, L Woodhouse, **A McCormick**, RJ Edmondson, NJ Curtin. Advanced ovarian cancer displays functional intra-tumour heterogeneity which correlates to *ex vivo* drug sensitivity. Int J Gynecol Cancer 2016
- FK Middleton, MJ Patterson, CJ Elstob, M Wade, **A McCormick**, RJ Edmondson, FE May, JM Allan, JR Pollard, NJ Curtin. Search for determinants of sensitivity to ATR inhibitor, VE-821, uncovers novel synthetic lethality with DNA-PKcs expression. Oncotarget. 2015; 6(32):32396-409
- RL O’Donnell, **A McCormick**, A Mukhopadhyay, LC Woodhouse, M Moat, A Grundy, M Dixon, A Kaufman, S Soohoo, A Elattar, B Uzir, NJ Curtin, RJ Edmondson. The use of ovarian cancer cells from patients undergoing surgery to generate primary cultures capable of undergoing functional analysis. Plos One 2014. 6; 9 (3):e90604
- **A McCormick**, P Cross, RJ Edmondson. Case report of uterine corpus metastasis in stage IA1 Squamous cervical carcinoma. Gynecologic Oncology Case Reports 2013; 6:31-33
- **A Cerbinskaite**, A Mukhopadhyay, ER Plummer, NJ Curtin, RJ Edmondson. Defective homologous recombination in human cancers. Cancer Treat Rev. 2012;38(2):89-100
- RJ Edmondson, A Mukhopadhyay, **A Cerbinskaite**, NJ Curtin. Implications of homologous recombination defectiveness in ovarian cancer. Gynaecological cancers: Biology and therapeutics. RCOG Press. 2011

- **A McCormick**, E Earp, K Elliot, RL O'Donnell, B Wilson, C Leeson, H Thomas, H Blair, S Fordham, J Lunec, JM Allan, RJ Edmondson. Functional characterisation of a novel ovarian cancer cell line, NUOC-1. **MANUSCRIPT SUBMITTED FOR PUBLICATION**
- **A McCormick**, NJ Sunter, R O'Sullivan, NJ Curtin, RJ Edmondson. Defects in the DNA double strand break end joining pathways in human cancers. **MANUSCRIPT BEING PREPARED FOR SUBMISSION**

Appendix 6: Published Abstracts

- **A McCormick**, E Earp, C Leeson, M Dixon, RL O'Donnell, A Kaufmann, RJ Edmondson. PTEN function is important in determining ovarian cancer sensitivity to cytotoxic agents. BJOG 12; 122:E11, 2015
- **A McCormick**, P Donoghue, M Dixon, RL O'Donnell, A Kaufmann, NJ Curtin, RJ Edmondson. Defects in non-homologous end joining pathway in ovarian cancers results in resistance to rucaparib. BJOG 12; 122:E12. 2015
- RL O'Donnell, A Kaufmann, LC Woodhouse, **A McCormick**, NJ Curtin, RJ Edmondson. Intra- and inter-tumour heterogeneity in epithelial ovarian cancer: consequences for biomarker-dependent stratification of therapies. BJOG 12; 122:E2, 2015
- LC. Woodhouse, **A McCormick**, RL O'Donnell, A Kaufmann, RJ Edmondson. Development of a Functional Assay to Determine the Nucleotide Excision Repair Status of Epithelial Ovarian Cancer. Int J Gynecol Cancer 24; 9:164, 2014
- **A McCormick**, M Dixon, RL O'Donnell, NJ Curtin, RJ Edmondson. Ovarian cancers harbor defects in non-homologous end joining resulting in error prone repair and resistance to rucaparib. Clin Cancer Research. 19: PR06, 2013
- **A McCormick**, E Earp, C Leeson, M Dixon, RL O'Donnell, RJ Edmondson. PTEN expression level is important in determining sensitivity to cytotoxic agents *in vitro*, but is not representative of PTEN function observed in primary ovarian cancer cultures. Clin Cancer Research. 19: B9. 2013
- RL O'Donnell, LC Woodhouse, **A McCormick**, A Kaufmann, M Dixon, A Mukhopadhyay, NJ Curtin, RJ Edmondson. Intra- and inter-tumour heterogeneity in epithelial ovarian cancer: Consequences for biomarker-dependent stratification of therapies. Clin Cancer Research. 19: PR10. 2013
- RL O'Donnell, JCC Murray, AGB Buskin, S Frame, DG Blake, M Dixon, **A McCormick**, A Kaufmann, ER Plummer, RJ Edmondson, NJ Curtin. Therapeutic potential of sapacitabine in ovarian cancers defective in homologous recombination. Clin Cancer Research. 19: A33. 2013

- RL O'Donnell, LC Woodhouse, **A McCormick**, A Mukhopadhyay, M Dixon, A Kaufmann, NJ Curtin, RJ Edmondson. Functional Intra-Tumour Heterogeneity in Ovarian Cancer: What Is a Representative Tumour Sample? Int J Gynecol Cancer 23; 8:S1, 2013
- **A McCormick**, NJ Curtin, RJ Edmondson. Inhibition of DNA-PK Recovers HR Function and Results in Platinum Resistance in an Ovarian Cancer Cell Line Model. Int J Gynecol Cancer 23; 8:S1, 2013
- E Earp, **A McCormick**, C Leeson, RJ Edmondson. Inhibiting Double Strand Break (DSB) Repair Pathways and PTEN Sensitises Ovarian Clear Cell Carcinoma (OCCC) to Cytotoxic Agents. Int J Gynecol Cancer 23; 8:S1, 2013
- **A McCormick**, NJ Curtin, RJ Edmondson. Non homologous end joining assessment in ovarian cancer. BJOG 6; 119:E8, 2012

Appendix 7: Oral Presentations

- **A McCormick**, E Earp, C Leeson, M Dixon, RL O'Donnell, R J Edmondson. PTEN is a potential target for ovarian cancer sensitisation to cytotoxic agents. ESGO, 2015
- **A McCormick**, P Donnohue, M Dixon, R O'Donnell, A Kaufman, NJ. Curtin, R J. Edmondson. Defects in non homologous end joining pathway in ovarian cancers results in resistance to rucaparib. Blair Bell RCOG Academic Meeting, 2014
- **A McCormick**, NJ Curtin, RJ Edmondson. Inhibition of DNA-PK recovers HR function and results in platinum resistance in an ovarian cancer cell line model. ESGO, 2013
- **A McCormick**, M Dixon, R O'Donnell, NJ Curtin, RJ Edmondson. Ovarian cancers harbor defect in nonhomologous end joining resulting in error prone repair and resistance to rucaparib. AACR: Ovarian cancer – concept to clinic, 2013
- **A McCormick**, NJ Curtin, RJ Edmondson. Ovarian cancers harbor defects in non homologous end joining. Frank Stabler Meeting, 2013

Frank Stabler Prize
- **A McCormick**, NJCurtin, RJ Edmondson. Ovarian cancers harbor defects in non homologous end joining. CRUK Clinical Fellows Meeting, 2012

Appendix 8: Poster Presentations

- **A McCormick**, S. Nakjang, P. Donoghue, NJ. Curtin, RJ Edmondson. The role of homologous recombination recovery in cisplatin and rucaparib resistance in ovarian cancer. ESGO, 2015
- J Burgon, A Herriott, D Jamieson, **A McCormick**, M Moat, R O'Donnell, NJ Curtin, Y Drew. Targeting the Mismatch Repair Pathway in Ovarian Cancer. NCRI 2015
- **A McCormick**, M Dixon, RL O'Donnell, NJ Curtin, RJ Edmondson. Defects in the non homologous end joining pathway in ovarian cancers results in resistance to PARP inhibitor, rucaparib. BGCS, 2015
- **A McCormick**, E Earp, C Leeson, M Dixon, RL O'Donnell, R J Edmondson. PTEN is a potential target for ovarian cancer sensitisation to cytotoxic agents. BGCS, 2015
- L. Woodhouse, **A McCormick**, A Kaufmann, P Donoghue, R O'Donnell, RJ Edmondson. Development of a functional assay to determine the nucleotide excision repair status of ovarian cancer cells. IGCS, 2014
- RP O'Sullivan, **A McCormick**, P Donoghue, A Kaufmann, NJ Curtin, RJ Edmondson. DNA-PK as a biomarker of non homologous end joining in ovarian cancer. NCRI 2014
- **A McCormick**, E Earp, C Leeson, M Dixon, R O'Donnell, RJ Edmondson. PTEN function is important in determining ovarian cancer sensitivity to cytotoxic agents *in vitro*. Blair Bell RCOG Academic Meeting. 2014
- **A McCormick**, M Dixon, R O'Donnell, NJ Curtin, RJ Edmondson. Ovarian cancers harbor defect in nonhomologous end joining resulting in error prone repair and resistance to rucaparib. AACR: Ovarian cancer – concept to clinic, 2013
- **A McCormick**, E Earp, C Leeson, M Dixon, R O'Donnell, RJ Edmondson. PTEN expression level is important in determining sensitivity to cytotoxic agents *in vitro*, but is not representative of PTEN function observed in primary ovarian cancer cultures. AACR: Ovarian cancer – concept to clinic, 2013

- RL O'Donnell, LC Woodhouse, **A McCormick**, A Kaufmann, M Dixon, A Mukhopadhyay, NJ Curtin, RJ Edmondson. Intra- and inter-tumour heterogeneity in epithelial ovarian cancer: Consequences for biomarker-dependent stratification of therapies. AACR: Ovarian cancer – concept to clinic, 2013
- RL O'Donnell, JCC Murray, AGB Buskin, S Frame, DG Blake, M Dixon, **A McCormick**, A Kaufmann, ER Plummer, RJ Edmondson, NJ Curtin. Therapeutic potential of sapacitabine in ovarian cancers defective in homologous recombination. AACR: Ovarian cancer – concept to clinic, 2013
- RL O'Donnell, L Woodhouse, **A McCormick**, A Mukhopadhyay, M Dixon, A Kaufmann, NJ Curtin, RJ Edmondson. Functional intra-tumour heterogeneity in ovarian cancer: what is a representative sample?. ESGO, 2013
- E Earp, **A McCormick**, C Leeson, RJ Edmondson. Inhibiting double strand break (DSB) repair pathways and PTEN sensitises Ovarian Clear Cell Carcinoma (OCCC) to cytotoxic agents. ESGO, 2013
- **A McCormick** J. Goodfellow, J. Gradwell, T. Chaloub, M. Roberts. HPV triage – colposcopic and biopsy and outcome. ESGO, 2013
- KE Elliot, C Hutton, **A McCormick**, RJ Edmondson, J Lunec. Response to MDM2 antagonism as a single agent or in combination with cisplatin in a panel of ovarian cancer cell lines. NCRI, 2013
- E Earp, **A McCormick**, C Leeson, RJ Edmondson. Ovarian Clear Cell Carcinoma (OCCC) is sensitised to cytotoxic agents through inhibition of double strand break (DSB) repair pathways and PTEN. NCRI, 2013
- RL O'Donnell, L Woodhouse, **A McCormick**, A Mukhopadhyay, M Dixon, A Kaufmann, NJ Curtin, RJ Edmondson. Functional intra-tumour heterogeneity in ovarian cancer: are our expectations of novel therapies too high?. BGCS, 2013
- E Earp, **A McCormick**, C Leeson, RJ Edmondson. Inhibiting the double strand break (DSB) repair pathways sensitises Ovarian Clear Cell Carcinoma (OCCC) to cytotoxic agents. Sylvia Lawder Prize Evening, 2013

- **A McCormick**, R O'Donnell, A Grundy, L Woodhouse, NJ Curtin, RJ Edmondson. Ovarian cancers harbor defects in non homologous end joining. NCRI, Liverpool, 2012
- L Woodhouse, A Grundy, **A McCormick**, R O'Donnell, NJ Curtin, RJ Edmondson. Validating the use of solid tissue explants to determine the homologous recombination status of epithelial ovarian carcinomas. NCRI, Liverpool, 2012
- A Grundy, L Woodhouse, **A McCormick**, R O'Donnell, NJ Curtin, RJ Edmondson. Development of a clinically applicable method to determine the homologous recombination status of epithelial ovarian cancers. NCRI, Liverpool, 2012
- R O'Donnell, AGB Buskin, JCC Murray, **A McCormick**, S Frame, A Mukhopadhyaya, ER Plummer, DG Blake, RJ Edmondson, NJ Curtin. Therapeutic potential of sapacitabine in ovarian cancers defective in homologous recombination. NCRI, Liverpool, 2012
- **A McCormick**, NJ Curtin, RJ Edmondson. Non homologous end joining defects in ovarian cancer. DNA repair meeting, Oxford, 2012

REFERENCES

- ABBA, M. C., LACUNZA, E., NUNEZ, M. I., COLUSSI, A., ISLA-LARRAIN, M., SEGAL-EIRAS, A., CROCE, M. V. & ALDAZ, C. M. 2009. Rhomboid domain containing 2 (RHBD2): A novel cancer-related gene over-expressed in breast cancer. *Biochimica Et Biophysica Acta-Molecular Basis of Disease*, 1792, 988-997.
- ABKEVICH, V., TIMMS, K. M., HENNESSY, B. T., POTTER, J., CAREY, M. S., MEYER, L. A., SMITH-MCCUNE, K., BROADDUS, R., LU, K. H., CHEN, J., TRAN, T. V., WILLIAMS, D., ILIEV, D., JAMMULAPATI, S., FITZGERALD, L. M., KRIVAK, T., DELOIA, J. A., GUTIN, A., MILLS, G. B. & LANCHBURY, J. S. 2012. Patterns of genomic loss of heterozygosity predict homologous recombination repair defects in epithelial ovarian cancer. *British Journal of Cancer*, 107, 1776-1782.
- AGHAJANIAN, C., BLANK, S. V., GOFF, B. A., JUDSON, P. L., TENERIELLO, M. G., HUSAIN, A., SOVAK, M. A., YI, J. & NYCUM, L. R. 2012. OCEANS: a randomized, double-blind, placebo-controlled phase III trial of chemotherapy with or without bevacizumab in patients with platinum-sensitive recurrent epithelial ovarian, primary peritoneal, or fallopian tube cancer. *J Clin Oncol*, 30, 2039-45.
- AHMED, A. A., BECKER, C. M. & BAST, R. C., JR. 2012. The origin of ovarian cancer. *BJOG*, 119, 134-6.
- AHMED, A. A., ETEMADMOGHADAM, D., TEMPLE, J., LYNCH, A. G., RIAD, M., SHARMA, R., STEWART, C., FEREDAY, S., CALDAS, C., DEFAZIO, A., BOWTELL, D. & BRENTON, J. D. 2010. Driver mutations in TP53 are ubiquitous in high grade serous carcinoma of the ovary. *J Pathol*, 221, 49-56.
- AHNESORG, P., SMITH, P. & JACKSON, S. P. 2006. XLF interacts with the XRCC4-DNA ligase IV complex to promote DNA nonhomologous end-joining. *Cell*, 124, 301-13.
- AL-ATTAR, A., GOSSAGE, L., FAREED, K. R., SHEHATA, M., MOHAMMED, M., ZAITOUN, A. M., SOOMRO, I., LOBO, D. N., ABBOTTS, R., CHAN, S. & MADHUSUDAN, S. 2010. Human apurinic/apyrimidinic endonuclease (APE1) is a prognostic factor in ovarian, gastro-oesophageal and pancreatico-biliary cancers. *Br J Cancer*, 102, 704-9.
- AL-BAHLANI, S., FRASER, M., WONG, A. Y. C., SAYAN, B. S., BERGERON, R., MELINO, G. & TSANG, B. K. 2011. P73 regulates cisplatin-induced apoptosis in ovarian cancer cells via a calcium/calpain-dependent mechanism. *Oncogene*, 30, 4219-4230.
- AL RAWAHI, T., LOPES, A. D., BRISTOW, R. E., BRYANT, A., ELATTAR, A., CHATTOPADHYAY, S. & GALAAL, K. 2013. Surgical cytoreduction for recurrent epithelial ovarian cancer. *Cochrane Database Syst Rev*, 2, CD008765.
- ALLEN, C., HALBROOK, J. & NICKOLOFF, J. A. 2003. Interactive competition between homologous recombination and non-homologous end joining. *Molecular Cancer Research*, 1, 913-920.
- ALTER, B. P. 1996. Fanconi's anemia and malignancies. *Am J Hematol*, 53, 99-110.
- ALTHAUS, F. R., HOFFERER, L., KLECZKOWSKA, H. E., MALANGA, M., NAEGELI, H., PANZETER, P. & REALINI, C. 1993. Histone shuttle driven by the automodification cycle of poly(ADP-ribose)polymerase. *Environ Mol Mutagen*, 22, 278-82.
- ALY, A. & GANESAN, S. 2011. BRCA1, PARP, and 53BP1: conditional synthetic lethality and synthetic viability. *J Mol Cell Biol*, 3, 66-74.
- AME, J. C., SPENLEHAUER, C. & DE MURCIA, G. 2004. The PARP superfamily. *Bioessays*, 26, 882-93.
- AMES, B. N. & GOLD, L. S. 1991. Endogenous mutagens and the causes of aging and cancer. *Mutat Res*, 250, 3-16.

- ANASTAS, J. N. & MOON, R. T. 2013. WNT signalling pathways as therapeutic targets in cancer. *Nature Reviews Cancer*, 13, 11-26.
- ANDREAE, J., VARON, R., SPERLING, K. & SEEGER, K. 2007. Polymorphisms in the DNA ligase IV gene might influence the risk of acute lymphoblastic leukemia in children. *Leukemia*, 21, 2226-7.
- ANGLESIO, M. S., CAREY, M. S., KOBEL, M., MACKAY, H. & HUNTSMAN, D. G. 2011. Clear cell carcinoma of the ovary: a report from the first Ovarian Clear Cell Symposium, June 24th, 2010. *Gynecol Oncol*, 121, 407-15.
- ANTHONEY, D. A., MCILWRATH, A. J., GALLAGHER, W. M., EDLIN, A. R. & BROWN, R. 1996. Microsatellite instability, apoptosis, and loss of p53 function in drug-resistant tumor cells. *Cancer Res*, 56, 1374-81.
- ARIAS-LOPEZ, C., LAZARO-TRUEBA, I., KERR, P., LORD, C. J., DEXTER, T., IRAVANI, M., ASHWORTH, A. & SILVA, A. 2006. P53 modulates homologous recombination by transcriptional regulation of the RAD51 gene. *Embo Reports*, 7, 219-224.
- ARORA, S., BISANZ, K. M., PERALTA, L. A., BASU, G. D., CHOUDHARY, A., TIBES, R. & AZORSA, D. O. 2010. RNAi screening of the kinome identifies modulators of cisplatin response in ovarian cancer cells. *Gynecologic Oncology*, 118, 220-227.
- ASHWORTH, A. 2008a. Drug resistance caused by reversion mutation. *Cancer Res*, 68, 10021-3.
- ASHWORTH, A. 2008b. A synthetic lethal therapeutic approach: poly(ADP) ribose polymerase inhibitors for the treatment of cancers deficient in DNA double-strand break repair. *J Clin Oncol*, 26, 3785-90.
- AUCKLEY, D. H., CROWELL, R. E., HEAPHY, E. R., STIDLEY, C. A., LECHNER, J. F., GILLILAND, F. D. & BELINSKY, S. A. 2001. Reduced DNA-dependent protein kinase activity is associated with lung cancer. *Carcinogenesis*, 22, 723-7.
- AUDEBERT, M., SALLES, B. & CALSOU, P. 2004. Involvement of poly(ADP-ribose) polymerase-1 and XRCC1/DNA ligase III in an alternative route for DNA double-strand breaks rejoining. *J Biol Chem*, 279, 55117-26.
- AUDEBERT, M., SALLES, B. & CALSOU, P. 2008. Effect of double-strand break DNA sequence on the PARP-1 NHEJ pathway. *Biochem Biophys Res Commun*, 369, 982-8.
- AUDEBERT, M., SALLES, B., WEINFELD, M. & CALSOU, P. 2006. Involvement of polynucleotide kinase in a poly(ADP-ribose) polymerase-1-dependent DNA double-strand breaks rejoining pathway. *J Mol Biol*, 356, 257-65.
- AUDEH, M. W., CARMICHAEL, J., PENSON, R. T., FRIEDLANDER, M., POWELL, B., BELL-MCGUINN, K. M., SCOTT, C., WEITZEL, J. N., OAKNIN, A., LOMAN, N., LU, K., SCHMUTZLER, R. K., MATULONIS, U., WICKENS, M. & TUTT, A. 2010. Oral poly(ADP-ribose) polymerase inhibitor olaparib in patients with BRCA1 or BRCA2 mutations and recurrent ovarian cancer: a proof-of-concept trial. *Lancet*, 376, 245-251.
- AUER, B., NAGL, U., HERZOG, H., SCHNEIDER, R. & SCHWEIGER, M. 1989. Human nuclear NAD⁺ ADP-ribosyltransferase(polymerizing): organization of the gene. *DNA*, 8, 575-80.
- AYOUB, N., RAJENDRA, E., SU, X., JEYASEKHARAN, A. D., MAHEN, R. & VENKITARAMAN, A. R. 2009. The carboxyl terminus of Brca2 links the disassembly of Rad51 complexes to mitotic entry. *Curr Biol*, 19, 1075-85.
- BALKWILL, F., BAST, R. C., BEREK, J., CHENEVIX-TRENCH, G., GORE, M., HAMILTON, T., JACOBS, I., MILLS, G., SOUHAMI, R., URBAN, N., ORSULIC, S. & SMYTH, J. 2004. Current research and treatment for epithelial ovarian cancer. A position paper from the Helene Harris Memorial Trust (vol 39, pg 1818, 2003). *European Journal of Cancer*, 40, 628-628.

- BAN, S., SHINOHARA, T., HIRAI, Y., MORITAKU, Y., COLOGNE, J. B. & MACPHEE, D. G. 2001. Chromosomal instability in BRCA1- or BRCA2-defective human cancer cells detected by spontaneous micronucleus assay. *Mutat Res*, 474, 15-23.
- BARBER, L. J., SANDHU, S., CHEN, L., CAMPBELL, J., KOZAREWA, I., FENWICK, K., ASSIOTIS, I., RODRIGUES, D. N., REIS FILHO, J. S., MORENO, V., MATEO, J., MOLIFE, L. R., DE BONO, J., KAYE, S., LORD, C. J. & ASHWORTH, A. 2013. Secondary mutations in BRCA2 associated with clinical resistance to a PARP inhibitor. *J Pathol*, 229, 422-9.
- BARTKOVA, J., HOREJSI, Z., KOED, K., KRAMER, A., TORT, F., ZIEGER, K., GULDBERG, P., SEHESTED, M., NESLAND, J. M., LUKAS, C., ORNTOF, T., LUKAS, J. & BARTEK, J. 2005. DNA damage response as a candidate anti-cancer barrier in early human tumorigenesis. *Nature*, 434, 864-70.
- BAU, D. T., FU, Y. P., CHEN, S. T., CHENG, T. C., YU, J. C., WU, P. E. & SHEN, C. Y. 2004. Breast cancer risk and the DNA double-strand break end-joining capacity of nonhomologous end-joining genes are affected by BRCA1. *Cancer Res*, 64, 5013-9.
- BAU, D. T., MAU, Y. C., DING, S. L., WU, P. E. & SHEN, C. Y. 2007. DNA double-strand break repair capacity and risk of breast cancer. *Carcinogenesis*, 28, 1726-30.
- BAU, D. T., MAU, Y. C. & SHEN, C. Y. 2006. The role of BRCA1 in non-homologous end-joining. *Cancer Lett*, 240, 1-8.
- BAU, D. T., YANG, M. D., TSOU, Y. A., LIN, S. S., WU, C. N., HSIEH, H. H., WANG, R. F., TSAI, C. W., CHANG, W. S., HSIEH, H. M., SUN, S. S. & TSAI, R. Y. 2010. Colorectal Cancer and Genetic Polymorphism of DNA Double-strand Break Repair Gene XRCC4 in Taiwan. *Anticancer Res*, 30, 2727-2730.
- BAUMANN, P. & WEST, S. C. 1998. DNA end-joining catalyzed by human cell-free extracts. *Proc Natl Acad Sci U S A*, 95, 14066-70.
- BAUTE, J. & DEPICKER, A. 2008. Base excision repair and its role in maintaining genome stability. *Crit Rev Biochem Mol Biol*, 43, 239-276.
- BEE, L., FABRIS, S., CHERUBINI, R., MOGNATO, M. & CELOTTI, L. 2013. The efficiency of homologous recombination and non-homologous end joining systems in repairing double-strand breaks during cell cycle progression. *PLoS One*, 8, e69061.
- BENAFIF, S. & HALL, M. 2015. An update on PARP inhibitors for the treatment of cancer. *Oncotargets and Therapy*, 8, 519-528.
- BENARD, J., DA SILVA, J., DE BLOIS, M. C., BOYER, P., DUVILLARD, P., CHIRIC, E. & RIOU, G. 1985. Characterization of a human ovarian adenocarcinoma line, IGROV1, in tissue culture and in nude mice. *Cancer Res*, 45, 4970-9.
- BENJAMIN, R. C. & GILL, D. M. 1980. Poly(ADP-ribose) synthesis in vitro programmed by damaged DNA. A comparison of DNA molecules containing different types of strand breaks. *J Biol Chem*, 255, 10502-8.
- BENTLEY, J., DIGGLE, C. P., HARNDEN, P., KNOWLES, M. A. & KILTIE, A. E. 2004. DNA double strand break repair in human bladder cancer is error prone and involves microhomology-associated end-joining. *Nucleic Acids Res*, 32, 5249-59.
- BENTLEY, J., L'HOTE, C., PLATT, F., HURST, C. D., LOWERY, J., TAYLOR, C., SAK, S. C., HARNDEN, P., KNOWLES, M. A. & KILTIE, A. E. 2009. Papillary and muscle invasive bladder tumors with distinct genomic stability profiles have different DNA repair fidelity and KU DNA-binding activities. *Genes Chromosomes Cancer*, 48, 310-21.
- BENTLEY, N. J., HOLTZMAN, D. A., FLAGGS, G., KEEGAN, K. S., DEMAGGIO, A., FORD, J. C., HOEKSTRA, M. & CARR, A. M. 1996. The Schizosaccharomyces pombe rad3 checkpoint gene. *Embo Journal*, 15, 6641-6651.
- BERNSTEIN, C., BERNSTEIN, H., PAYNE, C. M. & GAREWAL, H. 2002. DNA repair/pro-apoptotic dual-role proteins in five major DNA repair pathways: fail-safe protection

- against carcinogenesis. *Mutation Research-Reviews in Mutation Research*, 511, 145-178.
- BÉTERMIER, M., BERTRAND, P. & LOPEZ, B. S. 2014. Is Non-Homologous End-Joining Really an Inherently Error-Prone Process? *PLoS Genet*, 10, e1004086.
- BIECHE, I., DE MURCIA, G. & LIDERAU, R. 1996. Poly(ADP-ribose) polymerase gene expression status and genomic instability in human breast cancer. *Clin Cancer Res*, 2, 1163-7.
- BISHOP, A. J. & SCHIESTL, R. H. 2002. Homologous Recombination and Its Role in Carcinogenesis. *J Biomed Biotechnol*, 2, 75-85.
- BOHR, V. A. 2008. Rising from the RecQ-age: the role of human RecQ helicases in genome maintenance. *Trends Biochem Sci*, 33, 609-20.
- BOOKMAN, M. A., BRADY, M. F., MCGUIRE, W. P., HARPER, P. G., ALBERTS, D. S., FRIEDLANDER, M., COLOMBO, N., FOWLER, J. M., ARGENTA, P. A., DE GEEST, K., MUTCH, D. G., BURGER, R. A., SWART, A. M., TRIMBLE, E. L., ACCARIO-WINSLOW, C. & ROTH, L. M. 2009. Evaluation of new platinum-based treatment regimens in advanced-stage ovarian cancer: a Phase III Trial of the Gynecologic Cancer Intergroup. *J Clin Oncol*, 27, 1419-25.
- BOOKMAN, M. A., GREER, B. E. & OZOLS, R. F. 2003. Optimal therapy of advanced ovarian cancer: carboplatin and paclitaxel versus cisplatin and paclitaxel (GOG158) and an update on GOG0182-ICON5. *Int J Gynecol Cancer*, 13 Suppl 2, 149-55.
- BOULTON, S., KYLE, S. & DURKACZ, B. W. 1999. Interactive effects of inhibitors of poly(ADP-ribose) polymerase and DNA-dependent protein kinase on cellular responses to DNA damage. *Carcinogenesis*, 20, 199-203.
- BOULTON, S., KYLE, S. & DURKACZ, B. W. 2000. Mechanisms of enhancement of cytotoxicity in etoposide and ionising radiation-treated cells by the protein kinase inhibitor wortmannin. *Eur J Cancer*, 36, 535-41.
- BOUWMAN, P., ALY, A., ESCANDELL, J. M., PIETERSE, M., BARTKOVA, J., VAN DER GULDEN, H., HIDDINGH, S., THANASOULA, M., KULKARNI, A., YANG, Q., HAFETY, B. G., TOMMISKA, J., BLOMQVIST, C., DRAPKIN, R., ADAMS, D. J., NEVANLINNA, H., BARTEK, J., TARSOUNAS, M., GANESAN, S. & JONKERS, J. 2010. 53BP1 loss rescues BRCA1 deficiency and is associated with triple-negative and BRCA-mutated breast cancers. *Nat Struct Mol Biol*, 17, 688-95.
- BOYD, J., SONODA, Y., FEDERICI, M. G., BOGOMOLNIY, F., RHEI, E., MARESCO, D. L., SAIGO, P. E., ALMADRONES, L. A., BARAKAT, R. R., BROWN, C. L., CHI, D. S., CURTIN, J. P., POYNOR, E. A. & HOSKINS, W. J. 2000. Clinicopathologic features of BRCA-linked and sporadic ovarian cancer. *JAMA*, 283, 2260-5.
- BRANDSMA, I. & GENT, D. C. 2012. Pathway choice in DNA double strand break repair: observations of a balancing act. *Genome Integr*, 3, 9.
- BRISTOW, R. E., TOMACRUZ, R. S., ARMSTRONG, D. K., TRIMBLE, E. L. & MONTZ, F. J. 2002. Survival effect of maximal cytoreductive surgery for advanced ovarian carcinoma during the platinum era: a meta-analysis. *J Clin Oncol*, 20, 1248-59.
- BRONNER, C. E., BAKER, S. M., MORRISON, P. T., WARREN, G., SMITH, L. G., LESCOE, M. K., KANE, M., EARABINO, C., LIPFORD, J., LINDBLOM, A., TANNERGARD, P., BOLLAG, R. J., GODWIN, A. R., WARD, D. C., NORDENSKJOLD, M., FISHEL, R., KOLODNER, R. & LISKAY, R. M. 1994. Mutation in the DNA Mismatch Repair Gene Homolog Hmlh1 Is Associated with Hereditary Nonpolyposis Colon-Cancer. *Nature*, 368, 258-261.
- BROUGH, R., FRANKUM, J. R., COSTA-CABRAL, S., LORD, C. J. & ASHWORTH, A. 2011. Searching for synthetic lethality in cancer. *Curr Opin Genet Dev*, 21, 34-41.

- BROWN, E. J. & BALTIMORE, D. 2000. ATR disruption leads to chromosomal fragmentation and early embryonic lethality. *Genes & Development*, 14, 397-402.
- BROWN, E. J. & BALTIMORE, D. 2003. Essential and dispensable roles of ATR in cell cycle arrest and genome maintenance. *Genes & development*, 17, 615-628.
- BROWN, L. A., IRVING, J., PARKER, R., KIM, H., PRESS, J. Z., LONGACRE, T. A., CHIA, S., MAGLIOCCO, A., MAKRETISOV, N., GILKS, B., POLLACK, J. & HUNTSMAN, D. 2006. Amplification of EMSY, a novel oncogene on 11q13, in high grade ovarian surface epithelial carcinomas. *Gynecol Oncol*, 100, 264-70.
- BRYANT, H. E. & HELLEDAY, T. 2006. Inhibition of poly (ADP-ribose) polymerase activates ATM which is required for subsequent homologous recombination repair. *Nucleic Acids Res*, 34, 1685-91.
- BRYANT, H. E., PETERMANN, E., SCHULTZ, N., JEMTH, A. S., LOSEVA, O., ISSAEVA, N., JOHANSSON, F., FERNANDEZ, S., MCGLYNN, P. & HELLEDAY, T. 2009. PARP is activated at stalled forks to mediate Mre11-dependent replication restart and recombination. *EMBO J*, 28, 2601-15.
- BRYANT, H. E., SCHULTZ, N., THOMAS, H. D., PARKER, K. M., FLOWER, D., LOPEZ, E., KYLE, S., MEUTH, M., CURTIN, N. J. & HELLEDAY, T. 2005. Specific killing of BRCA2-deficient tumours with inhibitors of poly(ADP-ribose) polymerase. *Nature*, 434, 913-7.
- BUCK, D., MALIVERT, L., DE CHASSEVAL, R., BARRAUD, A., FONDANECHÉ, M. C., SANAL, O., PLEBANI, A., STEPHAN, J. L., HUFNAGEL, M., LE DEIST, F., FISCHER, A., DURANDY, A., DE VILLARTAY, J. P. & REVY, P. 2006. Cernunnos, a novel nonhomologous end-joining factor, is mutated in human immunodeficiency with microcephaly. *Cell*, 124, 287-99.
- BUI, H. X., REYNOLDS, J. P., HILL, G. A., PANCHANANTHAN, R. & CHOUBEY, D. 2009. IFI16: A Novel Growth Suppressor in Human Prostate Cancer. *Modern Pathology*, 22, 154a-154a.
- BULLER, R. E., SHAHIN, M. S., HOLMES, R. W., HATTERMAN, M., KIRBY, P. A. & SOOD, A. K. 2001. p53 Mutations and microsatellite instability in ovarian cancer: Yin and yang. *Am J Obstet Gynecol*, 184, 891-902; discussion 902-3.
- BULLER, R. E., SHAHIN, M. S., HOROWITZ, J. A., RUNNEBAUM, I. B., MAHAVNI, V., PETRAUSKAS, S., KREIENBERG, R., KARLAN, B., SLAMON, D. & PEGRAM, M. 2002. Long term follow-up of patients with recurrent ovarian cancer after Ad p53 gene replacement with SCH 58500. *Cancer Gene Therapy*, 9, 567-572.
- BUNTING, S. F., CALLEN, E., WONG, N., CHEN, H. T., POLATO, F., GUNN, A., BOTHMER, A., FELDHAHN, N., FERNANDEZ-CAPETILLO, O., CAO, L., XU, X., DENG, C. X., FINKEL, T., NUSSENZWEIG, M., STARK, J. M. & NUSSENZWEIG, A. 2010. 53BP1 inhibits homologous recombination in Brca1-deficient cells by blocking resection of DNA breaks. *Cell*, 141, 243-54.
- BURGER, R. A., BRADY, M. F., BOOKMAN, M. A., FLEMING, G. F., MONK, B. J., HUANG, H., MANNEL, R. S., HOMESLEY, H. D., FOWLER, J., GREER, B. E., BOENTE, M., BIRRER, M. J., LIANG, S. X. & GYNECOLOGIC ONCOLOGY, G. 2011. Incorporation of bevacizumab in the primary treatment of ovarian cancer. *N Engl J Med*, 365, 2473-83.
- BURGER, R. A., SILL, M. W., MONK, B. J., GREER, B. E. & SOROSKY, J. I. 2007. Phase II trial of bevacizumab in persistent or recurrent epithelial ovarian cancer or primary peritoneal cancer: a Gynecologic Oncology Group Study. *J Clin Oncol*, 25, 5165-71.
- BURMA, S., CHEN, B. P. & CHEN, D. J. 2006. Role of non-homologous end joining (NHEJ) in maintaining genomic integrity. *DNA Repair (Amst)*, 5, 1042-8.
- BURMA, S. & CHEN, D. J. 2004. Role of DNA-PK in the cellular response to DNA double-strand breaks. *DNA Repair (Amst)*, 3, 909-18.

- CANCER GENOME ATLAS RESEARCH, N. 2011. Integrated genomic analyses of ovarian carcinoma. *Nature*, 474, 609-15.
- CANNISTRA, S. A., MATULONIS, U. A., PENSON, R. T., HAMBLETON, J., DUPONT, J., MACKEY, H., DOUGLAS, J., BURGER, R. A., ARMSTRONG, D., WENHAM, R. & MCGUIRE, W. 2007. Phase II study of bevacizumab in patients with platinum-resistant ovarian cancer or peritoneal serous cancer. *J Clin Oncol*, 25, 5180-6.
- CARCANGIU, M. L., PEISSEL, B., PASINI, B., SPATTI, G., RADICE, P. & MANOUKIAN, S. 2006. Incidental carcinomas in prophylactic specimens in BRCA1 and BRCA2 germ-line mutation carriers, with emphasis on fallopian tube lesions - Report of 6 cases and review of the literature. *American Journal of Surgical Pathology*, 30, 1222-1230.
- CARDUNER, L., PICOT, C. R., LEROY-DUDAL, J., BLAY, L., KELLOUCHE, S. & CARREIRAS, F. 2014. Cell cycle arrest or survival signaling through alphav integrins, activation of PKC and ERK1/2 lead to anoikis resistance of ovarian cancer spheroids. *Exp Cell Res*, 320, 329-42.
- CARY, R. B., PETERSON, S. R., WANG, J., BEAR, D. G., BRADBURY, E. M. & CHEN, D. J. 1997. DNA looping by Ku and the DNA-dependent protein kinase. *Proc Natl Acad Sci U S A*, 94, 4267-72.
- CASS, I., BALDWIN, R. L., VARKEY, T., MOSLEHI, R., NAROD, S. A. & KARLAN, B. Y. 2003. Improved survival in women with BRCA-associated ovarian carcinoma. *Cancer*, 97, 2187-95.
- CASTELLS, M., THIBAUT, B., DELORD, J. P. & COUDERC, B. 2012. Implication of tumor microenvironment in chemoresistance: tumor-associated stromal cells protect tumor cells from cell death. *Int J Mol Sci*, 13, 9545-71.
- CECCALDI, R., LIU, J. C., AMUNUGAMA, R., HAJDU, I., PRIMACK, B., PETALCORIN, M. I., O'CONNOR, K. W., KONSTANTINOPOULOS, P. A., ELLEDGE, S. J., BOULTON, S. J., YUSUFZAI, T. & D'ANDREA, A. D. 2015a. Homologous-recombination-deficient tumours are dependent on Poltheta-mediated repair. *Nature*, 518, 258-62.
- CECCALDI, R., O'CONNOR, K. W., MOUW, K. W., LI, A. Y., MATULONIS, U. A., D'ANDREA, A. D. & KONSTANTINOPOULOS, P. A. 2015b. A unique subset of epithelial ovarian cancers with platinum sensitivity and PARP inhibitor resistance. *Cancer Res*, 75, 628-34.
- CERBINSKAITE, A., MUKHOPADHYAY, A., PLUMMER, E. R., CURTIN, N. J. & EDMONDSON, R. J. 2012. Defective homologous recombination in human cancers. *Cancer Treat Rev*, 38, 89-100.
- CHAN, N. & BRISTOW, R. G. 2010. "Contextual" synthetic lethality and/or loss of heterozygosity: tumor hypoxia and modification of DNA repair. *Clin Cancer Res*, 16, 4553-60.
- CHAN, N., KORITZINSKY, M., ZHAO, H., BINDRA, R., GLAZER, P. M., POWELL, S., BELMAAZA, A., WOUTERS, B. & BRISTOW, R. G. 2008. Chronic hypoxia decreases synthesis of homologous recombination proteins to offset chemoresistance and radioresistance. *Cancer Res*, 68, 605-14.
- CHANG, C. H., CHANG, C. L., TSAI, C. W., WU, H. C., CHIU, C. F., WANG, R. F., LIU, C. S., LIN, C. C. & BAU, D. T. 2009. Significant Association of an XRCC4 Single Nucleotide Polymorphism with Bladder Cancer Susceptibility in Taiwan. *Anticancer Res*, 29, 1777-1782.
- CHANG, C. H., CHIU, C. F., WU, H. C., TSENG, H. C., WANG, C. H., LIN, C. C., TSAI, C. W., LIANG, S. Y., WANG, C. L. & BAU, D. T. 2008a. Significant association of XRCC4 single nucleotide polymorphisms with prostate cancer susceptibility in Taiwanese males. *Mol Med Report*, 1, 525-530.

- CHANG, H. W., ROH, J. L., JEONG, E. J., LEE, S. W., KIM, S. W., CHOI, S. H., PARK, S. K. & KIM, S. Y. 2008b. Wnt signaling controls radiosensitivity via cyclooxygenase-2-mediated Ku expression in head and neck cancer. *International Journal of Cancer*, 122, 100-107.
- CHANG, W. S., KE, H. L., TSAI, C. W., LIEN, C. S., LIAO, W. L., LIN, H. H., LEE, M. H., WU, H. C., CHANG, C. H., CHEN, C. C., LEE, H. Z. & BAU, D. T. 2012. The Role of XRCC6 T-991C Functional Polymorphism in Renal Cell Carcinoma. *Anticancer Res*, 32, 3855-3860.
- CHAO, A., TSAI, C. L., JUNG, S. M., CHUANG, W. C., KAO, C., HSU, A., CHEN, S. H., LIN, C. Y., LEE, Y. C., LEE, Y. S., WANG, T. H., WANG, H. S. & LAI, C. H. 2015. BAI1-Associated Protein 2-Like 1 (BAIAP2L1) Is a Potential Biomarker in Ovarian Cancer. *Plos One*, 10.
- CHAPMAN, J. R., BARRAL, P., VANNIER, J. B., BOREL, V., STEGER, M., TOMAS-LOBA, A., SARTORI, A. A., ADAMS, I. R., BATISTA, F. D. & BOULTON, S. J. 2013. RIF1 Is Essential for 53BP1-Dependent Nonhomologous End Joining and Suppression of DNA Double-Strand Break Resection. *Molecular Cell*, 49, 858-871.
- CHAPMAN, J. R., SOSSICK, A. J., BOULTON, S. J. & JACKSON, S. P. 2012a. BRCA1-associated exclusion of 53BP1 from DNA damage sites underlies temporal control of DNA repair. *J Cell Sci*, 125, 3529-34.
- CHAPMAN, J. R., TAYLOR, M. R. G. & BOULTON, S. J. 2012b. Playing the End Game: DNA Double-Strand Break Repair Pathway Choice. *Molecular Cell*, 47, 497-510.
- CHEN, B. P., CHAN, D. W., KOBAYASHI, J., BURMA, S., ASAITHAMBY, A., MOROTOMI-YANO, K., BOTVINICK, E., QIN, J. & CHEN, D. J. 2005. Cell cycle dependence of DNA-dependent protein kinase phosphorylation in response to DNA double strand breaks. *J Biol Chem*, 280, 14709-15.
- CHEN, B. P., UEMATSU, N., KOBAYASHI, J., LERENTHAL, Y., KREMPLER, A., YAJIMA, H., LOBRICH, M., SHILOH, Y. & CHEN, D. J. 2007. Ataxia telangiectasia mutated (ATM) is essential for DNA-PKcs phosphorylations at the Thr-2609 cluster upon DNA double strand break. *J Biol Chem*, 282, 6582-7.
- CHEN, G., GHARIB, T. G., HUANG, C. C., TAYLOR, J. M., MISEK, D. E., KARDIA, S. L., GIORDANO, T. J., IANNETTONI, M. D., ORRINGER, M. B., HANASH, S. M. & BEER, D. G. 2002. Discordant protein and mRNA expression in lung adenocarcinomas. *Mol Cell Proteomics*, 1, 304-13.
- CHEN, T., STEPHENS, P. A., MIDDLETON, F. K. & CURTIN, N. J. 2012. Targeting the S and G2 checkpoint to treat cancer. *Drug Discovery Today*, 17, 194-202.
- CHEN, X. H., DU, H., LIU, B. J., ZOU, L., CHEN, W., YANG, Y., ZHU, Y., GONG, Y. J., TIAN, J. B., LI, F. & ZHONG, S. 2015. The Associations between RNA Splicing Complex Gene SF3A1 Polymorphisms and Colorectal Cancer Risk in a Chinese Population. *Plos One*, 10.
- CHENG, C. X., XUE, M., LI, K., LI, W. S. 2012. Predictive value of XRCC1 and XRCC3 gene polymorphisms for risk of ovarian cancer death after chemotherapy. *Asian Pac J Cancer Prev*, 13, 2541-5.
- CHENG, G. C., SUN, X. Q., WANG, J. L., XIAO, G., WANG, X. M., FAN, X. M., ZU, L. D., HAO, M. G., QU, Q., MAO, Y., XUE, Y. J. & WANG, J. H. 2014. HIC1 Silencing in Triple-Negative Breast Cancer Drives Progression through Misregulation of LCN2. *Cancer Research*, 74, 862-872.
- CHENG, J. Q., GODWIN, A. K., BELLACOSA, A., TAGUCHI, T., FRANKE, T. F., HAMILTON, T. C., TSICHLIS, P. N. & TESTA, J. R. 1992. AKT2, a putative oncogene encoding a member of a subfamily of protein-serine/threonine kinases, is amplified in human ovarian carcinomas. *Proc Natl Acad Sci U S A*, 89, 9267-71.
- CHENG, W. J., LIU, J. S., YOSHIDA, H., ROSEN, D. & NAORA, H. 2005. Lineage infidelity of epithelial ovarian cancers is controlled by HOX genes that specify regional identity in the reproductive tract. *Nature Medicine*, 11, 531-537.

- CHEONG, N., PERRAULT, A. R., WANG, H., WACHSBERGER, P., MAMMEN, P., JACKSON, I. & ILIAKIS, G. 1999. DNA-PK-independent rejoining of DNA double-strand breaks in human cell extracts in vitro. *Int J Radiat Biol*, 75, 67-81.
- CHIARUGI, A. 2012. A snapshot of chemoresistance to PARP inhibitors. *Trends Pharmacol Sci*, 33, 42-8.
- CHIOU, V. L., KOHN, E. C., ANNUNZIATA, C. M., MINASIAN, L. M., LIPKOWITZ, S., YU, M., GORDON, N., HOUSTON, N. D. & LEE, J. M. 2015. Phase I/Ib study of the PARP inhibitor (PARPi) olaparib (O) with carboplatin (C) in heavily pretreated high-grade serous ovarian cancer (HGSOC) at low genetic risk (NCT01445418). *Journal of Clinical Oncology*, 33.
- CHISTIAKOV, D. A., VORONOVA, N. V. & CHISTIAKOV, P. A. 2008. Genetic variations in DNA repair genes, radiosensitivity to cancer and susceptibility to acute tissue reactions in radiotherapy-treated cancer patients. *Acta Oncol*, 47, 809-24.
- CHIU, C. F., TSAI, M. H., TSENG, H. C., WANG, C. L., WANG, C. H., WU, C. N., LIN, C. C. & BAU, D. T. 2008a. A novel single nucleotide polymorphism in XRCC4 gene is associated with oral cancer susceptibility in Taiwanese patients. *Oral Oncology*, 44, 898-902.
- CHIU, C. F., WANG, C. H., WANG, C. L., LIN, C. C., HSU, N. Y., WENG, J. R. & BAU, D. T. 2008b. A novel single nucleotide polymorphism in XRCC4 gene is associated with gastric cancer susceptibility in Taiwan. *Ann Surg Oncol*, 15, 514-518.
- CHO, N. H., CORDON-CARDO, C., LI, G. C. & KIM, S. H. 2002. Allotype imbalance or microsatellite mutation in low-grade soft tissue sarcomas of the extremities in adults. *J Pathol*, 198, 21-9.
- CHOU, J. L., HUANG, R. L., SHAY, J., CHEN, L. Y., LIN, S. J., YAN, P. S., CHAO, W. T., LAI, Y. H., LAI, Y. L., CHAO, T. K., LEE, C. I., TAI, C. K., WU, S. F., NEPHEW, K. P., HUANG, T. H. M., LAI, H. C. & CHAN, M. W. Y. 2015. Hypermethylation of the TGF-beta target, ABCA1 is associated with poor prognosis in ovarian cancer patients. *Clinical Epigenetics*, 7.
- CHOUDHURY, A., ZHAO, H. L., JALALI, F., RASHID, S. A., RAN, J., SUPLOT, S., KILTIE, A. E. & BRISTOW, R. G. 2009. Targeting homologous recombination using imatinib results in enhanced tumor cell chemosensitivity and radiosensitivity. *Molecular Cancer Therapeutics*, 8, 203-213.
- CHRISTMANN, M., TOMICIC, M. T., ROOS, W. P. & KAINA, B. 2003. Mechanisms of human DNA repair: an update. *Toxicology*, 193, 3-34.
- CLINICAL_TRIALS.GOV. 2012. *Results database of federally and privately supported clinical trials conducted in the United States and around the world for PARP inhibitors and ovarian cancer* [Online].
- CLINICALTRIALS.GOV. NCT00628251. *Dose-finding Study Comparing Efficacy and Safety of a PARP Inhibitor Against Doxil in BRCA+ve Advanced Ovarian Cancer (ICEBERG 3)* [Online].
- CLINICALTRIALS.GOV. NCT00664781. *Rucaparib(CO-338;Formally Called AG-014699 or PF-0136738) in Treating Patients With Locally Advanced or Metastatic Breast Cancer or Advanced Ovarian Cancer* [Online].
- CLINICALTRIALS.GOV NCT01891344. *A Study of Rucaparib in Patients With Platinum-Sensitive, Relapsed, High-Grade Epithelial Ovarian, Fallopian Tube, or Primary Peritoneal Cancer (ARIEL2)*.
- CLINICALTRIALS.GOV NCT01968213. *A Study of Rucaparib as Switch Maintenance Following Platinum-Based Chemotherapy in Patients With Platinum-Sensitive, High-Grade Serous or Endometrioid Epithelial Ovarian, Primary Peritoneal or Fallopian Tube Cancer (ARIEL3)*.

- COLEMAN, R. L., DUSKA, L. R., RAMIREZ, P. T., HEYMACH, J. V., KAMAT, A. A., MODESITT, S. C., SCHMELER, K. M., IYER, R. B., GARCIA, M. E., MILLER, D. L., JACKSON, E. F., NG, C. S., KUNDRA, V., JAFFE, R. & SOOD, A. K. 2011. Phase 1-2 study of docetaxel plus aflibercept in patients with recurrent ovarian, primary peritoneal, or fallopian tube cancer. *Lancet Oncol*, 12, 1109-17.
- COLLABORATORS, I. 2002. Paclitaxel plus carboplatin versus standard chemotherapy with either single-agent carboplatin or cyclophosphamide, doxorubicin, and cisplatin in women with ovarian cancer: the ICON3 randomised trial. *Lancet*, 360, 505-15.
- COLOMBO, N., GUTHRIE, D., CHIARI, S., PARMAR, M., QIAN, W., SWART, A. M., TORRI, V., WILLIAMS, C., LISSONI, A. & BONAZZI, C. 2003. International Collaborative Ovarian Neoplasm trial 1: a randomized trial of adjuvant chemotherapy in women with early-stage ovarian cancer. *J Natl Cancer Inst*, 95, 125-32.
- CONVERY, E., SHIN, E. K., DING, Q., WANG, W., DOUGLAS, P., DAVIS, L. S., NICKOLOFF, J. A., LEES-MILLER, S. P. & MEEK, K. 2005. Inhibition of homologous recombination by variants of the catalytic subunit of the DNA-dependent protein kinase (DNA-PKcs). *Proc Natl Acad Sci U S A*, 102, 1345-50.
- COOKE, S. L. & BRENTON, J. D. 2011. Evolution of platinum resistance in high-grade serous ovarian cancer. *Lancet Oncol*, 12, 1169-74.
- CORNELL, L., MUNCK, J. M., ALSINET, C., VILLANUEVA, A., OGLE, L., WILLOUGHBY, C. E., TELEVANTOU, D., THOMAS, H. D., JACKSON, J., BURT, A. D., NEWELL, D., ROSE, J., MANAS, D. M., SHAPIRO, G. I., CURTIN, N. J. & REEVES, H. L. 2015. DNA-PK-A candidate driver of hepatocarcinogenesis and tissue biomarker that predicts response to treatment and survival. *Clin Cancer Res*, 21, 925-33.
- CORNEO, B., WENDLAND, R. L., DERIANO, L., CUI, X., KLEIN, I. A., WONG, S. Y., ARNAL, S., HOLUB, A. J., WELLER, G. R., PANCAKE, B. A., SHAH, S., BRANDT, V. L., MEEK, K. & ROTH, D. B. 2007. Rag mutations reveal robust alternative end joining. *Nature*, 449, 483-6.
- CORTEZ, D. 2003. Caffeine inhibits checkpoint responses without inhibiting the ataxia-telangiectasia-mutated (ATM) and ATM- and Rad3-related (ATR) protein kinases. *J Biol Chem*, 278, 37139-45.
- CORTEZ, D. 2005. Unwind and slow down: checkpoint activation by helicase and polymerase uncoupling. *Genes Dev*, 19, 1007-12.
- CORTEZ, D., WANG, Y., QIN, J. & ELLEDGE, S. J. 1999. Requirement of ATM-dependent phosphorylation of brca1 in the DNA damage response to double-strand breaks. *Science*, 286, 1162-6.
- COUPIER, I., BALDEYRON, C., ROUSSEAU, A., MOSSERI, V., PAGES-BERHOUE, S., CAUX-MONCOUTIER, V., PAPADOPOULOU, D. & STOPPA-LYONNET, D. 2004. Fidelity of DNA double-strand break repair in heterozygous cell lines harbouring BRCA1 missense mutations. *Oncogene*, 23, 914-9.
- COUTO, C. A., WANG, H. Y., GREEN, J. C., KIELY, R., SIDDAWAY, R., BORER, C., PEARS, C. J. & LAKIN, N. D. 2011. PARP regulates nonhomologous end joining through retention of Ku at double-strand breaks. *J Cell Biol*, 194, 367-75.
- CRAWFORD, R. S., ALBADAWI, H., ATKINS, M. D., JONES, J. E., YOO, H. J., CONRAD, M. F., AUSTEN, W. G., JR. & WATKINS, M. T. 2010. Postischemic poly (ADP-ribose) polymerase (PARP) inhibition reduces ischemia reperfusion injury in a hind-limb ischemia model. *Surgery*, 148, 110-8.
- CRUM, C. P., DRAPKIN, R., MIRON, A., INCE, T. A., MUTO, M., KINDELBERGER, D. W. & LEE, Y. 2007. The distal fallopian tube: a new model for pelvic serous carcinogenesis. *Curr Opin Obstet Gynecol*, 19, 3-9.

- CSETE, B., LENGUEL, Z., KADAR, Z. & BATTYANI, Z. 2009. Poly(adenosine diphosphate-ribose) polymerase-1 expression in cutaneous malignant melanomas as a new molecular marker of aggressive tumor. *Pathol Oncol Res*, 15, 47-53.
- CURTIN, N. J. 2012. DNA repair dysregulation from cancer driver to therapeutic target. *Nat Rev Cancer*, 12, 801-17.
- CYR, J. L., BROWN, G. D., STROOP, J. & HEINEN, C. D. 2011. The predicted truncation from a cancer-associated variant of the MSH2 initiation codon alters activity of the MSH2-MSH6 mismatch repair complex. *Mol Carcinog*.
- DABHOLKAR, M., VIONNET, J., BOSTICK-BRUTON, F., YU, J. J. & REED, E. 1994. Messenger RNA levels of XPAC and ERCC1 in ovarian cancer tissue correlate with response to platinum-based chemotherapy. *J Clin Invest*, 94, 703-8.
- DAMIA, G., GUIDI, G., D'INCALCI, M. 1998. Expression of genes involved in nucleotide excision repair and sensitivity to cisplatin and melphalan in human cancer cell lines. *Eur J Cancer*, 34, 1783-8.
- DANIEL, V. C., MARCHIONNI, L., HIERMAN, J. S., RHODES, J. T., DEVEREUX, W. L., RUDIN, C. M., YUNG, R., PARMIGIANI, G., DORSCH, M., PEACOCK, C. D. & WATKINS, D. N. 2009. A Primary Xenograft Model of Small-Cell Lung Cancer Reveals Irreversible Changes in Gene Expression Imposed by Culture In vitro. *Cancer Research*, 69, 3364-3373.
- DANOY, P., MICHELIS, S., DESSEN, P., PIGNAT, C., BOULET, T., MONET, M., BOUCHARDY, C., LATHROP, M., SARASIN, A. & BENHAMOU, S. 2008. Variants in DNA double-strand break repair and DNA damage-response genes and susceptibility to lung and head and neck cancers. *Int J Cancer*, 123, 457-63.
- DANTZER, F., DE LA RUBIA, G., MENISSIER-DE MURCIA, J., HOSTOMSKY, Z., DE MURCIA, G. & SCHREIBER, V. 2000. Base excision repair is impaired in mammalian cells lacking Poly(ADP-ribose) polymerase-1. *Biochemistry*, 39, 7559-69.
- DAVIES, A. A., MASSON, J. Y., MCILWRAITH, M. J., STASIAK, A. Z., STASIAK, A., VENKITARAMAN, A. R. & WEST, S. C. 2001. Role of BRCA2 in control of the RAD51 recombination and DNA repair protein. *Mol Cell*, 7, 273-82.
- DAVIES, B. R., STEELE, I. A., EDMONDSON, R. J., ZWOLINSKI, S. A., SARETZKI, G., VON ZGLINICKI, T. & O'HARE, M. J. 2003. Immortalisation of human ovarian surface epithelium with telomerase and temperature-sensitive SV40 large T antigen. *Exp Cell Res*, 288, 390-402.
- DAVIES, H., BIGNELL, G. R., COX, C., STEPHENS, P., EDKINS, S., CLEGG, S., TEAGUE, J., WOFFENDIN, H., GARNETT, M. J., BOTTOMLEY, W., DAVIS, N., DICKS, E., EWING, R., FLOYD, Y., GRAY, K., HALL, S., HAWES, R., HUGHES, J., KOSMIDOU, V., MENZIES, A., MOULD, C., PARKER, A., STEVENS, C., WATT, S., HOOPER, S., WILSON, R., JAYATILAKE, H., GUSTERSON, B. A., COOPER, C., SHIPLEY, J., HARGRAVE, D., PRITCHARD-JONES, K., MAITLAND, N., CHENEVIX-TRENCH, G., RIGGINS, G. J., BIGNER, D. D., PALMIERI, G., COSSU, A., FLANAGAN, A., NICHOLSON, A., HO, J. W., LEUNG, S. Y., YUEN, S. T., WEBER, B. L., SEIGLER, H. F., DARROW, T. L., PATERSON, H., MARAIS, R., MARSHALL, C. J., WOOSTER, R., STRATTON, M. R. & FUTREAL, P. A. 2002. Mutations of the BRAF gene in human cancer. *Nature*, 417, 949-54.
- DE LUCA, A., MAIELLO, M. R., D'ALESSIO, A., PERGAMENO, M. & NORMANNO, N. 2012. The RAS/RAF/MEK/ERK and the PI3K/AKT signalling pathways: role in cancer pathogenesis and implications for therapeutic approaches. *Expert Opin Ther Targets*, 16 Suppl 2, S17-27.
- DE RONDE, J. J., LIPS, E. H., MULDER, L., VINCENT, A. D., WESSELING, J., NIEUWLAND, M., KERKHOVEN, R., PEETERS, M. J. T. F. D. V., SONKE, G. S., RODENHUIS, S. & WESSELS, L. F. A. 2013. SERPINA6, BEX1, AGTR1, SLC26A3, and LAPTM4B are markers of

- resistance to neoadjuvant chemotherapy in HER2-negative breast cancer. *Breast Cancer Research and Treatment*, 137, 213-223.
- DE TOLEDO, M. C. S., SARIAN, L. O., SALLUM, L. F., ANDRADE, L. L. A., VASSALLO, J., SILVA, G. R. D., PINTO, G. A., SOARES, F. A., FONSECA, C. D. P. & DERCHAIN, S. F. M. 2014. Analysis of the contribution of immunologically-detectable HER2, steroid receptors and of the "triple-negative" tumor status to disease-free and overall survival of women with epithelial ovarian cancer. *Acta Histochemica*, 116, 440-447.
- DE VOS, M., SCHREIBER, V. & DANTZER, F. 2012. The diverse roles and clinical relevance of PARPs in DNA damage repair: current state of the art. *Biochem Pharmacol*, 84, 137-46.
- DEBERNARDIS, D., SIRE, E. G., DEFEUDIS, P., VIKHANSKAYA, F., VALENTI, M., RUSSO, P., PARODI, S., DINCALCI, M. & BROGGINI, M. 1997. p53 status does not affect sensitivity of human ovarian cancer cell lines to paclitaxel. *Cancer Research*, 57, 870-874.
- DEGER, R. B., FARUQI, S. A. & NOUMOFF, J. S. 1997. Karyotypic analysis of 32 malignant epithelial ovarian tumors. *Cancer Genet Cytogenet*, 96, 166-73.
- DELLORUSSO, C., WELCSH, P. L., WANG, W., GARCIA, R. L., KING, M. C. & SWISHER, E. M. 2007. Functional characterization of a novel BRCA1-null ovarian cancer cell line in response to ionizing radiation. *Mol Cancer Res*, 5, 35-45.
- DERIANO, L., GUIPAUD, O., MERLE-BERAL, H., BINET, J. L., RICOUL, M., POTOCKI-VERONESE, G., FAVAUDON, V., MACIOROWSKI, Z., MULLER, C., SALLES, B., SABATIER, L. & DELIC, J. 2005. Human chronic lymphocytic leukemia B cells can escape DNA damage-induced apoptosis through the nonhomologous end-joining DNA repair pathway. *Blood*, 105, 4776-83.
- DEROSE, Y. S., WANG, G. Y., LIN, Y. C., BERNARD, P. S., BUYS, S. S., EBBERT, M. T. W., FACTOR, R., MATSEN, C., MILASH, B. A., NELSON, E., NEUMAYER, L., RANDALL, R. L., STIJLEMAN, I. J., WELM, B. E. & WELM, A. L. 2011. Tumor grafts derived from women with breast cancer authentically reflect tumor pathology, growth, metastasis and disease outcomes. *Nature Medicine*, 17, 1514-U227.
- DEUTSCH, E., DUGRAY, A., ABDULKARIM, B., MARANGONI, E., MAGGIORELLA, L., VAGANAY, S., M'KACHER, R., RASY, S. D., ESCHWEGE, F., VAINCHENKER, W., TURHAN, A. G. & BOURHIS, J. 2001. BCR-ABL down-regulates the DNA repair protein DNA-PKcs. *Blood*, 97, 2084-90.
- DEVAPATLA, B. K., JAIPRASART, P. & WOO, S. 2014. Gene and protein expression profiling identifies molecular signature of resistance to anti-VEGF therapy in ovarian cancer. *Cancer Research*, 74.
- DIER, U., UUSITALO, L., GIROUX, C. & HEMPEL, N. 2013. Mitochondrial superoxide dismutase (Sod2) confers a survival advantage to ovarian cancer cells under stress conditions by enhancing mitochondrial respiratory reserve capacity. *Cancer Research*, 73.
- DIGGLE, C. P., BENTLEY, J. & KILTIE, A. E. 2003. Development of a rapid, small-scale DNA repair assay for use on clinical samples. *Nucleic Acids Res*, 31, e83.
- DIGGLE, C. P., BENTLEY, J., KNOWLES, M. A. & KILTIE, A. E. 2005. Inhibition of double-strand break non-homologous end-joining by cisplatin adducts in human cell extracts. *Nucleic Acids Res*, 33, 2531-9.
- DIGWEED, M. & SPERLING, K. 2004. Nijmegen breakage syndrome: clinical manifestation of defective response to DNA double-strand breaks. *DNA Repair (Amst)*, 3, 1207-17.
- DIMOVA, I., RAITCHEVA, S., DIMITROV, R., DOGANOV, N., TONCHEVA, D. 2006. Correlations between c-myc gene copy-number and clinicopathological parameters of ovarian tumours. *Eur J Cancer*, 42, 674-9.

- DING, L., ELLIS, M. J., LI, S. Q., LARSON, D. E., CHEN, K., WALLIS, J., HARRIS, C. C., MCLELLAN, M. D., FULTON, R. S., FULTON, L. L., ABBOTT, R. M., HOOG, J., DOOLING, D. J., KOBOLDT, D. C., SCHMIDT, H., KALICKI, J., ZHANG, Q. Y., CHEN, L., LIN, L., WENDL, M. C., MCMICHAEL, J. F., MAGRINI, V. J., COOK, L., MCGRATH, S. D., VICKERY, T. L., APPELBAUM, E., DESCHRYVER, K., DAVIES, S., GUINTOLI, T., LIN, L., CROWDER, R., TAO, Y., SNIDER, J. E., SMITH, S. M., DUKES, A. F., SANDERSON, G. E., POHL, C. S., DELEHAUNTY, K. D., FRONICK, C. C., PAPE, K. A., REED, J. S., ROBINSON, J. S., HODGES, J. S., SCHIERDING, W., DEES, N. D., SHEN, D., LOCKE, D. P., WIECHERT, M. E., ELDRED, J. M., PECK, J. B., OBERKFELL, B. J., LOLOFIE, J. T., DU, F. Y., HAWKINS, A. E., O'LAUGHLIN, M. D., BERNARD, K. E., CUNNINGHAM, M., ELLIOTT, G., MASON, M. D., THOMPSON, D. M., IVANOVICH, J. L., GOODFELLOW, P. J., PEROU, C. M., WEINSTOCK, G. M., AFT, R., WATSON, M., LEY, T. J., WILSON, R. K. & MARDIS, E. R. 2010. Genome remodelling in a basal-like breast cancer metastasis and xenograft. *Nature*, 464, 999-1005.
- DINKELMANN, M., SPEHALSKI, E., STONEHAM, T., BUIS, J., WU, Y., SEKIGUCHI, J. M. & FERGUSON, D. O. 2009. Multiple functions of MRN in end-joining pathways during isotype class switching. *Nat Struct Mol Biol*, 16, 808-13.
- DOBZHANSKY, T. 1946. Genetics of Natural Populations. Xiii. Recombination and Variability in Populations of *Drosophila Pseudoobscura*. *Genetics*, 31, 269-90.
- DOLL, J. A., SUAREZ, B. K. & DONIS-KELLER, H. 1996. Association between prostate cancer in black Americans and an allele of the PADPRP pseudogene locus on chromosome 13. *Am J Hum Genet*, 58, 425-8.
- DOMCKE, S., SINHA, R., LEVINE, D. A., SANDER, C. & SCHULTZ, N. 2013. Evaluating cell lines as tumour models by comparison of genomic profiles. *Nature Communications*, 4.
- DONG, R., YU, J., PU, H., ZHANG, Z. & XU, X. 2012. Frequent SLIT2 Promoter Methylation in the Serum of Patients with Ovarian Cancer. *Journal of International Medical Research*, 40, 681-686.
- DREW, Y., MULLIGAN, E. A., VONG, W. T., THOMAS, H. D., KAHN, S., KYLE, S., MUKHOPADHYAY, A., LOS, G., HOSTOMSKY, Z., PLUMMER, E. R., EDMONDSON, R. J. & CURTIN, N. J. 2011. Therapeutic potential of poly(ADP-ribose) polymerase inhibitor AG014699 in human cancers with mutated or methylated BRCA1 or BRCA2. *J Natl Cancer Inst*, 103, 334-46.
- DU BOIS, A., QUINN, M., THIGPEN, T., VERMORKEN, J., AVALL-LUNDQVIST, E., BOOKMAN, M., BOWTELL, D., BRADY, M., CASADO, A., CERVANTES, A., EISENHAEUER, E., FRIEDLAENDER, M., FUJIWARA, K., GRENMAN, S., GUASTALLA, J. P., HARPER, P., HOGBERG, T., KAYE, S., KITCHENER, H., KRISTENSEN, G., MANNEL, R., MEIER, W., MILLER, B., NEIJT, J. P., OZA, A., OZOLS, R., PARMAR, M., PECORELLI, S., PFISTERER, J., POVEDA, A., PROVENCHER, D., PUJADE-LAURAIN, E., RANDALL, M., ROCHON, J., RUSTIN, G., SAGAE, S., STEHMAN, F., STUART, G., TRIMBLE, E., VASEY, P., VERGOTE, I., VERHEIJEN, R. & WAGNER, U. 2005. 2004 consensus statements on the management of ovarian cancer: final document of the 3rd International Gynecologic Cancer Intergroup Ovarian Cancer Consensus Conference (GCIg OCCC 2004). *Annals of Oncology*, 16, 7-12.
- DU BOIS, A., WEBER, B., ROCHON, J., MEIER, W., GOUPIL, A., OLBRICHT, S., BARATS, J. C., KUHN, W., ORFEUVRE, H., WAGNER, U., RICHTER, B., LUECK, H. J., PFISTERER, J., COSTA, S., SCHROEDER, W., KIMMIG, R., PUJADE-LAURAIN, E., ARBEITSGEMEINSCHAFT GYNAEKOLOGISCHE, O., OVARIAN CANCER STUDY, G. & GROUPE D'INVESTIGATEURS NATIONAUX POUR L'ETUDE DES CANCERS, O. 2006. Addition of epirubicin as a third drug to carboplatin-paclitaxel in first-line treatment

- of advanced ovarian cancer: a prospectively randomized gynecologic cancer intergroup trial by the Arbeitsgemeinschaft Gynaekologische Onkologie Ovarian Cancer Study Group and the Groupe d'Investigateurs Nationaux pour l'Etude des Cancers Ovariens. *J Clin Oncol*, 24, 1127-35.
- DUBEAU, L. 1999. The cell of origin of ovarian epithelial tumors and the ovarian surface epithelium dogma: does the emperor have no clothes? *Gynecol Oncol*, 72, 437-42.
- DUNFIELD, L. D., SHEPHERD, T. G. & NACHTIGAL, M. W. 2002. Primary culture and mRNA analysis of human ovarian cells. *Biol Proced Online*, 4, 55-61.
- DUNKERN, T. R., FRITZ, G. & KAINA, B. 2001. Ultraviolet light-induced DNA damage triggers apoptosis in nucleotide excision repair-deficient cells via Bcl-2 decline and caspase-3/-8 activation. *Oncogene*, 20, 6026-38.
- DUPRE, A., BOYER-CHATENET, L., SATTLER, R. M., MODI, A. P., LEE, J. H., NICOLETTE, M. L., KOPELOVICH, L., JASIN, M., BAER, R., PAULL, T. T. & GAUTIER, J. 2008. A forward chemical genetic screen reveals an inhibitor of the Mre11-Rad50-Nbs1 complex. *Nat Chem Biol*, 4, 119-25.
- DUQUET, A., MELOTTI, A., MISHRA, S., MALERBA, M., SETH, C., CONOD, A. & ALTABA, A. R. I. 2014. A novel genome-wide in vivo screen for metastatic suppressors in human colon cancer identifies the positive WNT-TCF pathway modulators TMED3 and SOX12. *Embo Molecular Medicine*, 6, 882-901.
- DUROCHER, F., LABRIE, Y., SOUCY, P., SINILNIKOVA, O., LABUDA, D., BESSETTE, P., CHIQUETTE, J., LAFRAMBOISE, R., LEPINE, J., LESPERANCE, B., OUELLETTE, G., PICHETTE, R., PLANTE, M., TAVTIGIAN, S. V. & SIMARD, J. 2006. Mutation analysis and characterization of ATR sequence variants in breast cancer cases from high-risk French Canadian breast/ovarian cancer families. *BMC Cancer*, 6, 230.
- DUVAL, A. & HAMELIN, R. 2002. Genetic instability in human mismatch repair deficient cancers. *Ann Genet*, 45, 71-5.
- EDWARDS, S. L., BROUGH, R., LORD, C. J., NATRAJAN, R., VATCHEVA, R., LEVINE, D. A., BOYD, J., REIS, J. S. & ASHWORTH, A. 2008. Resistance to therapy caused by intragenic deletion in BRCA2. *Nature*, 451, 1111-U8.
- EISENHAUER, E. A., THERASSE, P., BOGAERTS, J., SCHWARTZ, L. H., SARGENT, D., FORD, R., DANCEY, J., ARBUCK, S., GWYTHYER, S., MOONEY, M., RUBINSTEIN, L., SHANKAR, L., DODD, L., KAPLAN, R., LACOMBE, D., VERWEIJ, J. 2009. New response evaluation criteria in solid tumours: revised RECIST guideline (version 1.1). *Eur J Cancer*, 45, 228-47.
- EL-KHAMISY, S. F., MASUTANI, M., SUZUKI, H. & CALDECOTT, K. W. 2003. A requirement for PARP-1 for the assembly or stability of XRCC1 nuclear foci at sites of oxidative DNA damage. *Nucleic Acids Res*, 31, 5526-33.
- ELATTAR, A., BRYANT, A., WINTER-ROACH, B. A., HATEM, M. & NAIK, R. 2011. Optimal primary surgical treatment for advanced epithelial ovarian cancer. *Cochrane Database Syst Rev*, CD007565.
- ENSHAEI, A., ROBSON, C. N., EDMONDSON, R. J. 2015. Artificial Intelligence Systems as Prognostic and Predictive Tools in Ovarian Cancer. *Ann Surg Oncol*.
- ERTEL, A., DEAN, J. L., RUI, H., LIU, C., WITKIEWICZ, A. K., KNUDSEN, K. E. & KNUDSEN, E. S. 2010. RB-pathway disruption in breast cancer: differential association with disease subtypes, disease-specific prognosis and therapeutic response. *Cell Cycle*, 9, 4153-63.
- ERTEL, A., VERGHESE, A., BYERS, S. W., OCHS, M. & TOZEREN, A. 2006. Pathway-specific differences between tumor cell lines and normal and tumor tissue cells. *Molecular Cancer*, 5.

- FARLEY, J., OZBUN, L. L. & BIRRER, M. J. 2008. Genomic analysis of epithelial ovarian cancer. *Cell Res*, 18, 538-48.
- FARMER, H., MCCABE, N., LORD, C. J., TUTT, A. N., JOHNSON, D. A., RICHARDSON, T. B., SANTAROSA, M., DILLON, K. J., HICKSON, I., KNIGHTS, C., MARTIN, N. M., JACKSON, S. P., SMITH, G. C. & ASHWORTH, A. 2005. Targeting the DNA repair defect in BRCA mutant cells as a therapeutic strategy. *Nature*, 434, 917-21.
- FATHALLA, M. F. 1971. Incessant ovulation--a factor in ovarian neoplasia? *Lancet*, 2, 163.
- FERRY, K. V., HAMILTON, T. C., JOHNSON, S. W. 2000. Increased nucleotide excision repair in cisplatin-resistant ovarian cancer cells: role of ERCC1-XPF. *Biochem Pharmacol*, 60, 1305-13.
- FLAVIN, R. J., SMYTH, P. C., FINN, S. P., LAIOS, A., O'TOOLE, S. A., BARRETT, C., RING, M., DENNING, K. M., LI, J., AHERNE, S. T., AZIZ, N. A., ALHADI, A., SHEPPARD, B. L., LODA, M., MARTIN, C., SHEILS, O. M. & O'LEARY, J. J. 2008. Altered eIF6 and Dicer expression is associated with clinicopathological features in ovarian serous carcinoma patients. *Modern Pathology*, 21, 676-684.
- FOLKINS, A. K., JARBOE, E. A., SALEEMUDDIN, A., LEE, Y., CALLAHAN, M. J., DRAPKIN, R., GARBER, J. E., MUTO, M. G., TWOROGGER, S. & CRUM, C. P. 2008. A candidate precursor to pelvic serous cancer (p53 signature) and its prevalence in ovaries and fallopian tubes from women with BRCA mutations. *Gynecol Oncol*, 109, 168-173.
- FOLKINS, A. K., SALEEMUDDIN, A., GARRETT, L. A., GARBER, J. E., MUTO, M. G., TWOROGGER, S. S., CRUM, C. P. 2009. Epidemiologic correlates of ovarian cortical inclusion cysts (CICs) support a dual precursor pathway to pelvic epithelial cancer. *Gynecol Oncol*, 115, 108-11.
- FONG, P. C., BOSS, D. S., YAP, T. A., TUTT, A., WU, P., MERGUI-ROELVINK, M., MORTIMER, P., SWAISLAND, H., LAU, A., O'CONNOR, M. J., ASHWORTH, A., CARMICHAEL, J., KAYE, S. B., SCHELLENS, J. H. & DE BONO, J. S. 2009. Inhibition of poly(ADP-ribose) polymerase in tumors from BRCA mutation carriers. *N Engl J Med*, 361, 123-34.
- FONG, P. C., YAP, T. A., BOSS, D. S., CARDEN, C. P., MERGUI-ROELVINK, M., GOURLEY, C., DE GREVE, J., LUBINSKI, J., SHANLEY, S., MESSIOU, C., A'HERN, R., TUTT, A., ASHWORTH, A., STONE, J., CARMICHAEL, J., SCHELLENS, J. H. M., DE BONO, J. S. & KAYE, S. B. 2010. Poly(ADP)-Ribose Polymerase Inhibition: Frequent Durable Responses in BRCA Carrier Ovarian Cancer Correlating With Platinum-Free Interval. *Journal of Clinical Oncology*, 28, 2512-2519.
- FRASER, M., ZHAO, H., LUOTO, K. R., LUNDIN, C., COACKLEY, C., CHAN, N., JOSHUA, A. M., BISMAR, T. A., EVANS, A. & HELLEDAY, T. 2012. PTEN deletion in prostate cancer cells does not associate with loss of RAD51 function: implications for radiotherapy and chemotherapy. *Clinical Cancer Research*, 18, 1015-1027.
- FRESE, K. K. & TUVESON, D. A. 2007. Maximizing mouse cancer models. *Nat Rev Cancer*, 7, 645-58.
- FU, Y. P., YU, J. C., CHENG, T. C., LOU, M. A., HSU, G. C., WU, C. Y., CHEN, S. T., WU, H. S., WU, P. E. & SHEN, C. Y. 2003. Breast cancer risk associated with genotypic polymorphism of the nonhomologous end-joining genes: a multigenic study on cancer susceptibility. *Cancer Res*, 63, 2440-6.
- FURUKAWA, R., MASELLI, A., THOMSON, S. A. M., LIM, R. W. L., STOKES, J. V. & FECHHEIMER, M. 2003. Calcium regulation of actin crosslinking is important for function of the actin cytoskeleton in Dictyostelium. *Journal of Cell Science*, 116, 187-196.
- GAGNE, J. P., ISABELLE, M., LO, K. S., BOURASSA, S., HENDZEL, M. J., DAWSON, V. L., DAWSON, T. M. & POIRIER, G. G. 2008. Proteome-wide identification of poly(ADP-

- ribose) binding proteins and poly(ADP-ribose)-associated protein complexes. *Nucleic Acids Res*, 36, 6959-76.
- GALANDE, S. & KOHWI-SHIGEMATSU, T. 1999. Poly(ADP-ribose) polymerase and Ku autoantigen form a complex and synergistically bind to matrix attachment sequences. *J Biol Chem*, 274, 20521-8.
- GATEI, M., YOUNG, D., CEROSALETI, K. M., DESAI-MEHTA, A., SPRING, K., KOZLOV, S., LAVIN, M. F., GATTI, R. A., CONCANNON, P. & KHANNA, K. 2000. ATM-dependent phosphorylation of nibrin in response to radiation exposure. *Nat Genet*, 25, 115-9.
- GAYARRE, J., KAMIENIAK, M. M., CAZORLA-JIMENEZ, A., MUNOZ-REPETO, I., BORREGO, S., GARCIA-DONAS, J., HERNANDO, S., ROBLES-DIAZ, L., GARCIA-BUENO, J. M., RAMON, Y. C. T., HERNANDEZ-AGUDO, E., HEREDIA SOTO, V., MARQUEZ-RODAS, I., ECHARRI, M. J., LACAMBRA-CALVET, C., SAEZ, R., CUSIDO, M., REDONDO, A., PAZ-ARES, L., HARDISSON, D., MENDIOLA, M., PALACIOS, J., BENITEZ, J. & GARCIA, M. J. 2016. The NER-related gene GTF2H5 predicts survival in high-grade serous ovarian cancer patients. *J Gynecol Oncol*, 27, e7.
- GAYMES, T. J., MUFTI, G. J. & RASSOOL, F. V. 2002. Myeloid leukemias have increased activity of the nonhomologous end-joining pathway and concomitant DNA misrepair that is dependent on the Ku70/86 heterodimer. *Cancer Res*, 62, 2791-7.
- GAYTHER, S. A. & PHAROAH, P. D. 2010. The inherited genetics of ovarian and endometrial cancer. *Current Opinions in Genetics & Development*, 20, 231-238.
- GAYTHER, S. A., RUSSELL, P., HARRINGTON, P., ANTONIOU, A. C., EASTON, D. F. & PONDER, B. A. 1999. The contribution of germline BRCA1 and BRCA2 mutations to familial ovarian cancer: no evidence for other ovarian cancer-susceptibility genes. *Am J Hum Genet*, 65, 1021-9.
- GEISLER, J. P., GOODHEART, M. J., SOOD, A. K., HOLMES, R. J., HATTERMAN-ZOGG, M. A. & BULLER, R. E. 2003. Mismatch repair gene expression defects contribute to microsatellite instability in ovarian carcinoma. *Cancer*, 98, 2199-206.
- GELMON, K. A., TISCHKOWITZ, M., MACKAY, H., SWENERTON, K., ROBIDOUX, A., TONKIN, K., HIRTE, H., HUNTSMAN, D., CLEMONS, M., GILKS, B., YERUSHALMI, R., MACPHERSON, E., CARMICHAEL, J., OZA, A. 2011. Olaparib in patients with recurrent high-grade serous or poorly differentiated ovarian carcinoma or triple-negative breast cancer: a phase 2, multicentre, open-label, non-randomised study. *Lancet Oncol*, 12, 852-61.
- GEMIGNANI, M. L., SCHLAERTH, A. C., BOGOMOLNIY, F., BARAKAT, R. R., LIN, O., SOSLOW, R., VENKATRAMAN, E., BOYD, J. 2003. Role of KRAS and BRAF gene mutations in mucinous ovarian carcinoma. *Gynecol Oncol*, 90, 378-81.
- GEYER, J. T., LOPEZ-GARCIA, M. A., SANCHEZ-ESTEVEZ, C., SARRIO, D., MORENO-BUENO, G., FRANCESCHETTI, I., PALACIOS, J. & OLIVA, E. 2009. Pathogenetic pathways in ovarian endometrioid adenocarcinoma: a molecular study of 29 cases. *Am J Surg Pathol*, 33, 1157-63.
- GIANSANTI, V., DONA, F., TILLHON, M. & SCOVASSI, A. I. 2010. PARP inhibitors: new tools to protect from inflammation. *Biochem Pharmacol*, 80, 1869-77.
- GILAD, O., NABET, B. Y., RAGLAND, R. L., SCHOPPY, D. W., SMITH, K. D., DURHAM, A. C. & BROWN, E. J. 2010. Combining ATR suppression with oncogenic Ras synergistically increases genomic instability, causing synthetic lethality or tumorigenesis in a dosage-dependent manner. *Cancer Res*, 70, 9693-702.
- GILLET, J. P., CALCAGNO, A. M., VARMA, S., MARINO, M., GREEN, L. J., VORA, M. I., PATEL, C., ORINA, J. N., ELISEEVA, T. A., SINGAL, V., PADMANABHAN, R., DAVIDSON, B., GANAPATHI, R., SOOD, A. K., RUEDA, B. R., AMBUDKAR, S. V. & GOTTESMAN, M. M. 2011. Redefining the relevance of established cancer cell lines to the study of

- mechanisms of clinical anti-cancer drug resistance. *Proceedings of the National Academy of Sciences of the United States of America*, 108, 18708-18713.
- GILMAN, A. 1963. The initial clinical trial of nitrogen mustard. *Am J Surg*, 105, 574-8.
- GOHRIG, A., DETJEN, K. M., HILFENHAUS, G., KORNER, J. L., WELZEL, M., ARSENIC, R., SCHMUCK, R., BAHRA, M., WU, J. Y., WIEDENMANN, B. & FISCHER, C. 2014. Axon Guidance Factor SLIT2 Inhibits Neural Invasion and Metastasis in Pancreatic Cancer. *Cancer Research*, 74, 1529-1540.
- GOLMARD, L., CAUX-MONCOUTIER, V., DAVY, G., AL AGEELI, E., POIROT, B., TIRAPO, C., MICHAUX, D., BARBAROUX, C., D'ENGHIEN, C. D., NICOLAS, A., CASTERA, L., SASTRE-GARAU, X., STERN, M. H., HOUDAYER, C. & STOPPA-LYONNET, D. 2013. Germline mutation in the RAD51B gene confers predisposition to breast cancer. *Bmc Cancer*, 13.
- GOMES, B. C., SILVA, S. N., AZEVEDO, A. P., MANITA, I., GIL, O. M., FERREIRA, T. C., LIMBERT, E., RUEFF, J. & GASPAR, J. F. 2010. The role of common variants of non-homologous end-joining repair genes XRCC4, LIG4 and Ku80 in thyroid cancer risk. *Oncol Rep*, 24, 1079-1085.
- GONIN, V., BACHELIER, R., DEUX, B., CONTIE, S., BONNELYE, E., RABBITS, P., WU, J. & CLEZARDIN, P. 2010. Involvement of the SLIT2/ROBO1 Pathway in Breast Cancer Bone Metastasis. *Bone*, 47, S273-S273.
- GOODE, E. L., DUNNING, A. M., KUSCHEL, B., HEALEY, C. S., DAY, N. E., PONDER, B. A., EASTON, D. F. & PHAROAH, P. P. 2002. Effect of germ-line genetic variation on breast cancer survival in a population-based study. *Cancer Res*, 62, 3052-7.
- GORE, M., MAINWARING, P., A'HERN, R., MACFARLANE, V., SLEVIN, M., HARPER, P., OSBORNE, R., MANSI, J., BLAKE, P., WILTSHAW, E., SHEPHERD, J. & GRP, L. G. O. 1998. Randomized trial of dose-intensity with single-agent carboplatin in patients with epithelial ovarian cancer. *Journal of Clinical Oncology*, 16, 2426-2434.
- GORRINGE, K. L., JACOBS, S., THOMPSON, E. R., SRIDHAR, A., QIU, W., CHOONG, D. Y. & CAMPBELL, I. G. 2007. High-resolution single nucleotide polymorphism array analysis of epithelial ovarian cancer reveals numerous microdeletions and amplifications. *Clin Cancer Res*, 13, 4731-9.
- GOTTIPATI, P., VISCHIONI, B., SCHULTZ, N., SOLOMONS, J., BRYANT, H. E., DJUREINOVIC, T., ISSAEVA, N., SLEETH, K., SHARMA, R. A. & HELLEDAY, T. 2010. Poly(ADP-ribose) polymerase is hyperactivated in homologous recombination-defective cells. *Cancer Res*, 70, 5389-98.
- GOWEN, L. C., JOHNSON, B. L., LATOUR, A. M., SULIK, K. K. & KOLLER, B. H. 1996. Brca1 deficiency results in early embryonic lethality characterized by neuroepithelial abnormalities. *Nat Genet*, 12, 191-4.
- GRAWUNDER, U., ZIMMER, D., KULESZA, P. & LIEBER, M. R. 1998. Requirement for an interaction of XRCC4 with DNA ligase IV for wild-type V(D)J recombination and DNA double-strand break repair in vivo. *J Biol Chem*, 273, 24708-14.
- GRISHAM, R. N., GARG, K., ZHOU, Q., IASONOS, A., BERGER, M. F., DAO, F., HYMAN, D. M., LEVINE, D. A., SOLIT, D. B., AGHAJANIAN, C. & IYER, G. 2012. A comprehensive analysis of BRAF and KRAS mutation status in low-grade serous (LGS) and serous borderline (SB) ovarian cancer (OC). *Journal of Clinical Oncology*, 30.
- GU, J., LU, H., TIPPIN, B., SHIMAZAKI, N., GOODMAN, M. F. & LIEBER, M. R. 2007a. XRCC4:DNA ligase IV can ligate incompatible DNA ends and can ligate across gaps. *EMBO J*, 26, 1010-23.

- GU, J., LU, H., TSAI, A. G., SCHWARZ, K. & LIEBER, M. R. 2007b. Single-stranded DNA ligation and XLF-stimulated incompatible DNA end ligation by the XRCC4-DNA ligase IV complex: influence of terminal DNA sequence. *Nucleic Acids Res*, 35, 5755-62.
- GUAN, B., WANG, T. L. & SHIH IE, M. 2011. ARID1A, a factor that promotes formation of SWI/SNF-mediated chromatin remodeling, is a tumor suppressor in gynecologic cancers. *Cancer Res*, 71, 6718-27.
- GUO, L. L., LIU, Y. G., BAI, Y. F., SUN, Y. Q., XIAO, F. M. & GUO, Y. 2010. Gene expression profiling of drug-resistant small cell lung cancer cells by combining microRNA and cDNA expression analysis. *European Journal of Cancer*, 46, 1692-1702.
- GUO, Y. F., XIAO, P., LEI, S. F., DENG, F. Y., XIAO, G. G., LIU, Y. Z., CHEN, X. D., LI, L. M., WU, S., CHEN, Y., JIANG, H., TAN, L. J., XIE, J. Y., ZHU, X. Z., LIANG, S. P. & DENG, H. W. 2008. How is mRNA expression predictive for protein expression? A correlation study on human circulating monocytes. *Acta Biochimica Et Biophysica Sinica*, 40, 426-436.
- HAFFNER, M. C., PETRIDOU, B., PEYRAT, J. P., REVILLION, F., MULLER-HOLZNER, E., DAXENBICHLER, G., MARTH, C. & DOPPLER, W. 2007. Favorable prognostic value of SOCS2 and IGF-I in breast cancer. *Bmc Cancer*, 7.
- HAINCE, J. F., MCDONALD, D., RODRIGUE, A., DERY, U., MASSON, J. Y., HENDZEL, M. J. & POIRIER, G. G. 2008. PARP1-dependent kinetics of recruitment of MRE11 and NBS1 proteins to multiple DNA damage sites. *J Biol Chem*, 283, 1197-208.
- HAN, J., HANKINSON, S. E., RANU, H., DE VIVO, I. & HUNTER, D. J. 2004. Polymorphisms in DNA double-strand break repair genes and breast cancer risk in the Nurses' Health Study. *Carcinogenesis*, 25, 189-95.
- HANAHAN, D. & WEINBERG, R. A. 2011. Hallmarks of cancer: the next generation. *Cell*, 144, 646-74.
- HARDISTY, J. F. 1985. Factors influencing laboratory animal spontaneous tumor profiles. *Toxicol Pathol*, 13, 95-104.
- HARTER, P., DU BOIS, A., HAHMANN, M., HASENBURG, A., BURGESS, A., LOIBL, S., GROPP, M., HUOBER, J., FINK, D., SCHRODER, W., MUENSTEDT, K., SCHMALFELDT, B., EMONS, G., PFISTERER, J., WOLLSCHLAEGER, K., MEERPOHL, H. G., BREITBACH, G. P., TANNER, B. & SEHOULI, J. 2006. Surgery in recurrent ovarian cancer: the Arbeitsgemeinschaft Gynaekologische Onkologie (AGO) DESKTOP OVAR trial. *Ann Surg Oncol*, 13, 1702-10.
- HARTLERODE, A. J. & SCULLY, R. 2009. Mechanisms of double-strand break repair in somatic mammalian cells. *Biochem J*, 423, 157-68.
- HARTLEY, A., ROLLASON, T. & SPOONER, D. 2000. Clear cell carcinoma of the fimbria of the fallopian tube in a BRCA1 carrier undergoing prophylactic surgery. *Clinical Oncology*, 12, 58-59.
- HE, J. X., KANG, X., YIN, Y. X., CHAO, K. S. C. & SHEN, W. H. 2015. PTEN regulates DNA replication progression and stalled fork recovery. *Nature Communications*, 6.
- HECHT, J. L., KOTSOPOULOS, J., GATES, M. A., HANKINSON, S. E. & TWOROGGER, S. S. 2008. Validation of tissue microarray technology in ovarian cancer: results from the Nurses' Health Study. *Cancer Epidemiol Biomarkers Prev*, 17, 3043-50.
- HEDDITCH, E. L., HENDERSON, M. J., RUSSELL, A. J., GAO, B., EMMANUEL, C., WILLIAMS, R. T., FLEMMING, C., JOHNATTY, S., GEORGE, J., MACGREGOR, S., BOWTELL, D., CHENEVIX-TRENCH, G., DEFAZIO, A., NORRIS, M. D., HABER, M. & GRP, A. O. C. S. 2015. Association of Abca1 Cholesterol Transporter with Poor Outcome and Aggressive Phenotype in Serous Ovarian Cancer. *Asia-Pacific Journal of Clinical Oncology*, 11, 114-114.

- HEGAN, D. C., LU, Y., STACHELEK, G. C., CROSBY, M. E., BINDRA, R. S. & GLAZER, P. M. 2010. Inhibition of poly(ADP-ribose) polymerase down-regulates BRCA1 and RAD51 in a pathway mediated by E2F4 and p130. *Proc Natl Acad Sci U S A*, 107, 2201-6.
- HEIKKINEN, K., KARPPINEN, S. M., SOINI, Y., MAKINEN, M. & WINQVIST, R. 2003. Mutation screening of Mre11 complex genes: indication of RAD50 involvement in breast and ovarian cancer susceptibility. *J Med Genet*, 40, e131.
- HEIKKINEN, K., MANSIKKA, V., KARPPINEN, S. M., RAPAKKO, K. & WINQVIST, R. 2005. Mutation analysis of the ATR gene in breast and ovarian cancer families. *Breast Cancer Res*, 7, R495-501.
- HEIKKINEN, K., RAPAKKO, K., KARPPINEN, S. M., ERKKO, H., KNUUTILA, S., LUNDAN, T., MANNERMAA, A., BORRESEN-DALE, A. L., BORG, A., BARKARDOTTIR, R. B., PETRINI, J. & WINQVIST, R. 2006. RAD50 and NBS1 are breast cancer susceptibility genes associated with genomic instability. *Carcinogenesis*, 27, 1593-9.
- HELLEDAY, T. 2010. Homologous recombination in cancer development, treatment and development of drug resistance. *Carcinogenesis*, 31, 955-60.
- HELLEDAY, T. 2011. The underlying mechanism for the PARP and BRCA synthetic lethality: clearing up the misunderstandings. *Mol Oncol*, 5, 387-93.
- HELLEDAY, T., BRYANT, H. E. & SCHULTZ, N. 2005. Poly(ADP-ribose) polymerase (PARP-1) in homologous recombination and as a target for cancer therapy. *Cell Cycle*, 4, 1176-8.
- HELLEDAY, T., PETERMANN, E., LUNDIN, C., HODGSON, B. & SHARMA, R. A. 2008. DNA repair pathways as targets for cancer therapy. *Nat Rev Cancer*, 8, 193-204.
- HELLEMAN, J., VAN STAVEREN, I. L., DINJENS, W. N., VAN KUIJK, P. F., RITSTIER, K., EWING, P. C., VAN DER BURG, M. E., STOTER, G. & BERNIS, E. M. 2006. Mismatch repair and treatment resistance in ovarian cancer. *BMC Cancer*, 6, 201.
- HENNESSY, B. T., COLEMAN, R. L. & MARKMAN, M. 2009. Ovarian cancer. *Lancet*, 374, 1371-82.
- HENNESSY, B. T., TIMMS, K. M., CAREY, M. S., GUTIN, A., MEYER, L. A., FLAKE, D. D., 2ND, ABKEVICH, V., POTTER, J., PRUSS, D., GLENN, P., LI, Y., LI, J., GONZALEZ-ANGULO, A. M., MCCUNE, K. S., MARKMAN, M., BROADDUS, R. R., LANCHBURY, J. S., LU, K. H. & MILLS, G. B. 2010. Somatic mutations in BRCA1 and BRCA2 could expand the number of patients that benefit from poly (ADP ribose) polymerase inhibitors in ovarian cancer. *J Clin Oncol*, 28, 3570-6.
- HERRINGTON, C. S., MCCLUGGAGE, W. G. 2010. The emerging role of the distal Fallopian tube and p53 in pelvic serous carcinogenesis. *J Pathol*, 220, 5-6.
- HERZOG, T. J. 2004. Recurrent ovarian cancer: how important is it to treat to disease progression? *Clin Cancer Res*, 10, 7439-49.
- HEYER, W. D., EHMTSEN, K. T. & LIU, J. 2010. Regulation of Homologous Recombination in Eukaryotes. *Annual Review of Genetics*, Vol 44, 44, 113-139.
- HIBBS, K., SKUBITZ, K. M., PAMBUCCIAN, S. E., CASEY, R. C., BURLESON, K. M., OEGEMA, T. R., JR., THIELE, J. J., GRINDLE, S. M., BLISS, R. L., SKUBITZ, A. P. 2004. Differential gene expression in ovarian carcinoma: identification of potential biomarkers. *Am J Pathol*, 165, 397-414.
- HICKSON, I., YAN, Z., RICHARDSON, C. J., GREEN, S. J., MARTIN, N. M. B., ORR, A. I., REAPER, P. M., JACKSON, S. P., CURTIN, N. J. & SMITH, G. C. M. 2004. Identification and characterization of a novel and specific inhibitor of the ataxia-telangiectasia mutated kinase ATM. *Cancer Research*, 64, 9152-9159.
- HILL, D. A., WANG, S. S., CERHAN, J. R., DAVIS, S., COZEN, W., SEVERSON, R. K., HARTGE, P., WACHOLDER, S., YEAGER, M., CHANOCK, S. J. & ROTHMAN, N. 2006. Risk of non-

- Hodgkin lymphoma (NHL) in relation to germline variation in DNA repair and related genes. *Blood*, 108, 3161-7.
- HILTON, J. L., GEISLER, J. P., RATHE, J. A., HATTERMANN-ZOGG, M. A., DEYOUNG, B. & BULLER, R. E. 2002. Inactivation of BRCA1 and BRCA2 in ovarian cancer. *J Natl Cancer Inst*, 94, 1396-406.
- HO, C. L., KURMAN, R. J., DEHARI, R., WANG, T. L. & SHIH IE, M. 2004. Mutations of BRAF and KRAS precede the development of ovarian serous borderline tumors. *Cancer Res*, 64, 6915-8.
- HOCHEGGER, H., DEJSUPHONG, D., FUKUSHIMA, T., MORRISON, C., SONODA, E., SCHREIBER, V., ZHAO, G. Y., SABERI, A., MASUTANI, M., ADACHI, N., KOYAMA, H., DE MURCIA, G. & TAKEDA, S. 2006. Parp-1 protects homologous recombination from interference by Ku and Ligase IV in vertebrate cells. *EMBO J*, 25, 1305-14.
- HOEFER, J., KERN, J., OFER, P., EDER, I. E., SCHAFER, G., DIETRICH, D., KRISTIANSEN, G., GELEY, S., RAINER, J., GUNSILIUS, E., KLOCKER, H., CULIG, Z. & PUHR, M. 2014. SOCS2 correlates with malignancy and exerts growth-promoting effects in prostate cancer. *Endocrine-Related Cancer*, 21, 175-187.
- HOEIJMAKERS, J. H. 2001. Genome maintenance mechanisms for preventing cancer. *Nature*, 411, 366-74.
- HOEIJMAKERS, J. H. 2009. DNA damage, aging, and cancer. *N Engl J Med*, 361, 1475-85.
- HOFFMANN, A. C., WILD, P., LEICHT, C., BERTZ, S., DANENBERG, K. D., DANENBERG, P. V., STOHR, R., STOCKLE, M., LEHMANN, J., SCHULER, M. & HARTMANN, A. 2010. MDR1 and ERCC1 expression predict outcome of patients with locally advanced bladder cancer receiving adjuvant chemotherapy. *Neoplasia*, 12, 628-36.
- HOLZER, A. K., KATANO, K., KLOMP, L. W. & HOWELL, S. B. 2004. Cisplatin rapidly down-regulates its own influx transporter hCTR1 in cultured human ovarian carcinoma cells. *Clin Cancer Res*, 10, 6744-9.
- HOLZER, A. K., MANOREK, G. H. & HOWELL, S. B. 2006. Contribution of the major copper influx transporter CTR1 to the cellular accumulation of cisplatin, carboplatin, and oxaliplatin. *Mol Pharmacol*, 70, 1390-4.
- HORTON, J. K. & WILSON, S. H. 2013. Strategic Combination of DNA-Damaging Agent and PARP Inhibitor Results in Enhanced Cytotoxicity. *Front Oncol*, 3, 257.
- HOSKINS, P., VERGOTE, I., CERVANTES, A., TU, D., STUART, G., ZOLA, P., POVEDA, A., PROVENCHER, D., KATSAROS, D., OJEDA, B., GHATAGE, P., GRIMSHAW, R., CASADO, A., ELIT, L., MENDIOLA, C., SUGIMOTO, A., D'HONDT, V., OZA, A., GERMA, J. R., ROY, M., BROTT, L., CHEN, D. & EISENHAEUER, E. A. 2010. Advanced ovarian cancer: phase III randomized study of sequential cisplatin-topotecan and carboplatin-paclitaxel vs carboplatin-paclitaxel. *J Natl Cancer Inst*, 102, 1547-56.
- HSU, N. Y., WANG, H. C., WANG, C. H., CHANG, C. L., CHIU, C. F., LEE, H. Z., TSAI, C. W. & BAU, D. T. 2009. Lung cancer susceptibility and genetic polymorphism of DNA repair gene XRCC4 in Taiwan. *Cancer Biomarkers*, 5, 159-165.
- HU, J. J., ROUSH, G. C., DUBIN, N., BERWICK, M., ROSES, D. F. & HARRIS, M. N. 1997. Poly(ADP-ribose) polymerase in human breast cancer: a case-control analysis. *Pharmacogenetics*, 7, 309-16.
- HU, L., ZALOUDEK, C., MILLS, G. B., GRAY, J., JAFFE, R. B. 2000. In vivo and in vitro ovarian carcinoma growth inhibition by a phosphatidylinositol 3-kinase inhibitor (LY294002). *Clin Cancer Res*, 6, 880-6.
- HUANG, F., MOTLEKAR, N. A., BURGWIN, C. M., NAPPER, A. D., DIAMOND, S. L. & MAZIN, A. V. 2011a. Identification of Specific Inhibitors of Human RAD51 Recombinase Using High-Throughput Screening. *Acs Chemical Biology*, 6, 628-635.

- HUANG, J., ZHANG, L., GRESHOCK, J., COLLIGON, T. A., WANG, Y., WARD, R., KATSAROS, D., LASSUS, H., BUTZOW, R. & GODWIN, A. K. 2011b. Frequent genetic abnormalities of the PI3K/AKT pathway in primary ovarian cancer predict patient outcome. *Genes, Chromosomes and Cancer*, 50, 606-618.
- HUNCHAREK, M., GESCHWIND, J. F., KUEPelnICK, B. 2003. Perineal application of cosmetic talc and risk of invasive epithelial ovarian cancer: a meta-analysis of 11,933 subjects from sixteen observational studies. *Anticancer Res*, 23, 1955-60.
- HUNT, C. R., GUPTA, A., HORIKOSHI, N. & PANDITA, T. K. 2012. Does PTEN loss impair DNA double-strand break repair by homologous recombination? *Clin Cancer Res*, 18, 920-2.
- IBRAGIMOVA, I. & CAIRNS, P. 2011. Assays for hypermethylation of the BRCA1 gene promoter in tumor cells to predict sensitivity to PARP-inhibitor therapy. *Methods Mol Biol*, 780, 277-91.
- IBRAHIM, Y. H., GARCIA-GARCIA, C., SERRA, V., HE, L., TORRES-LOCKHART, K., PRAT, A., ANTON, P., COZAR, P., GUZMAN, M., GRUESO, J., RODRIGUEZ, O., CALVO, M. T., AURA, C., DIEZ, O., RUBIO, I. T., PEREZ, J., RODON, J., CORTES, J., ELLISEN, L. W., SCALTRITI, M. & BASELGA, J. 2012. PI3K inhibition impairs BRCA1/2 expression and sensitizes BRCA-proficient triple-negative breast cancer to PARP inhibition. *Cancer Discov*, 2, 1036-47.
- ILIAKIS, G., WANG, H., PERRAULT, A. R., BOECKER, W., ROSIDI, B., WINDHOFER, F., WU, W., GUAN, J., TERZOUDI, G. & PANTELIS, G. 2004. Mechanisms of DNA double strand break repair and chromosome aberration formation. *Cytogenet Genome Res*, 104, 14-20.
- ILLUZZI, J. L. & WILSON, D. M., 3RD 2012. Base excision repair: contribution to tumorigenesis and target in anticancer treatment paradigms. *Curr Med Chem*, 19, 3922-36.
- INCE, T. A., SOUSA, A. D., JONES, M. A., HARRELL, J. C., AGOSTON, E. S., KROHN, M., SELFORS, L. M., LIU, W., CHEN, K., YONG, M., BUCHWALD, P., WANG, B., HALE, K. S., COHICK, E., SERGENT, P., WITT, A., KOZHEKBAEVA, Z., GAO, S., AGOSTON, A. T., MERRITT, M. A., FOSTER, R., RUEDA, B. R., CRUM, C. P., BRUGGE, J. S. & MILLS, G. B. 2015. Characterization of twenty-five ovarian tumour cell lines that phenocopy primary tumours. *Nat Commun*, 6, 7419.
- IP, S. C., RASS, U., BLANCO, M. G., FLYNN, H. R., SKEHEL, J. M. & WEST, S. C. 2008. Identification of Holliday junction resolvases from humans and yeast. *Nature*, 456, 357-61.
- ITAMOCHI, H., KIGAWA, J. & TERAOKAWA, N. 2008. Mechanisms of chemoresistance and poor prognosis in ovarian clear cell carcinoma. *Cancer Science*, 99, 653-658.
- JACINTO, F. V. & ESTELLER, M. 2007. Mutator pathways unleashed by epigenetic silencing in human cancer. *Mutagenesis*, 22, 247-53.
- JACQUEMONT, C. & TANIGUCHI, T. 2007. Proteasome function is required for DNA damage response and fanconi anemia pathway activation. *Cancer Res*, 67, 7395-405.
- JAMIESON, E. R. & LIPPARD, S. J. 1999. Structure, Recognition, and Processing of Cisplatin-DNA Adducts. *Chem Rev*, 99, 2467-98.
- JANEZIC, S. A., ZIOGAS, A., KRUMROY, L. M., KRASNER, M., PLUMMER, S. J., COHEN, P., GILDEA, M., BARKER, D., HAILE, R., CASEY, G. & ANTON-CULVER, H. 1999. Germline BRCA1 alterations in a population-based series of ovarian cancer cases. *Hum Mol Genet*, 8, 889-97.
- JASPERS, J. E., KERSBERGEN, A., BOON, U., SOL, W., VAN DEEMTER, L., ZANDER, S. A., DROST, R., WIJNTJENS, E., JI, J., ALY, A., DOROSHOW, J. H., CRANSTON, A., MARTIN, N. M., LAU, A., O'CONNOR, M. J., GANESAN, S., BORST, P., JONKERS, J. & ROTTENBERG, S.

2013. Loss of 53BP1 causes PARP inhibitor resistance in Brca1-mutated mouse mammary tumors. *Cancer Discov*, 3, 68-81.
- JAVLE, M. & CURTIN, N. J. 2011. The role of PARP in DNA repair and its therapeutic exploitation. *British Journal of Cancer*, 105, 1114-1122.
- JAZAERI, A. A., YEE, C. J., SOTIRIOU, C., BRANTLEY, K. R., BOYD, J., LIU, E. T. 2002. Gene expression profiles of BRCA1-linked, BRCA2-linked, and sporadic ovarian cancers. *J Natl Cancer Inst*, 94, 990-1000.
- JEGGO, P. A., CALDECOTT, K., PIDSLEY, S. & BANKS, G. R. 1989. Sensitivity of Chinese hamster ovary mutants defective in DNA double strand break repair to topoisomerase II inhibitors. *Cancer Res*, 49, 7057-63.
- JEGGO, P. A., O'DRISCOLL, M., GENNERY, A. R., SEIDEL, J. & CONCANNON, P. 2004. An overview of three new disorders associated with genetic instability: LIG4 syndrome, RS-SCID and ATR-Seckel syndrome. *DNA Repair*, 3, 1227-1235.
- JEMAL, A., SIEGEL, R., WARD, E., HAO, Y., XU, J. & THUN, M. J. 2009. Cancer statistics, 2009. *CA Cancer J Clin*, 59, 225-49.
- JIAN, H., ZHAO, Y., LIU, B. & LU, S. 2015. SEMA4B inhibits growth of non-small cell lung cancer in vitro and in vivo. *Cellular Signalling*, 27, 1208-1213.
- JIN, H., SUH, D. S., KIM, T. H., YEOM, J. H., LEE, K. & BAE, J. 2015. IER3 is a crucial mediator of TAp73 beta-induced apoptosis in cervical cancer and confers etoposide sensitivity. *Scientific Reports*, 5.
- JOHNSON, N., LI, Y. C., WALTON, Z. E., CHENG, K. A., LI, D. A., RODIG, S. J., MOREAU, L. A., UNITT, C., BRONSON, R. T., THOMAS, H. D., NEWELL, D. R., D'ANDREA, A. D., CURTIN, N. J., WONG, K. K. & SHAPIRO, G. I. 2011. Compromised CDK1 activity sensitizes BRCA-proficient cancers to PARP inhibition. *Nature Medicine*, 17, 875-U257.
- JONES, S., WANG, T.-L., SHIH, I.-M., MAO, T.-L., NAKAYAMA, K., RODEN, R., GLAS, R., SLAMON, D., DIAZ JR, L. A. & VOGELSTEIN, B. 2010. Frequent mutations of chromatin remodeling gene ARID1A in ovarian clear cell carcinoma. *Science Signaling*, 330, 228.
- JONKERS, J. & BERNIS, A. 2002. Conditional mouse models of sporadic cancer. *Nature Reviews Cancer*, 2, 251-265.
- KACHNIC, L. A., WU, B., WUNSCH, H., MEKEEL, K. L., DEFRANK, J. S., TANG, W. & POWELL, S. N. 1999. The ability of p53 to activate downstream genes p21(WAF1/cip1) and MDM2, and cell cycle arrest following DNA damage is delayed and attenuated in scid cells deficient in the DNA-dependent protein kinase. *J Biol Chem*, 274, 13111-7.
- KAE LIN, W. G., JR. 2005. The concept of synthetic lethality in the context of anticancer therapy. *Nat Rev Cancer*, 5, 689-98.
- KANAAR, R., HOEIJMAKERS, J. H. & VAN GENT, D. C. 1998. Molecular mechanisms of DNA double strand break repair. *Trends Cell Biol*, 8, 483-9.
- KANG, J., D'ANDREA, A. D., KOZONO, D. 2012. A DNA repair pathway-focused score for prediction of outcomes in ovarian cancer treated with platinum-based chemotherapy. *J Natl Cancer Inst*, 104, 670-81.
- KARAGOL, H., SAIP, P., UYGUN, K., CALOGLU, M., ERALP, Y., TAS, F., AYDINER, A. & TOPUZ, E. 2007. The efficacy of tamoxifen in patients with advanced epithelial ovarian cancer. *Med Oncol*, 24, 39-43.
- KARLAN, B. Y., OZA, A. M., RICHARDSON, G. E., PROVENCHER, D. M., HANSEN, V. L., BUCK, M., CHAMBERS, S. K., GHATAGE, P., PIPPITT, C. H., JR., BROWN, J. V., 3RD, COVENS, A., NAGARKAR, R. V., DAVY, M., LEATH, C. A., 3RD, NGUYEN, H., STEPAN, D. E., WEINREICH, D. M., TASSOUDJI, M., SUN, Y. N. & VERGOTE, I. B. 2012. Randomized, double-blind, placebo-controlled phase II study of AMG 386 combined with weekly paclitaxel in patients with recurrent ovarian cancer. *J Clin Oncol*, 30, 362-71.

- KASHISHIAN, A., DOUANGPANYA, H., CLARK, D., SCHLACHTER, S. T., EARY, C. T., SCHIRO, J. G., HUANG, H., BURGESS, L. E., KESICKI, E. A. & HALBROOK, J. 2003. DNA-dependent protein kinase inhibitors as drug candidates for the treatment of cancer. *Mol Cancer Ther*, 2, 1257-64.
- KAUFMAN, B., SHAPIRA-FROMMER, R., SCHMUTZLER, R. K., AUDEH, M. W., FRIEDLANDER, M., BALMANA, J., MITCHELL, G., FRIED, G., STEMMER, S. M., HUBERT, A., ROSENGARTEN, O., STEINER, M., LOMAN, N., BOWEN, K., FIELDING, A. & DOMCHEK, S. M. 2015. Olaparib Monotherapy in Patients With Advanced Cancer and a Germline BRCA1/2 Mutation. *Journal of Clinical Oncology*, 33, 244-U134.
- KAYE, S. B. 1996. Ovarian cancer, from the laboratory to the clinic: challenges for the future. *Ann Oncol*, 7, 9-13.
- KAYE, S. B., LUBINSKI, J., MATULONIS, U., ANG, J. E., GOURLEY, C., KARLAN, B. Y., AMNON, A., BELL-MCGUINN, K. M., CHEN, L. M., FRIEDLANDER, M., SAFRA, T., VERGOTE, I., WICKENS, M., LOWE, E. S., CARMICHAEL, J. & KAUFMAN, B. 2012. Phase II, Open-Label, Randomized, Multicenter Study Comparing the Efficacy and Safety of Olaparib, a Poly (ADP-Ribose) Polymerase Inhibitor, and Pegylated Liposomal Doxorubicin in Patients With BRCA1 or BRCA2 Mutations and Recurrent Ovarian Cancer. *Journal of Clinical Oncology*, 30, 372-379.
- KENDALL, S. D., ADAM, S. J. & COUNTER, C. M. 2006. Genetically engineered human cancer models utilizing mammalian transgene expression. *Cell Cycle*, 5, 1074-9.
- KENIRY, M. & PARSONS, R. 2008. The role of PTEN signaling perturbations in cancer and in targeted therapy. *Oncogene*, 27, 5477-5485.
- KENNEDY, R. D. & D'ANDREA, A. D. 2005. The Fanconi Anemia/BRCA pathway: new faces in the crowd. *Genes Dev*, 19, 2925-40.
- KENNEDY, R. D. & D'ANDREA, A. D. 2006. DNA repair pathways in clinical practice: lessons from pediatric cancer susceptibility syndromes. *J Clin Oncol*, 24, 3799-808.
- KHANNA, K. K. & JACKSON, S. P. 2001. DNA double-strand breaks: signaling, repair and the cancer connection. *Nat Genet*, 27, 247-54.
- KIM, G., ISON, G., MCKEE, A. E., ZHANG, H., TANG, S., GWISE, T., SRIDHARA, R., LEE, E., TZOU, A., PHILIP, R., CHIU, H. J., RICKS, T. K., PALMBY, T., RUSSELL, A. M., LADOUCEUR, G., PFUMA, E., LI, H., ZHAO, L., LIU, Q., VENUGOPAL, R., IBRAHIM, A. & PAZDUR, R. 2015. FDA Approval Summary: Olaparib Monotherapy in Patients with Deleterious Germline BRCA-Mutated Advanced Ovarian Cancer Treated with Three or More Lines of Chemotherapy. *Clin Cancer Res*.
- KIM, H. S., KIM, T. H., CHUNG, H. H. & SONG, Y. S. 2014. Risk and prognosis of ovarian cancer in women with endometriosis: a meta-analysis. *Br J Cancer*, 110, 1878-90.
- KIM, S. H., UM, J. H., DONG-WON, B., KWON, B. H., KIM, D. W., CHUNG, B. S. & KANG, C. D. 2000. Potentiation of chemosensitivity in multidrug-resistant human leukemia CEM cells by inhibition of DNA-dependent protein kinase using wortmannin. *Leuk Res*, 24, 917-25.
- KIM, S. T., LIM, D. S., CANMAN, C. E. & KASTAN, M. B. 1999. Substrate specificities and identification of putative substrates of ATM kinase family members. *J Biol Chem*, 274, 37538-43.
- KINDELBERGER, D. W., LEE, Y., MIRON, A., HIRSCH, M. S., FELTMATE, C., MEDEIROS, F., CALLAHAN, M. J., GARNER, E. O., GORDON, R. W., BIRCH, C., BERKOWITZ, R. S., MUTO, M. G., CRUM, C. P. 2007. Intraepithelial carcinoma of the fimbria and pelvic serous carcinoma: Evidence for a causal relationship. *Am J Surg Pathol*, 31, 161-9.
- KITCHENER, H. C. 2008. Survival from cancer of the ovary in England and Wales up to 2001. *Br J Cancer*, 99 Suppl 1, S73-4.

- KNAPPSKOG, S. & LONNING, P. E. 2012. P53 and its molecular basis to chemoresistance in breast cancer. *Expert Opin Ther Targets*, 16 Suppl 1, S23-30.
- KOBEL, M., KALLOGER, S. E., BOYD, N., MCKINNEY, S., MEHL, E., PALMER, C., LEUNG, S., BOWEN, N. J., IONESCU, D. N., RAJPUT, A., PRENTICE, L. M., MILLER, D., SANTOS, J., SWENERTON, K., GILKS, C. B. & HUNTSMAN, D. 2008. Ovarian carcinoma subtypes are different diseases: implications for biomarker studies. *PLoS Med*, 5, e232.
- KODAZ, H., HACIBEKIROGLU, I., TURKMEN, E., ERDOGAN, B., ELPEN, C., UZUNOGLU, S. & CICIN, I. 2015. Increased dose single-agent gemcitabine in platinum-taxane resistant metastatic ovarian cancer. *Tumori*, 101, 36-40.
- KOHN, E. C., SAROSY, G., BICHER, A., LINK, C., CHRISTIAN, M., STEINBERG, S. M., ROTHENBERG, M., ADAMO, D. O., DAVIS, P., OGNIBENE, F. P. & ET AL. 1994. Dose-intensive taxol: high response rate in patients with platinum-resistant recurrent ovarian cancer. *J Natl Cancer Inst*, 86, 18-24.
- KONSTANTINOPOULOS, P. A., SPENTZOS, D., KARLAN, B. Y., TANIGUCHI, T., FOUNTZILAS, E., FRANCOEUR, N., LEVINE, D. A. & CANNISTRA, S. A. 2010. Gene expression profile of BRCAness that correlates with responsiveness to chemotherapy and with outcome in patients with epithelial ovarian cancer. *J Clin Oncol*, 28, 3555-61.
- KONTOROVICH, T., COHEN, Y., NIR, U. & FRIEDMAN, E. 2008. Promoter methylation patterns of ATM, ATR, BRCA1, BRCA2 and P53 as putative cancer risk modifiers in Jewish BRCA1/BRCA2 mutation carriers. *Breast Cancer Res Treat*.
- KORCH, C., SPILLMAN, M. A., JACKSON, T. A., JACOBSEN, B. M., MURPHY, S. K., LESSEY, B. A., JORDAN, V. C. & BRADFORD, A. P. 2012. DNA profiling analysis of endometrial and ovarian cell lines reveals misidentification, redundancy and contamination. *Gynecol Oncol*, 127, 241-8.
- KORITA, P. V., WAKAI, T., SHIRAI, Y., MATSUDA, Y., SAKATA, J., TAKAMURA, M., YANO, M., SANPEI, A., AOYAGI, Y., HATAKEYAMA, K. & AJIOKA, Y. 2010. Multidrug resistance-associated protein 2 determines the efficacy of cisplatin in patients with hepatocellular carcinoma. *Oncol Rep*, 23, 965-72.
- KOUSSOUNADIS, A., LANGDON, S. P., HARRISON, D. J. & SMITH, V. A. 2014. Chemotherapy-induced dynamic gene expression changes in vivo are prognostic in ovarian cancer. *Br J Cancer*, 110, 2975-84.
- KRISHNAKUMAR, R. & KRAUS, W. L. 2010. The PARP side of the nucleus: molecular actions, physiological outcomes, and clinical targets. *Mol Cell*, 39, 8-24.
- KRZYWINSKI, M., SCHEIN, J., BIROL, I., CONNORS, J., GASCOYNE, R., HORSMAN, D., JONES, S. J. & MARRA, M. A. 2009. Circos: an information aesthetic for comparative genomics. *Genome Res*, 19, 1639-45.
- KUO, K.-T., MAO, T.-L., JONES, S., VERAS, E., AYHAN, A., WANG, T.-L., GLAS, R., SLAMON, D., VELCULESCU, V. E. & KUMAN, R. J. 2009. Frequent Activating Mutations of *PIK3CA* in Ovarian Clear Cell Carcinoma. *The American journal of pathology*, 174, 1597-1601.
- KURIMASA, A., OUYANG, H., DONG, L. J., WANG, S., LI, X., CORDON-CARDO, C., CHEN, D. J. & LI, G. C. 1999. Catalytic subunit of DNA-dependent protein kinase: impact on lymphocyte development and tumorigenesis. *Proc Natl Acad Sci U S A*, 96, 1403-8.
- KURMAN, R. J. & SHIH, I.-M. 2010. The Origin and pathogenesis of epithelial ovarian cancer-a proposed unifying theory. *The American journal of surgical pathology*, 34, 433.
- KURMAN, R. J. & SHIH, I. M. 2011. Molecular pathogenesis and extraovarian origin of epithelial ovarian cancer--shifting the paradigm. *Hum Pathol*, 42, 918-31.
- KUSCHEL, B., AURANEN, A., MCBRIDE, S., NOVIK, K. L., ANTONIOU, A., LIPSCOMBE, J. M., DAY, N. E., EASTON, D. F., PONDER, B. A., PHAROAH, P. D. & DUNNING, A. 2002.

- Variants in DNA double-strand break repair genes and breast cancer susceptibility. *Hum Mol Genet*, 11, 1399-407.
- KUSSIE, P. H., GORINA, S., MARECHAL, V., ELENBAAS, B., MOREAU, J., LEVINE, A. J. & PAVLETICH, N. P. 1996. Structure of the MDM2 oncoprotein bound to the p53 tumor suppressor transactivation domain. *Science*, 274, 948-53.
- KUTLER, D. I., SINGH, B., SATAGOPAN, J., BATISH, S. D., BERWICK, M., GIAMPIETRO, P. F., HANENBERG, H. & AUERBACH, A. D. 2003. A 20-year perspective on the International Fanconi Anemia Registry (IFAR). *Blood*, 101, 1249-56.
- LABHART, P. 1999. Nonhomologous DNA end joining in cell-free systems. *Eur J Biochem*, 265, 849-61.
- LACUNZA, E., CANZONERI, R., RABASSA, M. E., ZWENGER, A., SEGAL-EIRAS, A., CROCE, M. V. & ABBA, M. C. 2012. RHBDD2: a 5-fluorouracil responsive gene overexpressed in the advanced stages of colorectal cancer. *Tumor Biology*, 33, 2393-2399.
- LAHMANN, P. H., CUST, A. E., FRIEDENREICH, C. M., SCHULZ, M., LUKANOVA, A., KAAKS, R., LUNDIN, E., TJONNELAND, A., HALKJAER, J., SPENCER, E., RINALDI, S., SLIMANI, N., CHAJES, V., MICHAUD, D., NORAT, T., RIBOLI, E. 2010. Anthropometric measures and epithelial ovarian cancer risk in the European Prospective Investigation into Cancer and Nutrition. *Int J Cancer*, 126, 2404-15.
- LAI, D., VISSER-GRIEVE, S. & YANG, X. 2012. Tumour suppressor genes in chemotherapeutic drug response. *Biosci Rep*, 32, 361-74.
- LAKS, D. R., MASTERMAN-SMITH, M., VISNYEI, K., ANGENIEUX, B., OROZCO, N. M., FORAN, I., YONG, W. H., VINTERS, H. V., LIAU, L. M., LAZAREFF, J. A., MISCHER, P. S., CLOUGHESY, T. F., HORVATH, S. & KORNBLUM, H. I. 2009. Neurosphere Formation Is an Independent Predictor of Clinical Outcome in Malignant Glioma. *Stem Cells*, 27, 980-987.
- LAMBRECHTS, D., LENZ, H. J., DE HAAS, S., CARMELIET, P. & SCHERER, S. J. 2013. Markers of Response for the Antiangiogenic Agent Bevacizumab. *Journal of Clinical Oncology*, 31, 1219-1230.
- LAVOIE, J. N., L'ALLEMAIN, G., BRUNET, A., MULLER, R., POUYSSEUR, J. 1996. Cyclin D1 expression is regulated positively by the p42/p44MAPK and negatively by the p38/HOGMAPK pathway. *J Biol Chem*, 271, 20608-16.
- LE PAGE, C., OUELLET, V., MADORE, J., REN, F., HUDSON, T. J., TONIN, P. N., PROVENCHER, D. M. & MES-MASSON, A. M. 2006. Gene expression profiling of primary cultures of ovarian epithelial cells identifies novel molecular classifiers of ovarian cancer. *Br J Cancer*, 94, 436-45.
- LE PAGE, F., KWOH, E. E., AVRUTSKAYA, A., GENTIL, A., LEADON, S. A., SARASIN, A. & COOPER, P. K. 2000. Transcription-coupled repair of 8-oxoguanine: requirement for XPG, TFIIH, and CSB and implications for Cockayne syndrome. *Cell*, 101, 159-71.
- LEAHY, J. J. J., GOLDING, B. T., GRIFFIN, R. J., HARDCASTLE, I. R., RICHARDSON, C., RIGOREAU, L. & SMITH, G. C. M. 2004. Identification of a highly potent and selective DNA-dependent protein kinase (DNA-PK) inhibitor (NU7441) by screening of chromenone libraries. *Bioorganic & Medicinal Chemistry Letters*, 14, 6083-6087.
- LEARY, A., AUCLIN, E., PAUTIER, P. & LHOMMÉ, C. 2013. The PI3K/Akt/mTOR Pathway in Ovarian Cancer: Biological Rationale and Therapeutic Opportunities.
- LEDERMANN, J., HARTER, P., GOURLEY, C., FRIEDLANDER, M., VERGOTE, I., RUSTIN, G., SCOTT, C., MEIER, W., SHAPIRA-FROMMER, R., SAFRA, T., MATEI, D., MACPHERSON, E., WATKINS, C., CARMICHAEL, J. & MATULONIS, U. 2012. Olaparib Maintenance Therapy in Platinum-Sensitive Relapsed Ovarian Cancer. *New England Journal of Medicine*, 366, 1382-1392.

- LEDERMANN, J. A. & KRISTELEIT, R. S. 2010. Optimal treatment for relapsing ovarian cancer. *Annals of Oncology*, 21, 218-222.
- LEE, H. S., CHOE, G., PARK, K. U., PARK DO, J., YANG, H. K., LEE, B. L. & KIM, W. H. 2007a. Altered expression of DNA-dependent protein kinase catalytic subunit (DNA-PKcs) during gastric carcinogenesis and its clinical implications on gastric cancer. *Int J Oncol*, 31, 859-66.
- LEE, H. S., YANG, H. K., KIM, W. H. & CHOE, G. 2005. Loss of DNA-dependent protein kinase catalytic subunit (DNA-PKcs) expression in gastric cancers. *Cancer Res Treat*, 37, 98-102.
- LEE, M., WILLIAMS, K., HU, Y., ANDREAS, J., PATEL, S., ZHANG, S. Y. & CRAWFORD, N. 2015. GNL3 and SKA3 are novel prostate cancer metastasis susceptibility genes. *Clinical & Experimental Metastasis*, 32, 769-782.
- LEE, Y., MIRON, A., DRAPKIN, R., NUCCI, M. R., MEDEIROS, F., SALEEMUDDIN, A., GARBER, J., BIRCH, C., MOU, H., GORDON, R. W., CRAMER, D. W., MCKEON, F. D. & CRUM, C. P. 2007b. A candidate precursor to serous carcinoma that originates in the distal fallopian tube. *J Pathol*, 211, 26-35.
- LENGAUER, C., KINZLER, K. W. & VOGELSTEIN, B. 1998. Genetic instabilities in human cancers. *Nature*, 396, 643-9.
- LEUNG, C. S., YEUNG, T. L., YIP, K. P., PRADEEP, S., BALASUBRAMANIAN, L., LIU, J. S., WONG, K. K., MANGALA, L. S., ARMAIZ-PENA, G. N., LOPEZ-BERESTEIN, G., SOOD, A. K., BIRRER, M. J. & MOK, S. C. 2014. Calcium-dependent FAK/CREB/TNNC1 signalling mediates the effect of stromal MFAP5 on ovarian cancer metastatic potential. *Nature Communications*, 5.
- LEWIS, K. A., MULLANY, S., THOMAS, B., CHIEN, J., LOEWEN, R., SHRIDHAR, V. & CLIBY, W. A. 2005. Heterozygous ATR mutations in mismatch repair-deficient cancer cells have functional significance. *Cancer Res*, 65, 7091-5.
- LEWIS, T. S., SHAPIRO, P. S., AHN, N. G. 1998. Signal transduction through MAP kinase cascades. *Adv Cancer Res*, 74, 49-139.
- LI, B., NAVARRO, S., KASAHARA, N. & COMAI, L. 2004a. Identification and biochemical characterization of a Werner's syndrome protein complex with Ku70/80 and poly(ADP-ribose) polymerase-1. *J Biol Chem*, 279, 13659-67.
- LI, C. C., YANG, J. C., LU, M. C., LEE, C. L., PENG, C. Y., HSU, W. Y., DAI, Y. H., CHANG, F. R., ZHANG, D. Y., WU, W. J. & WU, Y. C. 2016. ATR-Chk1 signaling inhibition as a therapeutic strategy to enhance cisplatin chemosensitivity in urothelial bladder cancer. *Oncotarget*, 7, 1947-59.
- LI, D., SUZUKI, H., LIU, B., MORRIS, J., LIU, J., OKAZAKI, T., LI, Y., CHANG, P. & ABBRUZZESE, J. L. 2009a. DNA repair gene polymorphisms and risk of pancreatic cancer. *Clin Cancer Res*, 15, 740-6.
- LI, H. R., SHAGISULTANOVA, E. I., YAMASHITA, K., PIAO, Z., PERUCHO, M. & MALKHOSYAN, S. R. 2004b. Hypersensitivity of tumor cell lines with microsatellite instability to DNA double strand break producing chemotherapeutic agent bleomycin. *Cancer Res*, 64, 4760-7.
- LI, J., WOOD, W. H., BECKER, K. G., WEERARATNA, A. T. & MORIN, P. J. 2007. Gene expression response to cisplatin treatment in drug-sensitive and drug-resistant ovarian cancer cells. *Oncogene*, 26, 2860-2872.
- LI, M., BALCH, C., MONTGOMERY, J. S., JEONG, M., CHUNG, J. H., YAN, P., HUANG, T. H., KIM, S. & NEPHEW, K. P. 2009b. Integrated analysis of DNA methylation and gene expression reveals specific signaling pathways associated with platinum resistance in ovarian cancer. *BMC Med Genomics*, 2, 34.

- LI, Q., YU, J. J., MU, C., YUNMBAM, M. K., SLAVSKY, D., CROSS, C. L., BOSTICK-BRUTON, F. & REED, E. 2000. Association between the level of ERCC-1 expression and the repair of cisplatin-induced DNA damage in human ovarian cancer cells. *Anticancer Res*, 20, 645-52.
- LI, X., HEYER, W. D. 2008. Homologous recombination in DNA repair and DNA damage tolerance. *Cell Res*, 18, 99-113.
- LIANG, F. & JASIN, M. 1996. Ku80-deficient cells exhibit excess degradation of extrachromosomal DNA. *Journal of Biological Chemistry*, 271, 14405-14411.
- LIEBER, M. R. 2008. The mechanism of human nonhomologous DNA end joining. *J Biol Chem*, 283, 1-5.
- LIEBER, M. R. 2010. The mechanism of double-strand DNA break repair by the nonhomologous DNA end-joining pathway. *Annu Rev Biochem*, 79, 181-211.
- LIEBER, M. R., MA, Y., PANNICKE, U. & SCHWARZ, K. 2003. Mechanism and regulation of human non-homologous DNA end-joining. *Nat Rev Mol Cell Biol*, 4, 712-20.
- LIU, C. F., LOU, W., ZHU, Y. Z., YANG, J. C., NADIMINTY, N., GAIKWAD, N. W., EVANS, C. P. & GAO, A. C. 2015. Intracrine Androgens and AKR1C3 Activation Confer Resistance to Enzalutamide in Prostate Cancer. *Cancer Research*, 75, 1413-1422.
- LIU, J., BARRY, W. T., BIRRER, M. J., LEE, J. M., BUCKANOVICH, R. J., FLEMING, G. F., RIME, B., BUSS, M. K., NATIAM, S. R., HURTEAU, J., LUO, W. X., QUY, P., OBERMAYER, E., WHALEN, C., LEE, H., WINER, E. P., KOHN, E. C., IVY, S. P. & MATULONIS, U. 2014. A randomized phase 2 trial comparing efficacy of the combination of the PARP inhibitor olaparib and the antiangiogenic cediranib against olaparib alone in recurrent platinum-sensitive ovarian cancer. *Journal of Clinical Oncology*, 32.
- LIU, X., HAN, E. K., ANDERSON, M., SHI, Y., SEMIZAROV, D., WANG, G., MCGONIGAL, T., ROBERTS, L., LASKO, L., PALMA, J., ZHU, G. D., PENNING, T., ROSENBERG, S., GIRANDA, V. L., LUO, Y., LEVERSON, J., JOHNSON, E. F. & SHOEMAKER, A. R. 2009. Acquired resistance to combination treatment with temozolomide and ABT-888 is mediated by both base excision repair and homologous recombination DNA repair pathways. *Mol Cancer Res*, 7, 1686-92.
- LIU, Y., KADYROV, F. A. & MODRICH, P. 2011. PARP-1 enhances the mismatch-dependence of 5'-directed excision in human mismatch repair in vitro. *DNA Repair (Amst)*, 10, 1145-53.
- LIU, Y., ZHOU, K., ZHANG, H., SHUGART, Y. Y., CHEN, L., XU, Z., ZHONG, Y., LIU, H., JIN, L., WEI, Q., HUANG, F., LU, D. & ZHOU, L. 2008. Polymorphisms of LIG4 and XRCC4 involved in the NHEJ pathway interact to modify risk of glioma. *Hum Mutat*, 29, 381-9.
- LIU, Z., PHAN, S., FAMILI, F., PAN, Y., LENFERINK, A. E., CANTIN, C., COLLINS, C., O'CONNOR-MCCOURT, M. D. 2010. A multi-strategy approach to informative gene identification from gene expression data. *J Bioinform Comput Biol*, 8, 19-38.
- LIVAK, K. J. & SCHMITTGEN, T. D. 2001. Analysis of relative gene expression data using real-time quantitative PCR and the 2(-Delta Delta C(T)) Method. *Methods*, 25, 402-8.
- LOCKETT, K. L., HALL, M. C., XU, J., ZHENG, S. L., BERWICK, M., CHUANG, S. C., CLARK, P. E., CRAMER, S. D., LOHMAN, K. & HU, J. J. 2004. The ADPRT V762A genetic variant contributes to prostate cancer susceptibility and deficient enzyme function. *Cancer Res*, 64, 6344-8.
- LORUSSO, D., MANCINI, M., DI ROCCO, R., FONTANELLI, R. & RASPAGLIESI, F. 2012. The role of secondary surgery in recurrent ovarian cancer. *Int J Surg Oncol*, 2012, 613980.
- LOUKOPOULOS, P., KANETAKA, K., TAKAMURA, M., SHIBATA, T., SAKAMOTO, M. & HIROHASHI, S. 2004. Orthotopic transplantation models of pancreatic

- adenocarcinoma derived from cell lines and primary tumors and displaying varying metastatic activity. *Pancreas*, 29, 193-203.
- LU, H. R., WANG, X. & WANG, Y. 2006. A stronger DNA damage-induced G(2) checkpoint due to over-activated CHK1 in the absence of PARP-1. *Cell Cycle*, 5, 2364-2370.
- LUPACHYK, S., SHEVALYE, H., MAKSIMCHYK, Y., DREL, V. R. & OBROSOVA, I. G. 2011. PARP inhibition alleviates diabetes-induced systemic oxidative stress and neural tissue 4-hydroxynonenal adduct accumulation: correlation with peripheral nerve function. *Free Radic Biol Med*, 50, 1400-9.
- LYN, D., CHERNEY, B. W., LALANDE, M., BERENSON, J. R., LICHTENSTEIN, A., LUPOLD, S., BHATIA, K. G. & SMULSON, M. 1993. A duplicated region is responsible for the poly(ADP-ribose) polymerase polymorphism, on chromosome 13, associated with a predisposition to cancer. *Am J Hum Genet*, 52, 124-34.
- MA, Y., PANNICKE, U., SCHWARZ, K. & LIEBER, M. R. 2002. Hairpin opening and overhang processing by an Artemis/DNA-dependent protein kinase complex in nonhomologous end joining and V(D)J recombination. *Cell*, 108, 781-94.
- MA, Y., SCHWARZ, K. & LIEBER, M. R. 2005. The Artemis:DNA-PKcs endonuclease cleaves DNA loops, flaps, and gaps. *DNA Repair (Amst)*, 4, 845-51.
- MABUCHI, S., ALTOMARE, D. A., CONNOLLY, D. C., KLEIN-SZANTO, A., LITWIN, S., HOELZLE, M. K., HENSLEY, H. H., HAMILTON, T. C., TESTA, J. R. 2007. RAD001 (Everolimus) delays tumor onset and progression in a transgenic mouse model of ovarian cancer. *Cancer Res*, 67, 2408-13.
- MACALUSO, M., MONTANARI, M., CINTI, C. & GIORDANO, A. 2005. Modulation of cell cycle components by epigenetic and genetic events. *Semin Oncol*, 32, 452-7.
- MANDAL, R. K., SINGH, V., KAPOOR, R. & MITTAL, R. D. 2011. Do polymorphisms in XRCC4 influence prostate cancer susceptibility in North Indian population? *Biomarkers*, 16, 236-242.
- MANSOUR, W. Y., RHEIN, T. & DAHM-DAPHI, J. 2010. The alternative end-joining pathway for repair of DNA double-strand breaks requires PARP1 but is not dependent upon microhomologies. *Nucleic Acids Research*, 38, 6065-6077.
- MAO, Z., BOZZELLA, M., SELUANOV, A. & GORBUNOVA, V. 2008. Comparison of nonhomologous end joining and homologous recombination in human cells. *DNA Repair (Amst)*, 7, 1765-71.
- MARKMAN, M. 2009. Optimal management of recurrent ovarian cancer. *Int J Gynecol Cancer*, 19 Suppl 2, S40-3.
- MARKMAN, M., KENNEDY, A., WEBSTER, K., KULP, B., PETERSON, G. & BELINSON, J. 2000. Phase 2 evaluation of topotecan administered on a 3-day schedule in the treatment of platinum- and paclitaxel-refractory ovarian cancer. *Gynecol Oncol*, 79, 116-9.
- MARKMAN, M., ROTHMAN, R., HAKES, T., REICHMAN, B., HOSKINS, W., RUBIN, S., JONES, W., ALMADRONES, L. & LEWIS, J. L., JR. 1991. Second-line platinum therapy in patients with ovarian cancer previously treated with cisplatin. *J Clin Oncol*, 9, 389-93.
- MARKMAN, M., WEBSTER, K., ZANOTTI, K., ROHL, J. & BELINSON, J. 2004. Use of tamoxifen in asymptomatic patients with recurrent small-volume ovarian cancer. *Gynecol Oncol*, 93, 390-3.
- MASSAGUE, J. 2004. G1 cell-cycle control and cancer. *Nature*, 432, 298-306.
- MATEO, J., CARREIRA, S., SANDHU, S., MIRANDA, S., MOSSOP, H., PEREZ-LOPEZ, R., RODRIGUES, D. N., ROBINSON, D., OMLIN, A., TUNARIU, N., BOYSEN, G., PORTA, N., FLOHR, P., GILLMAN, A., FIGUEIREDO, I., PAULDING, C., SEED, G., JAIN, S., RALPH, C., PROTHEROE, A., HUSSAIN, S., JONES, R., ELLIOTT, T., MCGOVERN, U., BIANCHINI, D., GOODALL, J., ZAFEIRIOU, Z., WILLIAMSON, C. T., FERRALDESCHI, R., RIISNAES, R.,

- EBBS, B., FOWLER, G., RODA, D., YUAN, W., WU, Y. M., CAO, X., BROUGH, R., PEMBERTON, H., A'HERN, R., SWAIN, A., KUNJU, L. P., EELES, R., ATTARD, G., LORD, C. J., ASHWORTH, A., RUBIN, M. A., KNUDSEN, K. E., FENG, F. Y., CHINNAIYAN, A. M., HALL, E. & DE BONO, J. S. 2015. DNA-Repair Defects and Olaparib in Metastatic Prostate Cancer. *New England Journal of Medicine*, 373, 1697-1708.
- MATEOS-GOMEZ, P. A., GONG, F., NAIR, N., MILLER, K. M., LAZZERINI-DENCHI, E. & SFEIR, A. 2015. Mammalian polymerase theta promotes alternative NHEJ and suppresses recombination. *Nature*, 518, 254-7.
- MAYR, D., HIRSCHMANN, A., LOHRS, U., DIEBOLD, J. 2006. KRAS and BRAF mutations in ovarian tumors: a comprehensive study of invasive carcinomas, borderline tumors and extraovarian implants. *Gynecol Oncol*, 103, 883-7.
- MCCABE, N., TURNER, N. C., LORD, C. J., KLUZEK, K., BIALKOWSKA, A., SWIFT, S., GIAVARA, S., O'CONNOR, M. J., TUTT, A. N., ZDZIENICKA, M. Z., SMITH, G. C. & ASHWORTH, A. 2006. Deficiency in the repair of DNA damage by homologous recombination and sensitivity to poly(ADP-ribose) polymerase inhibition. *Cancer Res*, 66, 8109-15.
- MCCARTY, K. S., JR., SZABO, E., FLOWERS, J. L., COX, E. B., LEIGHT, G. S., MILLER, L., KONRATH, J., SOPER, J. T., BUDWIT, D. A., CREASMAN, W. T. & ET AL. 1986. Use of a monoclonal anti-estrogen receptor antibody in the immunohistochemical evaluation of human tumors. *Cancer Res*, 46, 4244s-4248s.
- MCCLUGGAGE, W. G. 2011. Morphological subtypes of ovarian carcinoma: a review with emphasis on new developments and pathogenesis. *Pathology*, 43, 420-32.
- MCCORMICK, A., EARP, E., LEESON, C., DIXON, M., O'DONNELL, R., KAUFMANN, A. & EDMONDSON, R. J. 2016. Phosphatase and Tensin Homolog Is a Potential Target for Ovarian Cancer Sensitization to Cytotoxic Agents. *Int J Gynecol Cancer*.
- MCELLIN, B., CAMACHO, C. V., MUKHERJEE, B., HAHM, B., TOMIMATSU, N., BACHOO, R. M. & BURMA, S. 2010. PTEN loss compromises homologous recombination repair in astrocytes: implications for glioblastoma therapy with temozolomide or poly(ADP-ribose) polymerase inhibitors. *Cancer Res*, 70, 5457-64.
- MCGLYNN, P. & LLOYD, R. G. 2002. Recombinational repair and restart of damaged replication forks. *Nature Reviews Molecular Cell Biology*, 3, 859-870.
- MCGUIRE, W. P., HOSKINS, W. J., BRADY, M. F., KUCERA, P. R., PARTRIDGE, E. E., LOOK, K. Y., CLARKE-PEARSON, D. L. & DAVIDSON, M. 1996. Cyclophosphamide and cisplatin compared with paclitaxel and cisplatin in patients with stage III and stage IV ovarian cancer. *N Engl J Med*, 334, 1-6.
- MCKEAN-COWDIN, R., BARNHOLTZ-SLOAN, J., INSKIP, P. D., RUDER, A. M., BUTLER, M., RAJARAMAN, P., RAZAVI, P., PATOKA, J., WIENCKE, J. K., BONDY, M. L. & WRENSCH, M. 2009. Associations between polymorphisms in DNA repair genes and glioblastoma. *Cancer Epidemiol Biomarkers Prev*, 18, 1118-26.
- MCMENAMIN, M. E., SOUNG, P., PERERA, S., KAPLAN, I., LODA, M. & SELLERS, W. R. 1999. Loss of PTEN expression in paraffin-embedded primary prostate cancer correlates with high Gleason score and advanced stage. *Cancer Res*, 59, 4291-6.
- MENG, Q., XIA, C., FANG, J., ROJANASAKUL, Y., JIANG, B. H. 2006. Role of PI3K and AKT specific isoforms in ovarian cancer cell migration, invasion and proliferation through the p70S6K1 pathway. *Cell Signal*, 18, 2262-71.
- MENON, U., GENTRY-MAHARAJ, A., HALLETT, R., RYAN, A., BURNELL, M., SHARMA, A., LEWIS, S., DAVIES, S., PHILPOTT, S., LOPES, A., GODFREY, K., ORAM, D., HEROD, J., WILLIAMSON, K., SEIF, M. W., SCOTT, I., MOULD, T., WOOLAS, R., MURDOCH, J., DOBBS, S., AMSO, N. N., LEESON, S., CRUICKSHANK, D., MCGUIRE, A., CAMPBELL, S., FALLOWFIELD, L., SINGH, N., DAWNAY, A., SKATES, S. J., PARMAR, M. & JACOBS, I.

2009. Sensitivity and specificity of multimodal and ultrasound screening for ovarian cancer, and stage distribution of detected cancers: results of the prevalence screen of the UK Collaborative Trial of Ovarian Cancer Screening (UKCTOCS). *Lancet Oncol*, 10, 327-40.
- MENOYO, A., ALAZZOZI, H., ESPIN, E., ARMENGOL, M., YAMAMOTO, H. & SCHWARTZ, S., JR. 2001. Somatic mutations in the DNA damage-response genes ATR and CHK1 in sporadic stomach tumors with microsatellite instability. *Cancer Res*, 61, 7727-30.
- MIAR, A., HEVIA, D., MUNOZ-CIMADEVILLA, H., ASTUDILLO, A., VELASCO, J., SAINZ, R. M. & MAYO, J. C. 2015. Manganese superoxide dismutase (SOD2/MnSOD)/catalase and SOD2/GPx1 ratios as biomarkers for tumor progression and metastasis in prostate, colon, and lung cancer. *Free Radical Biology and Medicine*, 85, 45-55.
- MIDDLETON, F. K., PATTERSON, M. J., ELSTOB, C. J., FORDHAM, S., HERRIOTT, A., WADE, M. A., MCCORMICK, A., EDMONDSON, R., MAY, F. E., ALLAN, J. M., POLLARD, J. R. & CURTIN, N. J. 2015. Common cancer-associated imbalances in the DNA damage response confer sensitivity to single agent ATR inhibition. *Oncotarget*, 6, 32396-409.
- MILNE, R. L. 2009. Variants in the ATM gene and breast cancer susceptibility. *Genome Med*, 1, 12.
- MINAMI, A., NAKANISHI, A., OGURA, Y., KITAGISHI, Y. & MATSUDA, S. 2014. Connection between Tumor Suppressor BRCA1 and PTEN in Damaged DNA Repair. *Front Oncol*, 4, 318.
- MINCA, E. C. & KOWALSKI, D. 2011. Replication fork stalling by bulky DNA damage: localization at active origins and checkpoint modulation. *Nucleic Acids Res*, 39, 2610-23.
- MIRONOV, N., JANSEN, L. A., ZHU, W. B., AGUELON, A. M., REGUER, G. & YAMASAKI, H. 1999. A novel sensitive method to detect frameshift mutations in exonic repeat sequences of cancer-related genes. *Carcinogenesis*, 20, 2189-92.
- MITCHELL, J., SMITH, G. C. & CURTIN, N. J. 2009a. Poly(ADP-Ribose) polymerase-1 and DNA-dependent protein kinase have equivalent roles in double strand break repair following ionizing radiation. *Int J Radiat Oncol Biol Phys*, 75, 1520-7.
- MITCHELL, J., SMITH, G. C. M. & CURTIN, N. J. 2009b. Poly(Adp-Ribose) Polymerase-1 and DNA-Dependent Protein Kinase Have Equivalent Roles in Double Strand Break Repair Following Ionizing Radiation. *International Journal of Radiation Oncology Biology Physics*, 75, 1520-1527.
- MITTAL, R. D., GANGWAR, R., MANDAL, R. K., SRIVASTAVA, P. & AHIRWAR, D. K. 2012. Gene variants of XRCC4 and XRCC3 and their association with risk for urothelial bladder cancer. *Mol Biol Rep*, 39, 1667-1675.
- MOHAMMED, A. E. S., EGUCHI, H., WADA, S., KOYAMA, N., SHIMIZU, M., OTANI, K., OHTAKI, M., TANIMOTO, K., HIYAMA, K., GABER, M. S. & NISHIYAMA, M. 2012. TMEM158 and FBLP1 as novel marker genes of cisplatin sensitivity in non-small cell lung cancer cells. *Experimental Lung Research*, 38, 463-474.
- MOHNI, K. N., KAVANAUGH, G. M. & CORTEZ, D. 2014. ATR pathway inhibition is synthetically lethal in cancer cells with ERCC1 deficiency. *Cancer Res*, 74, 2835-45.
- MOLL, U., LAU, R., SYPES, M. A., GUPTA, M. M. & ANDERSON, C. W. 1999. DNA-PK, the DNA-activated protein kinase, is differentially expressed in normal and malignant human tissues. *Oncogene*, 18, 3114-26.
- MONGIAT-ARTUS, P., MIQUEL, C., VAN DER AA, M., BUHARD, O., HAMELIN, R., SOLIMAN, H., BANGMA, C., JANIN, A., TEILLAC, P., VAN DER KWAST, T. & PRAZ, F. 2006. Microsatellite instability and mutation analysis of candidate genes in urothelial cell carcinomas of upper urinary tract. *Oncogene*, 25, 2113-8.

- MONK, B. J., PUJADE-LAURINE, E. & BURGER, R. A. 2013. Integrating bevacizumab into the management of epithelial ovarian cancer: the controversy of front-line versus recurrent disease. *Ann Oncol*, 24 Suppl 10, x53-x58.
- MONSEES, G. M., KRAFT, P., CHANOCK, S. J., HUNTER, D. J. & HAN, J. 2011. Comprehensive screen of genetic variation in DNA repair pathway genes and postmenopausal breast cancer risk. *Breast Cancer Res Treat*, 125, 207-14.
- MONTONI, A., ROBU, M., POULIOT, E. & SHAH, G. M. 2013. Resistance to PARP-Inhibitors in Cancer Therapy. *Front Pharmacol*, 4, 18.
- MOSKWA, P., BUFFA, F. M., PAN, Y., PANCHAKSHARI, R., GOTTIPATI, P., MUSCHEL, R. J., BEECH, J., KULSHRESTHA, R., ABDELMOHSEN, K., WEINSTOCK, D. M., GOROSPE, M., HARRIS, A. L., HELLEDAY, T. & CHOWDHURY, D. 2011. miR-182-mediated downregulation of BRCA1 impacts DNA repair and sensitivity to PARP inhibitors. *Mol Cell*, 41, 210-20.
- MOULD, E., BERRY, P., JAMIESON, D., HILL, C., CANO, C., TAN, N., ELLIOTT, S., DURKACZ, B., NEWELL, D. & WILLMORE, E. 2014. Identification of dual DNA-PK MDR1 inhibitors for the potentiation of cytotoxic drug activity. *Biochemical Pharmacology*, 88, 58-65.
- MOYNAHAN, M. E. & JASIN, M. 1997. Loss of heterozygosity induced by a chromosomal double-strand break. *Proc Natl Acad Sci U S A*, 94, 8988-93.
- MUKHOPADHYAY, A., CURTIN, N., PLUMMER, R. & EDMONDSON, R. J. 2011. PARP inhibitors and epithelial ovarian cancer: an approach to targeted chemotherapy and personalised medicine. *BJOG: An International Journal of Obstetrics & Gynaecology*, 118, 429-432.
- MUKHOPADHYAY, A., ELATTAR, A., CERBINSKAITE, A., WILKINSON, S. J., DREW, Y., KYLE, S., LOS, G., HOSTOMSKY, Z., EDMONDSON, R. J. & CURTIN, N. J. 2010. Development of a functional assay for homologous recombination status in primary cultures of epithelial ovarian tumor and correlation with sensitivity to poly(ADP-ribose) polymerase inhibitors. *Clin Cancer Res*, 16, 2344-51.
- MUKHOPADHYAY, A., PLUMMER, E. R., ELATTAR, A., SOOHOO, S., UZIR, B., QUINN, J. E., MCCLUGGAGE, W. G., MAXWELL, P., ANEKE, H., CURTIN, N. J. & EDMONDSON, R. J. 2012. Clinicopathological features of homologous recombination-deficient epithelial ovarian cancers: sensitivity to PARP inhibitors, platinum, and survival. *Cancer Res*, 72, 5675-82.
- MUNCK, J. M., BATEY, M. A., ZHAO, Y., JENKINS, H., RICHARDSON, C. J., CANO, C., TAVECCHIO, M., BARBEAU, J., BARDOS, J., CORNELL, L., GRIFFIN, R. J., MENEAR, K., SLADE, A., THOMMES, P., MARTIN, N. M., NEWELL, D. R., SMITH, G. C. & CURTIN, N. J. 2012. Chemosensitization of Cancer Cells by KU-0060648, a Dual Inhibitor of DNA-PK and PI-3K. *Mol Cancer Ther*, 11, 1789-98.
- MUNKSGAARD, P. S. & BLAAKAER, J. 2012. The association between endometriosis and ovarian cancer: A review of histological, genetic and molecular alterations. *Gynecologic Oncology*, 124, 164-169.
- MURUGAN, P., LIN, H. K., WU, W., MILLER, V., YANG, Q. & FUNG, K. M. 2012. Type 2 3a/Type 5 17 beta-HSD (AKR1C3) Is a Negative Regulator of Breast Cancer Proliferation: An Immunohistochemical and In Vitro Study. *Laboratory Investigation*, 92, 55a-55a.
- NAGAHARA, A., NAKAYAMA, M., OKA, D., TSUCHIYA, M., KAWASHIMA, A., MUKAI, M., NAKAI, Y., TAKAYAMA, H., NISHIMURA, K., JO, Y., NAGAI, A., OKUYAMA, A. & NONOMURA, N. 2010. SERPINE2 is a possible candidate promotor for lymph node metastasis in testicular cancer. *Biochemical and Biophysical Research Communications*, 391, 1641-1646.

- NAGARAJU, G., HARTLERODE, A., KWOK, A., CHANDRAMOULY, G. & SCULLY, R. 2009. XRCC2 and XRCC3 regulate the balance between short- and long-tract gene conversions between sister chromatids. *Mol Cell Biol*, 29, 4283-94.
- NAGATA, Y., LAN, K. H., ZHOU, X., TAN, M., ESTEVA, F. J., SAHIN, A. A., KLOS, K. S., LI, P., MONIA, B. P., NGUYEN, N. T., HORTOBAGYI, G. N., HUNG, M. C. & YU, D. 2004. PTEN activation contributes to tumor inhibition by trastuzumab, and loss of PTEN predicts trastuzumab resistance in patients. *Cancer Cell*, 6, 117-27.
- NAKAYAMA, K., NAKAYAMA, N., KURMAN, R. J., COPE, L., POHL, G., SAMUELS, Y., VELCULESCU, V. E., WANG, T. L. & SHIH IE, M. 2006. Sequence mutations and amplification of PIK3CA and AKT2 genes in purified ovarian serous neoplasms. *Cancer Biol Ther*, 5, 779-85.
- NAKAYAMA, N., NAKAYAMA, K., YEASMIN, S., ISHIBASHI, M., KATAGIRI, A., IIDA, K., FUKUMOTO, M. & MIYAZAKI, K. 2008. KRAS or BRAF mutation status is a useful predictor of sensitivity to MEK inhibition in ovarian cancer. *Br J Cancer*, 99, 2020-8.
- NATIONAL_CANCER_INSTITUTE. *Surveillance, Epidemiology, and End Results Program. SEER Stat Fact Sheets: Ovary Cancer*.
- NEAL, J. A., DANG, V., DOUGLAS, P., WOLD, M. S., LEES-MILLER, S. P. & MEEK, K. 2011. Inhibition of homologous recombination by DNA-dependent protein kinase requires kinase activity, is titratable, and is modulated by autophosphorylation. *Mol Cell Biol*, 31, 1719-33.
- NIK-ZAINAL, S., ALEXANDROV, L. B., WEDGE, D. C., VAN LOO, P., GREENMAN, C. D., RAINE, K., JONES, D., HINTON, J., MARSHALL, J., STEBBINGS, L. A., MENZIES, A., MARTIN, S., LEUNG, K., CHEN, L., LEROY, C., RAMAKRISHNA, M., RANCE, R., LAU, K. W., MUDIE, L. J., VARELA, I., MCBRIDE, D. J., BIGNELL, G. R., COOKE, S. L., SHLIEN, A., GAMBLE, J., WHITMORE, I., MADDISON, M., TARPEY, P. S., DAVIES, H. R., PAPAEMMANUIL, E., STEPHENS, P. J., MCLAREN, S., BUTLER, A. P., TEAGUE, J. W., JONSSON, G., GARBER, J. E., SILVER, D., MIRON, P., FATIMA, A., BOYALT, S., LANGEROD, A., TUTT, A., MARTENS, J. W., APARICIO, S. A., BORG, A., SALOMON, A. V., THOMAS, G., BORRESEN-DALE, A. L., RICHARDSON, A. L., NEUBERGER, M. S., FUTREAL, P. A., CAMPBELL, P. J., STRATTON, M. R. & BREAST CANCER WORKING GROUP OF THE INTERNATIONAL CANCER GENOME, C. 2012. Mutational processes molding the genomes of 21 breast cancers. *Cell*, 149, 979-93.
- NORQUIST, B., WURZ, K. A., PENNIL, C. C., GARCIA, R., GROSS, J., SAKAI, W., KARLAN, B. Y., TANIGUCHI, T. & SWISHER, E. M. 2011. Secondary somatic mutations restoring BRCA1/2 predict chemotherapy resistance in hereditary ovarian carcinomas. *J Clin Oncol*, 29, 3008-15.
- NOWSHEEN, S., COOPER, T., BONNER, J. A., LOBUGLIO, A. F. & YANG, E. S. 2012. HER2 overexpression renders human breast cancers sensitive to PARP inhibition independently of any defect in homologous recombination DNA repair. *Cancer Res*, 72, 4796-806.
- NUNEZ, R. 2001. DNA measurement and cell cycle analysis by flow cytometry. *Curr Issues Mol Biol*, 3, 67-70.
- O'DONNELL, R., KAUFMANN, A., WOODHOUSE, L., MCCORMICK, A., CURTIN, N. & EDMONDSON, R. 2015. Intra- and inter-tumour heterogeneity in epithelial ovarian cancer: consequences for biomarker-dependent stratification of therapies. *BJOG-an International Journal of Obstetrics and Gynaecology*, 122, E3-E3.
- O'DRISCOLL, M., GENNERY, A. R., SEIDEL, J., CONCANNON, P. & JEGGO, P. A. 2004. An overview of three new disorders associated with genetic instability: LIG4 syndrome, RS-SCID and ATR-Seckel syndrome. *DNA Repair (Amst)*, 3, 1227-35.

- O'DRISCOLL, M., RUIZ-PEREZ, V. L., WOODS, C. G., JEGGO, P. A. & GOODSHIP, J. A. 2003. A splicing mutation affecting expression of ataxia-telangiectasia and Rad3-related protein (ATR) results in Seckel syndrome. *Nature Genetics*, 33, 497-501.
- ODONNELL, R. L., MCCORMICK, A., MUKHOPADHYAY, A., WOODHOUSE, L. C., MOAT, M., GRUNDY, A., DIXON, M., KAUFMAN, A., SOOHOO, S., ELATTAR, A., CURTIN, N. J. & EDMONDSON, R. J. 2014. The Use of Ovarian Cancer Cells from Patients Undergoing Surgery to Generate Primary Cultures Capable of Undergoing Functional Analysis. *Plos One*, 9.
- OHASHI, A., ZDZIENICKA, M. Z., CHEN, J. & COUCH, F. J. 2005. Fanconi anemia complementation group D2 (FANCD2) functions independently of BRCA2- and RAD51-associated homologous recombination in response to DNA damage. *J Biol Chem*, 280, 14877-83.
- OPLUSTILOVA, L., WOLANIN, K., MISTRIK, M., KORINKOVA, G., SIMKOVA, D., BOUCHAL, J., LENOBEL, R., BARTKOVA, J., LAU, A., O'CONNOR, M. J., LUKAS, J. & BARTEK, J. 2012. Evaluation of candidate biomarkers to predict cancer cell sensitivity or resistance to PARP-1 inhibitor treatment. *Cell Cycle*, 11, 3837-50.
- ORR, N., LEMNRAU, A., COOKE, R., FLETCHER, O., TOMCZYK, K., JONES, M., JOHNSON, N., LORD, C. J., MITSOPOULOS, C., ZVELEBIL, M., MCDADE, S. S., BUCK, G., BLANCHER, C., TRAINER, A. H., JAMES, P. A., BOJESSEN, S. E., BOKMAND, S., NEVANLINNA, H., MATTSO, J., FRIEDMAN, E., LAITMAN, Y., PALLI, D., MASALA, G., ZANNA, I., OTTINI, L., GIANNINI, G., HOLLESTELLE, A., VAN DEN OUWELAND, A. M. W., NOVAKOVIC, S., KRAJC, M., GAGO-DOMINGUEZ, M., CASTELAO, J. E., OLSSON, H., HEDENFALK, I., EASTON, D. F., PHAROAH, P. D. P., DUNNING, A. M., BISHOP, D. T., NEUHAUSEN, S. L., STEELE, L., HOULSTON, R. S., GARCIA-CLOSAS, M., ASHWORTH, A., SWERDLOW, A. J. & CONSORTIUM, K. 2012. Genome-wide association study identifies a common variant in RAD51B associated with male breast cancer risk. *Nature Genetics*, 44, 1182-1184.
- OZA, A. M., CIBULA, D., BENZAQUEN, A. O., POOLE, C. J., MATHIJSEN, R. H. J., SONKE, G. S., MACKAY, H., LOWE, E. S., READ, J. & FRIEDLANDER, M. 2013. Olaparib plus chemotherapy, followed by maintenance monotherapy, in women with platinum-sensitive recurrent serous ovarian cancer (PSR SOC): BRCA1/2 mutation (BRCAm) and interim overall survival analyses. *European Journal of Cancer*, 49, S712-S713.
- PACHER, P. & SZABO, C. 2007. Role of poly(ADP-ribose) polymerase 1 (PARP-1) in cardiovascular diseases: the therapeutic potential of PARP inhibitors. *Cardiovasc Drug Rev*, 25, 235-60.
- PANNUNZIO, N. R., LI, S., WATANABE, G. & LIEBER, M. R. 2014. Non-homologous end joining often uses microhomology: implications for alternative end joining. *DNA Repair (Amst)*, 17, 74-80.
- PARMAR, M. K., LEDERMANN, J. A., COLOMBO, N., DU BOIS, A., DELALOYE, J. F., KRISTENSEN, G. B., WHEELER, S., SWART, A. M., QIAN, W., TORRI, V., FLORIANI, I., JAYSON, G., LAMONT, A. & TROPE, C. 2003. Paclitaxel plus platinum-based chemotherapy versus conventional platinum-based chemotherapy in women with relapsed ovarian cancer: the ICON4/AGO-OVAR-2.2 trial. *Lancet*, 361, 2099-106.
- PATEL, A. G., SARKARIA, J. N. & KAUFMANN, S. H. 2011. Nonhomologous end joining drives poly(ADP-ribose) polymerase (PARP) inhibitor lethality in homologous recombination-deficient cells. *Proc Natl Acad Sci U S A*, 108, 3406-11.
- PATTERSON, M. J., SUTTON, R. E., FORREST, I., SHARROCK, R., LANE, M., KAUFMANN, A., O'DONNELL, R., EDMONDSON, R. J., WILSON, B. T. & CURTIN, N. J. 2014. Assessing

- the function of homologous recombination DNA repair in malignant pleural effusion (MPE) samples. *Br J Cancer*, 111, 94-100.
- PAULL, T. T., CORTEZ, D., BOWERS, B., ELLEDGE, S. J. & GELLERT, M. 2001. Direct DNA binding by Brca1. *Proc Natl Acad Sci U S A*, 98, 6086-91.
- PAULL, T. T. & LEE, J. H. 2005. The Mre11/Rad50/Nbs1 complex and its role as a DNA double-strand break sensor for ATM. *Cell Cycle*, 4, 737-40.
- PEASLAND, A., WANG, L. Z., ROWLING, E., KYLE, S., CHEN, T., HOPKINS, A., CLIBY, W. A., SARKARIA, J., BEALE, G., EDMONDSON, R. J. & CURTIN, N. J. 2011. Identification and evaluation of a potent novel ATR inhibitor, NU6027, in breast and ovarian cancer cell lines. *British Journal of Cancer*.
- PELTOMAKI, P. & VASEN, H. 2004. Mutations associated with HNPCC predisposition -- Update of ICG-HNPCC/INSIGHT mutation database. *Dis Markers*, 20, 269-76.
- PENNINGTON, K. P., WALSH, T., HARRELL, M. I., LEE, M. K., PENNIL, C. C., RENDI, M. H., THORNTON, A., NORQUIST, B. M., CASADEI, S., NORD, A. S., AGNEW, K. J., PRITCHARD, C. C., SCROGGINS, S., GARCIA, R. L., KING, M. C. & SWISHER, E. M. 2014. Germline and Somatic Mutations in Homologous Recombination Genes Predict Platinum Response and Survival in Ovarian, Fallopian Tube, and Peritoneal Carcinomas. *Clinical Cancer Research*, 20, 764-775.
- PEREIRA, C., QUEIROS, S., GALAGHAR, A., SOUSA, H., PIMENTEL-NUNES, P., BRANDAO, C., MOREIRA-DIAS, L., MEDEIROS, R. & DINIS-RIBEIRO, M. 2014. Genetic Variability in Key Genes in Prostaglandin E-2 Pathway (COX-2, HPGD, ABCC4 and SLCO2A1) and Their Involvement in Colorectal Cancer Development. *Plos One*, 9.
- PERRAULT, R., WANG, H. C., WANG, M. L., ROSIDI, B. & ILIAKIS, G. 2004. Backup pathways of NHEJ are suppressed by DNA-PK. *J Cell Biochem*, 92, 781-794.
- PERREN, T. J., SWART, A. M., PFISTERER, J., LEDERMANN, J. A., PUJADE-LAURINE, E., KRISTENSEN, G., CAREY, M. S., BEALE, P., CERVANTES, A., KURZEDER, C., DU BOIS, A., SEHOULI, J., KIMMIG, R., STAHL, A., COLLINSON, F., ESSAPEN, S., GOURLEY, C., LORTHOLARY, A., SELLE, F., MIRZA, M. R., LEMINEN, A., PLANTE, M., STARK, D., QIAN, W., PARMAR, M. K., OZA, A. M. & INVESTIGATORS, I. 2011. A phase 3 trial of bevacizumab in ovarian cancer. *N Engl J Med*, 365, 2484-96.
- PETERMANN, E., ORTA, M. L., ISSAEVA, N., SCHULTZ, N. & HELLEDAY, T. 2010. Hydroxyurea-Stalled Replication Forks Become Progressively Inactivated and Require Two Different RAD51-Mediated Pathways for Restart and Repair. *Molecular Cell*, 37, 492-502.
- PFISTERER, J., WEBER, B., REUSS, A., KIMMIG, R., DU BOIS, A., WAGNER, U., BOURGEOIS, H., MEIER, W., COSTA, S., BLOHMER, J. U., LORTHOLARY, A., OLBRICHT, S., STAHL, A., JACKISCH, C., HARDY-BESSARD, A. C., MOBUS, V., QUAAS, J., RICHTER, B., SCHRODER, W., GEAY, J. F., LUCK, H. J., KUHN, W., MEDEN, H., NITZ, U., PUJADE-LAURINE, E., AGO, O. & GINECO 2006. Randomized phase III trial of topotecan following carboplatin and paclitaxel in first-line treatment of advanced ovarian cancer: a gynecologic cancer intergroup trial of the AGO-OVAR and GINECO. *J Natl Cancer Inst*, 98, 1036-45.
- PFUETZER, R. H., MYERS, E. S., SHAPIRO, S. E., FINCH, R., ELLIS, I., KANT, J. A., NEOPTOLEMOS, J. P. & WHITCOMB, D. C. 2001. Novel cationic trypsinogen (PRSS1) mutations N29T and R122C confer autosomal dominant Hereditary Pancreatitis. *Gastroenterology*, 120, A33-A33.
- PICCART, M. J., BERTELSEN, K., JAMES, K., CASSIDY, J., MANGIONI, C., SIMONSEN, E., STUART, G., KAYE, S., VERGOTE, I., BLOM, R., GRIMSHAW, R., ATKINSON, R. J., SWENERTON, K. D., TROPE, C., NARDI, M., KAERN, J., TUMOLO, S., TIMMERS, P., ROY, J. A., LHOAS, F., LINDVALL, B., BACON, M., BIRT, A., ANDERSEN, J. E., ZEE, B., PAUL, J., BARON, B. &

- PECORELLI, S. 2000. Randomized intergroup trial of cisplatin-paclitaxel versus cisplatin-cyclophosphamide in women with advanced epithelial ovarian cancer: three-year results. *J Natl Cancer Inst*, 92, 699-708.
- PINES, A., VROUWE, M. G., MARTEIJN, J. A., TYPAS, D., LUIJSTERBURG, M. S., CANSOY, M., HENSBERGEN, P., DEELDER, A., DE GROOT, A., MATSUMOTO, S., SUGASAWA, K., THOMA, N., VERMEULEN, W., VRIELING, H. & MULLENDERS, L. 2012. PARP1 promotes nucleotide excision repair through DDB2 stabilization and recruitment of ALC1. *J Cell Biol*, 199, 235-49.
- PLESCHKE, J. M., KLECZKOWSKA, H. E., STROHM, M. & ALTHAUS, F. R. 2000. Poly(ADP-ribose) binds to specific domains in DNA damage checkpoint proteins. *J Biol Chem*, 275, 40974-80.
- PLO, I., LIAO, Z. Y., BARCELO, J. M., KOHLHAGEN, G., CALDECOTT, K. W., WEINFELD, M. & POMMIER, Y. 2003. Association of XRCC1 and tyrosyl DNA phosphodiesterase (Tdp1) for the repair of topoisomerase I-mediated DNA lesions. *DNA Repair (Amst)*, 2, 1087-100.
- PLUMB, J. A., STRATHDEE, G., SLUDDEN, J., KAYE, S. B. & BROWN, R. 2000. Reversal of drug resistance in human tumor xenografts by 2'-deoxy-5-azacytidine-induced demethylation of the hMLH1 gene promoter. *Cancer Res*, 60, 6039-44.
- PLUMMER, E. R. & CALVERT, H. 2007. Targeting Poly(ADP-Ribose) Polymerase: A Two-Armed Strategy for Cancer Therapy. *Clinical Cancer Research*, 13, 6252-6256.
- PLUMMER, E. R., MIDDLETON, M. R., JONES, C., OLSEN, A., HICKSON, I., MCHUGH, P., MARGISON, G. P., MCGOWN, G., THORNCROFT, M., WATSON, A. J., BODDY, A. V., CALVERT, A. H., HARRIS, A. L., NEWELL, D. R. & CURTIN, N. J. 2005. Temozolomide pharmacodynamics in patients with metastatic melanoma: dna damage and activity of repair enzymes O6-alkylguanine alkyltransferase and poly(ADP-ribose) polymerase-1. *Clin Cancer Res*, 11, 3402-9.
- PLUMMER, R., JONES, C., MIDDLETON, M., WILSON, R., EVANS, J., OLSEN, A., CURTIN, N., BODDY, A., MCHUGH, P., NEWELL, D., HARRIS, A., JOHNSON, P., STEINFELDT, H., DEWJI, R., WANG, D., ROBSON, L. & CALVERT, H. 2008. Phase I study of the poly(ADP-ribose) polymerase inhibitor, AG014699, in combination with temozolomide in patients with advanced solid tumors. *Clin Cancer Res*, 14, 7917-23.
- PRAT, J., FIGO COMMITTEE ON GYNECOLOGIC ONCOLOGY 2013. Staging classification for cancer of the ovary, fallopian tube, and peritoneum. *Int J Gynaecol Obstet*.
- PRICE, B. D. & YOUMELL, M. B. 1996. The phosphatidylinositol 3-kinase inhibitor wortmannin sensitizes murine fibroblasts and human tumor cells to radiation and blocks induction of p53 following DNA damage. *Cancer Res*, 56, 246-50.
- PRZYBYCIN, C. G., URMAN, R. J., RONNETT, B. M., SHIH IE, M., VANG, R. 2010. Are all pelvic (nonuterine) serous carcinomas of tubal origin? *Am J Surg Pathol*, 34, 1407-16.
- PUJADE-LAURINE, E., HILPERT, F., WEBER, B., REUSS, A., POVEDA, A., KRISTENSEN, G., SORIO, R., VERGOTE, I. B., WITTEVEEN, P., BAMIAS, A., PEREIRA, D., WIMBERGER, P., OAKNIN, A., MIRZA, M. R., FOLLANA, P., BOLLAG, D. T., RAY-COQUARD, I. & INVESTIGATORS, A. 2012. AURELIA: A randomized phase III trial evaluating bevacizumab (BEV) plus chemotherapy (CT) for platinum (PT)-resistant recurrent ovarian cancer (OC). *Journal of Clinical Oncology*, 30.
- QIN, F. X., ZHANG, H. K., MA, L., LIU, X. L., DAI, K., LI, W. L., GU, F., FU, L. & MA, Y. J. 2015. Low Expression of Slit2 and Robo1 is Associated with Poor Prognosis and Brain-specific Metastasis of Breast Cancer Patients. *Scientific Reports*, 5.

- QUENNET, V., BEUCHER, A., BARTON, O., TAKEDA, S. & LOBRICH, M. 2011. CtIP and MRN promote non-homologous end-joining of etoposide-induced DNA double-strand breaks in G1. *Nucleic Acids Res*, 39, 2144-52.
- RAI, R., ZHENG, H., HE, H., LUO, Y., MULTANI, A., CARPENTER, P. B. & CHANG, S. 2010. The function of classical and alternative non-homologous end-joining pathways in the fusion of dysfunctional telomeres. *EMBO J*, 29, 2598-610.
- RAINEY, M. D., CHARLTON, M. E., STANTON, R. V. & KASTAN, M. B. 2008. Transient inhibition of ATM kinase is sufficient to enhance cellular sensitivity to ionizing radiation. *Cancer Research*, 68, 7466-7474.
- RAJAEI-BEHBAHANI, N., SCHMEZER, P., RAMROTH, H., BURKLE, A., BARTSCH, H., DIETZ, A. & BECHER, H. 2002. Reduced poly(ADP-ribosyl)ation in lymphocytes of laryngeal cancer patients: results of a case-control study. *Int J Cancer*, 98, 780-4.
- RAJAGOPALAN, H., BARDELLI, A., LENGAUER, C., KINZLER, K. W., VOGELSTEIN, B., VELCULESCU, V. E. 2002. Tumorigenesis: RAF/RAS oncogenes and mismatch-repair status. *Nature*, 418, 934.
- RAMIREZ, I., CHON, H. S. & APTE, S. M. 2011. The role of surgery in the management of epithelial ovarian cancer. *Cancer Control*, 18, 22-30.
- RAMUS, S. J. & GAYTHER, S. A. 2009. The Contribution of BRCA1 and BRCA2 to Ovarian Cancer. *Molecular Oncology*, 3, 138-150.
- RASS, E., GRABARZ, A., PLO, I., GAUTIER, J., BERTRAND, P. & LOPEZ, B. S. 2009. Role of Mre11 in chromosomal nonhomologous end joining in mammalian cells. *Nat Struct Mol Biol*, 16, 819-24.
- RATNER, E. S., KEANE, F. K., LINDNER, R., TASSI, R. A., PARANJAPPE, T., GLASGOW, M., NALLUR, S., DENG, Y., LU, L., STEELE, L., SAND, S., MULLER, R. U., BIGNOTTI, E., NEUHAUSEN, S. L., SCHWARTZ, P. E., SLACK, F. J., SANTIN, A. D., WEIDHAAS, J. B. 2011. A KRAS variant is a biomarker of poor outcome, platinum chemotherapy resistance and a potential target for therapy in ovarian cancer. *Oncogene*.
- REAPER, P. M., GRIFFITHS, M. R., LONG, J. M., CHARRIER, J. D., MACCORMICK, S., CHARLTON, P. A., GOLEC, J. M. C. & POLLARD, J. R. 2011. Selective killing of ATM- or p53-deficient cancer cells through inhibition of ATR. *Nature Chemical Biology*, 7, 428-430.
- REBUCCI, M. & MICHIELS, C. 2013. Molecular aspects of cancer cell resistance to chemotherapy. *Biochem Pharmacol*, 85, 1219-26.
- REDMAN, C., DUFFY, S., BROMHAM, N. & FRANCIS, K. 2011. Recognition and initial management of ovarian cancer: summary of NICE guidance. *BMJ*, 342, d2073.
- RELES, A., WEN, W. H., SCHMIDER, A., GEE, C., RUNNEBAUM, I. B., KILIAN, U., JONES, L. A., EL-NAGGAR, A., MINGUILLON, C., SCHONBORN, I., REICH, O., KREIENBERG, R., LICHTENEGGER, W. & PRESS, M. F. 2001. Correlation of p53 mutations with resistance to platinum-based chemotherapy and shortened survival in ovarian cancer. *Clinical Cancer Research*, 7, 2984-2997.
- REN, B., YU, G., TSENG, G. C., CIEPLY, K., GAVEL, T., MICHALOPOULOS, G., YU, Y. P. & LUO, J. H. 2006. MCM7 amplification and overexpression are associated with prostate cancer progression. *Oncogene*, 25, 1090-1098.
- REYES-GONZALEZ, J. M., ARMAIZ-PENA, G. N., MANGALA, L. S., VALIYEVA, F., IVAN, C., PRADEEP, S., ECHEVARRIA-VARGAS, I. M., RIVERA-REYES, A., SOOD, A. K. & VIVAS-MEJIA, P. E. 2015. Targeting c-MYC in Platinum-Resistant Ovarian Cancer. *Mol Cancer Ther*, 14, 2260-9.
- RIBALLO, E., CRITCHLOW, S. E., TEO, S. H., DOHERTY, A. J., PRIESTLEY, A., BROUGHTON, B., KYSELA, B., BEAMISH, H., PLOWMAN, N., ARLETT, C. F., LEHMANN, A. R., JACKSON, S.

- P. & JEGGO, P. A. 1999. Identification of a defect in DNA ligase IV in a radiosensitive leukaemia patient. *Current Biology*, 9, 699-702.
- RISCH, H. A., MCLAUGHLIN, J. R., COLE, D. E., ROSEN, B., BRADLEY, L., KWAN, E., JACK, E., VESPRINI, D. J., KUPERSTEIN, G., ABRAHAMSON, J. L., FAN, I., WONG, B. & NAROD, S. A. 2001. Prevalence and penetrance of germline BRCA1 and BRCA2 mutations in a population series of 649 women with ovarian cancer. *Am J Hum Genet*, 68, 700-10.
- ROBINSON-BENNETT, B. L., DEFORD, J., DIAZ-ARRASTIA, C., LEVINE, L., WANG, H. Q., HANNIGAN, E. V. & PAPAConstantinou, J. 2008. Implications of tyrosine phosphoproteomics in cervical carcinogenesis. *J Carcinog*, 7, 2.
- ROBLES-DIAZ, L., GOLDFRANK, D. J., KAUFF, N. D., ROBSON, M., OFFIT, K. 2004. Hereditary ovarian cancer in Ashkenazi Jews. *Fam Cancer*, 3, 259-64.
- RODDAM, P. L., ROLLINSON, S., O'DRISCOLL, M., JEGGO, P. A., JACK, A. & MORGAN, G. J. 2002. Genetic variants of NHEJ DNA ligase IV can affect the risk of developing multiple myeloma, a tumour characterised by aberrant class switch recombination. *J Med Genet*, 39, 900-5.
- ROMERO, I. & BAST, R. C. 2012. Minireview: Human Ovarian Cancer: Biology, Current Management, and Paths to Personalizing Therapy. *Endocrinology*, 153, 1593-1602.
- ROODHART, J. M. L., DAENEN, L. G. M., STIGTER, E. C. A., PRINS, H. J., GERRITS, J., HOUTHUIJZEN, J. M., GERRITSEN, M. G., SCHIPPER, H. S., BACKER, M. J. G., VAN AMERSFOORT, M., VERMAAT, J. S. P., MOERER, P., ISHIHARA, K., KALKHOVEN, E., BEIJNEN, J. H., DERKSEN, P. W. B., MEDEMA, R. H., MARTENS, A. C., BRENNKMAN, A. B. & VOEST, E. E. 2011. Mesenchymal Stem Cells Induce Resistance to Chemotherapy through the Release of Platinum-Induced Fatty Acids. *Cancer Cell*, 20, 370-383.
- ROSENZWEIG, K. E., YOUNELL, M. B., PALAYOOR, S. T. & PRICE, B. D. 1997. Radiosensitization of human tumor cells by the phosphatidylinositol3-kinase inhibitors wortmannin and LY294002 correlates with inhibition of DNA-dependent protein kinase and prolonged G2-M delay. *Clin Cancer Res*, 3, 1149-56.
- ROSIDI, B., WANG, M., WU, W., SHARMA, A., WANG, H. & ILIAKIS, G. 2008. Histone H1 functions as a stimulatory factor in backup pathways of NHEJ. *Nucleic Acids Res*, 36, 1610-23.
- ROSKELLEY, C. D. & BISSELL, M. J. 2002. The dominance of the microenvironment in breast and ovarian cancer. *Seminars in Cancer Biology*, 12, 97-104.
- ROTTENBERG, S., JASPERS, J. E., KERSBERGEN, A., VAN DER BURG, E., NYGREN, A. O., ZANDER, S. A., DERKSEN, P. W., DE BRUIN, M., ZEVENHOVEN, J., LAU, A., BOULTER, R., CRANSTON, A., O'CONNOR, M. J., MARTIN, N. M., BORST, P. & JONKERS, J. 2008. High sensitivity of BRCA1-deficient mammary tumors to the PARP inhibitor AZD2281 alone and in combination with platinum drugs. *Proc Natl Acad Sci U S A*, 105, 17079-84.
- RUBIO-VIQUEIRA, B. & HIDALGO, M. 2009. Direct In Vivo Xenograft Tumor Model for Predicting Chemotherapeutic Drug Response in Cancer Patients. *Clinical Pharmacology & Therapeutics*, 85, 217-221.
- RUSCETTI, T., LEHNERT, B. E., HALBROOK, J., LE TRONG, H., HOEKSTRA, M. F., CHEN, D. J. & PETERSON, S. R. 1998. Stimulation of the DNA-dependent protein kinase by poly(ADP-ribose) polymerase. *J Biol Chem*, 273, 14461-7.
- SABERI, A., HOCHEGGER, H., SZUTS, D., LAN, L., YASUI, A., SALE, J. E., TANIGUCHI, Y., MURAKAWA, Y., ZENG, W., YOKOMORI, K., HELLEDAY, T., TERAOKA, H., ARAKAWA, H., BUERSTEDDE, J. M. & TAKEDA, S. 2007. RAD18 and poly(ADP-ribose) polymerase independently suppress the access of nonhomologous end joining to double-strand

- breaks and facilitate homologous recombination-mediated repair. *Mol Cell Biol*, 27, 2562-71.
- SAKAI, W., SWISHER, E. M., JACQUEMONT, C., CHANDRAMOHAN, K. V., COUCH, F. J., LANGDON, S. P., WURZ, K., HIGGINS, J., VILLEGAS, E. & TANIGUCHI, T. 2009. Functional restoration of BRCA2 protein by secondary BRCA2 mutations in BRCA2-mutated ovarian carcinoma. *Cancer Res*, 69, 6381-6.
- SAKAI, W., SWISHER, E. M., KARLAN, B. Y., AGARWAL, M. K., HIGGINS, J., FRIEDMAN, C., VILLEGAS, E., JACQUEMONT, C., FARRUGIA, D. J., COUCH, F. J., URBAN, N. & TANIGUCHI, T. 2008. Secondary mutations as a mechanism of cisplatin resistance in BRCA2-mutated cancers. *Nature*, 451, 1116-20.
- SAKATA, K., MATSUMOTO, Y., TAUCHI, H., SATOH, M., OUCHI, A., NAGAKURA, H., KOITO, K., HOSOI, Y., SUZUKI, N., KOMATSU, K. & HAREYAMA, M. 2001. Expression of genes involved in repair of DNA double-strand breaks in normal and tumor tissues. *Int J Radiat Oncol Biol Phys*, 49, 161-7.
- SAKIYAMA, T., KOHNO, T., MIMAKI, S., OHTA, T., YANAGITANI, N., SOBUE, T., KUNITOH, H., SAITO, R., SHIMIZU, K., HIRAMA, C., KIMURA, J., MAENO, G., HIROSE, H., EGUCHI, T., SAITO, D., OHKI, M. & YOKOTA, J. 2005. Association of amino acid substitution polymorphisms in DNA repair genes TP53, POLI, REV1 and LIG4 with lung cancer risk. *Int J Cancer*, 114, 730-7.
- SALEHI, F., DUNFIELD, L., PHILLIPS, K. P., KREWSKI, D., VANDERHYDEN, B. C. 2008. Risk factors for ovarian cancer: an overview with emphasis on hormonal factors. *J Toxicol Environ Health B Crit Rev*, 11, 301-21.
- SALLMYR, A., TOMKINSON, A. E. & RASSOOL, F. V. 2008. Up-regulation of WRN and DNA ligase IIIalpha in chronic myeloid leukemia: consequences for the repair of DNA double-strand breaks. *Blood*, 112, 1413-23.
- SAMIMI, G., KATANO, K., HOLZER, A. K., SAFAEI, R. & HOWELL, S. B. 2004. Modulation of the cellular pharmacology of cisplatin and its analogs by the copper exporters ATP7A and ATP7B. *Mol Pharmacol*, 66, 25-32.
- SAMIMI, G., VARKI, N. M., WILCZYNSKI, S., SAFAEI, R., ALBERTS, D. S. & HOWELL, S. B. 2003. Increase in expression of the copper transporter ATP7A during platinum drug-based treatment is associated with poor survival in ovarian cancer patients. *Clin Cancer Res*, 9, 5853-9.
- SAN FILIPPO, J., SUNG, P. & KLEIN, H. 2008. Mechanism of eukaryotic homologous recombination. *Annu Rev Biochem*, 77, 229-57.
- SANDBERG, R. & ERNBERG, I. 2005. Assessment of tumor characteristic gene expression in cell lines using a tissue similarity index (TSI). *Proceedings of the National Academy of Sciences of the United States of America*, 102, 2052-2057.
- SCARTOZZI, M., DE NICTOLIS, M., GALIZIA, E., CARASSAI, P., BIANCHI, F., BERARDI, R., GESUITA, R., PIGA, A., CELLERINO, R. & PORFIRI, E. 2003. Loss of hMLH1 expression correlates with improved survival in stage III-IV ovarian cancer patients. *Eur J Cancer*, 39, 1144-9.
- SCHILSKY, R. L. 2010. Personalized medicine in oncology: the future is now. *Nat Rev Drug Discov*, 9, 363-6.
- SCHREIBER, V., AME, J. C., DOLLE, P., SCHULTZ, I., RINALDI, B., FRAULOB, V., MENISSIER-DE MURCIA, J. & DE MURCIA, G. 2002. Poly(ADP-ribose) polymerase-2 (PARP-2) is required for efficient base excision DNA repair in association with PARP-1 and XRCC1. *J Biol Chem*, 277, 23028-36.
- SCOTT, C. L., SWISHER, E. M. & KAUFMANN, S. H. 2015. Poly (ADP-ribose) polymerase inhibitors: recent advances and future development. *J Clin Oncol*, 33, 1397-406.

- SEKIGUCHI, J. M. & FERGUSON, D. O. 2006. DNA double-strand break repair: a relentless hunt uncovers new prey. *Cell*, 124, 260-2.
- SELVAKUMARAN, M., PISARCIK, D. A., BAO, R., YEUNG, A. T. & HAMILTON, T. C. 2003. Enhanced cisplatin cytotoxicity by disturbing the nucleotide excision repair pathway in ovarian cancer cell lines. *Cancer Res*, 63, 1311-6.
- SHAH, G. M., KANDAN-KULANGARA, F., MONTONI, A., SHAH, R. G., BRIND'AMOUR, J., VODENICHAROV, M. D. & AFFAR EL, B. 2011. Approaches to detect PARP-1 activation in vivo, in situ, and in vitro. *Methods Mol Biol*, 780, 3-34.
- SHAHIN, M. S., HUGHES, J. H., SOOD, A. K. & BULLER, R. E. 2000. The prognostic significance of p53 tumor suppressor gene alterations in ovarian carcinoma. *Cancer*, 89, 2006-2017.
- SHARMA, M., JAIN, R., IONESCU, E. & SLOCUM, H. K. 1995. Capillary electrophoretic separation and laser-induced fluorescence detection of the major DNA adducts of cisplatin and carboplatin. *Anal Biochem*, 228, 307-11.
- SHARMA, S., SANTISKULVONG, C., BENTOLILA, L. A., RAO, J., DORIGO, O. & GIMZEWSKI, J. K. 2012. Correlative nanomechanical profiling with super-resolution F-actin imaging reveals novel insights into mechanisms of cisplatin resistance in ovarian cancer cells. *Nanomedicine*, 8, 757-66.
- SHAYESTEH, L., LU, Y., KUO, W. L., BALDOCCHI, R., GODFREY, T., COLLINS, C., PINKEL, D., POWELL, B., MILLS, G. B., GRAY, J. W. 1999. PIK3CA is implicated as an oncogene in ovarian cancer. *Nat Genet*, 21, 99-102.
- SHEN, D. W., POULIOT, L. M., HALL, M. D. & GOTTESMAN, M. M. 2012. Cisplatin Resistance: A Cellular Self-Defense Mechanism Resulting from Multiple Epigenetic and Genetic Changes. *Pharmacological Reviews*, 64, 706-721.
- SHEN, H., SCHULTZ, M., KRUH, G. D. & TEW, K. D. 1998. Increased expression of DNA-dependent protein kinase confers resistance to adriamycin. *Biochim Biophys Acta*, 1381, 131-8.
- SHENG, Q., ZHANG, Y., WANG, R., ZHANG, J., CHEN, B., WANG, J., ZHANG, W. & XIN, X. 2012. Prognostic significance of APE1 cytoplasmic localization in human epithelial ovarian cancer. *Med Oncol*, 29, 1265-71.
- SHERMAN-BAUST, C. A., BECKER, K. G., WOOD, W. H., ZHANG, Y. Q. & MORIN, P. J. 2011. Gene expression and pathway analysis of ovarian cancer cells selected for resistance to cisplatin, paclitaxel, or doxorubicin. *Journal of Ovarian Research*, 4.
- SHIH, I.-M. & KURMAN, R. J. 2004. Ovarian Tumorigenesis: A Proposed Model Based on Morphological and Molecular Genetic Analysis. *The American Journal of Pathology*, 164, 1511-1518.
- SHINOHARA, E. T., GENG, L., TAN, J., CHEN, H., SHIR, Y., EDWARDS, E., HALBROOK, J., KESICKI, E. A., KASHISHIAN, A. & HALLAHAN, D. E. 2005. DNA-dependent protein kinase is a molecular target for the development of noncytotoxic radiation-sensitizing drugs. *Cancer Res*, 65, 4987-92.
- SHINTANI, S., MIHARA, M., LI, C., NAKAHARA, Y., HINO, S., NAKASHIRO, K. & HAMAKAWA, H. 2003. Up-regulation of DNA-dependent protein kinase correlates with radiation resistance in oral squamous cell carcinoma. *Cancer Sci*, 94, 894-900.
- SHIVJI, M. K., MUKUND, S. R., RAJENDRA, E., CHEN, S., SHORT, J. M., SAVILL, J., KLENERMAN, D. & VENKITARAMAN, A. R. 2009. The BRC repeats of human BRCA2 differentially regulate RAD51 binding on single- versus double-stranded DNA to stimulate strand exchange. *Proc Natl Acad Sci U S A*, 106, 13254-9.
- SHRIVASTAV, M., DE HARO, L. P. & NICKOLOFF, J. A. 2008. Regulation of DNA double-strand break repair pathway choice. *Cell Res*, 18, 134-47.

- SIDDIK, Z. H. 2003. Cisplatin: mode of cytotoxic action and molecular basis of resistance. *Oncogene*, 22, 7265-7279.
- SKEHAN, P., STORENG, R., SCUDIERO, D., MONKS, A., MCMAHON, J., VISTICA, D., WARREN, J. T., BOKESCH, H., KENNEY, S. & BOYD, M. R. 1990. New Colorimetric Cytotoxicity Assay for Anticancer-Drug Screening. *Journal of the National Cancer Institute*, 82, 1107-1112.
- SLATER, E. P., FENDRICH, V., STRAUCH, K., ROSPLESZCZ, S., RAMASWAMY, A., MATTHAI, E., CHALLOUPKA, B., GRESS, T. M., LANGER, P. & BARTSCH, D. K. 2013. LCN2 and TIMP1 as Potential Serum Markers for the Early Detection of Familial Pancreatic Cancer. *Translational Oncology*, 6, 99-103.
- SMALLEY, K. S. 2003. A pivotal role for ERK in the oncogenic behaviour of malignant melanoma? *Int J Cancer*, 104, 527-32.
- SMITH, T. R., LEVINE, E. A., FREIMANIS, R. I., AKMAN, S. A., ALLEN, G. O., HOANG, K. N., LIU-MARES, W. & HU, J. J. 2008. Polygenic model of DNA repair genetic polymorphisms in human breast cancer risk. *Carcinogenesis*, 29, 2132-8.
- SOBCZUK, A., SMOLARZ, B., ROMANOWICZ, H., ZADROZNY, M., BASZCZYNSKI, J., WESTFAL, B. & PERTYNSKI, T. 2010. Analysis of the polymorphisms in non-homologous DNA end joining (NHEJ) gene Ku70 and Ligase IV in sporadic breast cancer in women. *Pol J Pathol*, 61, 27-31.
- SODHI, R. K., SINGH, N. & JAGGI, A. S. 2010. Poly(ADP-ribose) polymerase-1 (PARP-1) and its therapeutic implications. *Vascul Pharmacol*, 53, 77-87.
- SOMEYA, M., SAKATA, K., MATSUMOTO, Y., YAMAMOTO, H., MONOBE, M., IKEDA, H., ANDO, K., HOSOI, Y., SUZUKI, N. & HAREYAMA, M. 2006. The association of DNA-dependent protein kinase activity with chromosomal instability and risk of cancer. *Carcinogenesis*, 27, 117-22.
- SONG, H., RAMUS, S. J., TYRER, J., BOLTON, K. L., GENTRY-MAHARAJ, A., WOZNIAK, E., ANTON-CULVER, H., CHANG-CLAUDE, J., CRAMER, D. W., WILKENS, L. R., WU, A. H., YANG, H., AUSTRALIAN CANCER, STUDY, AUSTRALIAN OVARIAN CANCER STUDY, GROUP, OVARIAN CANCER ASSOCIATION, CONSORTIUM, HOULSTON, R., BERCHUCK, A., PHAROAH, P. D., GAYTHER, S. A. 2009. A genome-wide association study identifies a new ovarian cancer susceptibility locus on 9p22.2. *Nat Genet*, 41, 996-1000.
- SONG, I. S., SAVARAJ, N., SIDDIK, Z. H., LIU, P., WEI, Y., WU, C. J. & KUO, M. T. 2004. Role of human copper transporter Ctr1 in the transport of platinum-based antitumor agents in cisplatin-sensitive and cisplatin-resistant cells. *Mol Cancer Ther*, 3, 1543-9.
- SPAGNOLO, L., BARBEAU, J., CURTIN, N. J., MORRIS, E. P. & PEARL, L. H. 2012. Visualization of a DNA-PK/PARP1 complex. *Nucleic Acids Res*, 40, 4168-77.
- SPENTZOS, D., LEVINE, D. A., RAMONI, M. F., JOSEPH, M., GU, X., BOYD, J., LIBERMANN, T. A., CANNISTRA, S. A. 2004. Gene expression signature with independent prognostic significance in epithelial ovarian cancer. *J Clin Oncol*, 22, 4700-10.
- STAUFFER, D., CHANG, B., HUANG, J., DUNN, A. & THAYER, M. 2007. p300/CREB-binding protein interacts with ATR and is required for the DNA replication checkpoint. *Journal of Biological Chemistry*, 282, 9678-9687.
- STEFANSSON, O. A., JONASSON, J. G., JOHANNSSON, O. T., OLAFSDOTTIR, K., STEINARSDOTTIR, M., VALGEIRSDOTTIR, S. & EYFJORD, J. E. 2009. Genomic profiling of breast tumours in relation to BRCA abnormalities and phenotypes. *Breast Cancer Research*, 11.
- STEIN, W. D., LITMAN, T., FOJO, T. & BATES, S. E. 2004. Serial Analysis of Gene Expression (SAGE) database analysis of chemosensitivity: Comparing solid tumors with cell lines

- and comparing solid tumors from different tissue origins. *Cancer Research*, 64, 2805-2816.
- STEWART, D. J. 2007. Mechanisms of resistance to cisplatin and carboplatin. *Critical Reviews in Oncology/Hematology*, 63, 12-31.
- STORZ, P. 2005. Reactive oxygen species in tumor progression. *Front Biosci*, 10, 1881-96.
- STRATHDEE, G., MACKEAN, M. J., ILLAND, M. & BROWN, R. 1999. A role for methylation of the hMLH1 promoter in loss of hMLH1 expression and drug resistance in ovarian cancer. *Oncogene*, 18, 2335-41.
- STRATTON, J. F., GAYTHER, S. A., RUSSELL, P., DEARDEN, J., GORE, M., BLAKE, P., EASTON, D. & PONDER, B. A. 1997. Contribution of BRCA1 mutations to ovarian cancer. *N Engl J Med*, 336, 1125-30.
- STRAUSS, H. G., HEMSEN, A., KARBE, I., LAUTENSCHLAGER, C., PERSING, M. & THOMSEN, C. 2008. Phase II trial of biweekly pegylated liposomal doxorubicin in recurrent platinum-refractory ovarian and peritoneal cancer. *Anticancer Drugs*, 19, 541-5.
- STRONATI, L., GENSABELLA, G., LAMBERTI, C., BARATTINI, P., FRASCA, D., TANZARELLA, C., GIACOBINI, S., TOSCANO, M. G., SANTACROCE, C. & DANESI, D. T. 2001. Expression and DNA binding activity of the Ku heterodimer in bladder carcinoma. *Cancer*, 92, 2484-92.
- SUEBLINVONG, T., CARNEY, M.E. 2009. Current understanding of risk factors for ovarian cancer. *Curr Treat Options Oncol.*, 10, 67-81.
- SUGIMURA, K., TAKEBAYASHI, S., TAGUCHI, H., TAKEDA, S. & OKUMURA, K. 2008. PARP-1 ensures regulation of replication fork progression by homologous recombination on damaged DNA. *J Cell Biol*, 183, 1203-12.
- SULTANA, R., ABDEL-FATAH, T., PERRY, C., MOSELEY, P., ALBARAKTI, N., MOHAN, V., SEEDHOUSE, C., CHAN, S. & MADHUSUDAN, S. 2013. Ataxia Telangiectasia Mutated and Rad3 Related (ATR) Protein Kinase Inhibition Is Synthetically Lethal in XRCC1 Deficient Ovarian Cancer Cells. *PLoS ONE*, 8.
- SUN, M., WANG, G., PACIGA, J. E., FELDMAN, R. I., YUAN, Z. Q., MA, X. L., SHELLEY, S. A., JOVE, R., TSICHLIS, P. N., NICOSIA, S. V., CHENG, J. Q. 2001. AKT1/PKBalpha kinase is frequently elevated in human cancers and its constitutive activation is required for oncogenic transformation in NIH3T3 cells. *Am J Pathol*, 159, 431-7.
- SUNG, P. & KLEIN, H. 2006. Mechanism of homologous recombination: mediators and helicases take on regulatory functions. *Nat Rev Mol Cell Biol*, 7, 739-50.
- SWISHER, E. M., SAKAI, W., KARLAN, B. Y., WURZ, K., URBAN, N. & TANIGUCHI, T. 2008. Secondary BRCA1 mutations in BRCA1-mutated ovarian carcinomas with platinum resistance. *Cancer Research*, 68, 2581-2586.
- SYMINGTON, L. S. & GAUTIER, J. 2011. Double-strand break end resection and repair pathway choice. *Annu Rev Genet*, 45, 247-71.
- TAMURA, K., YAMAMOTO, H., SHIMIZU, C., KINOSHITA, T., ANDO, M., YUNOKAWA, M., KOIZUMI, F., MASUTOMI, K., TSUDA, H. & FUJIWARA, Y. 2010. Low Expression Level of Nucleostemin (Gnl3), Stimulator of Cancer Stem Cell Feather, Is a Promising Biomarker to Predict Pathologic Complete Response (Pcr) in Neoadjuvant Treatment with Breast Cancer. *Annals of Oncology*, 21, 88-88.
- TAN, D. S. P., MILLER, R. E. & KAYE, S. B. 2013. New perspectives on molecular targeted therapy in ovarian clear cell carcinoma. *Br J Cancer*, 108, 1553-1559.
- TANIGUCHI, T., TISCHKOWITZ, M., AMEZIANE, N., HODGSON, S. V., MATHEW, C. G., JOENJE, H., MOK, S. C. & D'ANDREA, A. D. 2003. Disruption of the Fanconi anemia-BRCA pathway in cisplatin-sensitive ovarian tumors. *Nat Med*, 9, 568-74.

- TAPIA, G., DIAZ-PADILLA, I. 2012. Molecular Mechanisms of Platinum Resistance in Ovarian Cancer. In: DIAZ-PADILLA, I. (ed.) *Ovarian Cancer - A Clinical and Translational Update*.
- TAVECCHIO, M., MUNCK, J. M., CANO, C., NEWELL, D. R. & CURTIN, N. J. 2012. Further characterisation of the cellular activity of the DNA-PK inhibitor, NU7441, reveals potential cross-talk with homologous recombination. *Cancer Chemother Pharmacol*, 69, 155-64.
- TAYLOR, A. M., GROOM, A. & BYRD, P. J. 2004. Ataxia-telangiectasia-like disorder (ATLD)-its clinical presentation and molecular basis. *DNA Repair (Amst)*, 3, 1219-25.
- TAYLOR, A. M., HARNDEN, D. G., ARLETT, C. F., HARCOURT, S. A., LEHMANN, A. R., STEVENS, S. & BRIDGES, B. A. 1975. Ataxia telangiectasia: a human mutation with abnormal radiation sensitivity. *Nature*, 258, 427-9.
- TELLI, M. L., TIMMS, K. M., REID, J. E., HENNESSY, B., MILLS, G. B., JENSEN, K. C., SZALLASI, Z., BARRY, W. T., WINER, E. P., TUNG, N., ISAKOFF, S. J., RYAN, P. D., GREENE-COLOZZI, A., GUTIN, A., SANGALE, Z., ILIEV, D., NEFF, C., ABKEVICH, V., JONES, J. T., LANCHBURY, J. S., HARTMAN, A. R., GARBER, J. E., FORD, J. M., SILVER, D. P. & RICHARDSON, A. L. 2016. Homologous Recombination Deficiency (HRD) Score Predicts Response to Platinum-Containing Neoadjuvant Chemotherapy in Patients with Triple Negative Breast Cancer. *Clin Cancer Res*.
- THACKER, J. & ZDZIENICKA, M. Z. 2003. The mammalian XRCC genes: their roles in DNA repair and genetic stability. *DNA Repair (Amst)*, 2, 655-72.
- THAVARAMARA, T., TANGJITGAMOL, S., MANUSIRIVITHAYA, S. & LEELAHAKORN, S. 2009. Oral etoposide for refractory or recurrent epithelial ovarian cancer. *J Med Assoc Thai*, 92, 1397-405.
- THOMPSON, L. H. 2012. Recognition, signaling, and repair of DNA double-strand breaks produced by ionizing radiation in mammalian cells: the molecular choreography. *Mutat Res*, 751, 158-246.
- TIAN, J., LIU, Y. P., ZHU, B. B., TIAN, Y., ZHONG, R., CHEN, W., LU, X. H., ZOU, L., SHEN, N., QIAN, J. M., LI, H., MIAO, X. P. & WANG, L. 2015. SF3A1 and pancreatic cancer: new evidence for the association of the spliceosome and cancer. *Oncotarget*, 6, 37750-37757.
- TIMMS, K. M., ABKEVICH, V., HUGHES, E., NEFF, C., REID, J., MORRIS, B., KALVA, S., POTTER, J., TRAN, T. V., CHEN, J., ILIEV, D., SANGALE, Z., TIKISHVILI, E., PERRY, M., ZHARKIKH, A., GUTIN, A. & LANCHBURY, J. S. 2014. Association of BRCA1/2 defects with genomic scores predictive of DNA damage repair deficiency among breast cancer subtypes. *Breast Cancer Research*, 16.
- TOLEDO, L. I., MURGA, M., ZUR, R., SORIA, R., RODRIGUEZ, A., MARTINEZ, S., OYARZABAL, J., PASTOR, J., BISCHOFF, J. R. & FERNANDEZ-CAPETILLO, O. 2011. A cell-based screen identifies ATR inhibitors with synthetic lethal properties for cancer-associated mutations. *Nat Struct Mol Biol*, 18, 721-7.
- TONEGAWA, S. 1983. Somatic generation of antibody diversity. *Nature*, 302, 575-81.
- TONG, X., SHINE, D. H., AGOULNIK, I., FREUND, C. T., HASENBURG, A., AGUILAR-CORDOVA, E., WOO, S. L. & KIEBACK, D. G. 1998. Adenovirus mediated thymidine kinase gene therapy may enhance sensitivity of ovarian cancer cells to chemotherapeutic agents. *Anticancer Res*, 18, 3421-6.
- TREECK, O., WACKWITZ, B., HAUS, U., ORTMANN, O. 2006. Effects of a combined treatment with mTOR inhibitor RAD001 and tamoxifen in vitro on growth and apoptosis of human cancer cells. *Gynecol Oncol*, 102, 292-9.

- TREISMAN, R. 1994. Ternary complex factors: growth factor regulated transcriptional activators. *Curr Opin Genet Dev*, 4, 96-101.
- TRIMBOS, J. B., VERGOTE, I., BOLIS, G., VERMORKEN, J. B., MANGIONI, C., MADRONAL, C., FRANCHI, M., TATEO, S., ZANETTA, G., SCARFONE, G., GIURGEA, L., TIMMERS, P., COENS, C. & PECORELLI, S. 2003. Impact of adjuvant chemotherapy and surgical staging in early-stage ovarian carcinoma: European Organisation for Research and Treatment of Cancer-Adjuvant ChemoTherapy in Ovarian Neoplasm trial. *J Natl Cancer Inst*, 95, 113-25.
- TSENG, H. C., TSAI, M. H., CHIU, C. F., WANG, C. H., CHANG, N. W., HUANG, C. Y., TSAI, C. W., LIANG, S. Y., WANG, C. L. & BAU, D. T. 2008. Association of XRCC4 codon 247 polymorphism with oral cancer susceptibility in Taiwan. *Anticancer Res*, 28, 1687-1691.
- TSENG, R. C., CHANG, J. M., CHEN, J. H., HUANG, W. R., TANG, Y. A., KUO, Y., YAN, J. J., LAI, W. W. & WANG, Y. C. 2015. Deregulation of SLIT2-Mediated Cdc42 Activity Is Associated with Esophageal Cancer Metastasis and Poor Prognosis. *Journal of Thoracic Oncology*, 10, 189-198.
- TSENG, R. C., HSIEH, F. J., SHIH, C. M., HSU, H. S., CHEN, C. Y. & WANG, Y. C. 2009. Lung cancer susceptibility and prognosis associated with polymorphisms in the nonhomologous end-joining pathway genes: a multiple genotype-phenotype study. *Cancer*, 115, 2939-48.
- TURNER, N., TUTT, A. & ASHWORTH, A. 2004. Hallmarks of 'BRCAness' in sporadic cancers. *Nature Reviews Cancer*, 4, 814-819.
- TURNER, N., TUTT, A. & ASHWORTH, A. 2005. Targeting the DNA repair defect of BRCA tumours. *Curr Opin Pharmacol*, 5, 388-93.
- TURNER, N. C., ASHWORTH, A. 2011. Biomarkers of PARP inhibitor sensitivity. *Breast Cancer Res Treat*, 127, 283-6.
- UM, J. H., KWON, J. K., KANG, C. D., KIM, M. J., JU, D. S., BAE, J. H., KIM, D. W., CHUNG, B. S. & KIM, S. H. 2004. Relationship between antiapoptotic molecules and metastatic potency and the involvement of DNA-dependent protein kinase in the chemosensitization of metastatic human cancer cells by epidermal growth factor receptor blockade. *J Pharmacol Exp Ther*, 311, 1062-70.
- VAINIO, P., MPINDI, J. P., KOHONEN, P., FEY, V., MIRTITI, T., ALANEN, K. A., PERALA, M., KALLIONIEMI, O. & ILJIN, K. 2012. High-Throughput Transcriptomic and RNAi Analysis Identifies AIM1, ERGIC1, TMED3 and TPX2 as Potential Drug Targets in Prostate Cancer. *Plos One*, 7.
- VALERIE, K. & POVIRK, L. F. 2003. Regulation and mechanisms of mammalian double-strand break repair. *Oncogene*, 22, 5792-5812.
- VANKRANEN, H. J., DEGRUIJL, F. R., DEVRIES, A., SONTAG, Y., WESTER, P. W., SENDEN, H. C. M., ROZEMULLER, E. & VANKREIJL, C. F. 1995. Frequent P53 Alterations but Low Incidence of Ras Mutations in Uv-B-Induced Skin Tumors of Hairless Mice. *Carcinogenesis*, 16, 1141-1147.
- VARMA, R. R., HECTOR, S. M., CLARK, K., GRECO, W. R., HAWTHORN, L. & PENDYALA, L. 2005. Gene expression profiling of a clonal isolate of oxaliplatin resistant ovarian carcinoma cell line A2780/C10. *Oncology Reports*, 14, 925-932.
- VASEY, P. A., SHULMAN, L. N., CAMPOS, S., DAVIS, J., GORE, M., JOHNSTON, S., KIRN, D. H., O'NEILL, V., SIDDIQUI, N., SEIDEN, M. V. & KAYE, S. B. 2002. Phase I trial of intraperitoneal injection of the E1B-55-kd-Gene - Deleted adenovirus ONYX-015 (dl1520) given on days 1 through 5 every 3 weeks in patients with

- recurrent/refractory epithelial ovarian cancer. *Journal of Clinical Oncology*, 20, 1562-1569.
- VASSILEV, L. T., VU, B. T., GRAVES, B., CARVAJAL, D., PODLASKI, F., FILIPOVIC, Z., KONG, N., KAMMLOTT, U., LUKACS, C., KLEIN, C., FOTOUHI, N. & LIU, E. A. 2004. In vivo activation of the p53 pathway by small-molecule antagonists of MDM2. *Science*, 303, 844-8.
- VASSILEVA, V., MILLAR, A., BRIOLLAIS, L., CHAPMAN, W. & BAPAT, B. 2002. Genes involved in DNA repair are mutational targets in endometrial cancers with microsatellite instability. *Cancer Res*, 62, 4095-9.
- VAUGHAN, S., COWARD, J. I., BAST, R. C., BERCHUCK, A., BEREK, J. S., BRENTON, J. D., COUKOS, G., CRUM, C. C., DRAPKIN, R., ETEMADMOGHADAM, D., FRIEDLANDER, M., GABRA, H., KAYE, S. B., LORD, C. J., LENGUEL, E., LEVINE, D. A., MCNEISH, I. A., MENON, U., MILLS, G. B., NEPHEW, K. P., OZA, A. M., SOOD, A. K., STRONACH, E. A., WALCZAK, H., BOWTELL, D. D. & BALKWILL, F. R. 2011. Rethinking ovarian cancer: recommendations for improving outcomes. *Nat Rev Cancer*, 11, 719-725.
- VERGOTE, I., TROPE, C. G., AMANT, F., KRISTENSEN, G. B., EHLEN, T., JOHNSON, N., VERHEIJEN, R. H., VAN DER BURG, M. E., LACAVE, A. J., PANICI, P. B., KENTER, G. G., CASADO, A., MENDIOLA, C., COENS, C., VERLEYE, L., STUART, G. C., PECORELLI, S., REED, N. S., EUROPEAN ORGANIZATION FOR, R., TREATMENT OF CANCER-GYNAECOLOGICAL CANCER, G. & GROUP, N. C. T. 2010. Neoadjuvant chemotherapy or primary surgery in stage IIIC or IV ovarian cancer. *N Engl J Med*, 363, 943-53.
- VEUGER, S. J., CURTIN, N. J., RICHARDSON, C. J., SMITH, G. C. & DURKACZ, B. W. 2003. Radiosensitization and DNA repair inhibition by the combined use of novel inhibitors of DNA-dependent protein kinase and poly(ADP-ribose) polymerase-1. *Cancer Res*, 63, 6008-15.
- VEUGER, S. J., CURTIN, N. J., SMITH, G. C. & DURKACZ, B. W. 2004. Effects of novel inhibitors of poly(ADP-ribose) polymerase-1 and the DNA-dependent protein kinase on enzyme activities and DNA repair. *Oncogene*, 23, 7322-9.
- VICHAJ, V. & KIRTIKARA, K. 2006. Sulforhodamine B colorimetric assay for cytotoxicity screening. *Nature Protocols*, 1, 1112-1116.
- VIRSIK-KOPP, P., RAVE-FRANK, M., HOFMAN-HUTHER, H. & SCHMIDBERGER, H. 2004. Role of DNA-dependent protein kinase in the process of radiation-induced aberration formation. *Int J Radiat Biol*, 80, 125-33.
- VOCKLEY, J. G., CREIGHTON, C. J., NICHOL, R., FISHER, S., UPFAL, E. & SAMAYOA, J. 2012. Integrated genomic analyses of ovarian carcinoma (vol 474, pg 609, 2011). *Nature*, 490, 292-292.
- VON HEIDEMAN, A., THOLANDER, B., GRUNDMARK, B., CAJANDER, S., GERDIN, E., HOLM, L., AXELSSON, A., ROSENBERG, P., MAHTEME, H., DANIEL, E., LARSSON, R., NYGREN, P. 2014. Chemotherapeutic drug sensitivity of primary cultures of epithelial ovarian cancer cells from patients in relation to tumour characteristics and therapeutic outcome. *Acta Oncol*, 53, 242-50.
- WADE, M. A., SUNTER, N. J., FORDHAM, S. E., LONG, A., MASIC, D., RUSSELL, L. J., HARRISON, C. J., RAND, V., ELSTOB, C., BOWN, N., ROWE, D., LOWE, C., CUTHBERT, G., BENNETT, S., CROSIER, S., BACON, C. M., ONEL, K., SCOTT, K., SCOTT, D., TRAVIS, L. B., MAY, F. E. & ALLAN, J. M. 2015. c-MYC is a radiosensitive locus in human breast cells. *Oncogene*, 34, 4985-94.
- WALKER, G., MACLEOD, K., WILLIAMS, A., CAMERON, D., SMYTH, J. & LANGDON, S. 2007. Estrogen-regulated gene expression predicts response to endocrine therapy in patients with ovarian cancer. *Gynecol Oncol*, 106, 461-468.

- WALKER, J. R., CORPINA, R. A. & GOLDBERG, J. 2001. Structure of the Ku heterodimer bound to DNA and its implications for double-strand break repair. *Nature*, 412, 607-14.
- WANG, C., HORIUCHI, A., IMAI, T., OHIRA, S., ITOH, K., NIKAI, T., KATSUYAMA, Y. & KONISHI, I. 2004a. Expression of BRCA1 protein in benign, borderline, and malignant epithelial ovarian neoplasms and its relationship to methylation and allelic loss of the BRCA1 gene. *J Pathol*, 202, 215-23.
- WANG, H., PERRAULT, A. R., TAKEDA, Y., QIN, W. & ILIAKIS, G. 2003. Biochemical evidence for Ku-independent backup pathways of NHEJ. *Nucleic Acids Res*, 31, 5377-88.
- WANG, H., ROSIDI, B., PERRAULT, R., WANG, M., ZHANG, L., WINDHOFFER, F. & ILIAKIS, G. 2005. DNA ligase III as a candidate component of backup pathways of nonhomologous end joining. *Cancer Res*, 65, 4020-30.
- WANG, H. C., CHOU, W. C., SHIEH, S. Y. & SHEN, C. Y. 2006a. Ataxia telangiectasia mutated and checkpoint kinase 2 regulate BRCA1 to promote the fidelity of DNA end-joining. *Cancer Res*, 66, 1391-400.
- WANG, H. Y., WANG, H. C., POWELL, S. N., ILIAKIS, G. & WANG, Y. 2004b. ATR affecting cell radiosensitivity is dependent on homologous recombination repair but independent of nonhomologous end joining. *Cancer Research*, 64, 7139-7143.
- WANG, M., WU, W., ROSIDI, B., ZHANG, L., WANG, H. & ILIAKIS, G. 2006b. PARP-1 and Ku compete for repair of DNA double strand breaks by distinct NHEJ pathways. *Nucleic Acids Res*, 34, 6170-82.
- WANG, W., GAO, Y., YAN, F., WANG, M., HU, F., WANG, D., CAO, Q., QIN, C., YIN, C., ZHANG, Z. & PAN, X. 2012. Association of Ku70 A-31G polymorphism and risk of renal cell carcinoma in a Chinese population. *DNA Cell Biol*, 31, 1314-20.
- WANG, X., PAN, L., MAO, N., SUN, L., QIN, X. & YIN, J. 2013a. Cell-cycle synchronization reverses Taxol resistance of human ovarian cancer cell lines. *Cancer Cell Int*, 13, 77.
- WANG, X. G., WANG, Z. Q., TONG, W. M. & SHEN, Y. 2007. PARP1 Val762Ala polymorphism reduces enzymatic activity. *Biochem Biophys Res Commun*, 354, 122-6.
- WANG, X. M., LI, J., YAN, M. X., LIU, L., JIA, D. S., GENG, Q., LIN, H. C., HE, X. H., LI, J. J. & YAO, M. 2013b. Integrative Analyses Identify Osteopontin, LAMB3 and ITGB1 as Critical Pro-Metastatic Genes for Lung Cancer. *Plos One*, 8.
- WATANABE, Y., KOI, M., HEMMI, H., HOSHAI, H. & NODA, K. 2001. A change in microsatellite instability caused by cisplatin-based chemotherapy of ovarian cancer. *Br J Cancer*, 85, 1064-9.
- WATKINS, J. A., IRSHAD, S., GRIGORIADIS, A. & TUTT, A. N. J. 2014. Genomic scars as biomarkers of homologous recombination deficiency and drug response in breast and ovarian cancers. *Breast Cancer Research*, 16.
- WATSON, P. & LYNCH, H. T. 2001. Cancer risk in mismatch repair gene mutation carriers. *Fam Cancer*, 1, 57-60.
- WEI, L., LAN, L., HONG, Z., YASUI, A., ISHIOKA, C. & CHIBA, N. 2008. Rapid recruitment of BRCA1 to DNA double-strand breaks is dependent on its association with Ku80. *Mol Cell Biol*, 28, 7380-93.
- WELLCOME TRUST SANGER INSTITUTE. 2013. *COSMIC (Catalogue of somatic mutations in cancer)*.
- WIECHEC, E., WIUF, C., OVERGAARD, J. & HANSEN, L. L. 2011. High-Resolution Melting Analysis for Mutation Screening of RGSL1, RGS16, and RGS8 in Breast Cancer. *Cancer Epidemiology Biomarkers & Prevention*, 20, 397-407.
- WIEGAND, K. C., SHAH, S. P., AL-AGHA, O. M., ZHAO, Y., TSE, K., ZENG, T., SENZ, J., MCCONECHY, M. K., ANGLESIO, M. S., KALLOGER, S. E., YANG, W., HERAVI-MOUSSAVI, A., GIULIANI, R., CHOW, C., FEE, J., ZAYED, A., PRENTICE, L., MELNYK, N.,

- TURASHVILI, G., DELANEY, A. D., MADORE, J., YIP, S., MCPHERSON, A. W., HA, G., BELL, L., FEREDAY, S., TAM, A., GALLETTA, L., TONIN, P. N., PROVENCHER, D., MILLER, D., JONES, S. J., MOORE, R. A., MORIN, G. B., OLOUMI, A., BOYD, N., APARICIO, S. A., SHIH IE, M., MES-MASSON, A. M., BOWTELL, D. D., HIRST, M., GILKS, B., MARRA, M. A. & HUNTSMAN, D. G. 2010. ARID1A mutations in endometriosis-associated ovarian carcinomas. *N Engl J Med*, 363, 1532-43.
- WILLEMS, P., CLAES, K., BAEYENS, A., VANDERSICKEL, V., WERBROUCK, J., DE RUYCK, K., POPPE, B., VAN DEN BROECKE, R., MAKAR, A., MARRAS, E., PERLETTI, G., THIERENS, H. & VRAL, A. 2008. Polymorphisms in nonhomologous end-joining genes associated with breast cancer risk and chromosomal radiosensitivity. *Genes Chromosomes Cancer*, 47, 137-48.
- WILLNER, J., WURZ, K., ALLISON, K. H., GALIC, V., GARCIA, R. L., GOFF, B. A. & SWISHER, E. M. 2007. Alternate molecular genetic pathways in ovarian carcinomas of common histological types. *Hum Pathol*, 38, 607-13.
- WINDHOFER, F., KRAUSE, S., HADER, C., SCHULZ, W. A. & FLORL, A. R. 2008. Distinctive differences in DNA double-strand break repair between normal urothelial and urothelial carcinoma cells. *Mutat Res*, 638, 56-65.
- WINDHOFER, F., WU, W., WANG, M., SINGH, S. K., SAHA, J., ROSIDI, B. & ILIAKIS, G. 2007. Marked dependence on growth state of backup pathways of NHEJ. *Int J Radiat Oncol Biol Phys*, 68, 1462-70.
- WISEMAN, H. & HALLIWELL, B. 1996. Damage to DNA by reactive oxygen and nitrogen species: role in inflammatory disease and progression to cancer. *Biochem J*, 313 (Pt 1), 17-29.
- WOODHOUSE, L., MCCORMICK, A., O'DONNELL, R., KAUFMANN, A. & EDMONDSON, R. 2014. Development of a Functional Assay to Determine the Nucleotide Excision Repair Status of Epithelial Ovarian Cancer. *International Journal of Gynecological Cancer*, 24, 169-170.
- WORLEY, M. J., WELCH, W. R., BERKOWITZ, R. S., NG, S. W. 2013. Endometriosis-associated ovarian cancer: a review of pathogenesis. *Int J Mol Sci*, 14, 5367-79.
- WU, J. N. & ROBERTS, C. W. 2013. ARID1A mutations in cancer: another epigenetic tumor suppressor? *Cancer Discov*, 3, 35-43.
- WU, L. & HICKSON, I. D. 2003. The Bloom's syndrome helicase suppresses crossing over during homologous recombination. *Nature*, 426, 870-4.
- WU, W., WANG, M., SINGH, S. K., MUSSFELDT, T. & ILIAKIS, G. 2008. Repair of radiation induced DNA double strand breaks by backup NHEJ is enhanced in G2. *DNA Repair (Amst)*, 7, 329-38.
- XING, J., WU, X., VAPORCIYAN, A. A., SPITZ, M. R. & GU, J. 2008. Prognostic significance of ataxia-telangiectasia mutated, DNA-dependent protein kinase catalytic subunit, and Ku heterodimeric regulatory complex 86-kD subunit expression in patients with nonsmall cell lung cancer. *Cancer*, 112, 2756-64.
- YAJIMA, H., LEE, K. J. & CHEN, B. P. C. 2006. ATR-dependent phosphorylation of DNA-dependent protein kinase catalytic subunit in response to UV-induced replication stress. *Molecular and Cellular Biology*, 26, 7520-7528.
- YAMAMOTO, K., WANG, Y., JIANG, W., LIU, X., DUBOIS, R. L., LIN, C. S., LUDWIG, T., BAKKENIST, C. J. & ZHA, S. 2012. Kinase-dead ATM protein causes genomic instability and early embryonic lethality in mice. *J Cell Biol*, 198, 305-13.
- YAN, C. T., BOBOILA, C., SOUZA, E. K., FRANCO, S., HICKERNELL, T. R., MURPHY, M., GUMASTE, S., GEYER, M., ZARRIN, A. A., MANIS, J. P., RAJEWSKY, K. & ALT, F. W.

2007. IgH class switching and translocations use a robust non-classical end-joining pathway. *Nature*, 449, 478-82.
- YANG, M. D., WANG, H. C., CHANG, W. S., TSAI, C. W. & BAU, D. T. 2011. Genetic polymorphisms of DNA double strand break gene Ku70 and gastric cancer in Taiwan. *BMC Cancer*, 11, 174.
- YAO, L., LAO, W. F., ZHANG, Y., TANG, X. R., HU, X. T., HE, C., HU, X. F. & XU, L. S. X. 2012. Identification of EFEMP2 as a Serum Biomarker for the Early Detection of Colorectal Cancer with Lectin Affinity Capture Assisted Secretome Analysis of Cultured Fresh Tissues. *Journal of Proteome Research*, 11, 3281-3294.
- YEPURU, M., WU, Z. Z., KULKARNI, A., YIN, F., BARRETT, C. M., KIM, J., STEINER, M. S., MILLER, D. D., DALTON, J. T. & NARAYANAN, R. 2013. Steroidogenic Enzyme AKR1C3 Is a Novel Androgen Receptor-Selective Coactivator that Promotes Prostate Cancer Growth. *Clinical Cancer Research*, 19, 5613-5625.
- YOKOMIZO, A., TINDALL, D. J., HARTMANN, L., JENKINS, R. B., SMITH, D. I., LIU, W. 1998. Mutation analysis of the putative tumor suppressor PTEN/MMAC1 in human ovarian cancer. *Int J Oncol*, 13, 101-5.
- YOSHIOKA, K., YOSHIOKA, Y. & HSIEH, P. 2006. ATR kinase activation mediated by MutS alpha and MutL alpha in response to cytotoxic O(6)-methylguanine adducts. *Molecular Cell*, 22, 501-510.
- YU, H. P., ZHAO, H., WANG, L. E., HAN, Y. H., CHEN, W. V., AMOS, C. I., RAFNAR, T., SULEM, P., STEFANSSON, K., LANDI, M. T., CAPORASO, N., ALBANES, D., THUN, M., MCKAY, J. D., BRENNAN, P., WANG, Y. F., HOULSTON, R. S., SPITZ, M. R. & WEI, Q. Y. 2011. An analysis of single nucleotide polymorphisms of 125 DNA repair genes in the Texas genome-wide association study of lung cancer with a replication for the XRCC4 SNPs. *DNA Repair*, 10, 398-407.
- ZAREMBA, T., THOMAS, H. D., COLE, M., COULTHARD, S. A., PLUMMER, E. R. & CURTIN, N. J. 2011. Poly(ADP-ribose) polymerase-1 (PARP-1) pharmacogenetics, activity and expression analysis in cancer patients and healthy volunteers. *Biochem J*, 436, 671-9.
- ZHAI, X., LIU, J., HU, Z., WANG, S., QING, J., WANG, X., JIN, G., GAO, J. & SHEN, H. 2006. Polymorphisms of ADPRT Val762Ala and XRCC1 Arg399Glu and risk of breast cancer in Chinese women: a case control analysis. *Oncol Rep*, 15, 247-52.
- ZHANG, H., ZHANG, S., CUI, J., ZHANG, A., SHEN, L. & YU, H. 2008. Expression and promoter methylation status of mismatch repair gene hMLH1 and hMSH2 in epithelial ovarian cancer. *Aust N Z J Obstet Gynaecol*, 48, 505-9.
- ZHANG, J., ZHANG, W. P., ZOU, D. J., CHEN, G. Y., WAN, T., ZHANG, M. H. & CAO, X. T. 2003. Cloning and functional characterization of GMPR2, a novel human guanosine monophosphate reductase, which promotes the monocytic differentiation of HL-60 leukemia cells. *Journal of Cancer Research and Clinical Oncology*, 129, 76-83.
- ZHANG, Y., NEWCOMB, P. A., EGAN, K. M., TITUS-ERNSTOFF, L., CHANOCK, S., WELCH, R., BRINTON, L. A., LISSOWSKA, J., BARDIN-MIKOLAJCZAK, A., PEPLONSKA, B., SZESZENIA-DABROWSKA, N., ZATONSKI, W. & GARCIA-CLOSAS, M. 2006. Genetic polymorphisms in base-excision repair pathway genes and risk of breast cancer. *Cancer Epidemiol Biomarkers Prev*, 15, 353-8.
- ZHANG, Y., WANG, J., XIANG, D., WANG, D. & XIN, X. 2009. Alterations in the expression of the apurinic/apyrimidinic endonuclease-1/redox factor-1 (APE1/Ref-1) in human ovarian cancer and indentification of the therapeutic potential of APE1/Ref-1 inhibitor. *Int J Oncol*, 35, 1069-79.

- ZHAO, H. & PIWNICA-WORMS, H. 2001. ATR-mediated checkpoint pathways regulate phosphorylation and activation of human Chk1. *Molecular and Cellular Biology*, 21, 4129-4139.
- ZHAO, Y., THOMAS, H. D., BATEY, M. A., COWELL, I. G., RICHARDSON, C. J., GRIFFIN, R. J., CALVERT, A. H., NEWELL, D. R., SMITH, G. C. & CURTIN, N. J. 2006. Preclinical evaluation of a potent novel DNA-dependent protein kinase inhibitor NU7441. *Cancer Res*, 66, 5354-62.
- ZHONG, Q., BOYER, T. G., CHEN, P. L. & LEE, W. H. 2002. Deficient nonhomologous end-joining activity in cell-free extracts from Brca1-null fibroblasts. *Cancer Res*, 62, 3966-70.
- ZHONG, Q., CHEN, C. F., LI, S., CHEN, Y., WANG, C. C., XIAO, J., CHEN, P. L., SHARP, Z. D. & LEE, W. H. 1999. Association of BRCA1 with the hRad50-hMre11-p95 complex and the DNA damage response. *Science*, 285, 747-50.
- ZHONG, T., XU, F. F., XU, J. H., LIU, L. & CHEN, Y. 2015. Aldo-keto reductase 1C3 (AKR1C3) is associated with the doxorubicin resistance in human breast cancer via PTEN Loss. *Biomedicine & Pharmacotherapy*, 69, 317-325.
- ZHOU, L. P., LUAN, H., DONG, X. H., JIN, G. J., MA, D. L. & SHANG, H. 2012. Association of Functional Polymorphisms of the XRCC4 Gene with the Risk of Breast Cancer: A Meta-analysis. *Asian Pac J Cancer Prev*, 13, 3431-6.
- ZHOU, X. Y., CHEN, X. J., HU, L. M., HAN, S. P., QIANG, F. L., WU, Y. L., PAN, L., SHEN, H. B., LI, Y. & HU, Z. B. 2010. Polymorphisms involved in the miR-218-LAMB3 pathway and susceptibility of cervical cancer, a case-control study in Chinese women. *Gynecologic Oncology*, 117, 287-290.
- ZHOU, X. Y., XIA, Y., LI, L. & ZHANG, G. X. 2015. MiR-101 inhibits cell growth and tumorigenesis of Helicobacter pylori related gastric cancer by repression of SOCS2. *Cancer Biology & Therapy*, 16, 160-169.
- ZHU, Q. L., LIANG, X., DAI, J. & GUAN, X. 2015. Prostaglandin transporter, SLCO2A1, mediates the invasion and apoptosis of lung cancer cells via PI3K/AKT/mTOR pathway. *International Journal of Clinical and Experimental Pathology*, 8, 9175-9181.
- ZHUANG, J., ZHANG, J., WILLERS, H., WANG, H., CHUNG, J. H., VAN GENT, D. C., HALLAHAN, D. E., POWELL, S. N. & XIA, F. 2006. Checkpoint kinase 2-mediated phosphorylation of BRCA1 regulates the fidelity of nonhomologous end-joining. *Cancer Res*, 66, 1401-8.